Astroparticle Physics with Multiple Messengers

Günter Sigl
II. Institut theoretische Physik, Universität Hamburg
http://www2.iap.fr/users/sigl/homepage.html

Astroparticle Physics with Multiple Messengers

- Cosmic radiation from our Galaxy
- Extragalactic Cosmic Radiation
- Open Questions: Nature of the sources, chemical composition
- Role of cosmic magnetic fields
- Ultra-High Energy Cosmic Rays and secondary γ-rays and neutrinos: Constraints and detection prospects with different experiments.
- Testing physics beyond the Standard Model: Cross sections at PeV scales, Lorentz symmetry violation

Günter Sigl

II. Institut theoretische Physik, Universität Hamburg

http://www2.iap.fr/users/sigl/homepage.html

The structure of the spectrum and scenarios of its origin

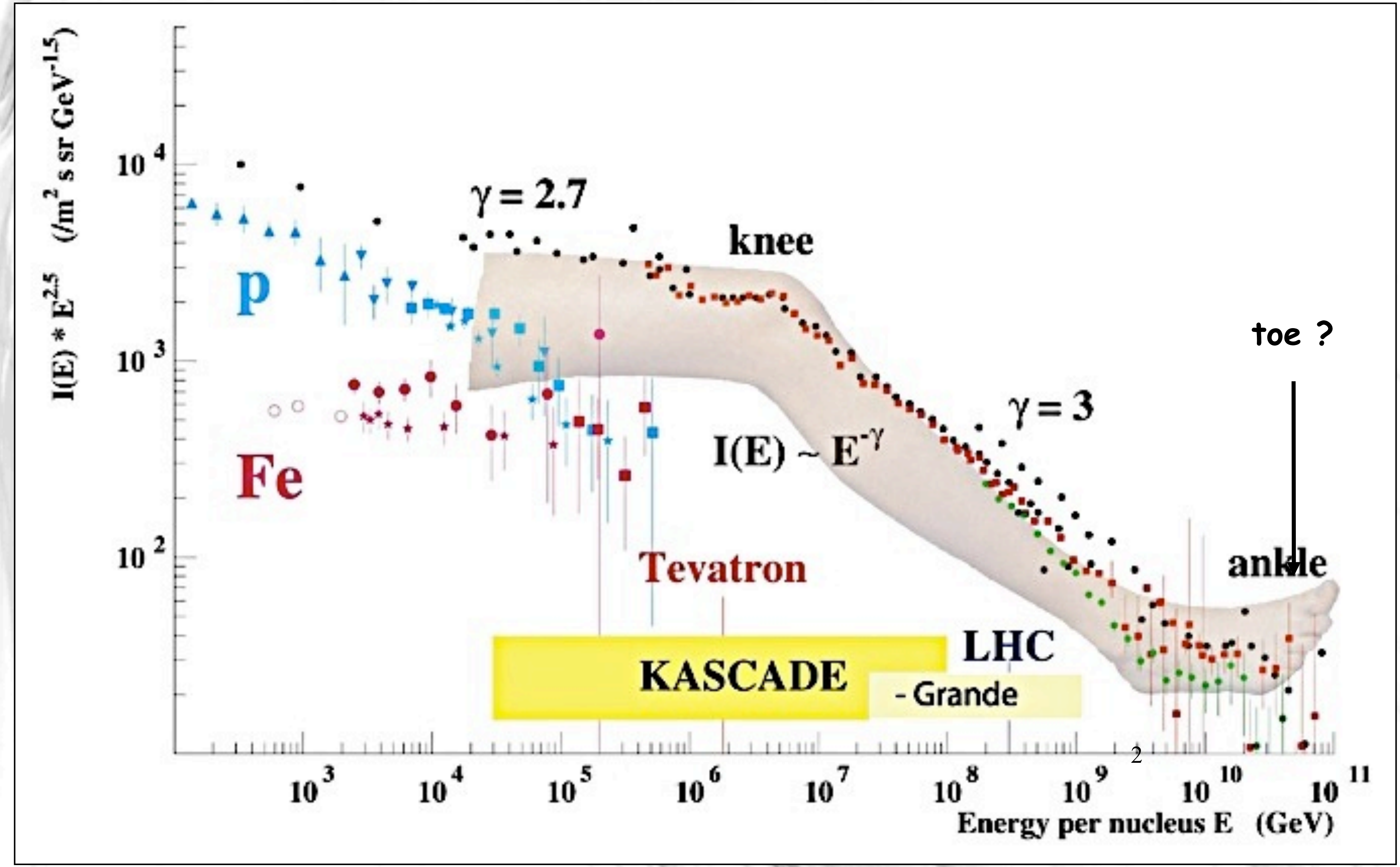

The structure of the spectrum and scenarios of its origin

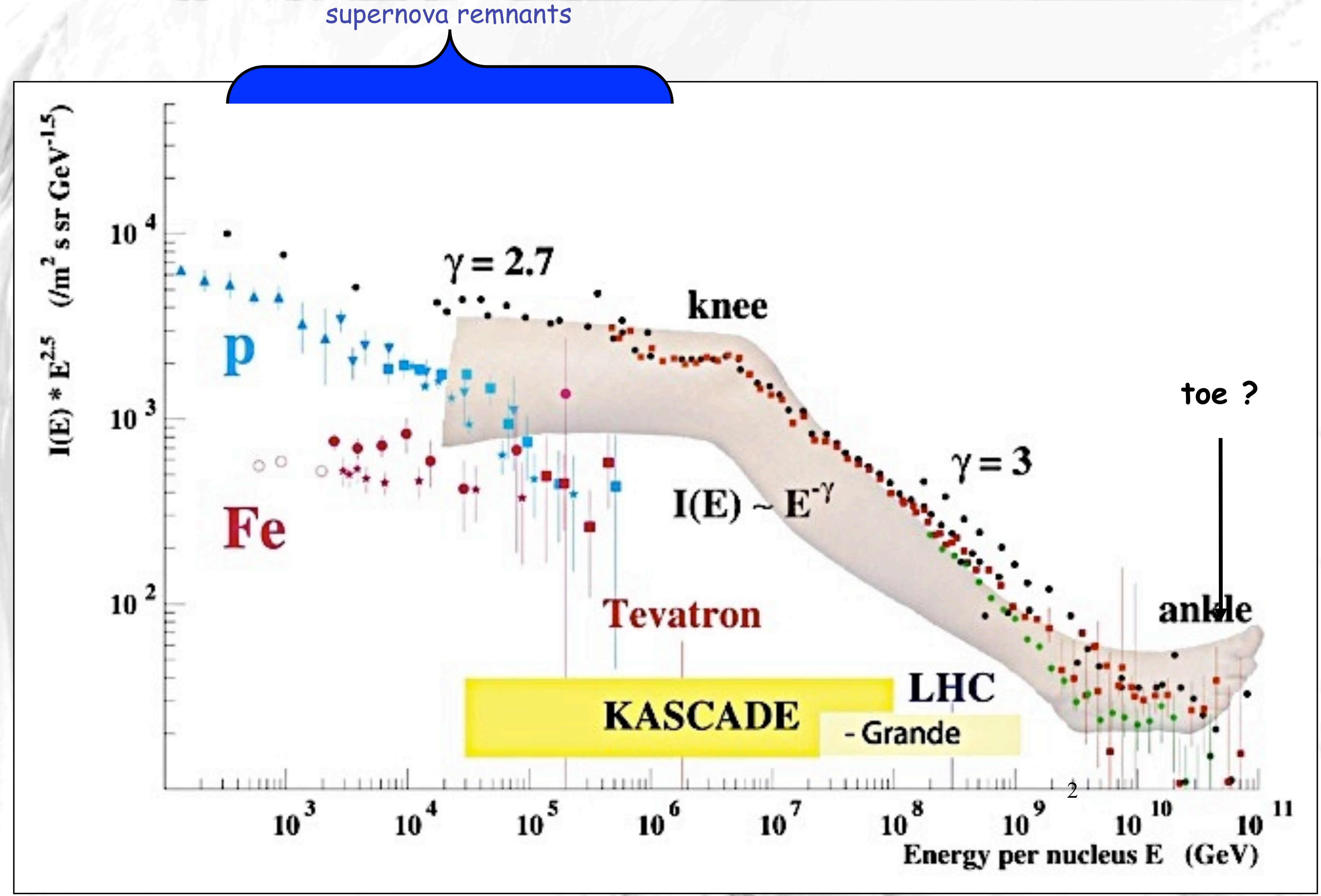

The structure of the spectrum and scenarios of its origin

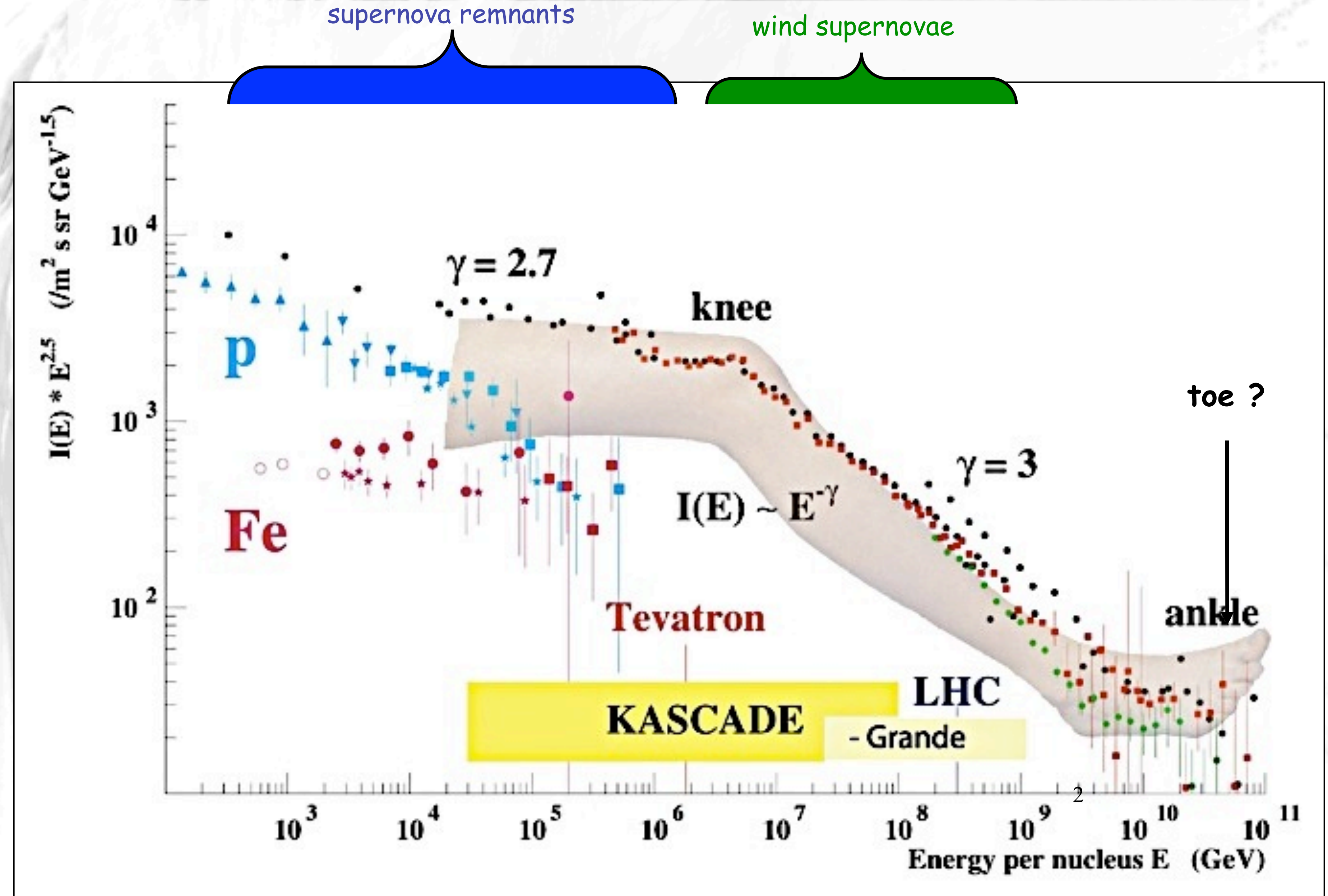

The structure of the spectrum and scenarios of its origin

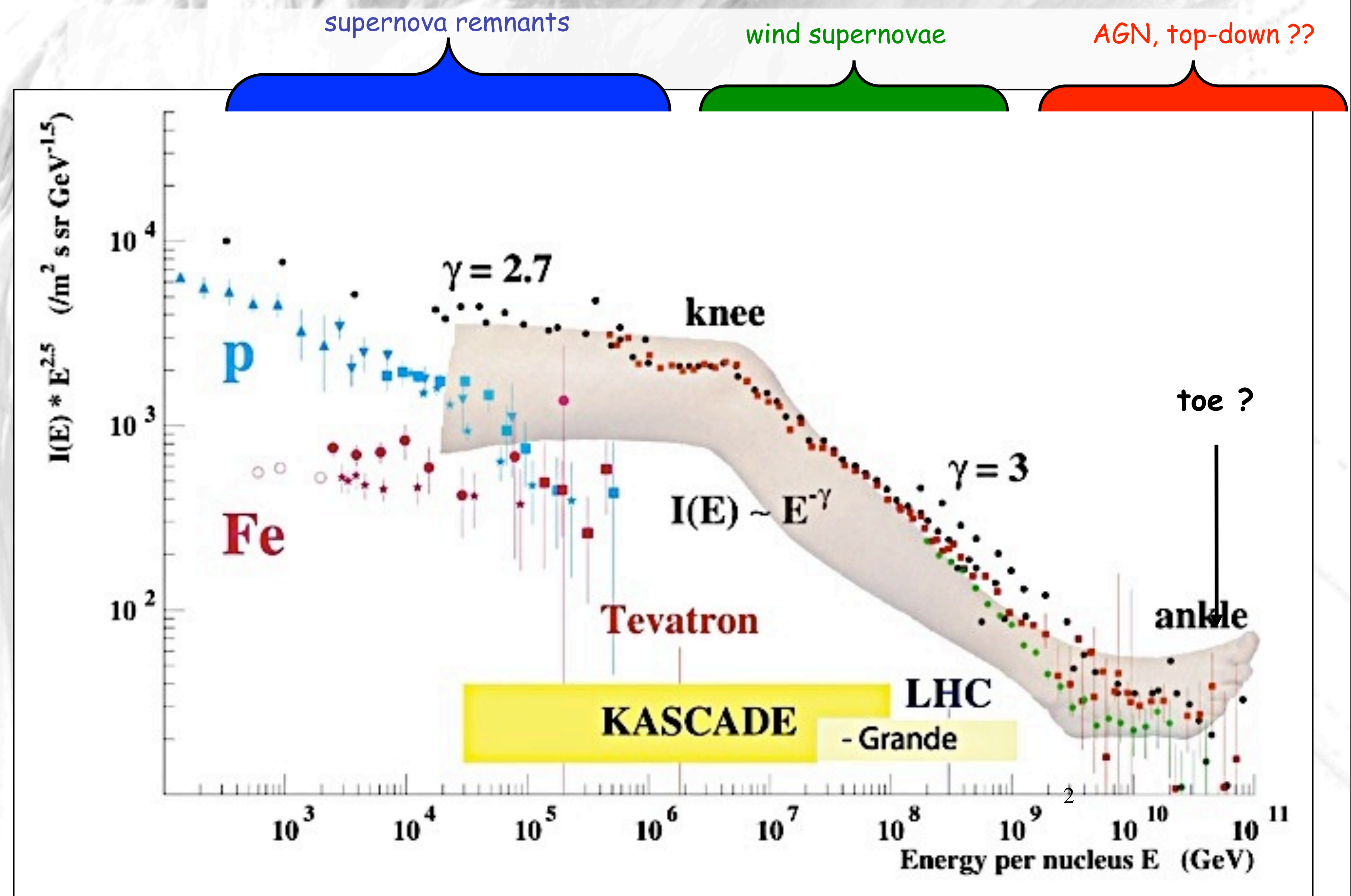

Another View of the All Particle Spectrum

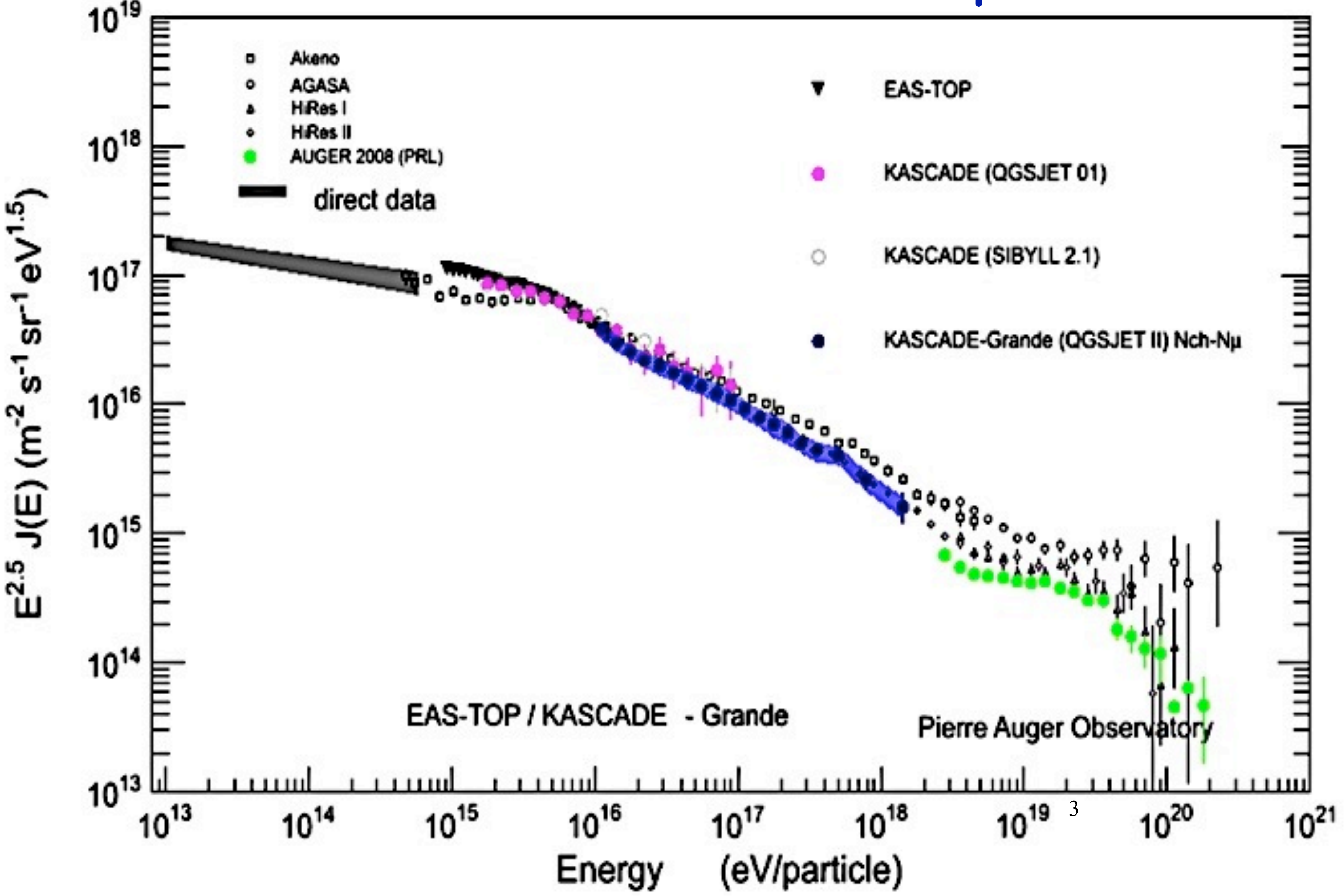

KASCADE-Grande collaboration, arXiv:1009.4716

Supernova Remnants and Galactic Cosmic and γ-Rays

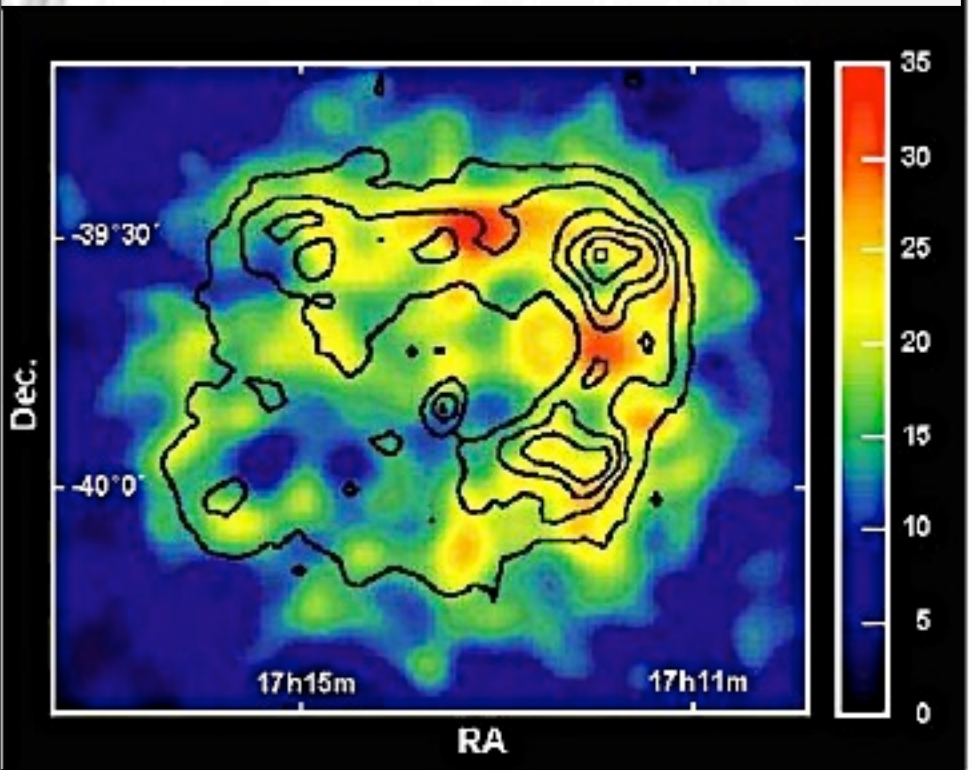

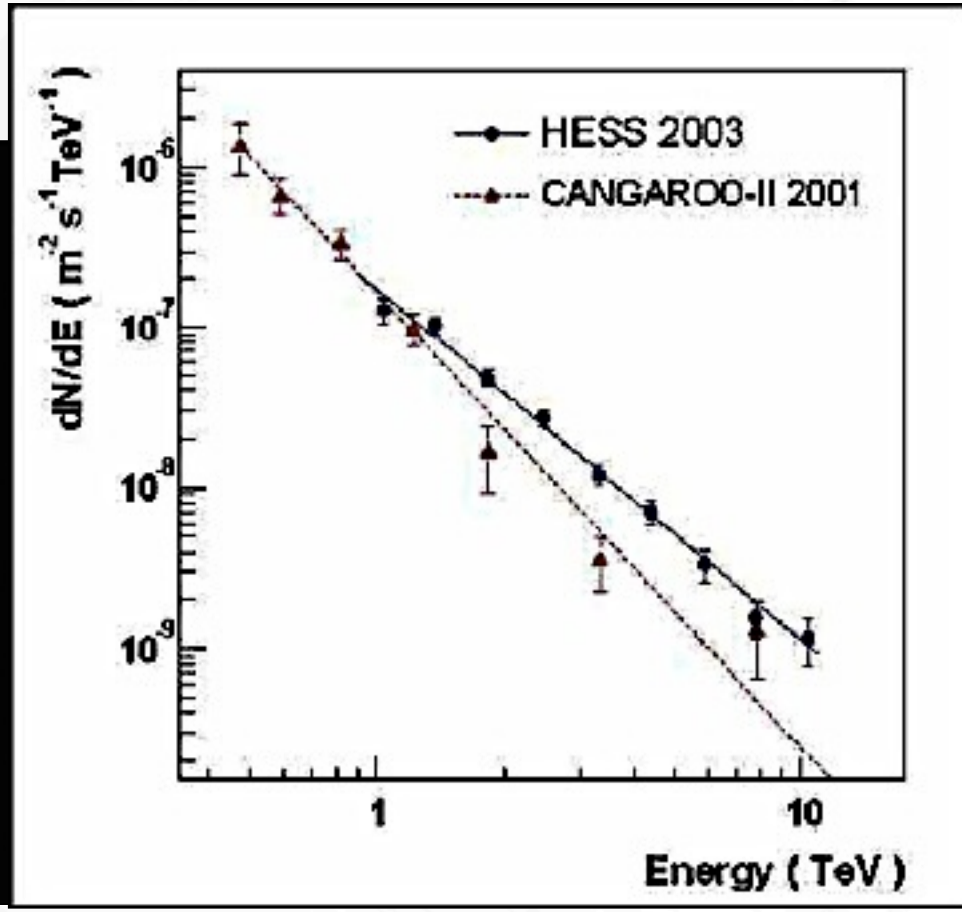

Aharonian et al., Nature 432 (2004) 75

Supernova remnants have been seen by HESS in γ-rays: The remnant RXJ1713-3946 has a spectrum ~$E^{-2.2}$: => Charged particles have been accelerated to > 100 TeV. Also seen in 1-3 keV X-rays (contour lines from ASCA)

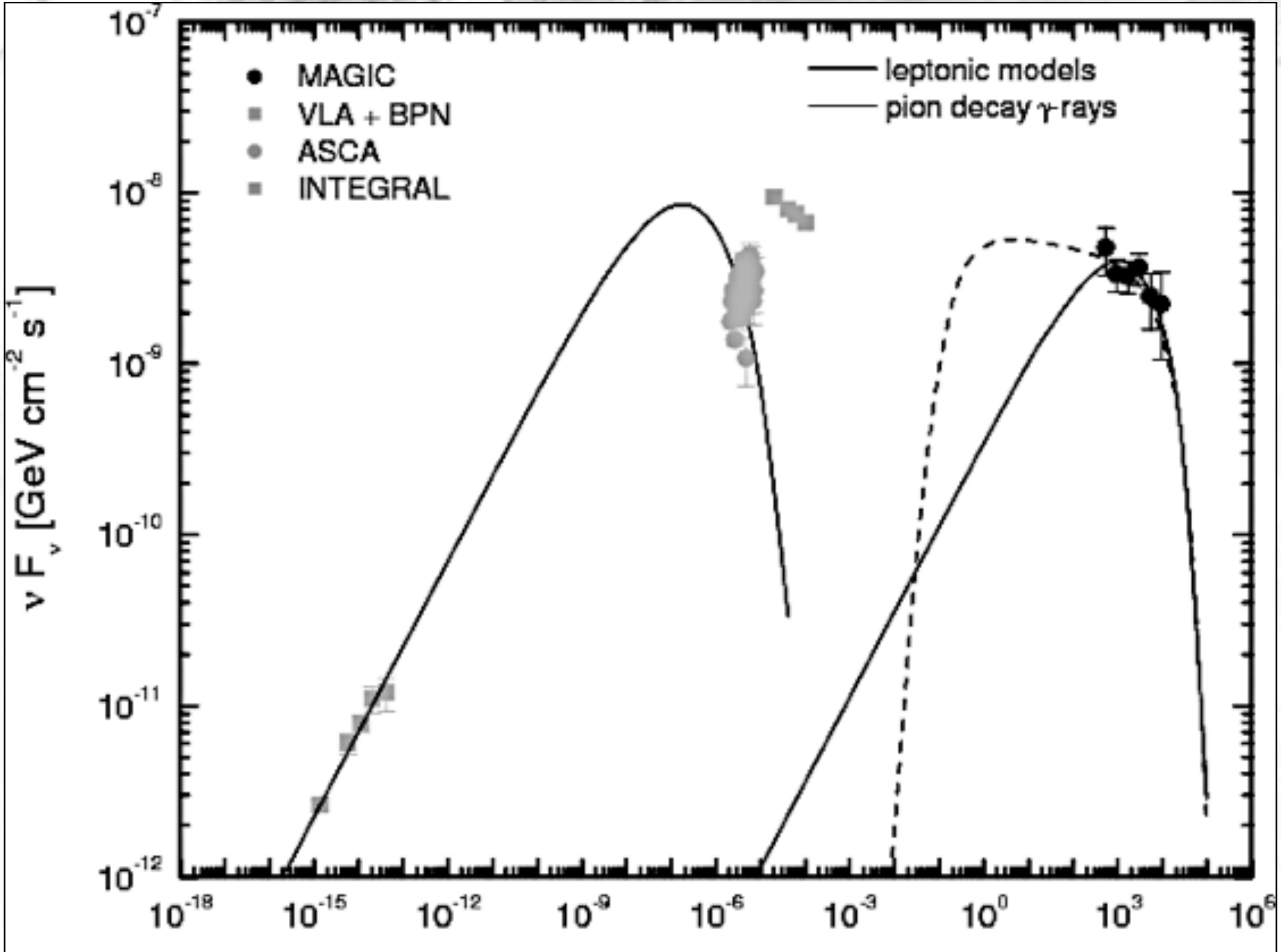

Albert et al., ApJ 637 (2006) L41

5

Hadronic versus leptonic model of SN remnant HESS J1813-178:
both are still possible

But in some supernova remnants the magnetic field needed to explain relative height of synchrotron and inverse Compton peak in the leptonic model would be too high:

$$\frac{P_{\text{synch}}}{P_{\text{IC}}} = \frac{u_B}{u_{\text{CMB+IR}}}$$

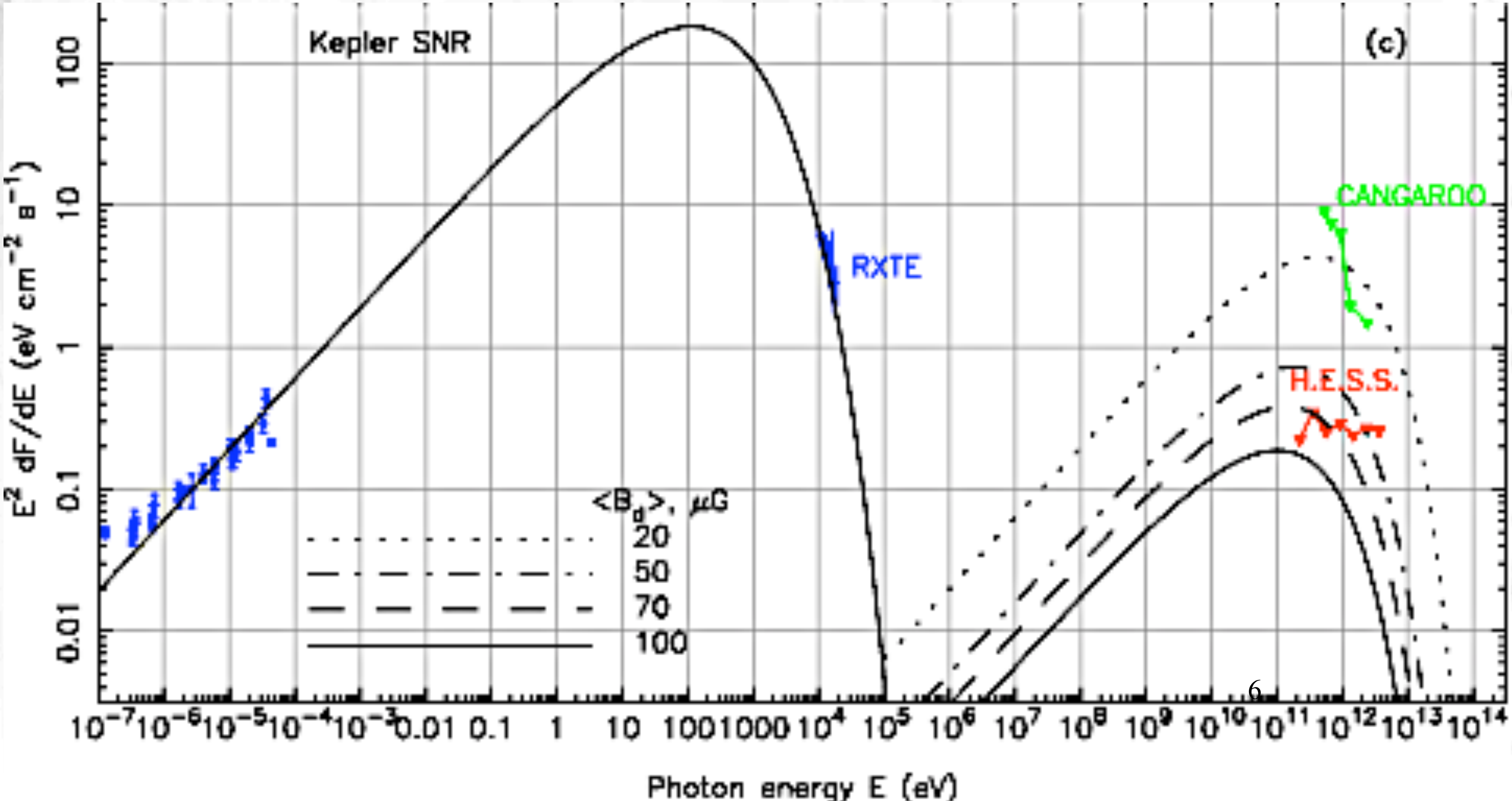

Voelk, Ksenofontov, Berezhko, Astron. Astrophys. 490 (2008) 515

„double-humped" spectra are also typical for AGNs

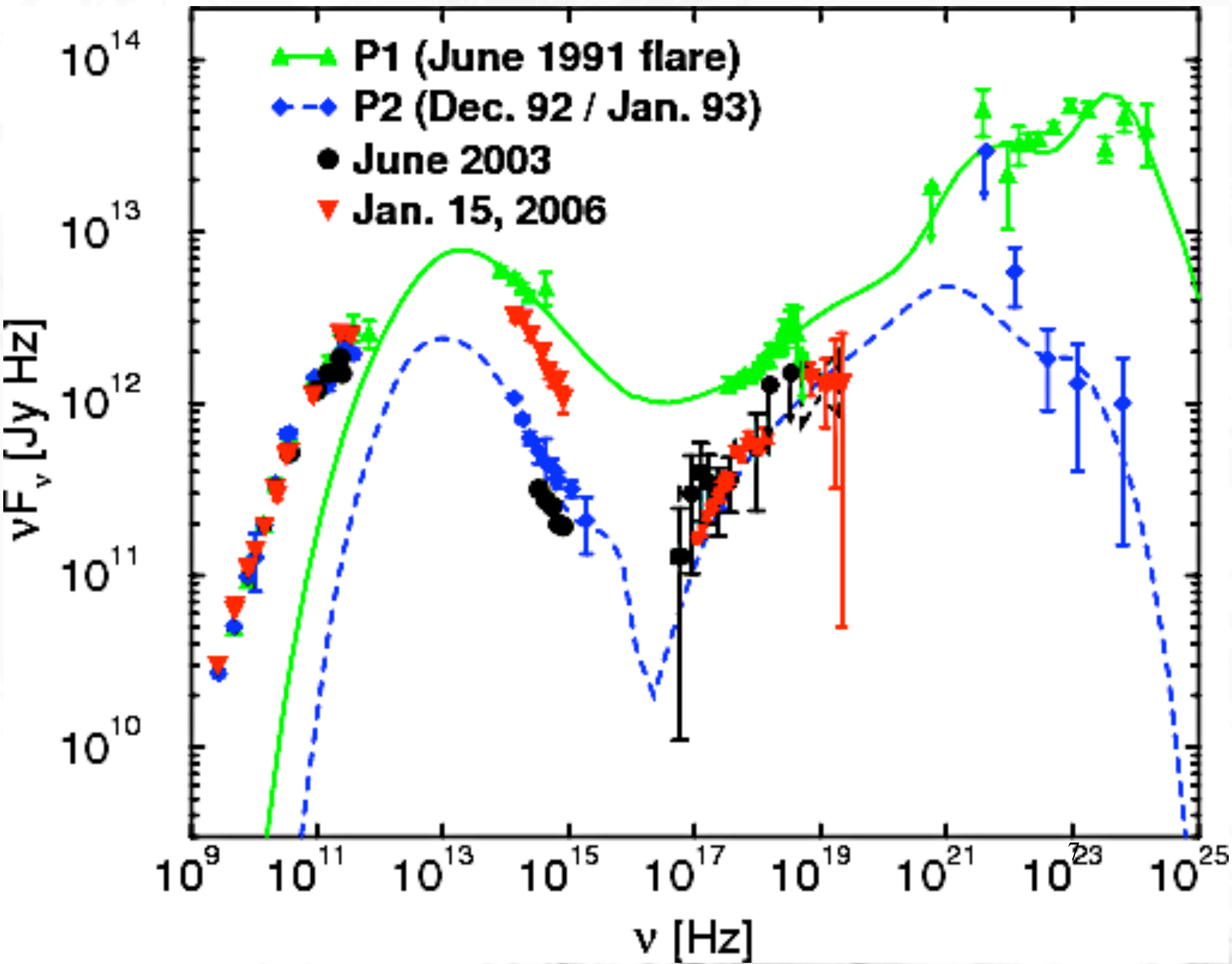

Latest example: Lobes of Centaurus A seen by Fermi-LAT

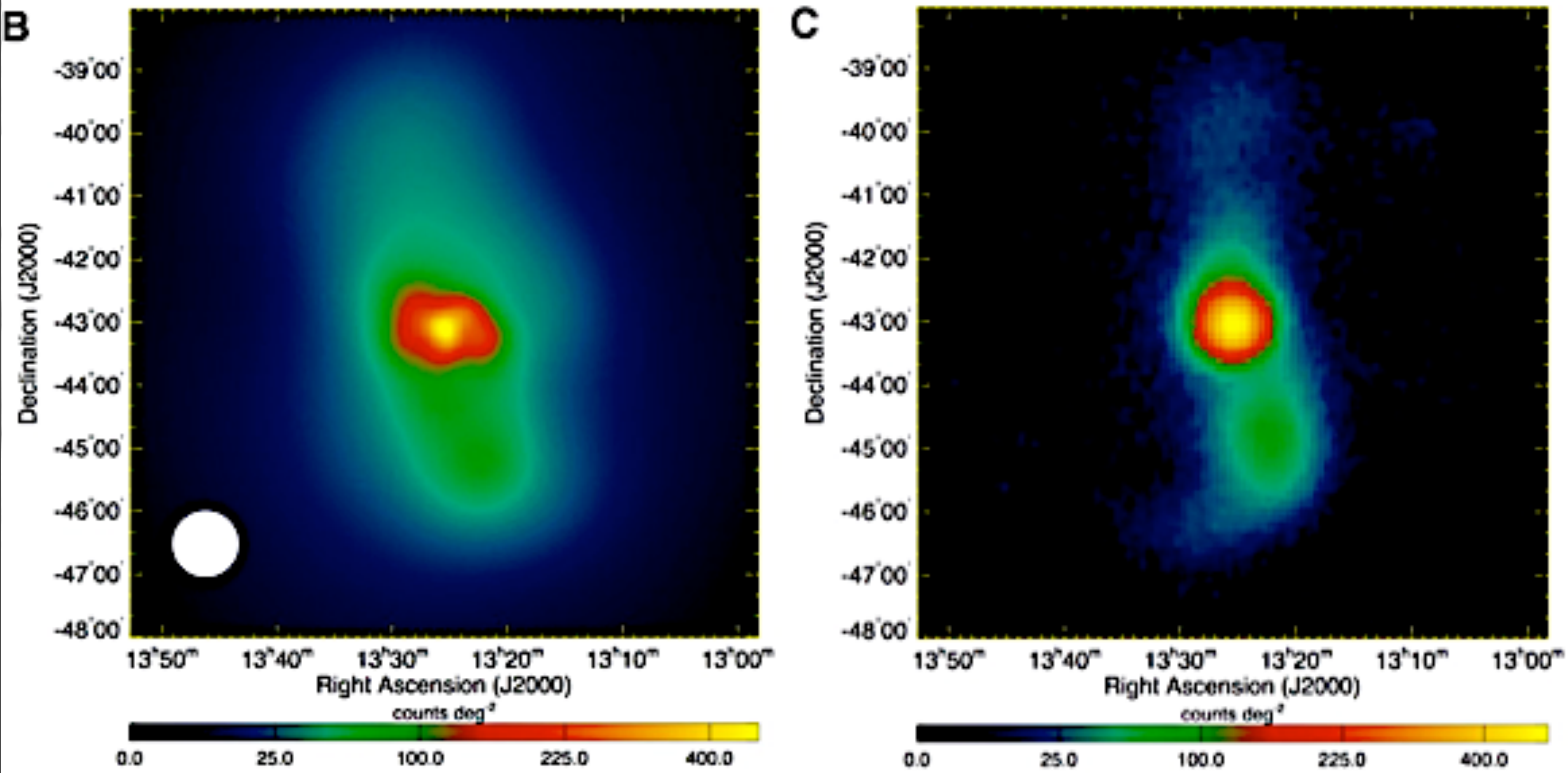

8

> 200 MeV γ-rays

Radio observations

Abdo et al., Science Express 1184656, April 1, 2010

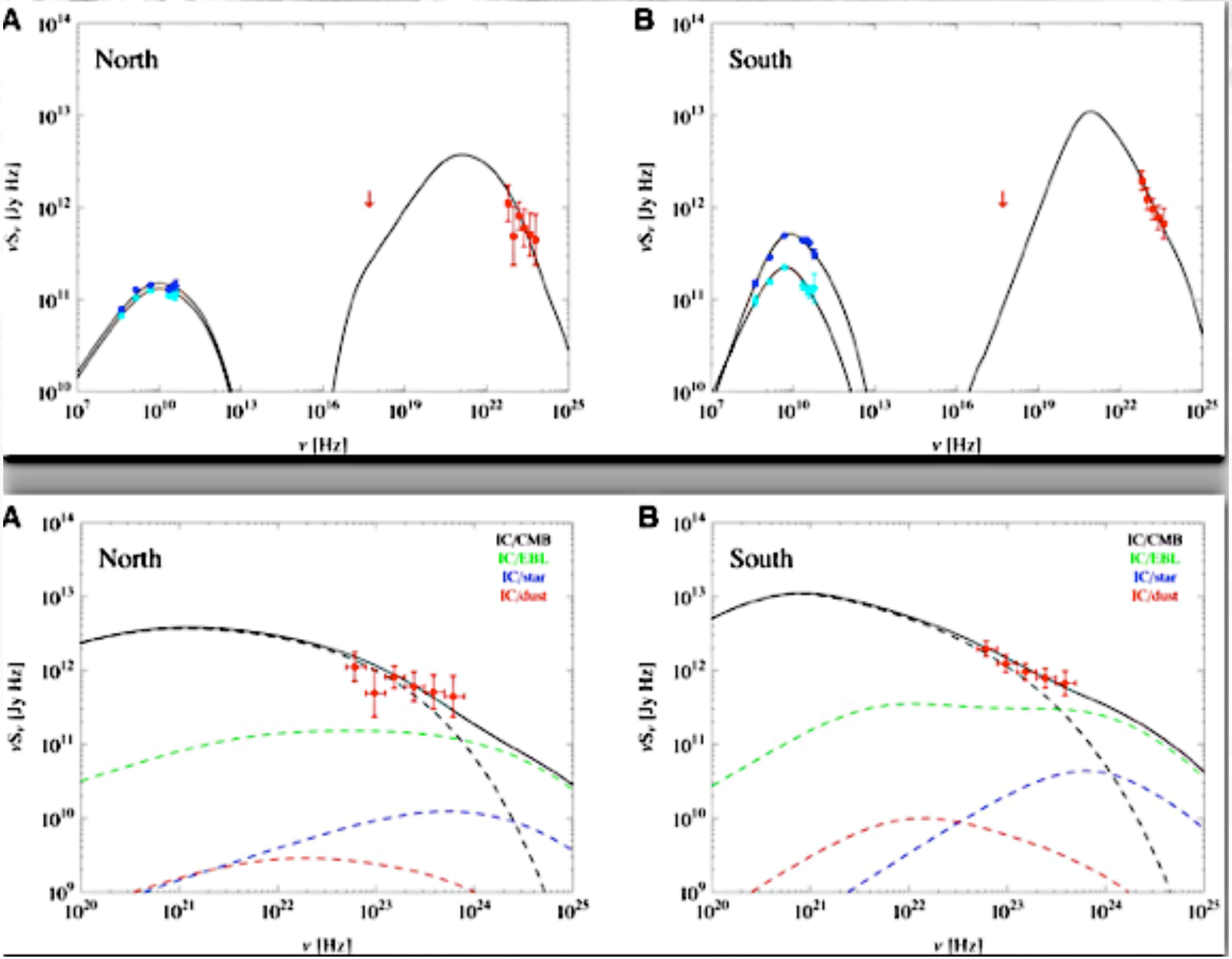

9

Low energy bump = synchrotron

high energy bump = inverse Compton on CMB in ~0.85μG field

Abdo et al., Science Express 1184656, April 1, 2010

Core of Centaurus A seen by Fermi-LAT

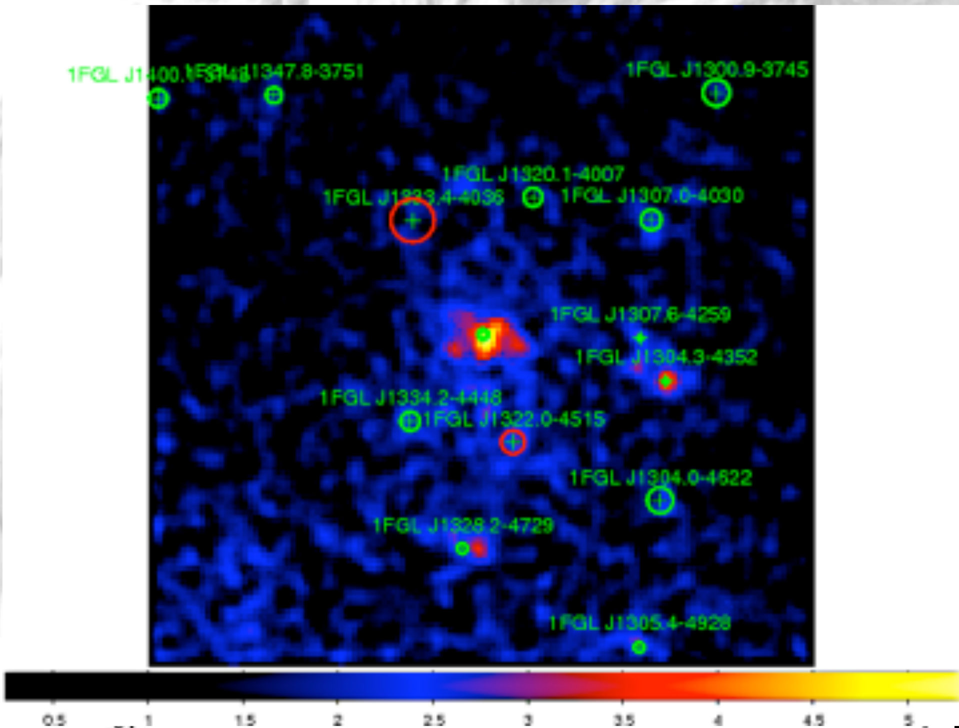

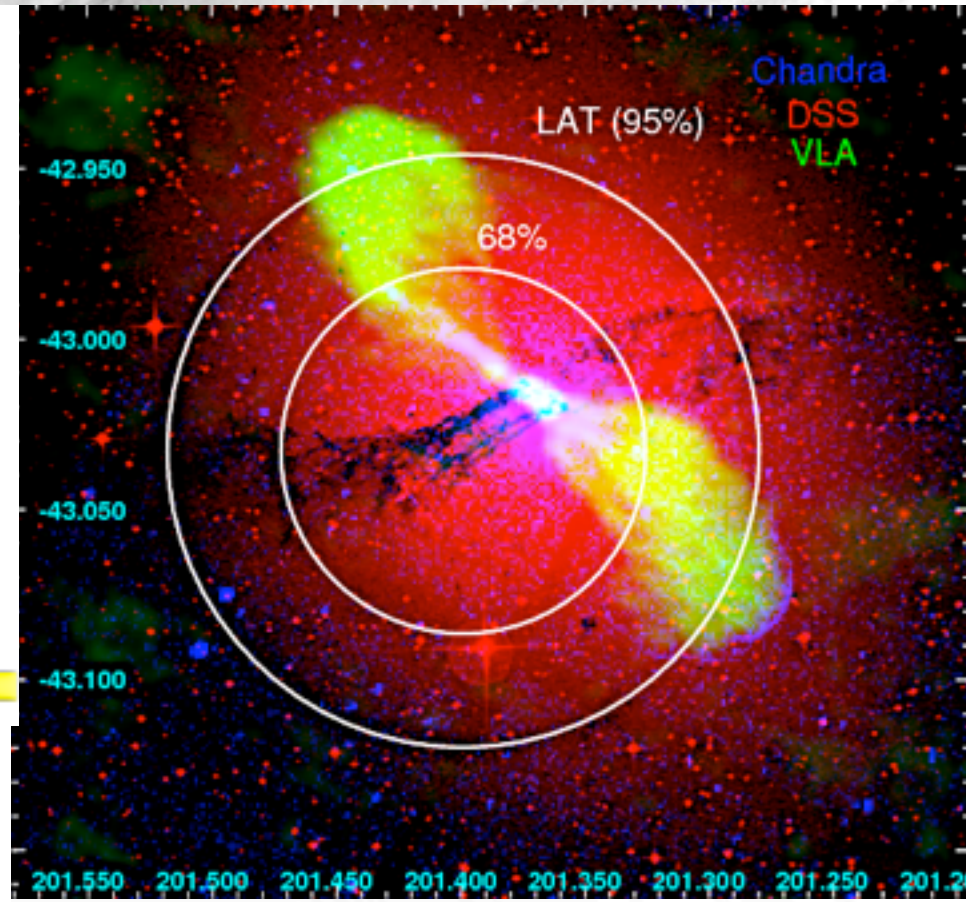

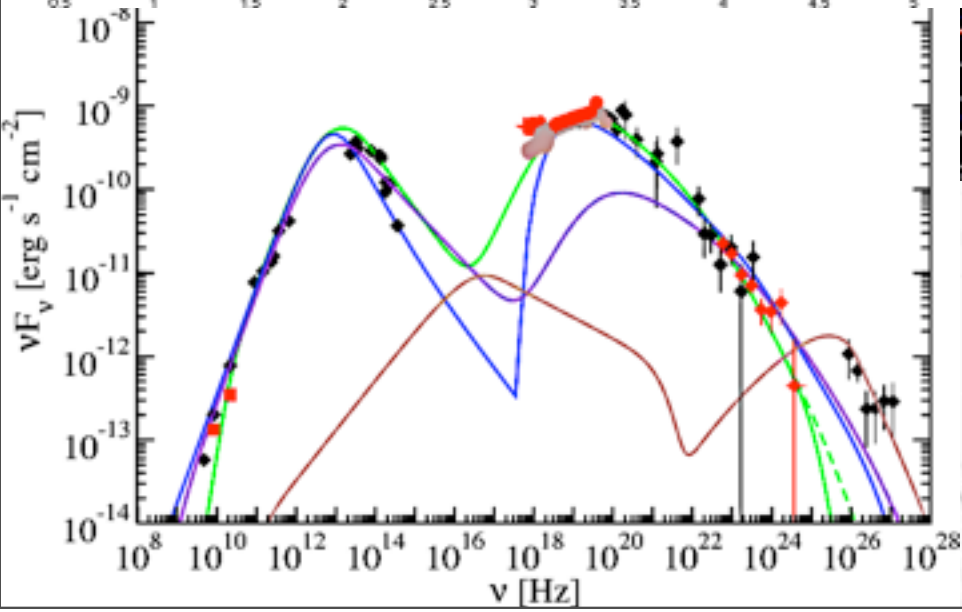

Can be explained by synchrotron self Compton except for HESS observation

10

Abdo et al., (Fermi LAT collaboration), arXiv:1006.5463

Interactions of Hadronic primary cosmic rays

γ-rays can be produced by **pp -> ppπ^0 -> ppγγ**

$$\sigma_{pp}(s) \simeq \left[35.49 + 0.307 \ln^2\left(s/28.94\,\mathrm{GeV}^2\right)\right]\ \mathrm{mb}$$

This cross section is almost constant -> secondary spectra roughly the same shape as primary fluxes as long as meson cooling time is much larger than decay time.

γ-rays can also be produced by **pγ interactions:**

For sub-MeV photons the cross section has a threshold and is typically ~ 100 mb and weakly energy dependent at energies much above the threshold

11

=> Secondary neutrino flux also has a (very high energy) threshold above which it roughly follows the primary spectrum.

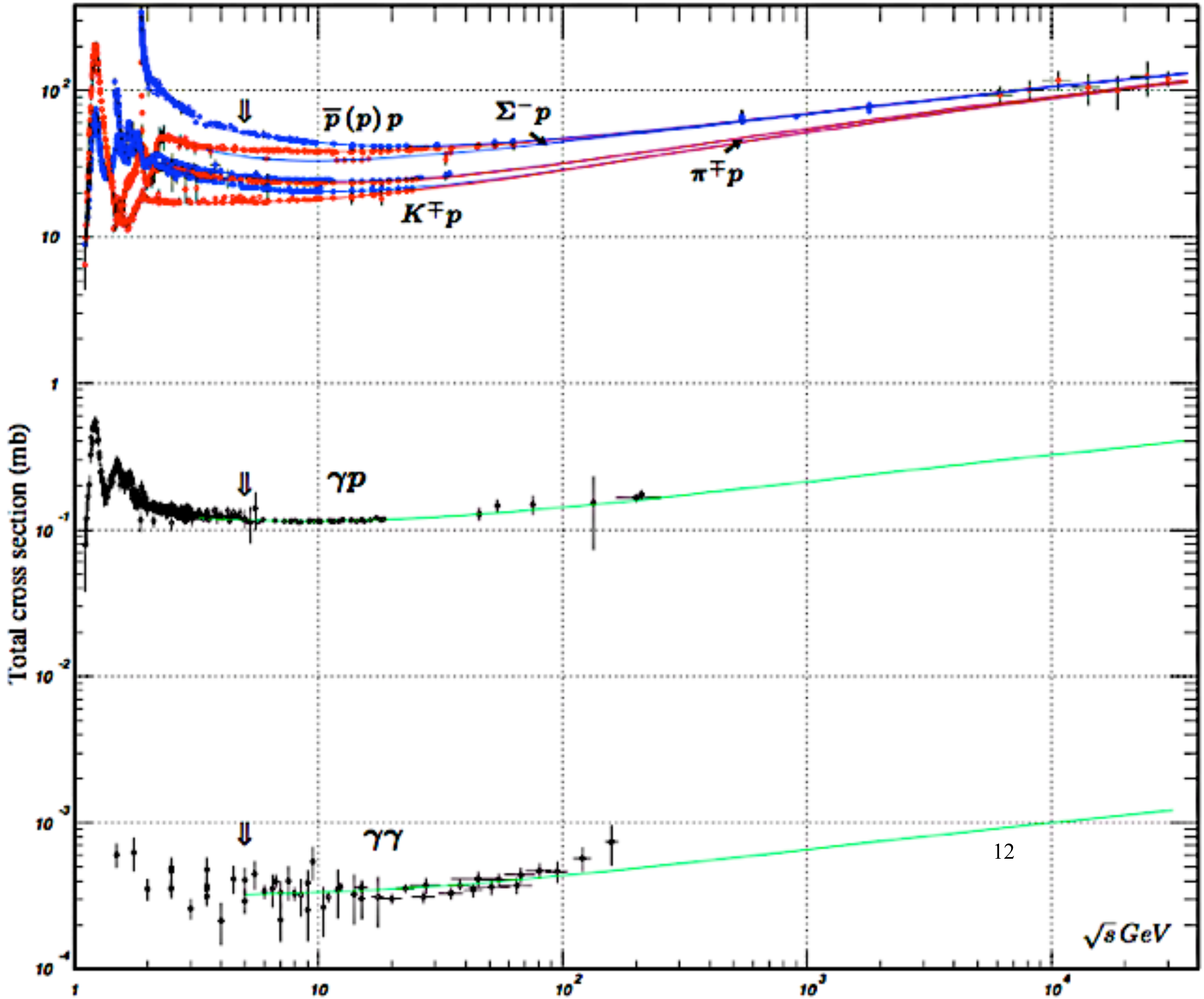
$\overline{p}\,(p)\,p$
$\Sigma^- p$
$\pi^\mp p$
$K^\mp p$
γp
$\gamma\gamma$
Total cross section (mb)
$\sqrt{s}$ GeV
12

HESS sources: X-ray binary LS 5039

Secondary γ-rays and neutrinos mostly produced by pp interactions in this model

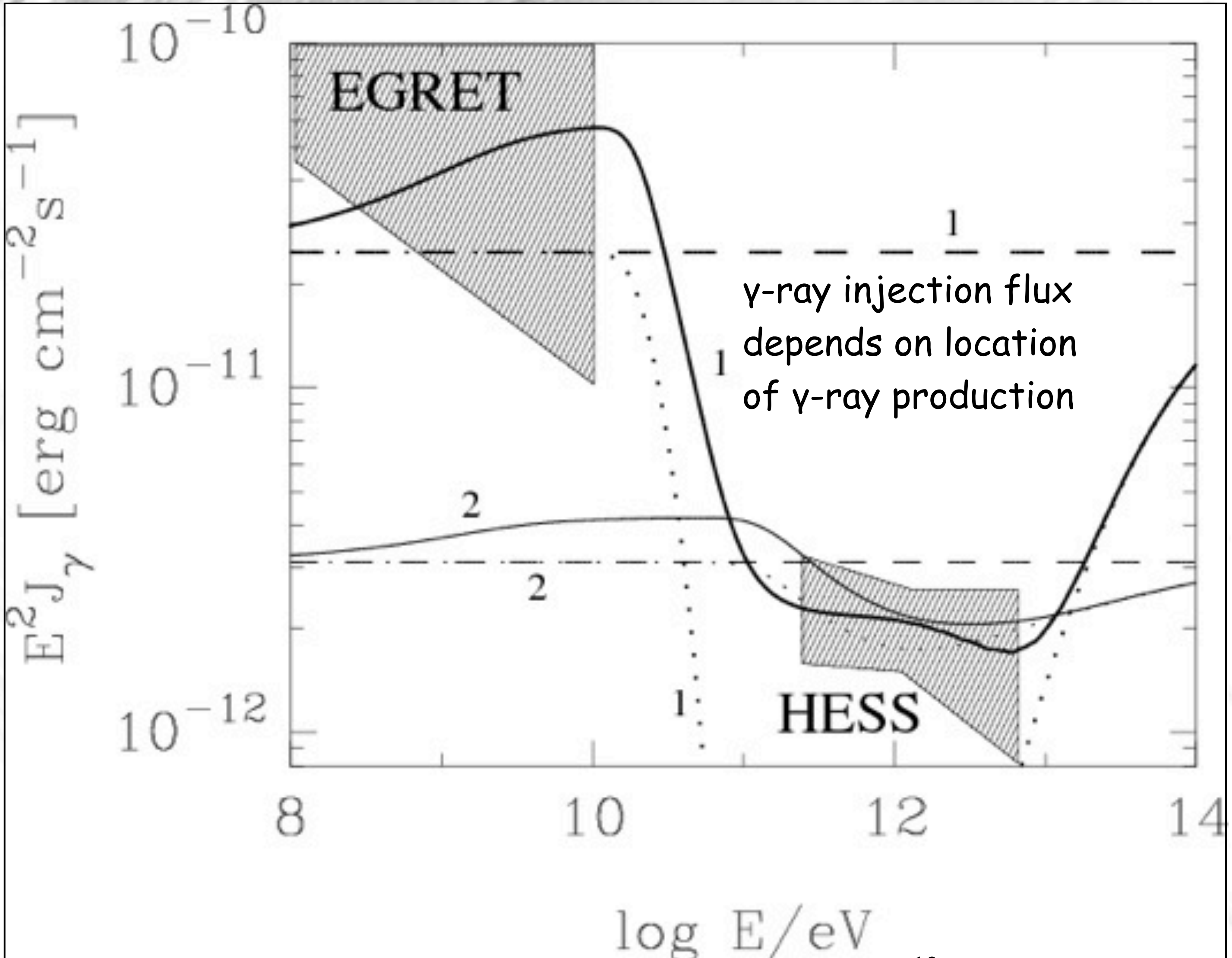

F.Aharonian et al., astro-ph/0508658

Expected neutrino fluxes above TeV ~10^{-9}-10^{-7} GeV cm^{-2}s^{-1}

Hadronic Interactions and Galactic Cosmic and γ-Rays

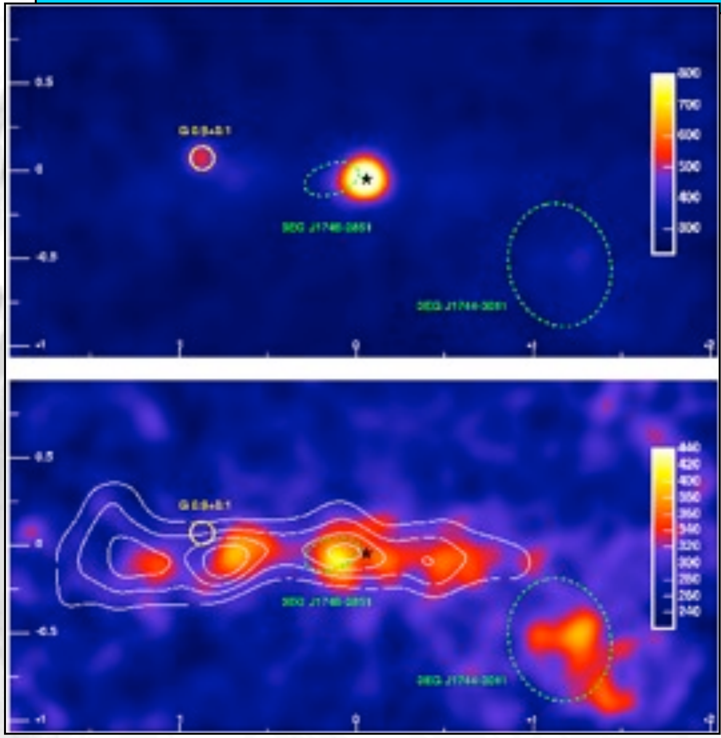

HESS has observed γ-rays from objects around the galactic centre which correlate well with the gas density in molecular clouds for a cosmic ray diffusion time of $T \sim R^2/D \sim 3\times10^3\ (\theta/1^o)^2/\eta$ years where $D = \eta\ 10^{30}\ cm^2/s$ is the diffusion coefficient for protons of a few TeV.

Aharonian et al., Nature 439 (2006) 695

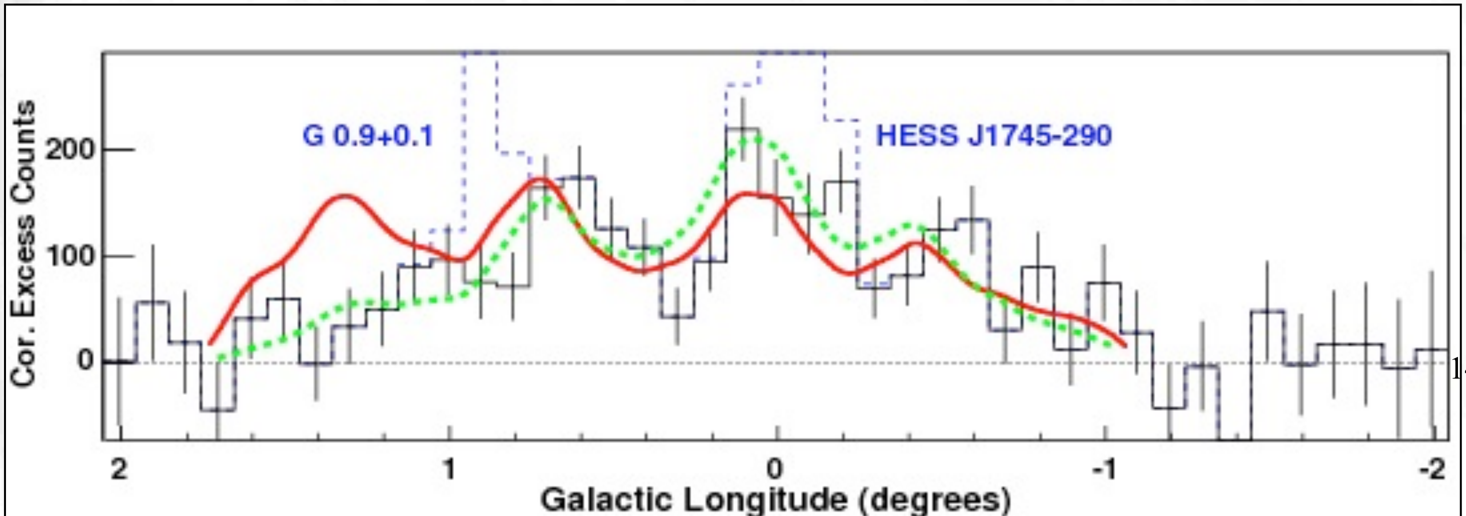

14

Identifying galactic sources from their secondary gamma-ray signatures

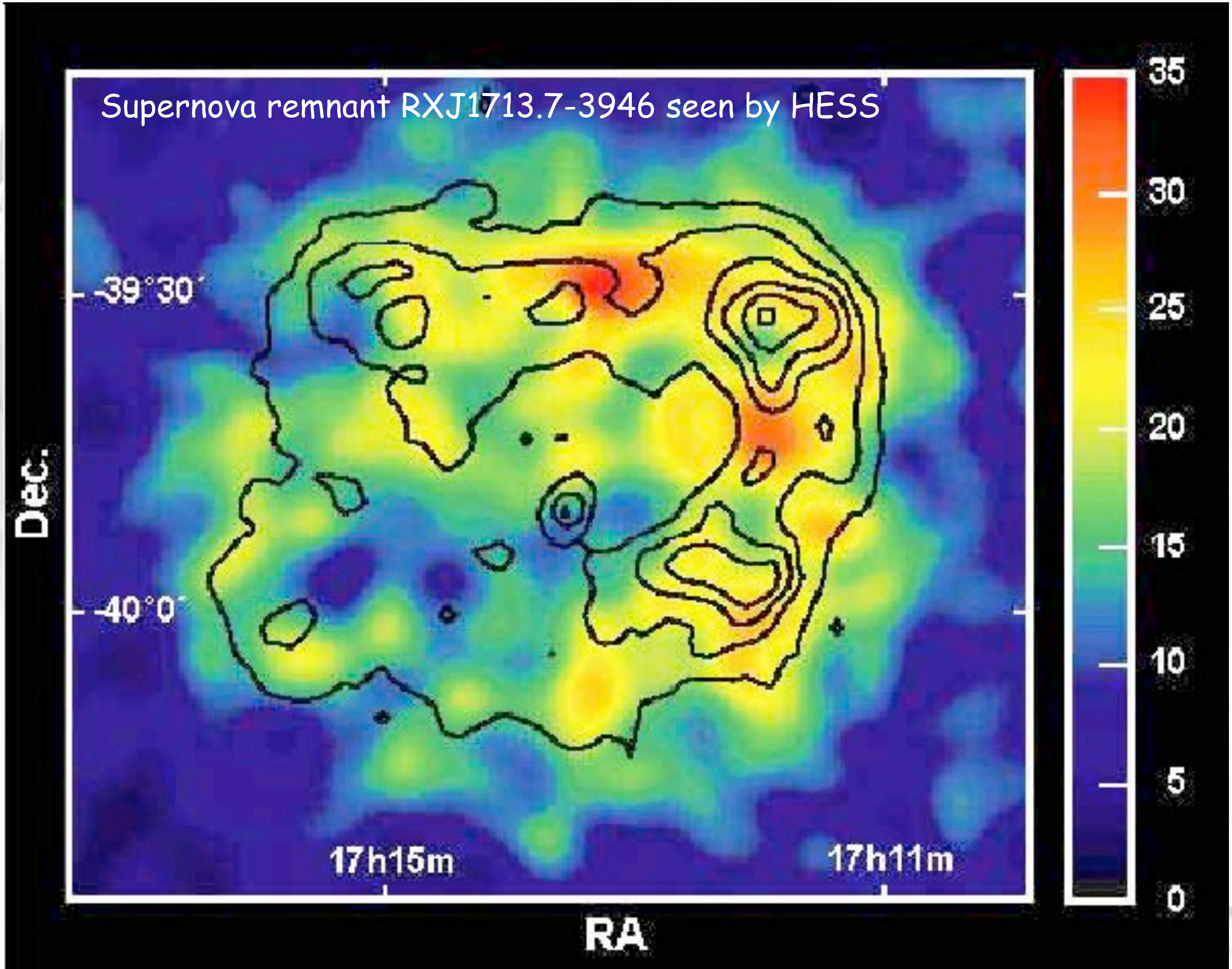

Identifying galactic sources from their secondary gamma-ray signatures

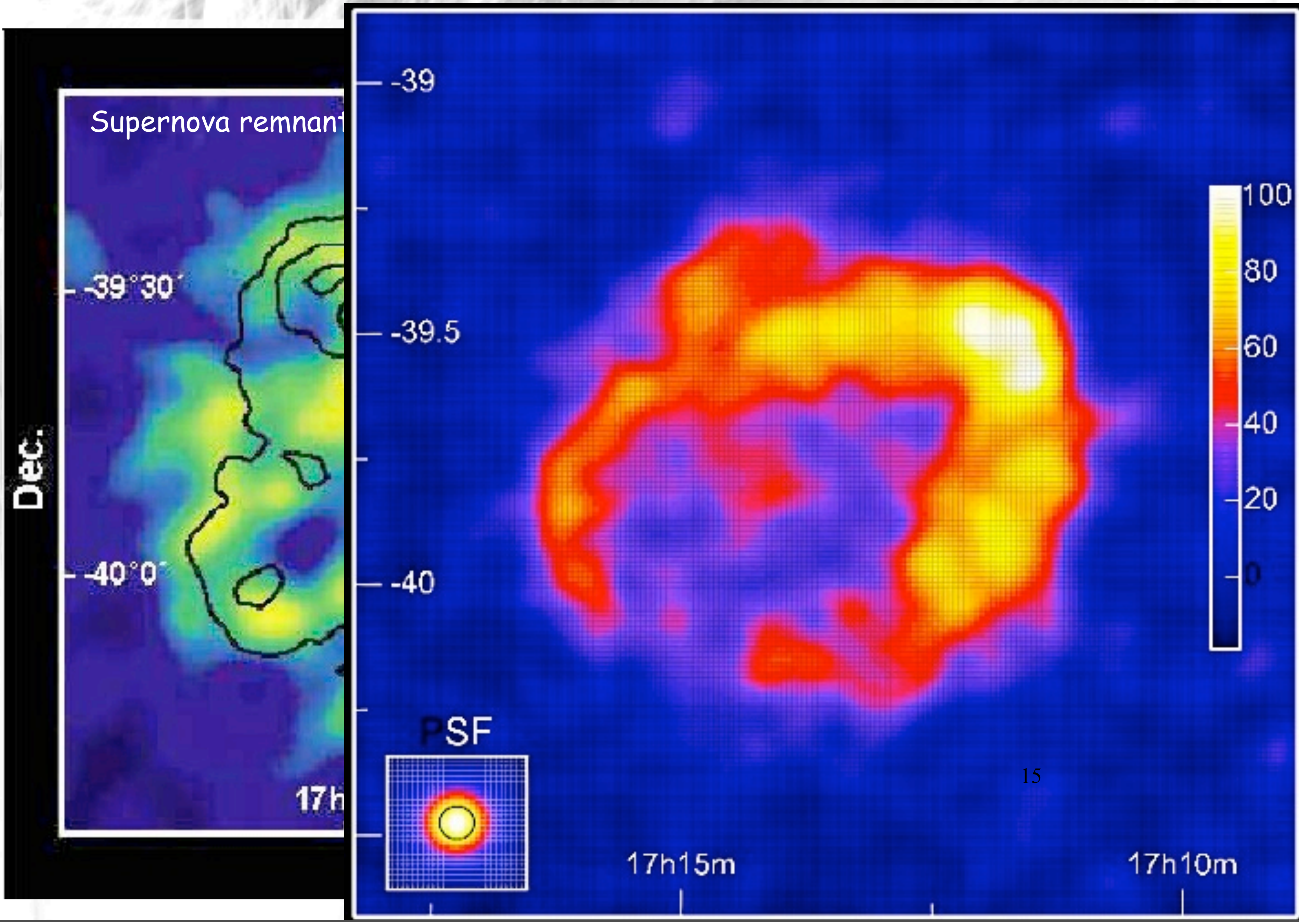

Shell-type supernova remnant RCW 86 seen by HESS

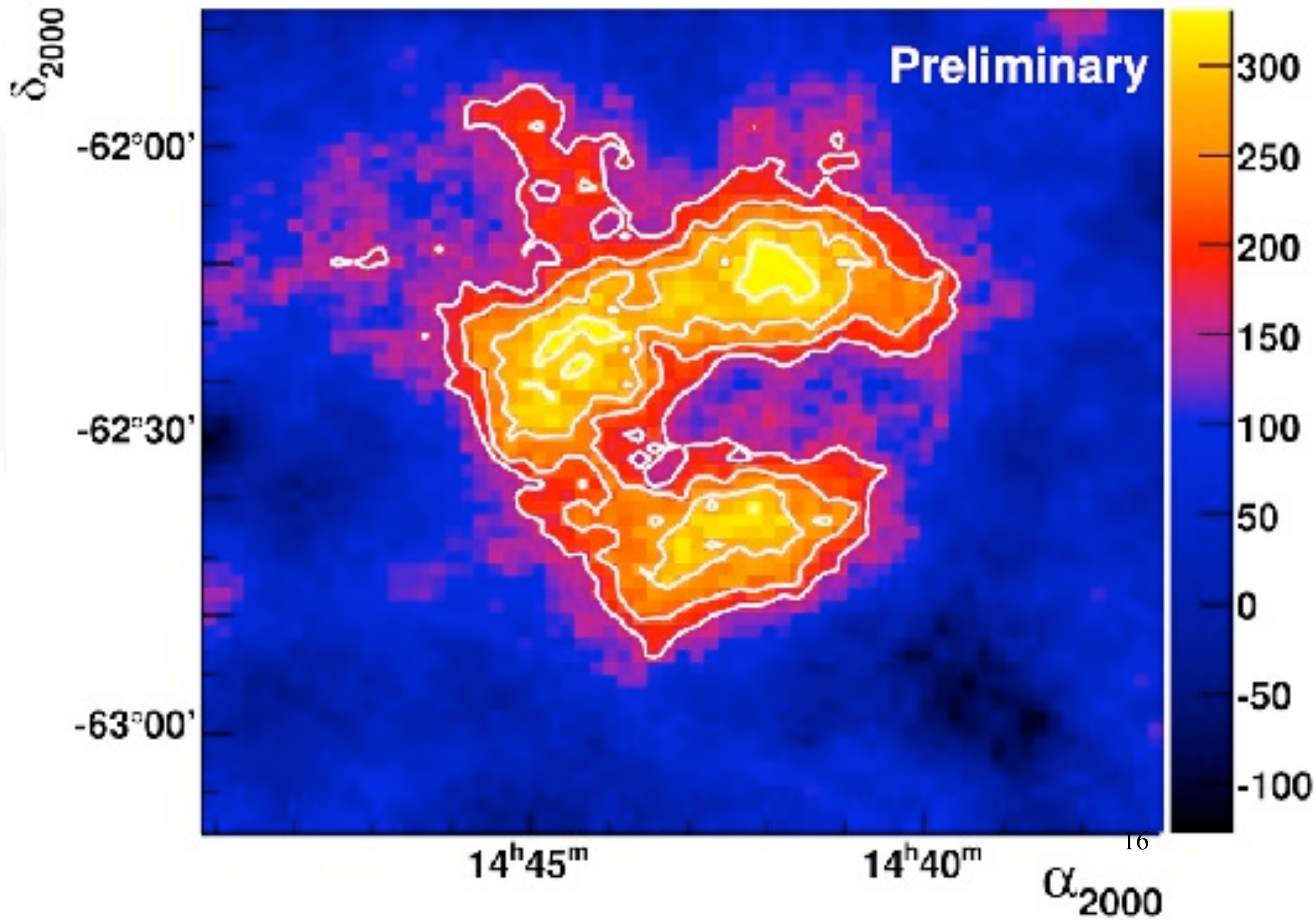

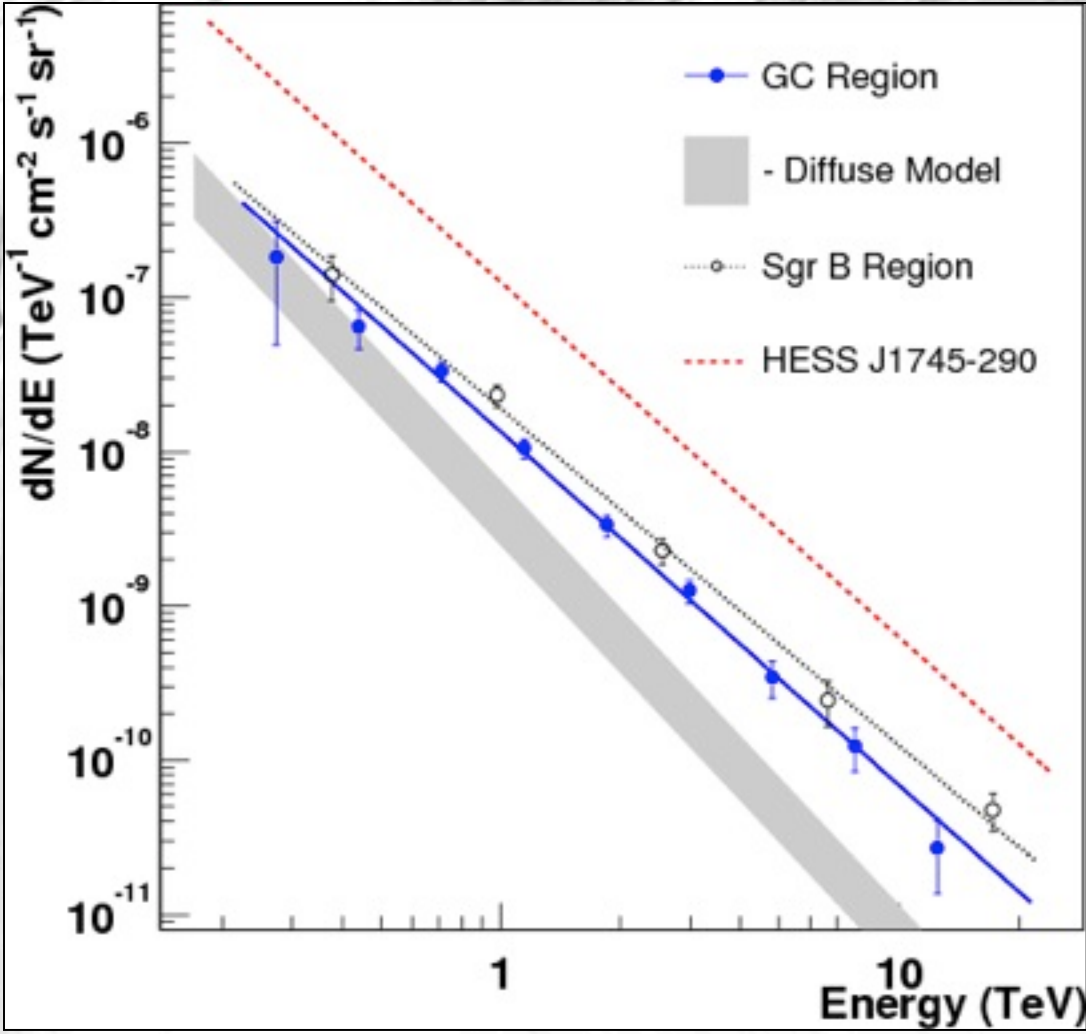

Given the observed spectrum $E^{-2.3}$, this can be interpreted as photons from π^0 decay produced in pp interactions where the TeV protons have the same spectrum and could have been produced in a SN event.

Note that this is consistent with the source spectrum both expected from shock acceleration theory and from the cosmic ray spectrum observed in the solar neighborhood, $E^{-2.7}$, corrected for diffusion in the galactic magnetic field, $j(E) \sim Q(E)/D(E)$.

Galactic Cosmic Ray Propagation and Signatures of Dark Matter Annihilation

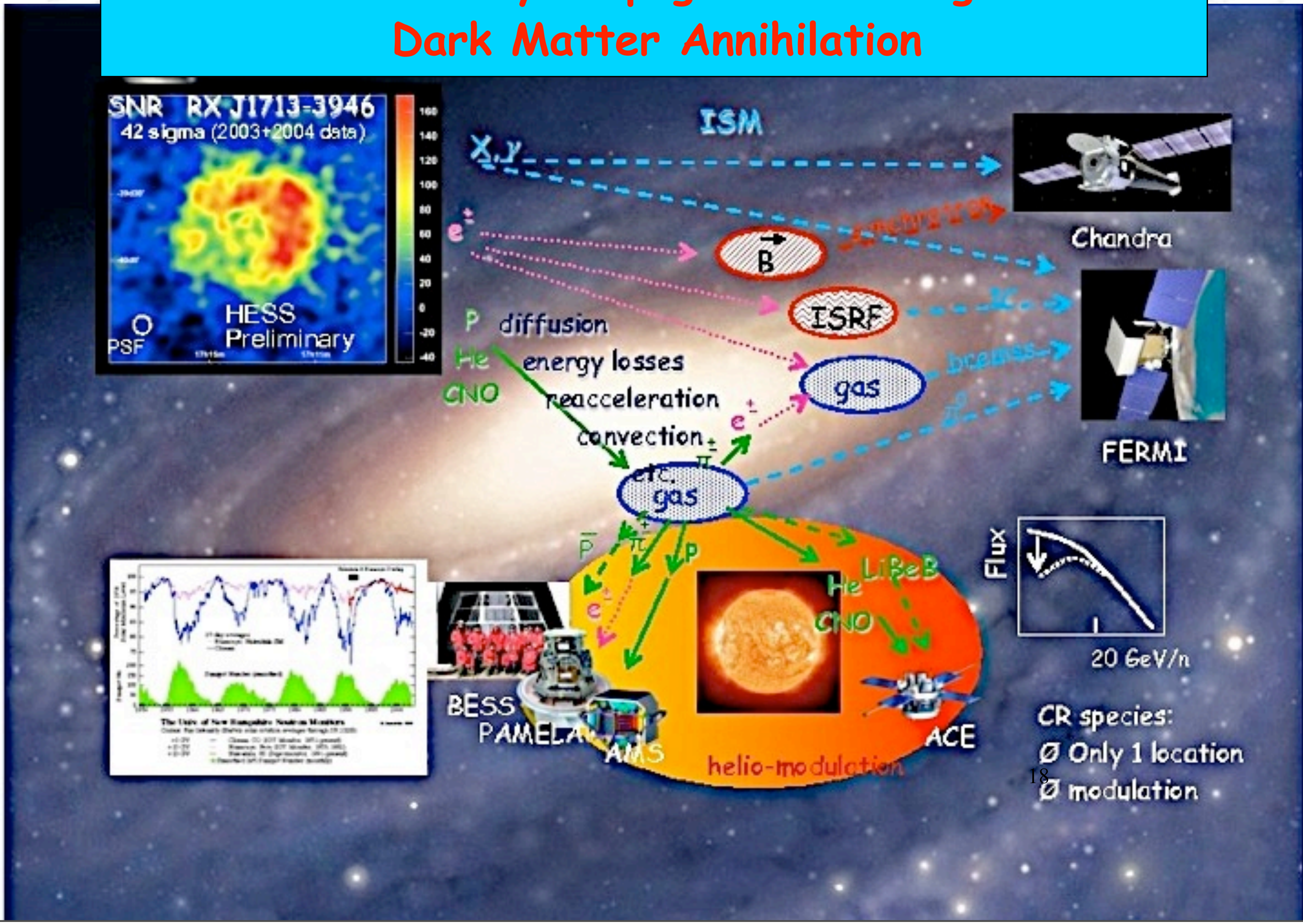

Galactic Cosmic Ray Propagation

Galactic propagation is described by solving the diffusion-convection-energy loss equation:

$$\partial_t n = \nabla \cdot (D_{xx} \nabla n - \mathbf{v_c}) + \partial_p \left(p^2 D_{pp} \partial_p \frac{n}{p^2} \right) - \partial_p \left[\dot{p}\, n - \frac{p}{3} (\nabla \cdot \mathbf{v_c} n) \right] + Q(\mathbf{r}, p)$$

spatial diffusion | convection | reacceleration | energy loss | adiabatic compression/ expansion | source term

This equation is solved in a cylindrical slab geometry with suitable boundary Conditions.

19

Out of the resulting electron/positron distribution one can compute synchrotron emission (and also inverse Compton scattering) along any line of sight.

Note: Propagation parameters are constrained by secondary to primary ratios:

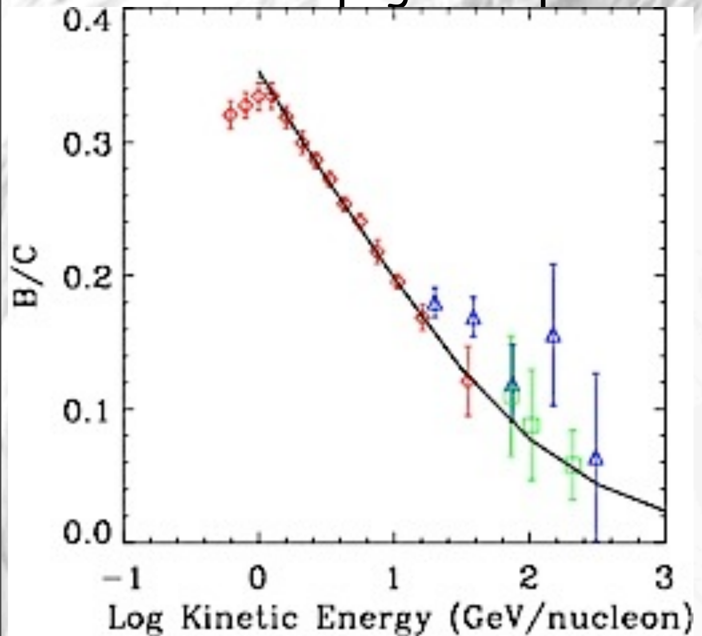

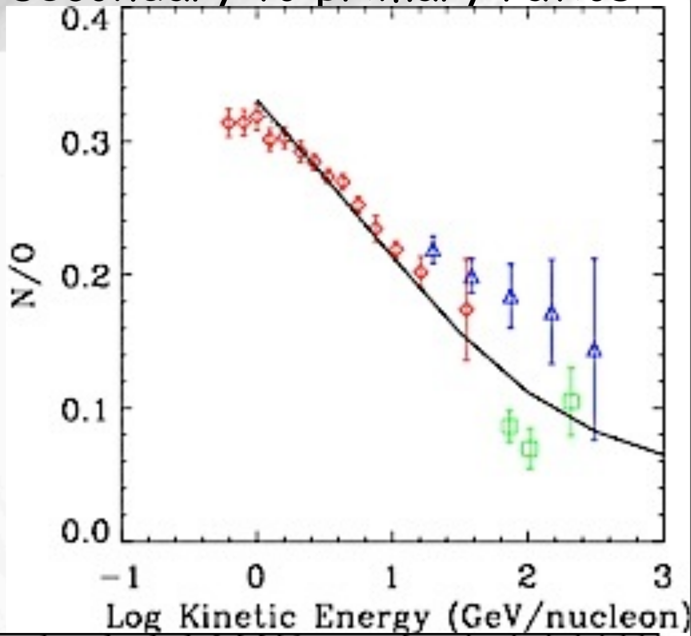

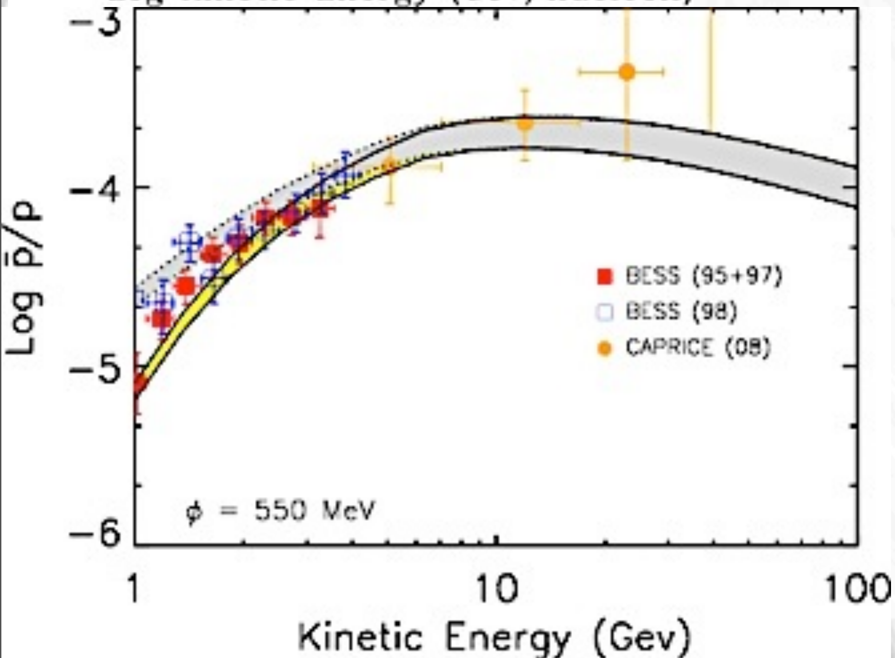

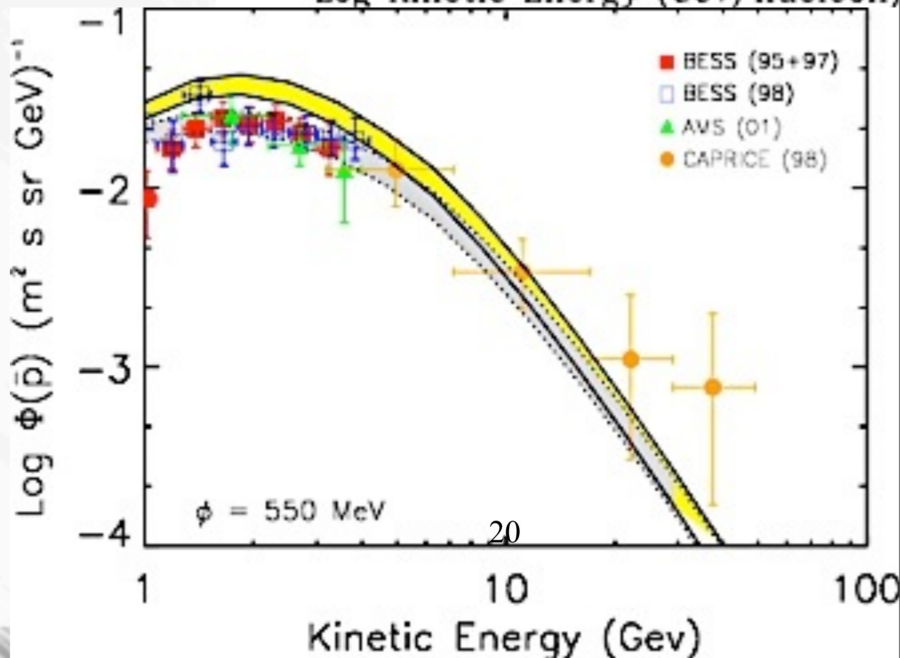

Evoli, Gaggero, Grasso, Maccione, JCAP 0810, 018 (2008)

Propagation Models

Definition of diffusion coefficients:

$$D_{xx} = \frac{v}{c_0} D_0 \left(\frac{E/Z}{\mathrm{GV}} \right)^{\delta}$$

$$D_{pp} = \frac{4p^2 v_A^2}{3\delta(4-\delta^2)(4-\delta) D_{xx}}$$

where v_A is the Alfven speed

Models often considered:

Model	δ§	D_0 [kpc^2/Myr]	R [kpc]	L [kpc]	V_c [km/s]	dV_c/dz km/s/kpc	V_a [km/s]
MIN	0.85/0.85	0.0016	20	1	13.5	0	22.4
MED	0.70/0.70	0.0112	20	4	12	0	52.9
MAX	0.46/0.46	0.0765	20	15	5	0	117.6
DC	0/0.55	0.0829	30	4	0	6[21]	0
DR	0.34/0.34	0.1823	30	4	0	0	32

All Particle Spectrum and chemical Composition

Heavy elements start to dominate above knee

Rigidity (E/Z) effect: combination of deconfinement and maximum energy

Hoerandel, astro-ph/0702370

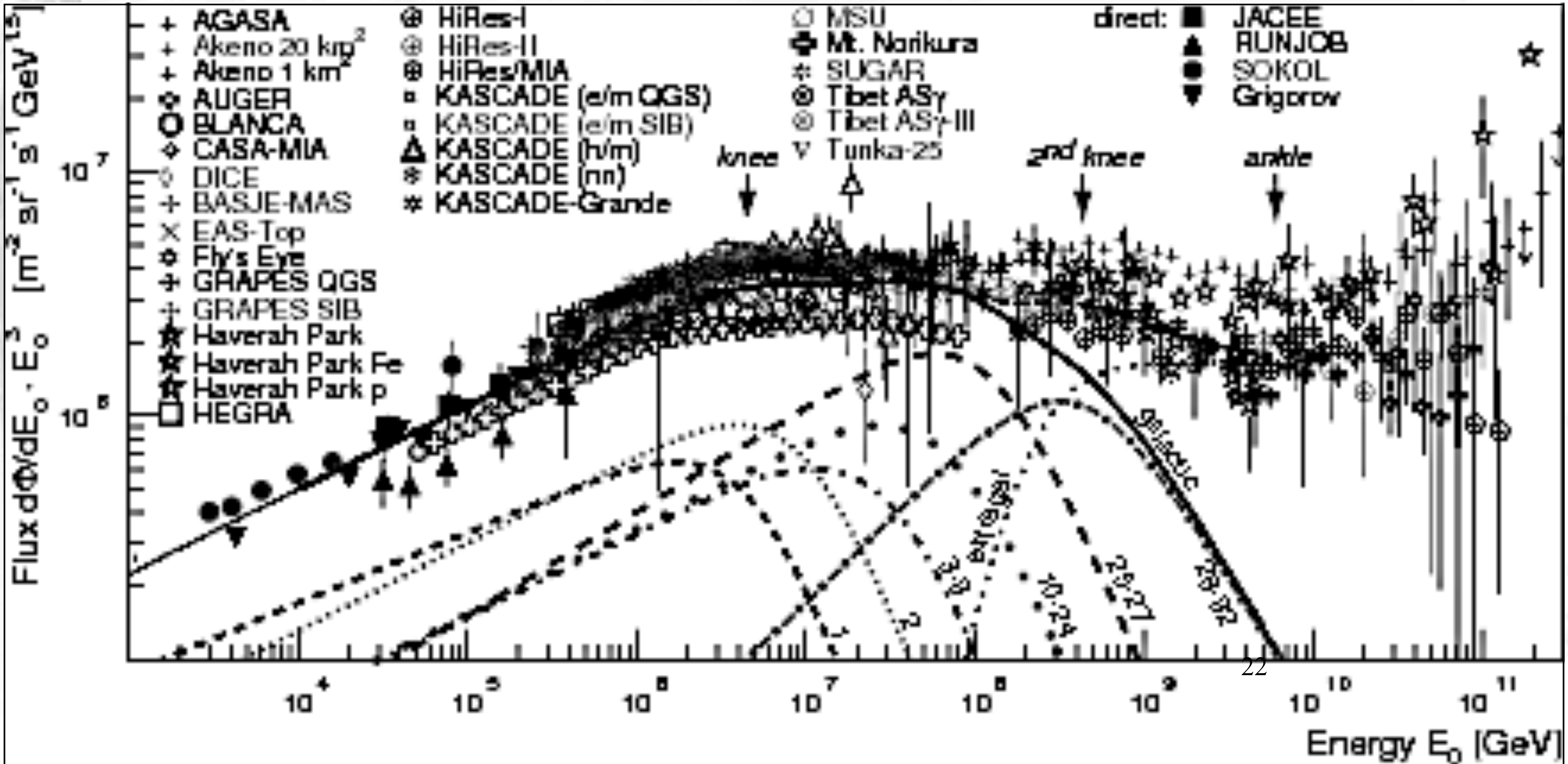

23

3.) The knee is probably a deconfinement effect in the galactic magnetic field as suggested by rigidity dependence measured by KASCADE:

3.) The knee is probably a deconfinement effect in the galactic magnetic field as suggested by rigidity dependence measured by KASCADE:

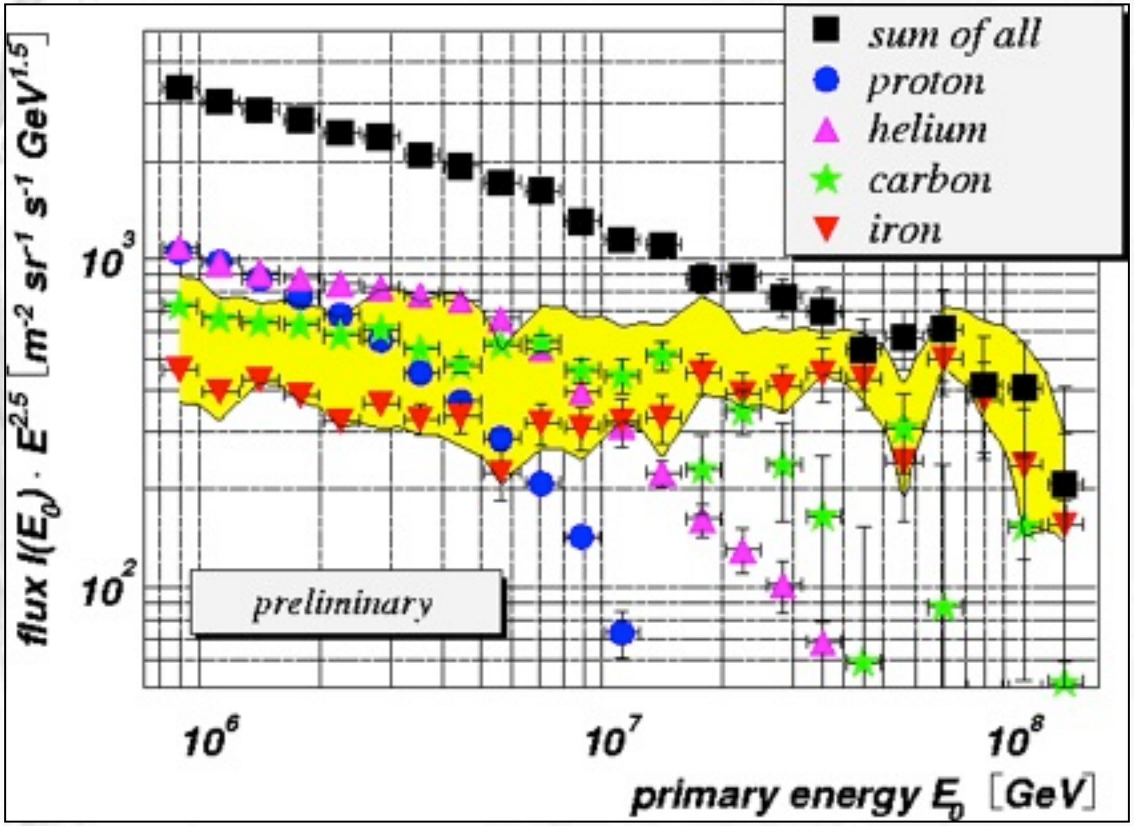

23

3.) The knee is probably a deconfinement effect in the galactic magnetic field as suggested by rigidity dependence measured by KASCADE:

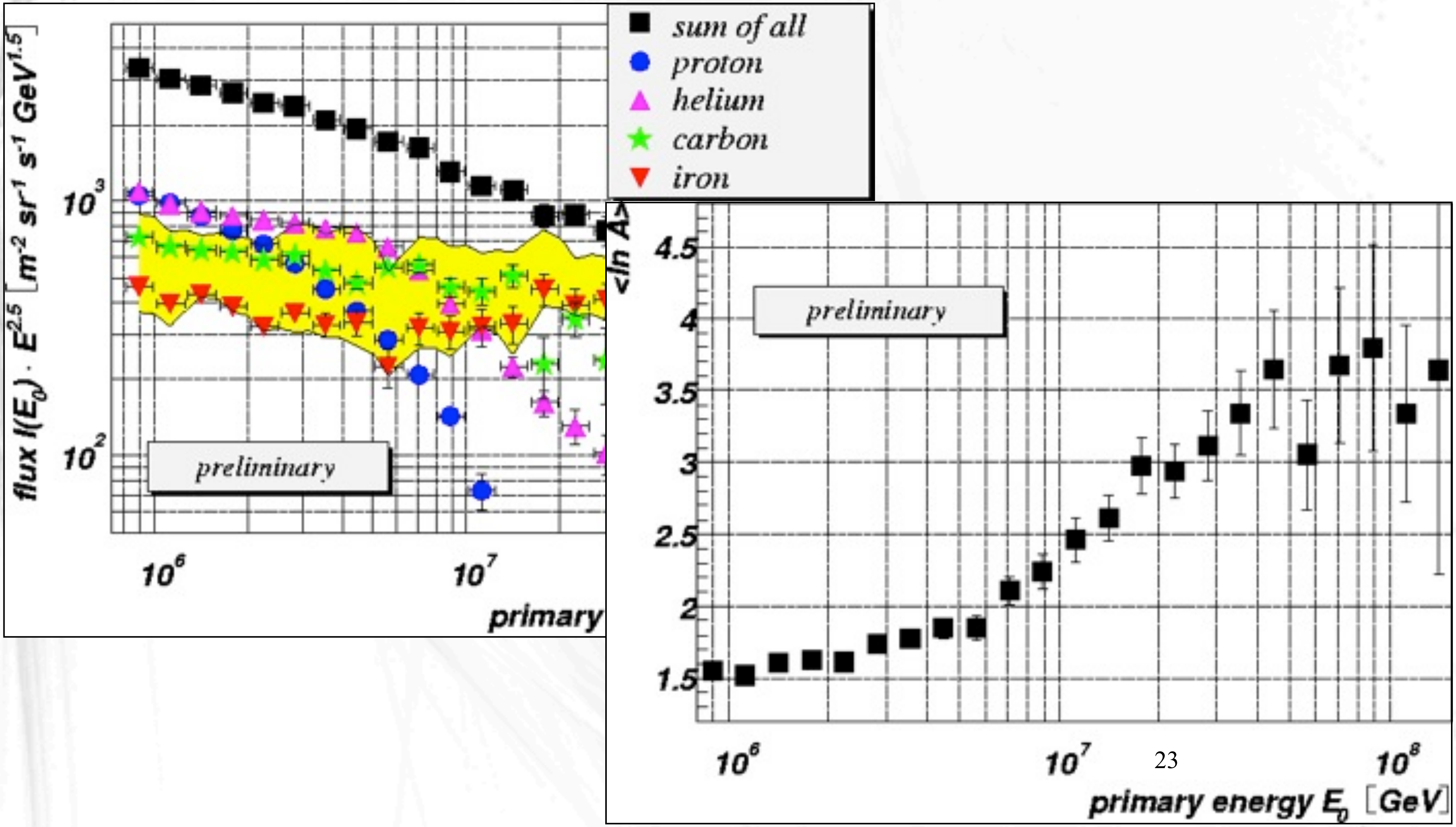

23

3.) The knee is … c magnetic
field as su… SCADE:

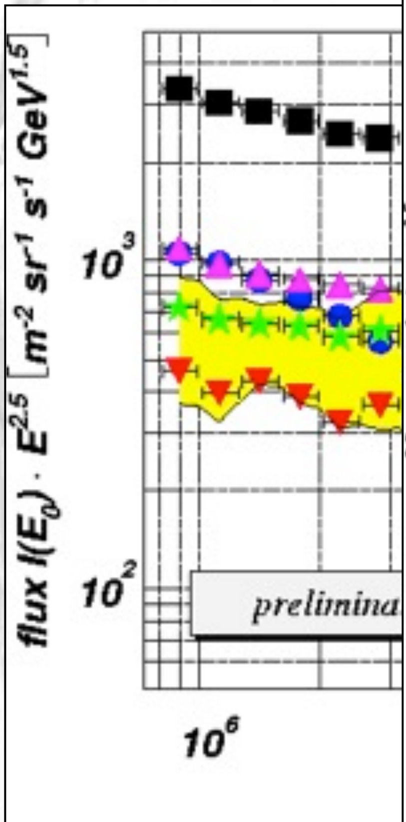

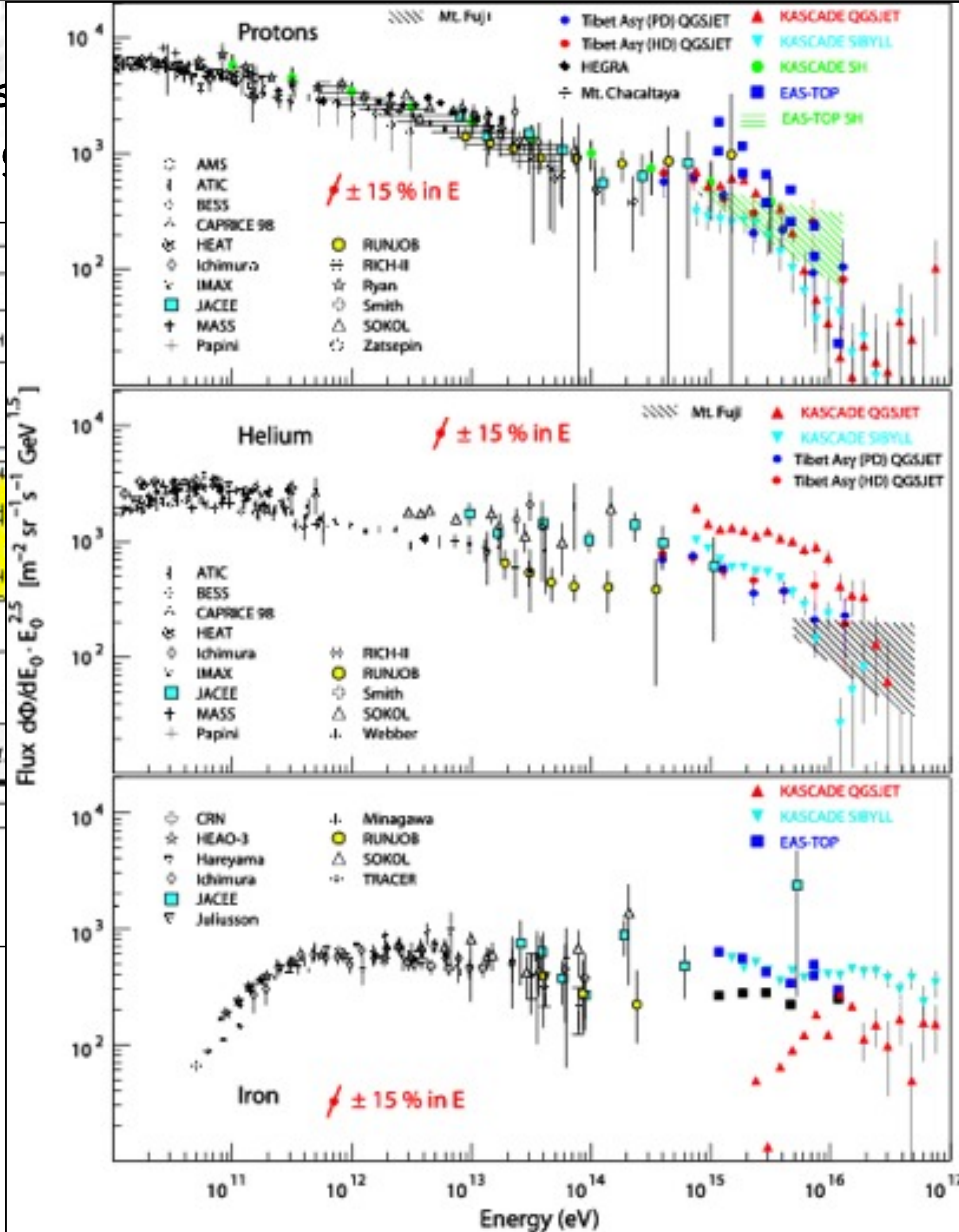

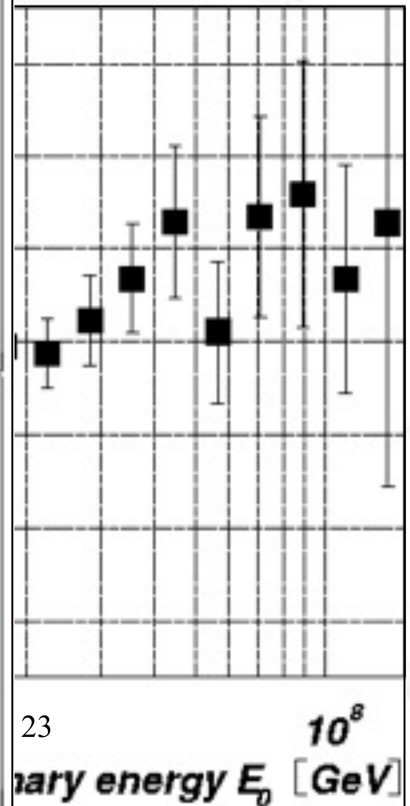

Do Cosmic Ray Anisotropies at 1-100 TeV reveal the Sources ?

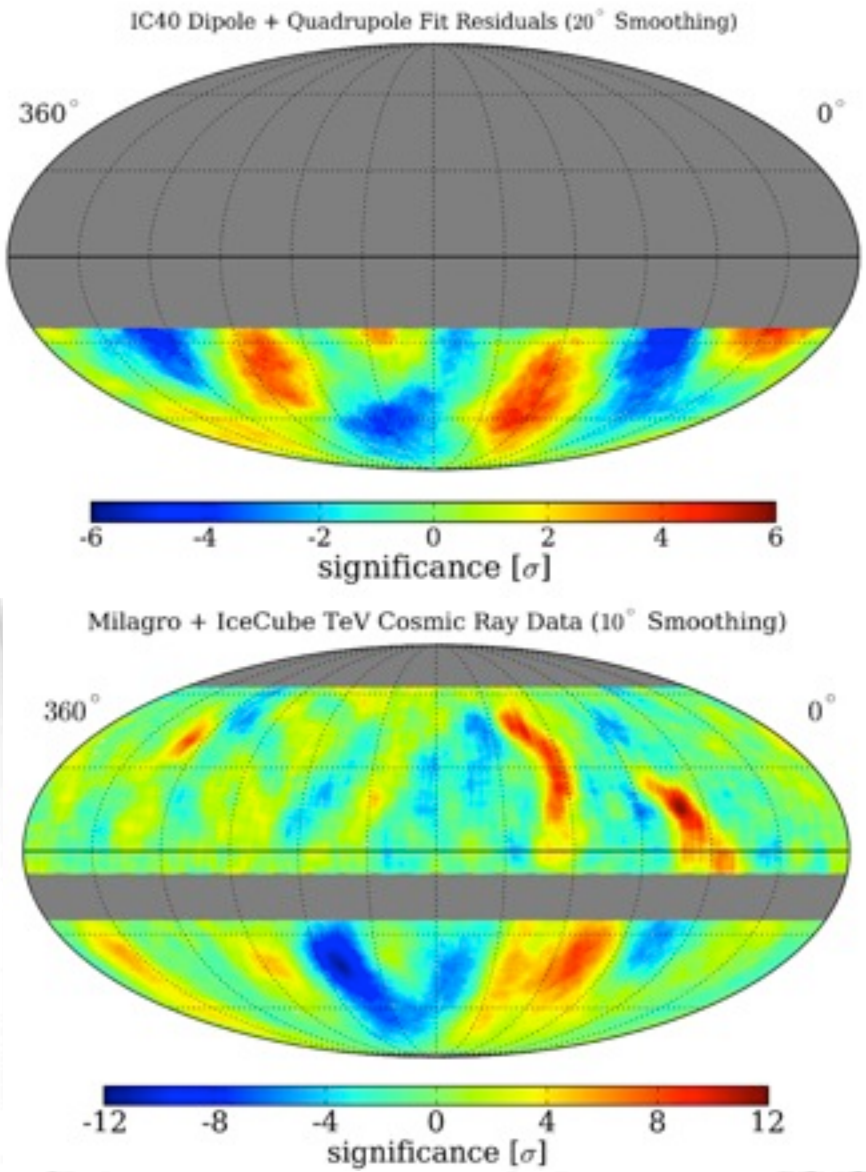

R. Abbasi et al, ICECUBE collaboration, arXiv:1105.2326

Observed level ~ 10^{-3} is surprisingly high and difficult to explain:

wrong structure for Compton-Getting effect

too large for sources like Vela and beyond (> 100 pc) because gyro-radius < 0.1 pc

propagation mode, magnetic field structure ?

24

Diffuse γ-ray spectra predicted and observed by EGRET

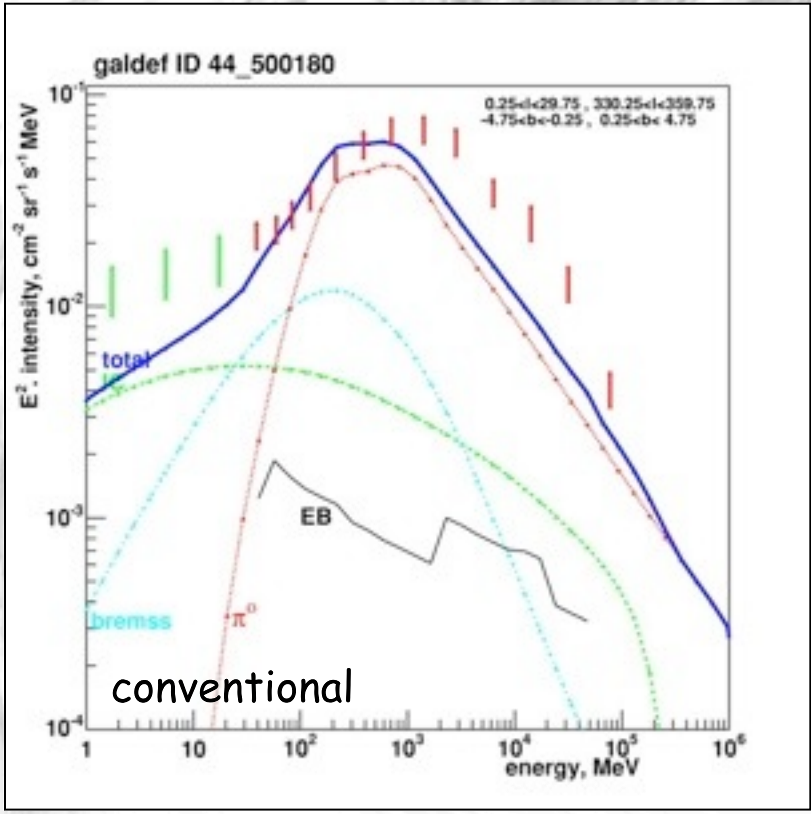

Above 100 MeV
dominated by
pp induced γ-rays

25

Strong, Moskalenko, and Reimer, ApJ 613 (2004) 962

Diffuse γ-ray spectra predicted and observed by EGRET

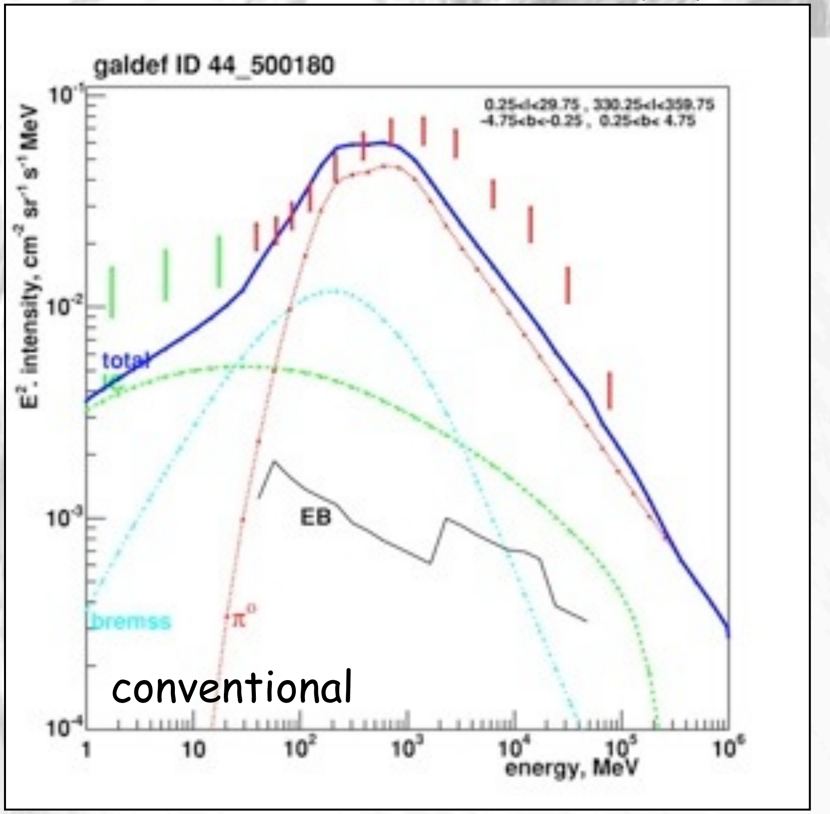

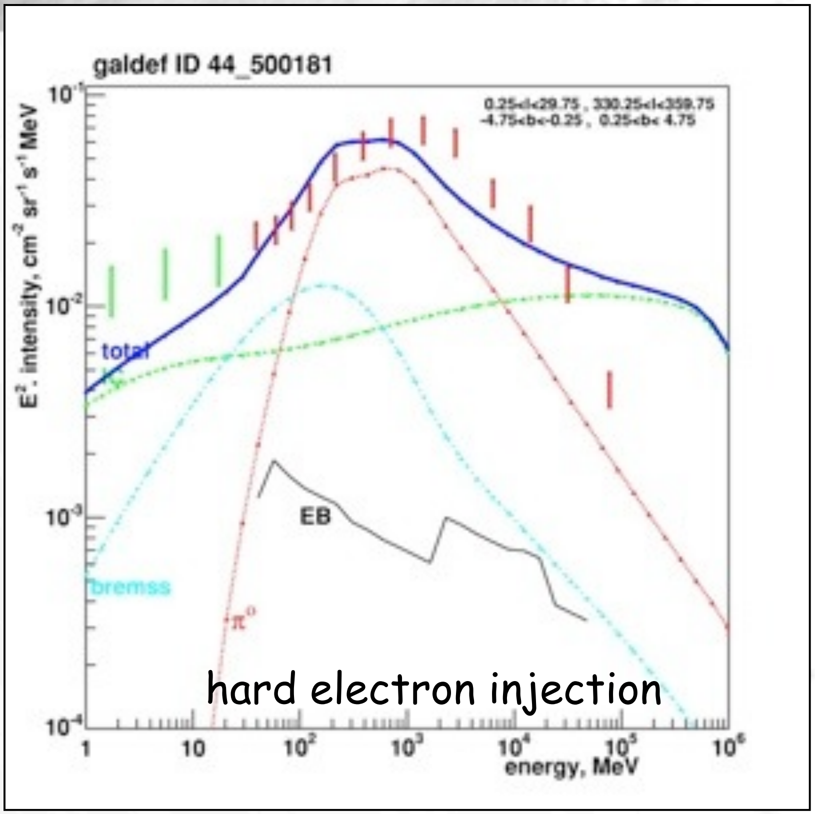

Above 100 MeV
dominated by
pp induced γ-rays

25

Strong, Moskalenko, and Reimer, ApJ 613 (2004) 962

Diffuse γ-ray spectra predicted and observed by EGRET

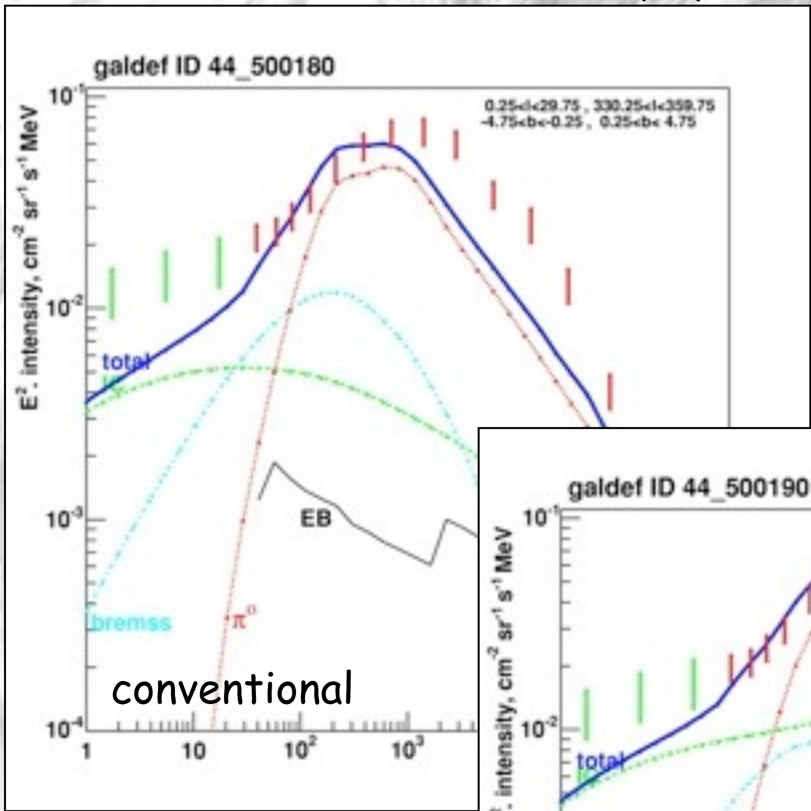

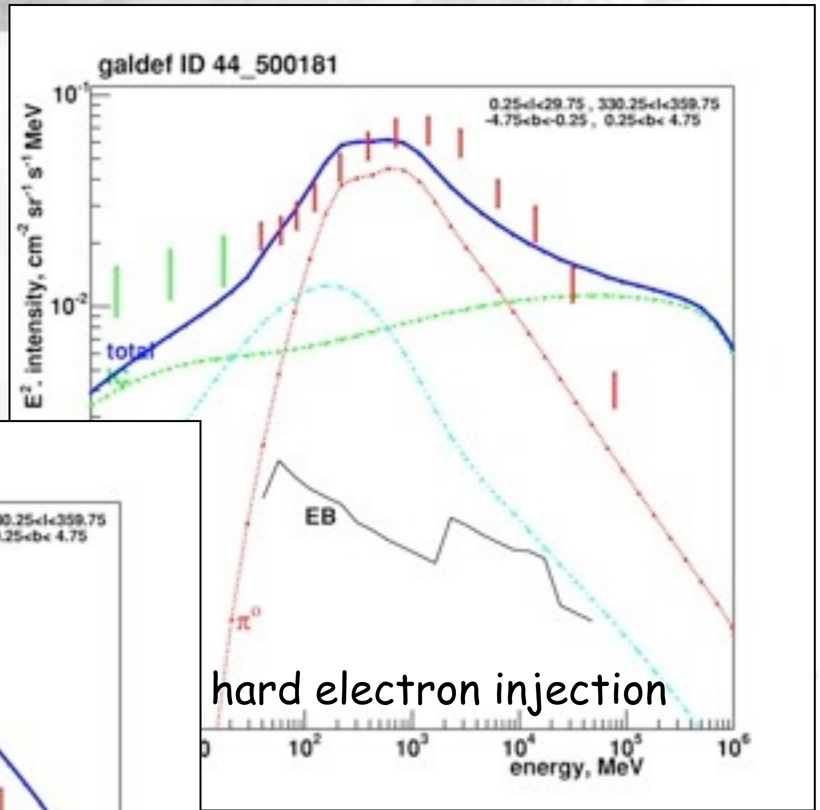

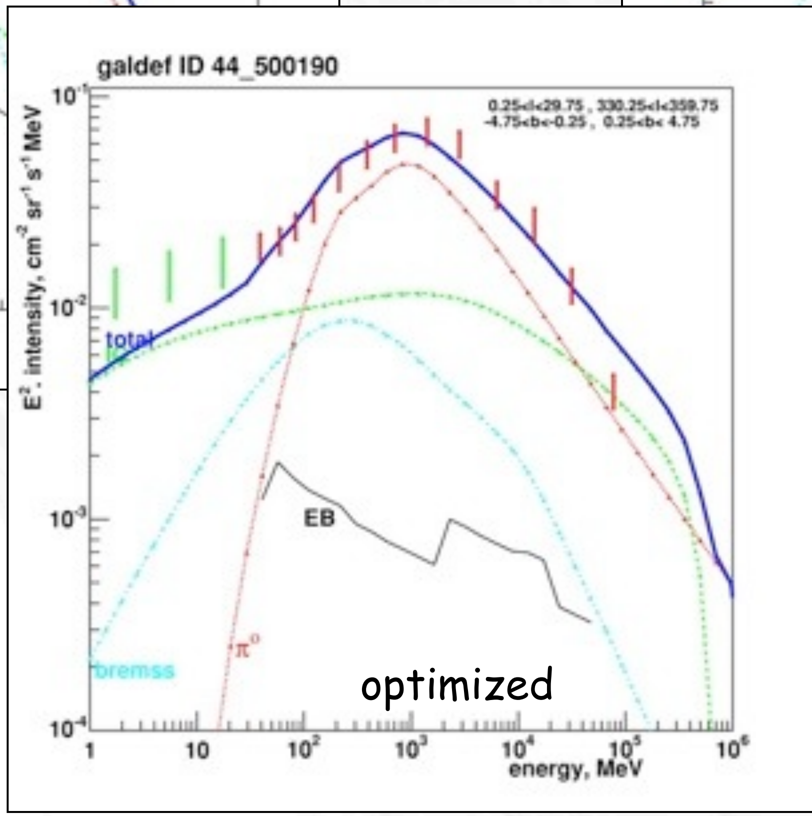

Above 100 MeV
dominated by
pp induced γ-rays

Strong, Moskalenko, and Reimer, ApJ 613 (2004) 962

But newest FERMI data do not show a GeV excess any more

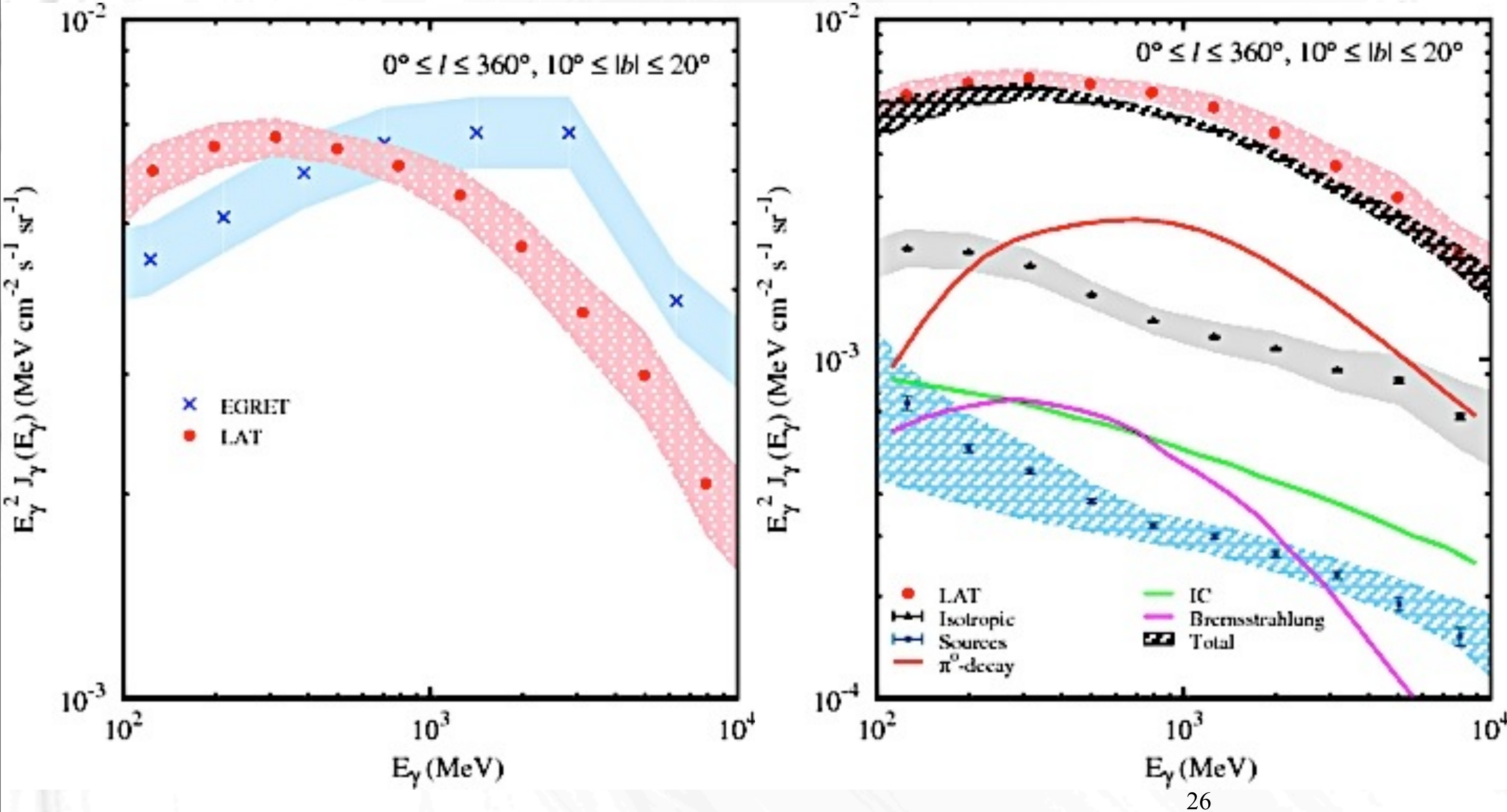

Porter et al., FERMI collaboration, arXiv:0907.0294

The galactic neutrino flux is comparable to the galactic diffuse γ-ray flux

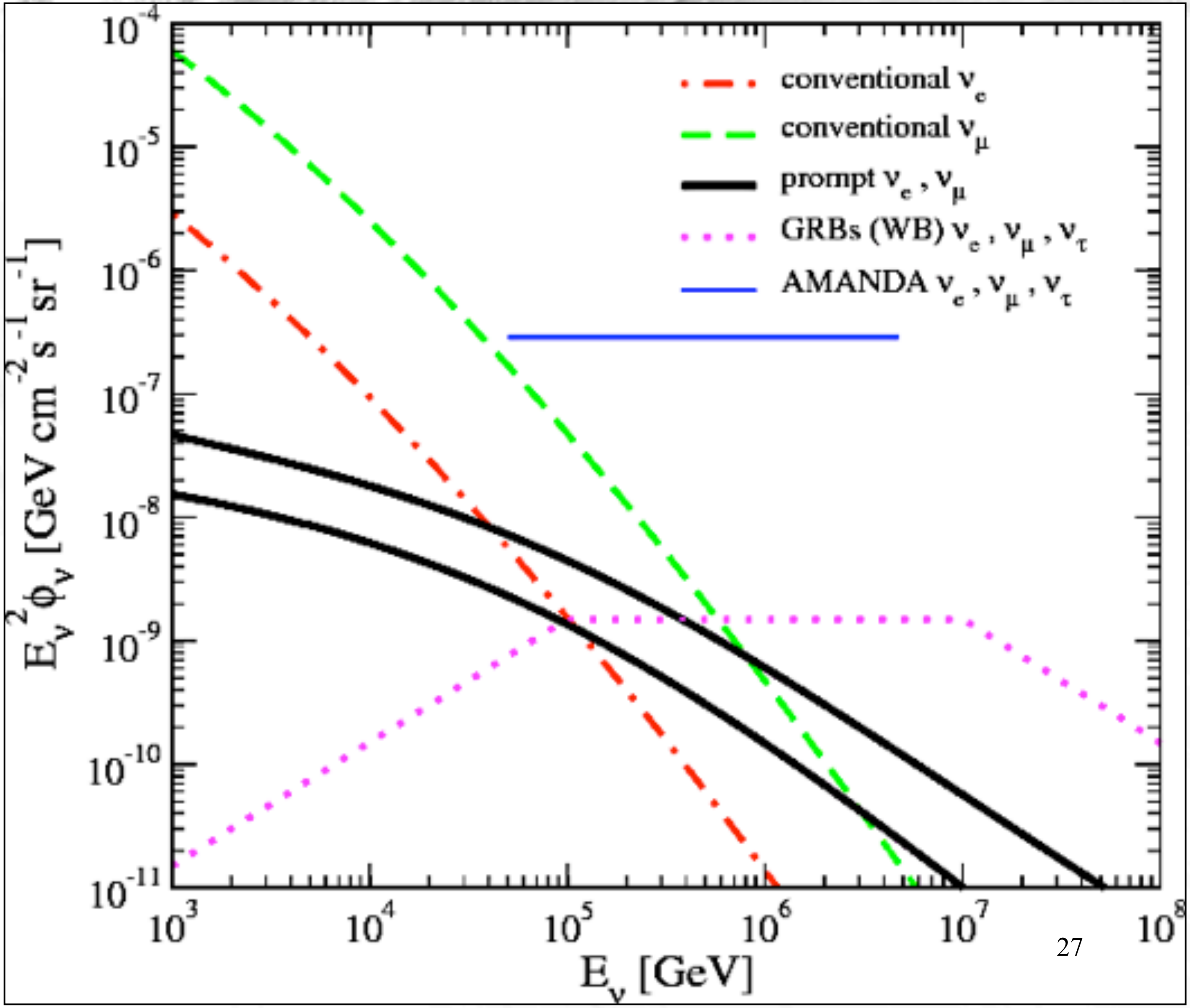

Candia and Beacom, JCAP 0411 (2004) 009

Recently Considered Indirect Signatures of Dark Matter

Gamma-ray flux from galactic centre observed by H.E.S.S.

511 keV annihilation line from near the galactic centre observed by INTGRAL

GeV galactic gamma-ray excess observed by EGRET, but not confirmed by Fermi-LAT; still, there may be a "Fermi haze"

The WMAP microwave haze of the inner Galaxy

Galactic positron excess observed by the PAMELA satellite (and earlier experiments)

An excess observed in the combined electron/positron flux observed by ATIC and FERMI/GLAST

28

Galactic Centre gamma-ray Flux

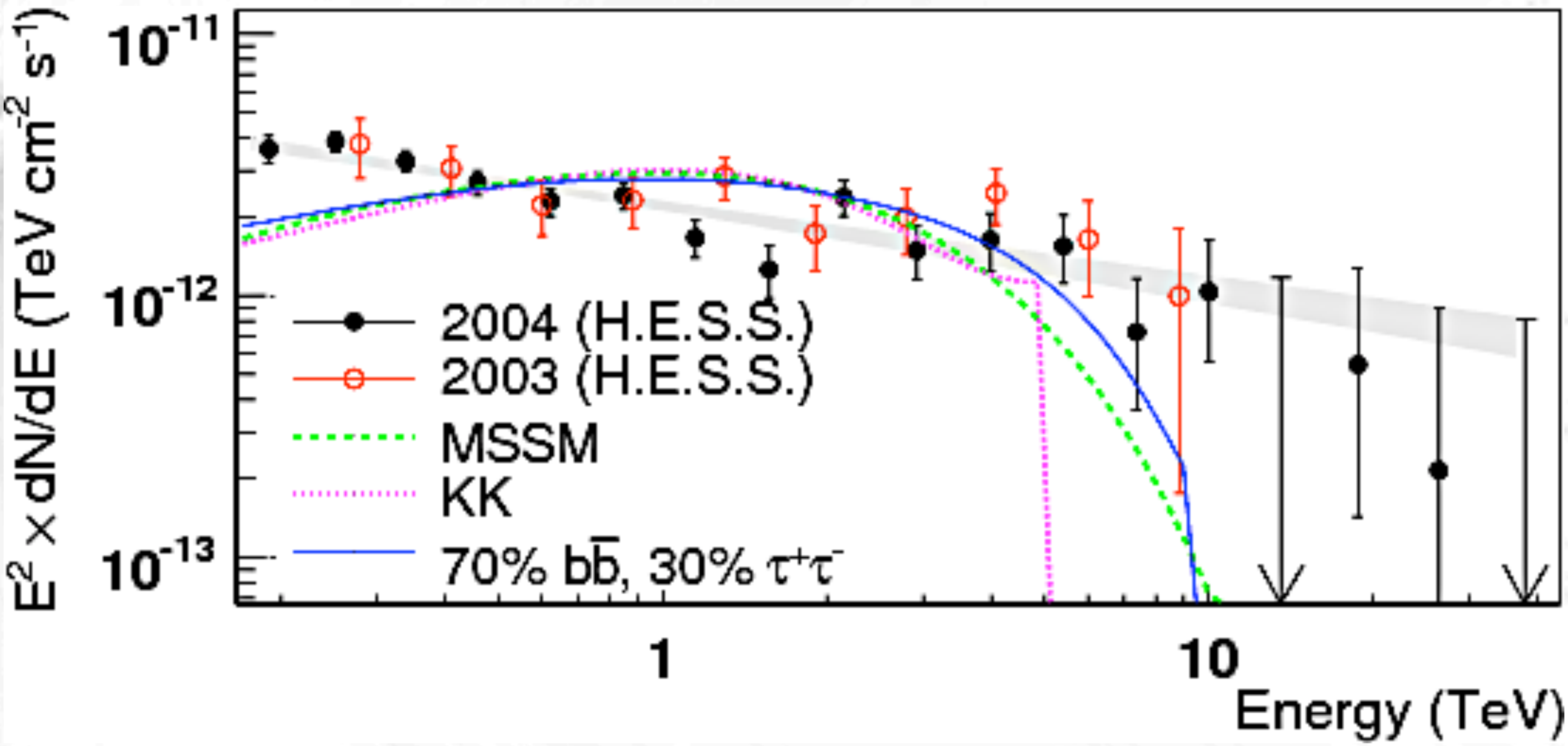

The H.E.S.S. data extends to beyond 30 TeV which is would require unnaturally large dark matter masses; newest data consistent with acceleration with cut-off.

Galactic Centre 511 keV Annihilation Line

But new INTEGRAL data shows line emission is not spherically symmetric as expected if from a dark matter halo. It seems instead to correlate with the Galactic bulge
[Weidenspointner et al., Nature 451, 159 (2008)]

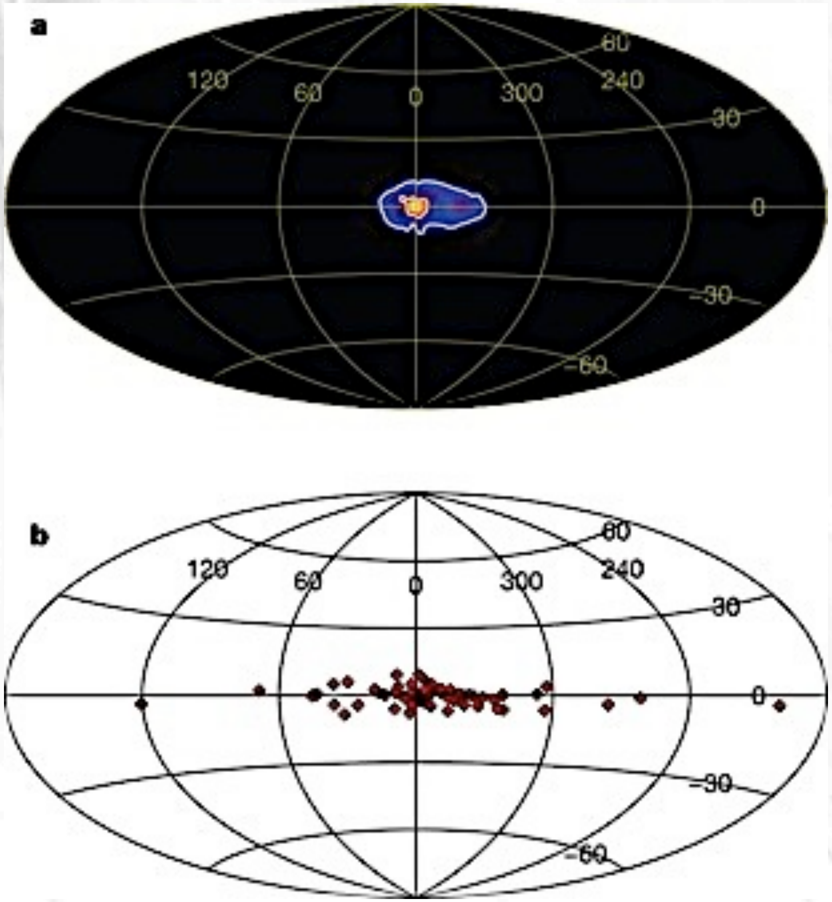

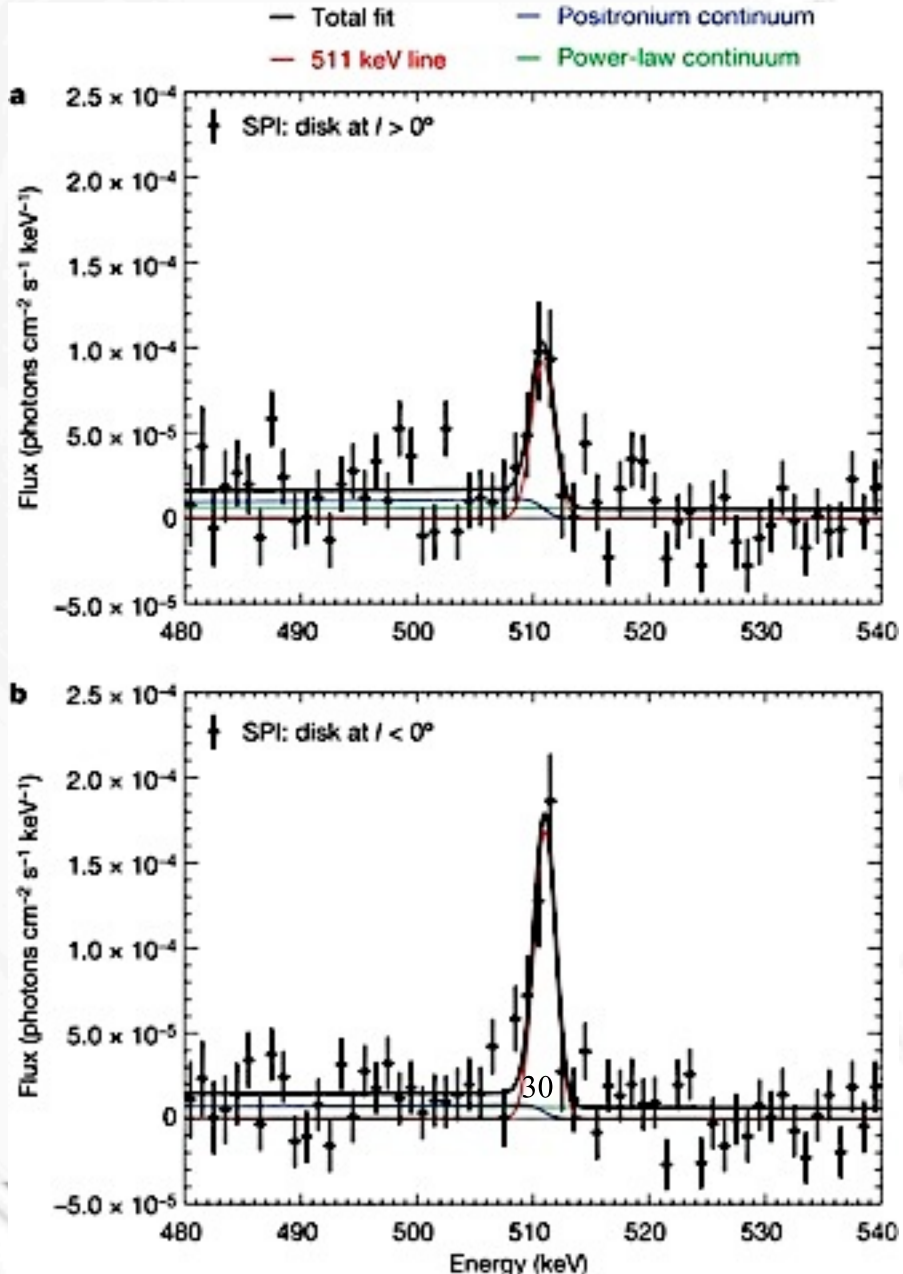

Galactic GeV gamma-ray excess seen by EGRET

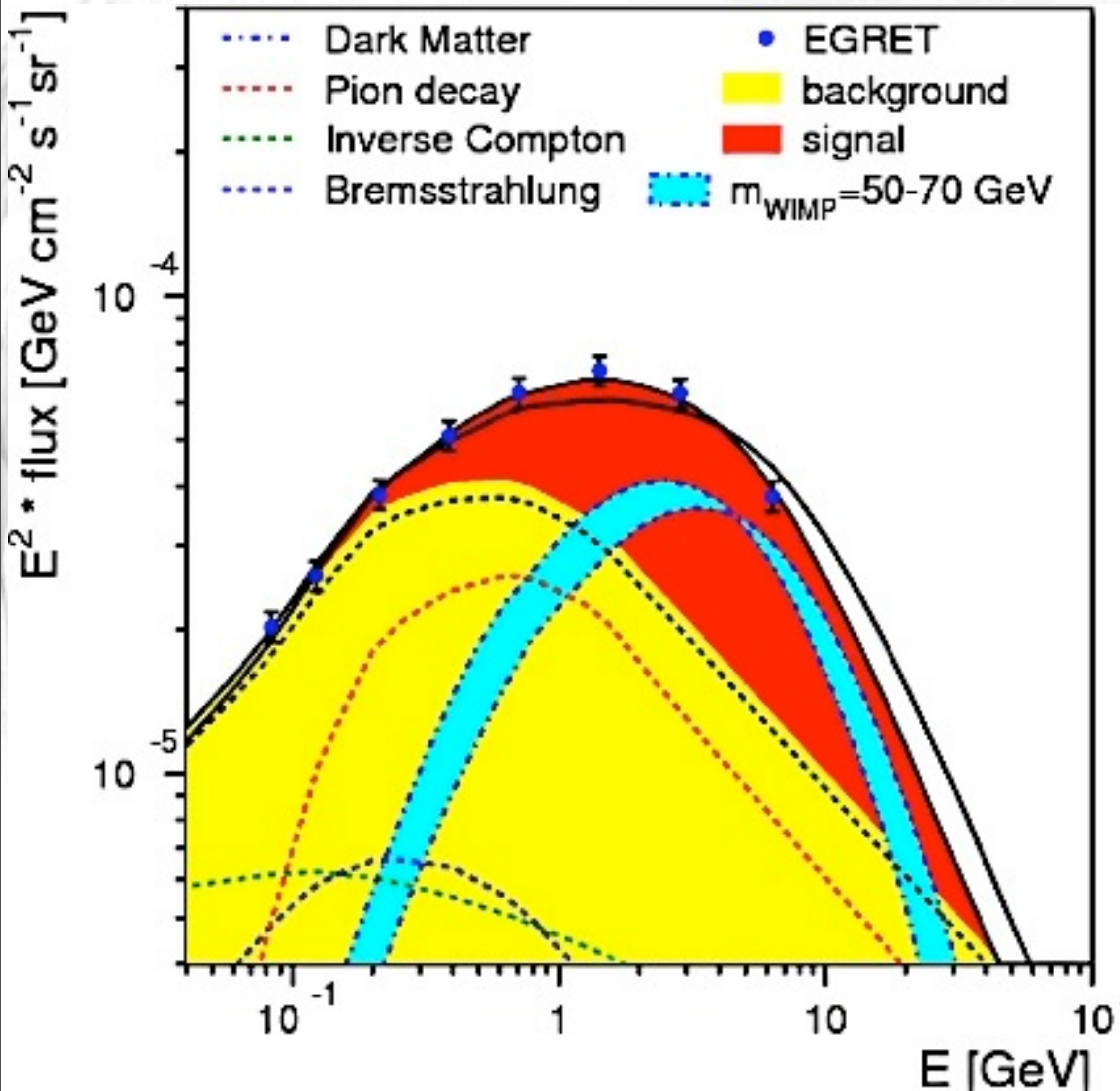

31

Signal ?

De Boer et al, Astron.Astrophys. 444, 51 (2005)

Or cosmic ray background ?

Strong, Moskalenko, and Reimer, ApJ 613 (2004) 962

Galactic GeV gamma-ray excess seen by EGRET

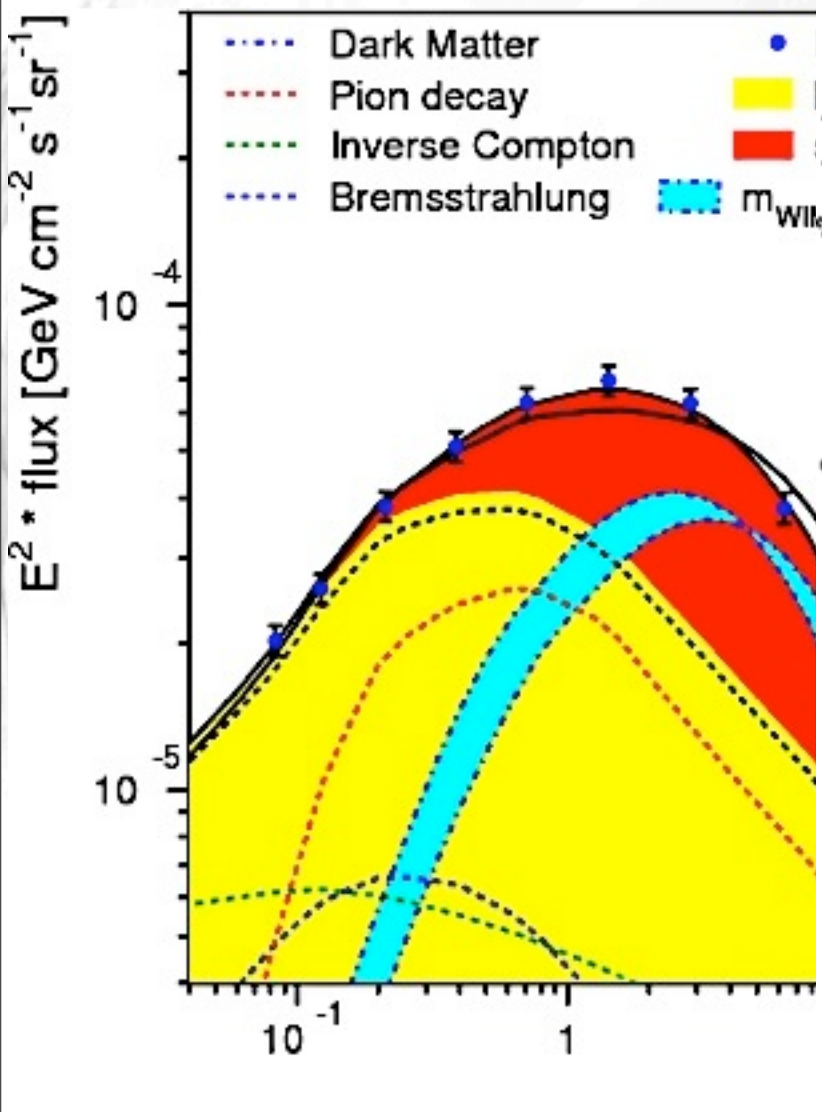

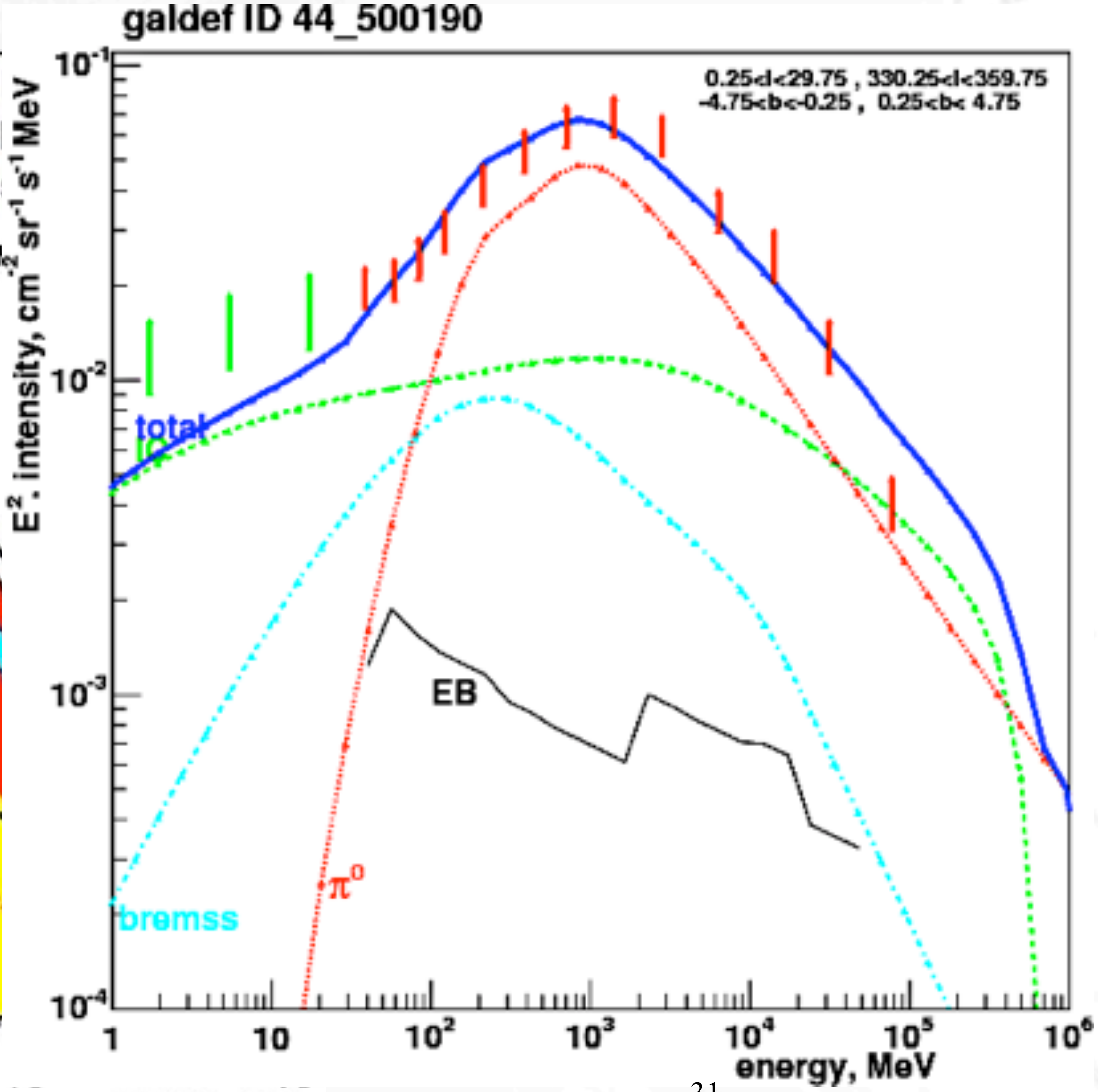

Signal ?

De Boer et al, Astron.Astrophys. 444, 51 (2005)

Or cosmic ray background ?

Strong, Moskalenko, and Reimer, ApJ 613 (2004) 962

Fermi haze residual after subtracting template from Fermi sky at 1-2 GeV itself, which should be dominated by π^0 channel

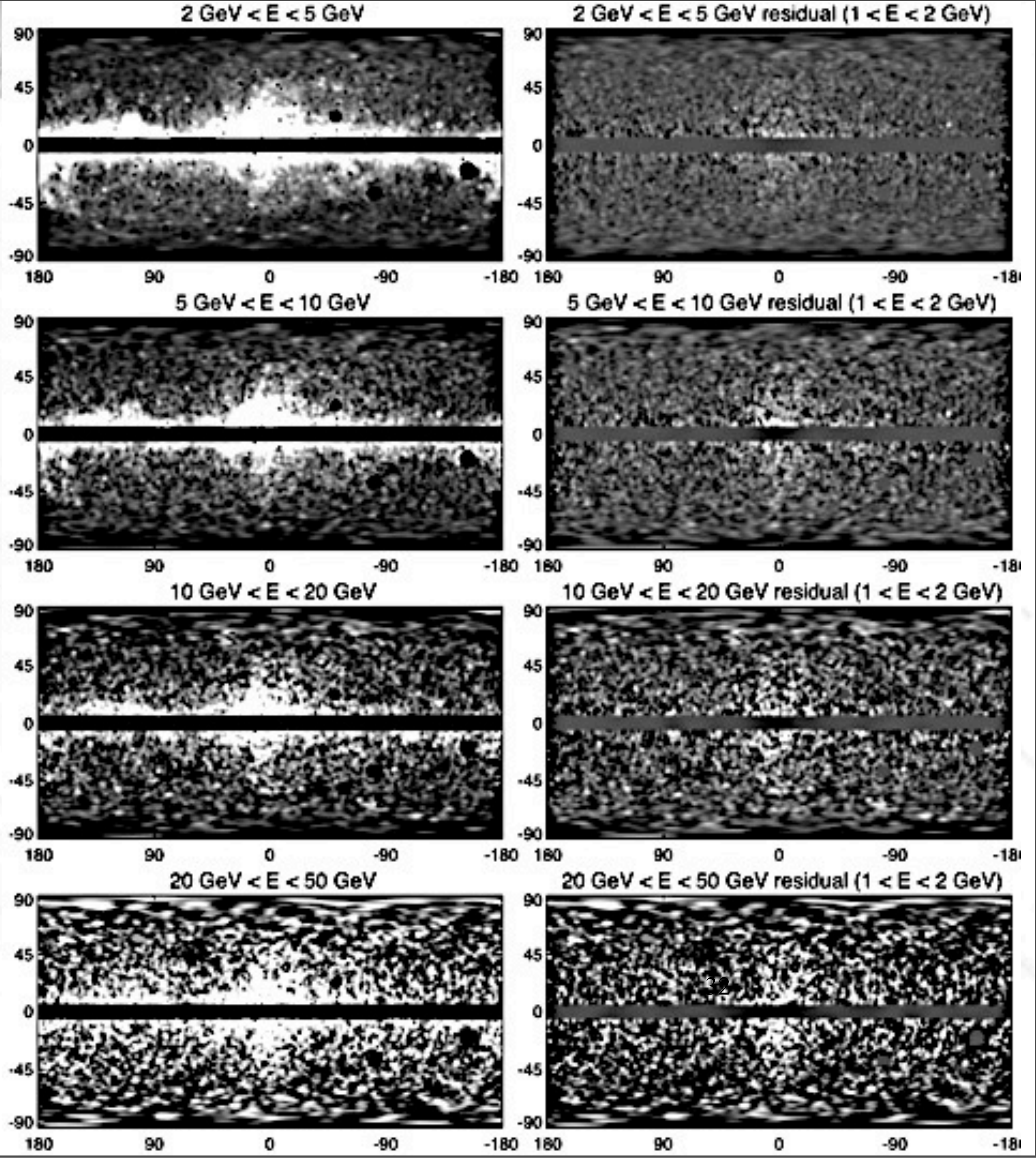

Dobler et al, arXiv:0910.4583

WMAP haze

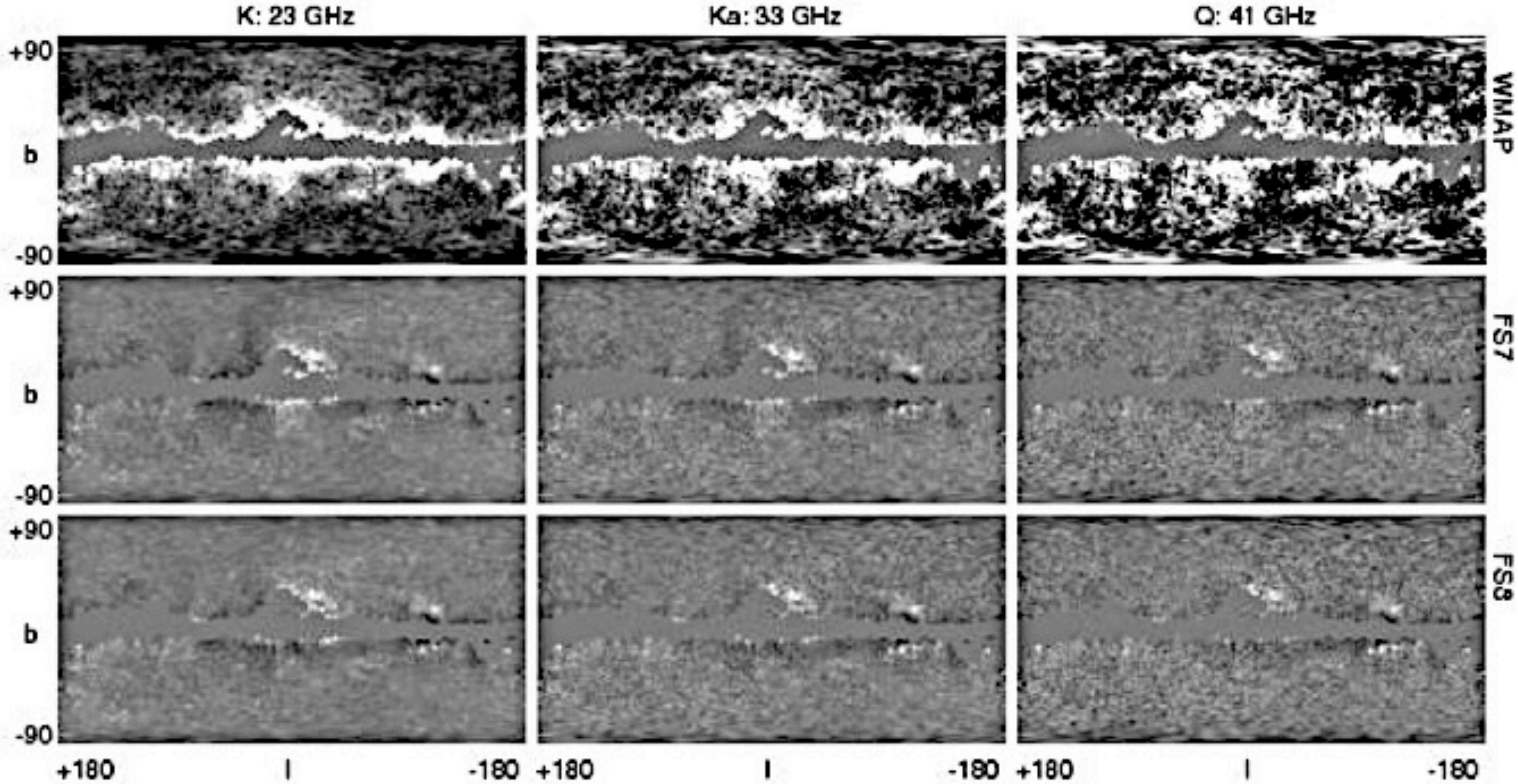

Dobler and Finkbeiner, ApJ 680 (2008) 1222

WMAP haze is the residual after subtracting a template obtained from extrapolating the Haslam 408 MHz map.
But distribution of primary electrons may be different for these energies, e.g. Mertsch and Sarkar arXiv:1004.3056

Morphology of Fermi haze and WMAP haze seem to correlate

An electron component harder than acceleration spectra could explain both due to synchrotron and inverse Compton, respectively

But excesses are of order the astrophysical background uncertainties

Dobler et al, arXiv:0910.4583

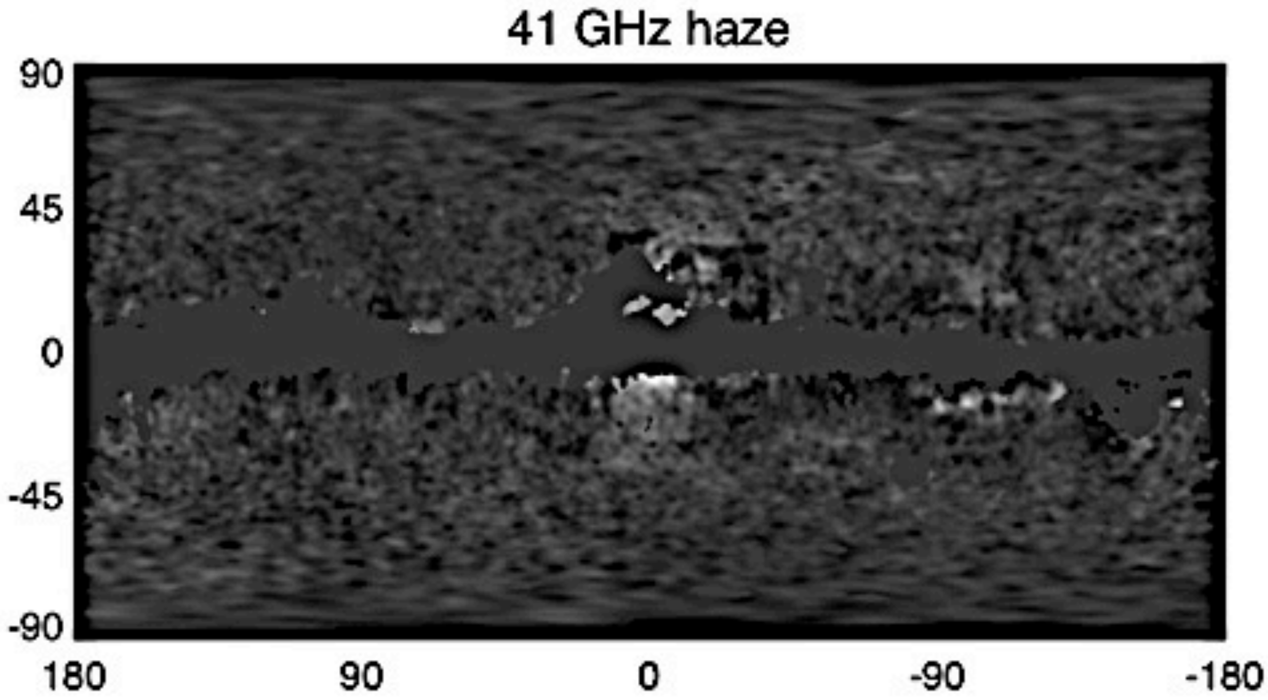

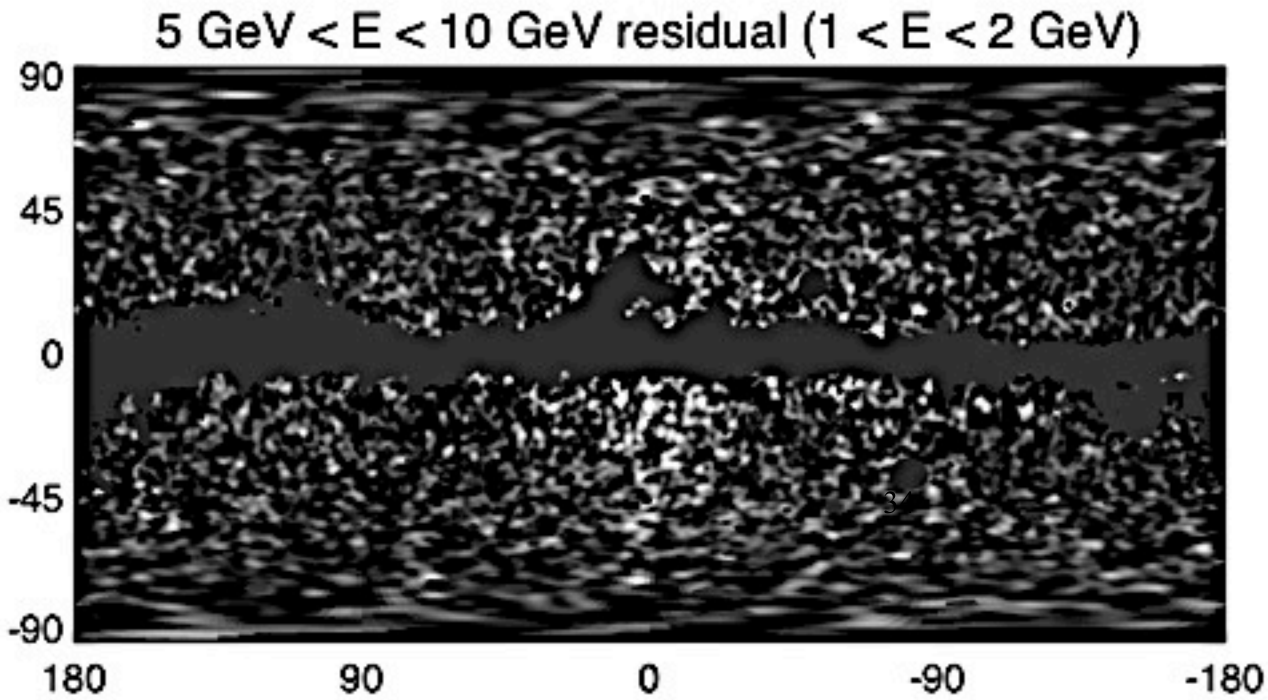

Galactic Positron Fraction Excess

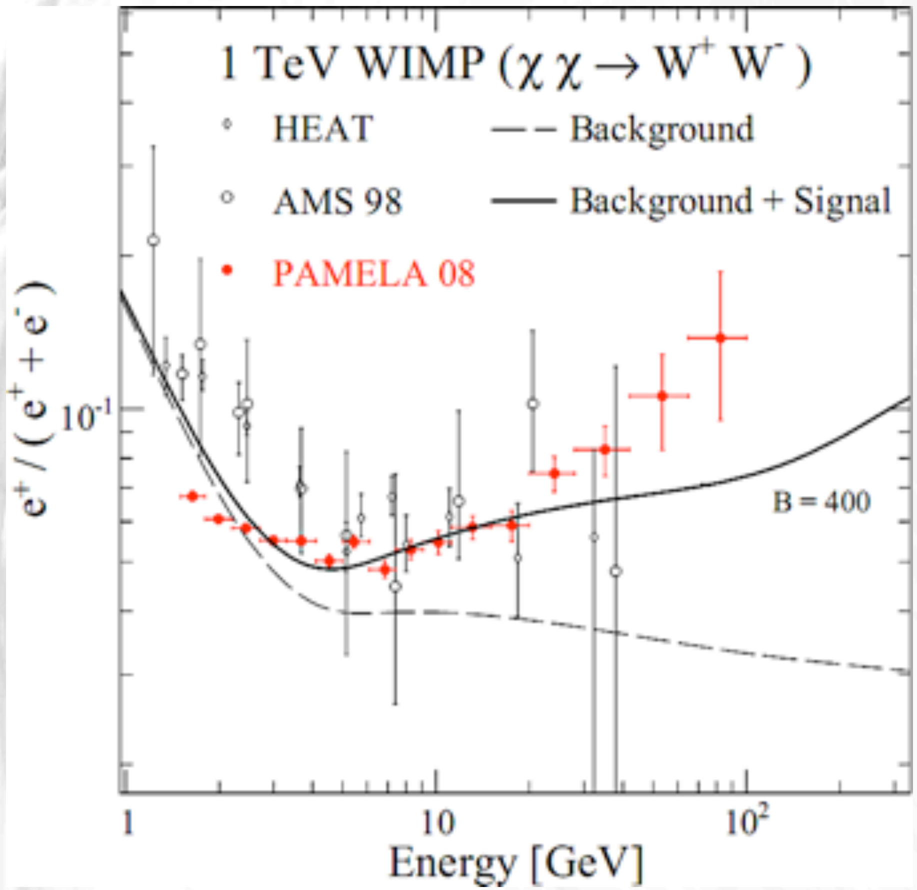

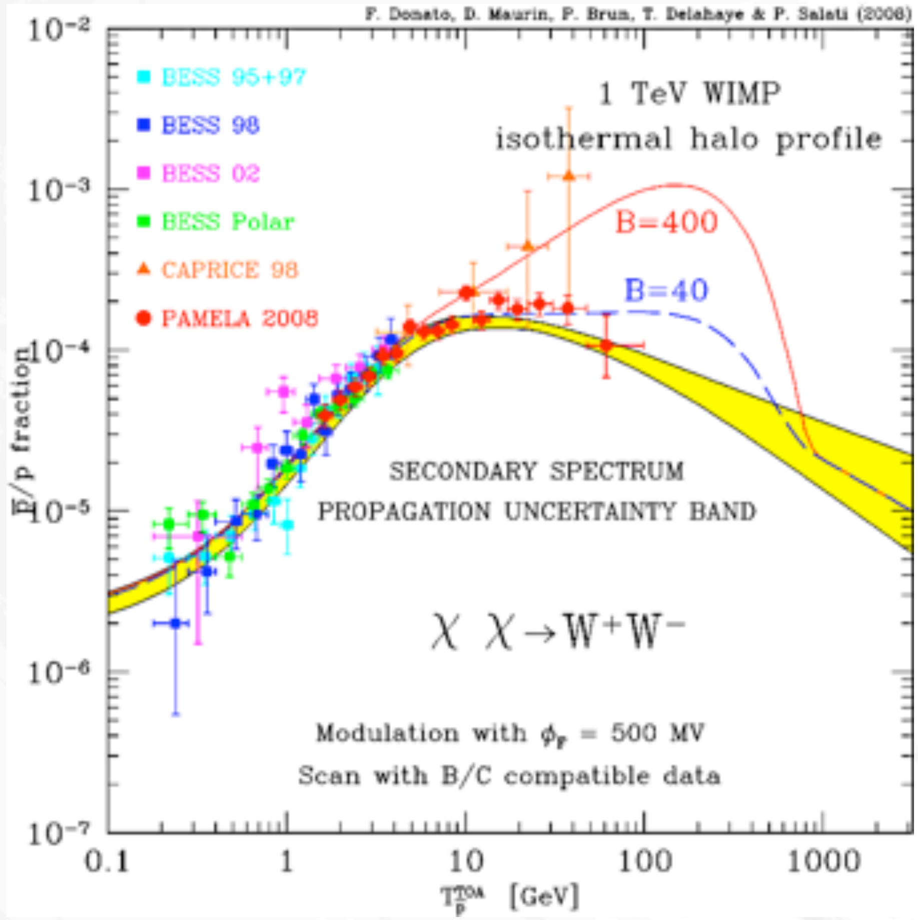

Positron fraction: Excess beyond expected secondary production from homogeneous cosmic ray source distribution

Antiproton fraction: No significant enhancement beyond expected secondary production by cosmic rays

Donato et al., Phys.Rev.Lett.102, 071301 (2009)

But no significant enhancement of anti-proton fraction observed:

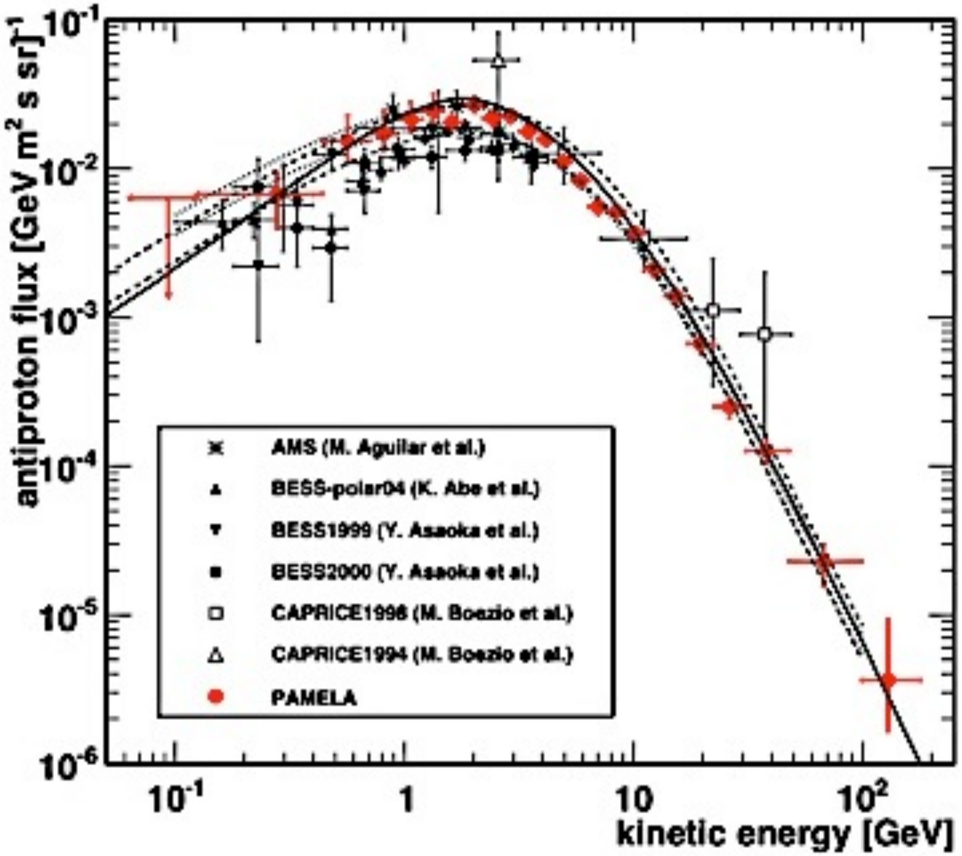

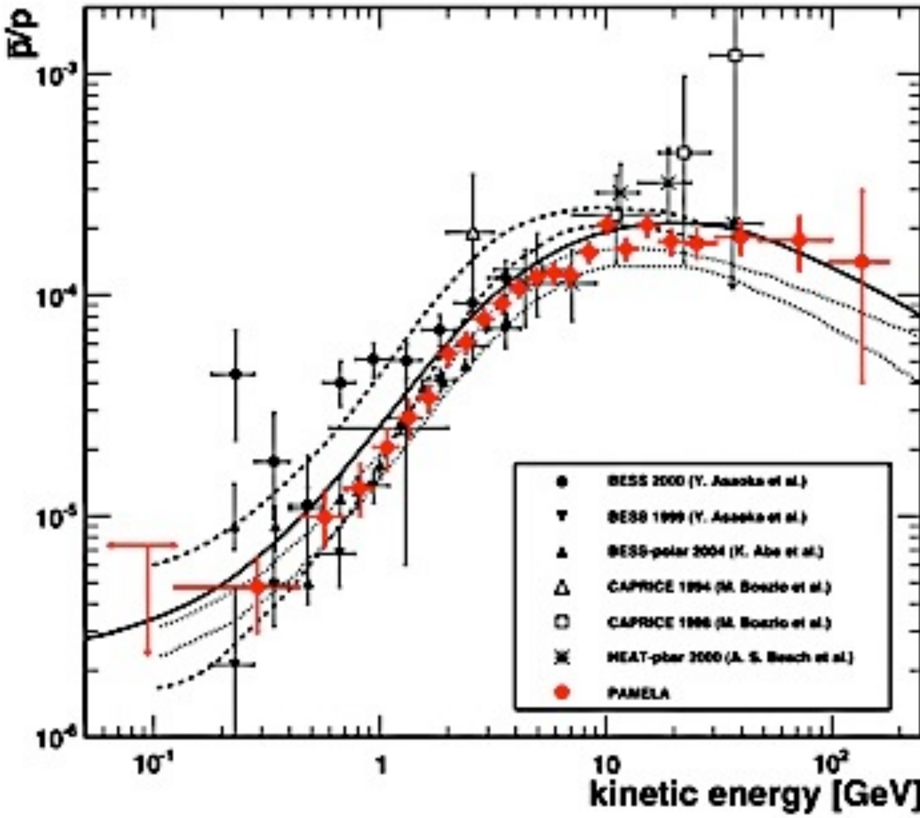

Pamela collaboration, Adriani et al., arXiv:1007.0821

36

Galactic Electron+Positron Flux requires at least two components

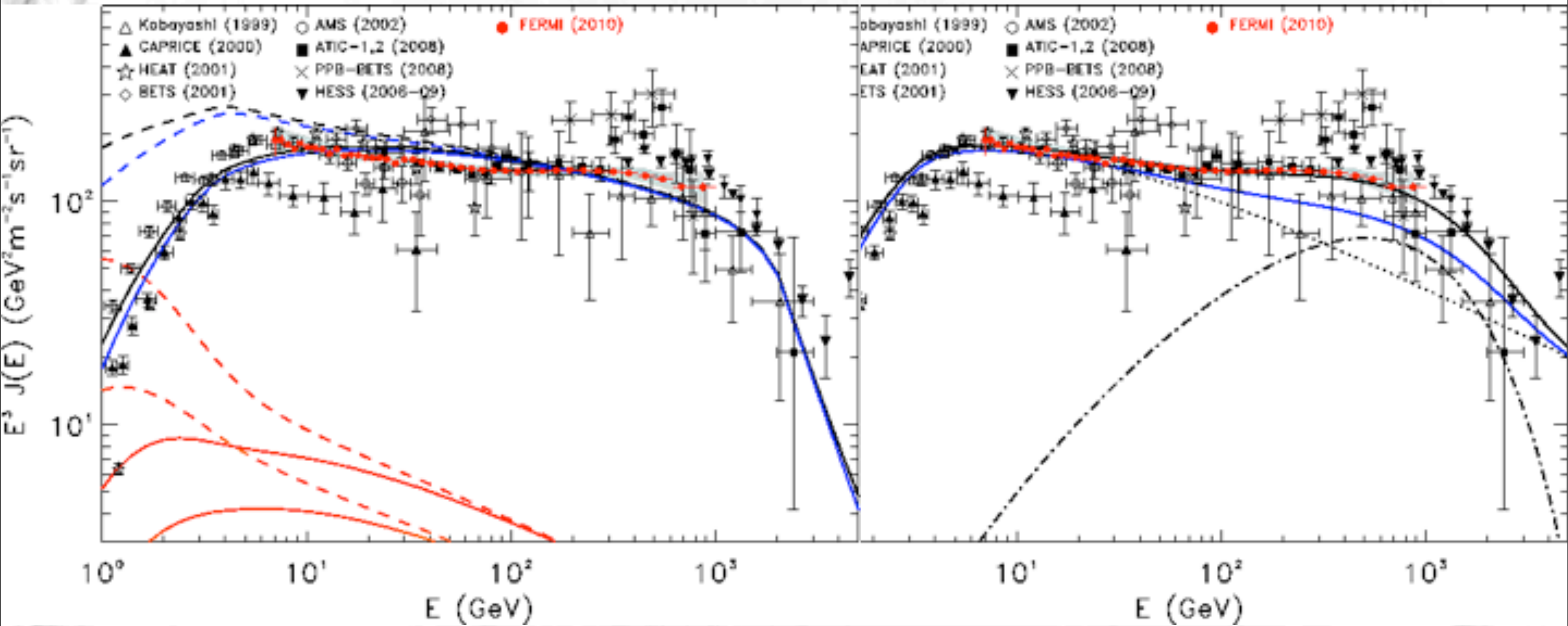

Fermi LAT collaboration, arXiv:1008.3999

37

Galactic Electron+Positron Excess

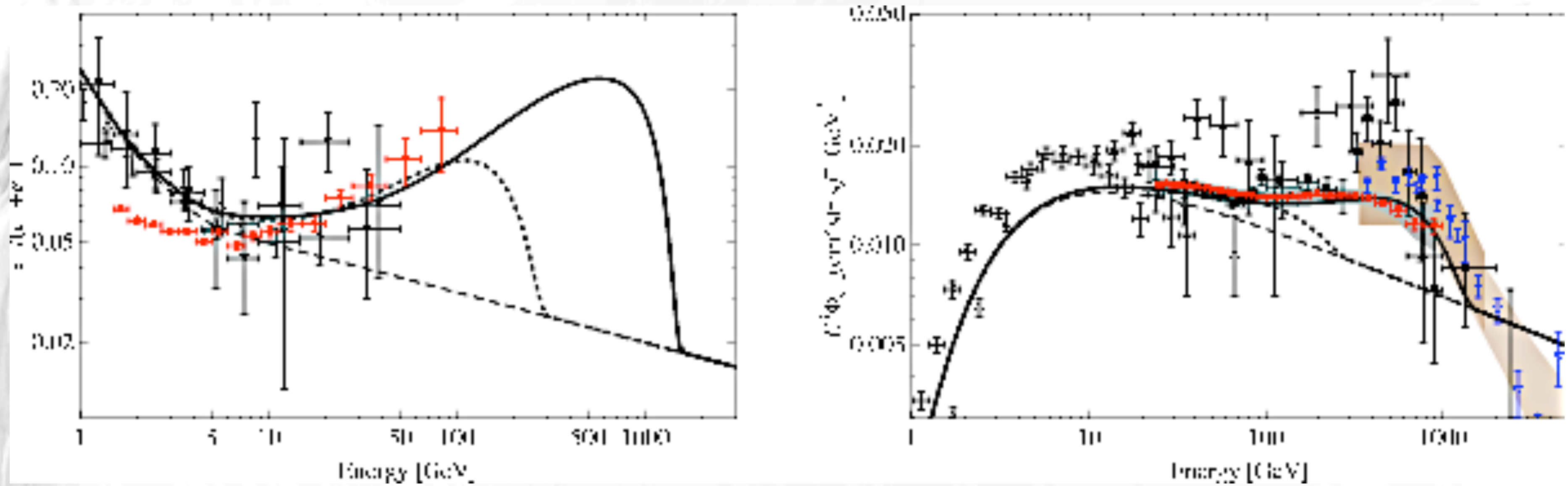

Ibarra, Tran, Weniger, arXiv:0906.1571

Decaying dark matter fits to positron fraction and electron-positron flux:
Decay into W^{+-} μ^{-+} with mass 600 GeV (dotted line) and 3000 GeV (solid line)

38

Direct Detection Limits and Modulation Signals in DAMA and CoGeNT

39

Farina et al., arXiv:1107.0715

Ultra-High Energy Cosmic Rays

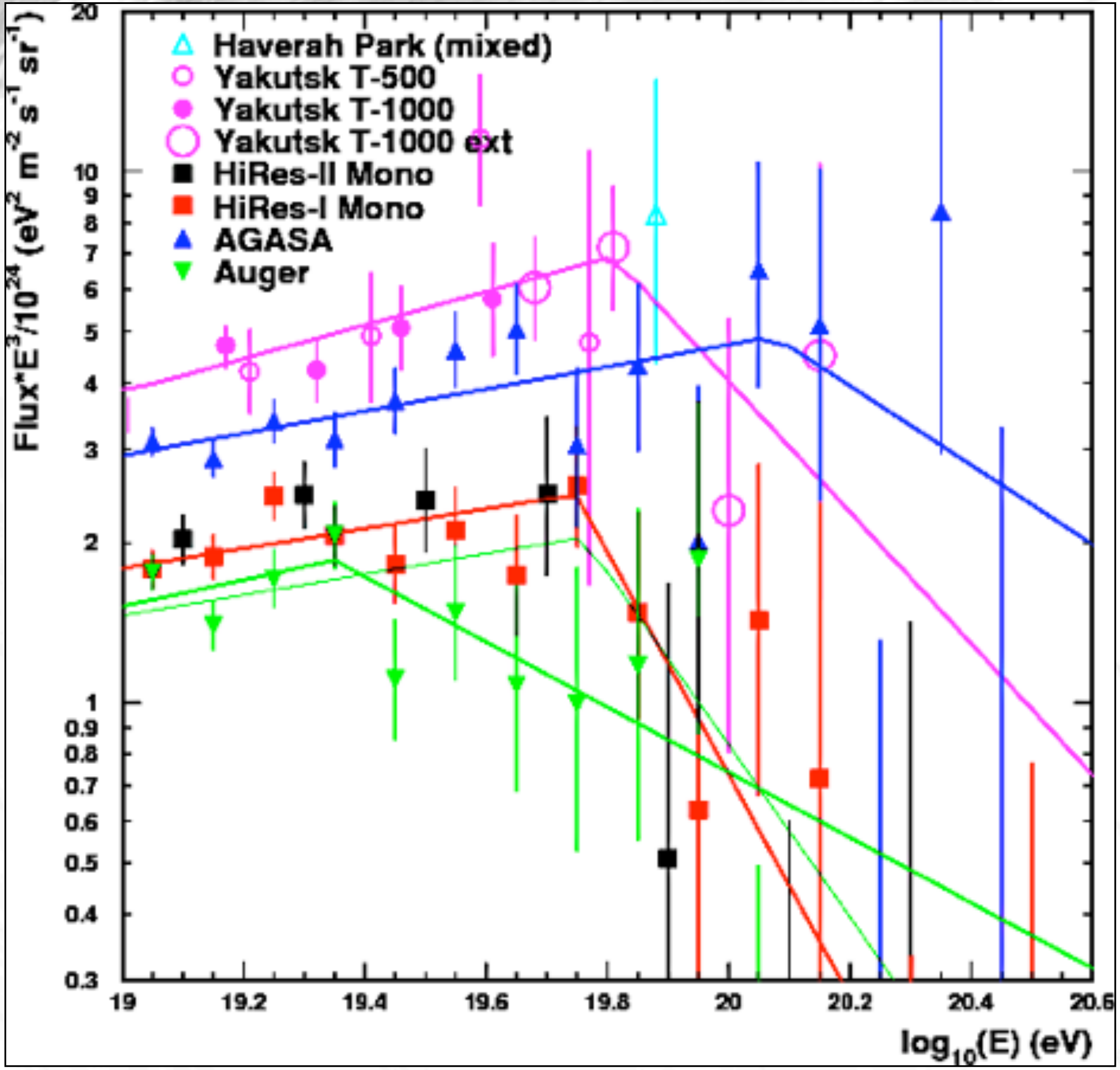

Lowering AGASA energy scale by about 20% brings it in accordance with HiRes up to the GZK cut-off, but maybe not beyond ?

Bergmann, Belz, J.Phys.G34 (2007) R359

41

May need an experiment combining ground array with fluorescence such as the Auger project to resolve this issue.

Comparison of Experimental Spectra at the Highest Energies

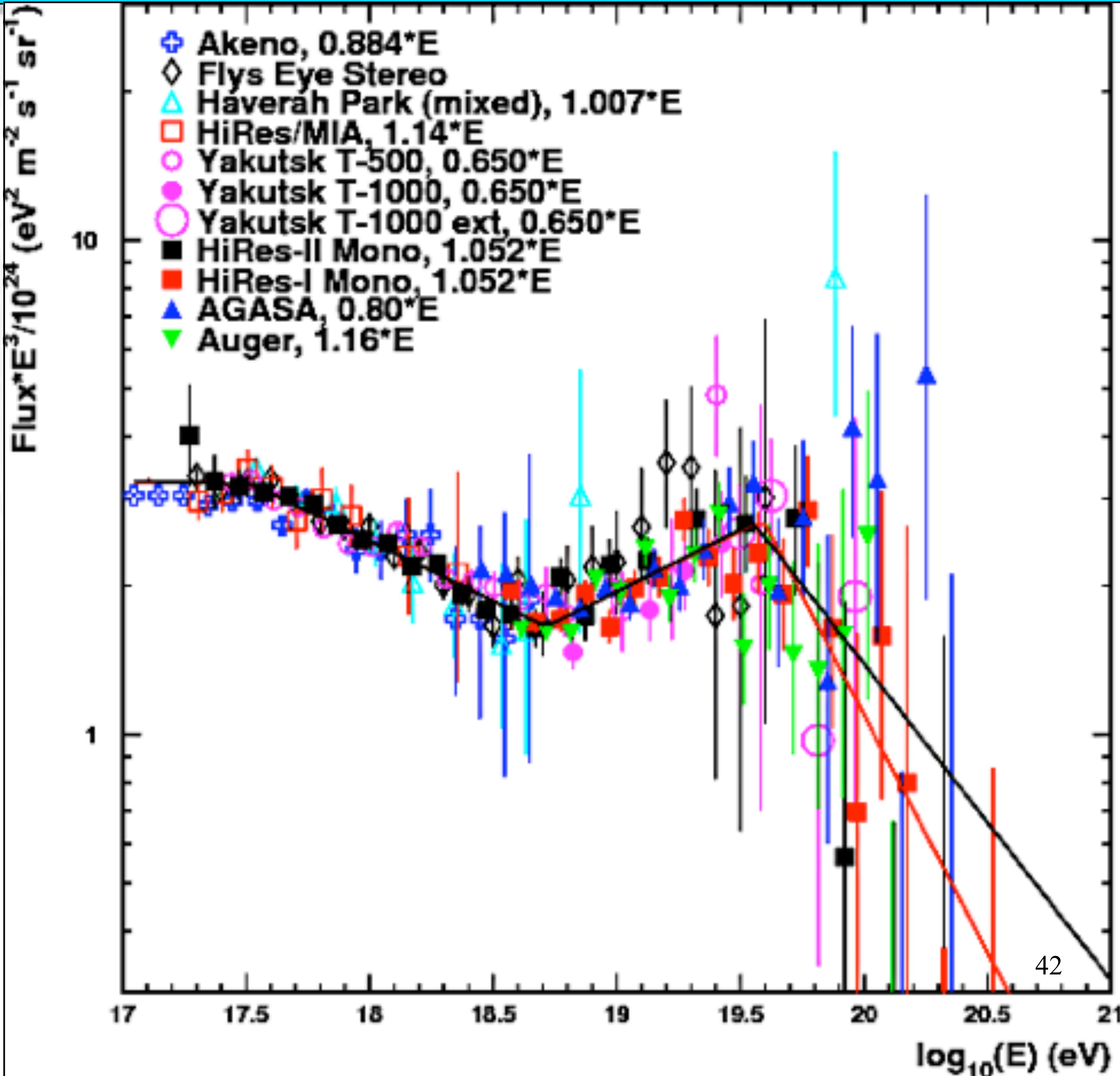

Bergmann, Belz, J.Phys.G34 (2007) R359

Auger and HiRes Spectra

Auger exposure = 12,790 km^2 sr yr up to December 2008

Pierre Auger Collaboration, PRL 101, 061101 (2008)
and Phys.Lett.B 685 (2010) 239

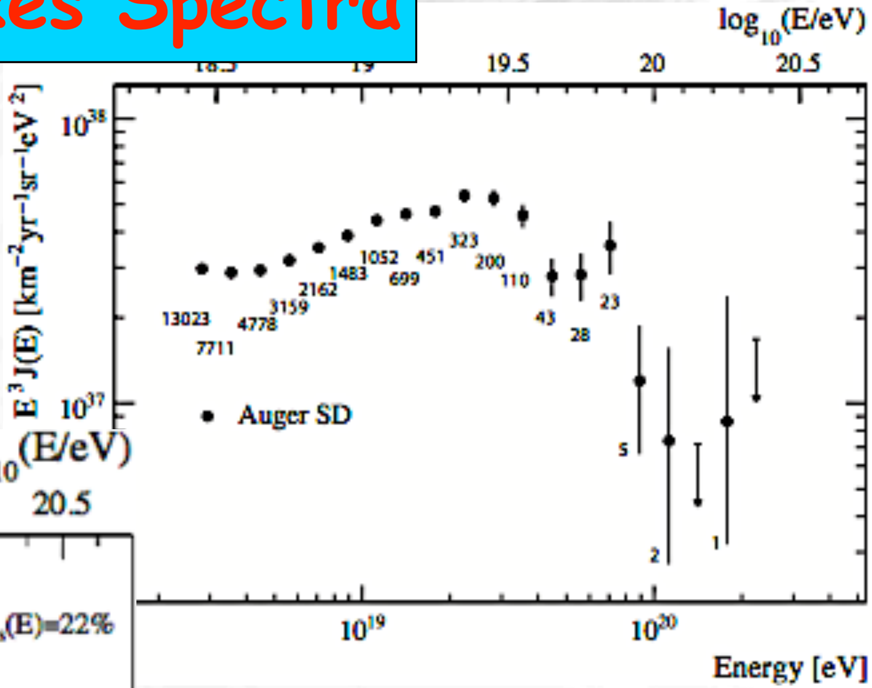

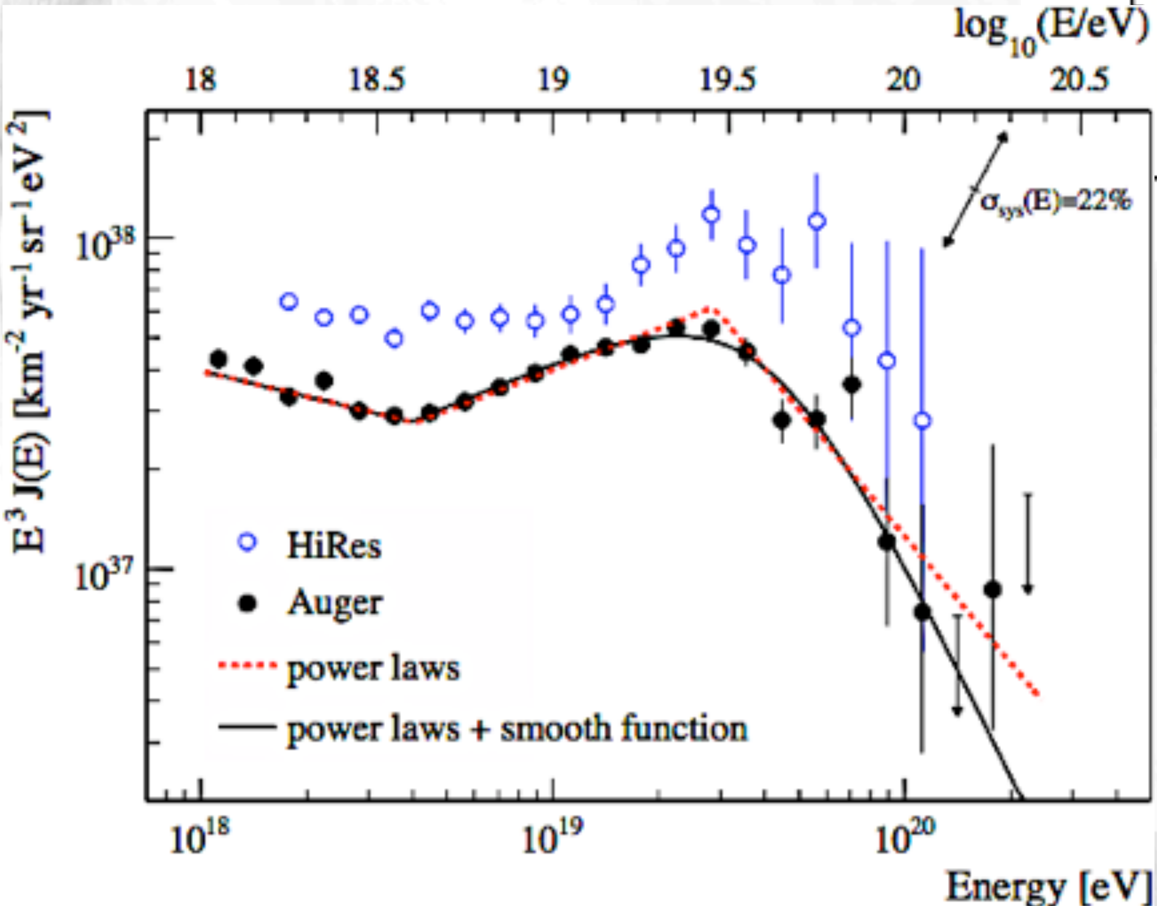

43

Atmospheric Showers and their Detection

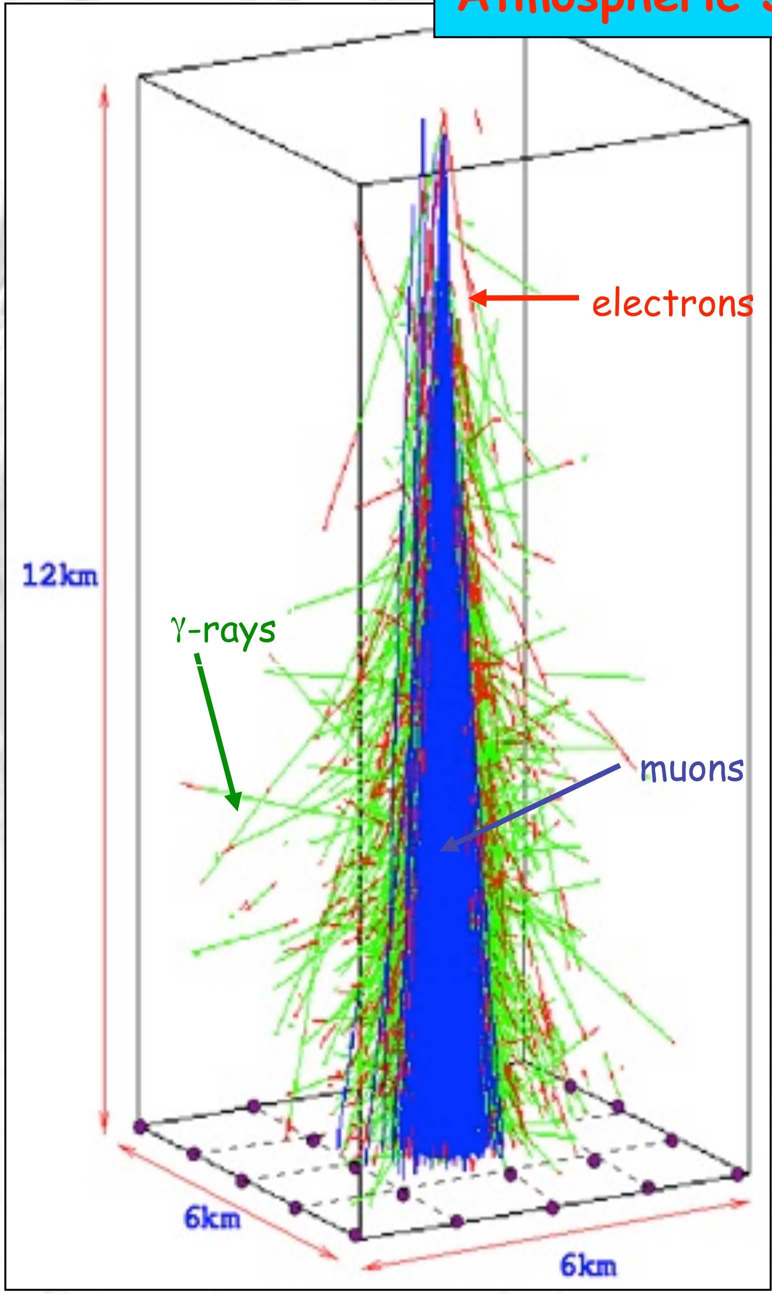

44

Atmospheric Showers and their Detection

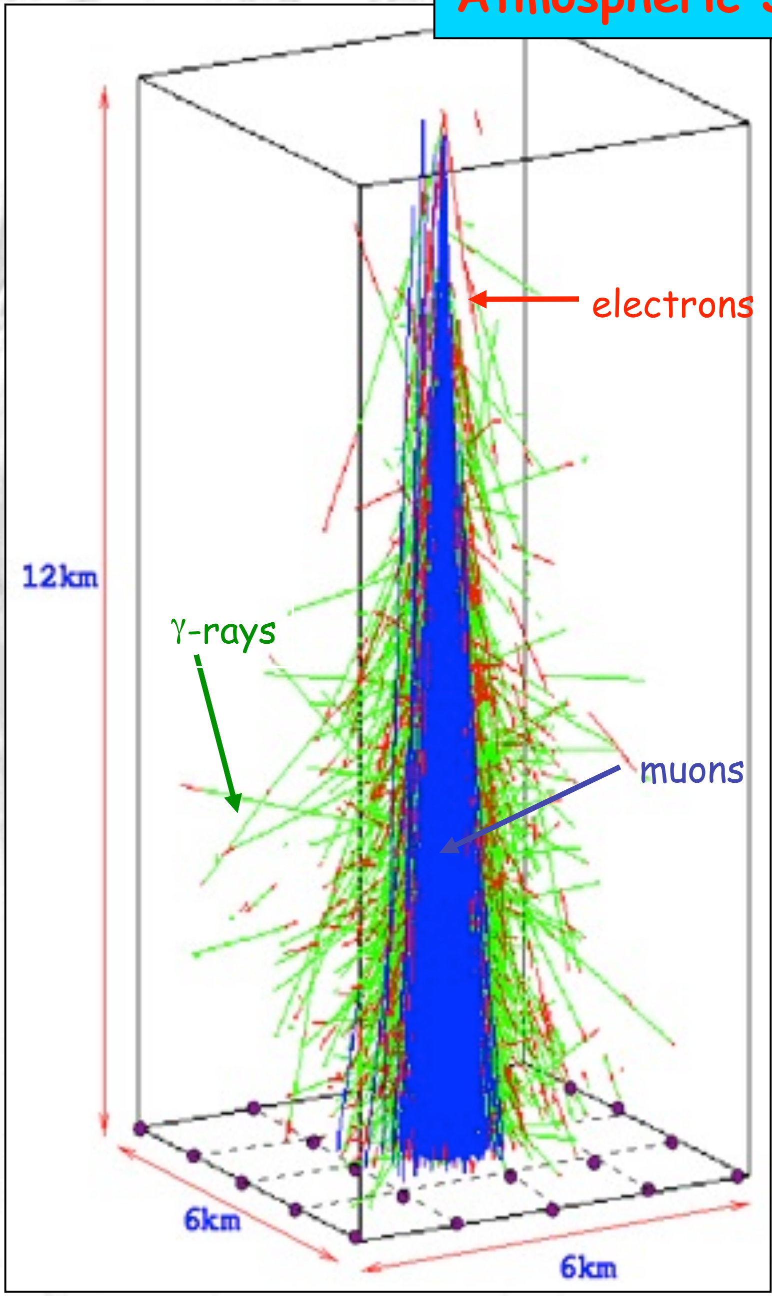

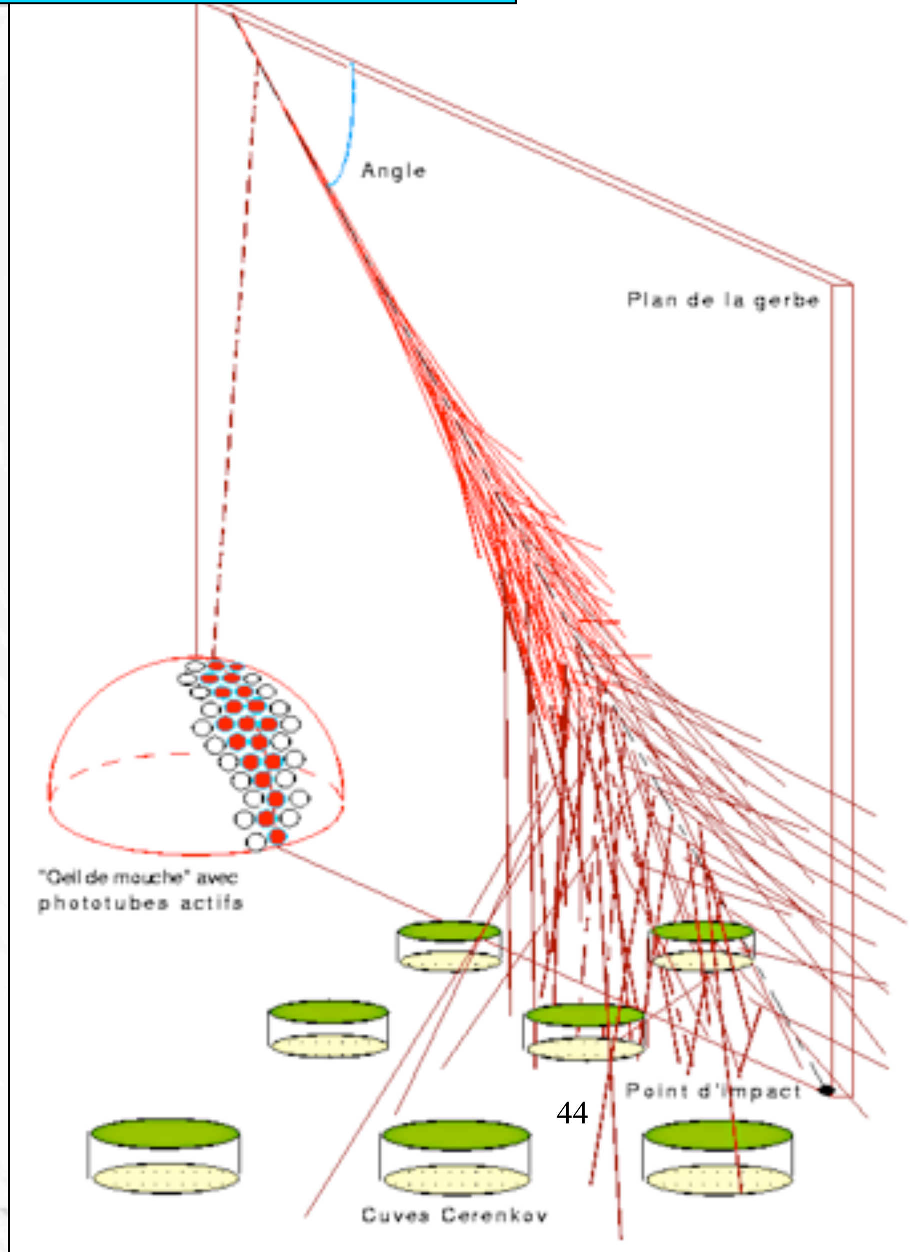

Atmospheric Showers and their Detection

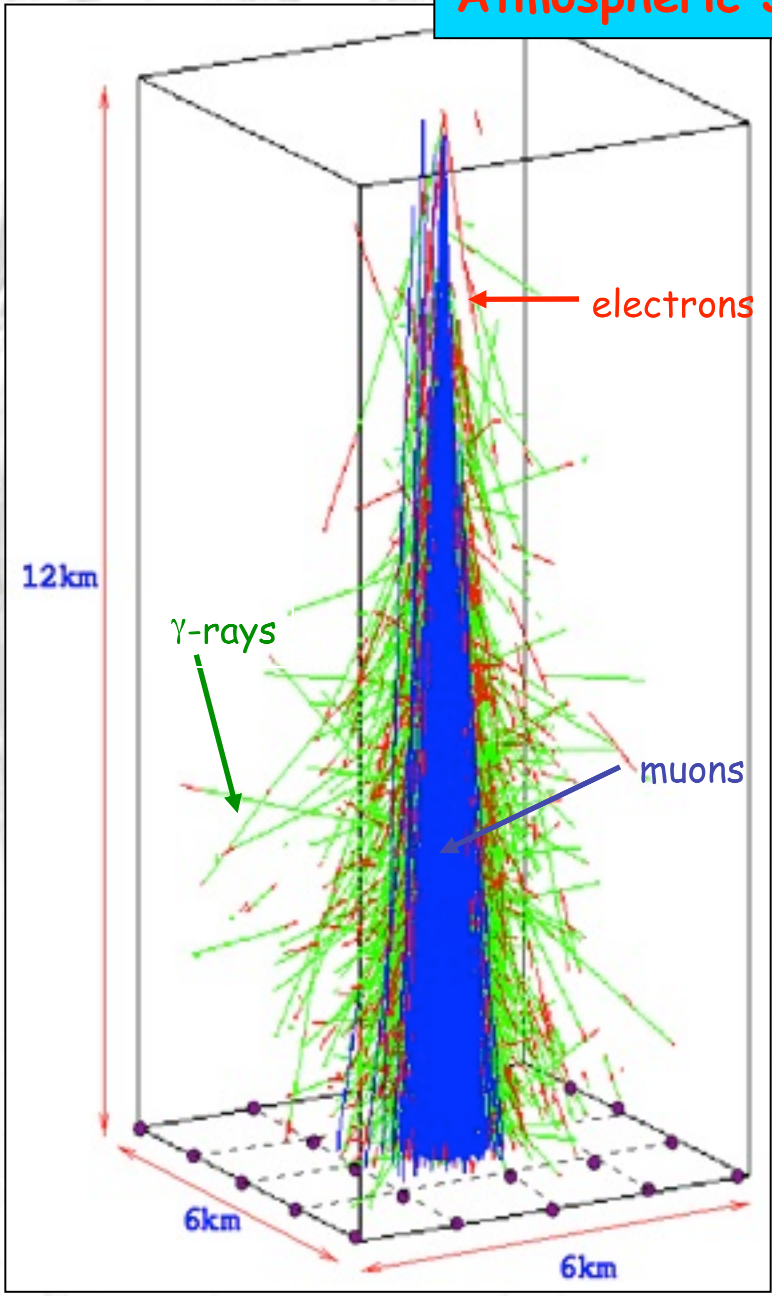

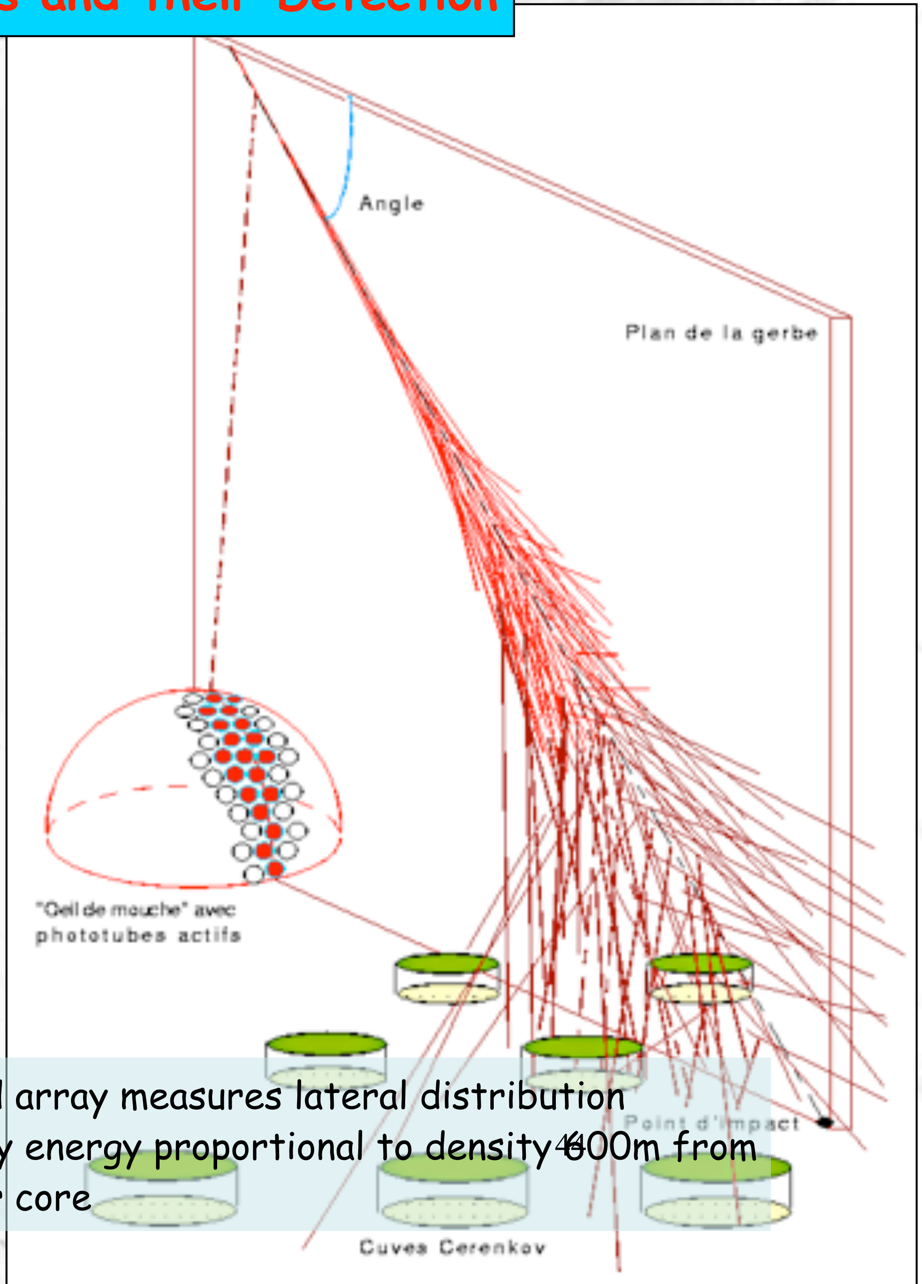

Ground array measures lateral distribution
Primary energy proportional to density 600m from shower core

Atmospheric Showers and their Detection

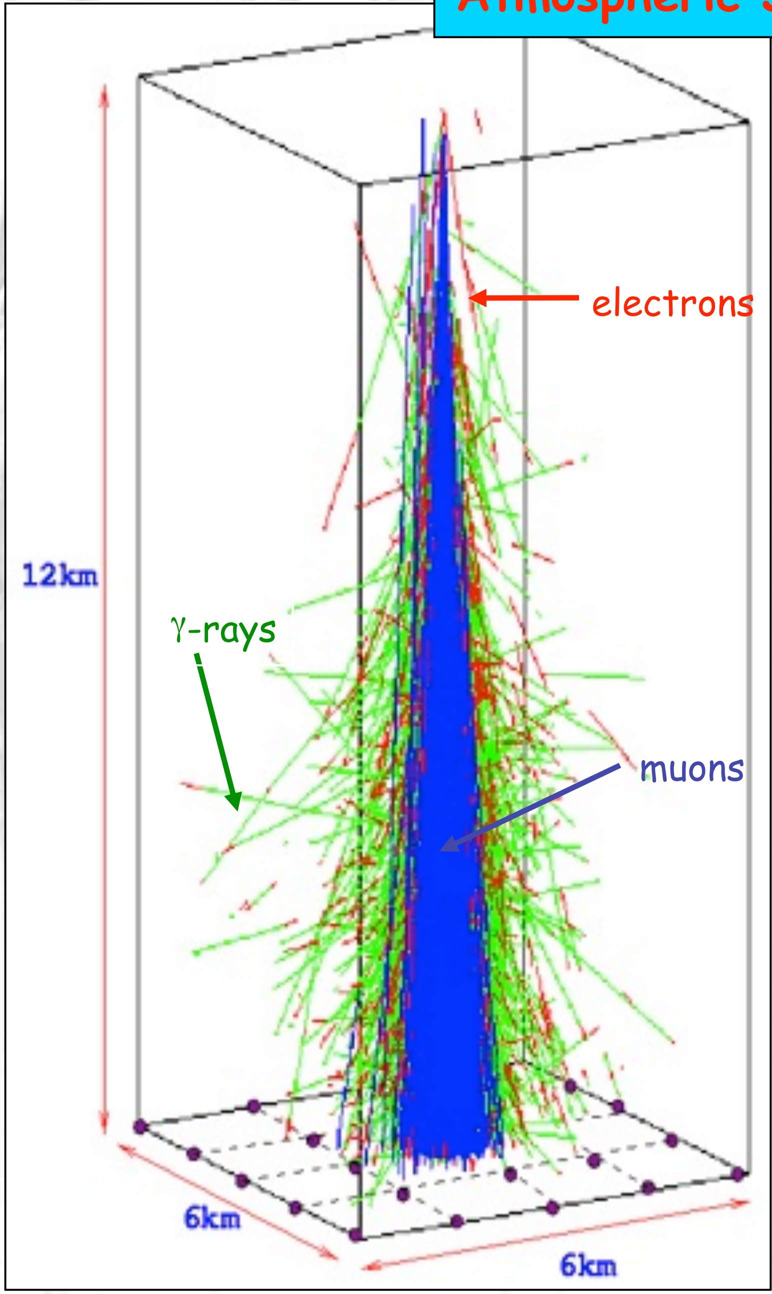

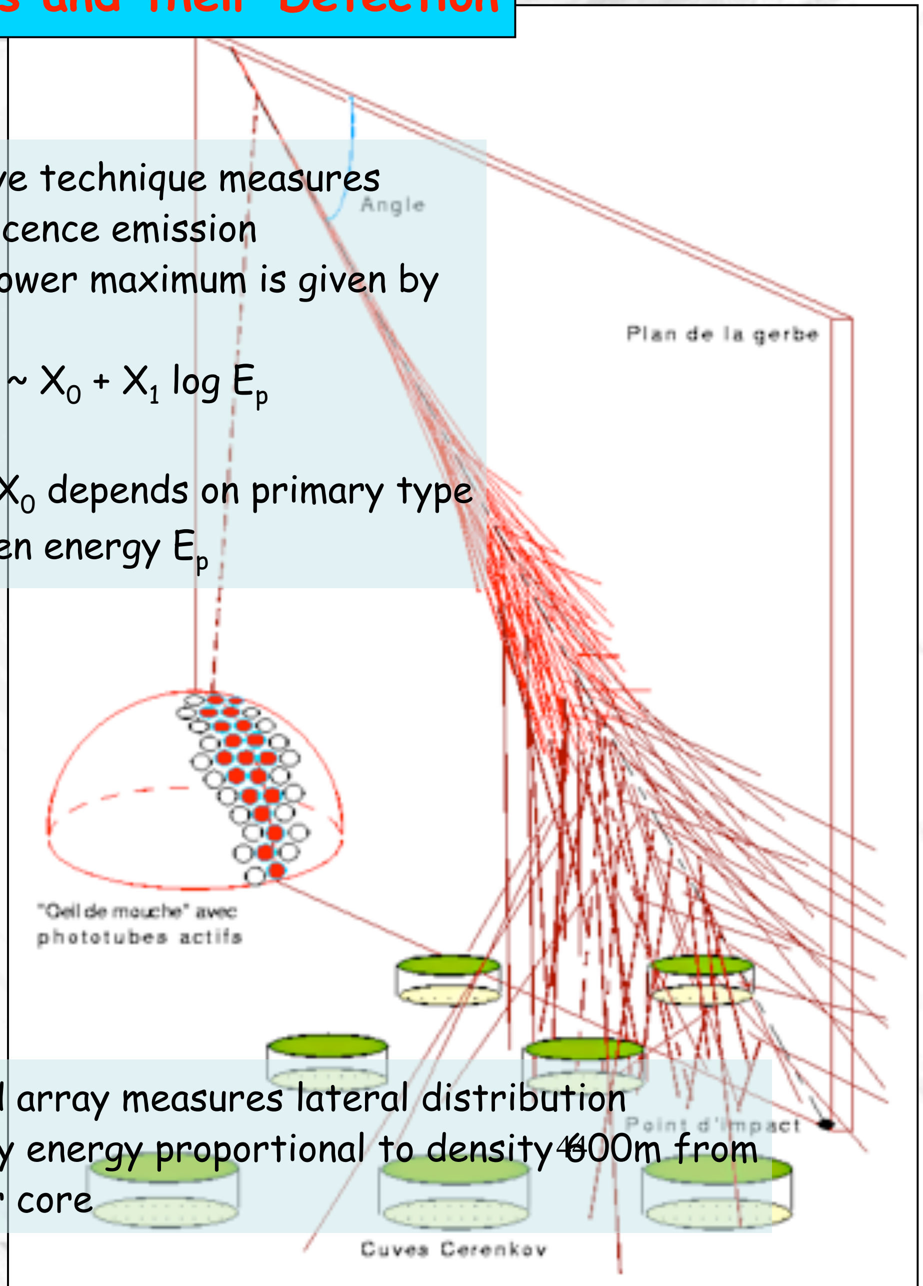

Fly's Eye technique measures fluorescence emission

The shower maximum is given by

$$X_{max} \sim X_0 + X_1 \log E_p$$

where X_0 depends on primary type for given energy E_p

Ground array measures lateral distribution

Primary energy proportional to density 600m from shower core

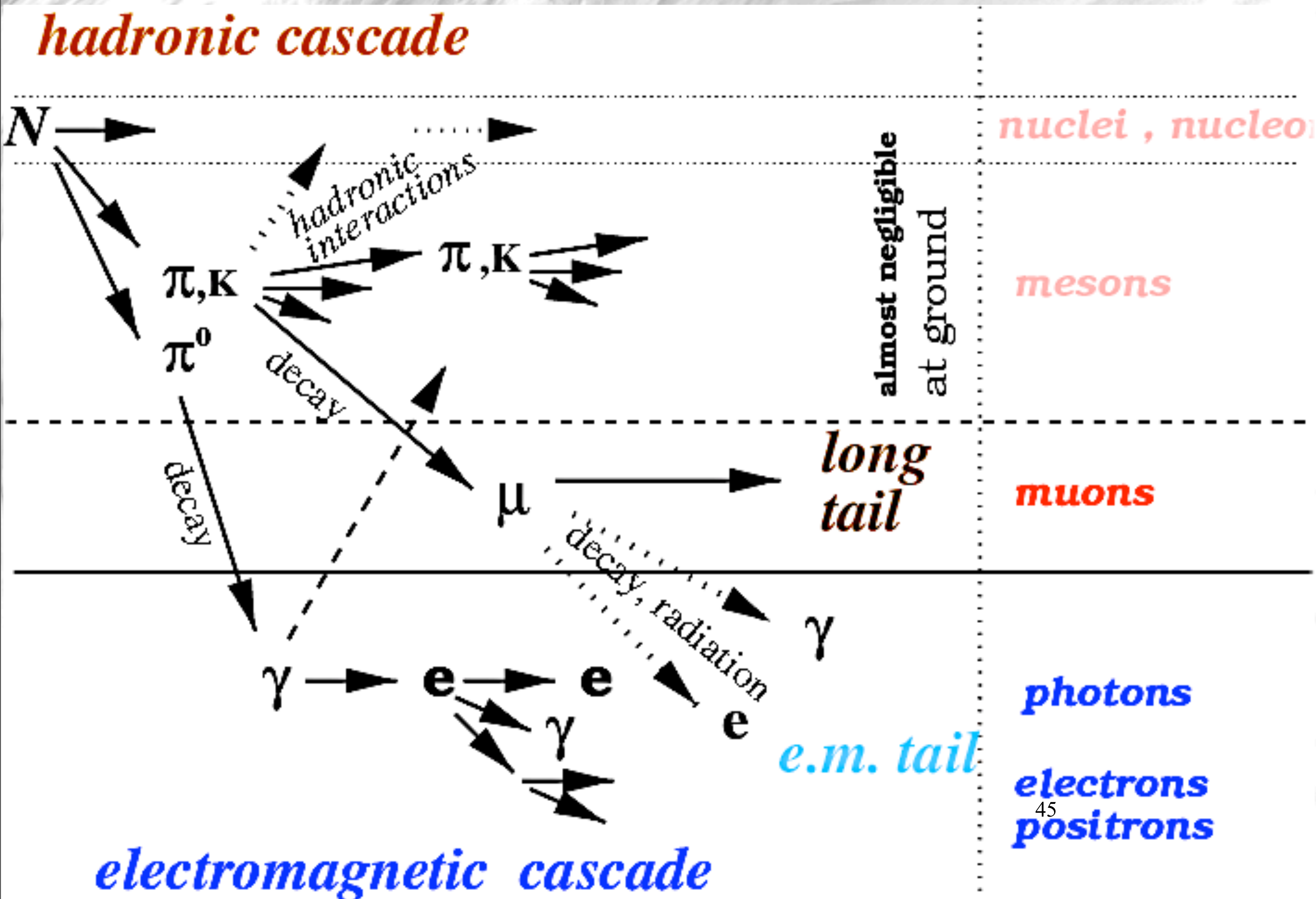
hadronic cascade
N
hadronic interactions
π,K
π ,K
π0
decay
decay
almost negligible at ground
long tail
μ
decay, radiation
γ
γ
e
e
γ
e
e.m. tail
nuclei , nucleo
mesons
muons
photons
electrons
positrons
45
electromagnetic cascade

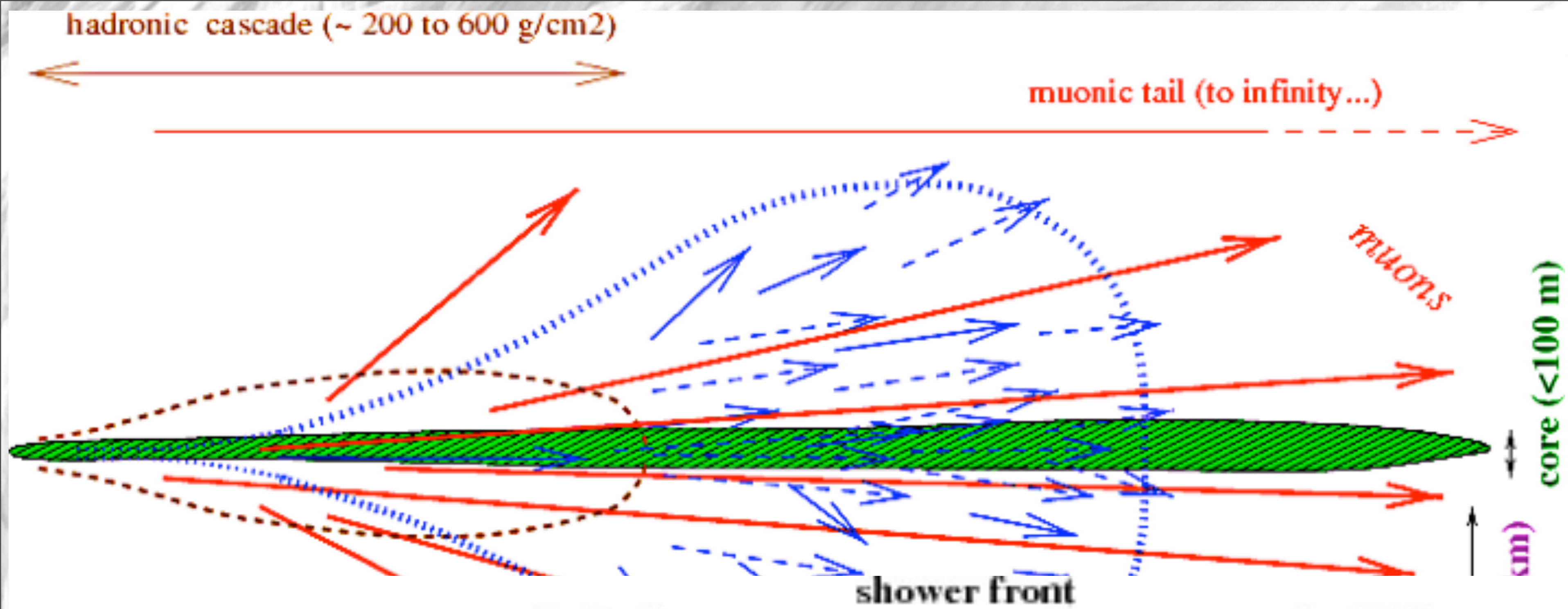
hadronic cascade (~ 200 to 600 g/cm2)
muonic tail (to infinity...)
muons
core (<100 m)
shower front

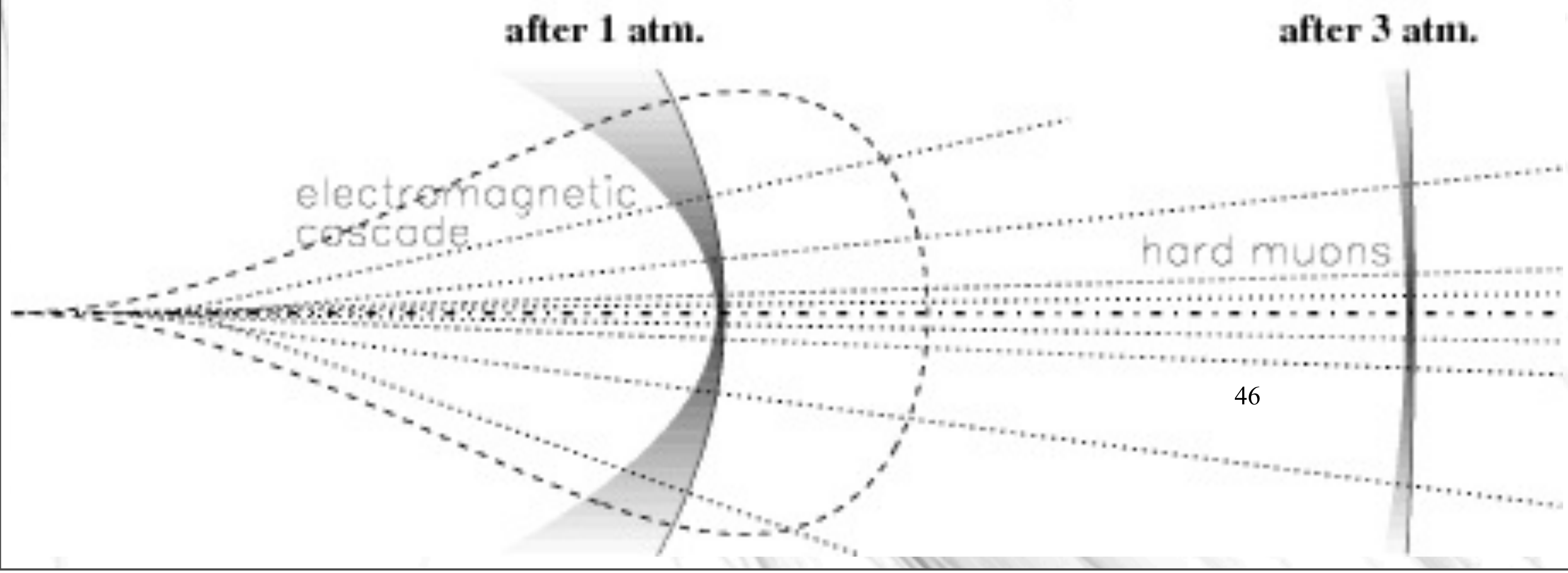
after 1 atm.
after 3 atm.
electromagnetic
cascade
hard muons
46

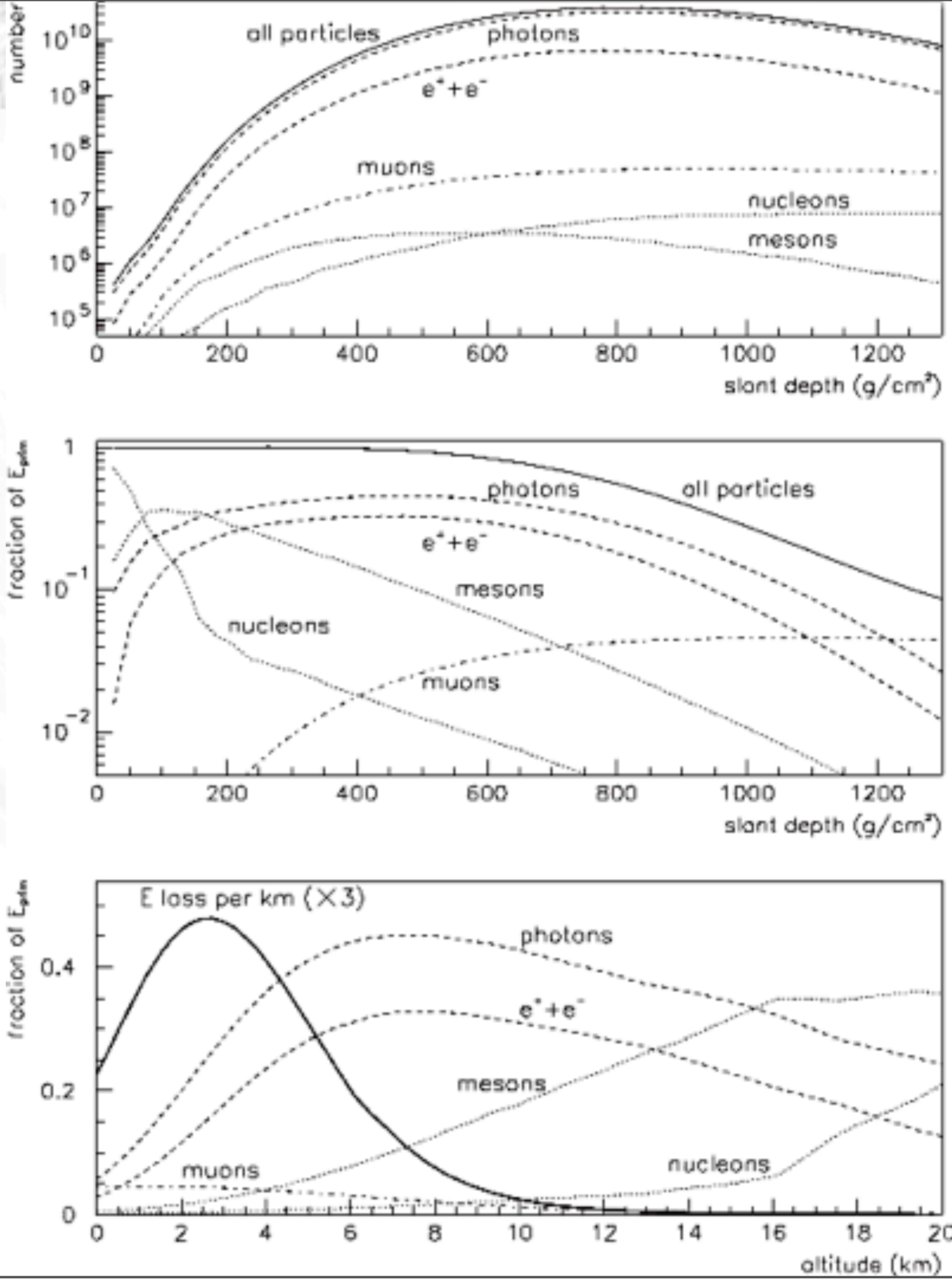

number
all particles
photons
$e^+ + e^-$
muons
nucleons
mesons
slant depth (g/cm²)
fraction of E_{prim}
photons
all particles
$e^+ + e^-$
mesons
nucleons
muons
slant depth (g/cm²)
fraction of E_{prim}
E loss per km (×3)
photons
$e^+ + e^-$
mesons
muons
nucleons
altitude (km)

47

Cosmic ray versus neutrino induced air showers

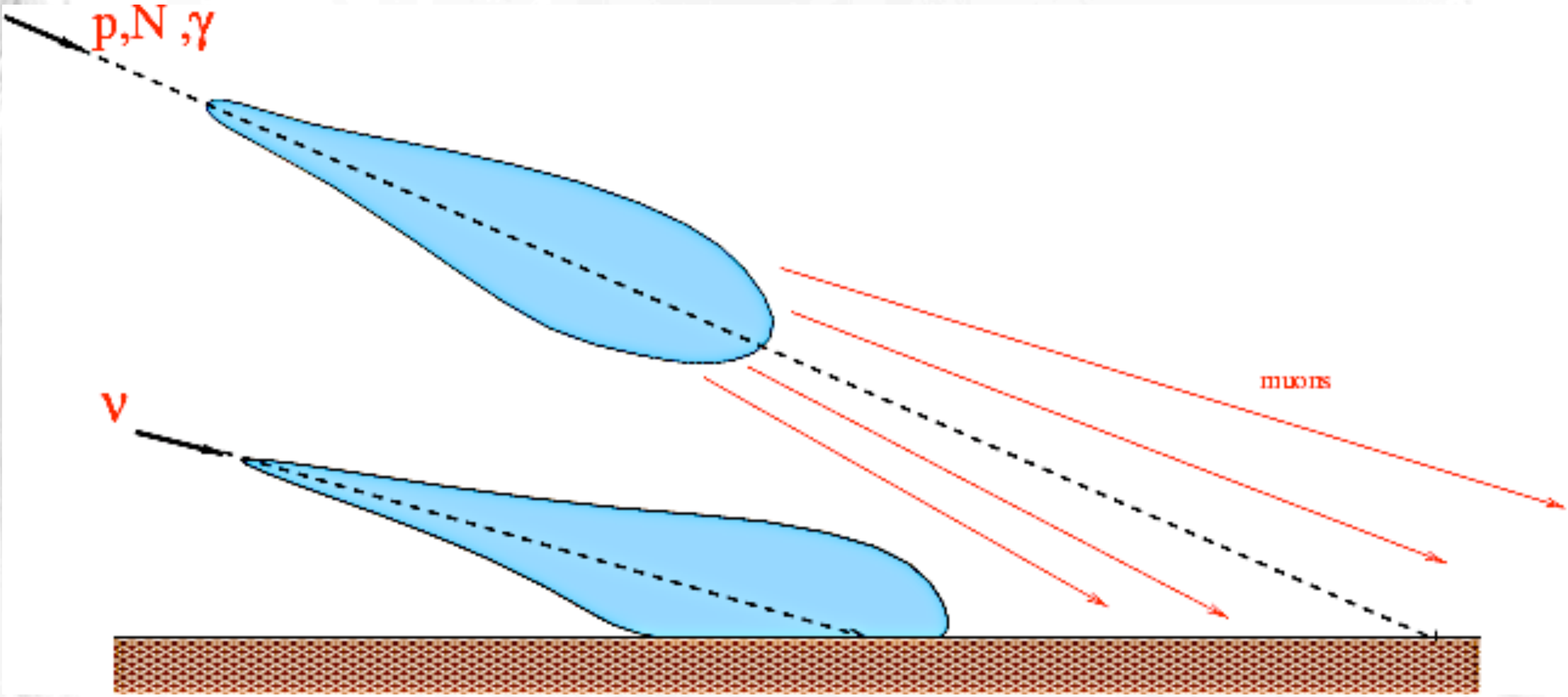

48

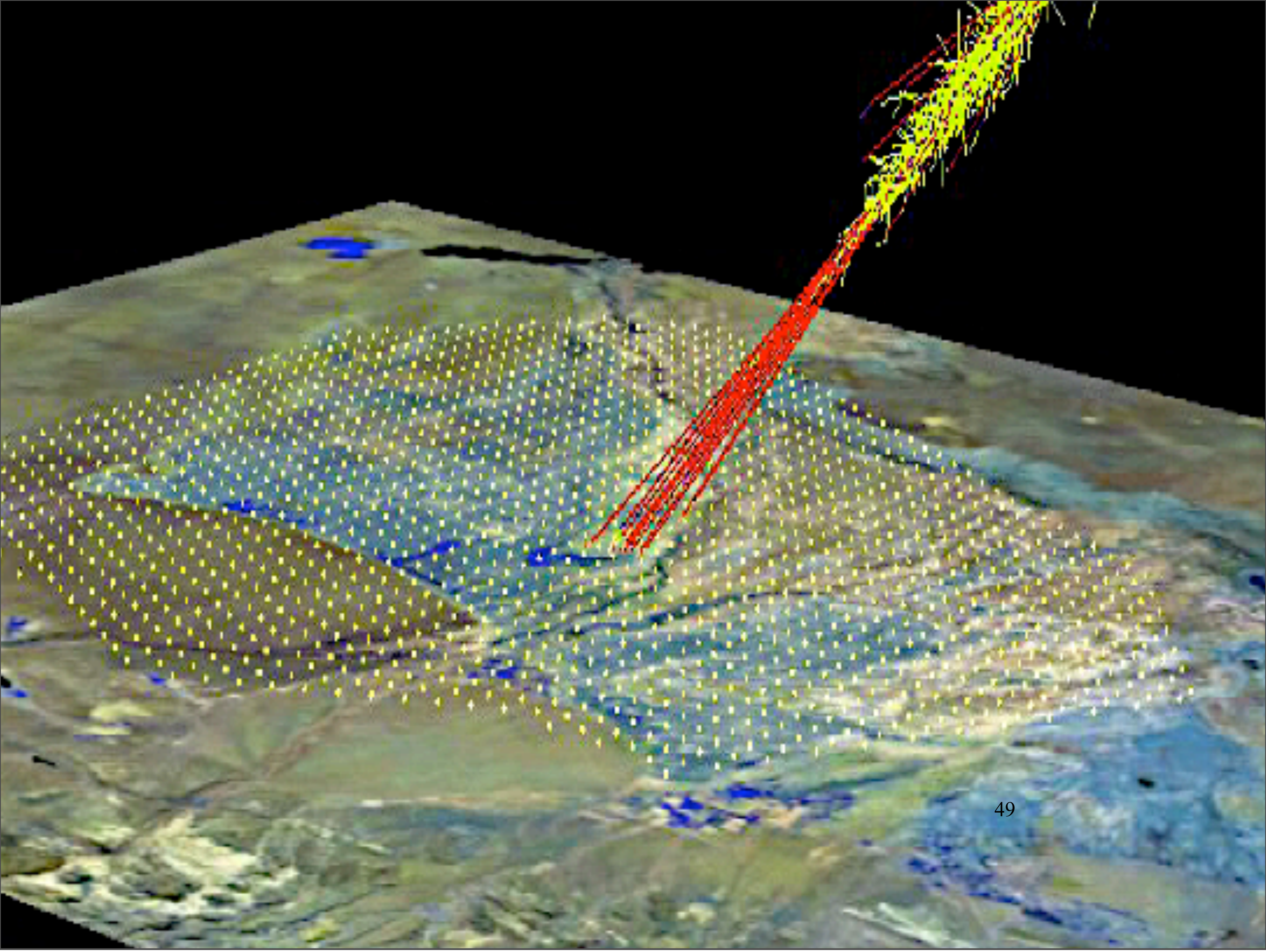
49

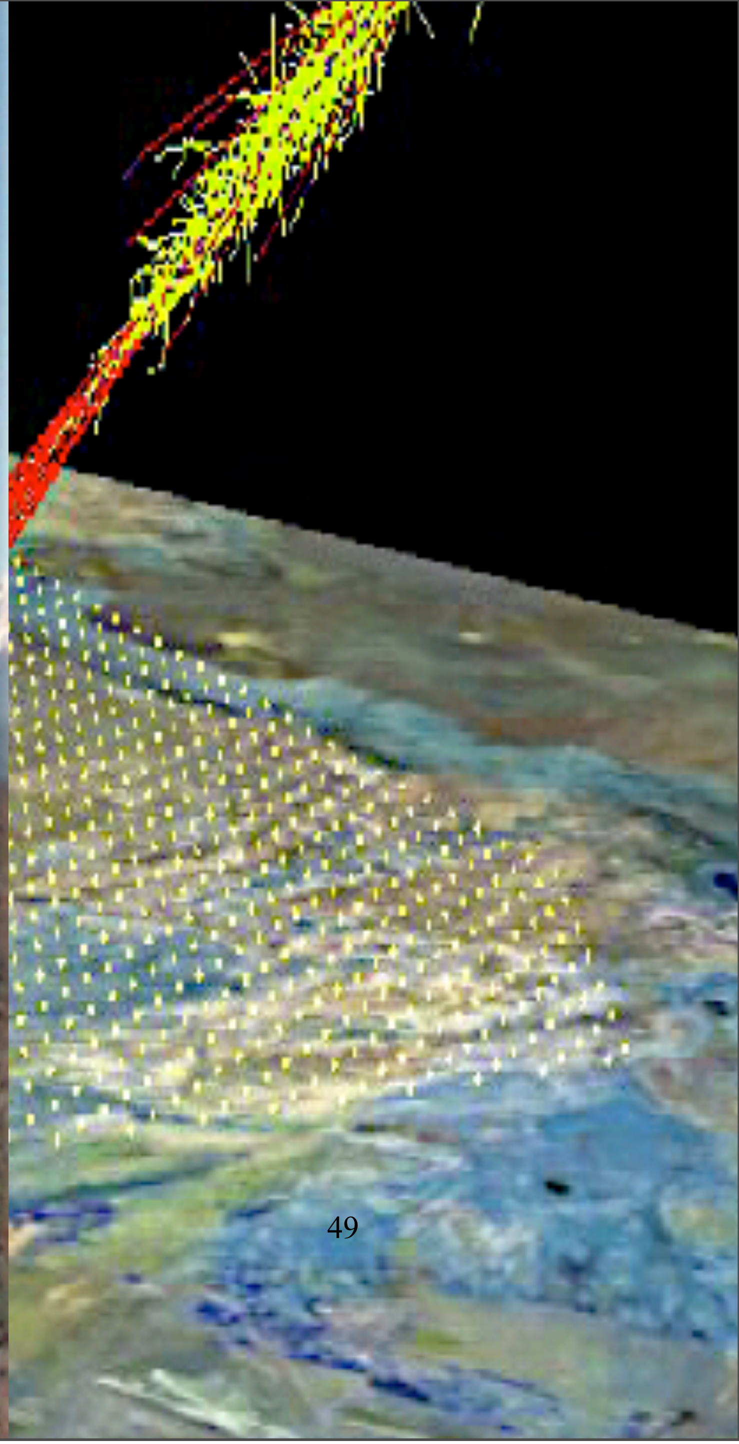
49

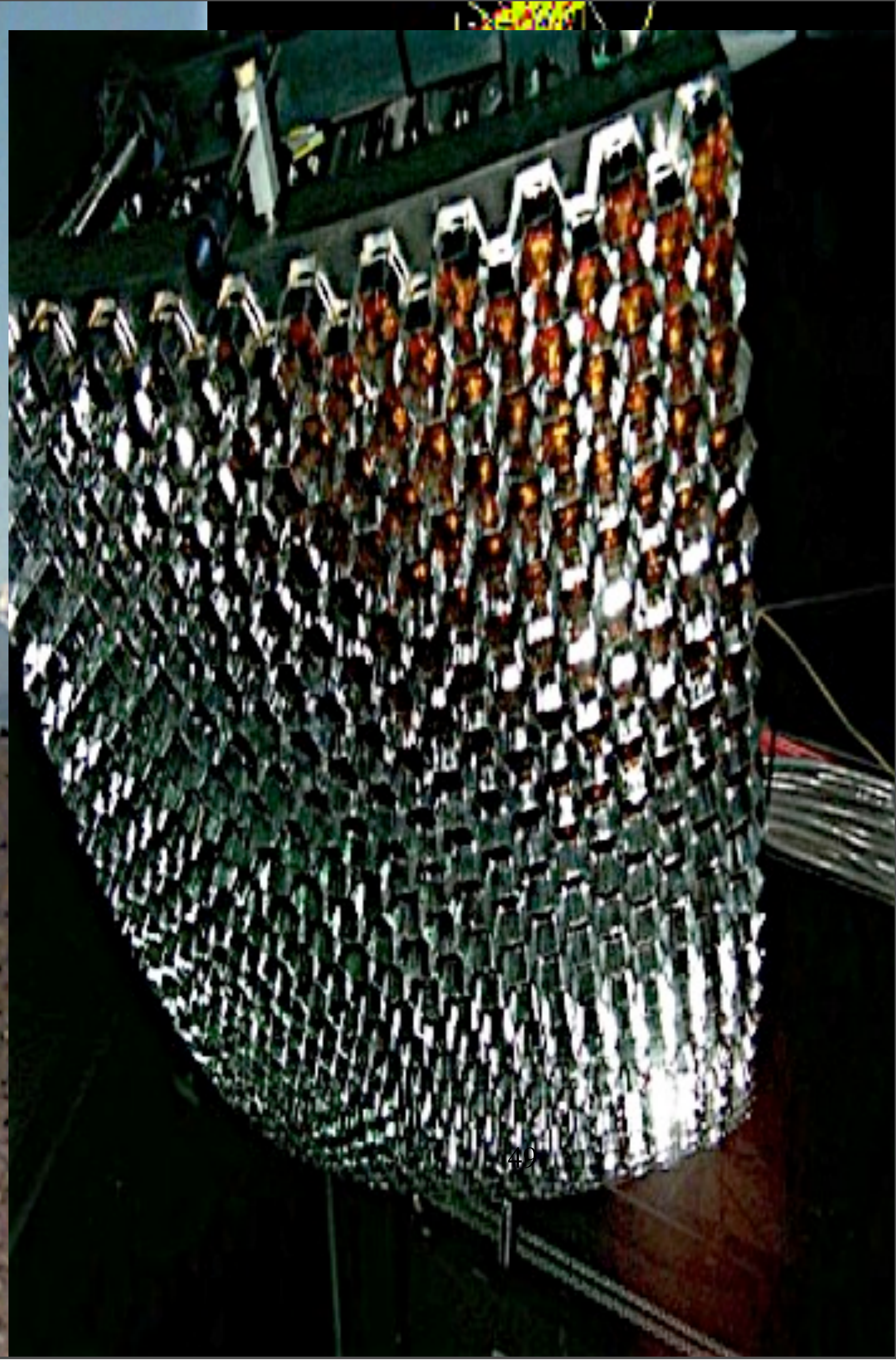

Southern Auger Site

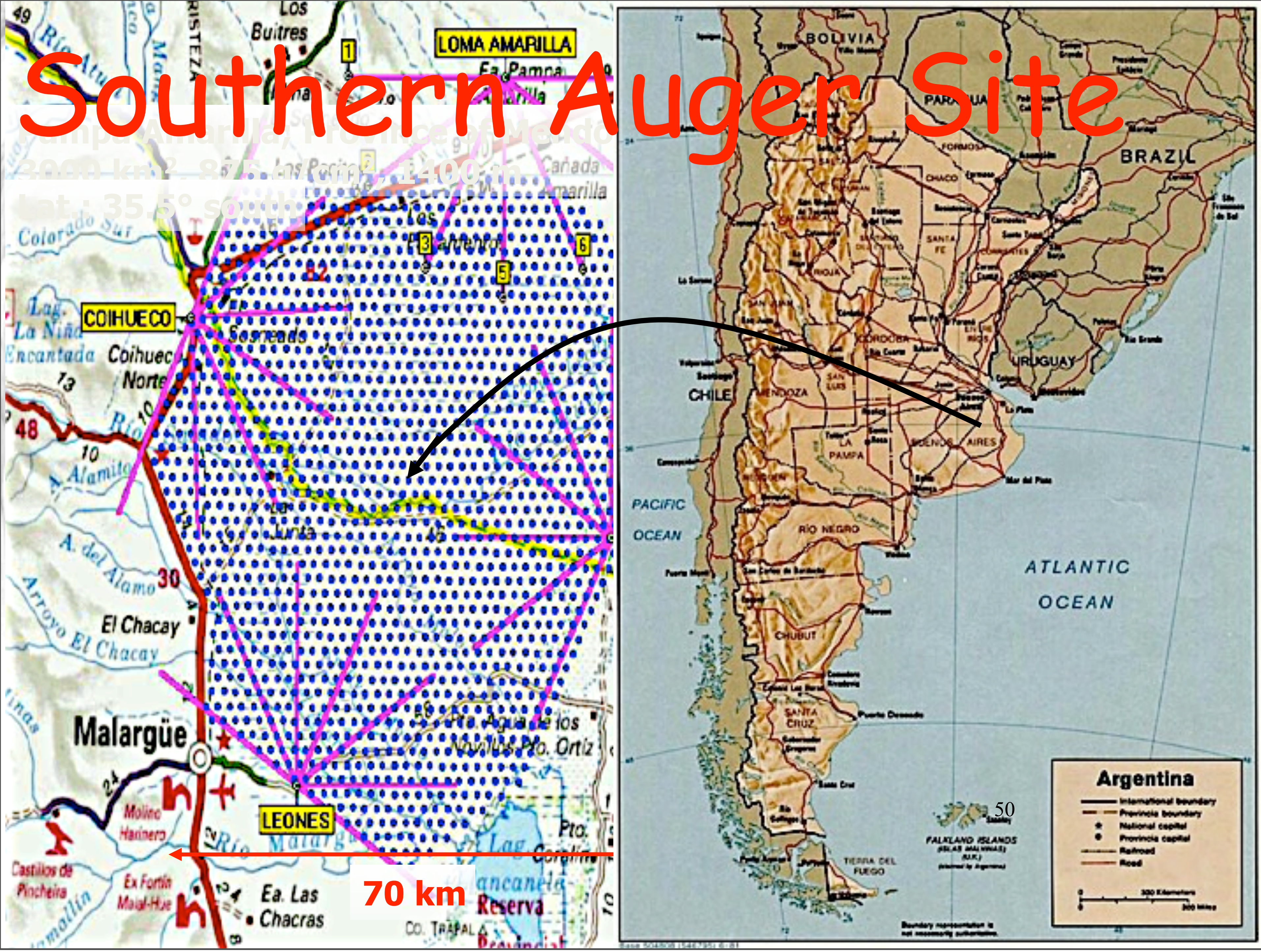

Southern Auger Site

Pampa Amarilla, Province of Mendoza
3000 km², 875 g/cm², 1400 m
Lat.: 35.5° south

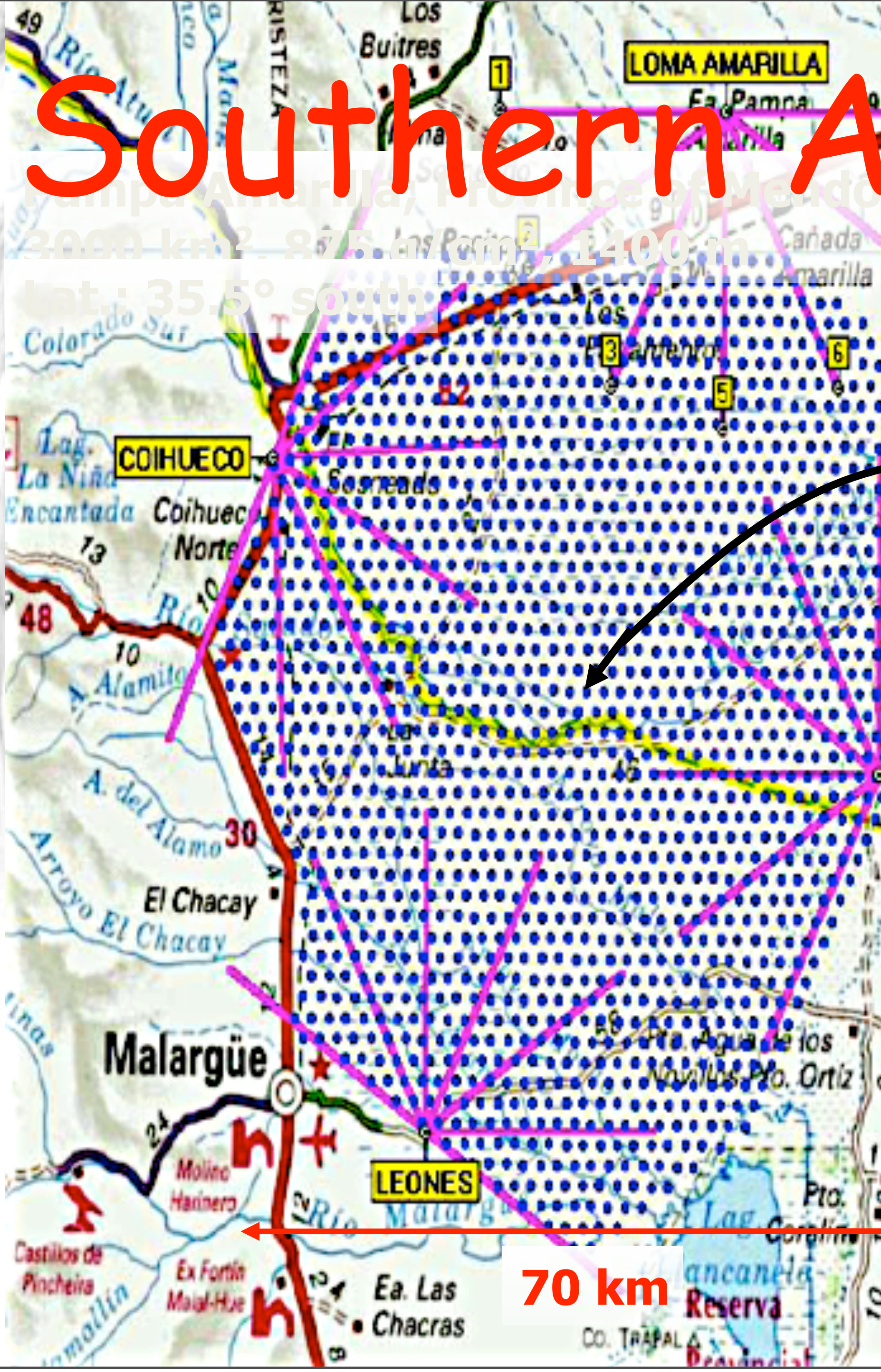

Surface Array (SD):
1600 Water Tanks
1.5 km spacing
3000 km^2

Southern Auger Site

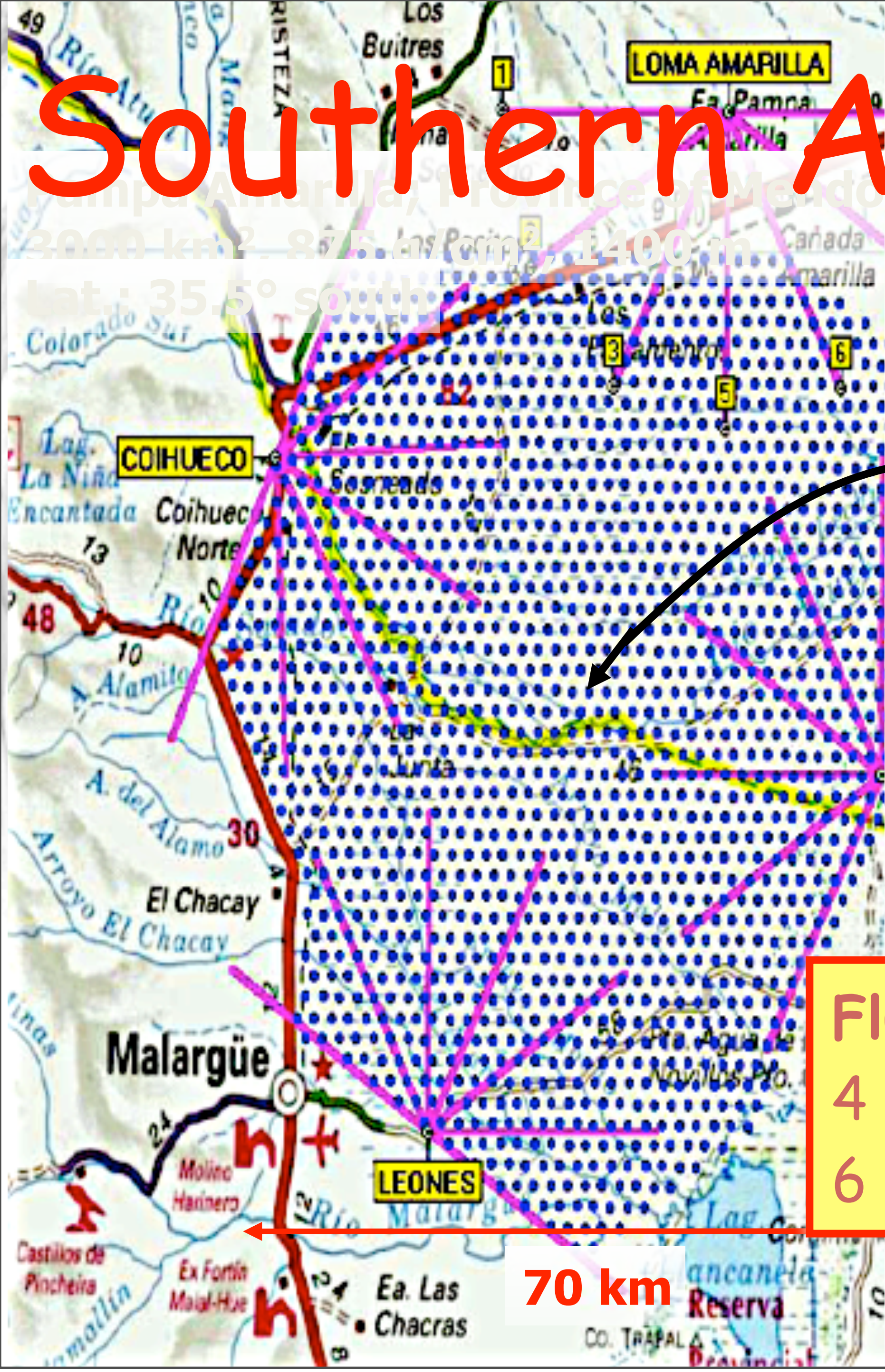

Surface Array (SD):
1600 Water Tanks
1.5 km spacing
3000 km^2

Fluorescence Detectors (FD):
4 Sites ("Eyes")
6 Telescopes per site (180° x 30°)

The Greisen-Zatsepin-Kuzmin (GZK) effect

Nucleons can produce pions on the cosmic microwave background

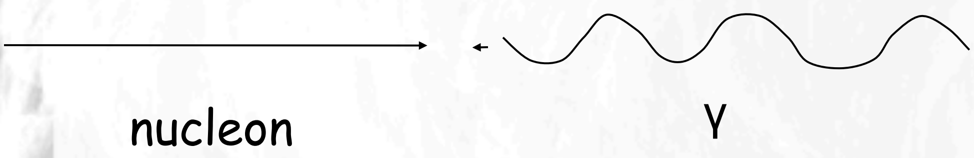

$$E_{\mathrm{th}} = \frac{2m_N m_\pi + m_\pi^2}{4\varepsilon} \simeq 4 \times 10^{19}\,\mathrm{eV}$$

The Greisen-Zatsepin-Kuzmin (GZK) effect

Nucleons can produce pions on the cosmic microwave background

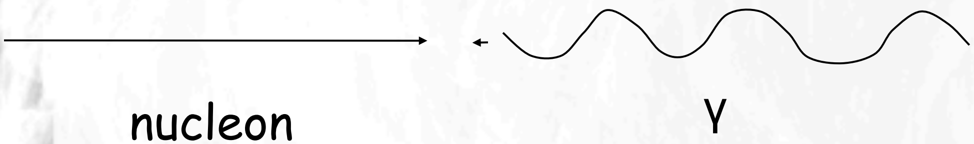

$$E_{\rm th} = \frac{2m_N m_\pi + m_\pi^2}{4\varepsilon} \simeq 4 \times 10^{19}\,{\rm eV}$$

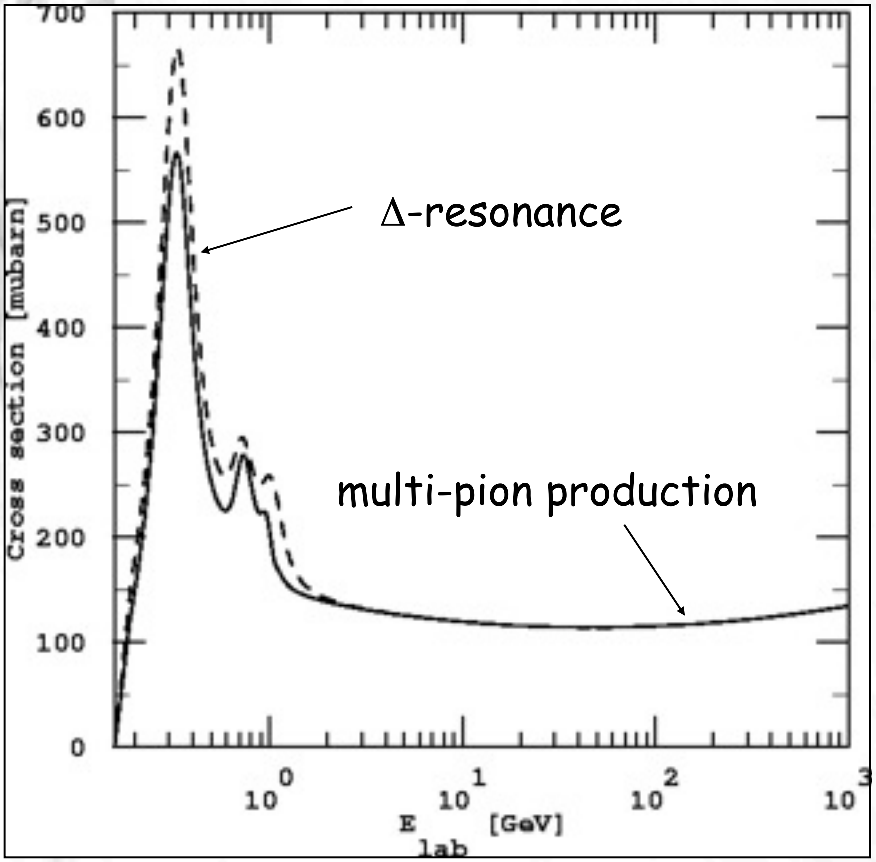

51

The Greisen-Zatsepin-Kuzmin (GZK) effect

Nucleons can produce pions on the cosmic microwave background

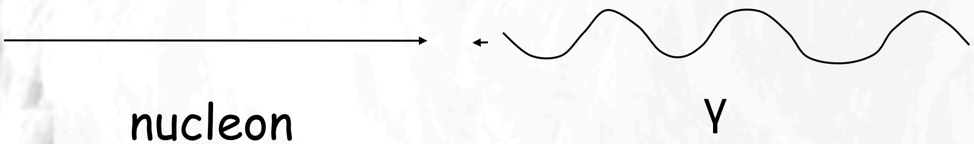

$$E_{\rm th} = \frac{2m_N m_\pi + m_\pi^2}{4\varepsilon} \simeq 4 \times 10^{19}\,\mathrm{eV}$$

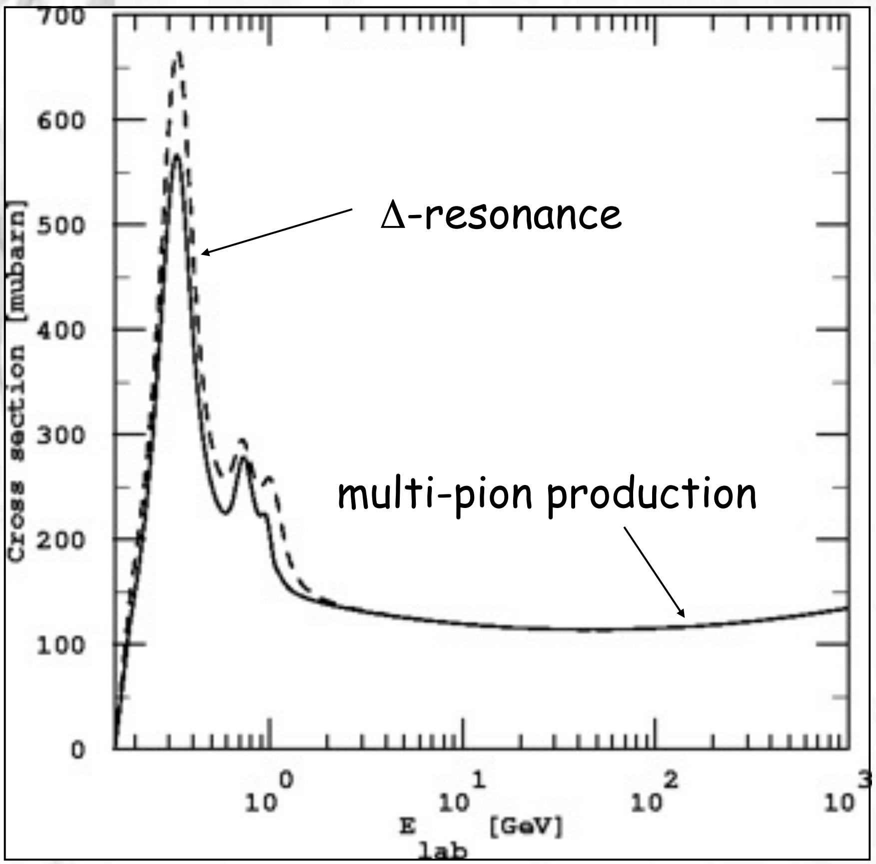

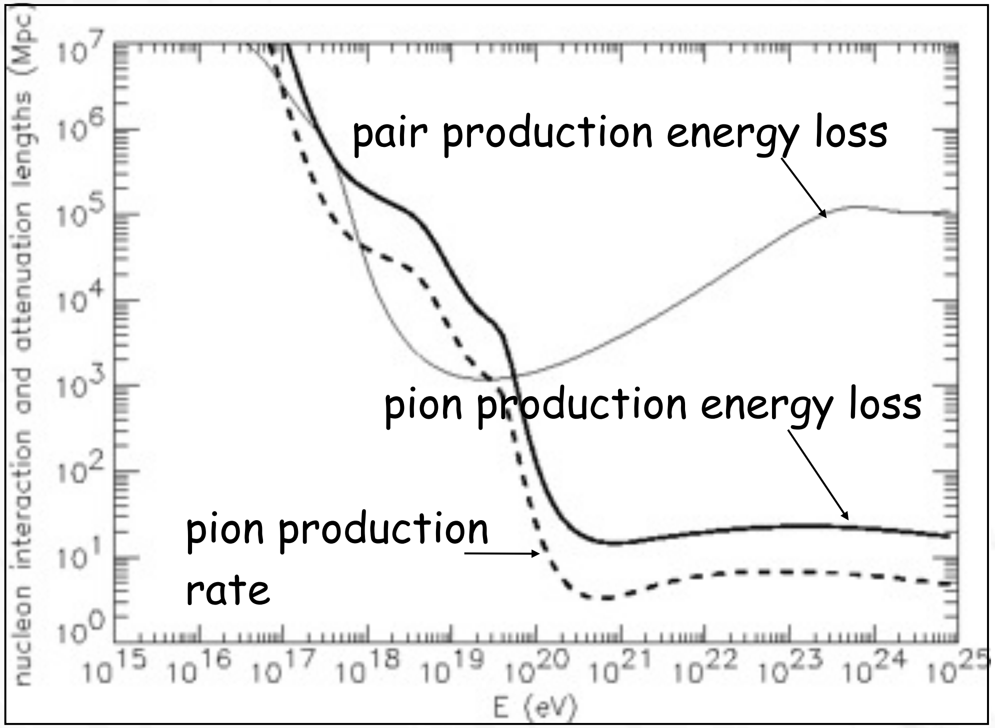

The Greisen-Zatsepin-Kuzmin (GZK) effect

Nucleons can produce pions on the cosmic microwave background

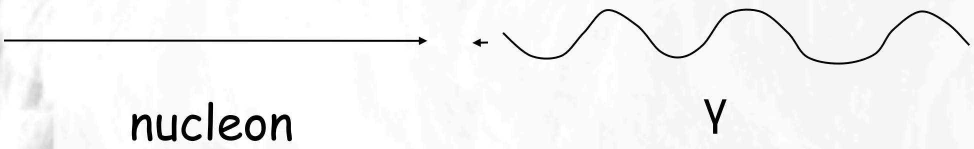

$$E_{\rm th} = \frac{2m_N m_\pi + m_\pi^2}{4\varepsilon} \simeq 4 \times 10^{19}\,\mathrm{eV}$$

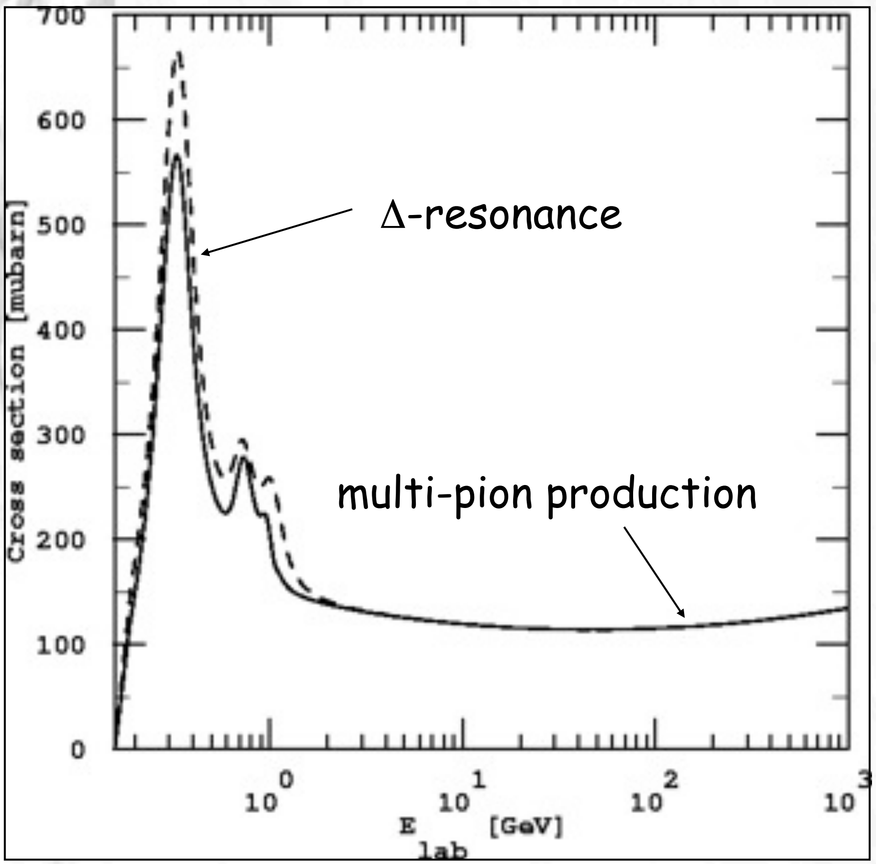

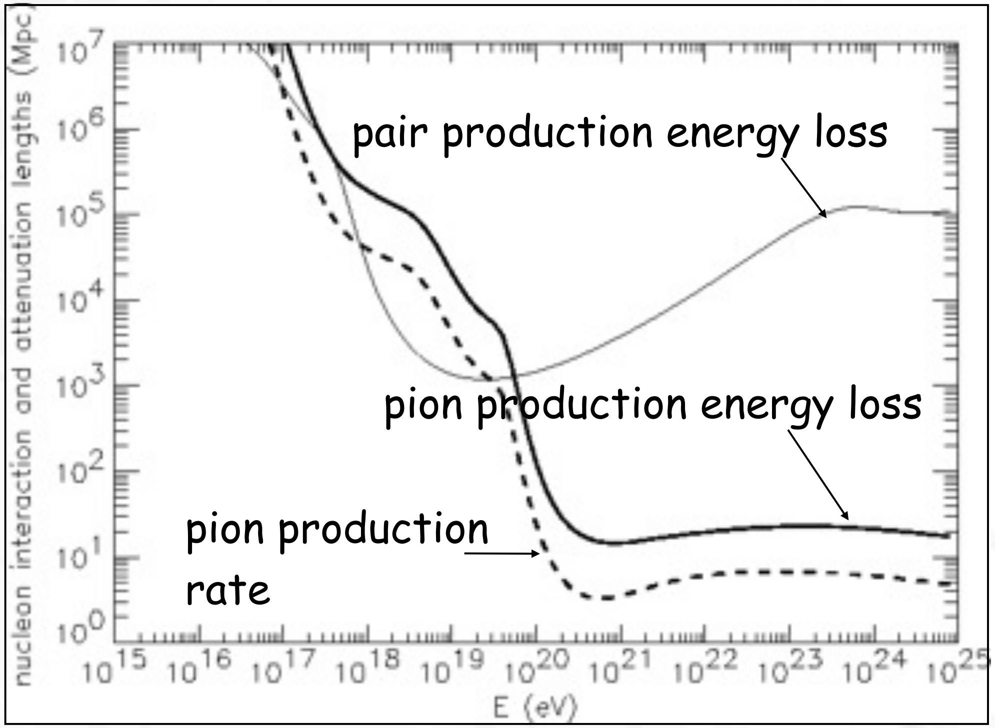

sources must be in cosmological backyard
Only Lorentz symmetry breaking at $\Gamma > 10^{11}$ could avoid this conclusion.

The Ultra-High Energy Cosmic Ray Mystery consists of (at least) Three Interrelated Challenges

52

The Ultra-High Energy Cosmic Ray Mystery consists of (at least) Three Interrelated Challenges

1.) electromagnetically or strongly interacting particles above 10^{20} eV loose energy within less than about 50 Mpc.

52

The Ultra-High Energy Cosmic Ray Mystery consists of (at least) Three Interrelated Challenges

1.) electromagnetically or strongly interacting particles above 10^{20} eV loose energy within less than about 50 Mpc.

2.) in most conventional scenarios exceptionally powerful acceleration sources within that distance are needed.

The Ultra-High Energy Cosmic Ray Mystery consists of (at least) Three Interrelated Challenges

1.) electromagnetically or strongly interacting particles above 10^{20} eV loose energy within less than about 50 Mpc.

2.) in most conventional scenarios exceptionally powerful acceleration sources within that distance are needed.

3.) The observed distribution does not yet reveal unambiguously the sources, although there is some correlation with local large scale structure

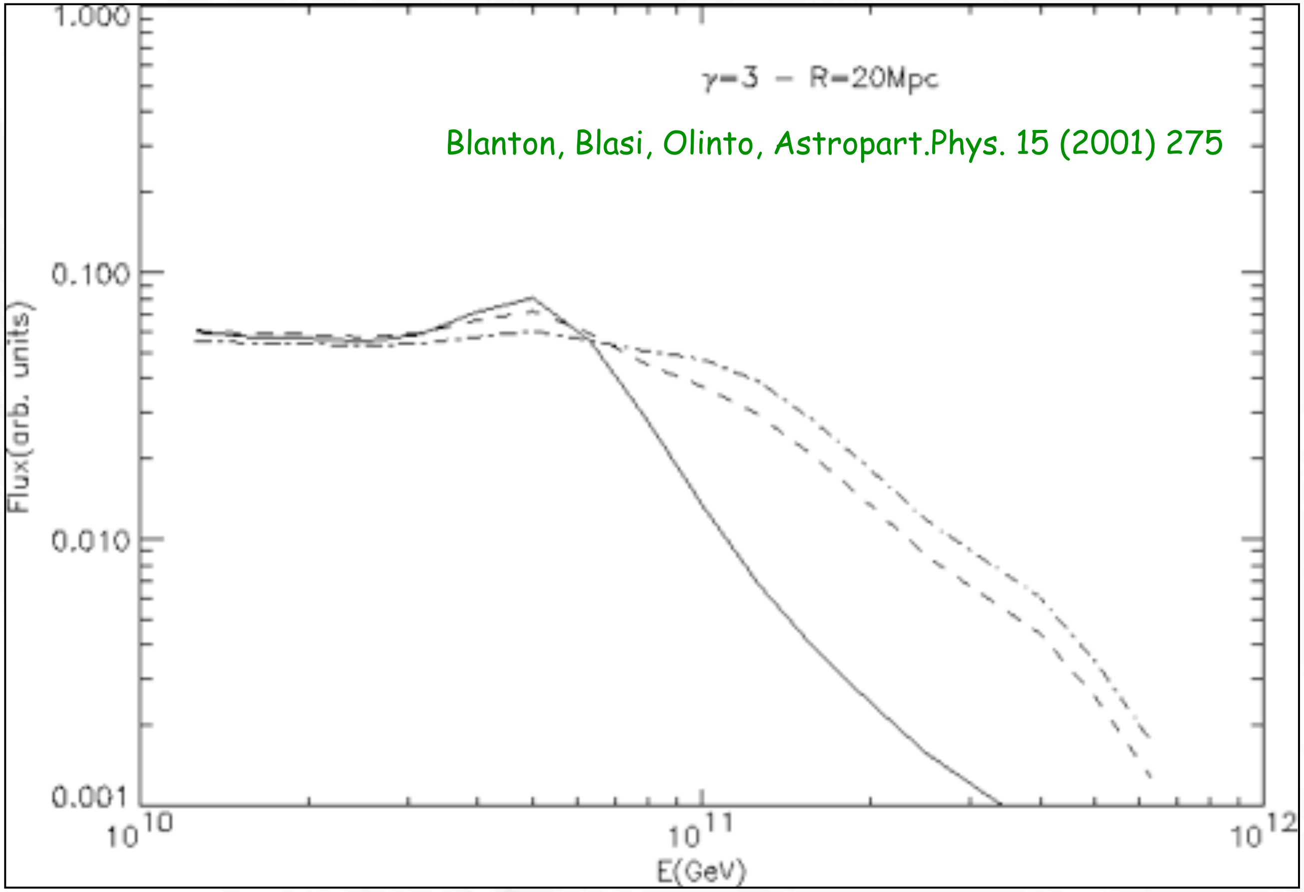

Observable spectrum for an E^{-3} injection spectrum for a distribution of sources with overdensities of 1, 10, 30 (bottom to top) within 20 Mpc, and otherwise homogeneous.

GZK "cut-off" is a misnomer because "conventional" astrophysics can create events above the "cut-off"

The GZK effect may tell us about the source distribution (in the absence of strong magnetic deflection)

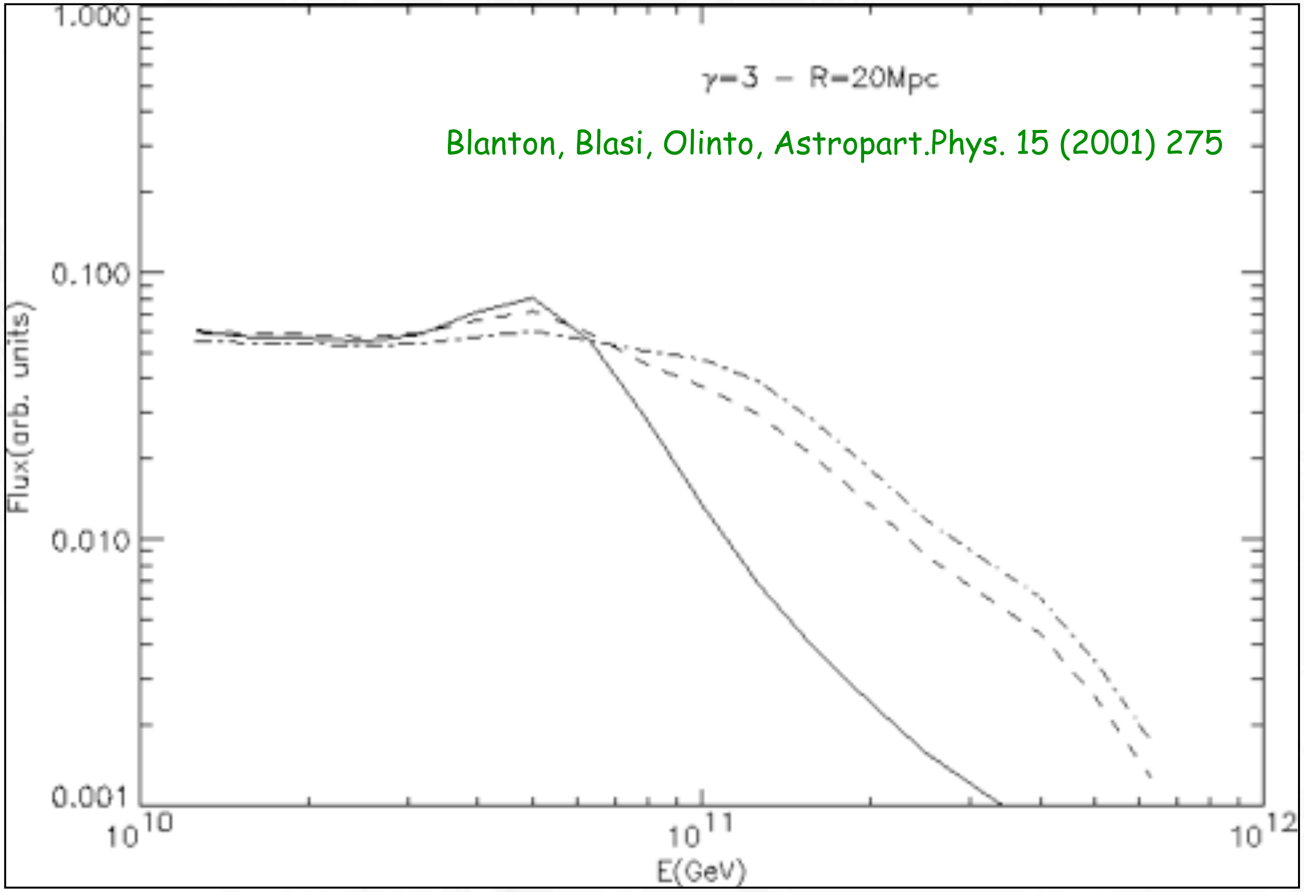

Observable spectrum for an E^{-3} injection spectrum for a distribution of sources with overdensities of 1, 10, 30 (bottom to top) within 20 Mpc, and otherwise homogeneous.

1st Order Fermi Shock Acceleration

The most widely accepted scenario of cosmic ray acceleration

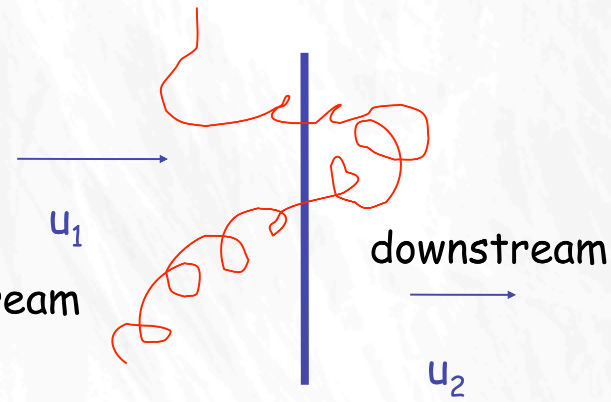

Fractional energy gain per shock crossing $\propto u_1 - u_2$ on a time scale r_L/u_2.

Together with downstream losses this leads to a spectrum E^{-q} with $q > 2$ typically.

When the gyro-radius r_L becomes comparable to the shock size L, the spectrum cuts off.

1^{st} Order Fermi Shock Acceleration

The most widely accepted scenario of cosmic ray acceleration

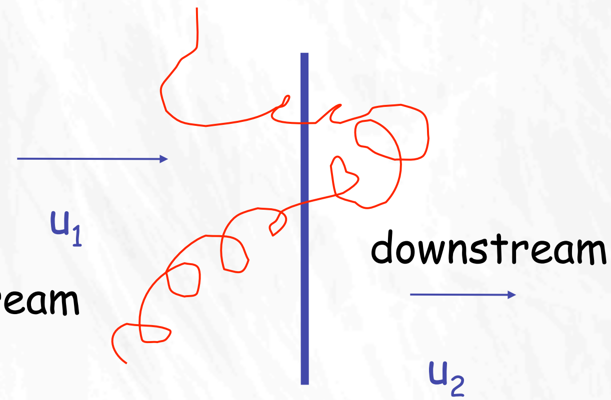

Fractional energy gain per shock crossing $\propto u_1 - u_2$ on a time scale r_L/u_2.

Together with downstream losses this leads to a spectrum E^{-q} with $q > 2$ typically.

When the gyro-radius r_L becomes comparable to the shock size L, the spectrum cuts off.

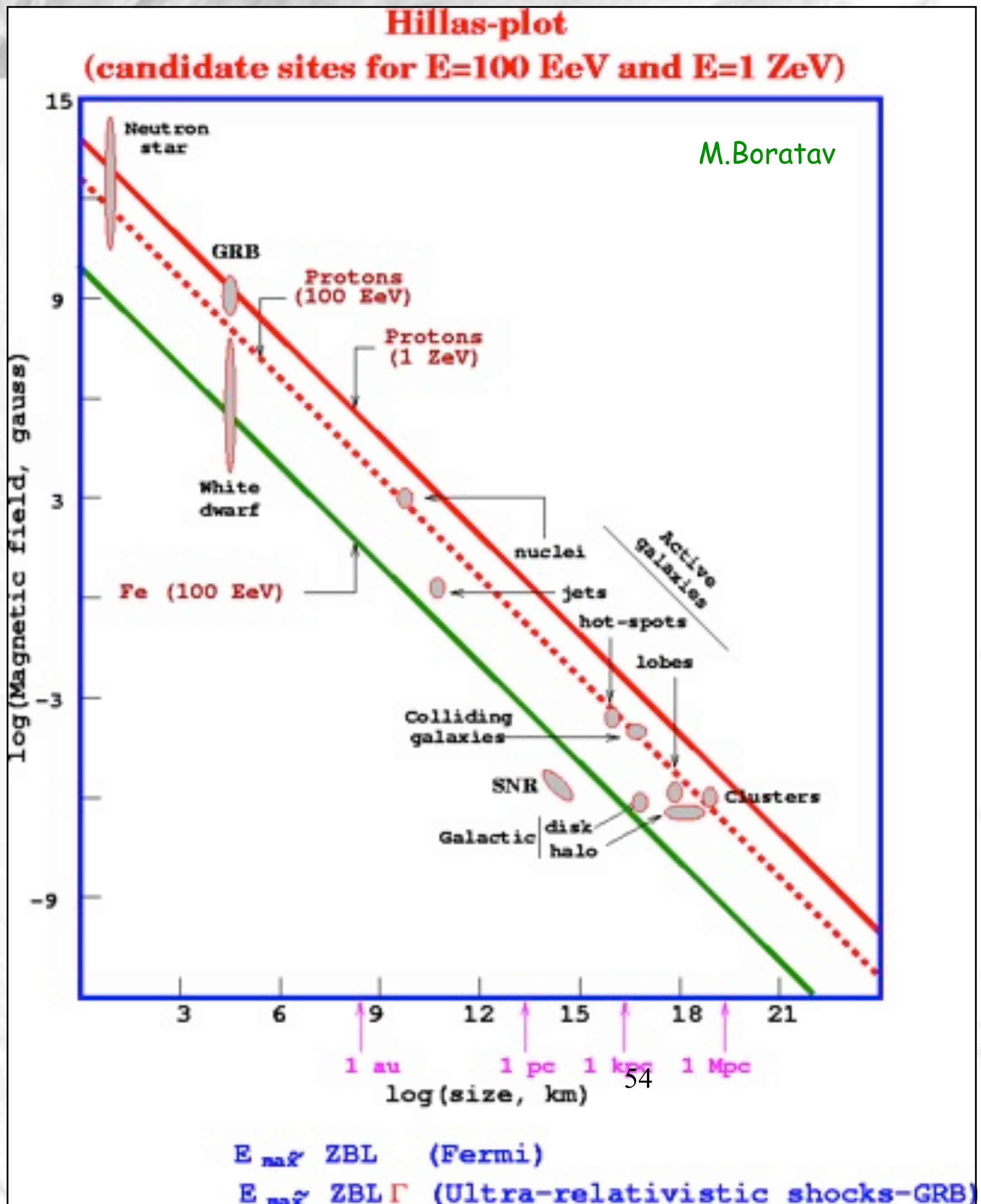

A possible acceleration site associated with shocks in hot spots of active galaxies

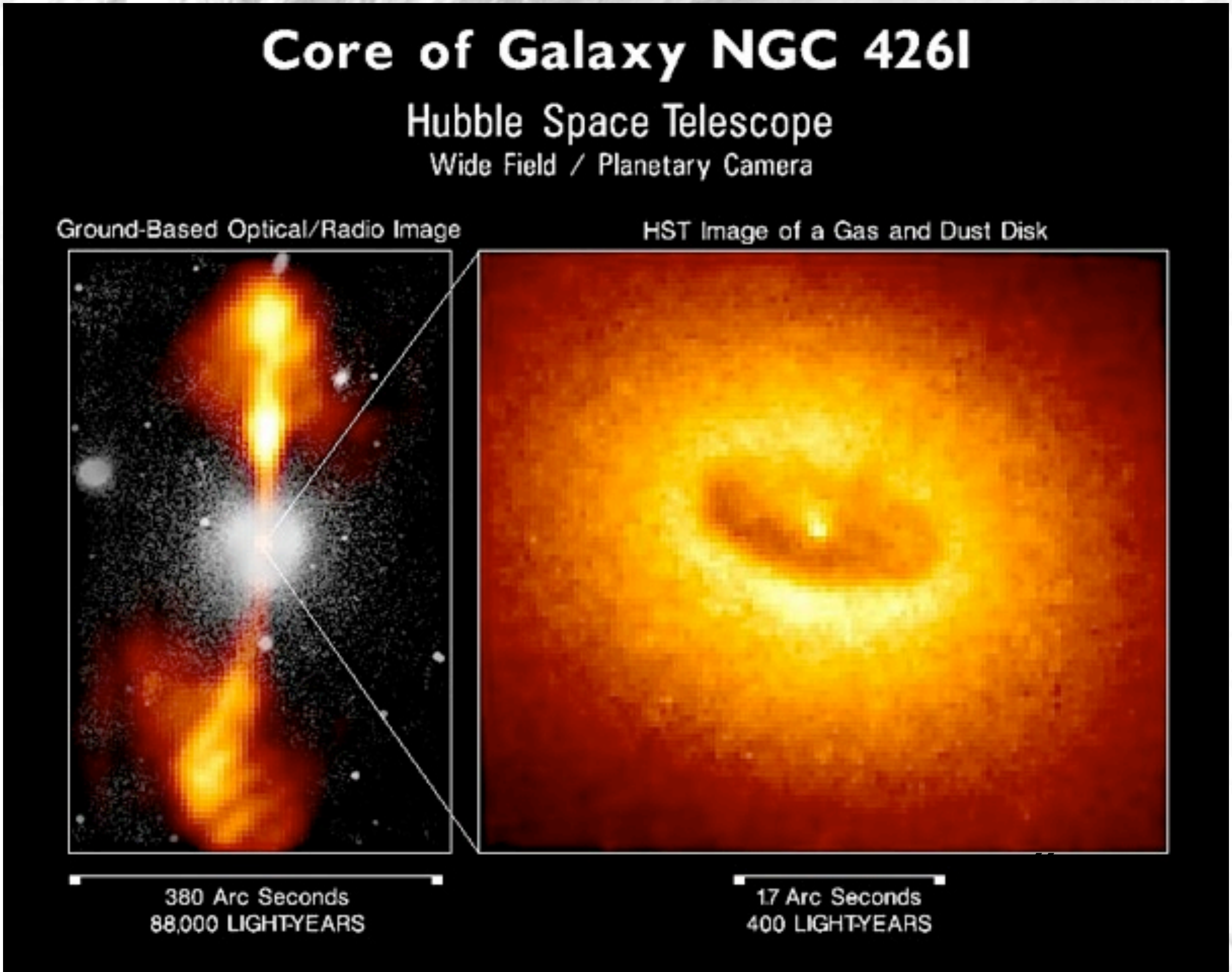

Or Cygnus A

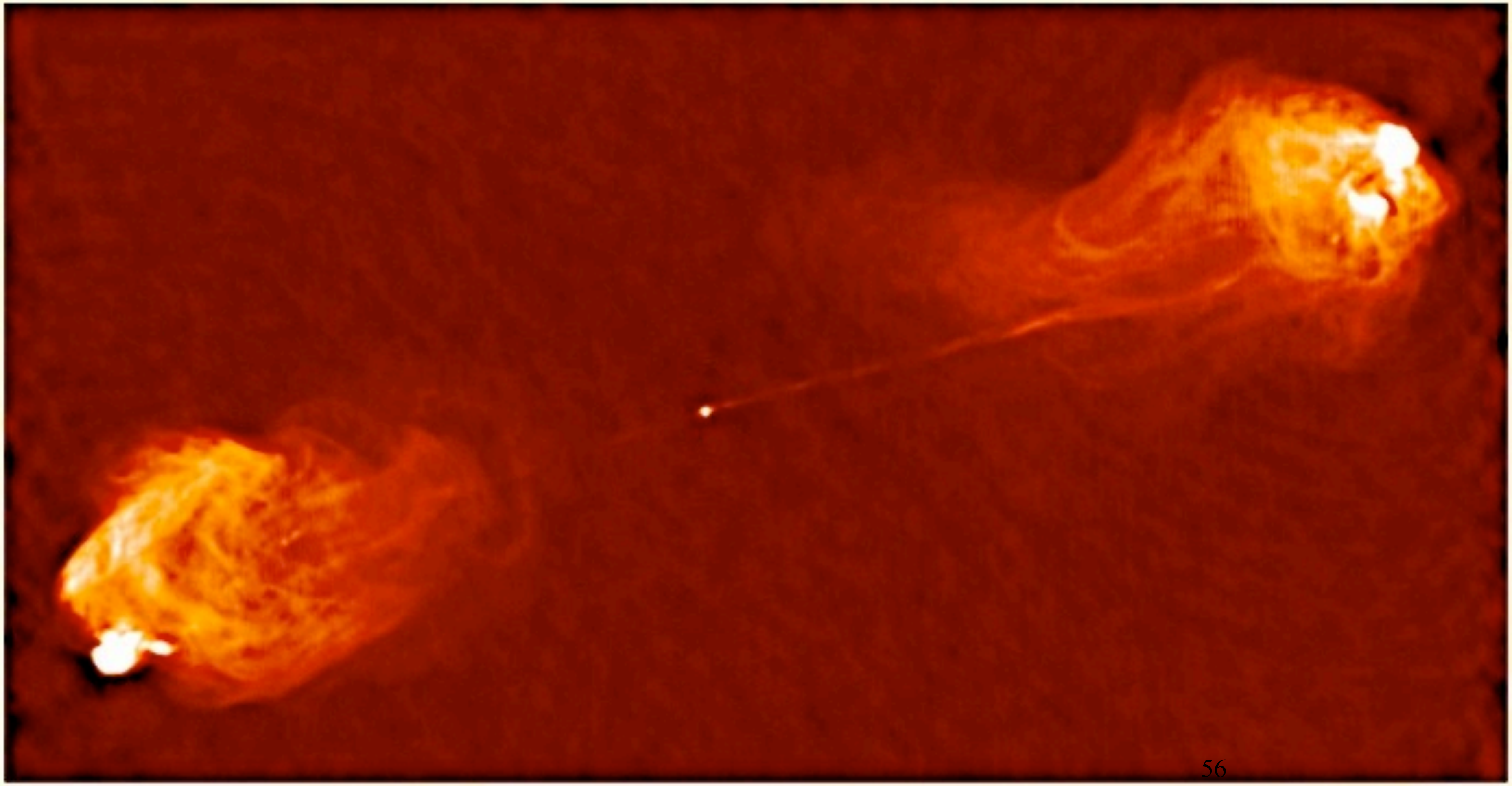

Shock Acceleration Theory

Monte Carlo Simulation Particle Trajectories

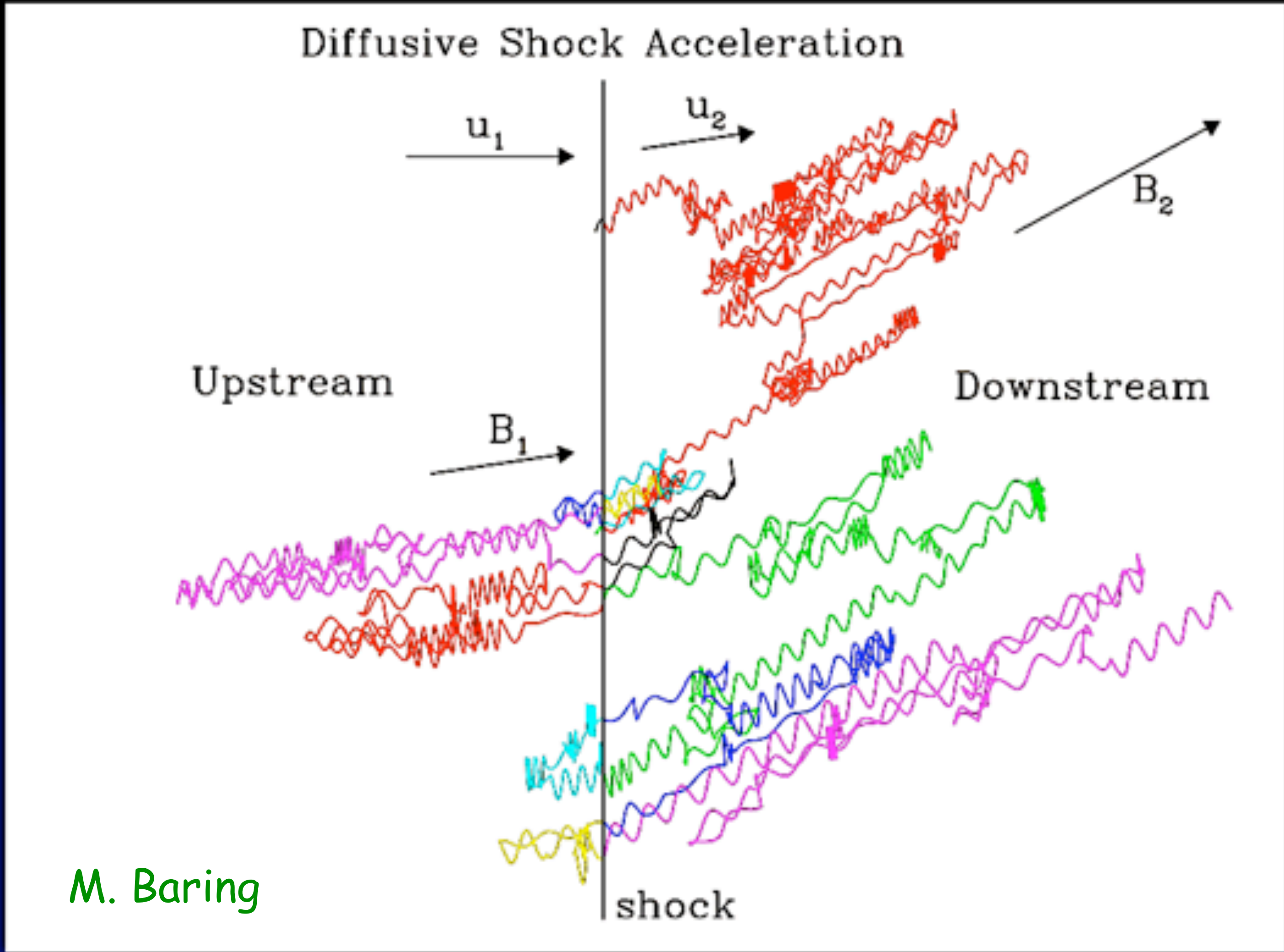

- Gyration in B-fields and diffusive transport modeled by a Monte Carlo technique; color-coded in Figure according to fluid frame energy.
- Shock crossings produce net energy gains (evident in the increase of gyroradii) according to principle of first-order Fermi mechanism.

Monte Carlo simulations of particle spectra for oblique mildly relativistic shocks

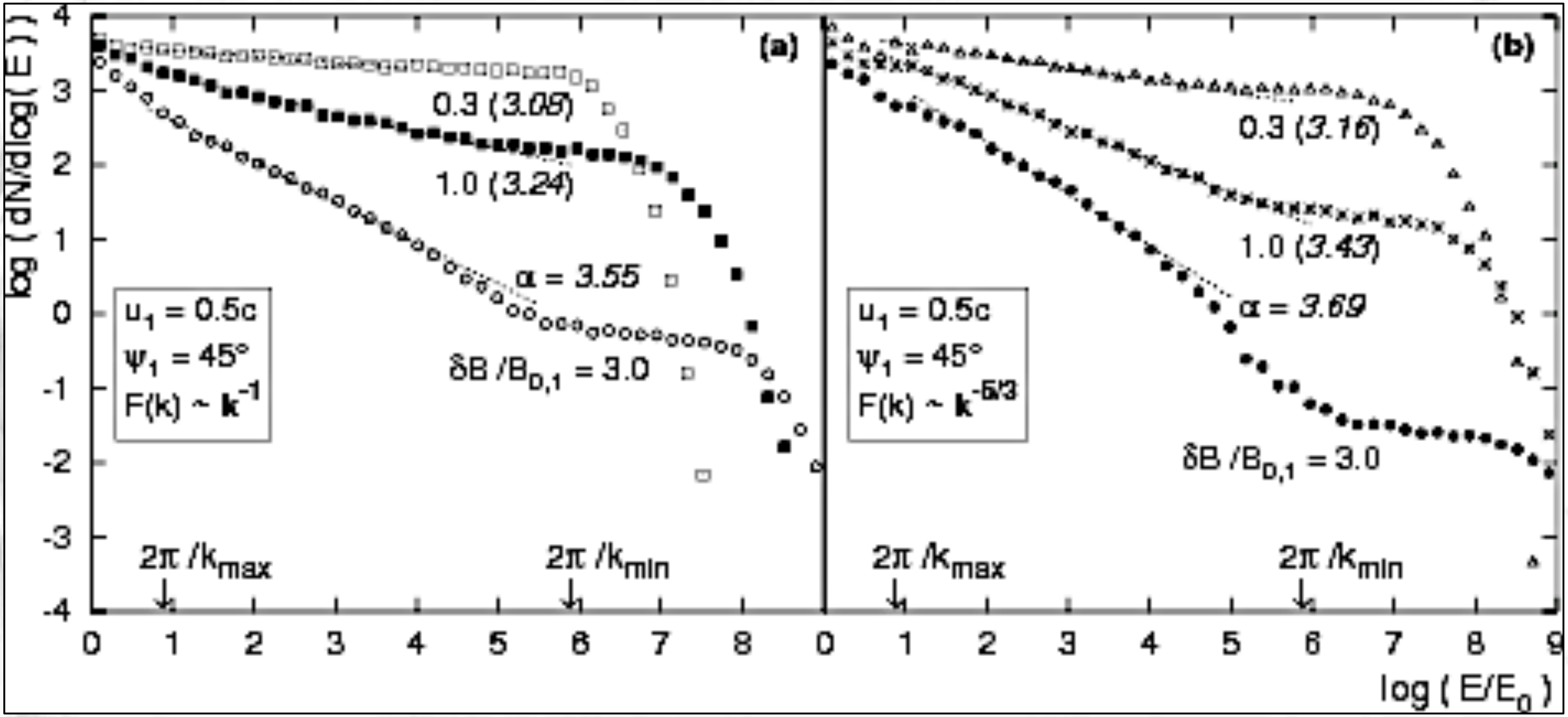

No “universal” spectral index α~4.2 as sometimes claimed

59

Niemiec and Ostrowski, e.g. arXiv:0801.1339

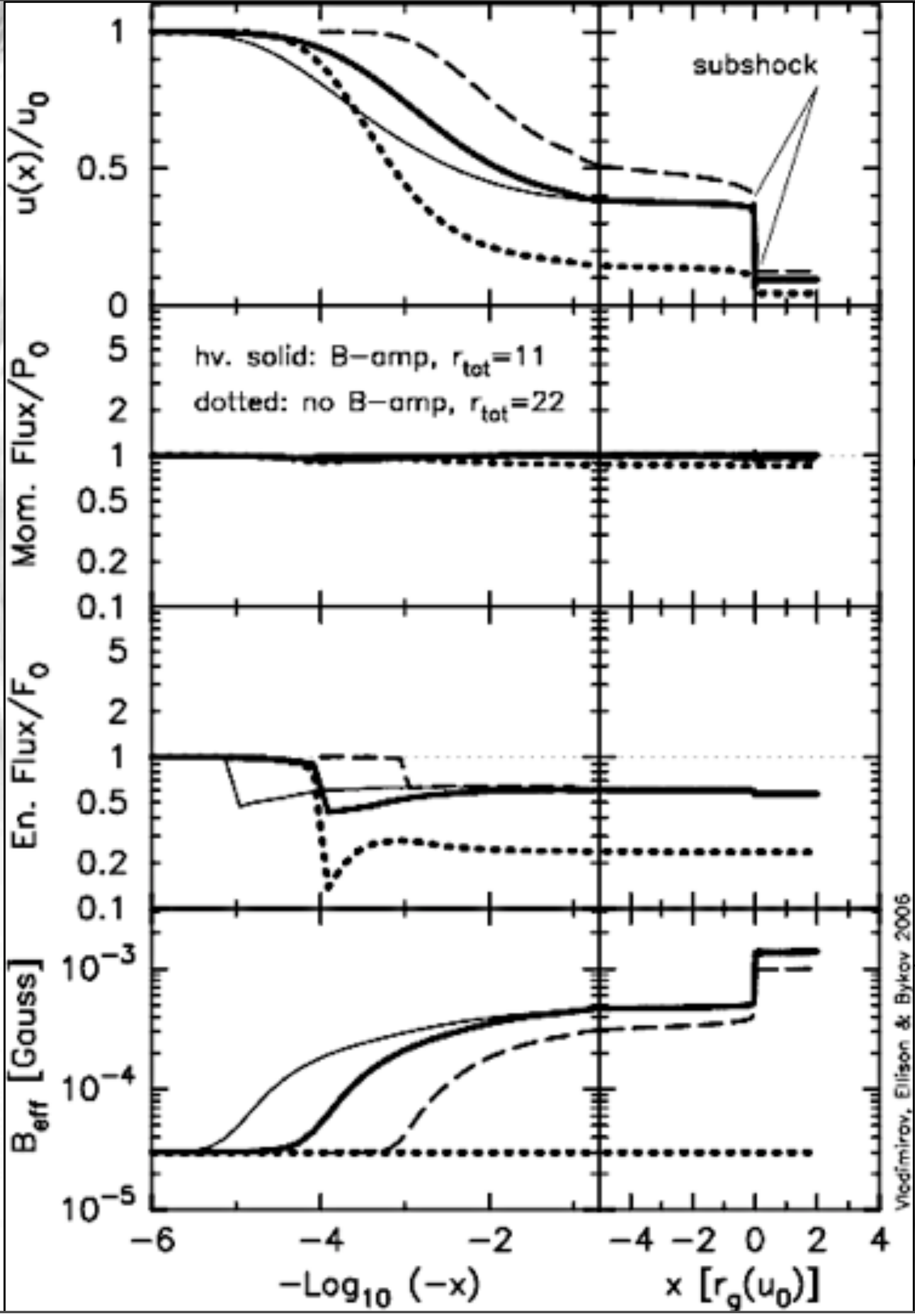

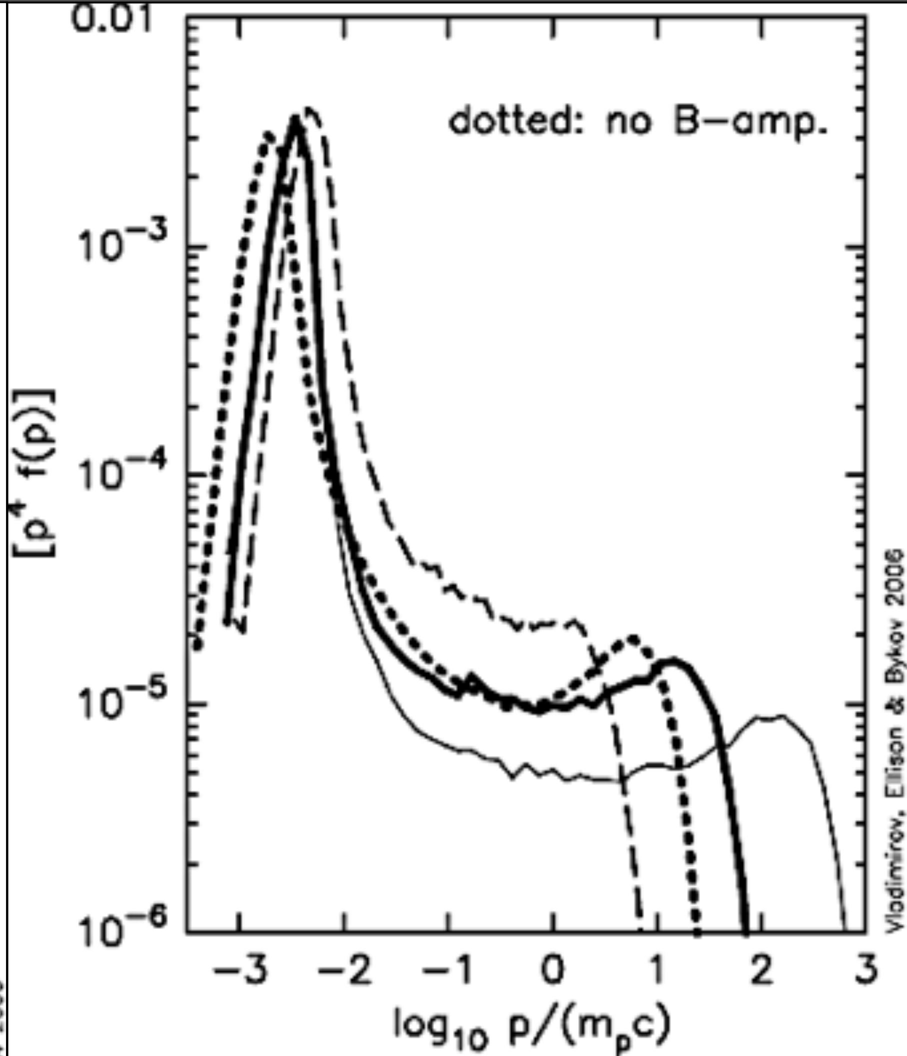

Vladimirov, Ellison, Bykov, Astrophys.J. 652 (2006) 1246

Monte Carlo simulations with backreaction on magnetic turbulence

Acceleration and energy loss rates for protons and oxygen nuclei in model for high luminosity gamma-ray bursts

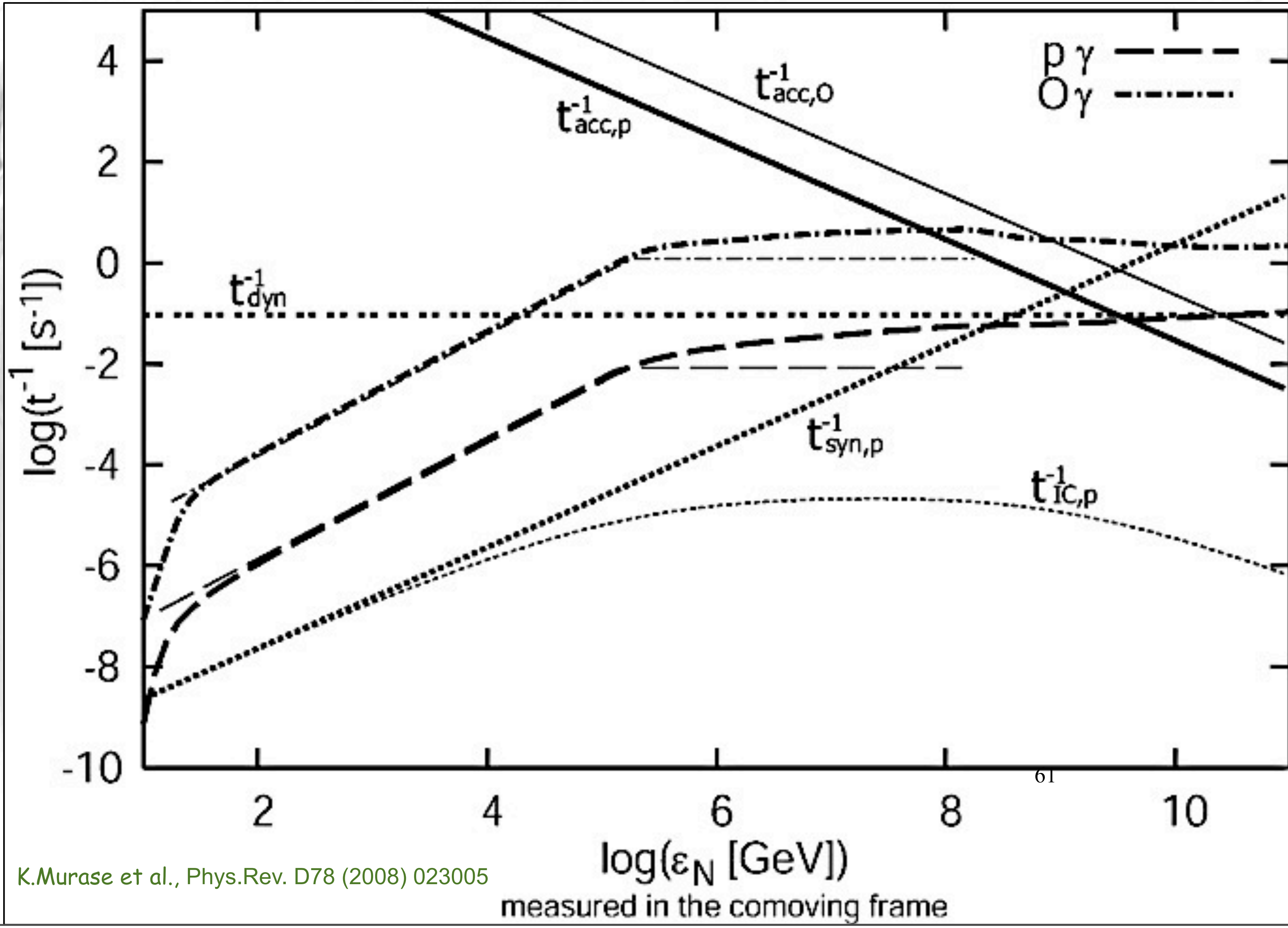

K.Murase et al., Phys.Rev. D78 (2008) 023005

Hillas plot with energy losses

one-shot, curvature-dominated only

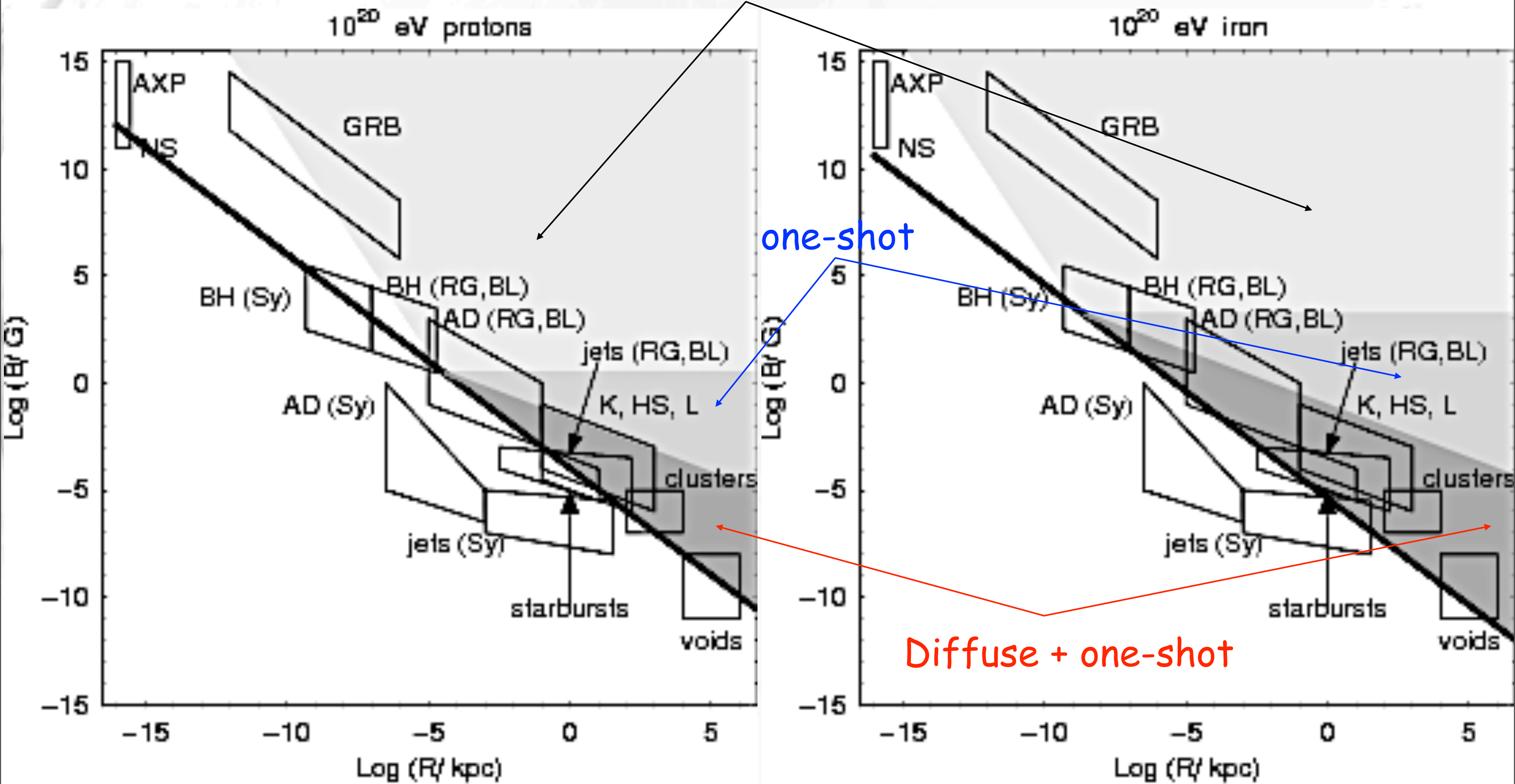

62

Observed events consistent with constraints on correlated sources for heavy primaries !

Ptitsyna, Troitsky., arXiv:0808.0367

Ultra-High Energy Cosmic Ray Sky Distribution

Pierre Auger Observatory update on correlations with nearby extragalactic matter: Pierre Auger Collaboration, arXiv:1009.1855

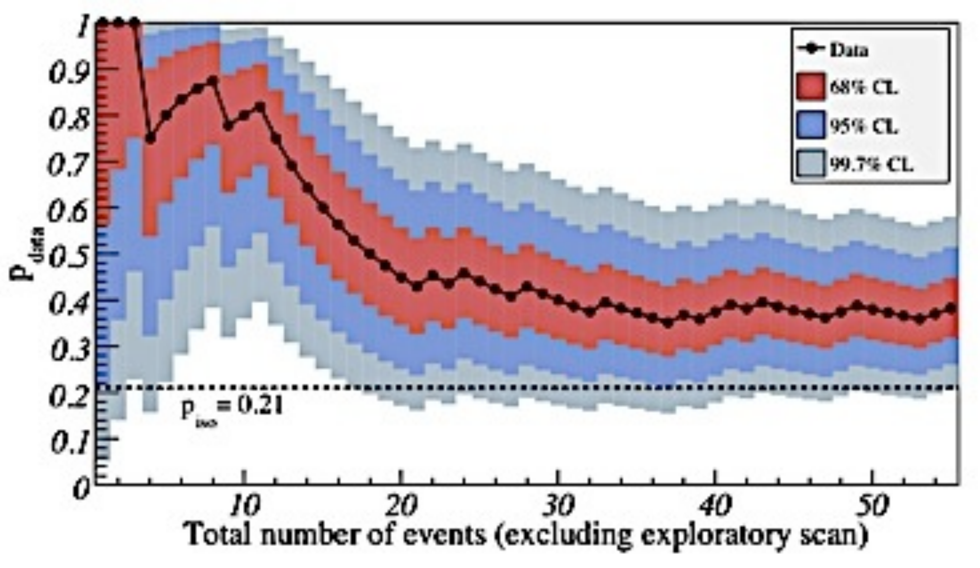

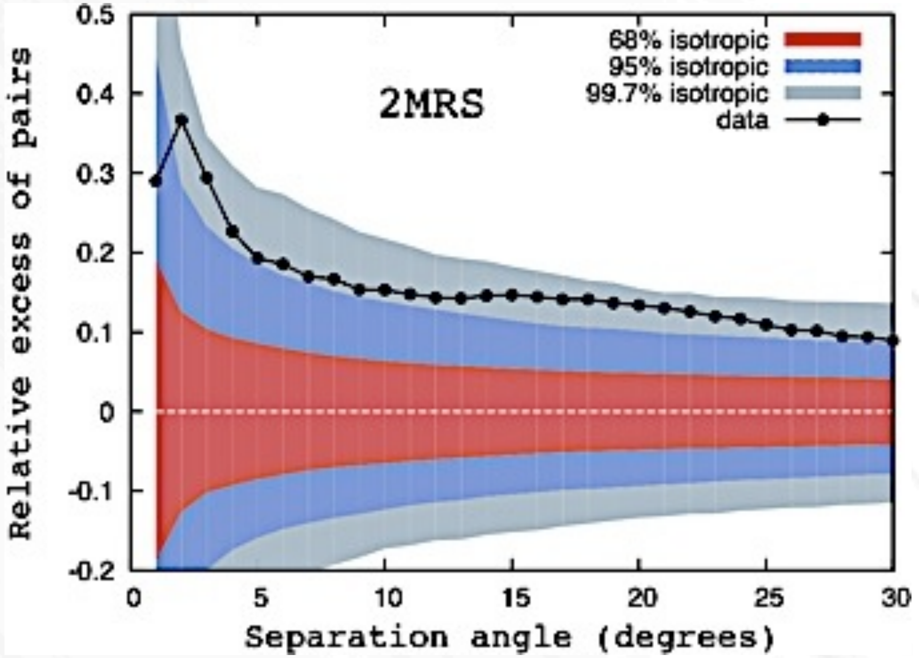

The case for anisotropy does not seem to have strengthened with more data: Fraction of events above 55 EeV correlating with the Veron Cetty Catalog has came down from 69+11-13% to 38+7-6% with 21% expected for isotropy. Excess of correlation also seen with 2MRS catalog at 95% CL.

Auger sees Correlations with AGNs !

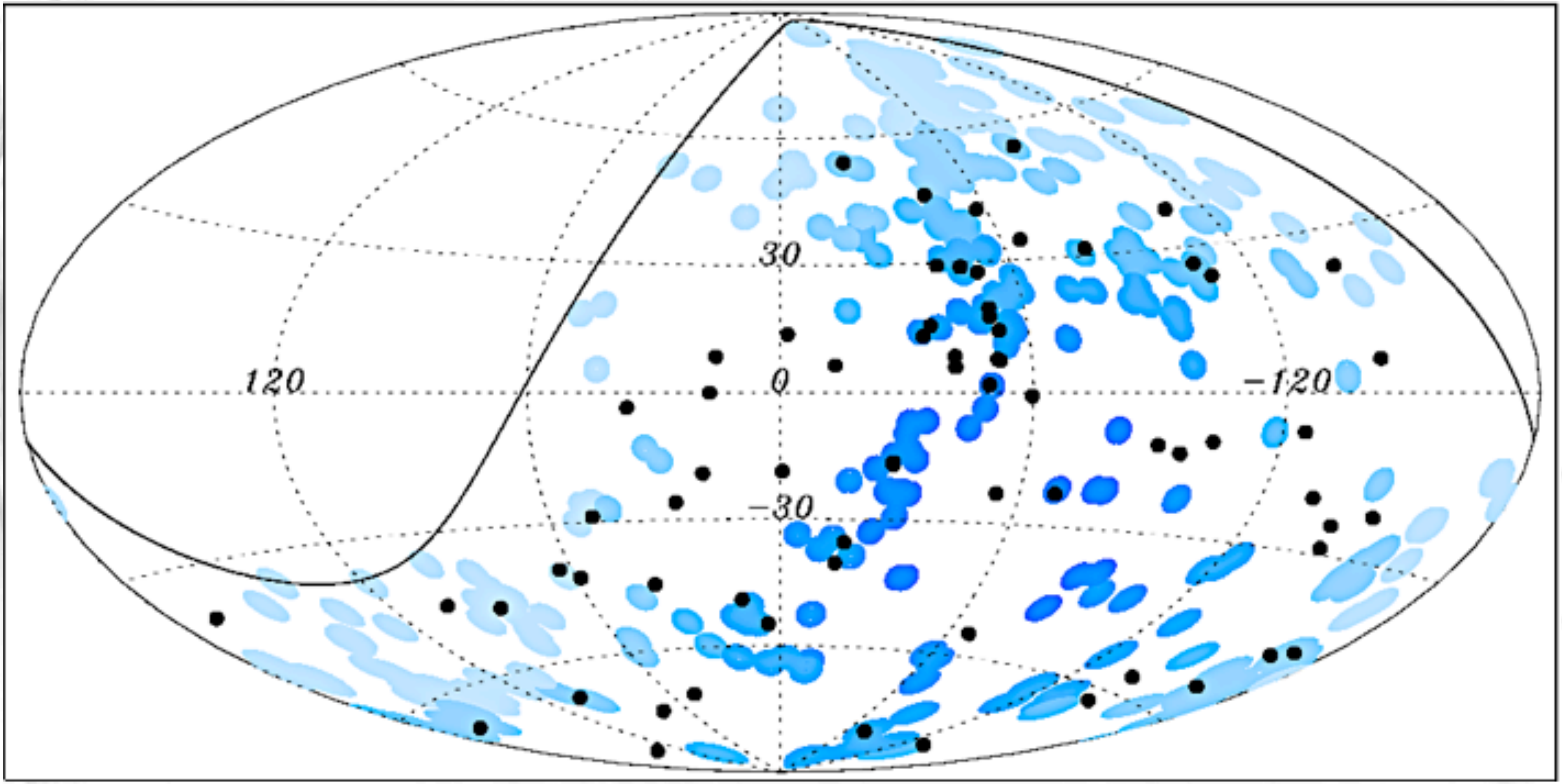

Blue 3.1 deg. circles = 318 AGNs from the Veron Cetty catalogue within 75 Mpc (exposure weighted color); black dots = 69 events above 55 EeV.[64]
29 events correlated within 3.1°, 14.5 expected for isotropy

Pierre Auger Collaboration, Astropart.Phys. 34 (2010) 314

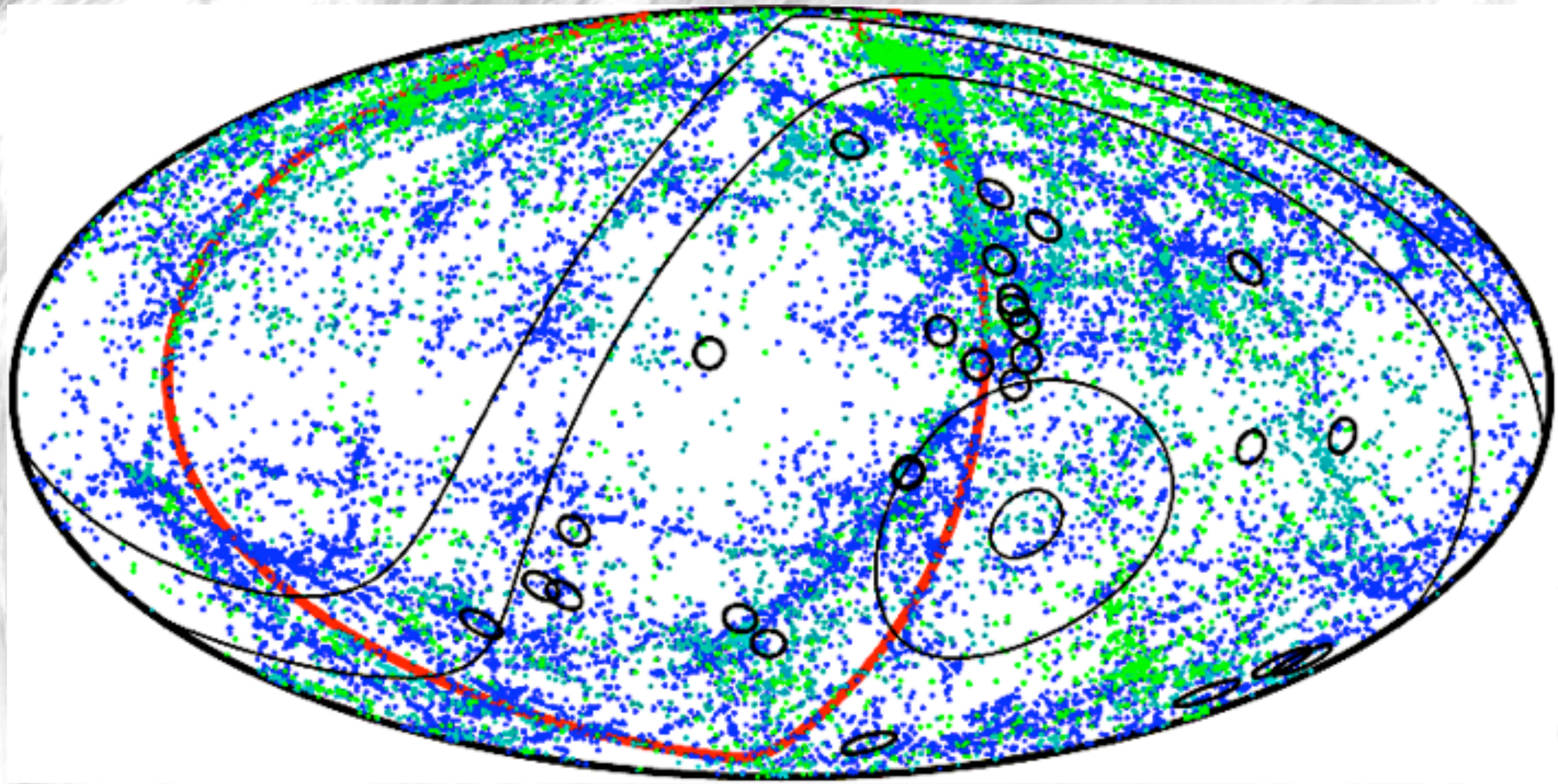

Points = galaxies with z < 0.015

Black circles = Auger events above 60 EeV.

Black lines = equal exposure contours

red line= supergalactic plane

Lipari, arXiv:0808.0417

65

But HiRes sees no Correlations !

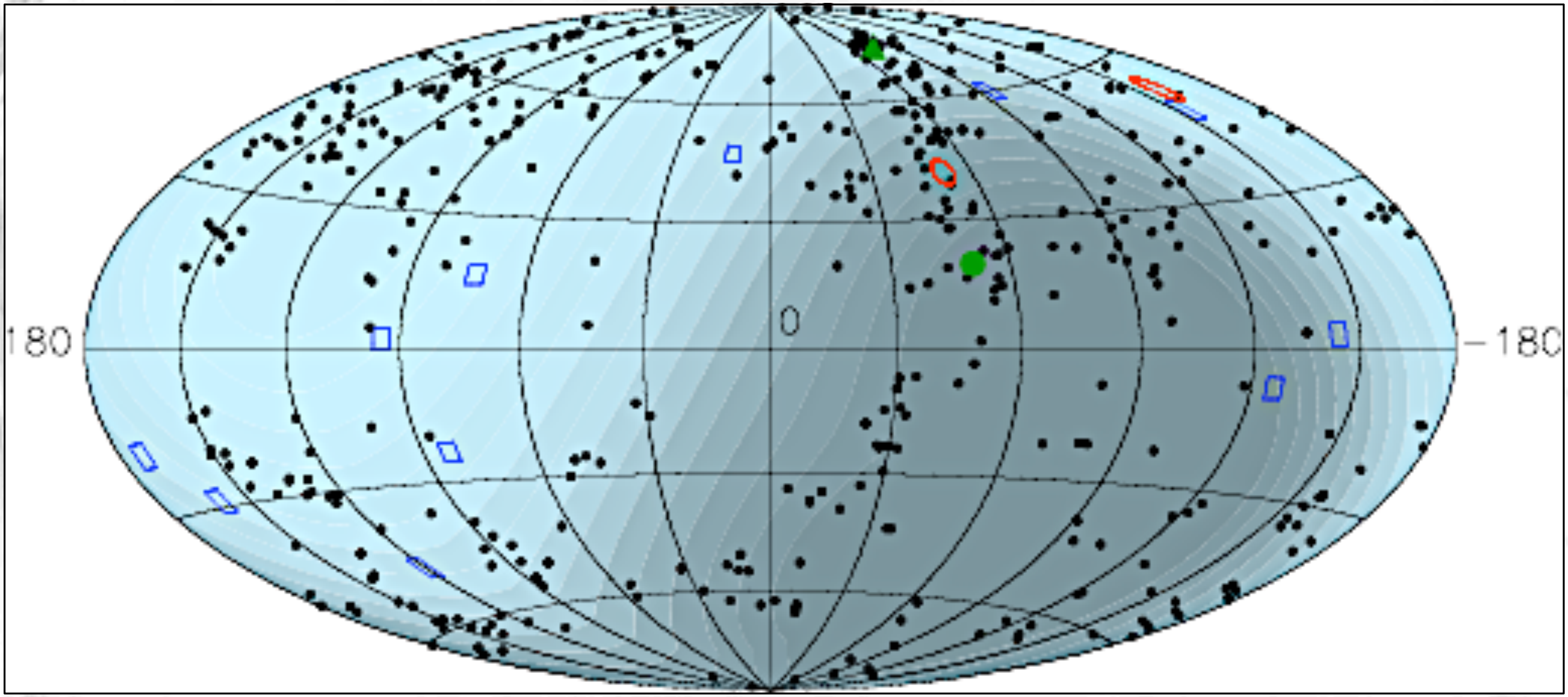

Black dots = 457 AGNs + 14 QSOs from the Veron Cetty catalogue for z < 0.018
red circles = 2 correlated events above 56 EeV within 3.1°, 66
blue squares = 11 uncorrelated events

HiRes Collaboration, Astropart.Phys. 30 (2008) 175

But HiRes sees no Correlations !

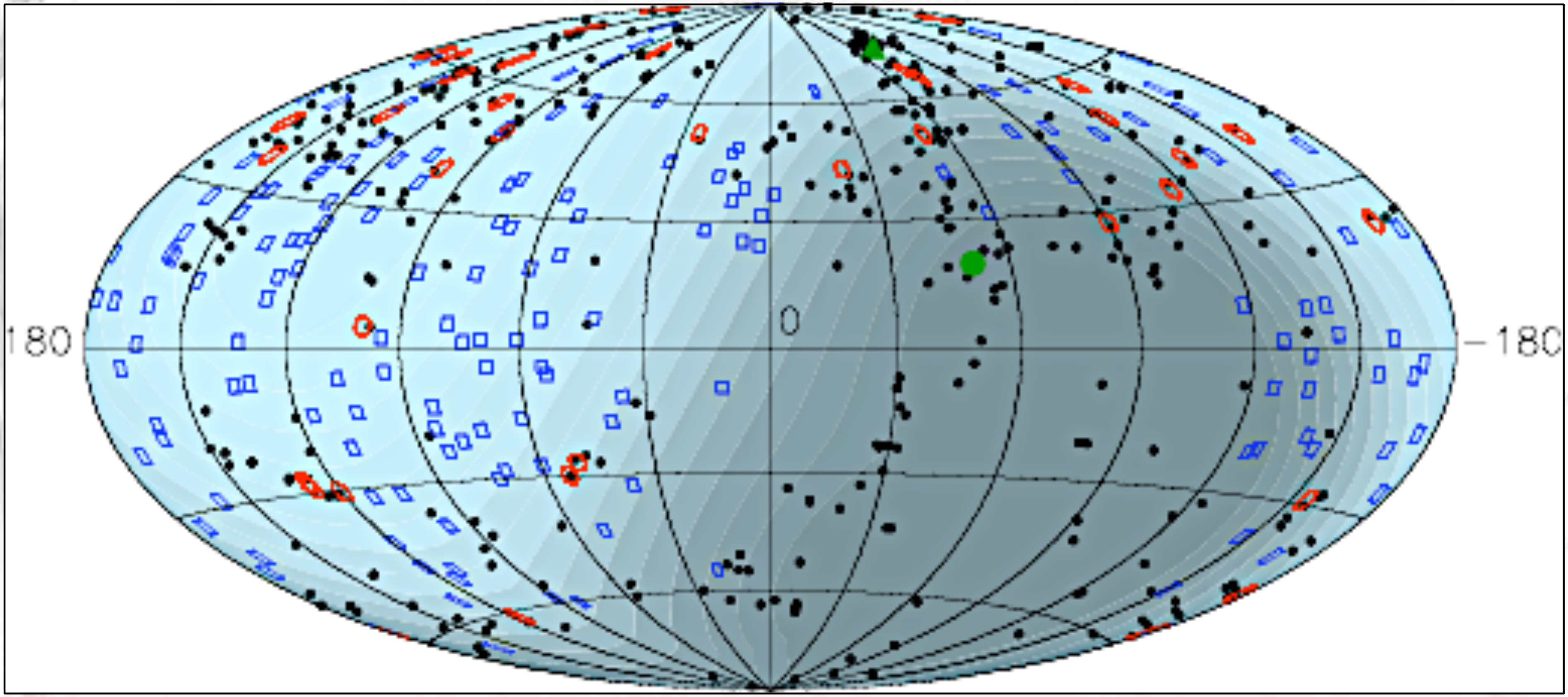

Black dots = 389 AGNs + 14 QSOs from the Veron Cetty catalogue for z < 0.016
red circles = 36 correlated events above 15.8 EeV within 2.0°, 67
blue squares = 162 uncorrelated events

HiRes Collaboration, Astropart.Phys. 30 (2008) 175

Correlation with supergalactic plane

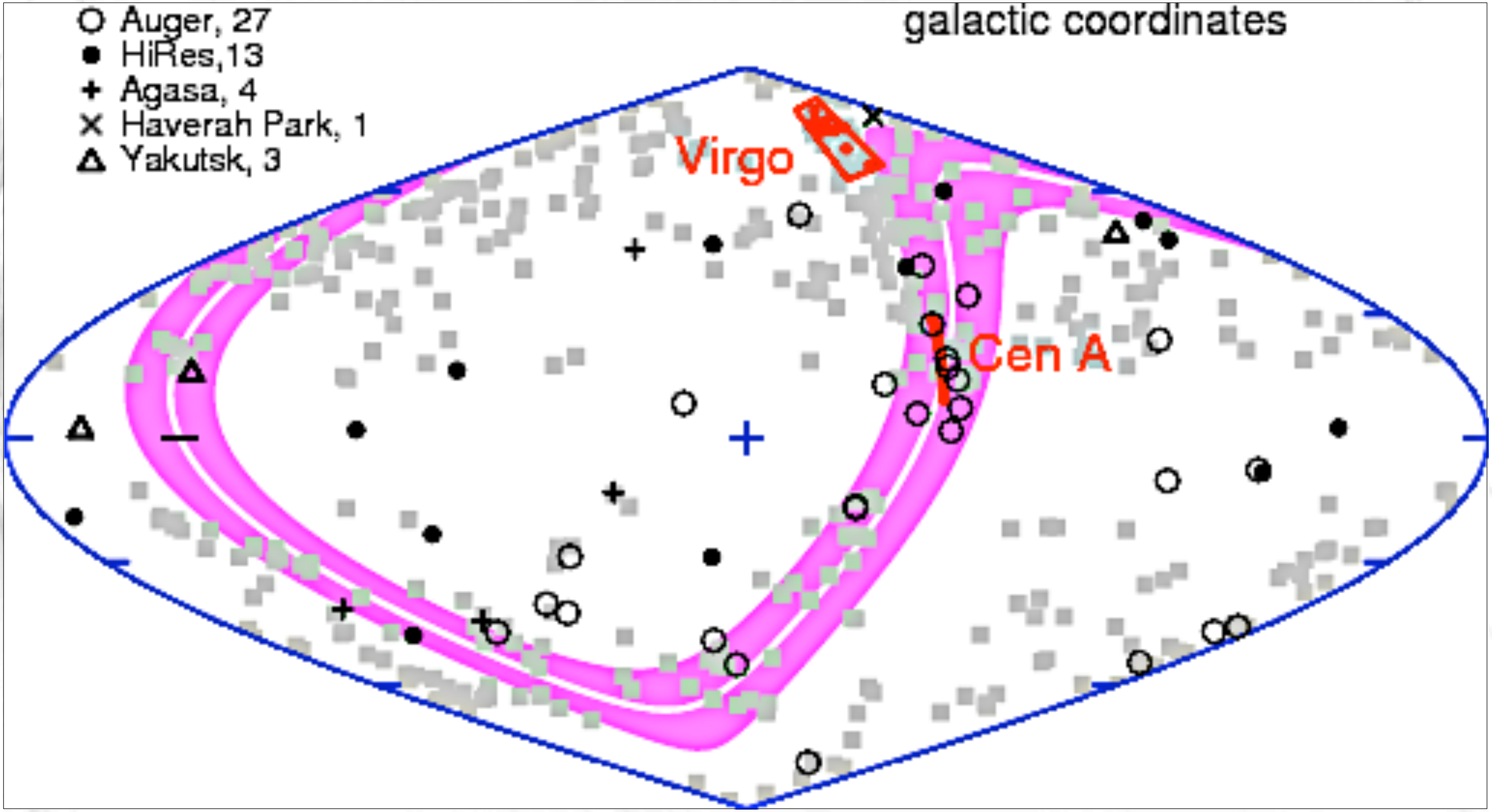

Correlation with supergalactic plane within 10° (15°) is improved from 2.0 (2.4) sigma to 3.6 (3.2) sigma when definition relates to structure within 70 Mpc.

Stanev, arXiv:0805.1746

Further Curiosities in the Sky Distributions

too few events from Virgo cluster, see
Gorbunov et al., JETP Lett. 87 (2007) 461

too many events from Centaurus A, e.g. Moskalenko et al., arXiv:0805.1260; Rachen, arXiv:0808.0348.

The AGNs with which Auger events correlate are not thought to be strong enough, see Moskalenko et al., arXiv:0805.1260; Zaw, Farrar, Greene, arXiv:0806.3470 (the latter arguing for flares)

According to Gureev and Troitsky, arXiv:0808.0481, the correlation of Auger events with AGNs is stronger when nearest neighbor sources only are counted, than when all AGN within given off-set are counted. According to them, this reveals individual sources rather than the population.

Some general estimates for sources

Accelerating particles of charge eZ to energy E_{max} requires induction $\varepsilon > E_{max}/eZ$. With $Z_0 \sim 100\Omega$ the vacuum impedance, this requires dissipation of minimum power of

$$L_{\rm min} \sim \frac{\epsilon^2}{Z_0} \simeq 10^{45}\, Z^{-2} \left(\frac{E_{\rm max}}{10^{20}\,{\rm eV}}\right)^2 \,{\rm erg\,s^{-1}}$$

This „Poynting" luminosity can also be obtained from $L_{min} \sim (BR)^2$ where BR is given by the „Hillas criterium":

$$BR > 3\times 10^{17}\,\Gamma^{-1}\left(\frac{E_{\rm max}}{10^{20}\,{\rm eV}}\right)\,{\rm Gauss\,cm}$$

where Γ is a possible beaming factor.
If most of this goes into electromagnetic channel, only AGNs and maybe gamma-ray bursts could be consistent with this.

70

In arXiv:1003.2500 Hardcastle estimates a corresponding lower limit on the radio luminosity:

$$L_{108\,\mathrm{MHz}} > 2 \times 10^{24}\,\epsilon \left(\frac{E/Z}{10^{20}\,\mathrm{eV}}\right)^{7/2} \left(\frac{r_{\mathrm{lobe}}}{100\,\mathrm{kpc}}\right)^{-1/2} \mathrm{W\,Hz^{-1}}$$

for an E^{-2} electron spectrum
with ε = energy in electrons / energy in magnetic field

He concludes: if protons, then very few sources which should be known and spectrum should cut off steeply at observed highest energies

If heavier nuclei then there are many radio galaxy sources but only Cen A may be identifiable

Centaurus A

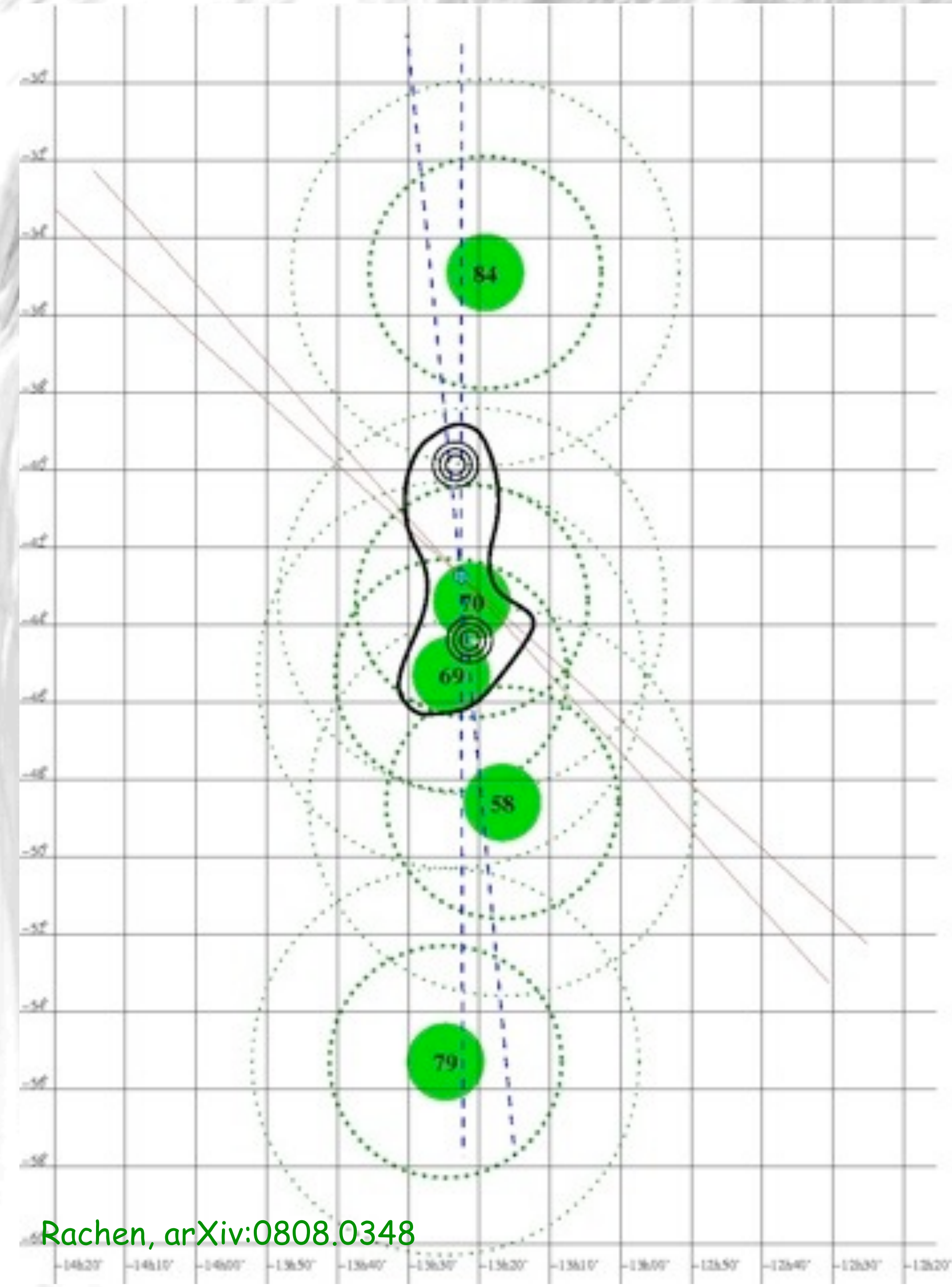

84
70
69
58
79
Rachen, arXiv:0808.0348

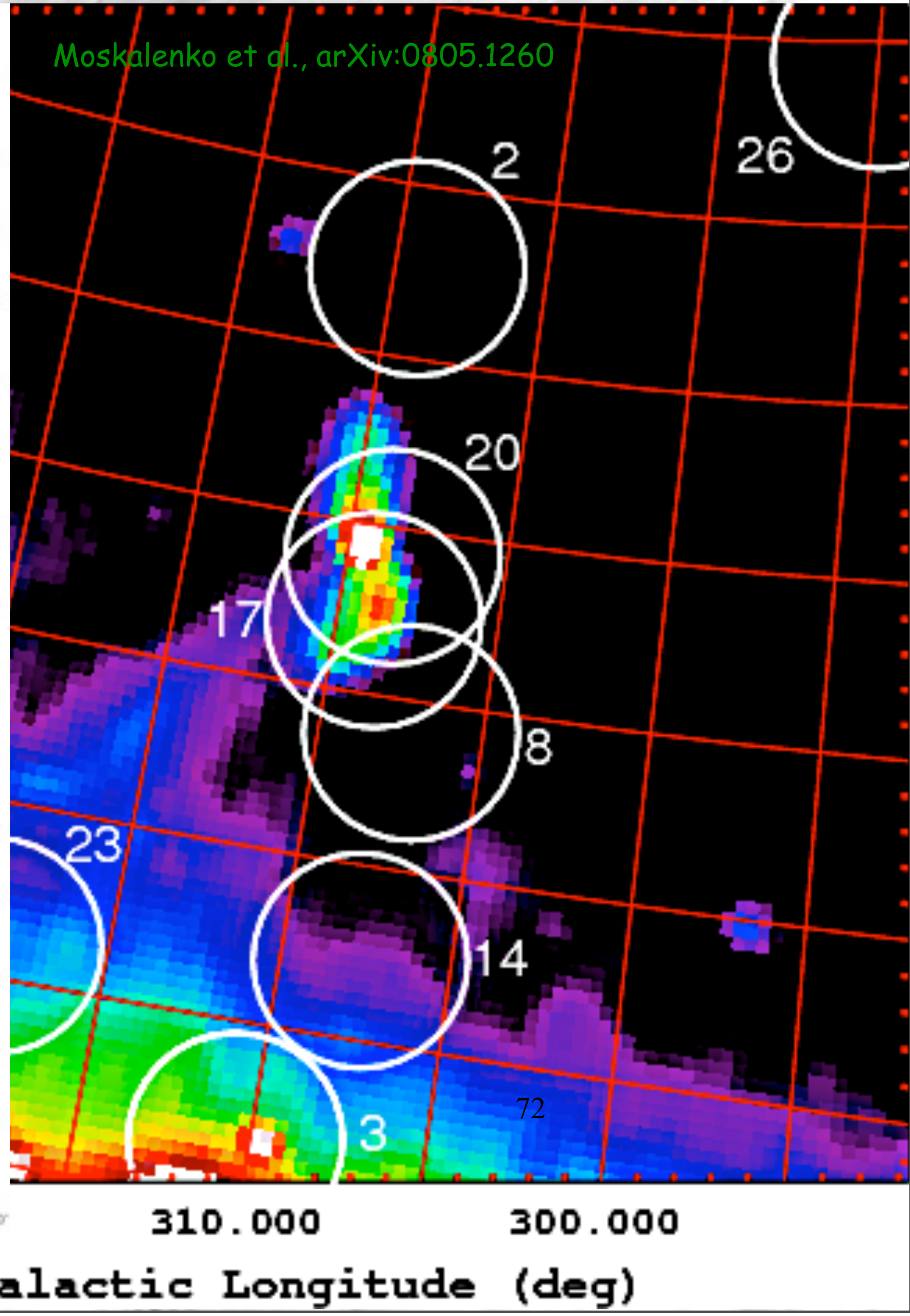

Moskalenko et al., arXiv:0805.1260
2
26
20
17
8
23
14
3
72
310.000
300.000
Galactic Longitude (deg)

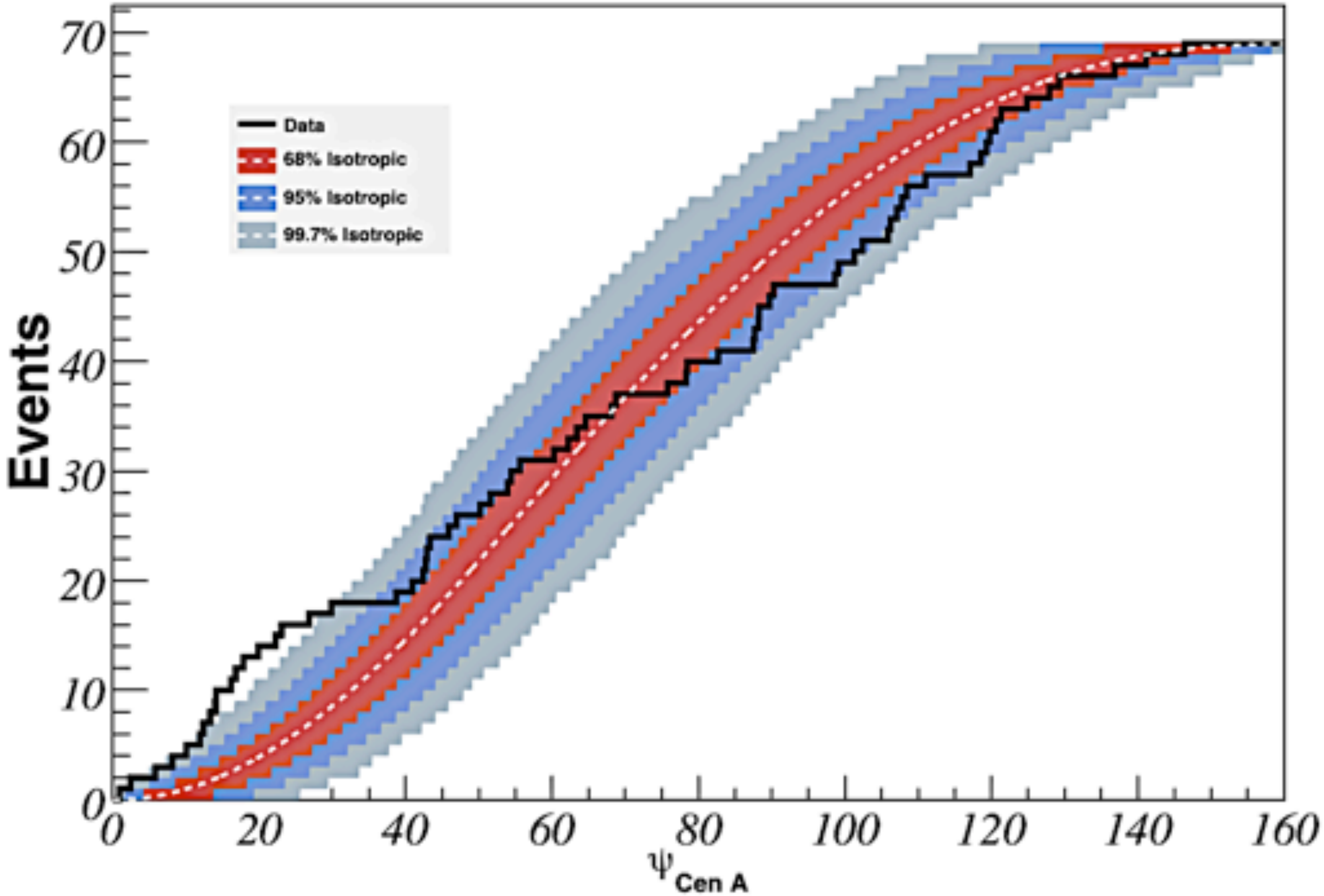

Pierre Auger sees a clear excess in the direction of Centaurus A.

Pierre Auger Collaboration, Astropart.Phys. 34 (2010) 314

Chemical Composition, Nature of the Ankle

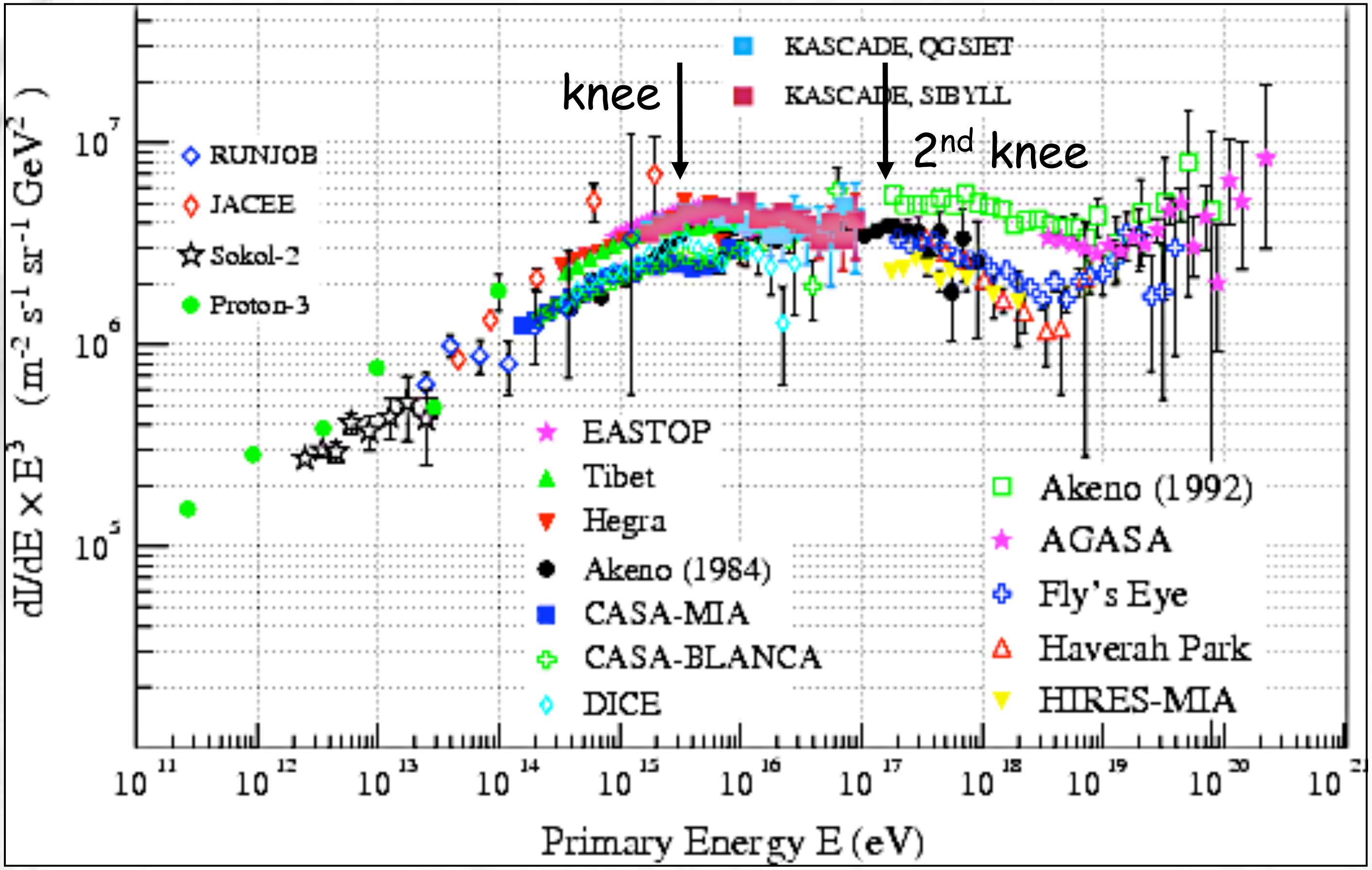

74

Chemical Composition, Nature of the Ankle

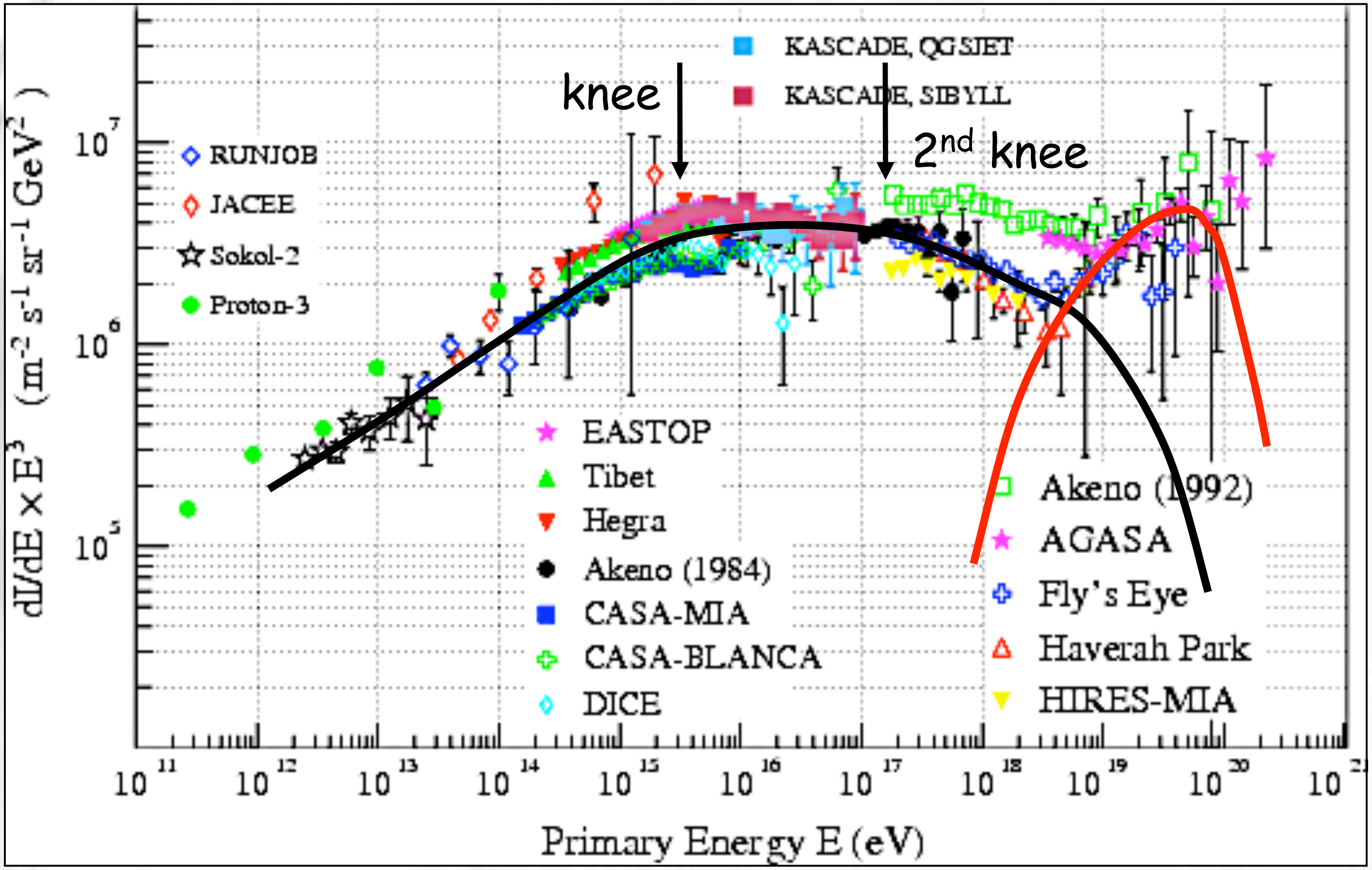

"Conventional Scenario":

The ankle at ~5×10^{18} eV is a cross-over from a heavy Galactic to a light extragalactic component.

74

Chemical Composition, Nature of the Ankle

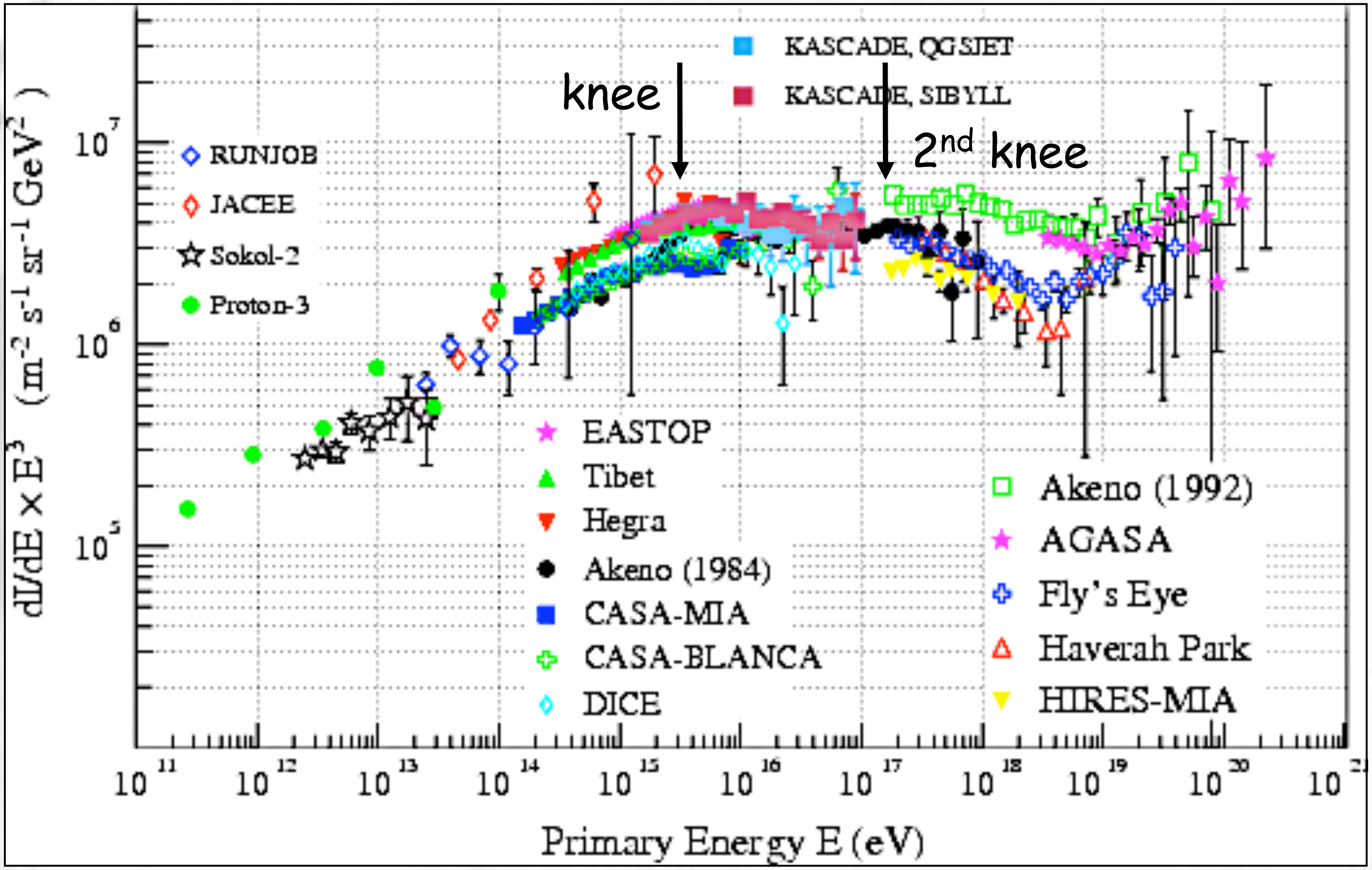

74

Chemical Composition, Nature of the Ankle

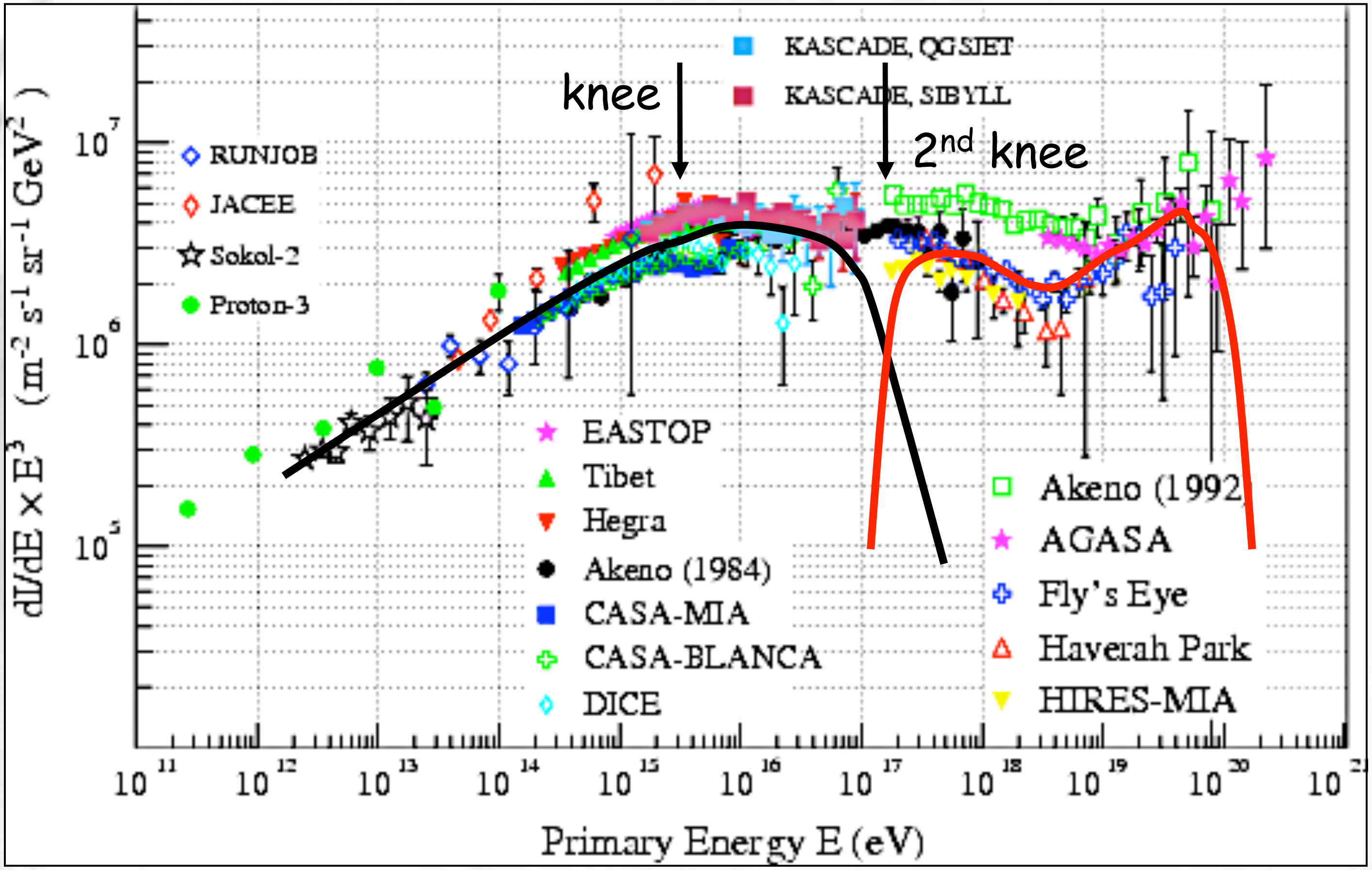

Scenario of Berezinsky et al.:
Galactic cosmic rays level out at the 2nd knee at $\sim 4\times10^{17}$ eV where dominated by heavy nuclei..
The ankle at $\sim 5\times10^{18}$ eV is due to pair production of extragalactic protons on the CMB. Requires >85% protons at the ankle.

There may be a significant heavy component at the highest energies:

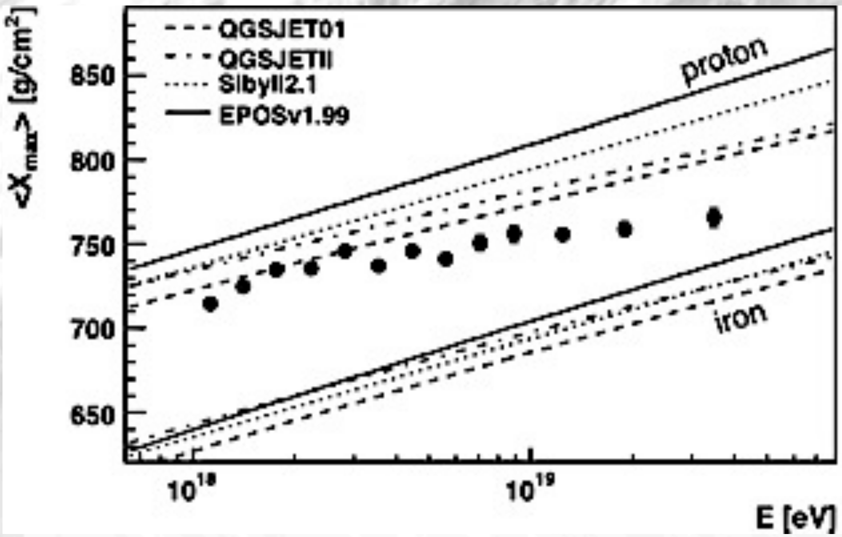

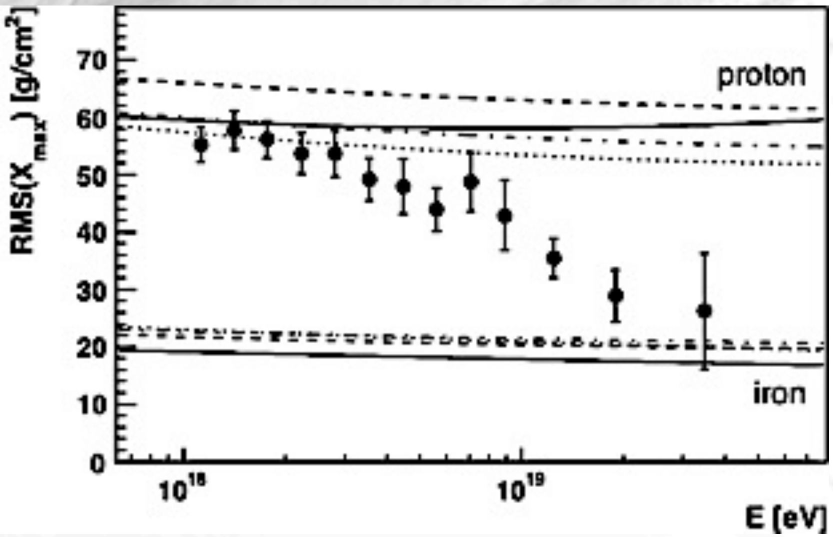

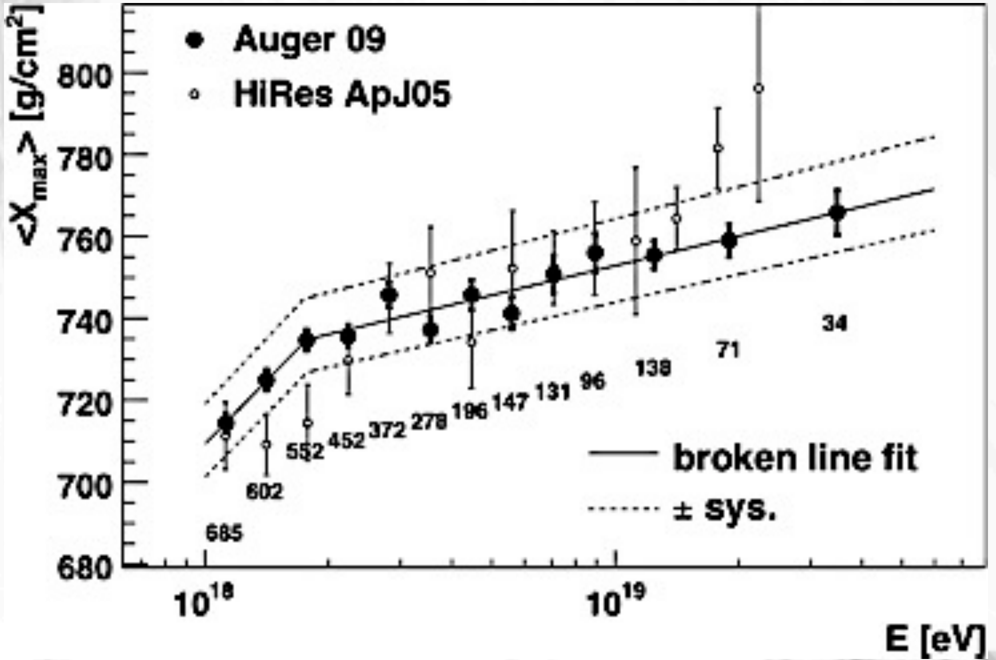

Auger data on composition seem to point to a quite heavy composition at the highest energies, whereas HiRes data seem consistent with a light composition.

Pierre Auger Collaboration,
Phys.Rev.Lett., 104 (2010) 091101

75

HiRes Collaboration,
Phys.Rev.Lett. 104 (2010) 161101

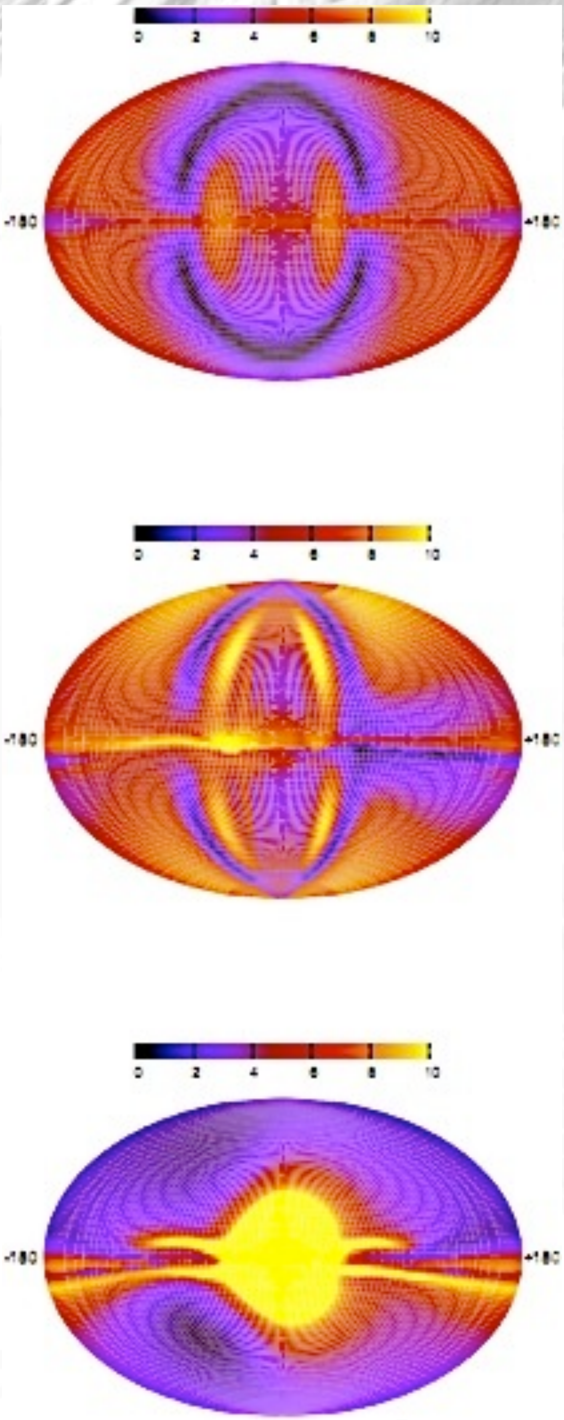

Consequences for Galactic Deflection

Deflection in **galactic magnetic field** is rather model dependent, here for E/Z=4 10^{19} eV for Models of

Tinyakov, Tkachev (top)

Harrari, Mollerach, Roulet (middle)

Prouza, Smida (bottom)

Deflection in **extragalactic fields** is even more uncertain

Kachelriess, Serpico, Teshima, Astropart. Phys. 26 (2006) 378

76

Deflection of iron in galactic magnetic field model of Prouza&Smida

Angular range between 0 and 100 degrees, galactic coordinates

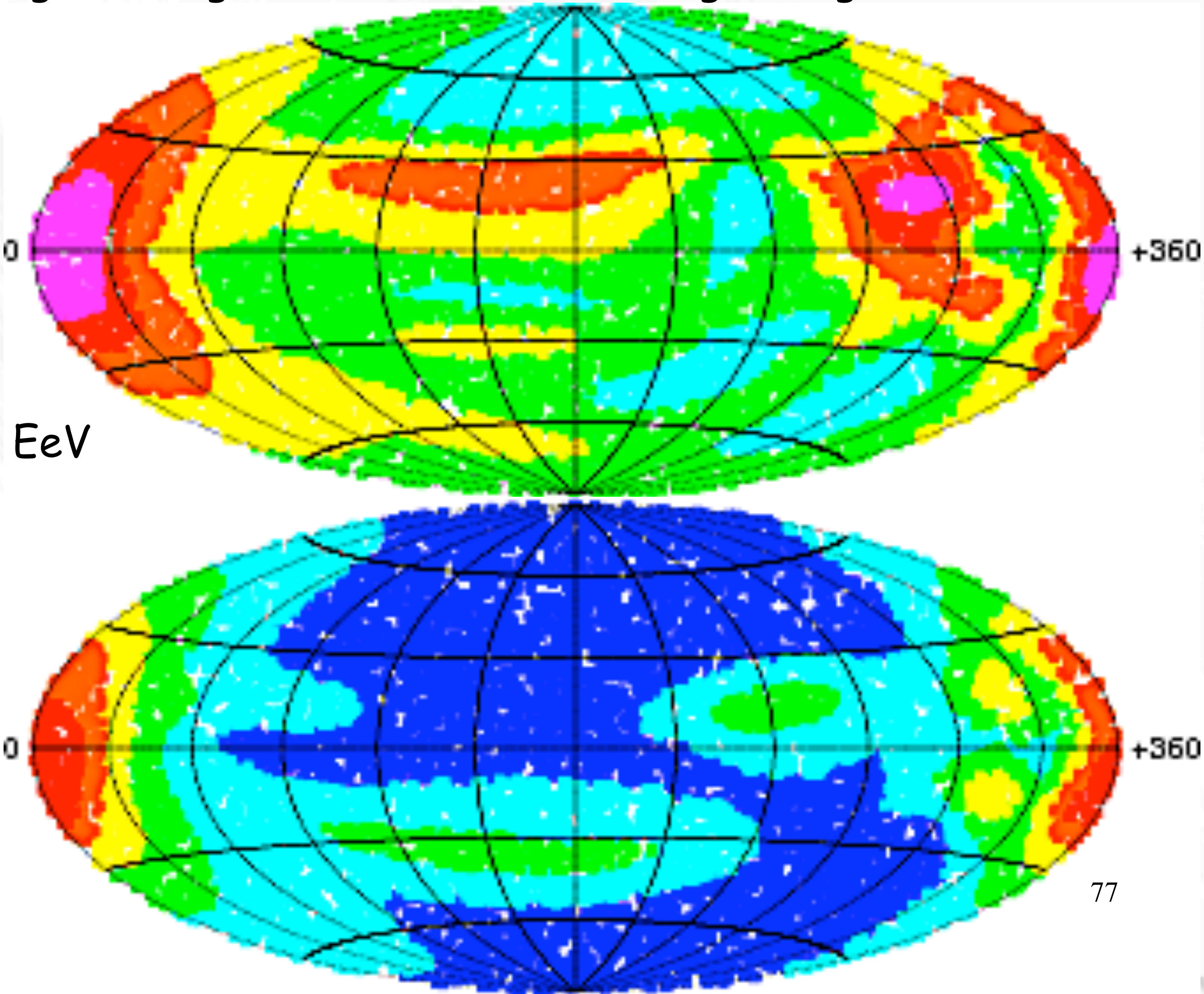

E=60 EeV

E=140 EeV

Giacinti, Kachelriess, Semikoz, Sigl, JCAP 1008 (2010) 036

Bachtracking of iron in galactic magnetic field model of Prouza&Smida

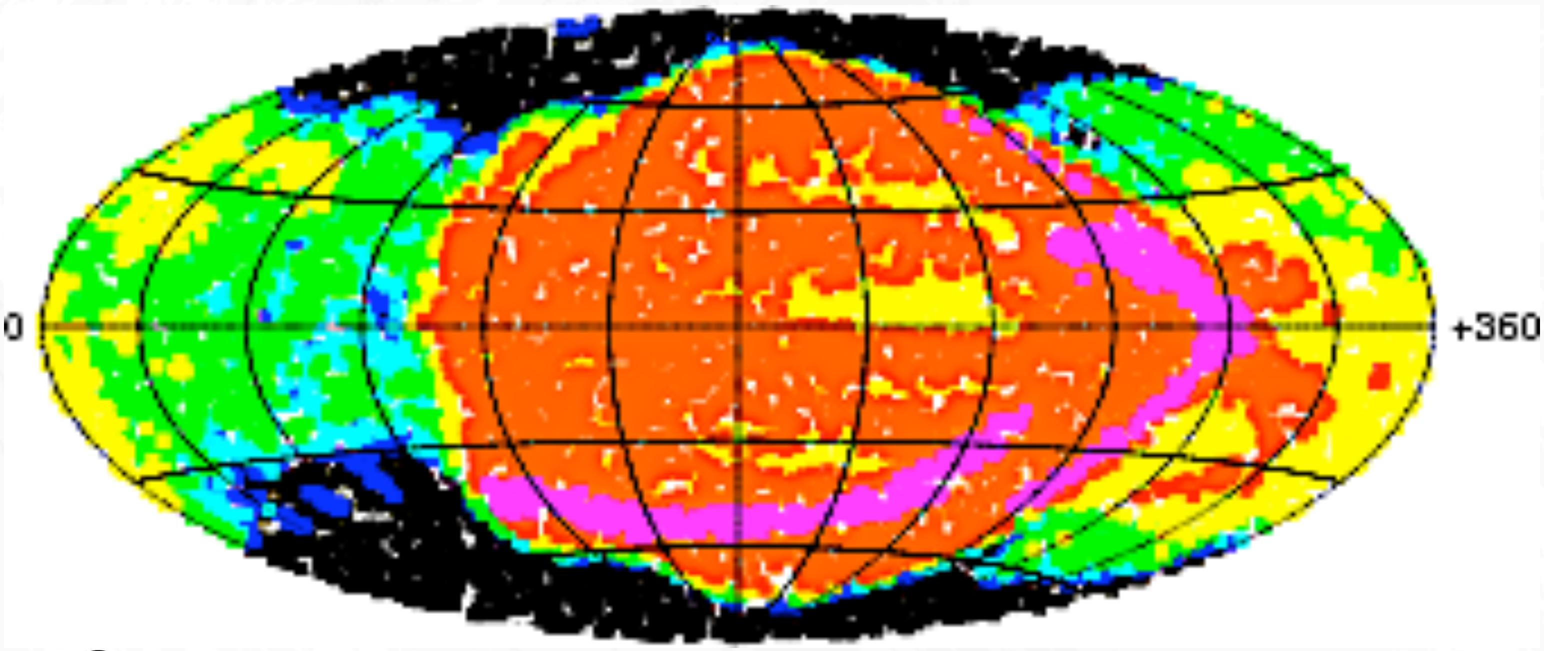

E=60 EeV

Giacinti, Kachelriess, Semikoz, Sigl, JCAP 1008 (2010) 036

Density range between 10^{-3} and $10^{0.5}$, galactic coordinates

Highly anisotropic picture

Empty backtracked regions are invisible from within the Galaxy !

78

“Iron Image” of galaxy cluster Abell0569 in two galactic field models

Energy range from 60 to 140 EeV

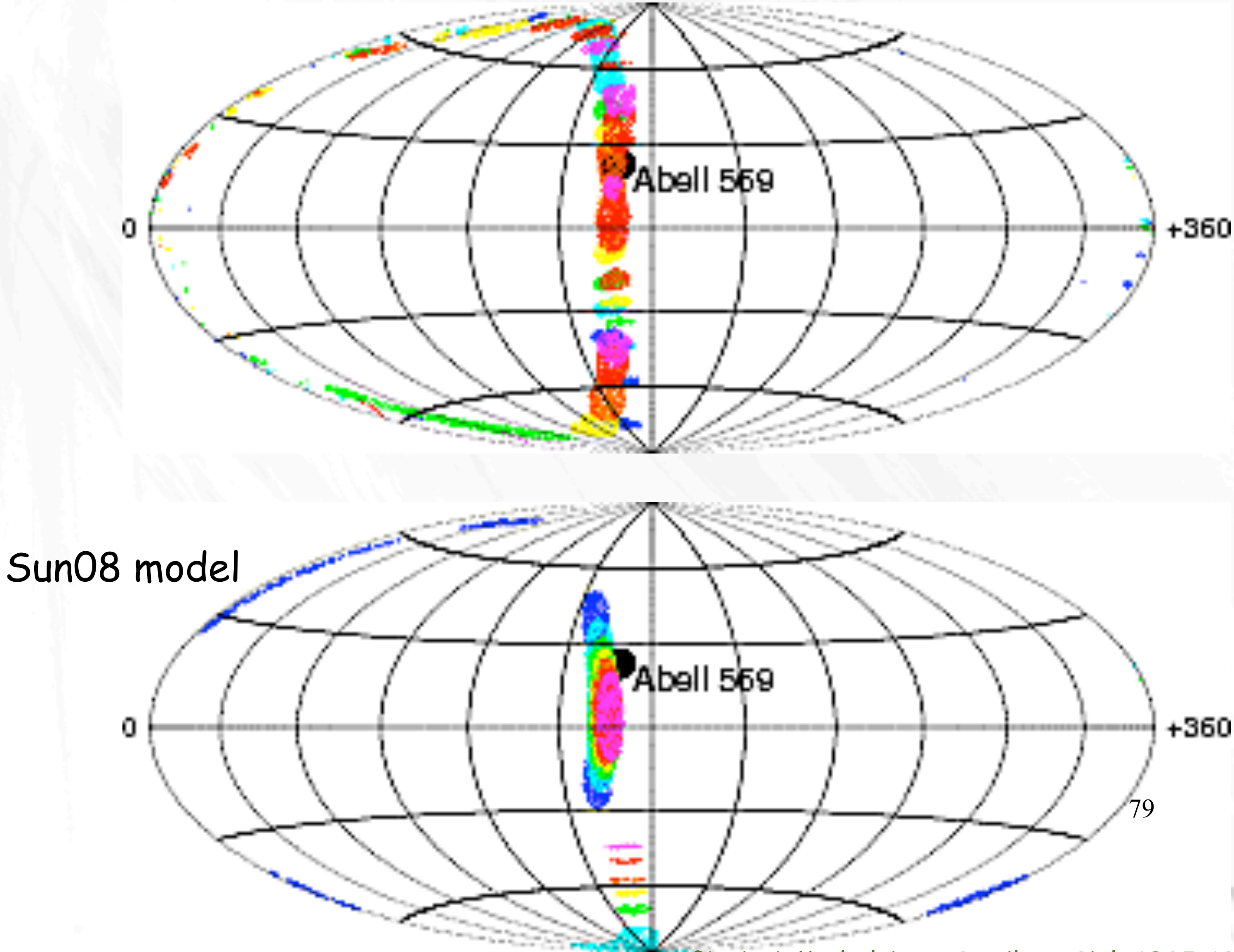

Giacinti, Kachelriess, Semikoz, Sigl, JCAP 1008 (2010) 036

"Iron image" of supergalactic plane in galactic magnetic field model of Prouza&Smida

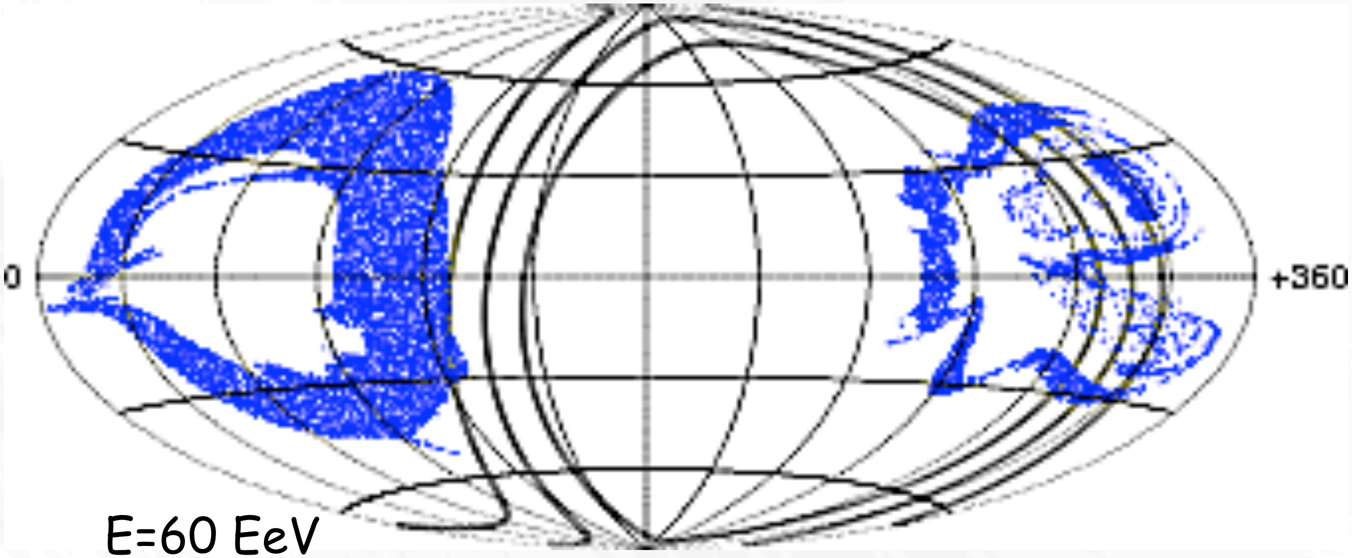

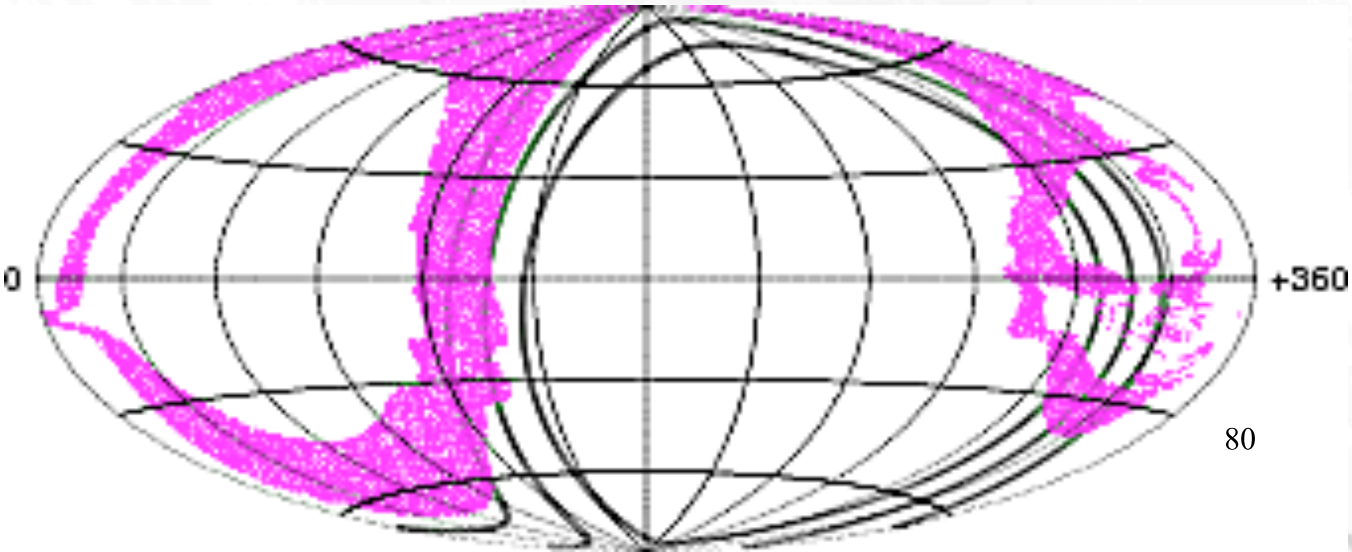

E=140 EeV

Giacinti, Kachelriess, Semikoz, Sigl, JCAP 1008 (2010) 036

"Conundrum":

If deflection is small and sources follow the local large scale structure then

a) primaries should be protons to avoid too much deflection in galactic field

b) but air shower measurements by Pierre Auger (but not HiRes) indicate mixed or heavy composition

c) Theory of AGN acceleration seem to necessitate heavier nuclei to reach observed energy

Extragalactic Ultra-High Energy Cosmic Ray Propagation and Magnetic Fields

Cosmic rays above ~10^{19} eV are probably extragalactic and may be deflected mostly by extragalactic fields B_{XG} rather than by galactic fields.

However, very little is known about about B_{XG}: It could be as small as 10^{-20} G (primordial seeds, Biermann battery) or up to fractions of micro Gauss if concentrated in clusters and filaments (equipartition with plasma).

Transition from rectilinear to diffusive propagation over distance d in a field of strength B and coherence length λ_c at:

$$E_c \sim 1.2 \times 10^{19} \left(\frac{Z}{26}\right)\left(\frac{d}{\mathrm{Mpc}}\right)^{1/2}\left(\frac{B_{\mathrm{rms}}}{\mathrm{nG}}\right)\left(\frac{\lambda_c}{\mathrm{Mpc}}\right)^{1/2} \mathrm{eV}$$

Example: Magnetic field of 10^{-10} Gauss,
coherence scale 1 Mpc,
burst source at 50 Mpc distance

time delay

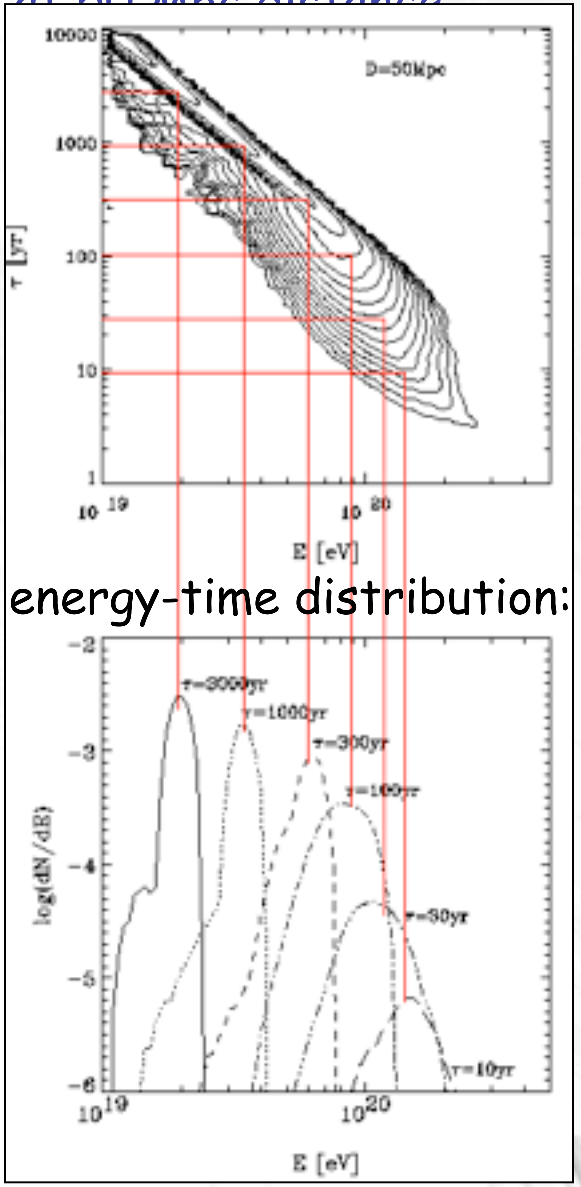

cuts through energy-time distribution:

differential spectrum

Lemoine, Sigl

83

Example: Magnetic field of 10^{-10} Gauss, coherence scale 1 Mpc, burst source at 50 Mpc distance

Typical numbers:

time delay

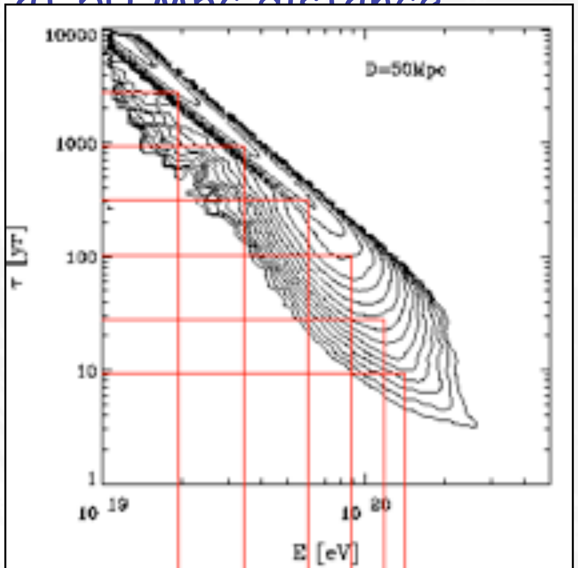

cuts through energy-time distribution:

differential spectrum

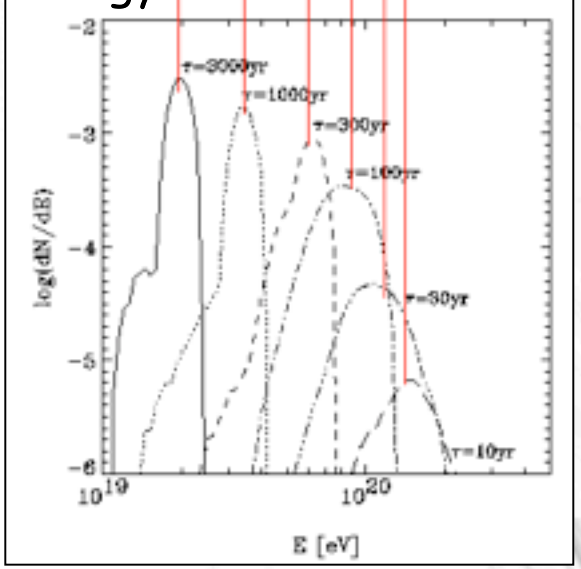

Lemoine, Sigl

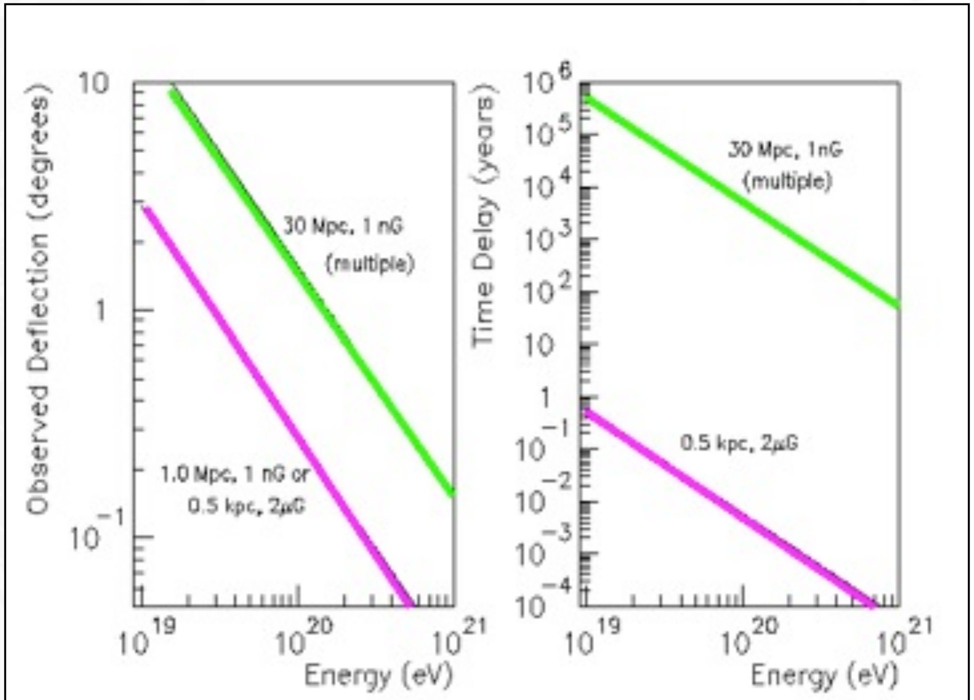

Δθ for a vertical shower:

	10 EeV	100 EeV
Array alone	2°	<1°
Hybrid	0.25°	0.20°

83

Neglect energy losses for simplicity.

Time delay over distance d in a field B_{rms} of coherence length λ_c for small deflection:

$$\tau(E,d) \simeq \frac{d\theta(E,d)^2}{4} \simeq 1.5 \times 10^3 \, Z^2 \left(\frac{E}{10^{20}\,\mathrm{eV}}\right)^{-2} \left(\frac{d}{10\,\mathrm{Mpc}}\right)^2 \left(\frac{B_{\rm rms}}{10^{-9}\,\mathrm{G}}\right)^2 \left(\frac{\lambda_c}{\mathrm{Mpc}}\right) \mathrm{yr}$$

This becomes comparable to distance d at energy E_c:

$$E_c \sim 4.7 \times 10^{19} \, Z \left(\frac{d}{10\,\mathrm{Mpc}}\right)^{1/2} \left(\frac{B_{\rm rms}}{10^{-7}\,\mathrm{G}}\right) \left(\frac{\lambda_c}{\mathrm{Mpc}}\right)^{1/2} \mathrm{eV}$$

In the rectilinear regime for total differential power Q(E) injected inside d, the differential flux reads

84

$$j(E) = \frac{Q(E)}{(4\pi d)^2}$$

In the diffusive regime characterized by a diffusion constant D(E), particles are confined during a time scale

$$\tau(E,d) \simeq \frac{d^2}{D(E)}$$

which leads to the flux

$$j(E) \simeq \frac{Q(E)\tau(E)}{(4\pi)^2 d^3} = \frac{Q(E)}{(4\pi)^2 d D(E)}$$

For a given power spectrum B(k) of the magnetic field an often used (very approximate) estimate of the diffusion coefficient is

$$D(E) \simeq \frac{r_g(E)}{3} \frac{B_{\rm rms}}{\int_{1/r_g(E)}^{\infty} dk k^2 \langle B^2(k)\rangle},$$

where $B_{rms}^2 = \int_0^\infty dk k^2 \langle B^2(k)\rangle$, and the gyroradius is

$$r_g(E) \simeq \frac{E}{ZeB_{\rm rms}} \simeq 110\, Z^{-1} \left(\frac{E}{10^{20}\,{\rm eV}}\right)\left(\frac{B_{\rm rms}}{10^{-6}\,{\rm G}}\right)^{-1} {\rm kpc}$$

85

IF $E \ll E_c$ and IF energy losses can be approximated as continuous, $dE/dt=-b(E)$ (this is not the case for pion production), the local cosmic ray density $n(E,\mathbf{r})$ obeys the diffusion equation

$$\partial_t n(E,\mathbf{r}) + \partial_E \left[b(E)n(E,\mathbf{r})\right] - \nabla \cdot \left[D(E,\mathbf{r})\nabla n(E,\mathbf{r})\right] = q(E,\mathbf{r})$$

Where now $q(E,\mathbf{r})$ is the differential injection rate per volume, $Q(E)=\int d^3\mathbf{r}\, q(E,\mathbf{r})$. Analytical solutions exist (Syrovatskii), but the necessary assumptions are in general too restrictive for ultra-high energy cosmic rays.

Monte Carlo codes are therefore in general indispensable.

Transition rectilinear-diffusive regime: Summary

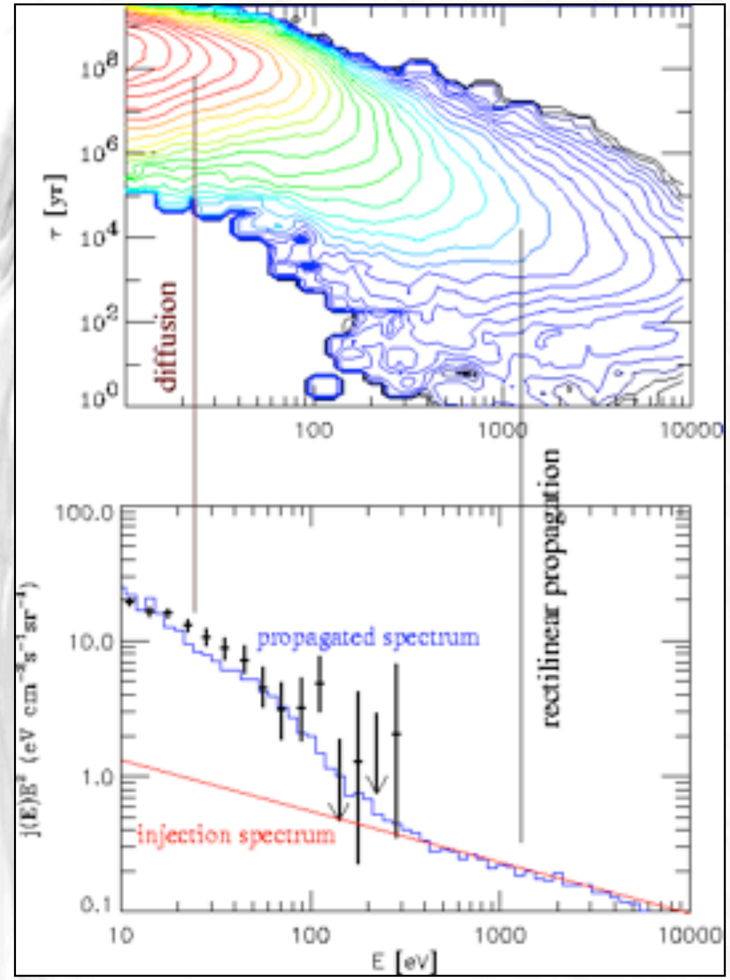

$$\tau(E) \propto d\theta^2 \propto \frac{d^2}{E^2}$$ in rectilinear regime

$$\tau(E,d) \simeq \frac{d^2}{D(E)}$$ in diffusive regime

$$j(E) \propto \frac{Q(E)}{d^2}$$ in rectilinear regime

$$j(E) \propto \frac{Q(E)\tau(E)}{d^3} \propto \frac{Q(E)}{dD(E)}$$ in diffusive regime

Simulated example: Continuous source distribution following Gaussian profile; $B=3\times10^{-7}$ G, d=10 Mpc, λ_c=1 Mpc.

Transition at energy $$E_c \sim 4.7\times10^{19}\, Z \left(\frac{d}{10\,\mathrm{Mpc}}\right)^{1/2} \left(\frac{B_{\rm rms}}{10^{-7}\,\mathrm{G}}\right) \left(\frac{\lambda_c}{\mathrm{Mpc}}\right)^{1/2} \mathrm{eV}$$

87

In the transition regime Monte Carlo codes are in general indispensable.

Principle of deflection Monte Carlo code

source

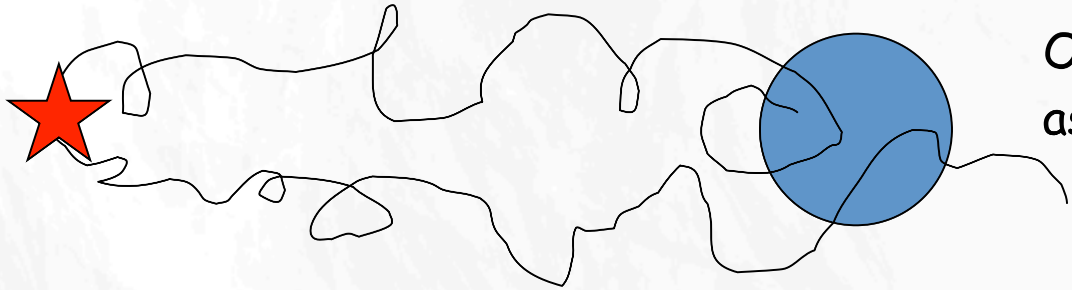

Observer is modelled as a sphere

A particle is registered every time a trajectory crosses the sphere around the observer. This version to be applied for individual source/magnetic field realizations and inhomogeneous structures.

Main Drawback: CPU-intensive if deflections are considerable because most trajectories are “lost”. But inevitable for accurate simulations in highly structured environments without symmetries.

Simulating Propagation of Ultrahigh Energy Cosmic Rays, Gamma-Rays and Neutrinos with CRPropa

CRPropa is a public code for UHE cosmic rays, neutrinos and γ-rays being extended to heavy nuclei and hadronic interactions

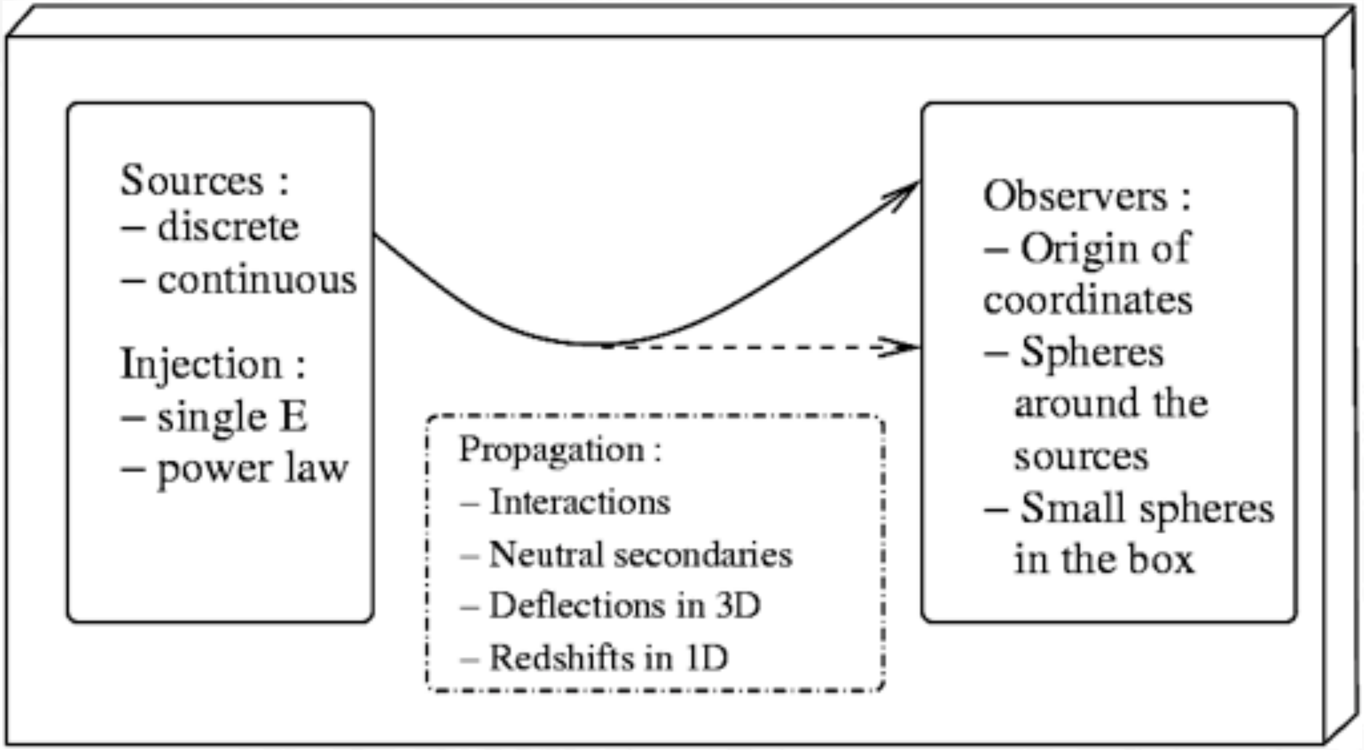

Eric Armengaud, Tristan Beau, Günter Sigl, Francesco Miniati, Astropart.Phys.28 (2007) 463.

89

http://apcauger.in2p3.fr/CRPropa/index.php

Now including: Jörg Kulbartz, Luca Maccione, Ricard Tomas, Mariam Tortola, Nils Nierstenhoefer, Karl-Heinz Kampert, ...

Effects of a single source: Numerical simulations

A source at 3.4 Mpc distance injecting protons with spectrum $E^{-2.4}$ up to 10^{22} eV
A uniform Kolmogorov magnetic field, $\langle B^2(k)\rangle \sim k^{-11/3}$, of rms strength 0.3 μG, and largest turbulent eddy size of 1 Mpc.

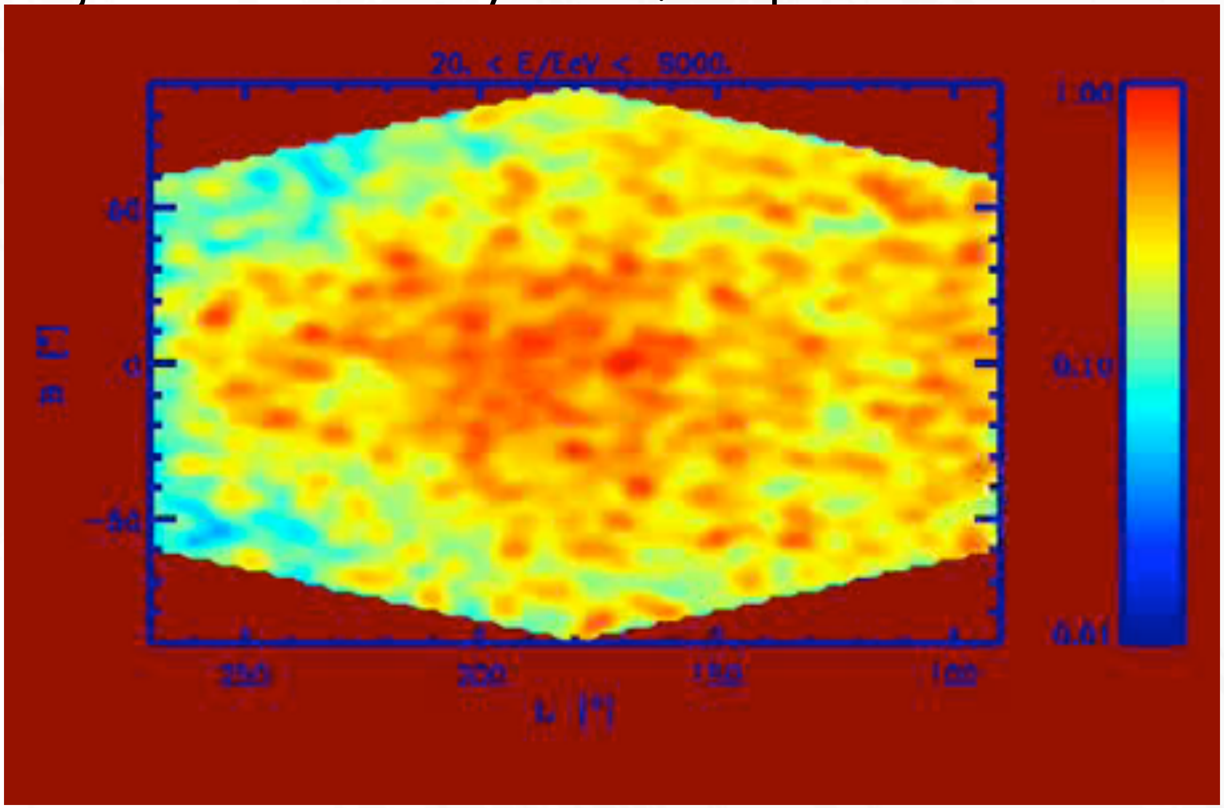

10^5 trajectories,
251 images between 20 and 300 EeV,
2.5° angular resolution

Isola, Lemoine, Sigl

Conclusions:

1.) Isotropy is inconsistent with only one source.
2.) Strong fields produce interesting lensing (clustering) effects.

The Universe is structured

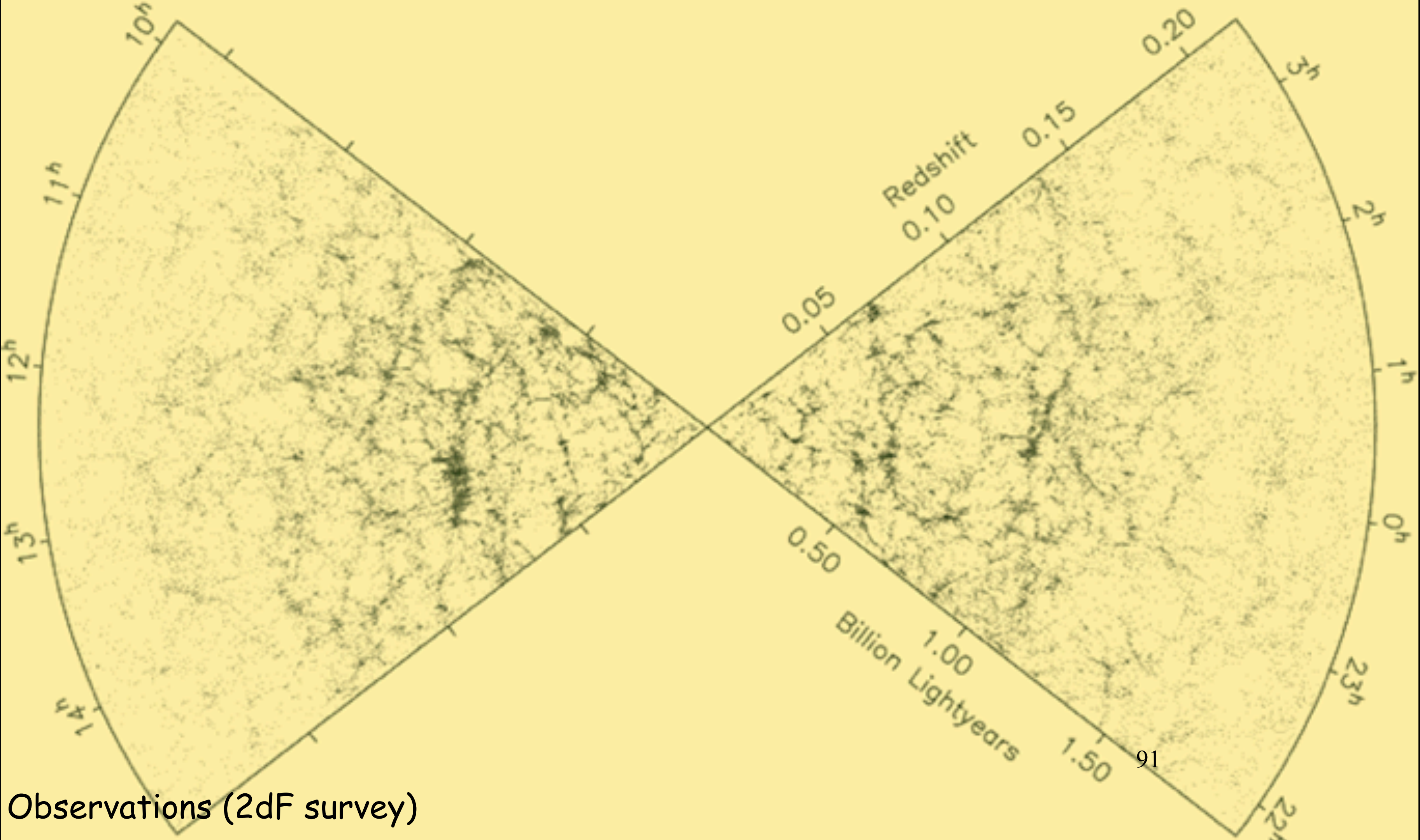

Observations (2dF survey)

The Universe is structured

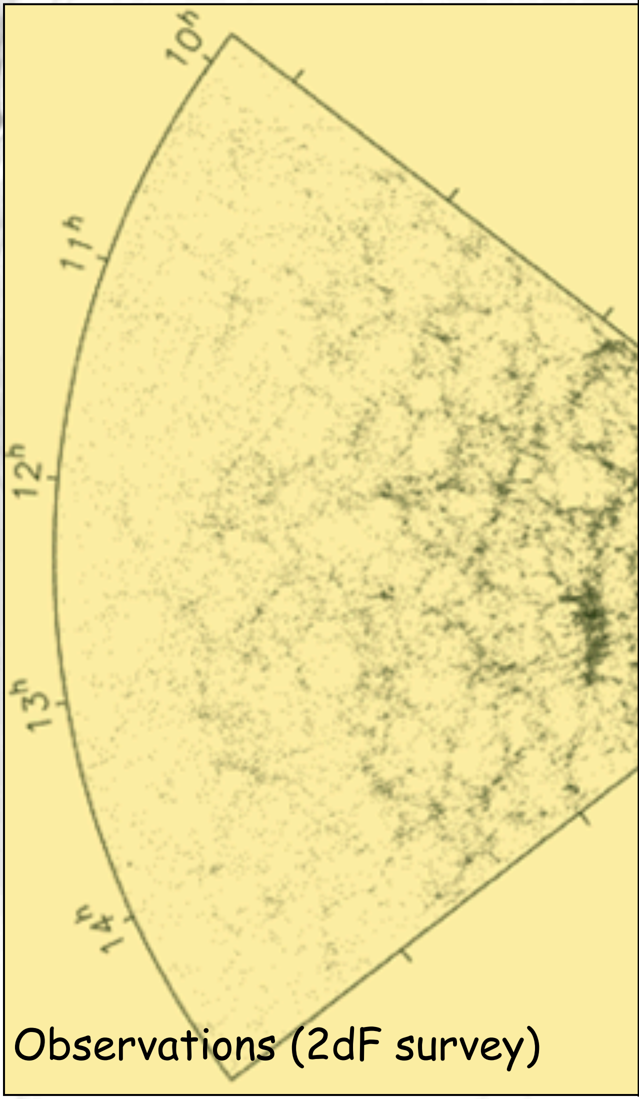

Observations (2dF survey)

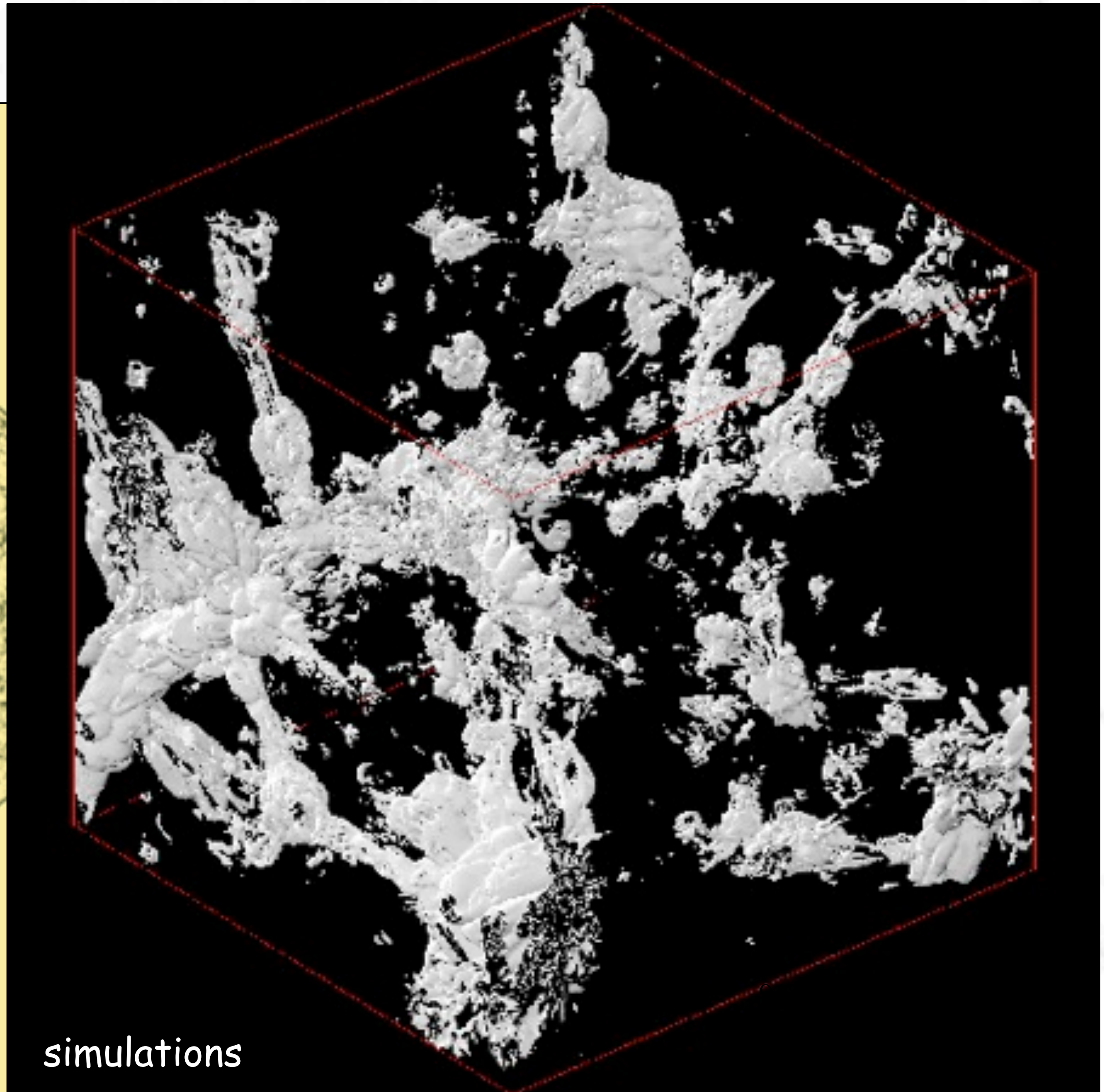

simulations

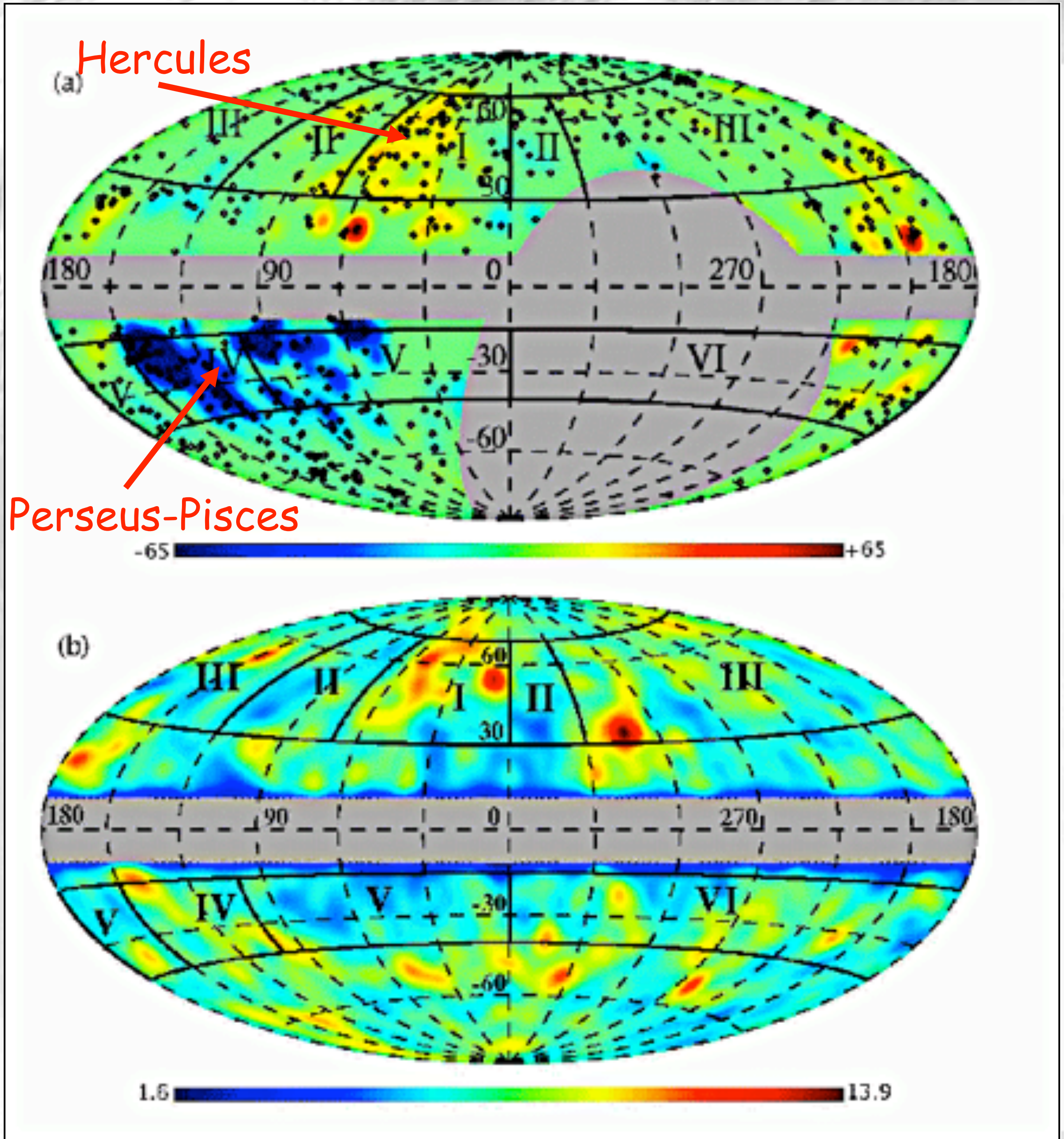

Smoothed rotation measure:
Possible signatures of ~0.1μG level on super-cluster scales!

Theoretical motivations from the Weibel instability which tends to drive field to fraction of thermal energy density

But need much more data from radio astronomy, e.g. Lofar, SKA

2MASS galaxy column density

92

Xu et al., astro-ph/0509826

Propagation in structured extragalactic magnetic fields

Scenarios of extragalactic magnetic fields using large scale structure simulations with magnetic fields reaching few micro Gauss in galaxy clusters.

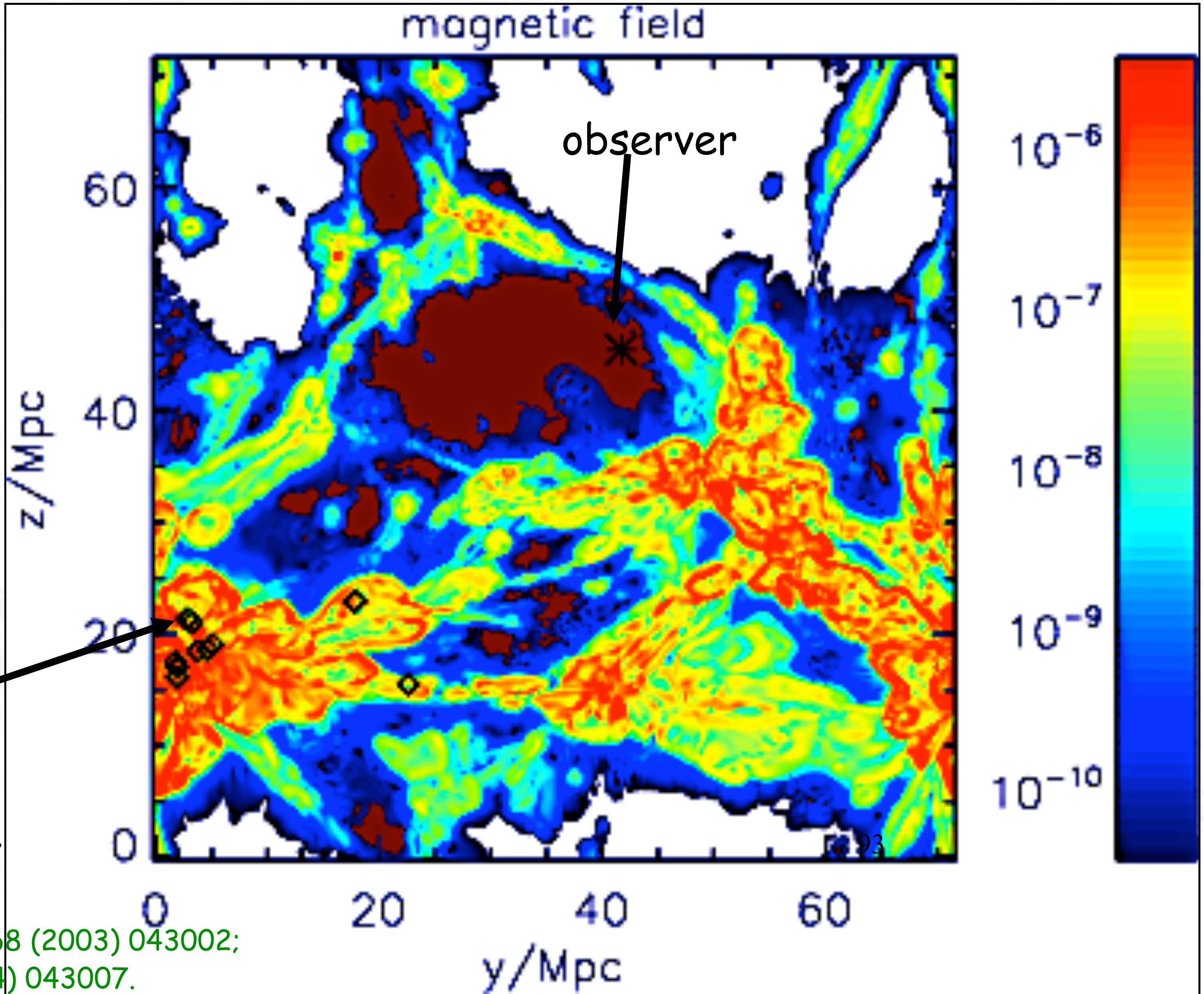

Discrete sources of density ~10^{-5} Mpc^{-3} follow baryon density, field at Earth ~10^{-11} G.

Sigl, Miniati, Ensslin, Phys.Rev.D 68 (2003) 043002; astro-ph/0309695; PRD 70 (2004) 043007.

The simulated sky above 4×10^{19} eV with structured sources of density 2.4×10^{-5} Mpc^{-3} : $\sim 2 \times 10^{5}$ simulated trajectories above 4×10^{19} eV.

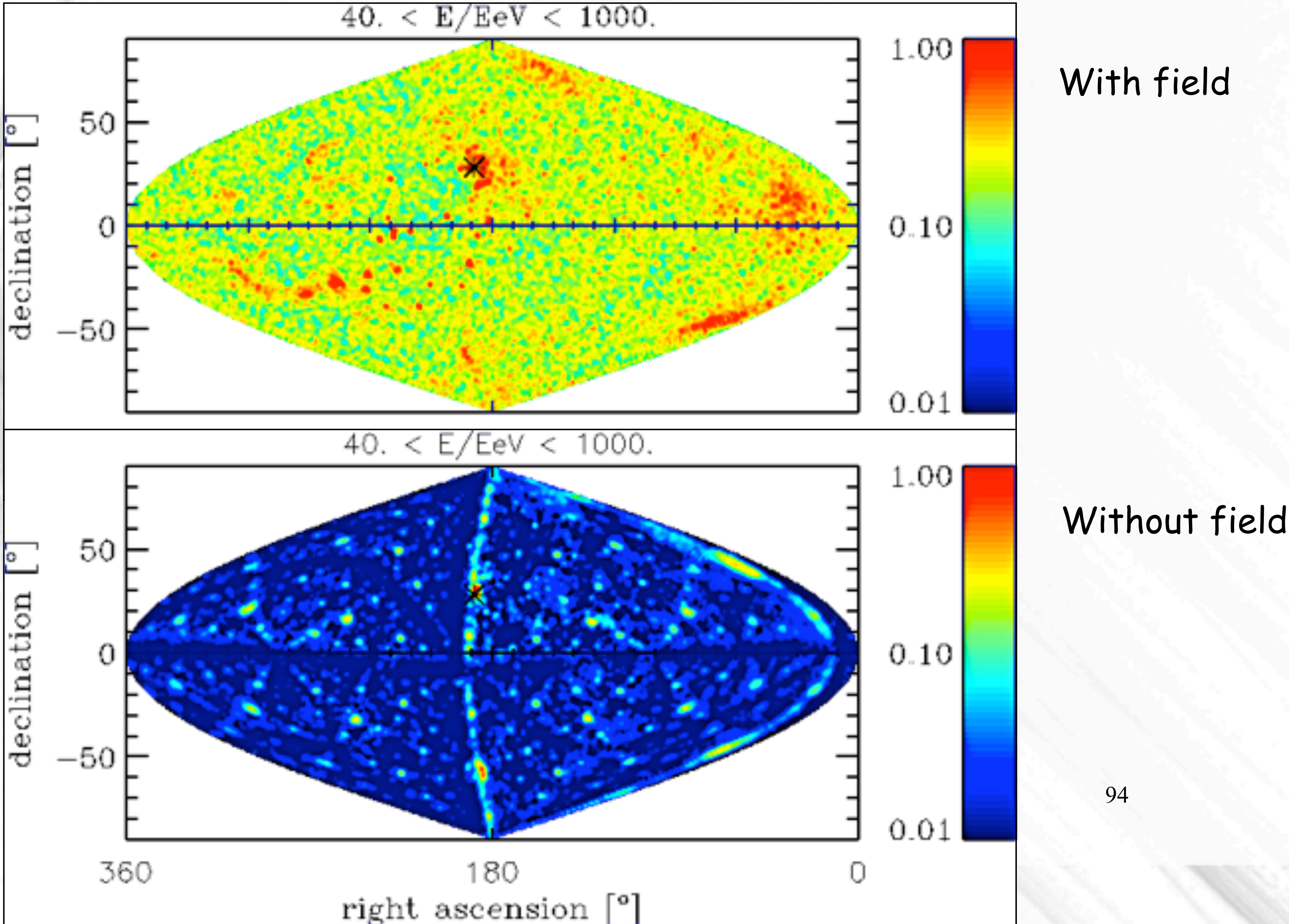

94

The simulated sky above 10^{20} eV with structured sources of density 2.4×10^{-5} Mpc^{-3} : ~2×10^{5} simulated trajectories above 10^{20} eV.

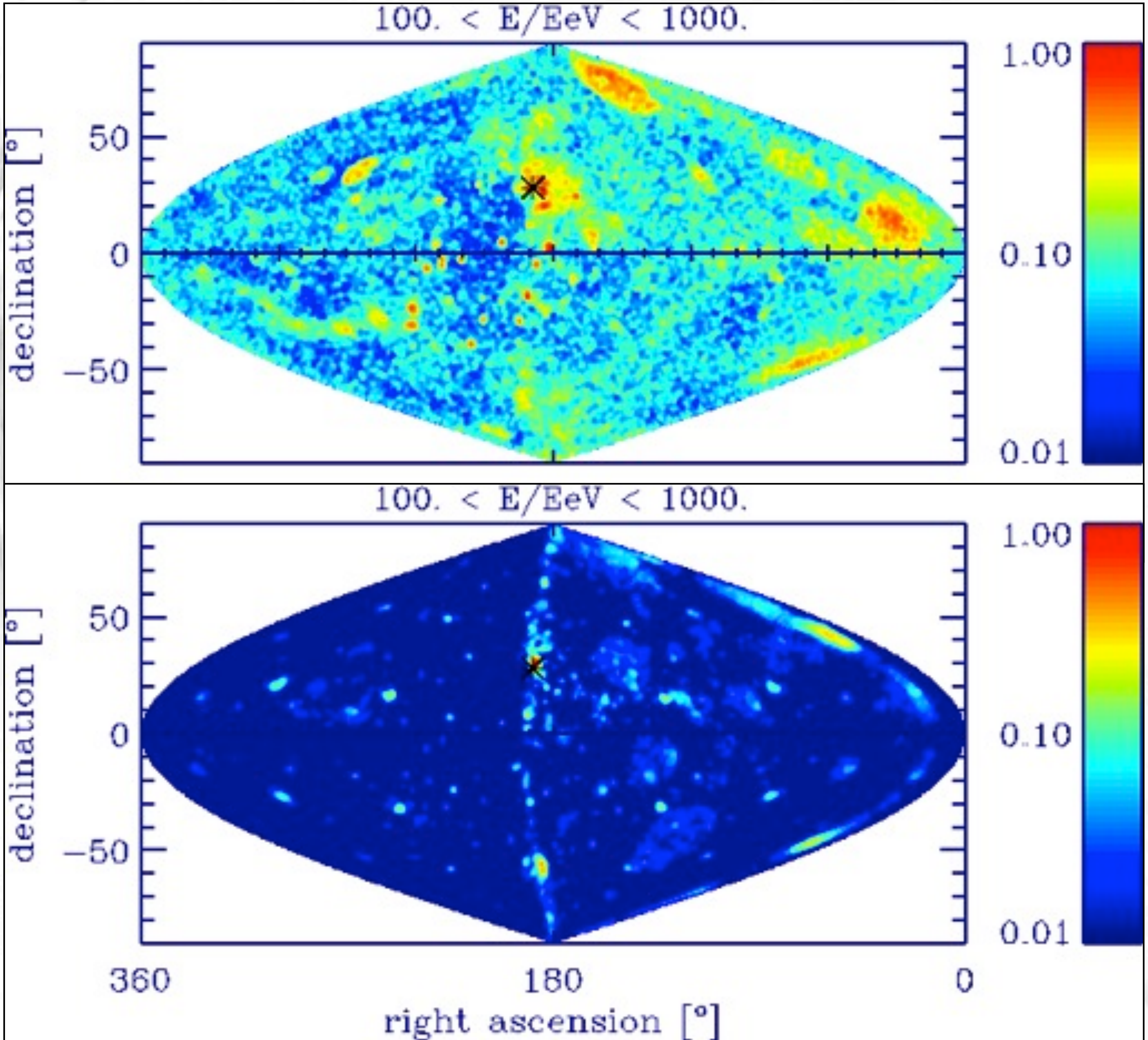

With field

Without field

95

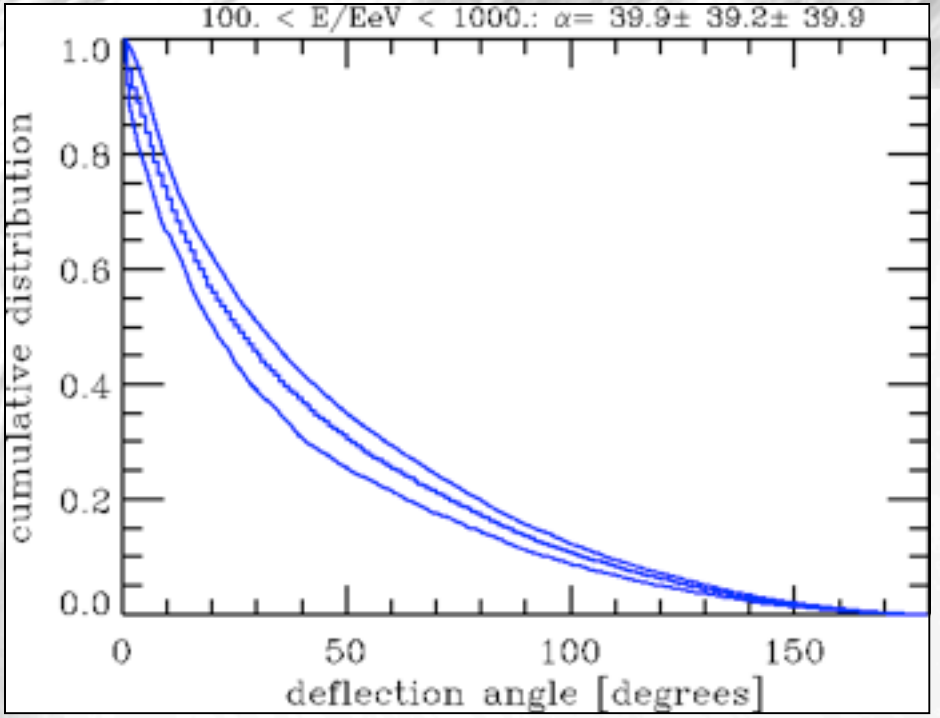

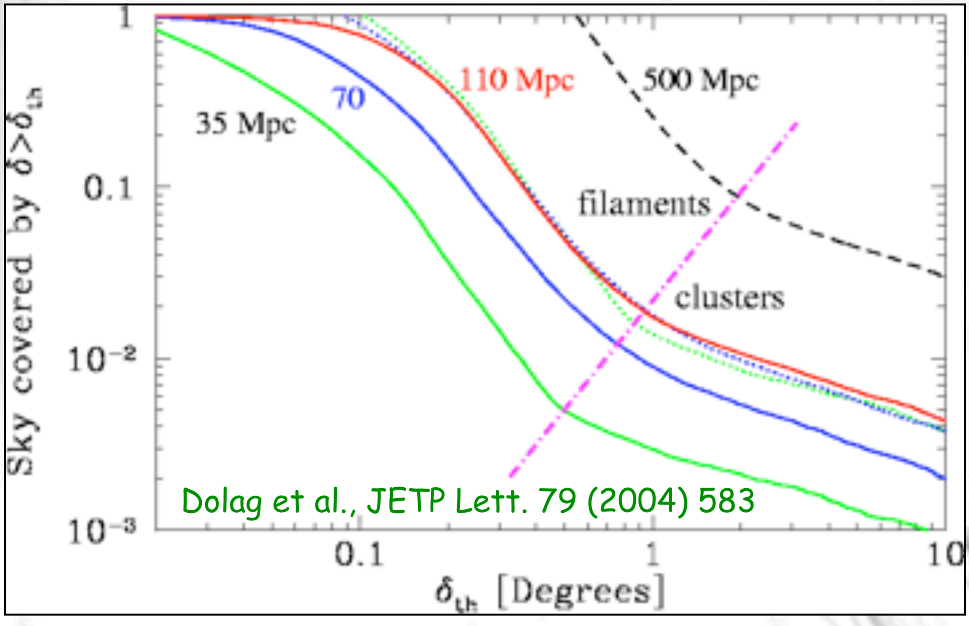

Cumulative deflection angle distributions for proton primaries

96

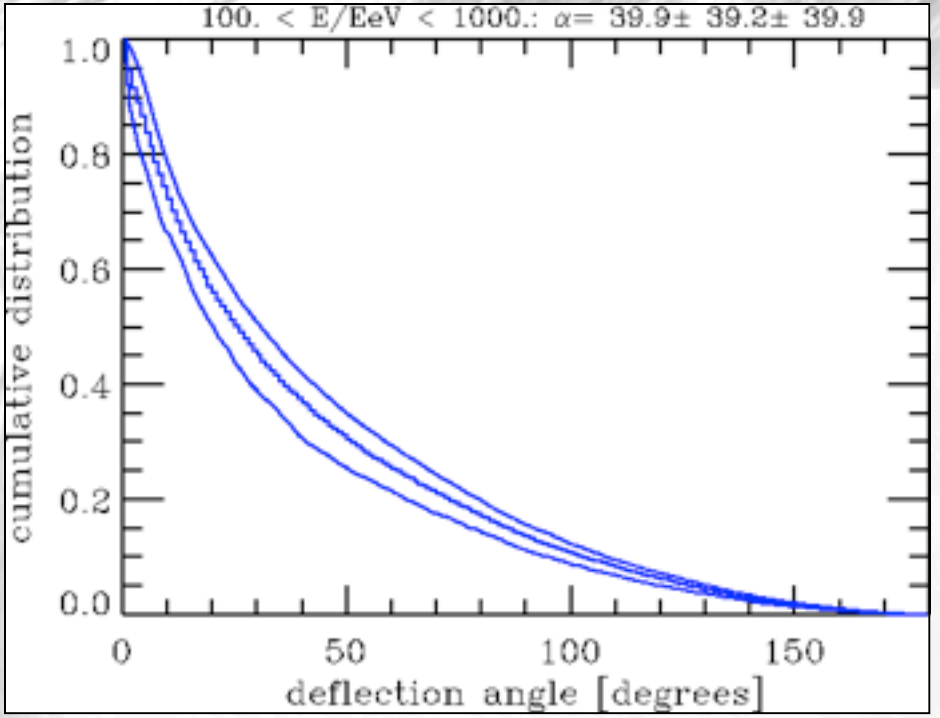

Deflection in magnetized structures surrounding the sources lead to off-sets of arrival direction from source direction up to >10 degrees up to 10^{20} eV in our simulations. This is contrast to Dolag et al., JETP Lett. 79 (2004) 583.

Particle astronomy not necessarily possible, especially for nuclei !

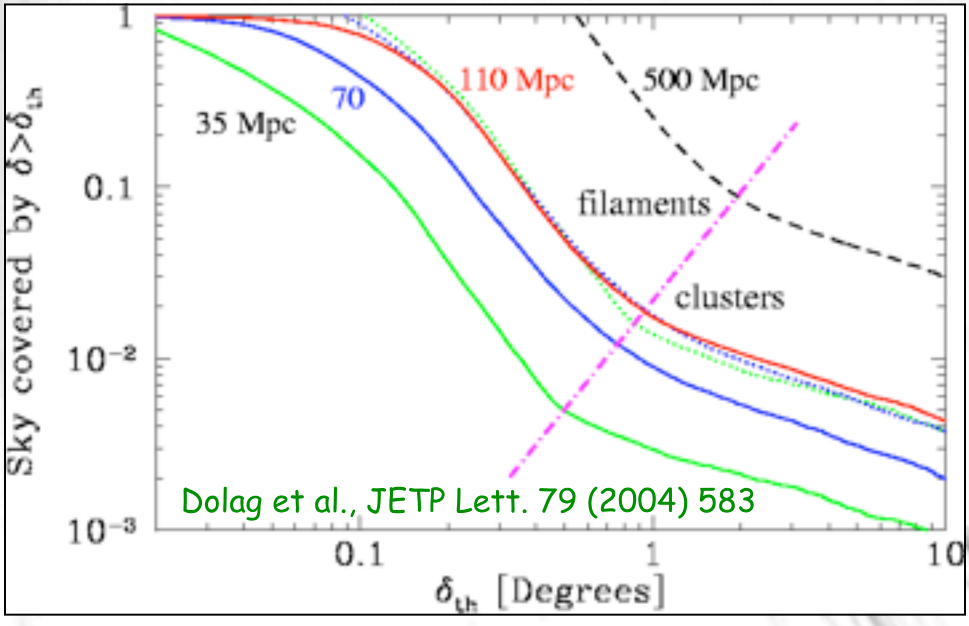

Cumulative deflection angle distributions for proton primaries

96

Recent results give intermediate and still significant deflections for proton primaries:

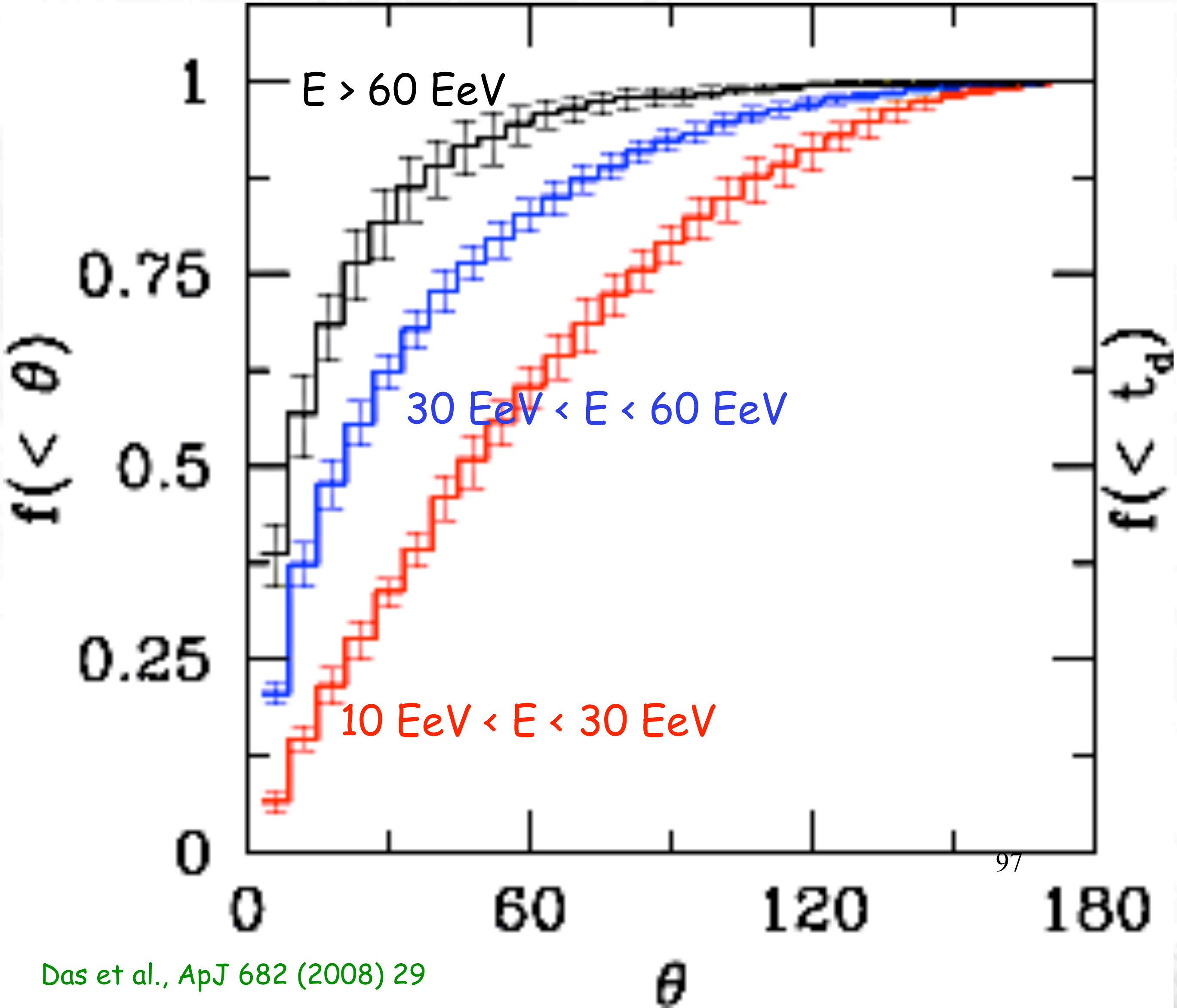

Das et al., ApJ 682 (2008) 29

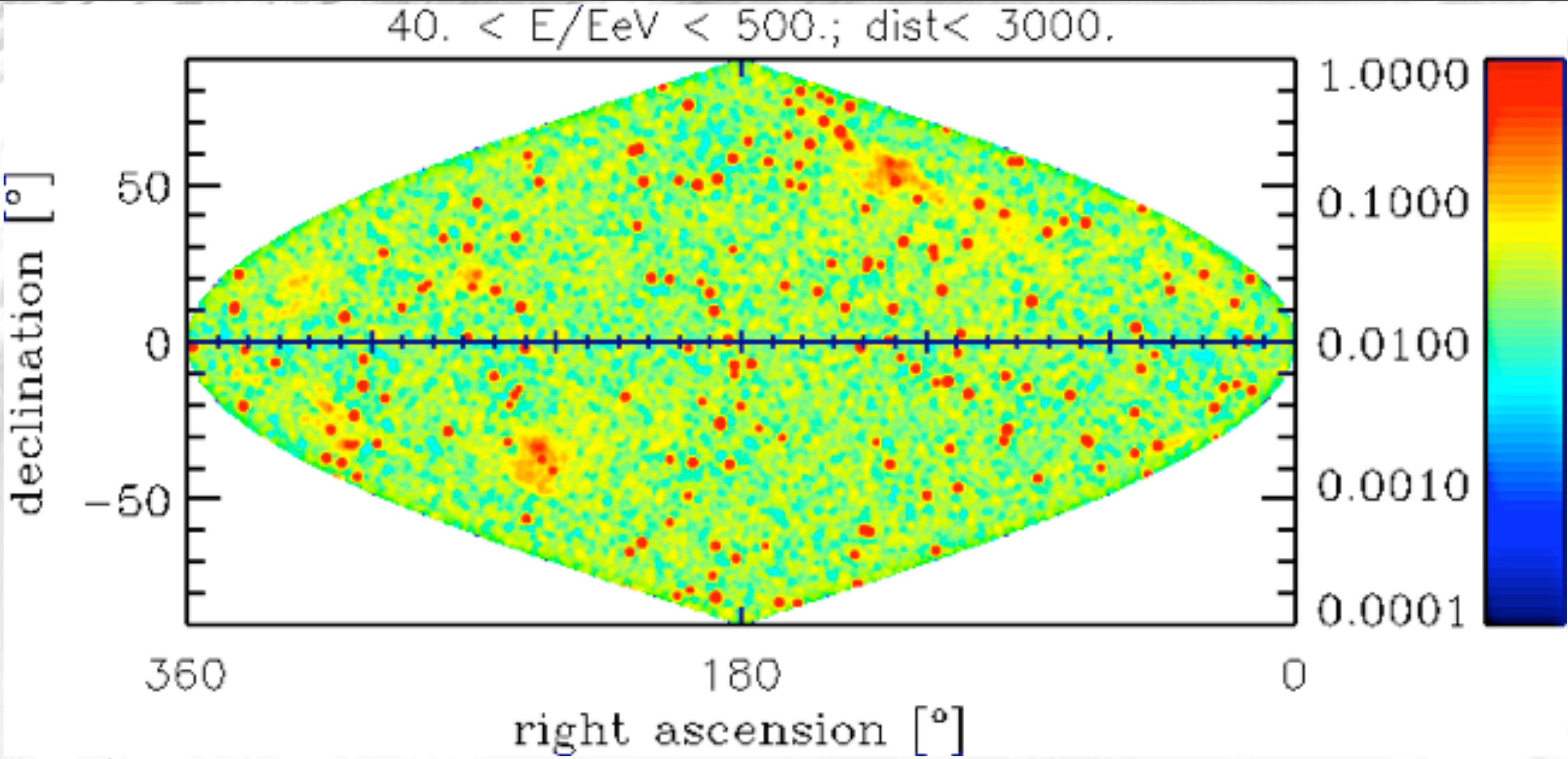

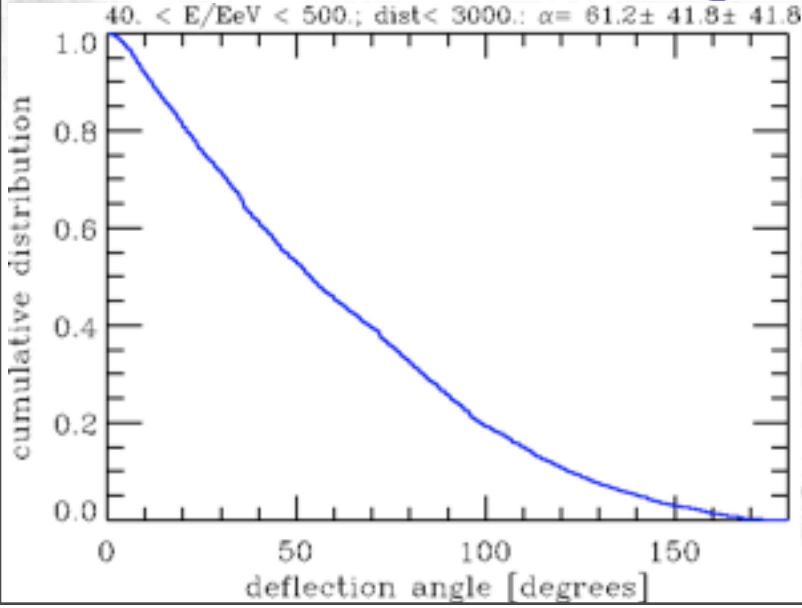

Sky distributions for iron primaries above 40 EeV, $E^{-2.2}$ injection up to 10^{22} eV

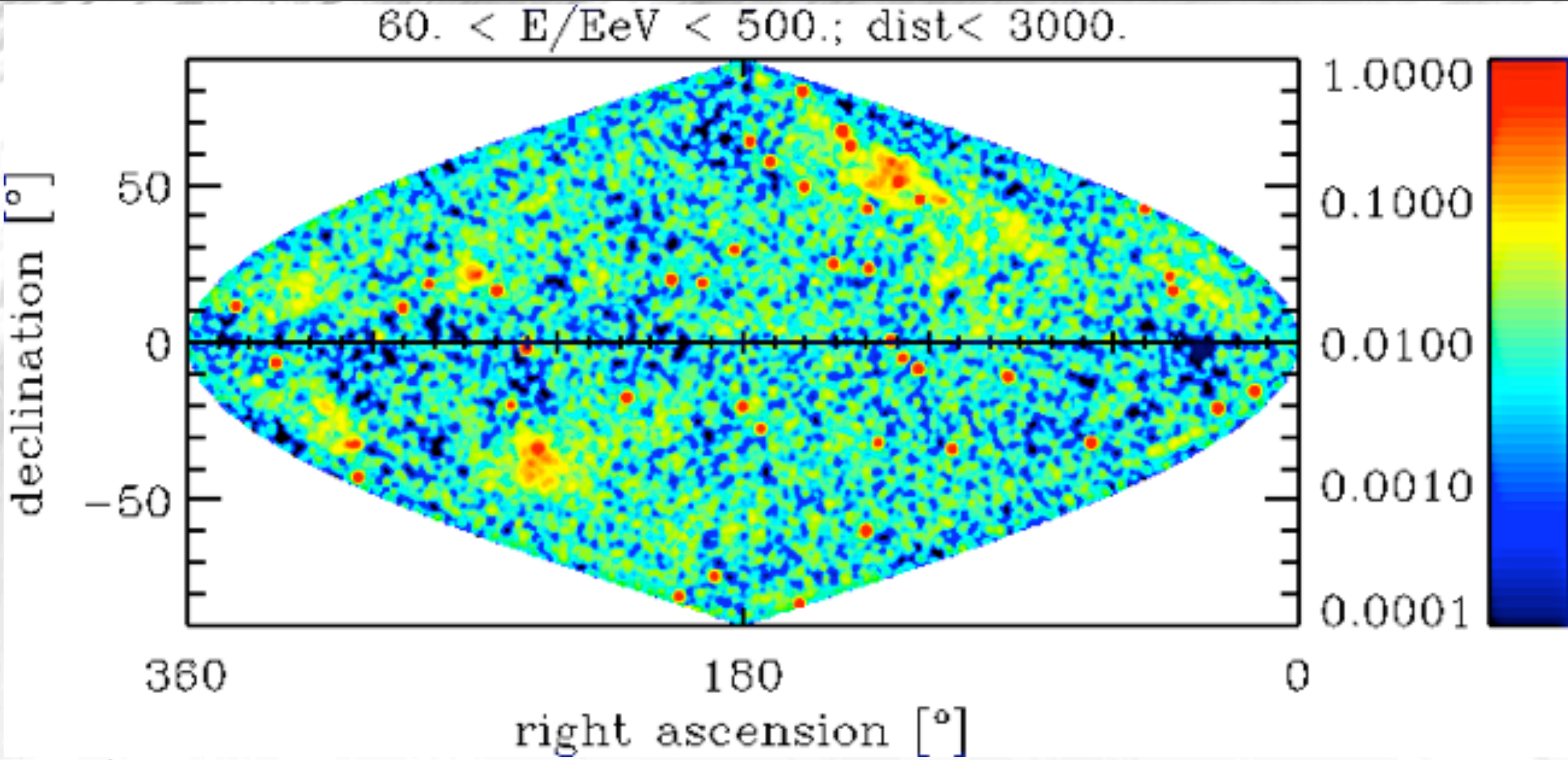

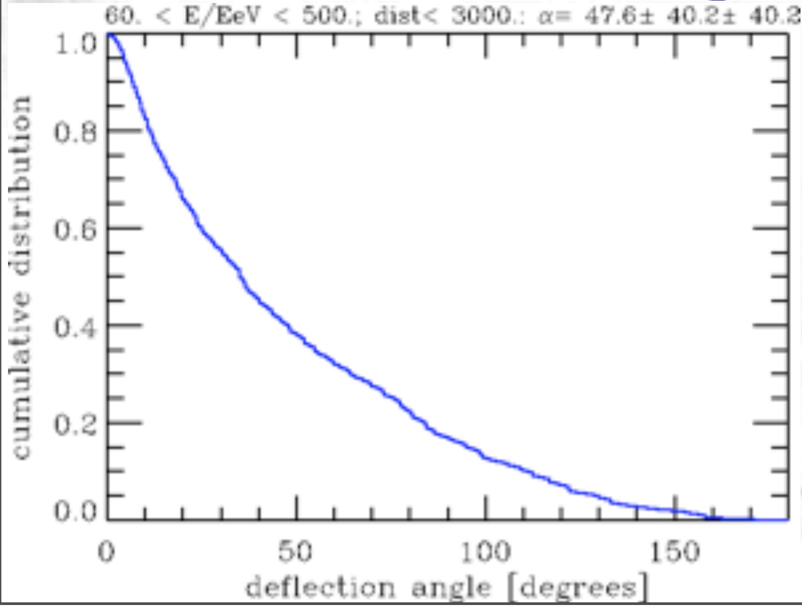

Sky distributions for iron primaries above 60 EeV, $E^{-2.2}$ injection up to 10^{22} eV

99

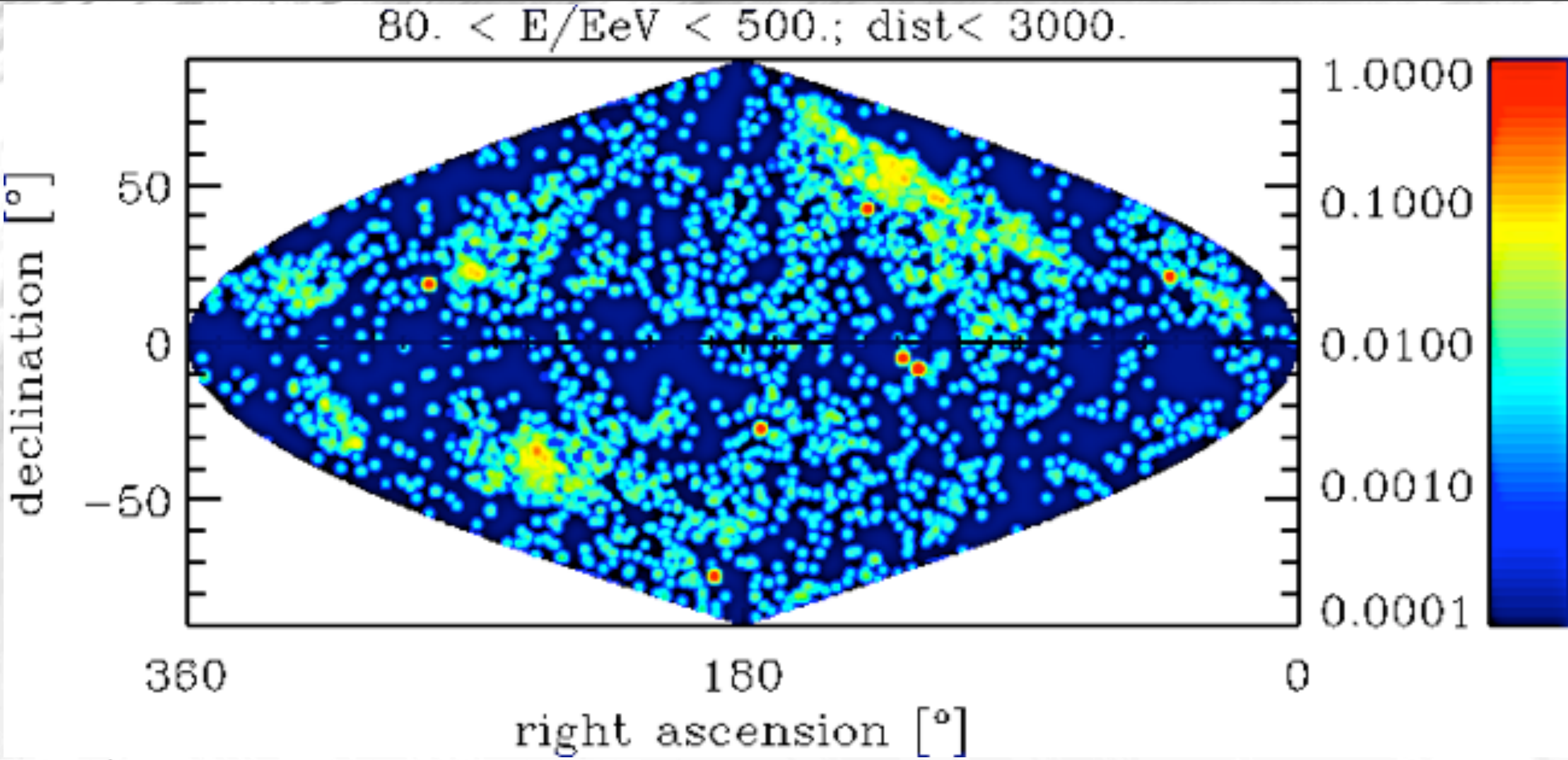

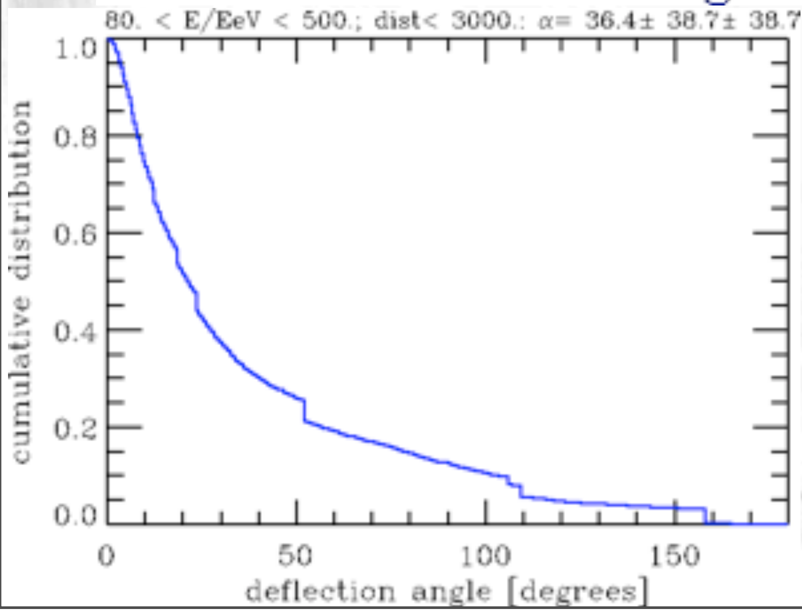

Sky distributions for iron primaries above 80 EeV, $E^{-2.2}$ injection up to 10^{22} eV

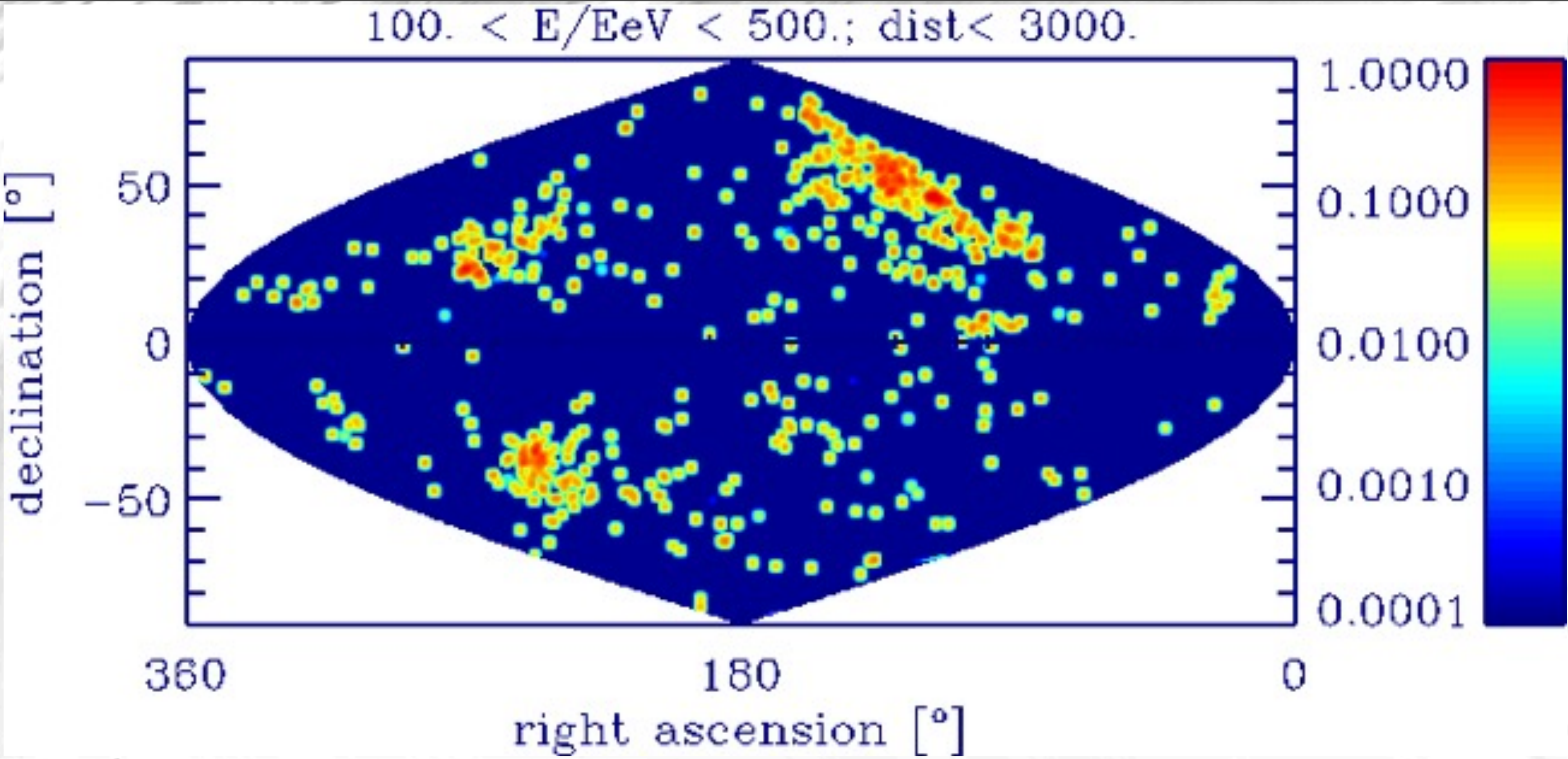

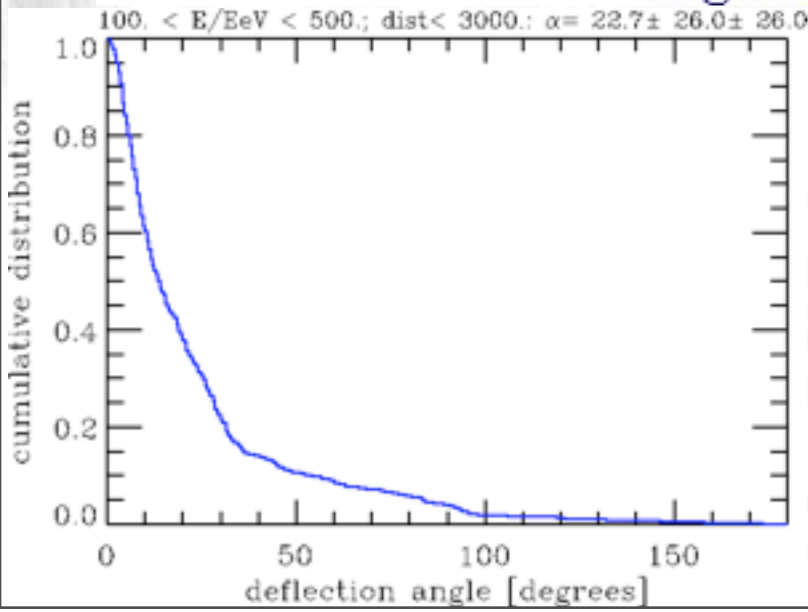

Sky distributions for iron primaries above 100 EeV, $E^{-2.2}$ injection up to 10^{22} eV

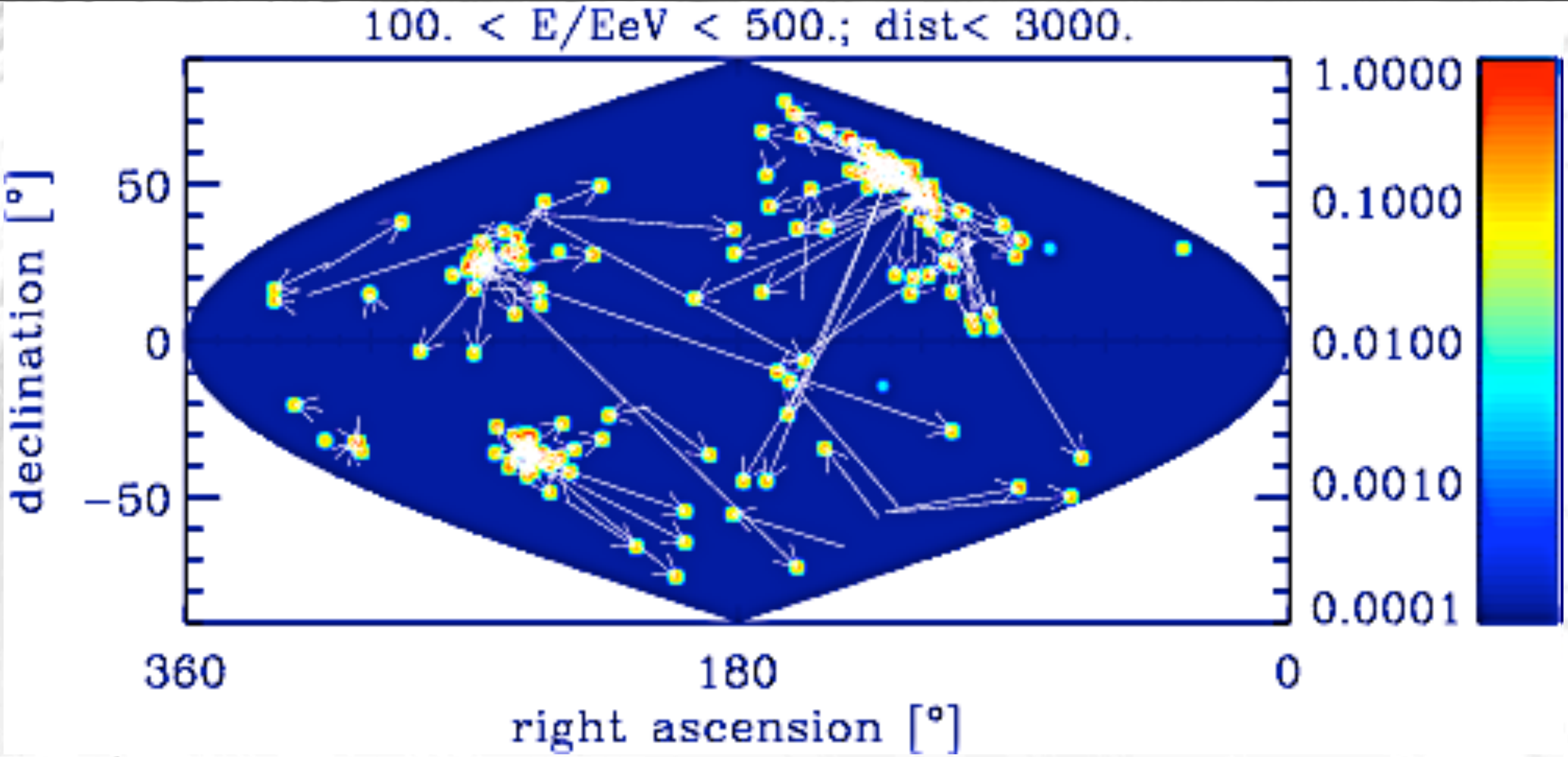

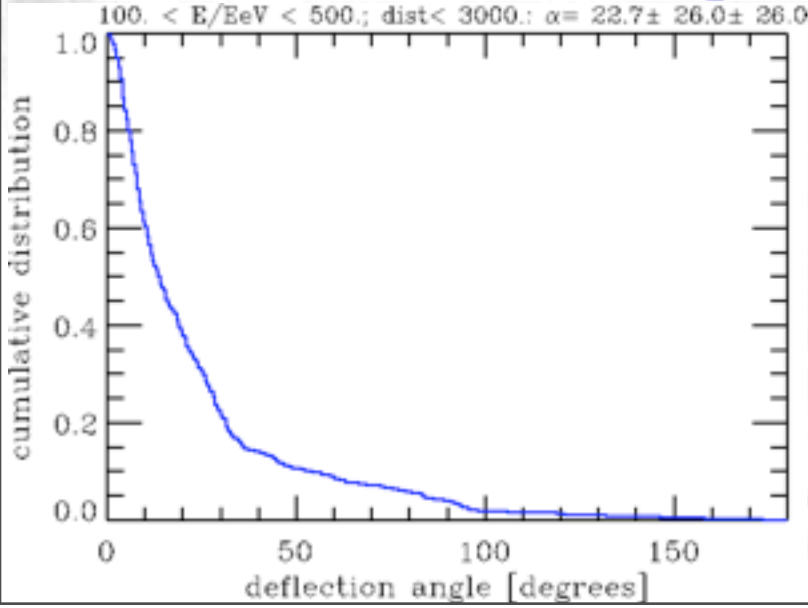

Sky distributions for iron primaries above 100 EeV, $E^{-2.2}$ injection up to 10^{22} eV

Conclusion:

A correleation with the local large scale structure is not necessarily destroyed by relatively large deflection, not even for iron, provided the field correlates with the large scale structure and deflection is mainly within that structure

It would mean that any correlation with specific sources does not identify particular sources, but only a source class that is distributed as the large scale structure

Instead of AGN it could be e.g. due to GRBs or magnetars

102

But galactic deflection is also large and in general does not align with with supergalactic plane

Injection of Solar Abundances for Magnetized Sources

For an injection spectrum $E^{-\alpha}$ elemental abundance at given energy E is modified to

$$\frac{dn_A}{dE}(E) = N\, x_A\, A^{\alpha-1}\, E^{-\alpha}$$

where x_A is the abundance at given energy per nucleon E/A.

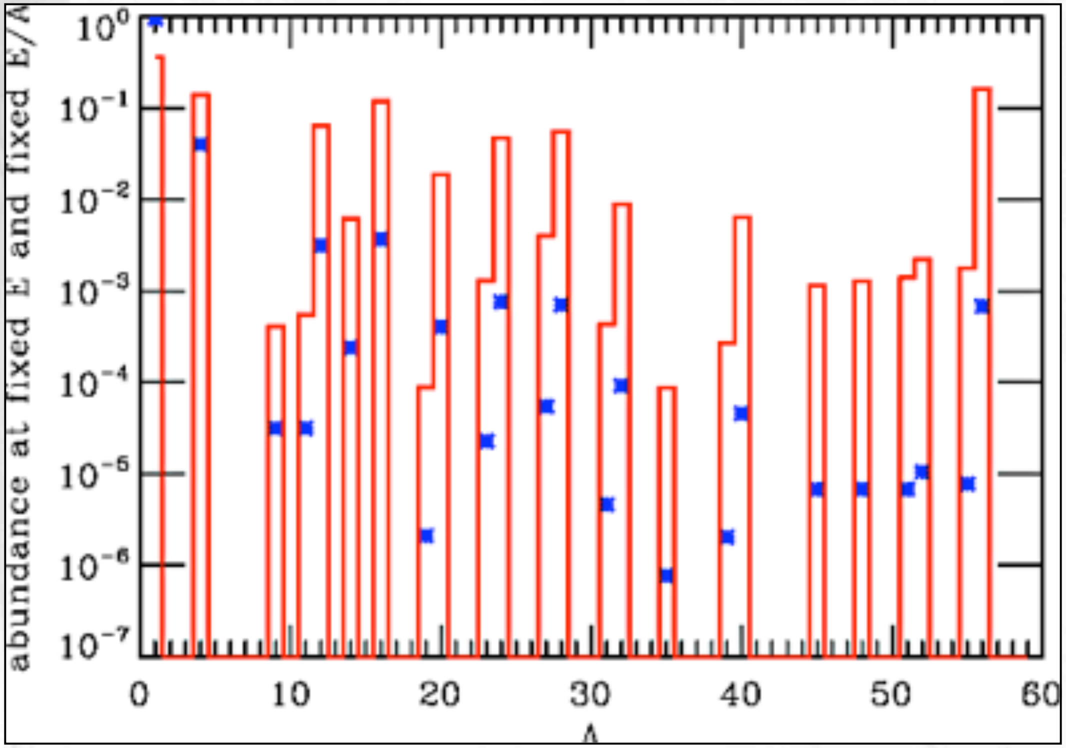

Composition at given E/A (blue), Composition at given E for an $E^{-2.6}$ injection spectrum (red).

Example: Acceleration of Mixed (Solar Metallicity) Composition at Cluster Accretion Shocks

Injection spectrum $E^{-1.7}$ with rigidity $E/Z < 5 \times 10^{18}$ eV (consistent with properties of cluster accretion shocks) and a source density ~ 2.4×10^{-6} Mpc^{-3}.

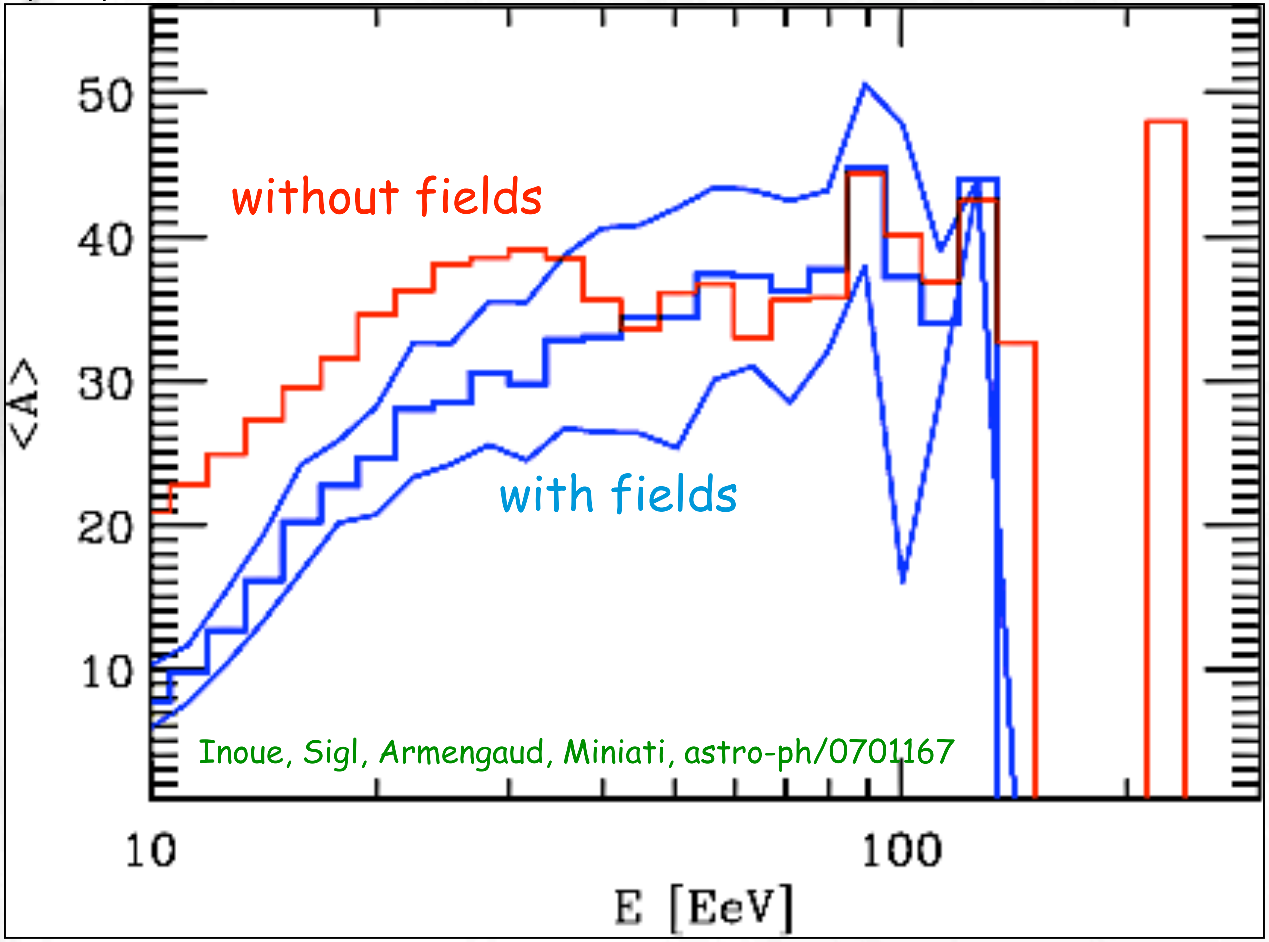

104

This scenario predicts an increasingly heavy composition at the highest energies.

A particular instance of the Mixed Composition Cluster Accretion Shocks Scenario

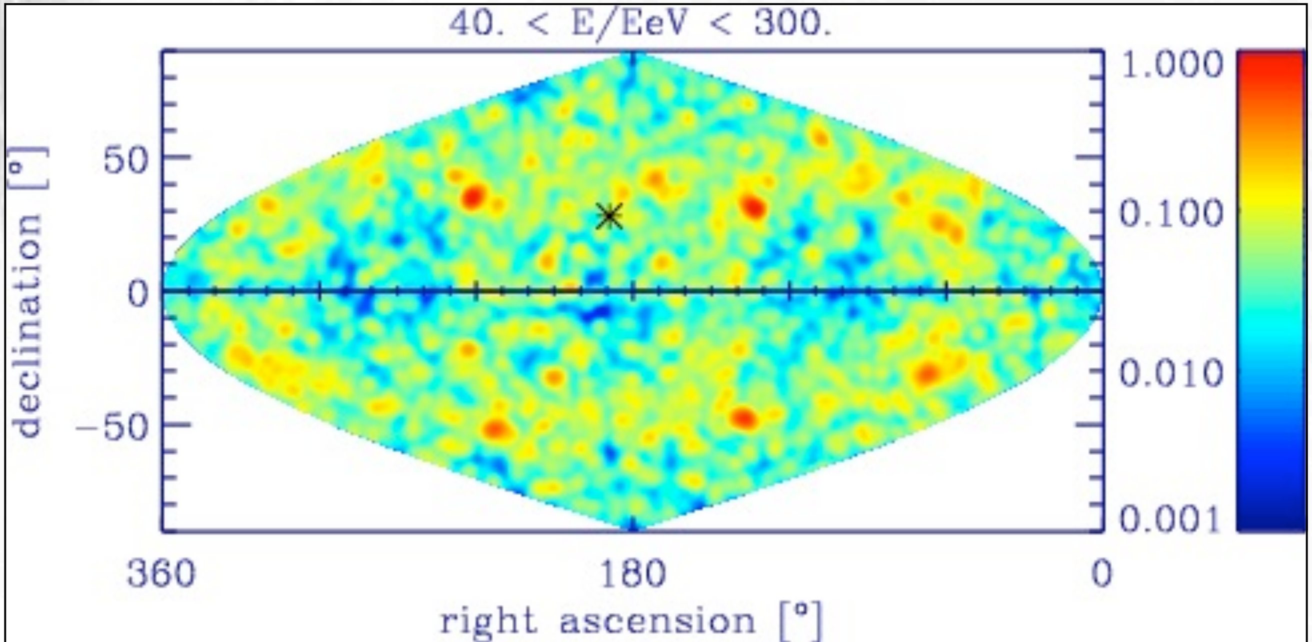

Without field: probably too anisotropic due to low source density

105

A particular instance of the Mixed Composition Cluster Accretion Shocks Scenario

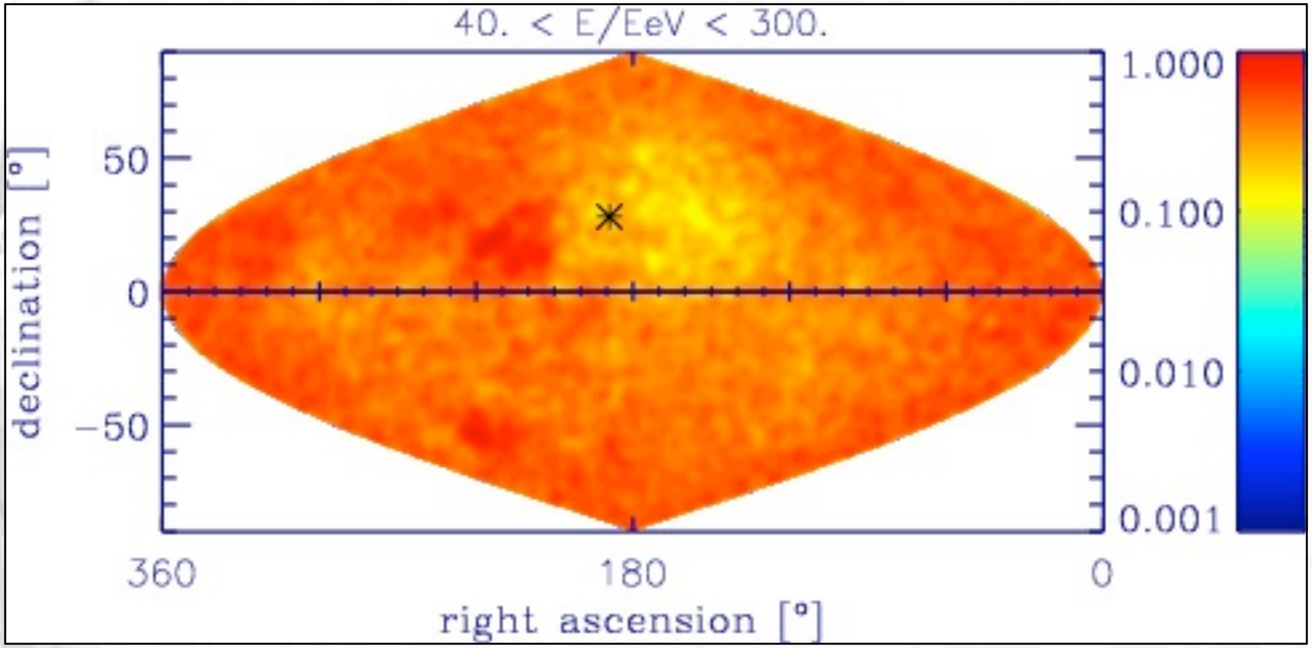

With field:

Almost isotropic; would be consistent with HiRes observations !

A particular instance of the Mixed Composition Cluster Accretion Shocks Scenario

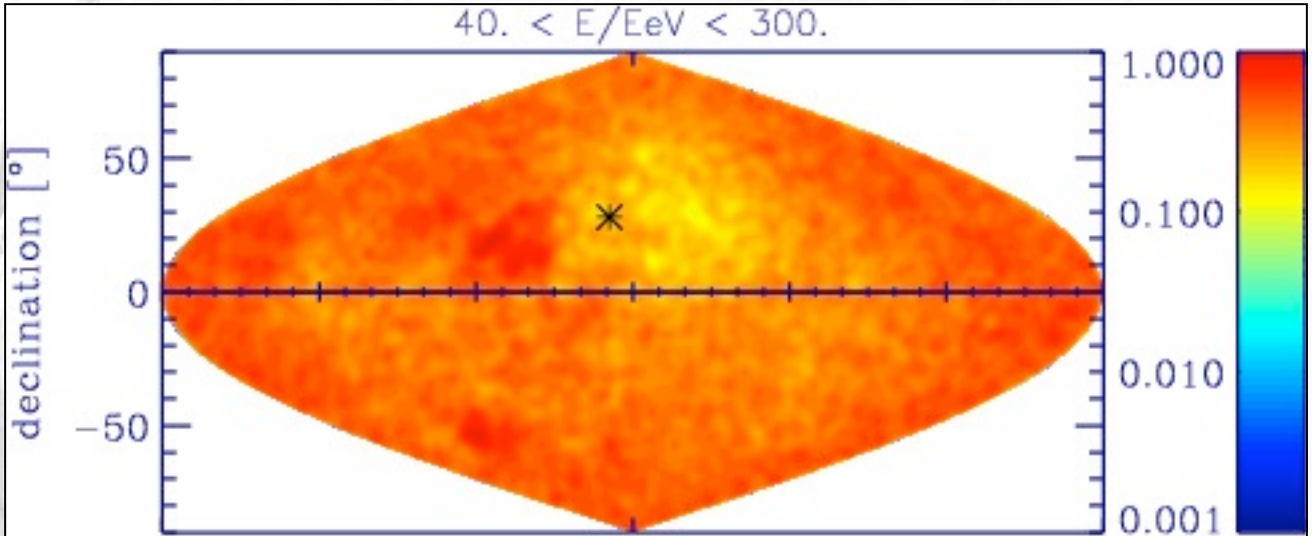

With field:

Almost isotropic; would be consistent with HiRes observations !

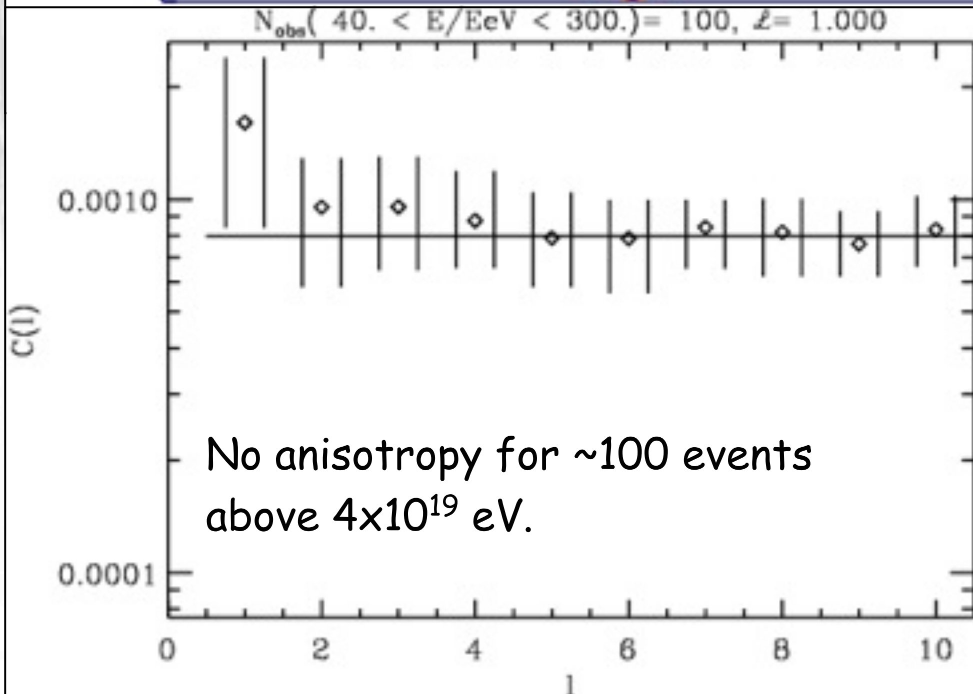

No anisotropy for ~100 events above 4×10^{19} eV.

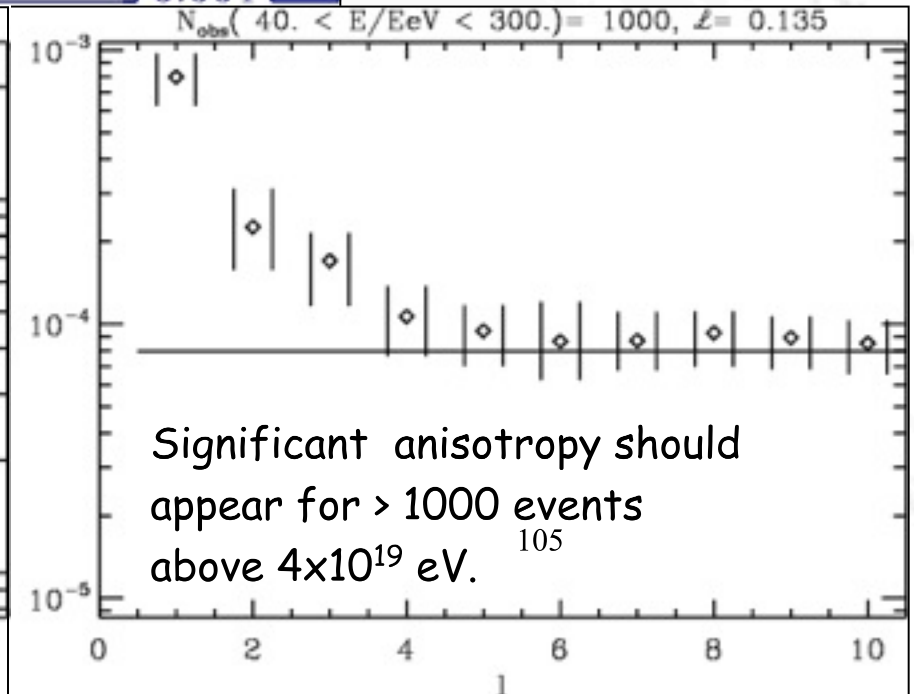

Significant anisotropy should appear for > 1000 events above 4×10^{19} eV.

105

Heavy Nuclei: Structured Fields and Individual Sources

Spectra and Composition of Fluxes from Single Discrete Sources considerably depend on Source Magnetization, especially for Sources within a few Mpc.

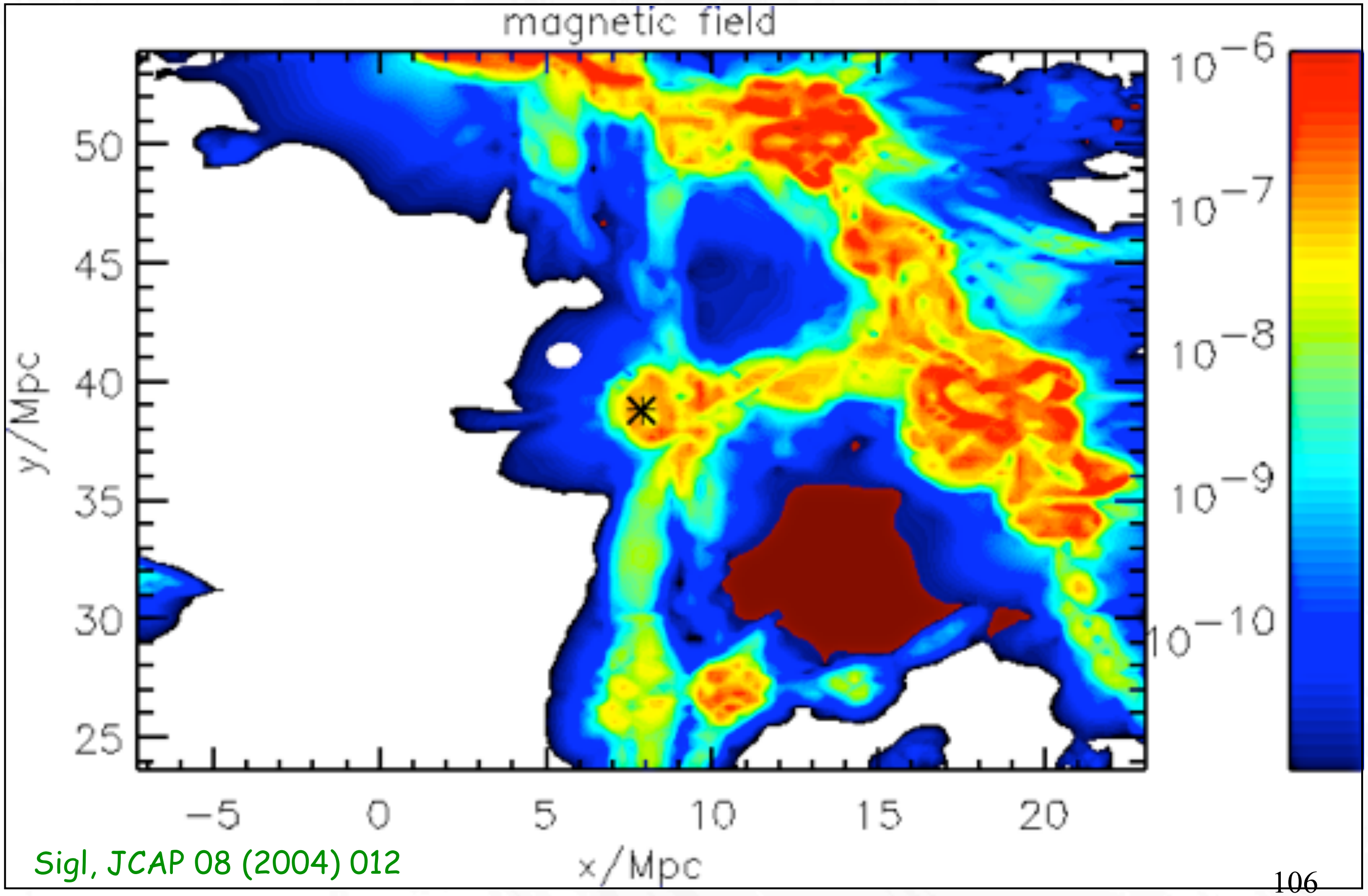

Sigl, JCAP 08 (2004) 012

106

Source in the center; weakly magnetized observer modelled as a sphere shown in white at 3.3 Mpc distance.

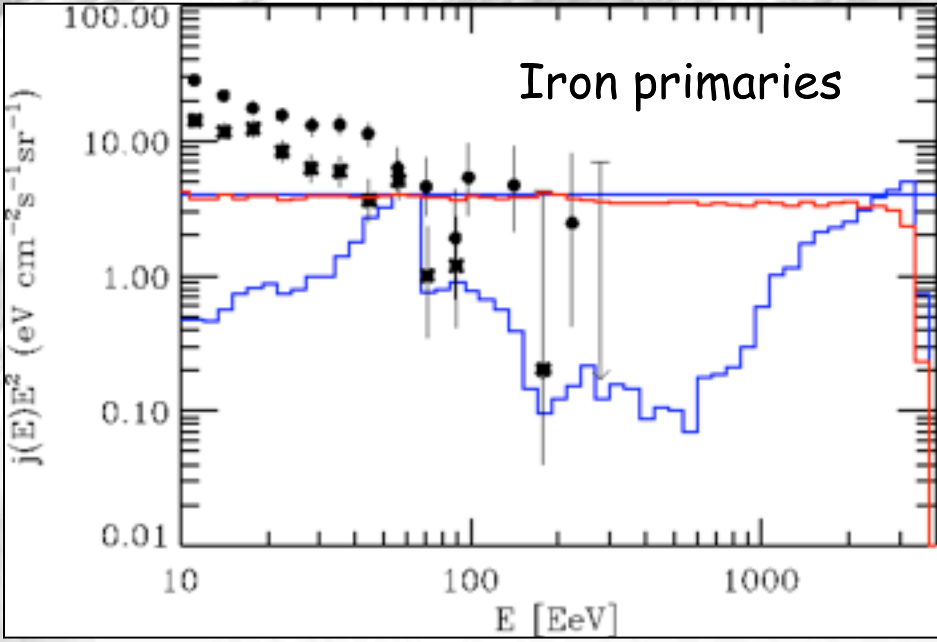

With field = blue

Without field = red

Injection spectrum = horizontal line

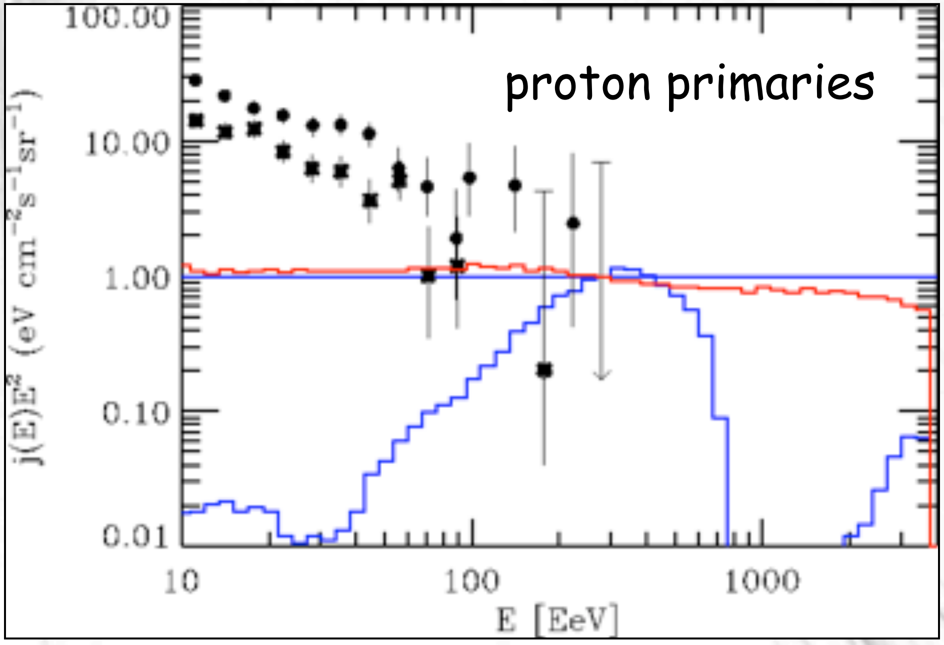

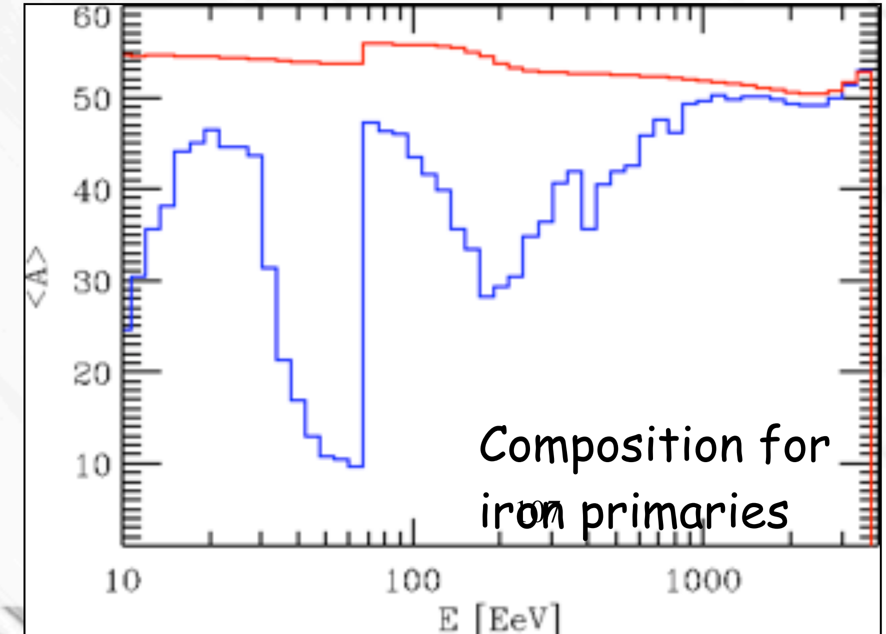

Importance of deflection obvious from comparing energy loss/spallation time scales with delay times

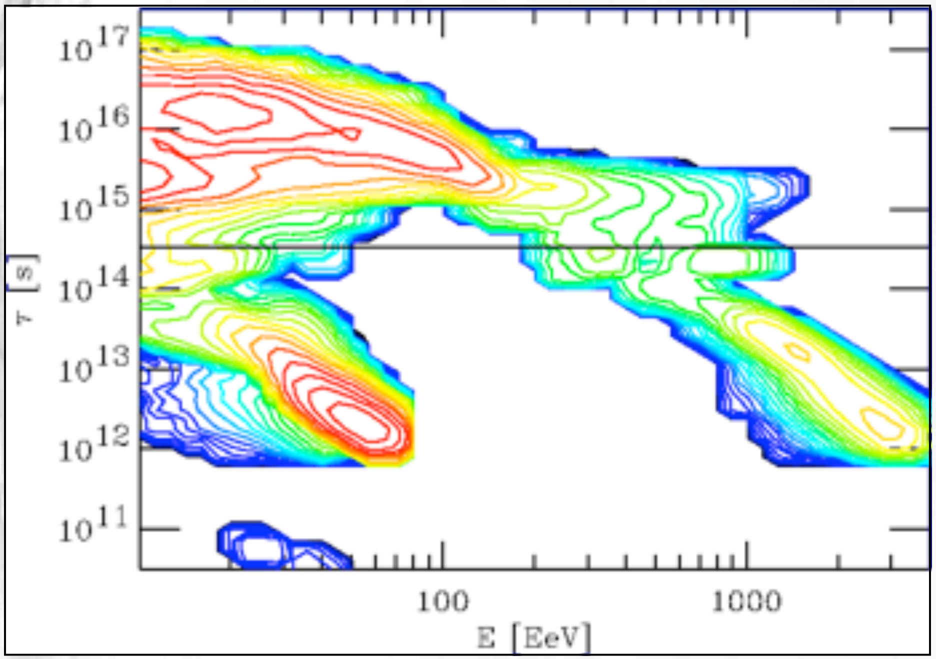

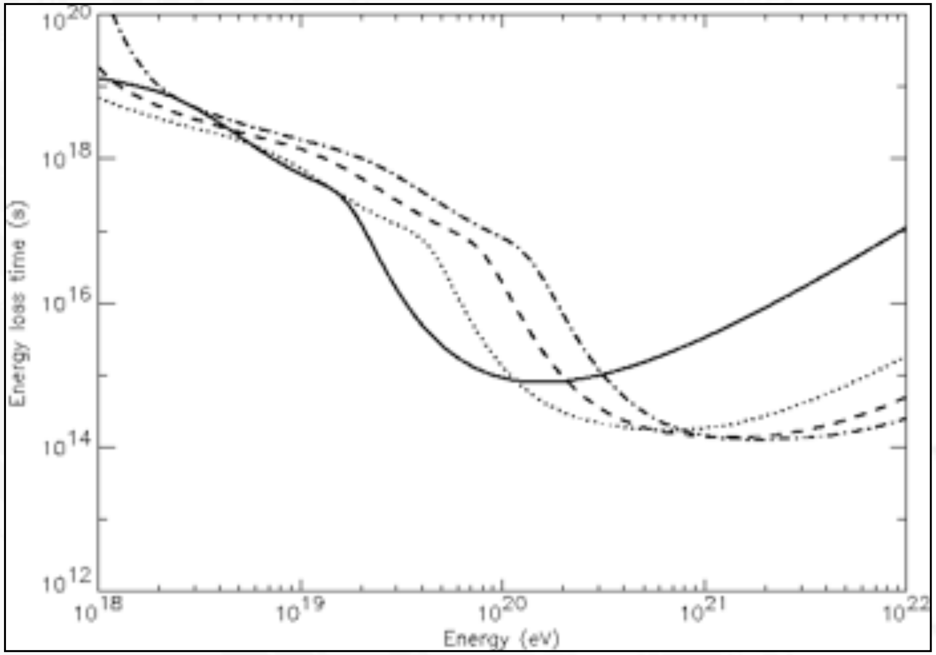

horizontal line=straight line propagation time

low delay-time spike at ~50 EeV due to spallation nucleons produced outside source field.

Energy loss times for helium (solid), carbon (dotted), silicon (dashed), and iron (dash-dotted).

Discrete Extragalactic High Energy Neutrino Sources

Rough estimate of neutrino flux from hadronic AGN jets: The "proton blazar"

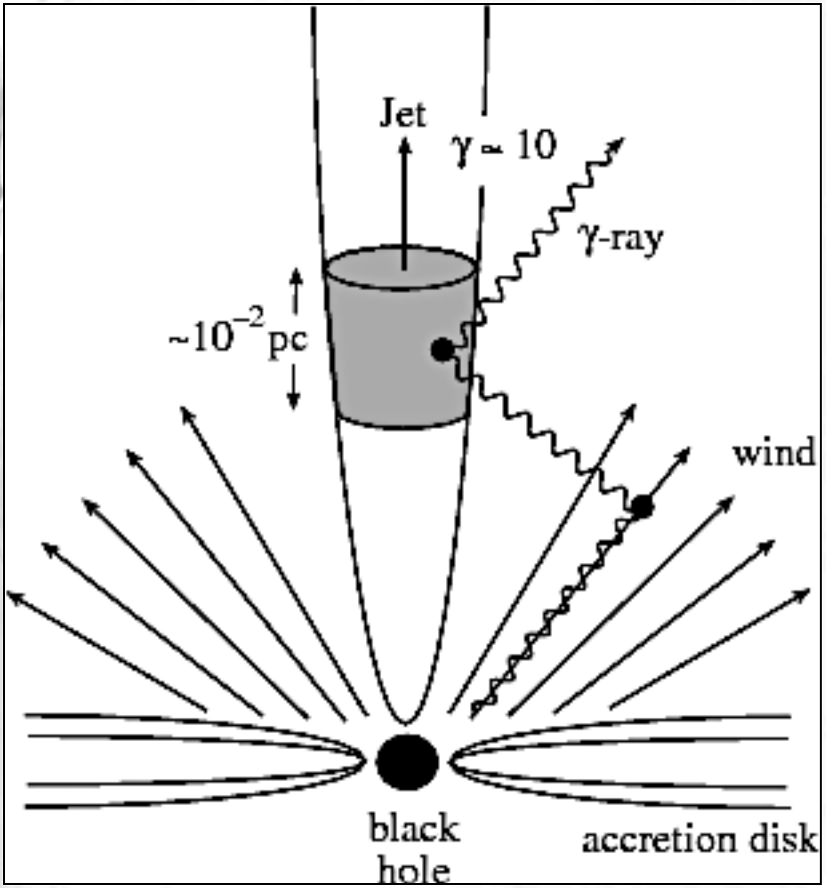

Following
Halzen and Zas, Astrophys.J. 488 (1997) 669

1. Size of accelerators $R \sim \Gamma T$, where jet boost factor $\Gamma \sim 10$ and duration of observed bursts $T \sim 1$ day

110

2. Magnetic field strength in jet $B^2 \sim \rho_{electron} \sim 1$ erg cm^{-3} (equipartition)

3. "Hillas condition" on maximal proton energy $E_{max} \sim eBR$ and from $p\gamma \to N\pi$ kinematics $E_{max,\nu} \sim 0.1\, E_{max} \sim 10^{18}$ eV.

4. Neutrino luminosity related to γ-ray luminosity by $L_\nu \sim 3L_\gamma/13$ from $p\gamma \to N\pi$ kinematics

5. Assume proton spectrum $dN_p/dE_p \propto E_p^{-2-\epsilon}$; γ–ray spectrum $dN_\gamma/d\epsilon \propto \epsilon^{-2-\alpha}$.
If jet is optically thin against $p\gamma$ then

$$\frac{dN_\nu}{dE_\nu} \propto \frac{dN_p}{dE_p}(10\,E_\nu)\int_{\epsilon_\gamma^{\rm thr}} d\epsilon_\gamma \frac{dN_\gamma}{d\epsilon_\gamma} \propto E_\nu^{-2-\epsilon}(\epsilon_\gamma^{\rm thr})^{-1-\alpha} \propto E_\nu^{-1-\epsilon+\alpha},$$

6. Combine with normalization:

$$\frac{dN_\nu}{dE_\nu} \sim \frac{3}{13}\frac{L_\gamma}{E_{\max,\nu}}\frac{1-\epsilon+\alpha}{E_\nu}\left(\frac{E_\nu}{E_{\max,\nu}}\right)^{-\epsilon+\alpha}.$$

7. Fold with luminosity function of AGNs in GeV γ-rays.

Diffuse Neutrino fluxes from AGN jets

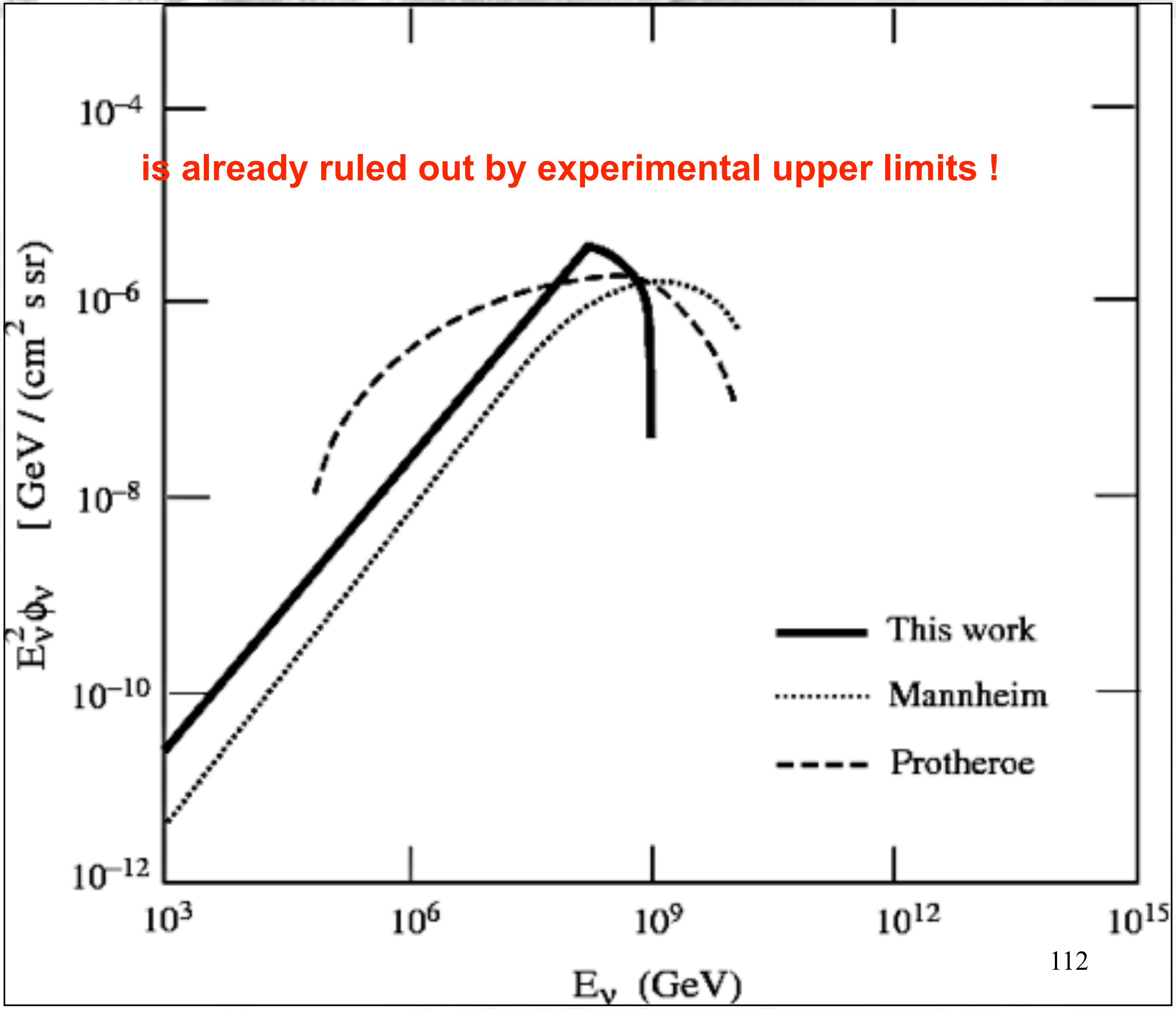

Halzen and Zas, Astrophys.J. 488 (1997) 669

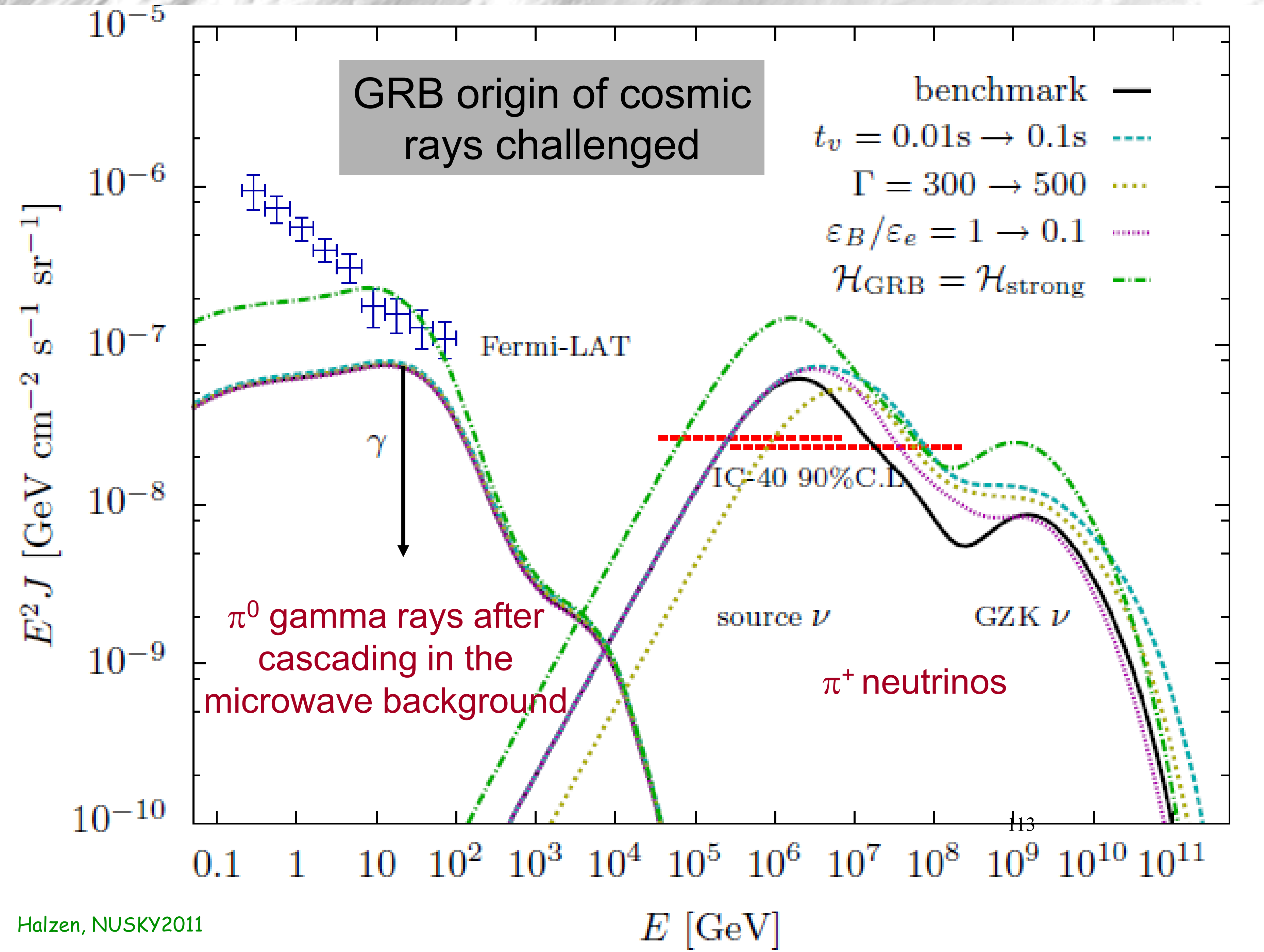

Halzen, NUSKY2011

The „grand unified" neutrino energy flux spectrum

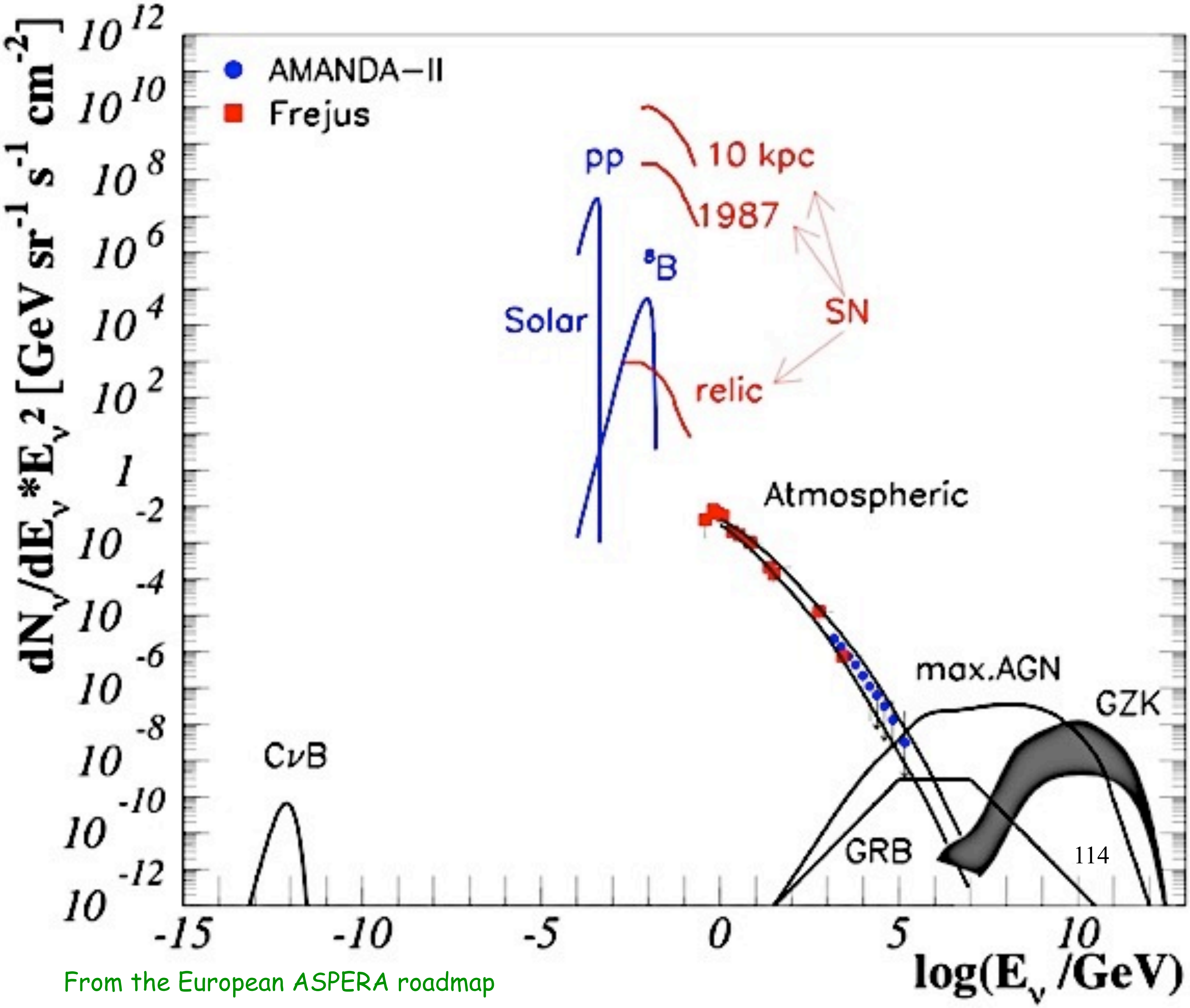

From the European ASPERA roadmap

The „grand unified“ differential neutrino number spectrum

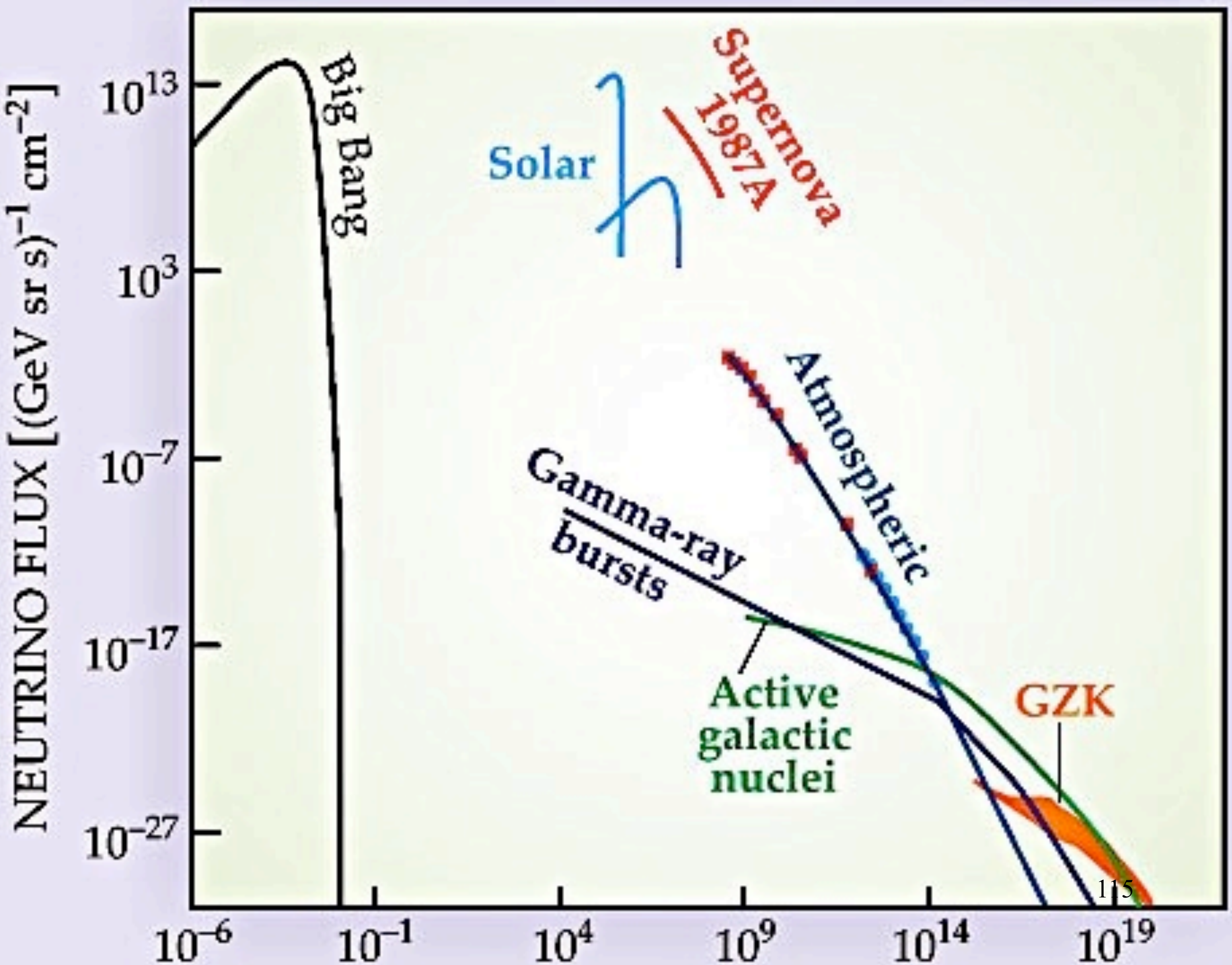

From Physics Today

Summary of neutrino production modes

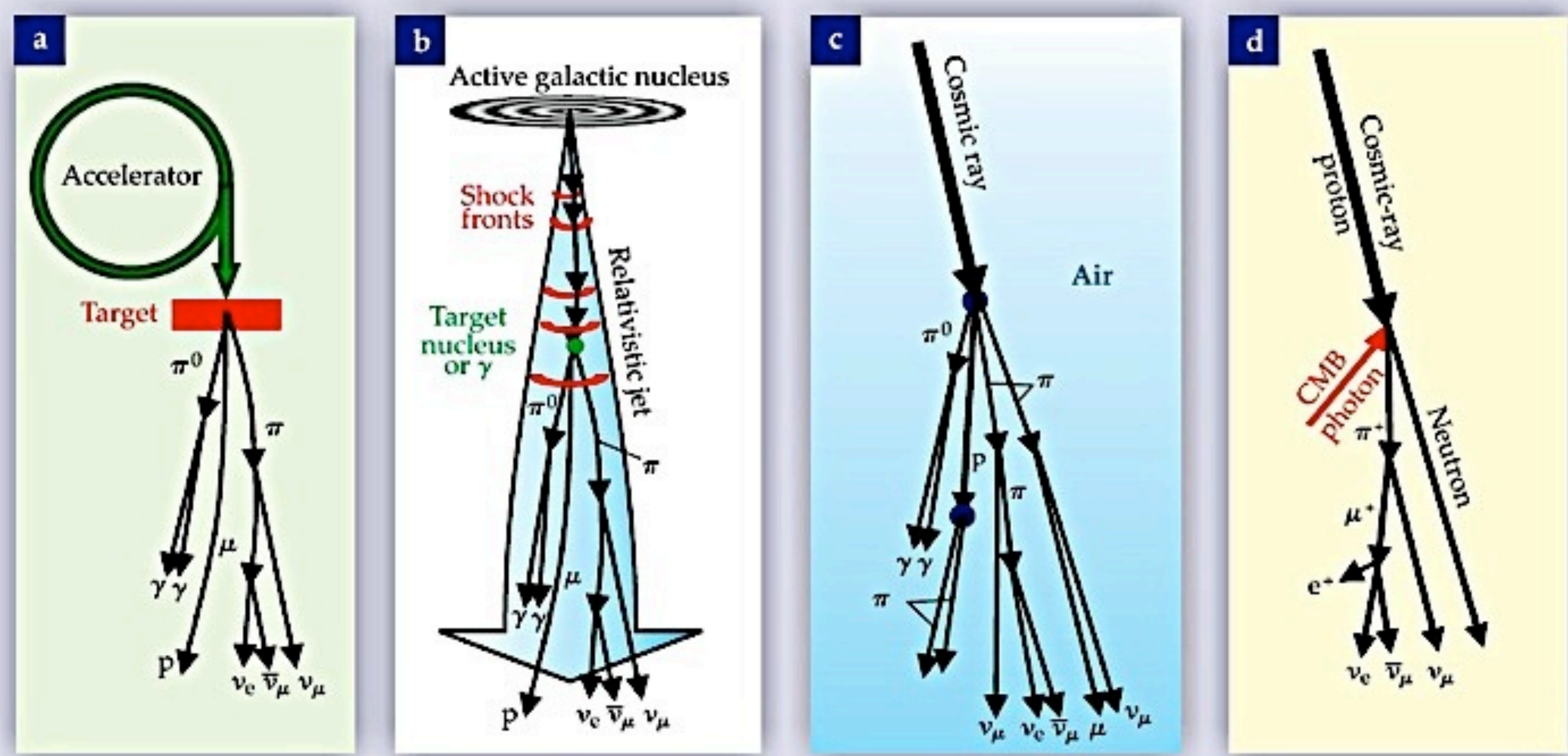

116

From Physics Today

Current Upper Limits at TeV-EeV energies

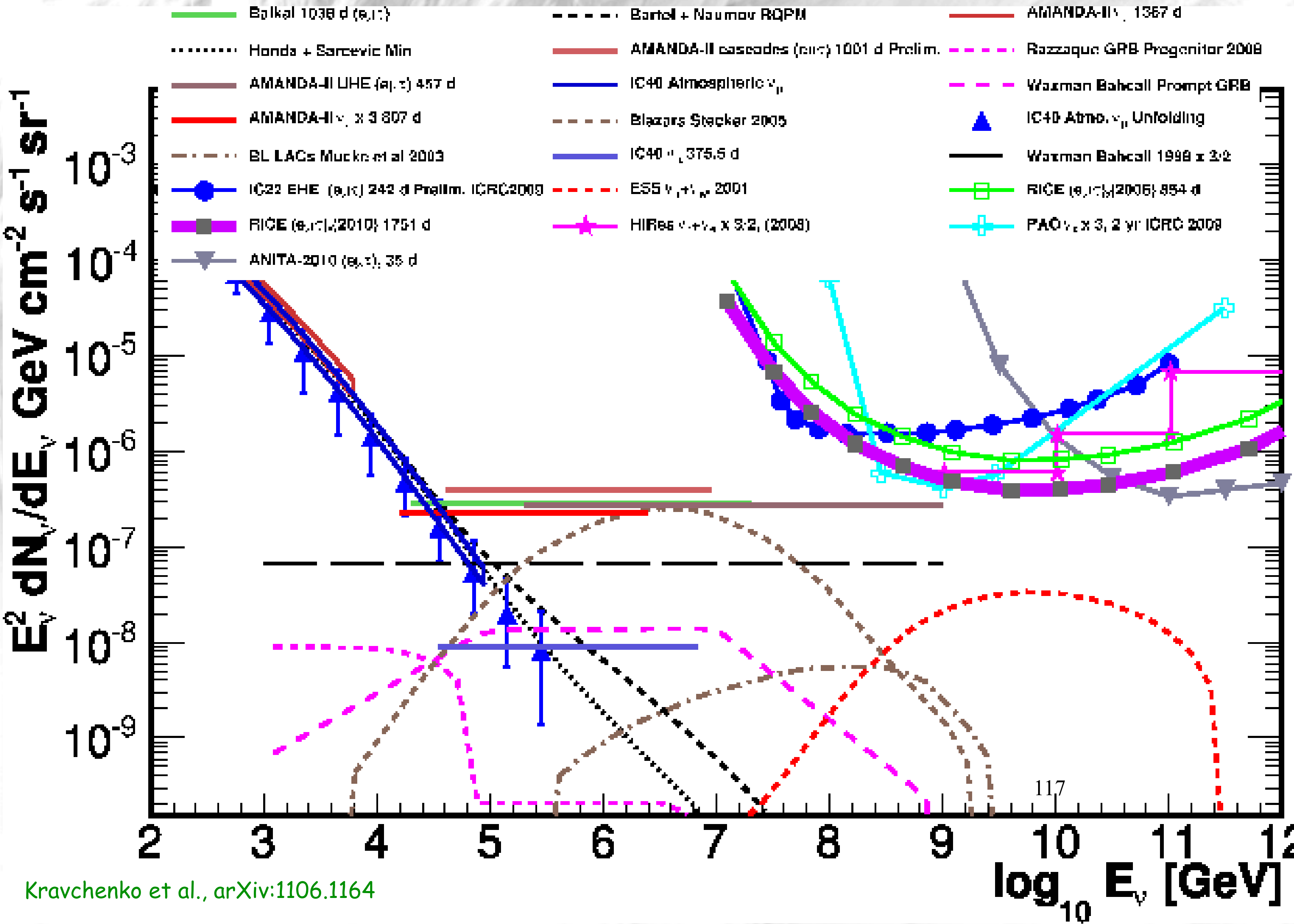

Kravchenko et al., arXiv:1106.1164

Note, however, that blazars promising as neutrino sources should be loud in GeV γ-rays, but NOT in γ-rays above TeV.

This is because such γ-rays pair produce with "blue bump" photons of ~10 eV energy with a cross section $\sim\sigma_{Th} \sim 1$ b about a factor 10^4 larger than the pγ cross section that produces the neutrinos => If loud in > TeV γ-rays, optical depth for neutrino production would be very small.

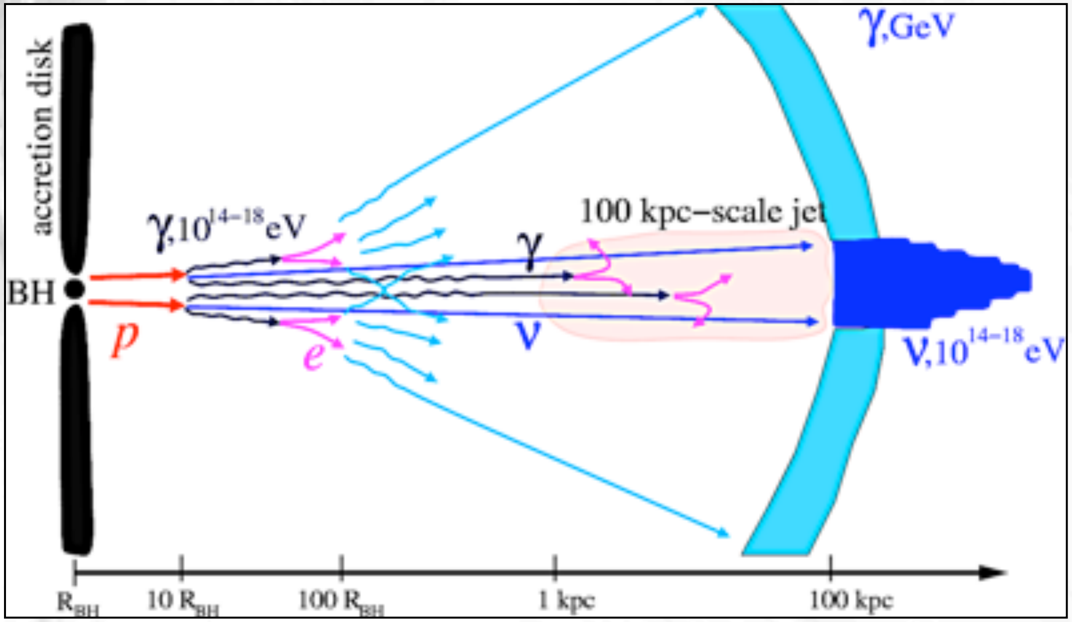

118

Neronov and Semikoz, Phys.Rev.D66 (2002) 123003

Note, however, that blazars promising as neutrino sources should be loud in GeV γ-rays, but NOT in γ-rays above TeV.

This is because such γ-rays pair produce with "blue bump" photons of ~10 eV energy with a cross section $\sim\sigma_{Th} \sim 1$ b about a factor 10^4 larger than the pγ cross section that produces the neutrinos => If loud in > TeV γ-rays, optical depth for neutrino production would be very small.

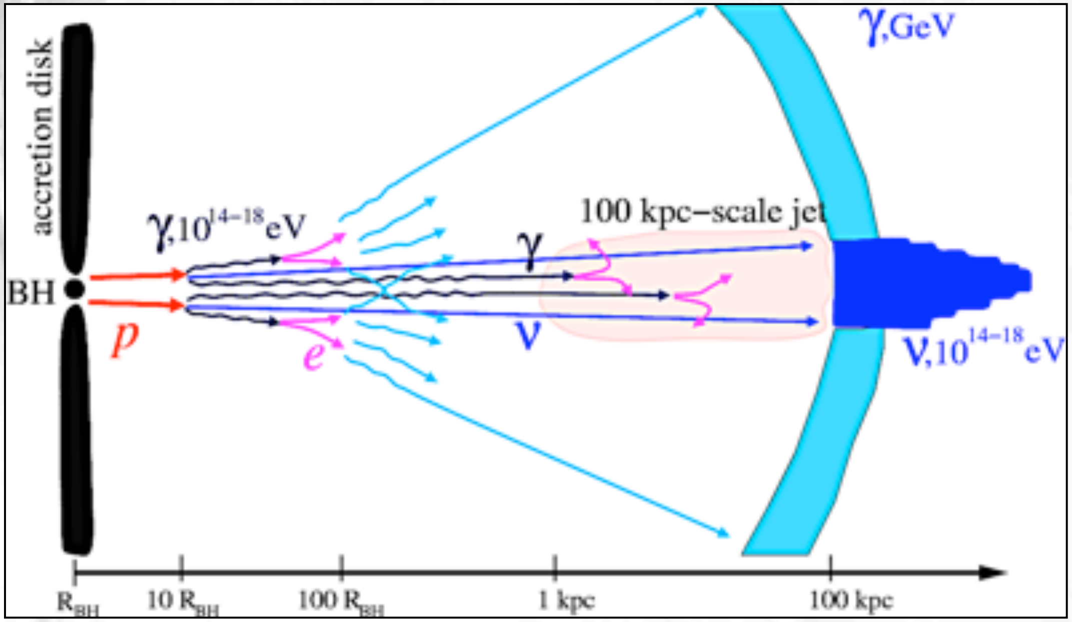

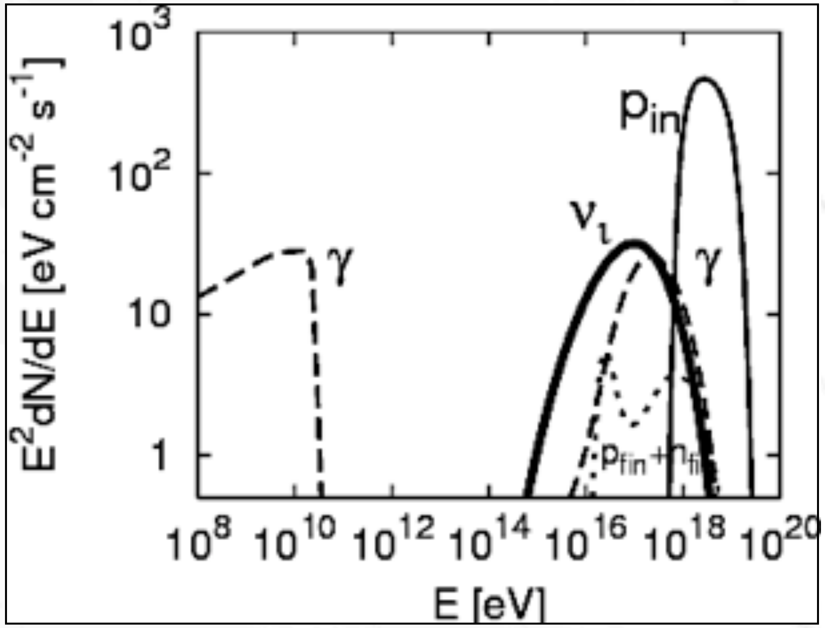

118

Neronov and Semikoz, Phys.Rev.D66 (2002) 123003

A “guaranteed” flux from starburst galaxies:

Idea: protons loose most of their energy in form of pions => secondary electrons produce radio synchrotron => can be related to secondary neutrinos

$$E_\nu \frac{dL}{dE_\nu}(E_\nu \simeq \mathrm{GeV}) \simeq 4\nu L_\nu(\nu \simeq \mathrm{GeV})$$

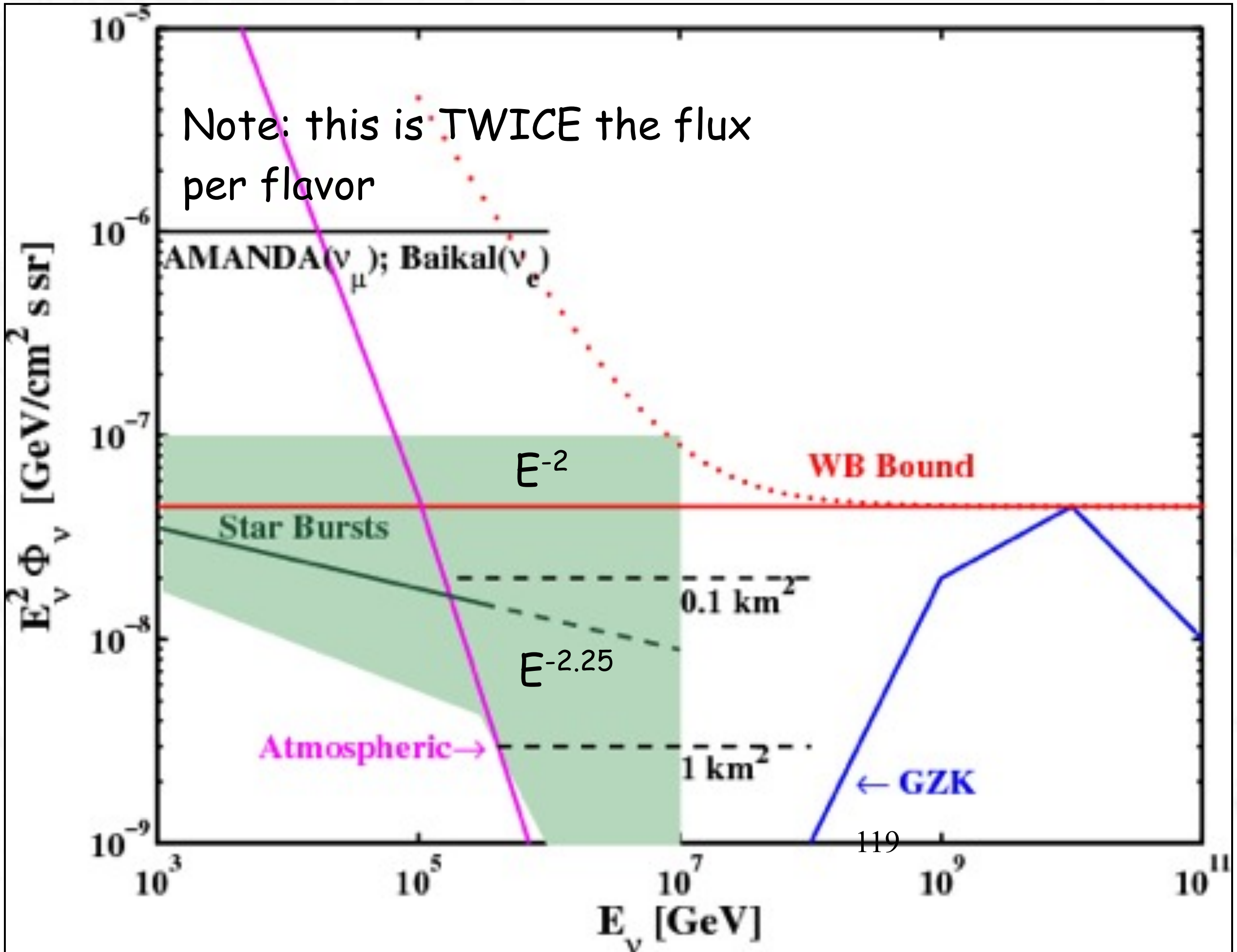

Loeb and Waxman, astro-ph/0601695

Another estimate of neutrino fluxes from continuous UHECR sources

If f is the ratio of cosmic rays interacting within the source to the cosmic ray flux leaving the source and $x_\nu \sim 0.05$ the average neutrino energy in units of primary energy, then

$$E^2 j_\nu^{\rm diff}(E) \simeq \frac{1}{6\pi H_0}\, f\, x_\nu^{\alpha-1}(\alpha-2) Q_{\rm UHE} \left(\frac{E}{10^{20}\,{\rm eV}}\right)^{2-\alpha}$$

In a water/ice detector the detection rate is

$$R_\nu(>E) \sim 2.3 \left(\frac{E}{10^{16}\,{\rm eV}}\right)^{-0.637} \left(\frac{V_{\rm eff}}{{\rm km}^3}\right) \left(\frac{E^2\, j_\nu^{\rm diff}(E)}{100\,{\rm eV\,cm^{-2}\,sr^{-1}\,s^{-1}}}\right) {\rm yr}^{-1}$$

If the ankle marks the transition from galactic to extragalactic cosmic rays then $\alpha \sim 2.2$ and the neutrino spectrum goes down to $\sim 10^{17}$ eV, with

$$R_\nu \sim 2\times 10^{-2} f\, {\rm yr}^{-1}\,{\rm km}^{-3} < 20\, Z^{-2} \left(\frac{L_{\rm tot}}{L_{\rm min}}\right) {\rm yr}^{-1}\,{\rm km}^{-3}$$

120

G.Sigl arXiv:0803.3800

where L_{tot} is the bolometric luminosity.

If the ankle is due to pair production of extragalactic cosmic rays, then α ~ 2.6 and the neutrino spectrum goes down to ~ 10^{16} eV, with

$$R_\nu \sim 5.5 f\,\mathrm{yr}^{-1}\,\mathrm{km}^{-3} < 180\,Z^{-2}\left(\frac{L_{\rm tot}}{L_{\rm min}}\right)\mathrm{yr}^{-1}\,\mathrm{km}^{-3}$$

The low cross-over scenario where flux is dominated by extragalactic protons above 4×10^{17} eV may be close to be ruled out by AMANDA.

This, however, assumes transparent sources which cosmic rays have to leave as neutrons which each come with one π^+ decaying into neutrinos.

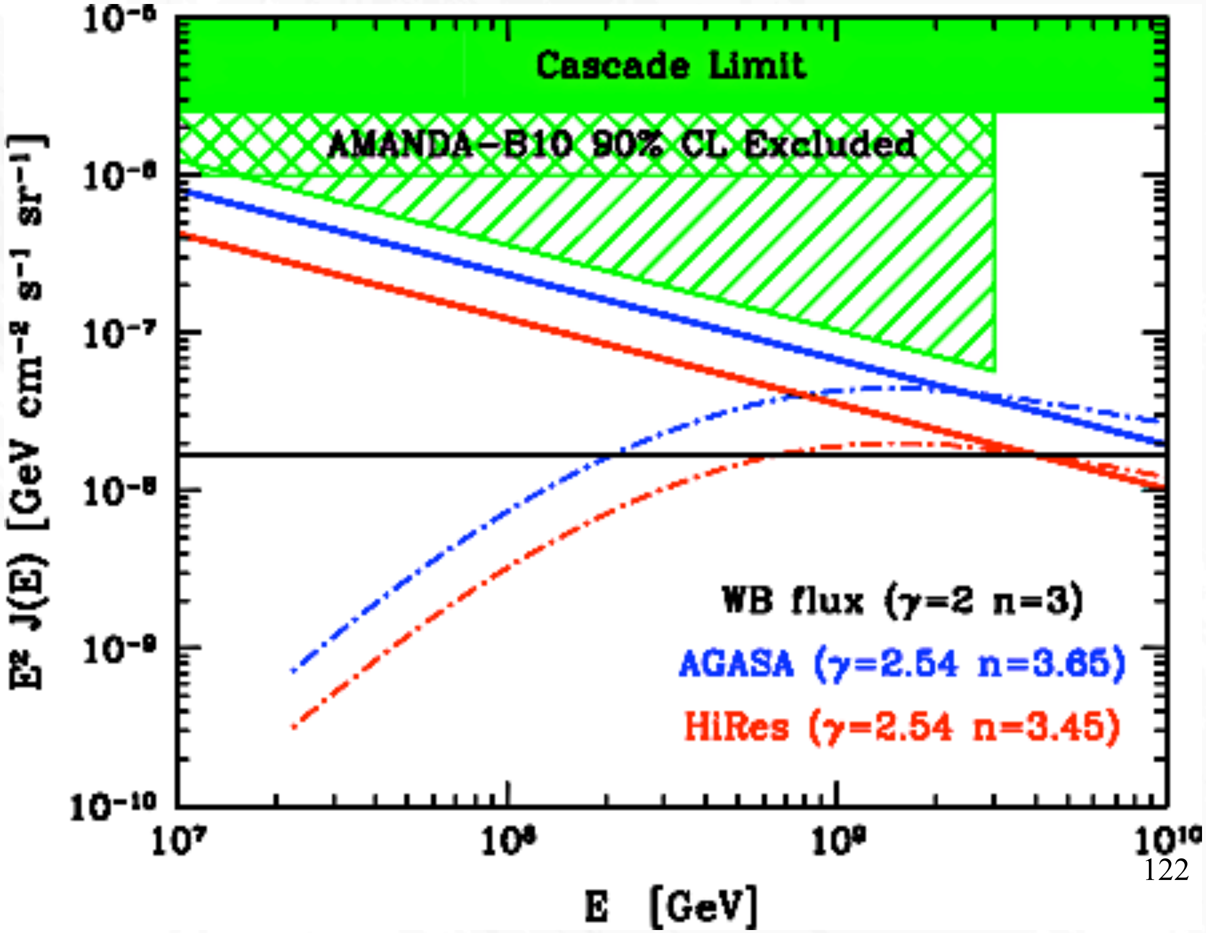

Ahlers et al., Phys.Rev. D72 (2005) 023001

Chemical Composition and Source Contributions to the Ultra-High Energy Neutrino Flux

In AGN sources, nuclei are disintegrated above ~10^{19} eV
In GRB sources, all nuclei are practically disintegrated (compact source)
In starburst galaxy sources, very few nuclei are disintegrated

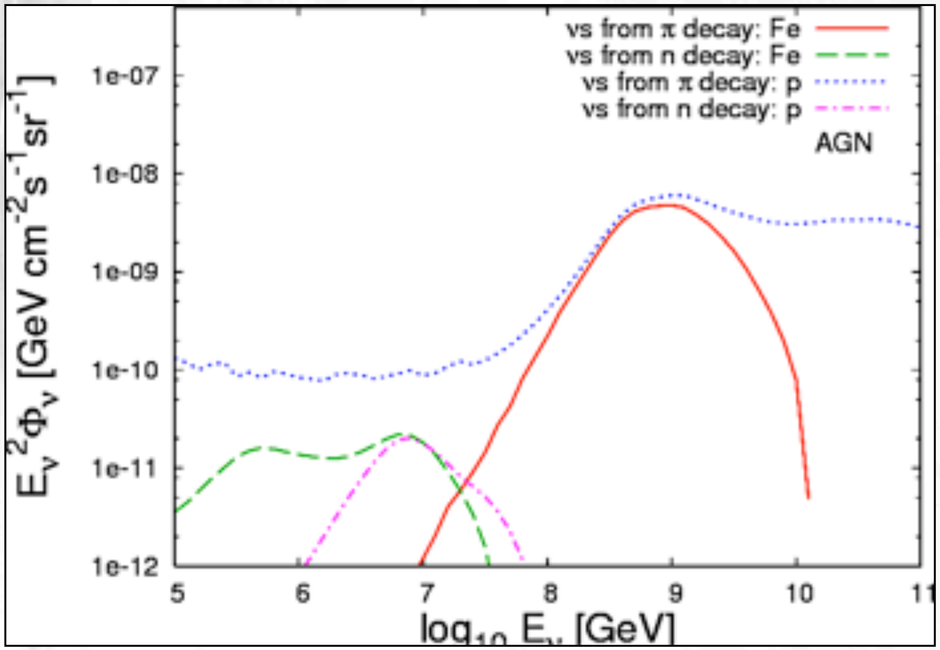

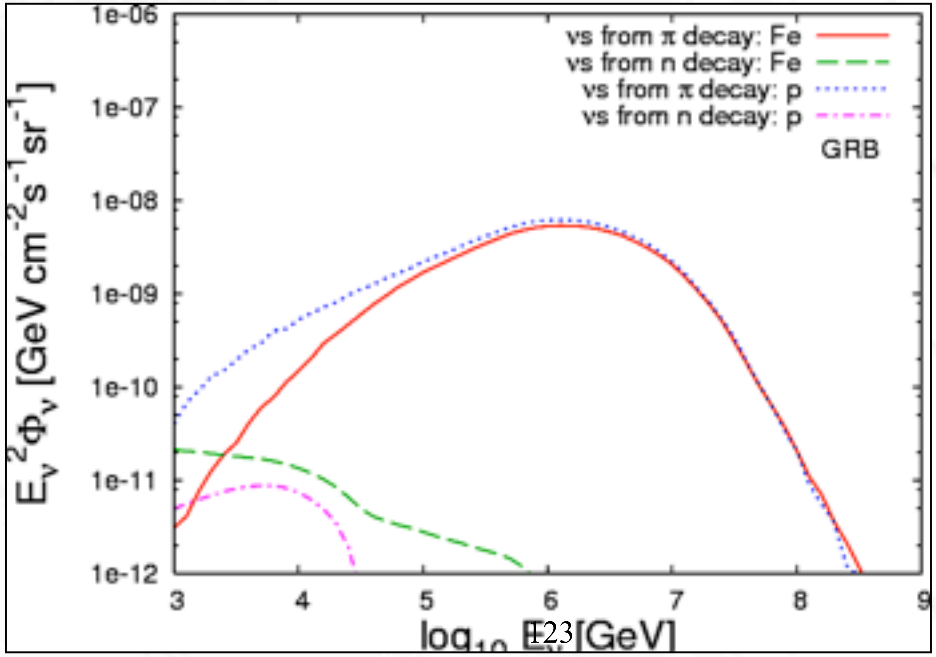

Anchordoqui, Goldberg, Hooper, Sarkar, Taylor, Phys.Rev. D76 (2007) 123008

Ultra-High Energy Cosmic Rays and the Connection to Diffuse Υ-ray and Neutrino Fluxes

accelerated nuclei interact:

$$
{}^{A}_{Z} + N,\gamma \rightarrow X + \left\{ \begin{array}{ll} \pi^{+} & \rightarrow \mathrm{neutrinos} \\ \pi^{0} & \rightarrow \gamma-\mathrm{rays} \end{array} \right.
$$

during propagation ("cosmogenic")
or in sources (AGN, GRB, ...)

=> energy fluences in γ-rays and neutrinos are comparable due to isospin symmetry.

Universe acts as a calorimeter for total injected electromagnetic energy above the pair threshold.
=> neutrino flux constraints.

Ultra-High Energy Cosmic Rays and the Connection to Diffuse γ-ray and Neutrino Fluxes

accelerated nuclei interact:

$$ {}^{A}_{Z} + N, \gamma \rightarrow X + \begin{cases} \pi^{+} & \rightarrow \text{neutrinos} \\ \pi^{0} & \rightarrow \gamma - \text{rays} \end{cases} $$

during propagation ("cosmogenic")
or in sources (AGN, GRB, ...)

=> energy fluences in γ-rays and neutrinos are comparable due to isospin symmetry.

Universe acts as a calorimeter for total injected electromagnetic energy above the pair threshold.
=> neutrino flux constraints.

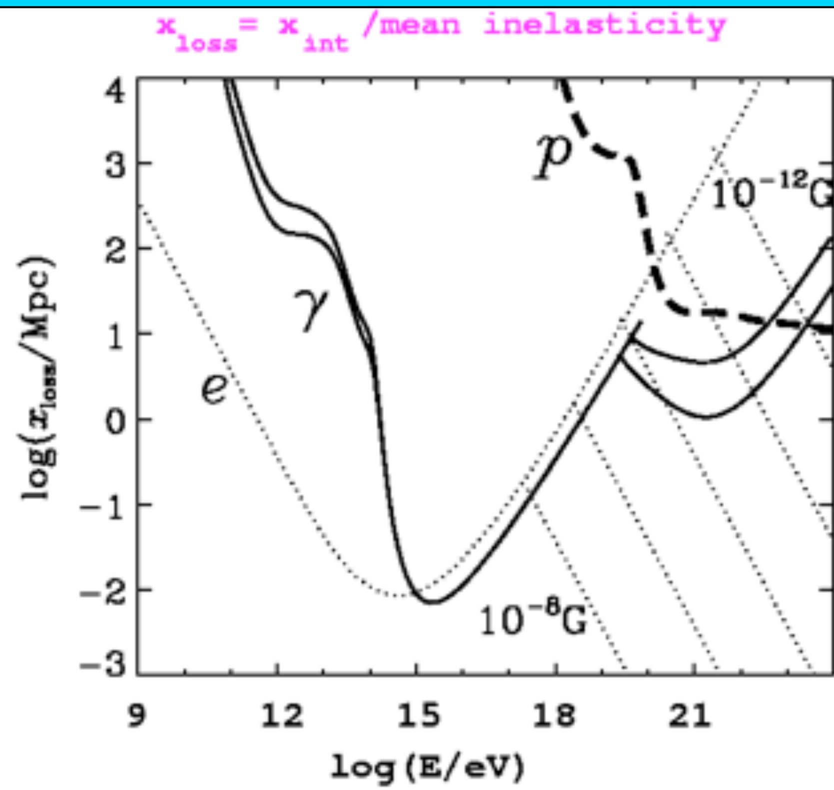

Included processes:

Electrons: inverse Compton; synchrotron rad (for fields from pG to 10 nG)

Gammas: pair-production through IR, CMB, and radio backgrounds 124

Protons: Bethe-Heitler pair production, pion photoproduction

Ultra-High Energy Cosmic Rays and the Connection to Diffuse γ-ray and Neutrino Fluxes

accelerated nuclei interact:

$$^A_Z + N,\gamma \to X + \left\{ \begin{array}{ll} \pi^+ & \to \text{neutrinos} \\ \pi^0 & \to \gamma - \text{rays} \end{array} \right.$$

during propagation ("cosmogenic")
or in sources (AGN, GRB, ...)

=> energy fluences in γ-rays and neutrinos are comparable due to isospin symmetry.

Neutrino spectrum is unmodified, γ-rays pile up below pair production threshold (on CMB at a few 10^{14} eV)

Universe acts as a calorimeter for total injected electromagnetic energy above the pair threshold.
=> neutrino flux constraints.

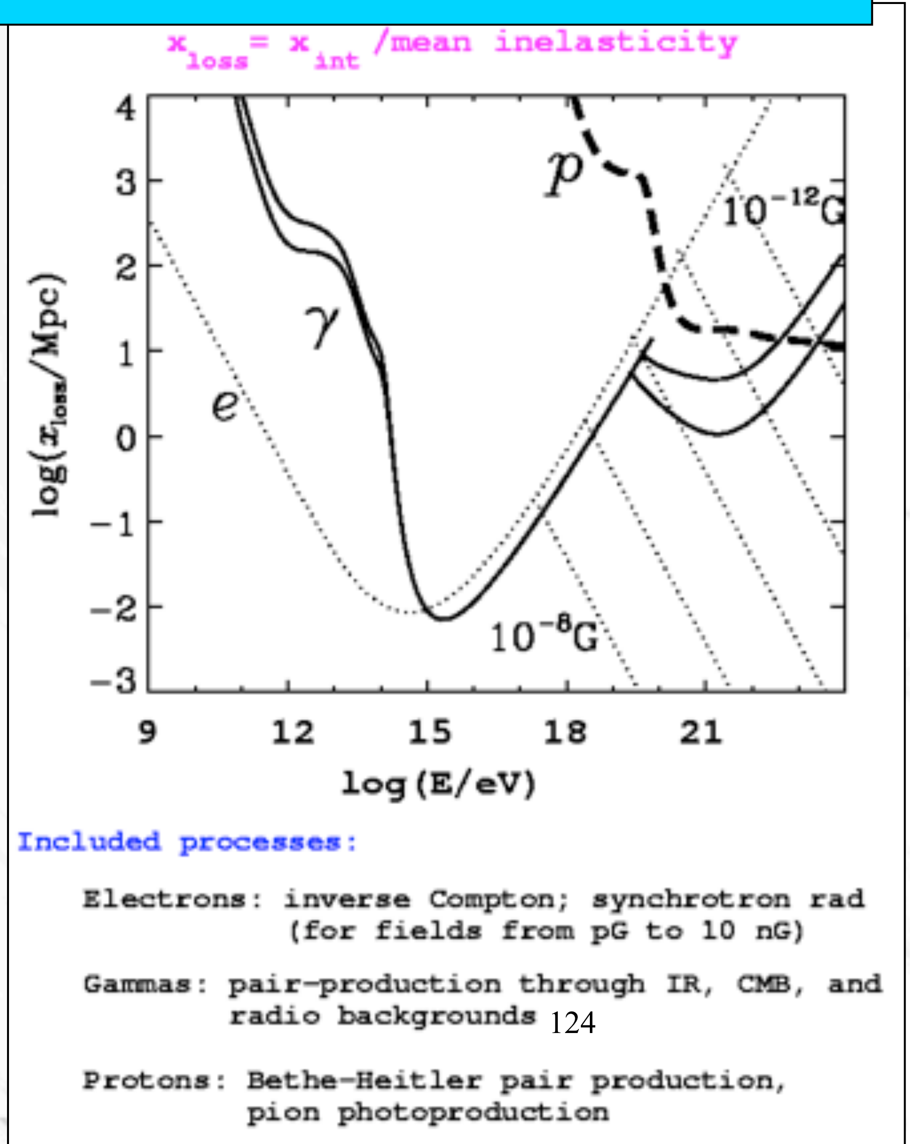

Interaction Horizons

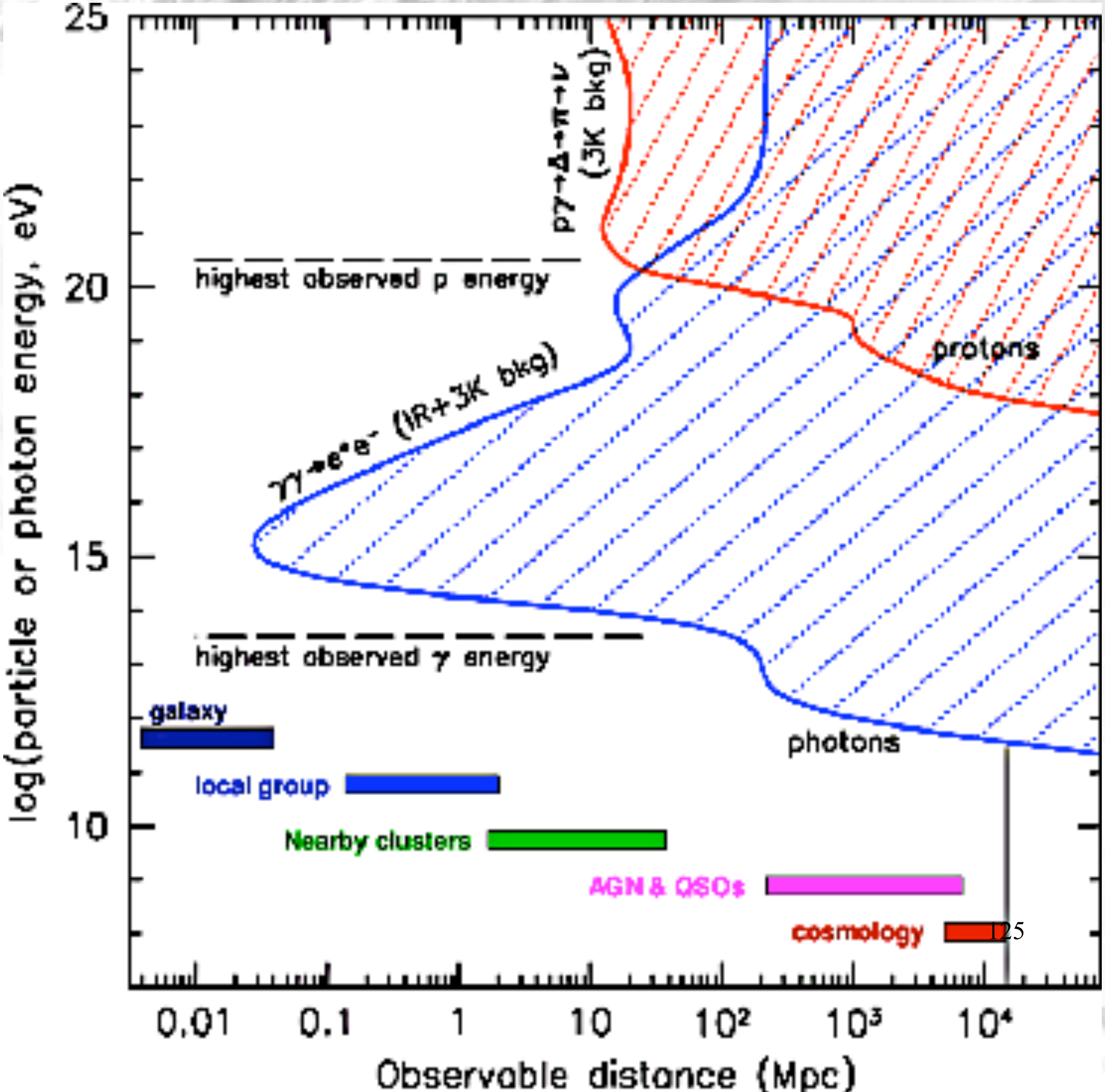

Propagation of nucleons, photons, electrons, and neutrinos

In one dimension propagation is governed by Boltzmann equations for differential spectrum of species i, $n_i(E)$:

$$\frac{\partial n_i(E)}{\partial t} = \Phi_i(E) - n_i(E)\int d\varepsilon n_b(\varepsilon)\int_{-1}^{+1} d\mu \frac{1-\mu\beta_b\beta_i}{2}\sum_j \sigma_{i\to j}\Big|_{s=\varepsilon E(1-\mu\beta_b\beta_i)}$$
$$+\int dE'\int d\varepsilon n_b(\varepsilon)\int_{-1}^{+1} d\mu \sum_j \frac{1-\mu\beta_b\beta_j'}{2} n_j(E')\left.\frac{d\sigma_{j\to i}(s,E)}{dE}\right|_{s=\varepsilon E'(1-\mu\beta_b\beta_j)},$$

where:

$\Phi_i(E)$ =injection spectrum,

$n_b(\varepsilon)$ =diffuse background neutrino or photon density at energy ε,

$\mu = \cos$(angle between background and in-particle),

β =particle velocities,

$\sigma_{i\to j}$ = cross sections for processes $i \to j$,

s =center of mass energy.

Background spectrum between $\sim 10^{-8}$ eV and ~ 10 eV

propagated particles between 100 MeV and 10^{16} GeV (GUT scale)

transport equations (including cosmology, i.e. redshift-distance relation) solved by implicit methods.

126

Processes taken into account

Nucleons:

- (multiple) pion production: $N\gamma_b \to N(n\pi)$ with subsequent pion decays: leads to "GZK-effect".
- pair production by protons: $p\gamma_b \to pe^+e^-$: relevant below GZK threshold (similar to triplet pair production below)
- Neutron decay: $n \to pe^-\bar{\nu}_e$

Electromagnetic channel:

- pair production and inverse Compton scattering: $\gamma\gamma_b \to e^+e^-$ and $e\gamma_b \to e\gamma$: leading order processes with

$$\sigma_{\rm PP} \simeq 2\sigma_{\rm ICS} \simeq \frac{3}{2}\sigma_T\frac{m_e^2}{s}\ln\frac{s}{2m_e^2} \quad (s \gg m_e^2)\,.$$

- double pair production: $\gamma\gamma_b \to e^+e^-e^+e^-$: dominates at highest energies with

$$\sigma_{\rm DPP} \simeq \frac{43\alpha^2}{24\pi^2}\sigma_T \quad (s \gg m_e^2)\,.$$

- triplet pair production: $e\gamma_b \to ee^+e^-$: dominant at highest energies with

$$\sigma_{\rm TPP} \simeq \frac{3\alpha}{8\pi}\sigma_T\left(\frac{28}{9}\ln\frac{s}{m_e^2} - \frac{218}{27}\right) \quad (s \gg m_e^2)\,,$$

  with fractional energy loss η of leading e

$$\eta \simeq 1.768\left(\frac{s}{m_e^2}\right)^{-3/4} \quad (s \gg m_e^2)\,.$$

- synchrotron loss of electrons and positrons in cosmic magnetic fields: $eB \to e\gamma$. 127
  Energy loss given by

$$\frac{dE}{dt} = -\frac{4}{3}\sigma_T\frac{B^2}{8\pi}\left(\frac{Zm_e}{m}\right)^4\left(\frac{E}{m_e}\right)^2\,.$$

The universal photon spectrum

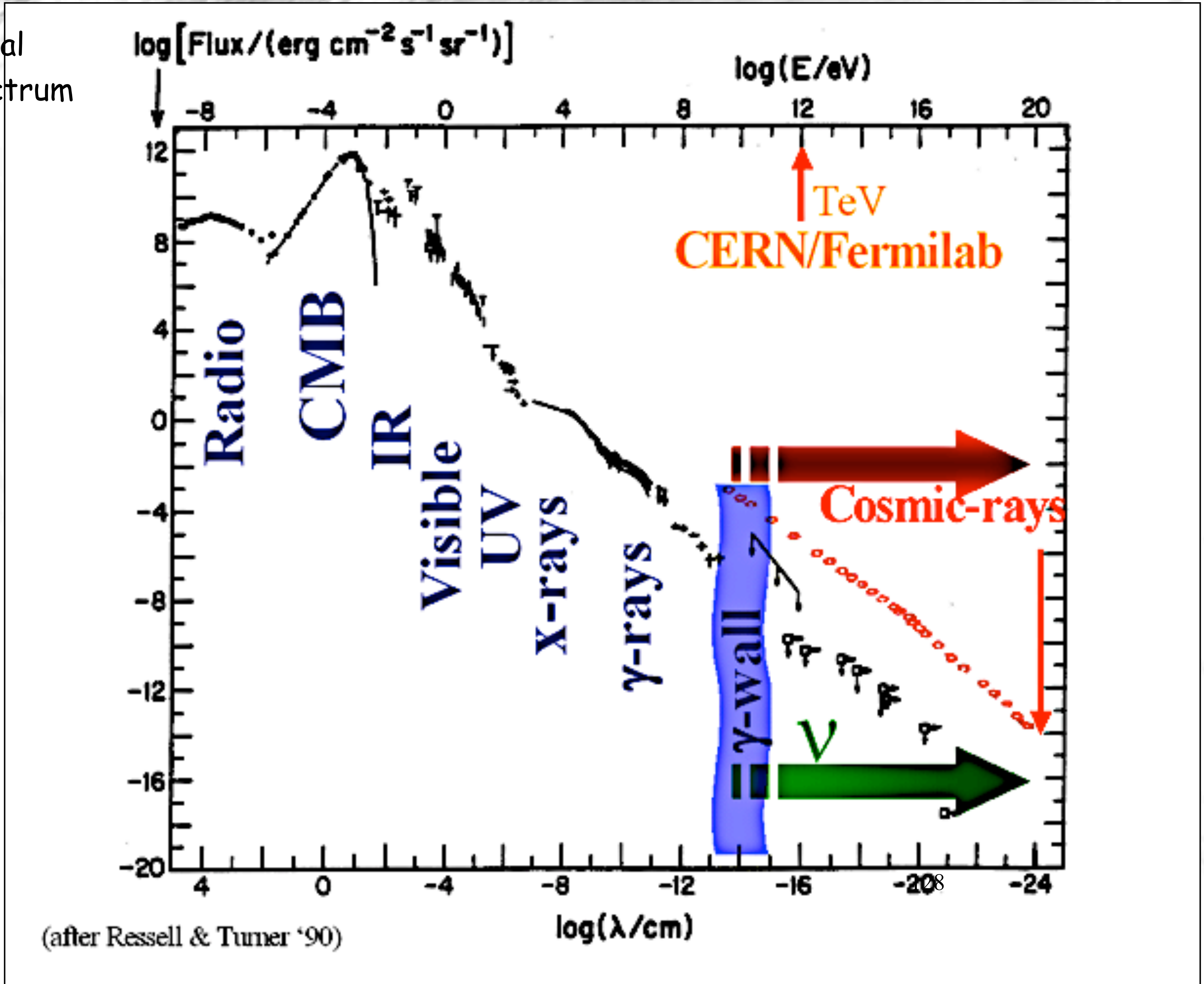

Low energy photon target: Diffuse fluxes

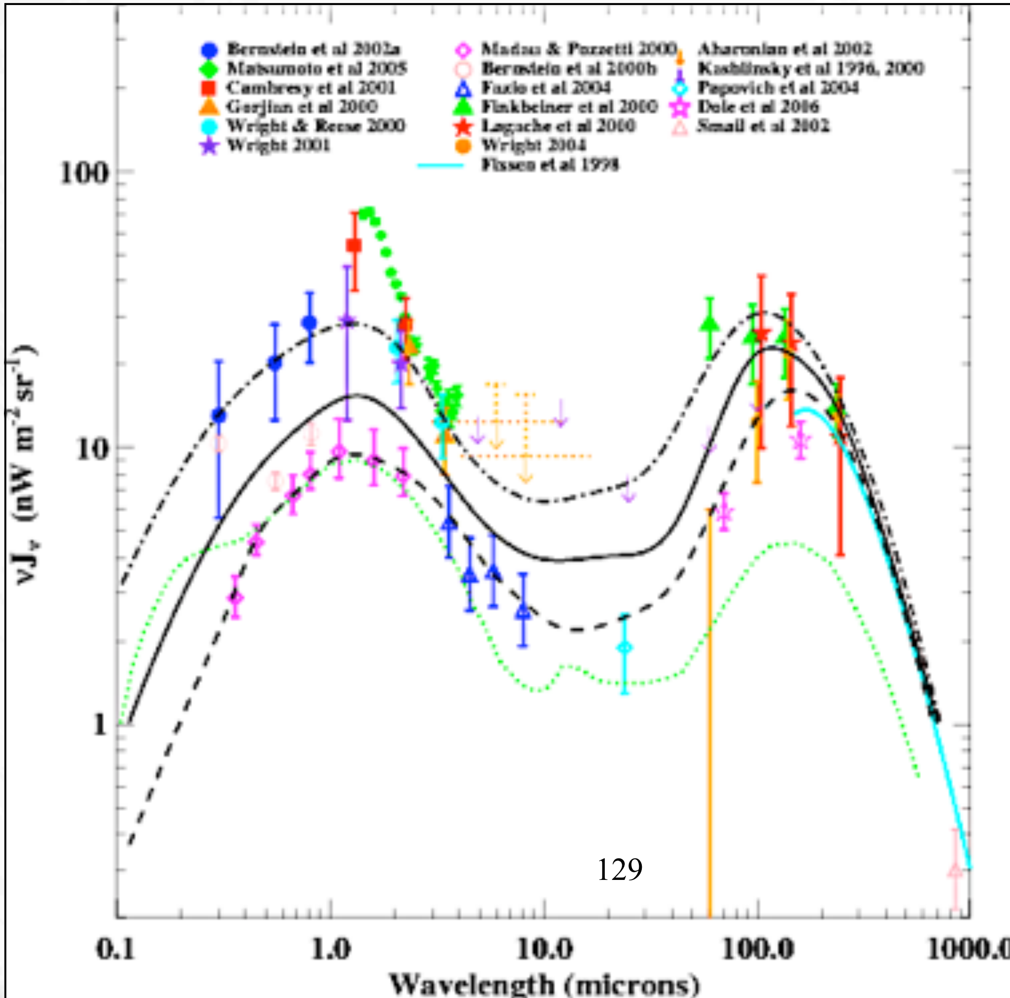

Low energy photon target: Diffuse fluxes

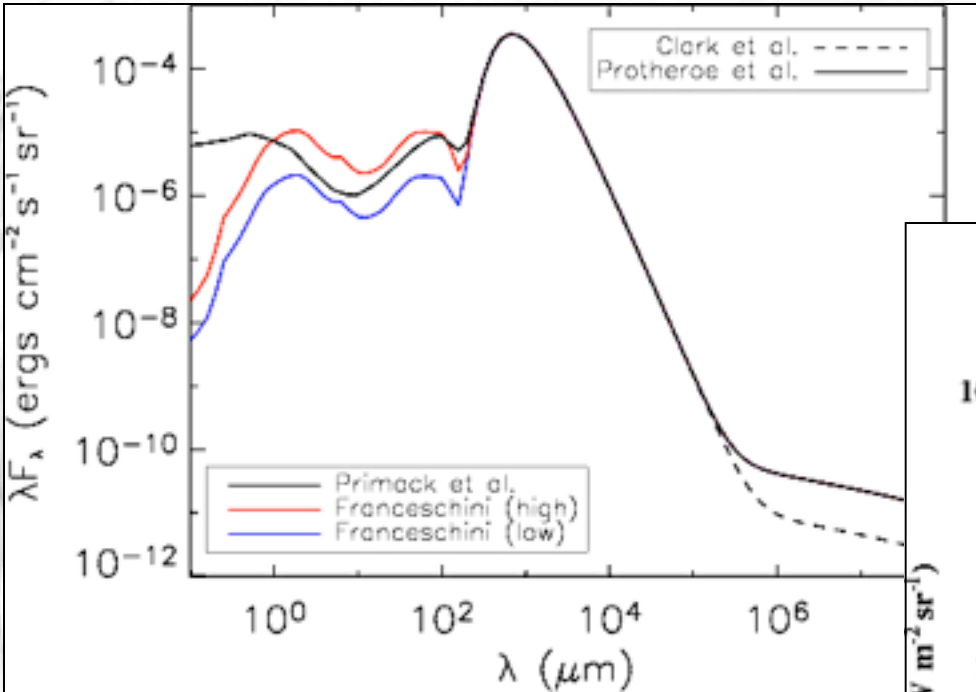

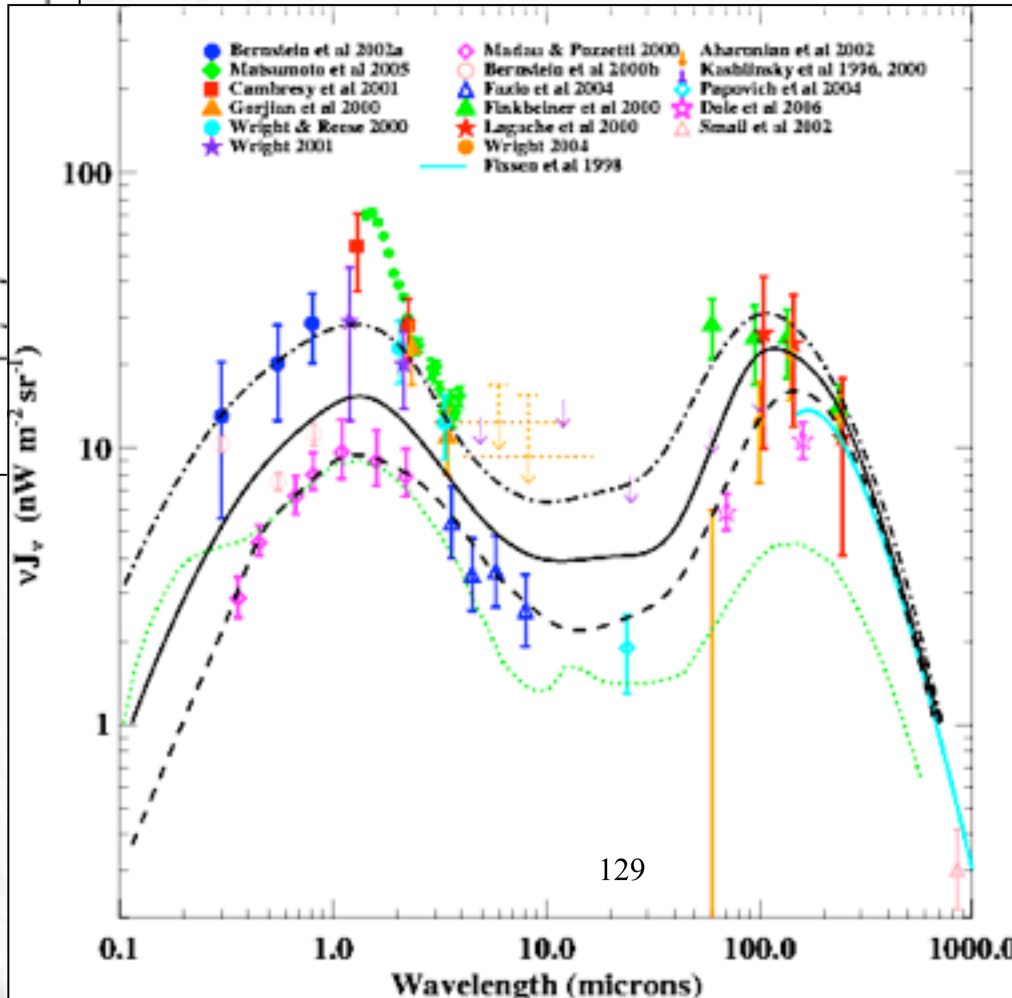

The diffuse photon background from keV to 100 GeV

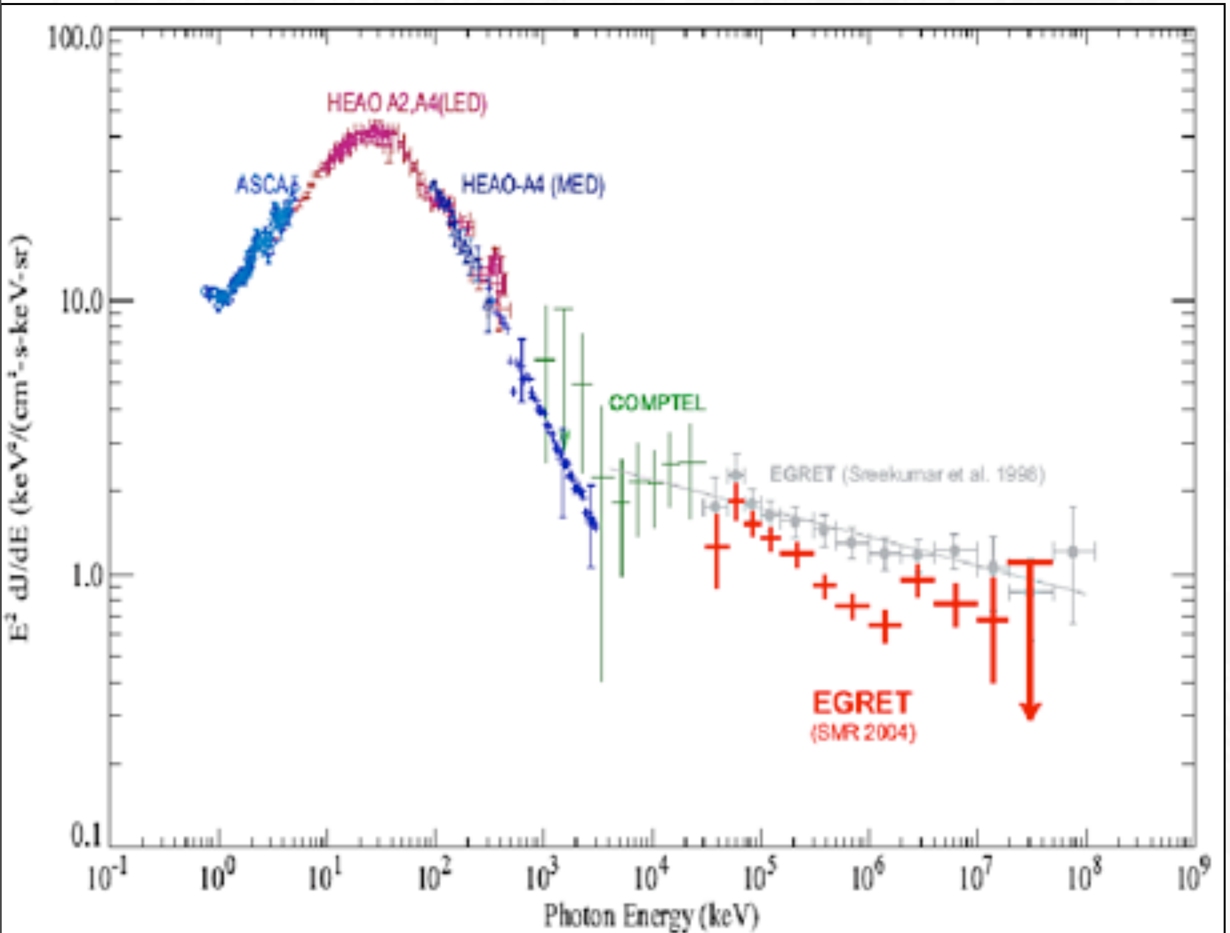

130

The diffuse photon background from keV to 100 GeV

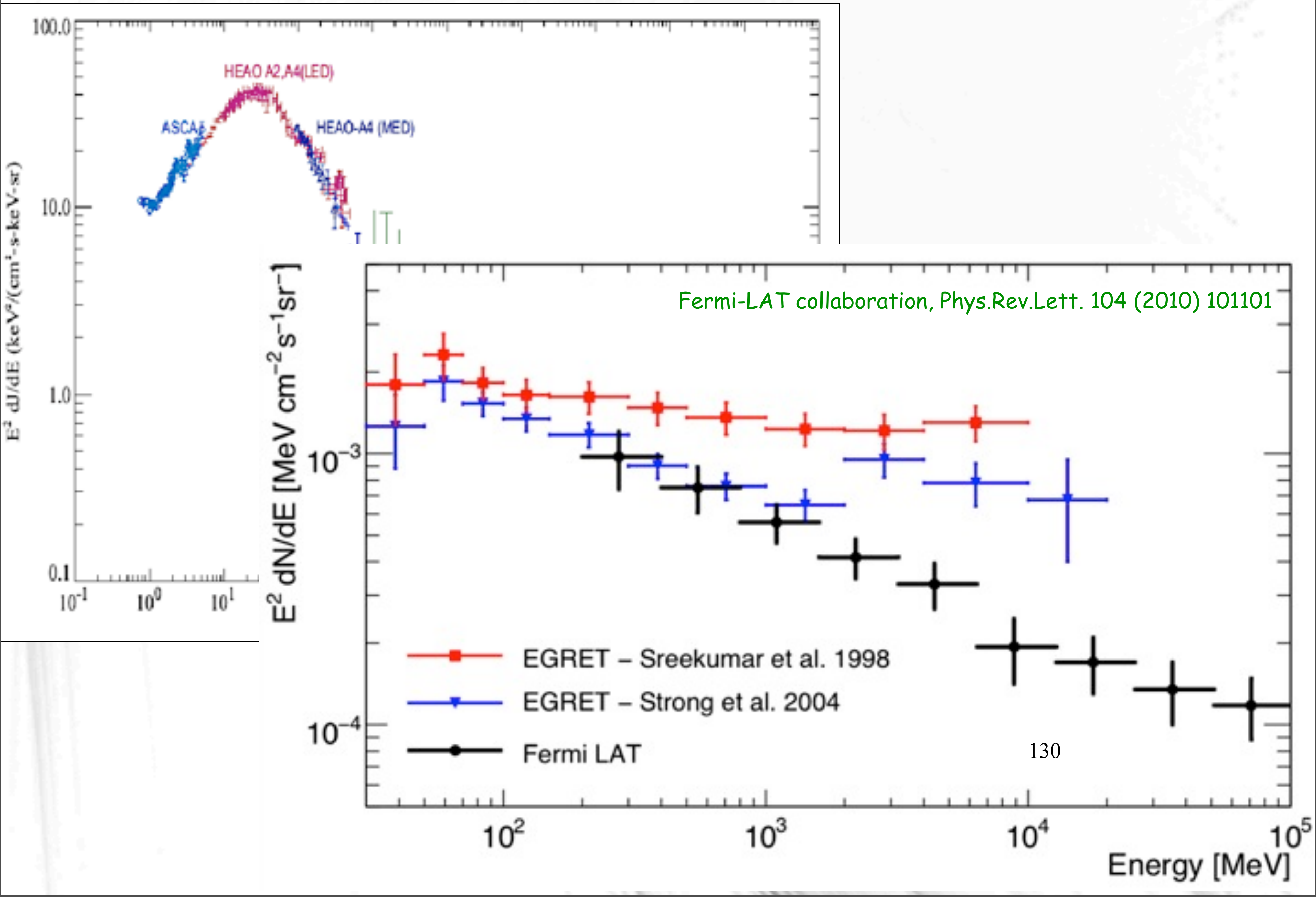

Theoretical Limits, Sensitivities, and "Realistic" Fluxes: A Summary

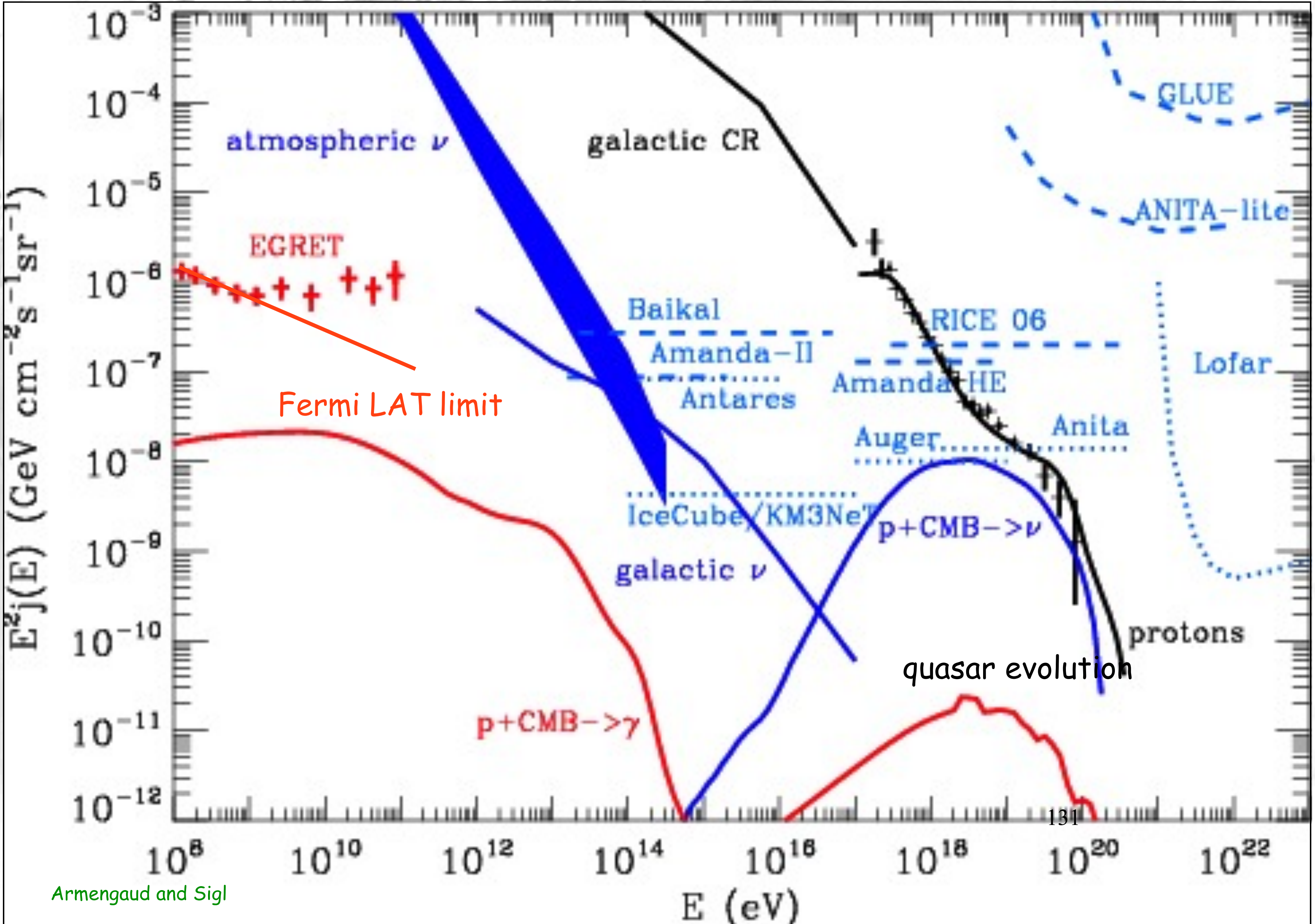

Armengaud and Sigl

Theoretical Limits, Sensitivities, and “Realistic” Fluxes: A Summary

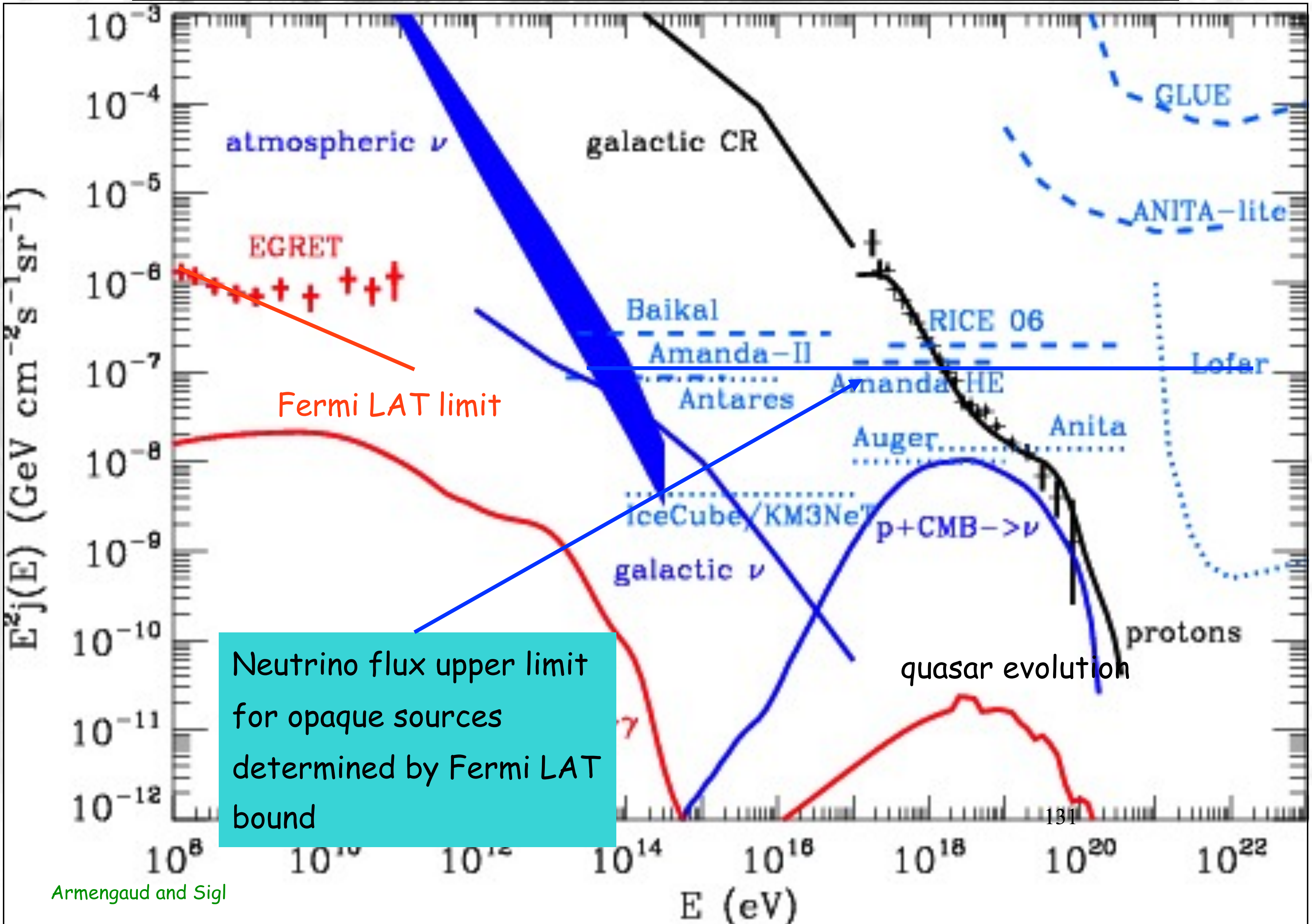

Theoretical Limits, Sensitivities, and "Realistic" Fluxes: A Summary

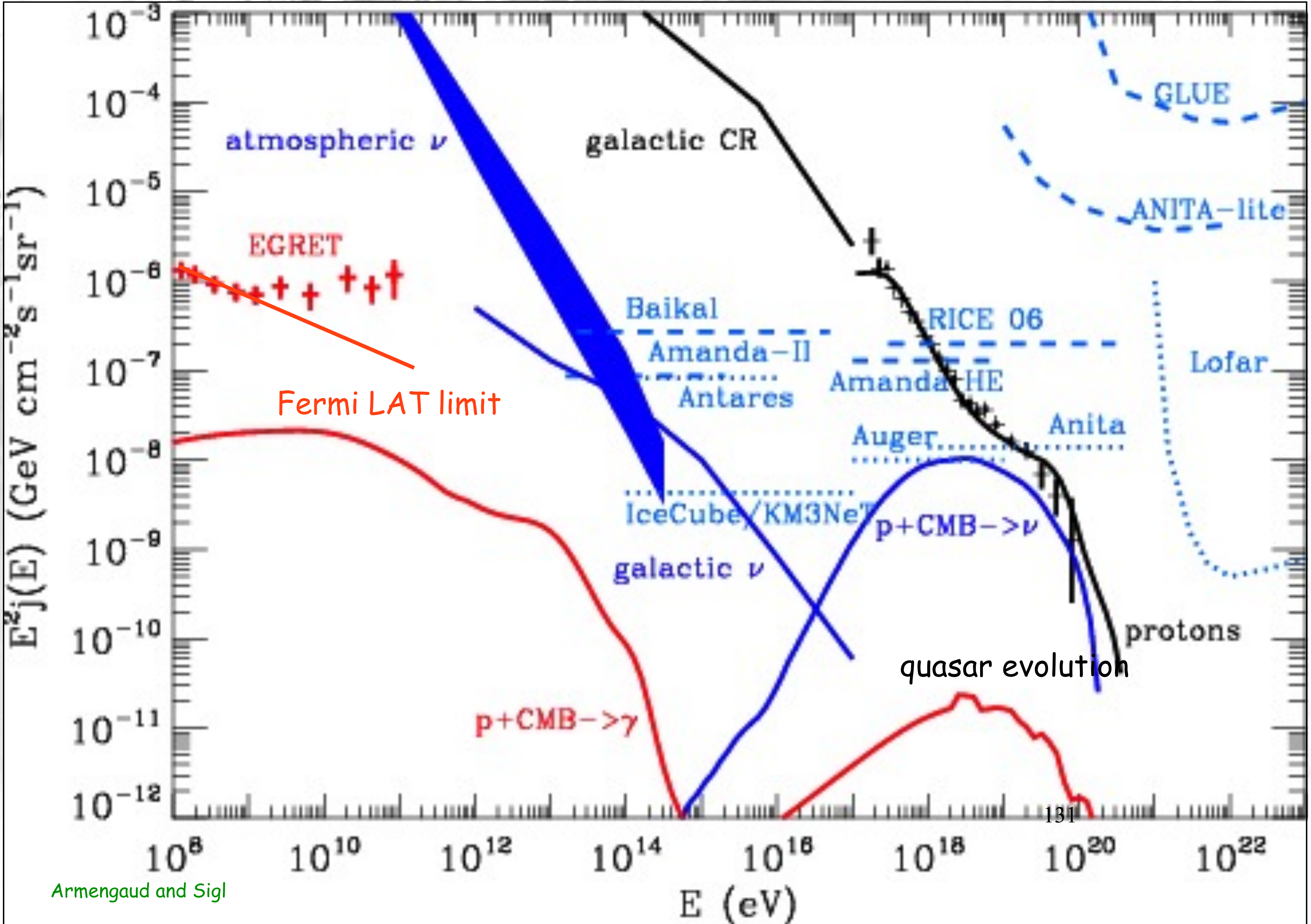

Theoretical Limits, Sensitivities, and "Realistic" Fluxes: A Summary

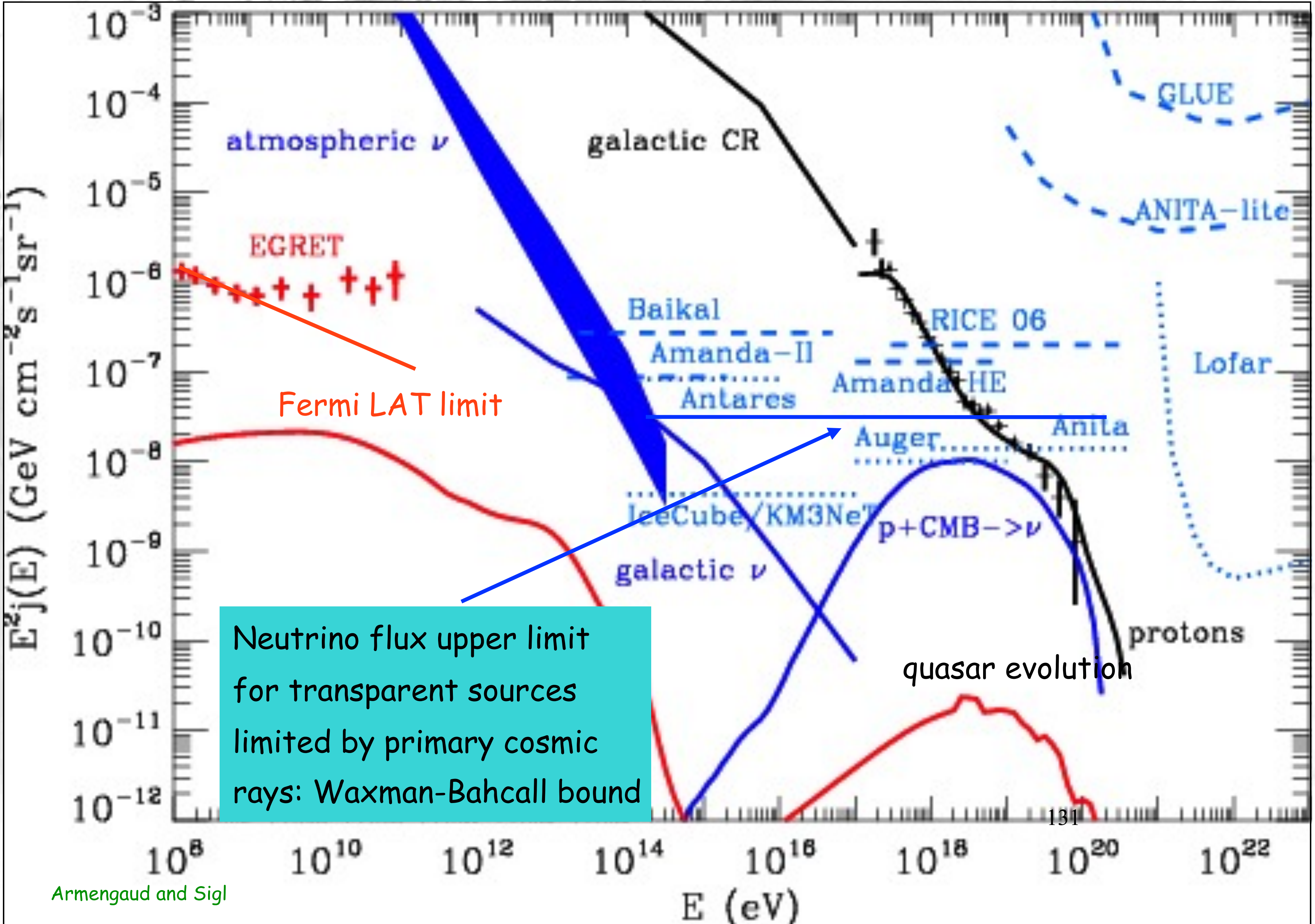

Armengaud and Sigl

Theoretical Limits, Sensitivities, and "Realistic" Fluxes: A Summary

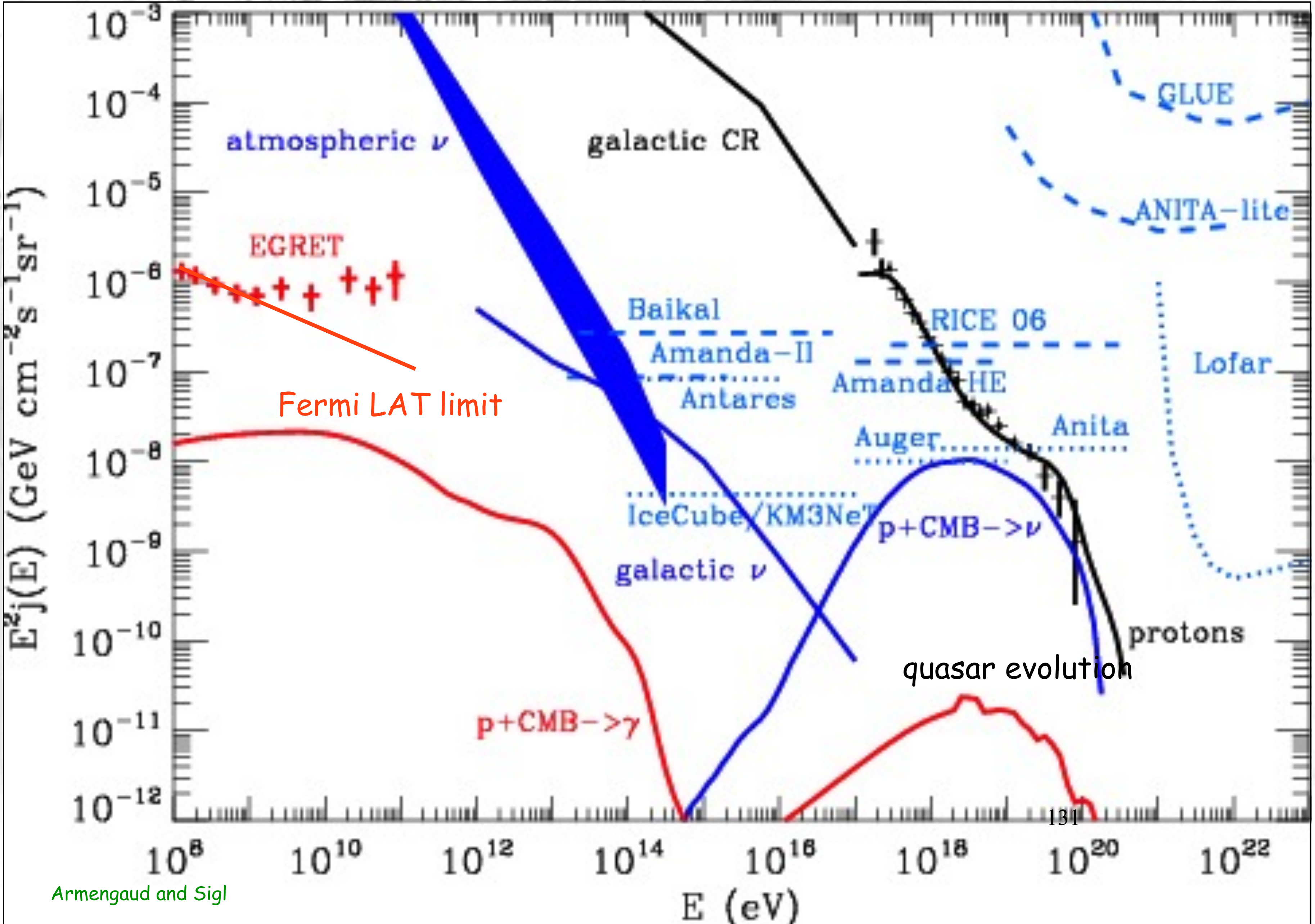

Armengaud and Sigl

Theoretical Limits, Sensitivities, and "Realistic" Fluxes: A Summary

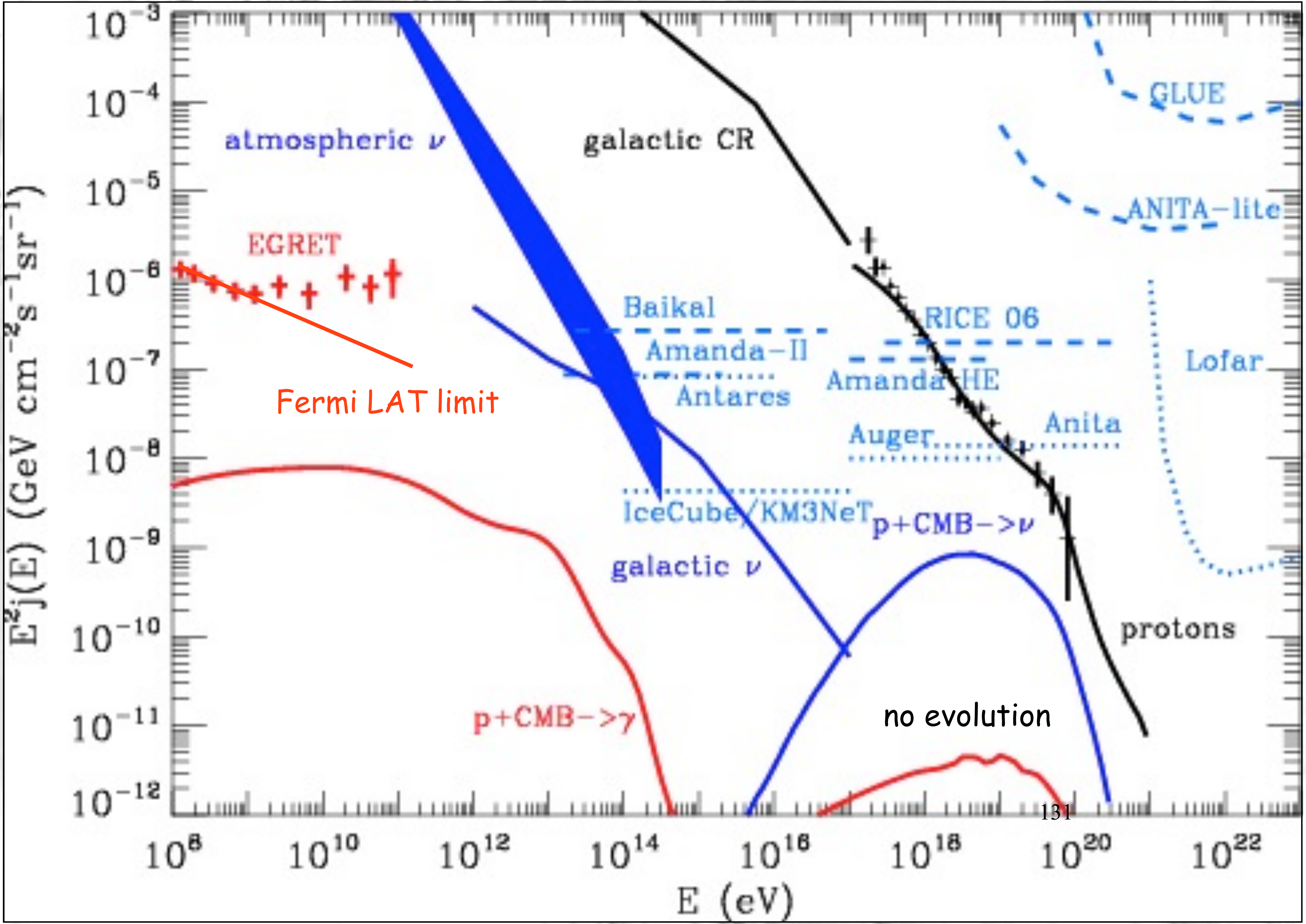

Physics with Diffuse Cosmogenic Neutrino Fluxes

Cosmogenic neutrino fluxes depend on number of nucleons produced above GZK threshold which is proportional to E_{max}/A

Further suppressed for heavy nuclei due to increased pair production

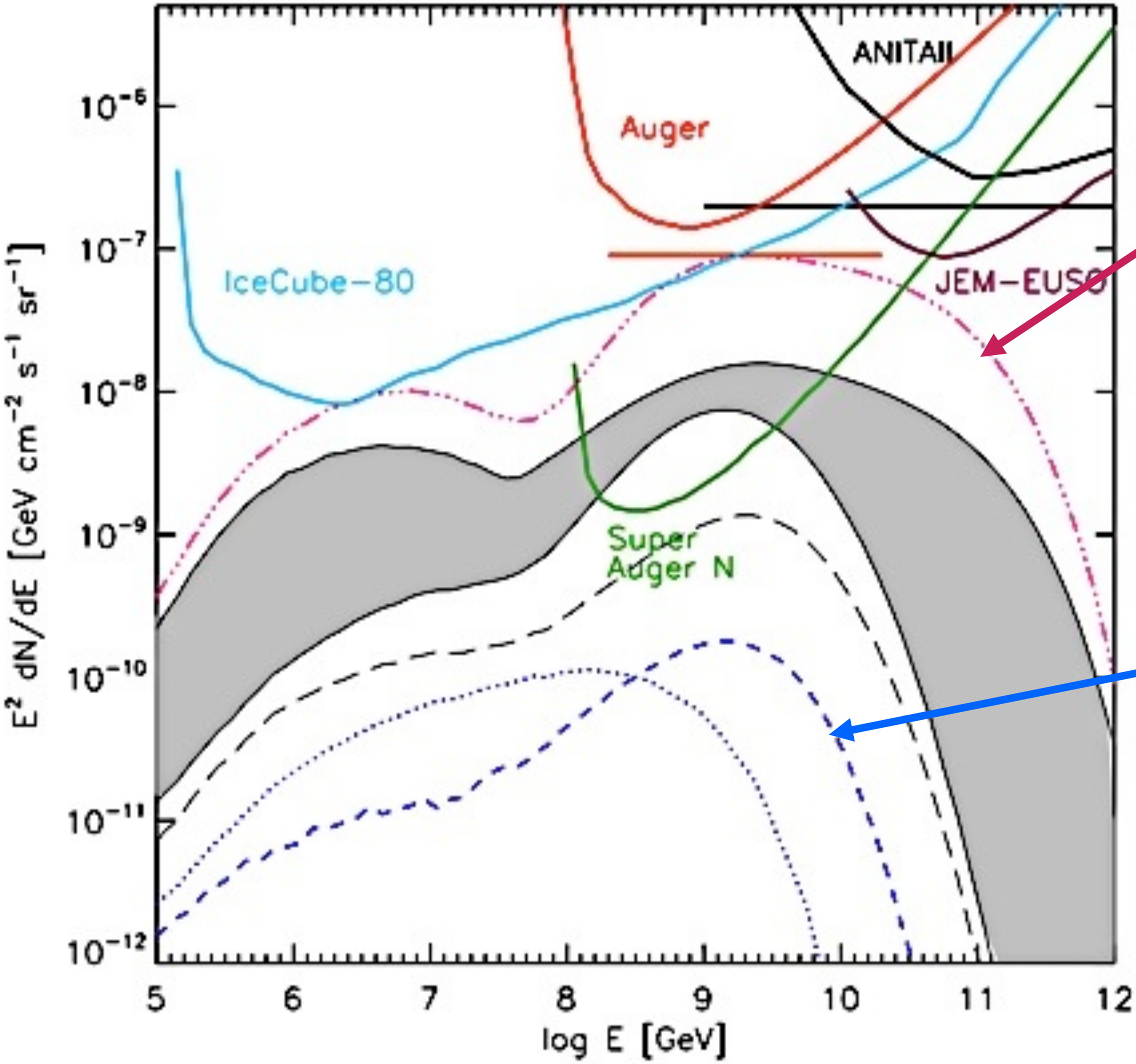

Pure protons, E_{max}=3 10^{21} eV, strong evolution

Pure iron, E_{max}= 10^{20}/26 eV, no evolution

132

Kotera, Allard, Olinto, JCAP 1010 (2010) 013

Expected Sensitivities to/Rates of UHE neutrino fluxes

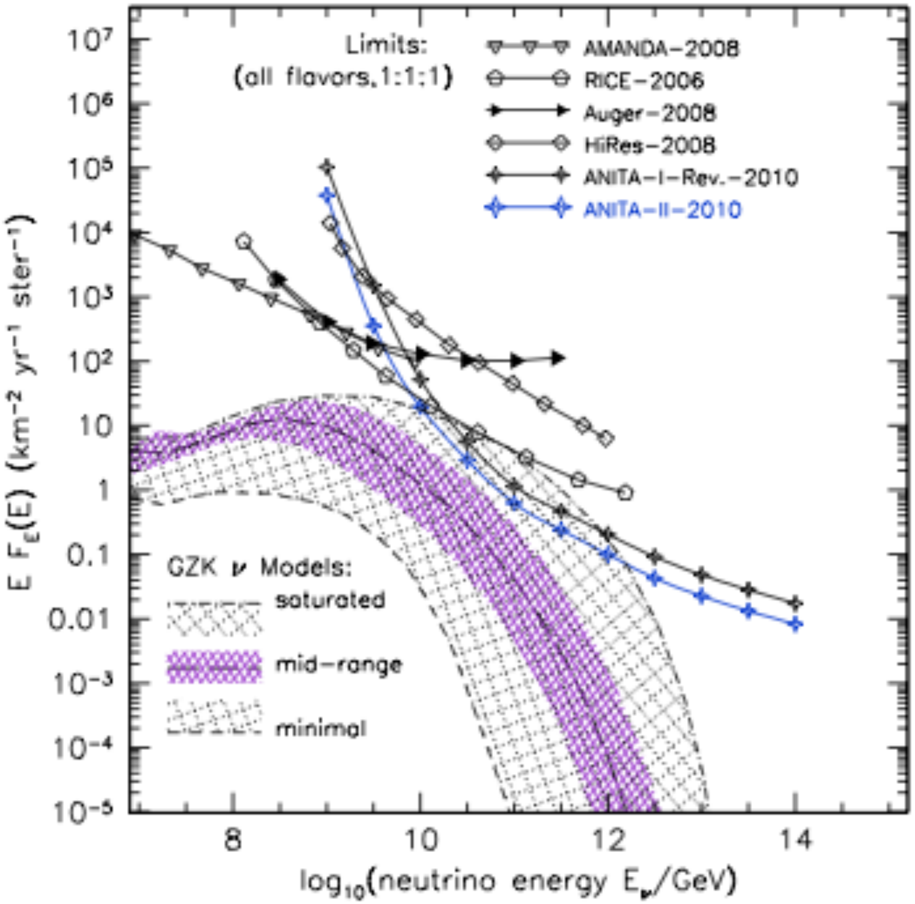

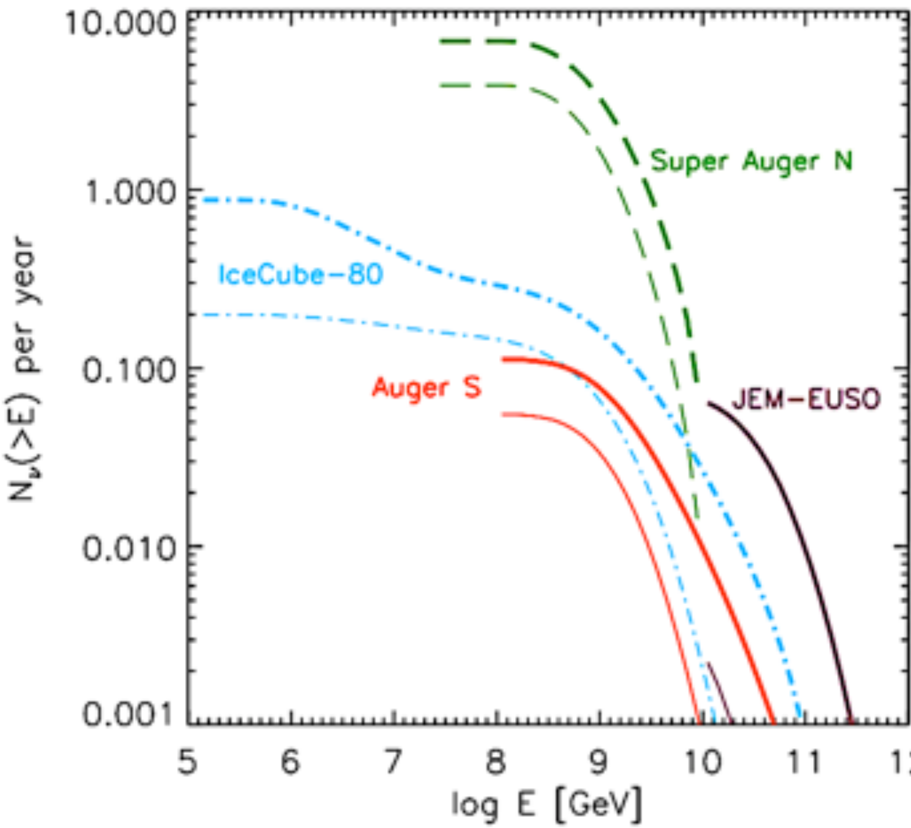

Rates for intermediate fluxes

P. Gorham et al, arXiv:1011.5004, Phys.Rev. D82 (2010) 022004

Kotera, Allard, Olinto, JCAP 1010 (2010) 013

133

TeV γ-ray fluxes also constrain cosmogenic neutrino fluxes

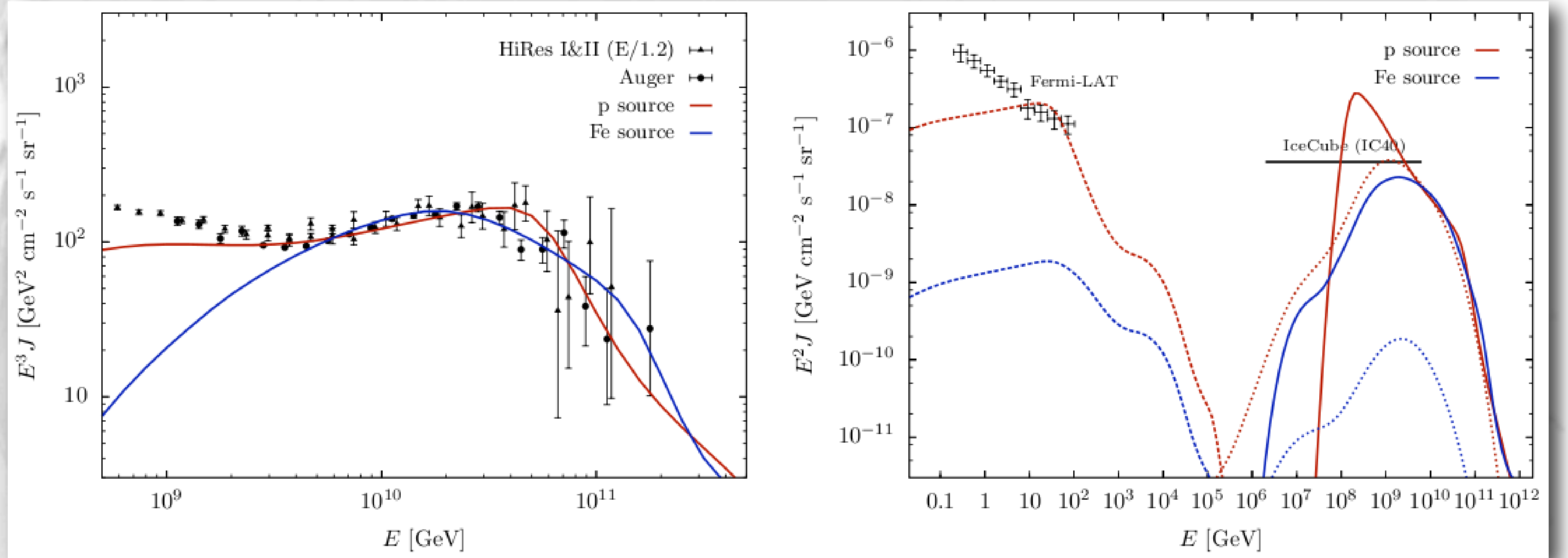

Ahlers and Salvado, arXiv:1105.5113

$$j_p(E) \propto \Theta(2-z)\,(1+z)^5\,E^{-2.3}\,\Theta\left(10^{20.5}\,\mathrm{eV}-E\right),$$

$$j_{\rm Fe}(E) \propto E^{-2.3}\,\Theta\left(26\times 10^{20.5}\,\mathrm{eV}-E\right).$$

134

Physics with Diffuse Secondary Gamma-Ray Fluxes

UHE gamma-ray fluxes depend on number of nucleons locally produced above GZK threshold which is proportional to E_{max}/A

Further suppressed for heavy nuclei due to increased pair production

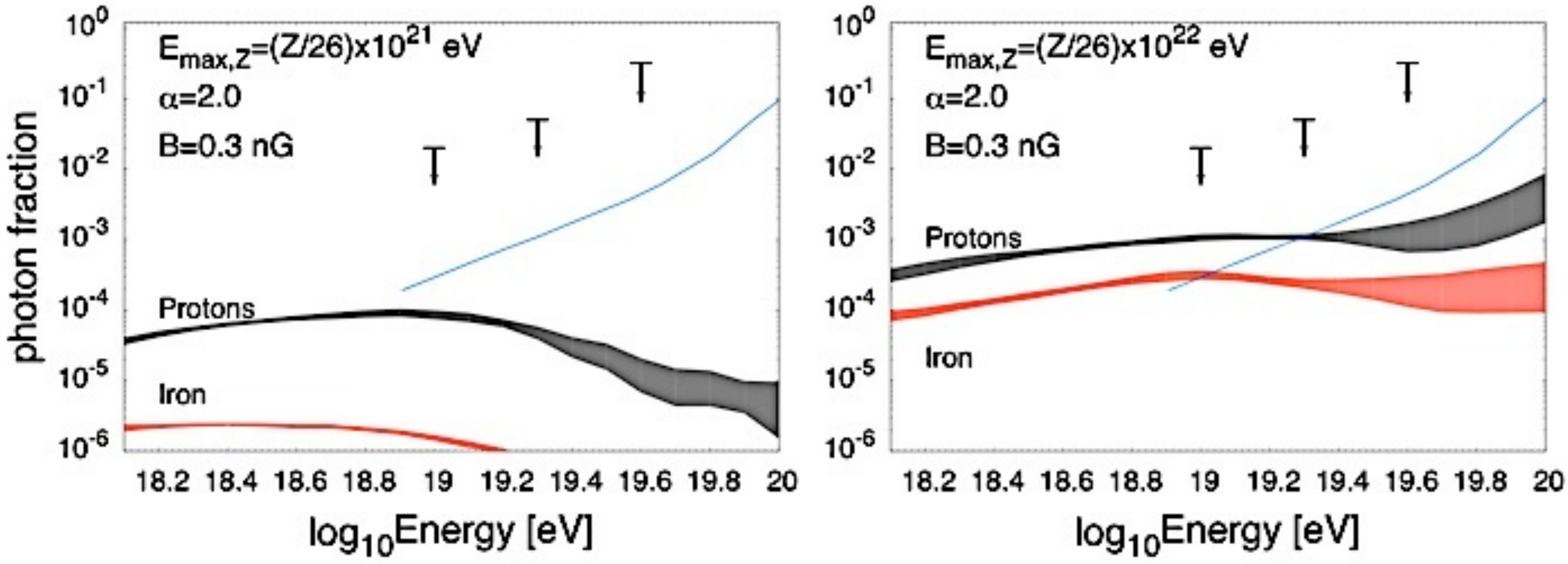

Hooper, Taylor, Sarkar, Astropart.Phys. 34 (2011) 340

The GZK neutrino flux can also be enhanced by magnetic fields surrounding the sources

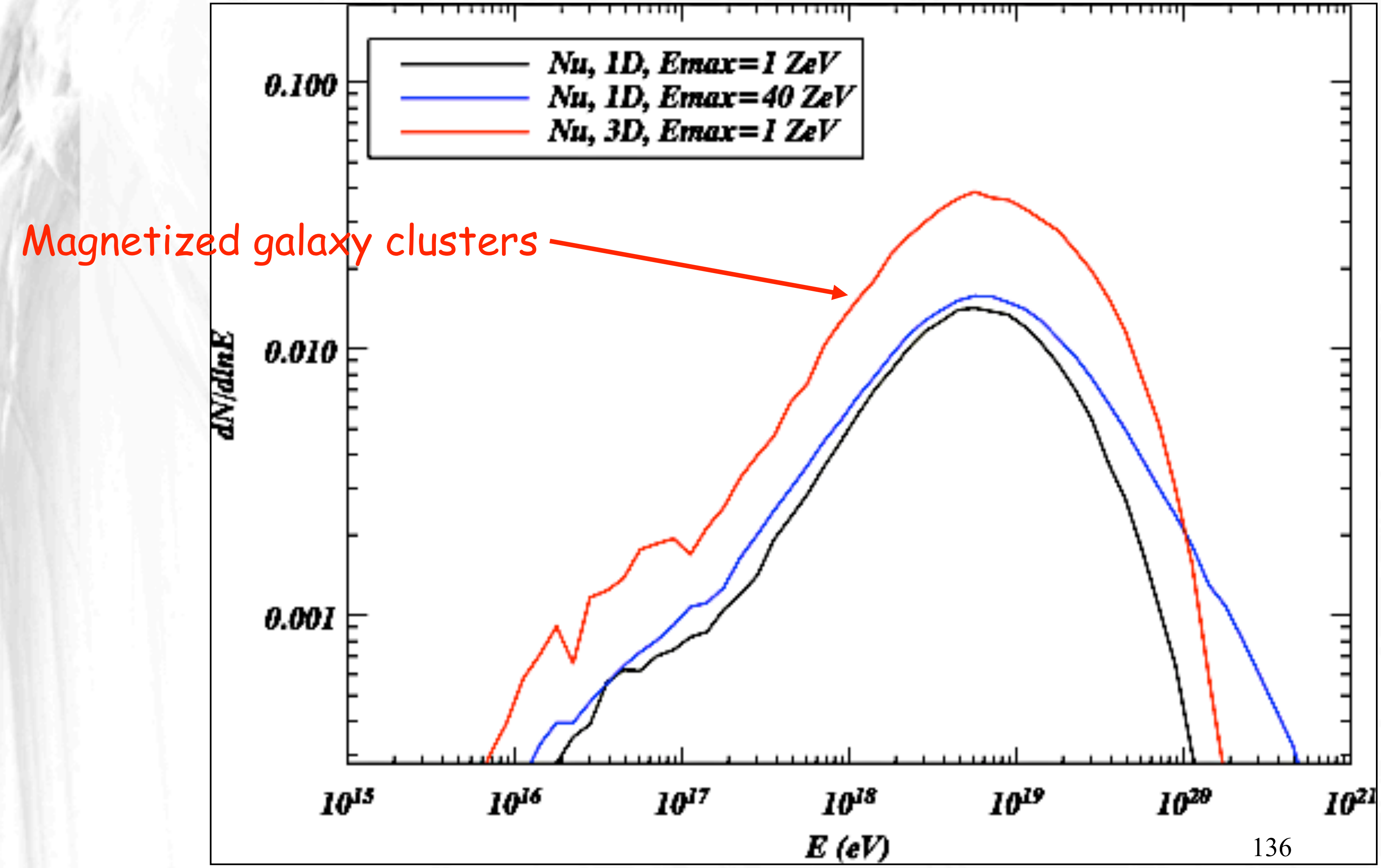

Armengaud and Sigl

Neutrino-Nucleon Cross Section and Required Detector Size

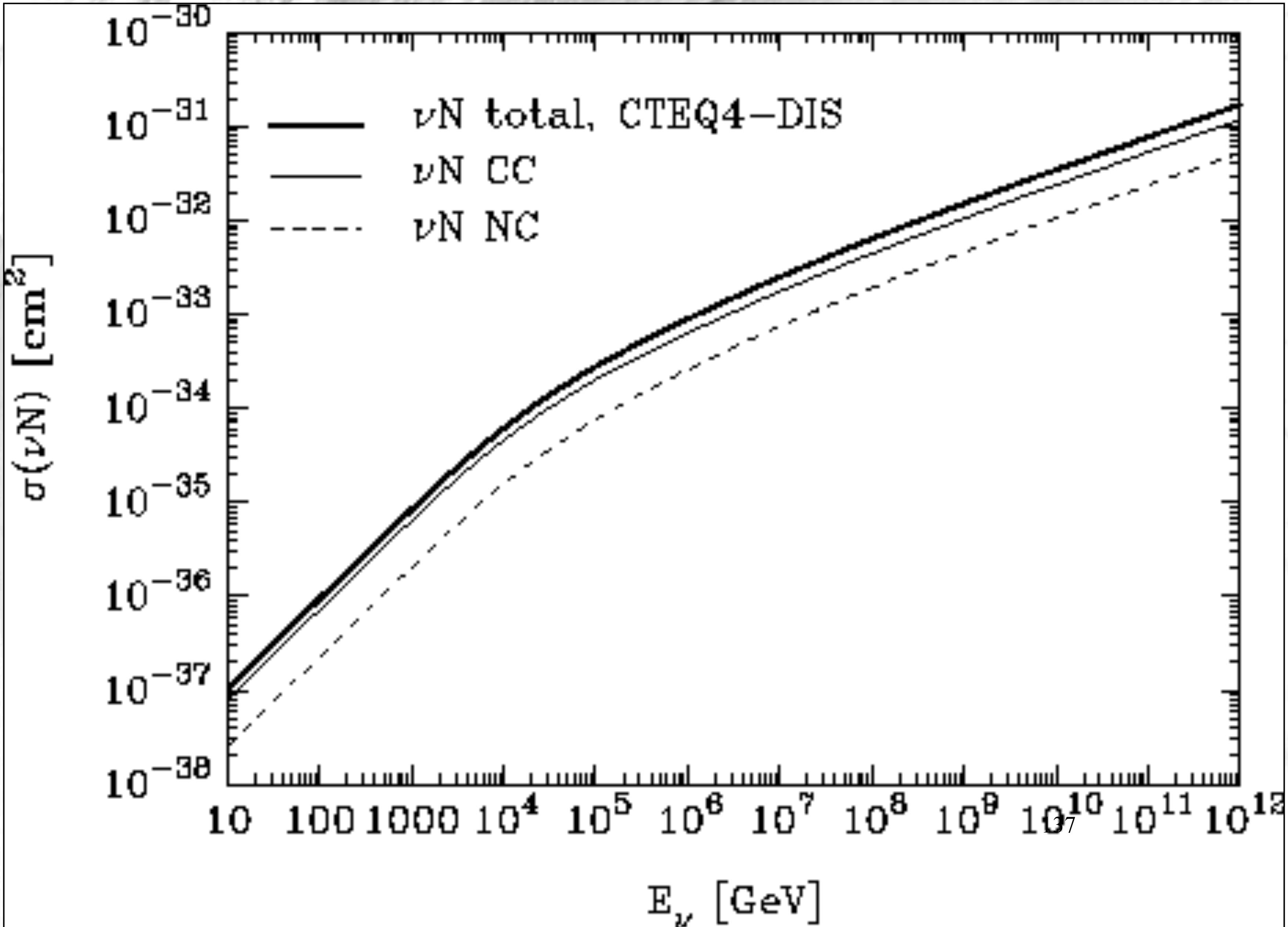

Ultra-High Energy Neutrino Detection: Traditional and New Ideas

Mostly uses the charged-current reactions: $\nu_i + N \text{ ® } l_i + N , \quad i = e, \mu, \tau$

Ultra-High Energy Neutrino Detection: Traditional and New Ideas

Mostly uses the charged-current reactions: $\nu_i + N \circledR\ l_i + N\,,\quad i = e, \mu, \tau$

1.) detect Cherenkov radiation from muons in deep sea or ice

AMANDA, ANTARES, BAIKAL, ICECUBE, KM3NeT

aims at 1 km^3 for E> 100 GeV to 1 TeV

138

Ultra-High Energy Neutrino Detection: Traditional and New Ideas

Mostly uses the charged-current reactions: $\nu_i + N \text{ ® } l_i + N\,,\quad i = e, \mu, \tau$

1.) detect Cherenkov radiation from muons in deep sea or ice
   AMANDA, ANTARES, BAIKAL, ICECUBE, KM3NeT
   aims at 1 km^3 for E> 100 GeV to 1 TeV

2.) horizontal air showers for electron and τ-neutrinos
   PIERRE AUGER
   for E> 10^{18} eV, increased efficiency for τ-neutrinos if surrounded by mountains on 100 km scale which is decay length of produced taus.

138

Ultra-High Energy Neutrino Detection: Traditional and New Ideas

Mostly uses the charged-current reactions: $\nu_i + N \rightarrow l_i + N\,, \quad i = e, \mu, \tau$

1.) detect Cherenkov radiation from muons in deep sea or ice

AMANDA, ANTARES, BAIKAL, ICECUBE, KM3NeT

aims at 1 km^3 for E> 100 GeV to 1 TeV

2.) horizontal air showers for electron and τ-neutrinos

PIERRE AUGER

for E> 10^{18} eV, increased efficiency for τ-neutrinos if surrounded by mountains on 100 km scale which is decay length of produced taus.

3.) detection of inclined showers from space for E>10^{20} eV

EUSO

138

Ultra-High Energy Neutrino Detection: Traditional and New Ideas

Mostly uses the charged-current reactions: $\nu_i + N \rightarrow l_i + N\,,\quad i = e, \mu, \tau$

1.) detect Cherenkov radiation from muons in deep sea or ice
   AMANDA, ANTARES, BAIKAL, ICECUBE, KM3NeT
   aims at 1 km^3 for E> 100 GeV to 1 TeV

2.) horizontal air showers for electron and τ-neutrinos
   PIERRE AUGER
   for E> 10^{18} eV, increased efficiency for τ-neutrinos if surrounded by mountains on 100 km scale which is decay length of produced taus.

3.) detection of inclined showers from space for E>10^{20} eV
   EUSO

4.) detection of radio emission from negative charge excess of showers produced in air, water, ice, or in skimming rock.
   RICE (in South-pole ice), GLUE (radio-telescope observing the moons rim)

Ultra-High Energy Neutrino Detection: Traditional and New Ideas

Mostly uses the charged-current reactions: $\nu_i + N \rightarrow l_i + N, \quad i = e, \mu, \tau$

1.) detect Cherenkov radiation from muons in deep sea or ice
AMANDA, ANTARES, BAIKAL, ICECUBE, KM3NeT
aims at 1 km^3 for E> 100 GeV to 1 TeV

2.) horizontal air showers for electron and τ-neutrinos
PIERRE AUGER
for E> 10^{18} eV, increased efficiency for τ-neutrinos if surrounded by mountains on 100 km scale which is decay length of produced taus.

3.) detection of inclined showers from space for E>10^{20} eV
EUSO

4.) detection of radio emission from negative charge excess of showers produced in air, water, ice, or in skimming rock.
RICE (in South-pole ice), GLUE (radio-telescope observing the moons rim)

5.) acoustic detection in water: hydrophonic arrays

Ultra-High Energy Neutrino Detection: Traditional and New Ideas

Mostly uses the charged-current reactions: $\nu_i + N \rightarrow l_i + N, \quad i = e, \mu, \tau$

1.) detect Cherenkov radiation from muons in deep sea or ice
AMANDA, ANTARES, BAIKAL, ICECUBE, KM3NeT
aims at 1 km^3 for E> 100 GeV to 1 TeV

2.) horizontal air showers for electron and τ-neutrinos
PIERRE AUGER
for E> 10^{18} eV, increased efficiency for τ-neutrinos if surrounded by mountains on 100 km scale which is decay length of produced taus.

3.) detection of inclined showers from space for E>10^{20} eV
EUSO

4.) detection of radio emission from negative charge excess of showers produced in air, water, ice, or in skimming rock.
RICE (in South-pole ice), GLUE (radio-telescope observing the moons rim)

5.) acoustic detection in water: hydrophonic arrays

6.) Earth-skimming events in ground arrays or fluorescence detectors.

Experimental Detection of E<10^{17}eV Neutrinos

139

Experimental Detection of E<10^{17}eV Neutrinos

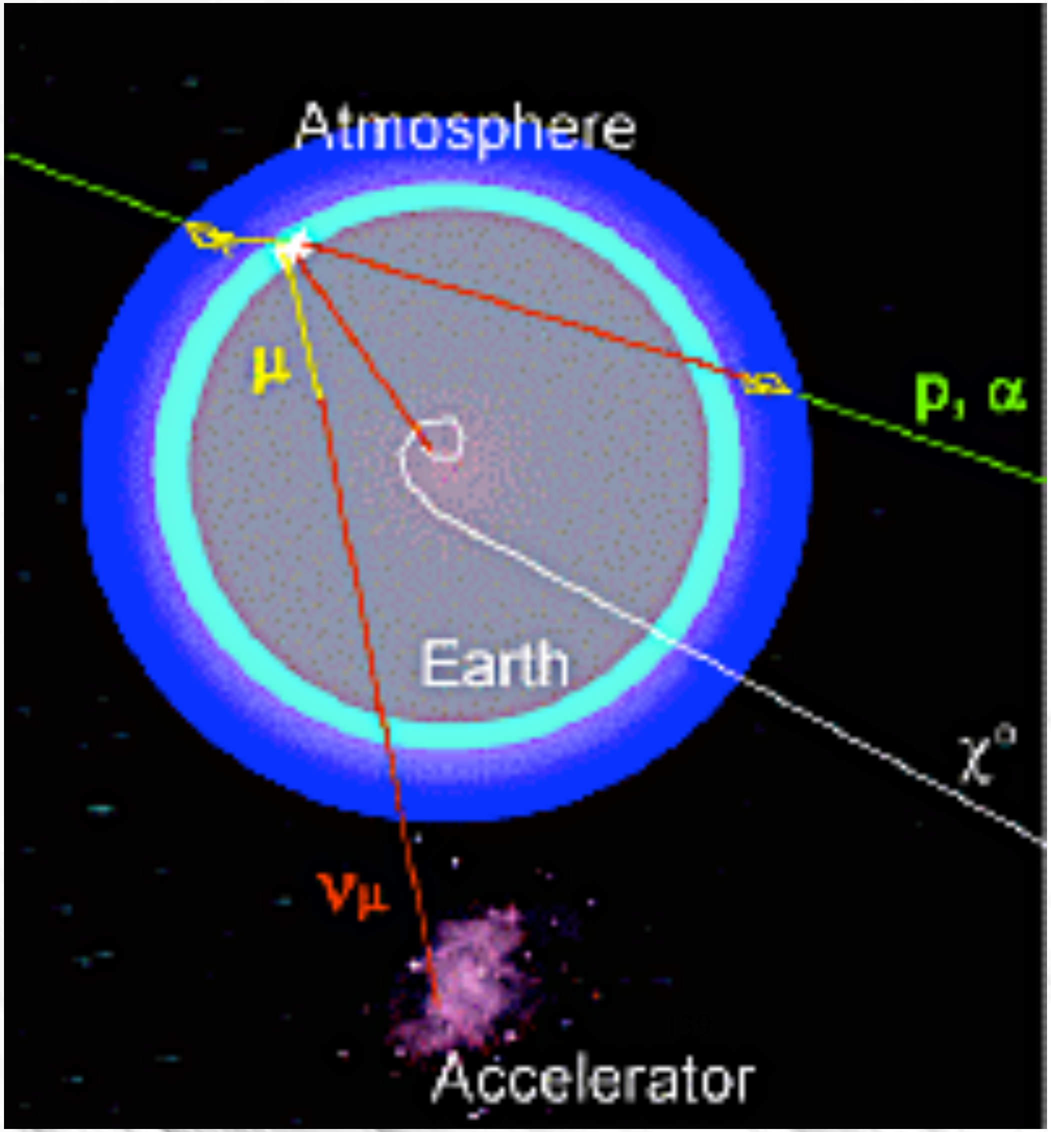

Experimental Detection of E<10^{17}eV Neutrinos

- Neutrinos coming from above are secondary from cosmic rays

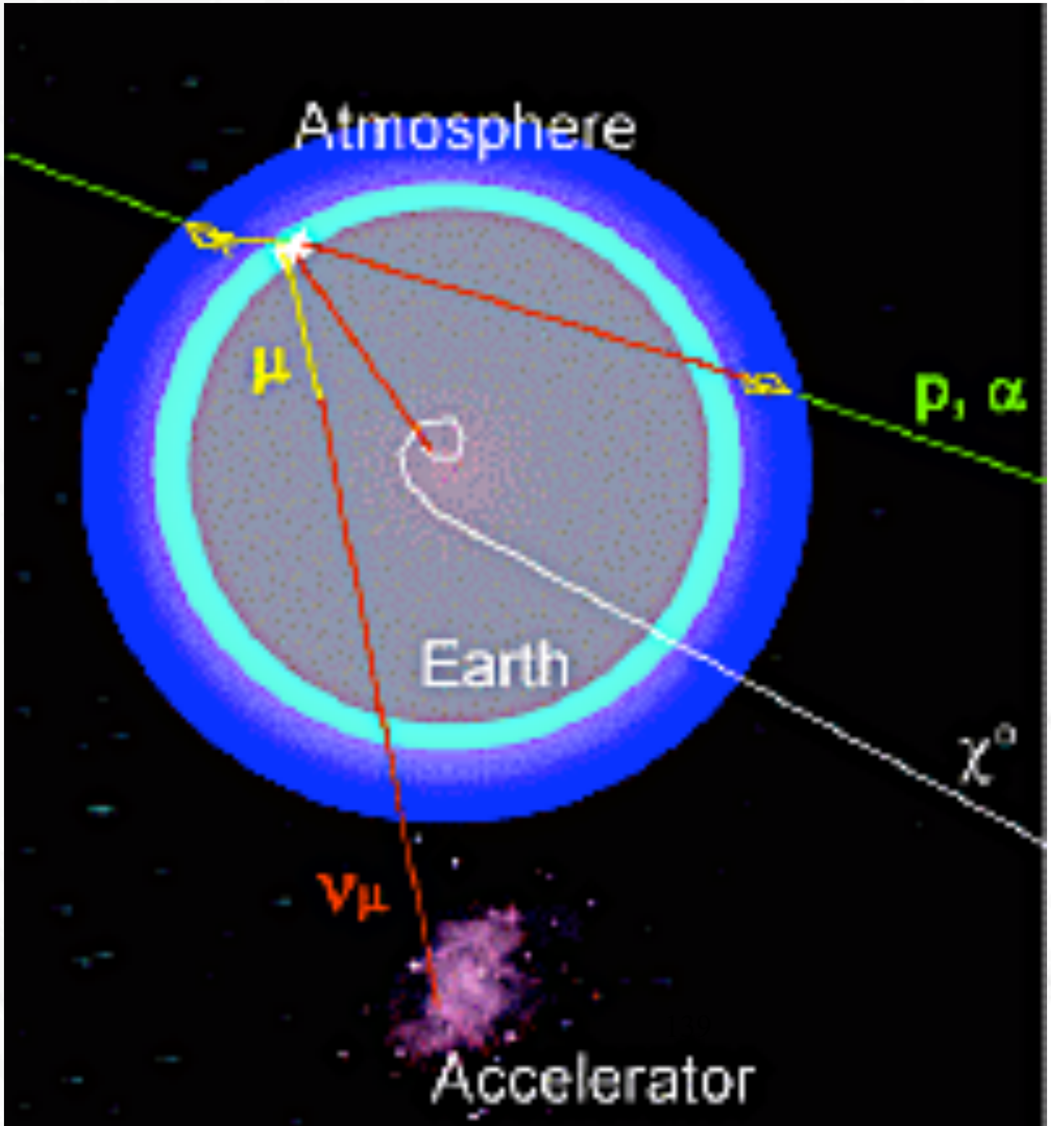

Experimental Detection of E<10^{17}eV Neutrinos

- Neutrinos coming from above are secondary from cosmic rays

- Neutrino coming from below are mixture of atmospheric neutrinos and HE neutrinos from space

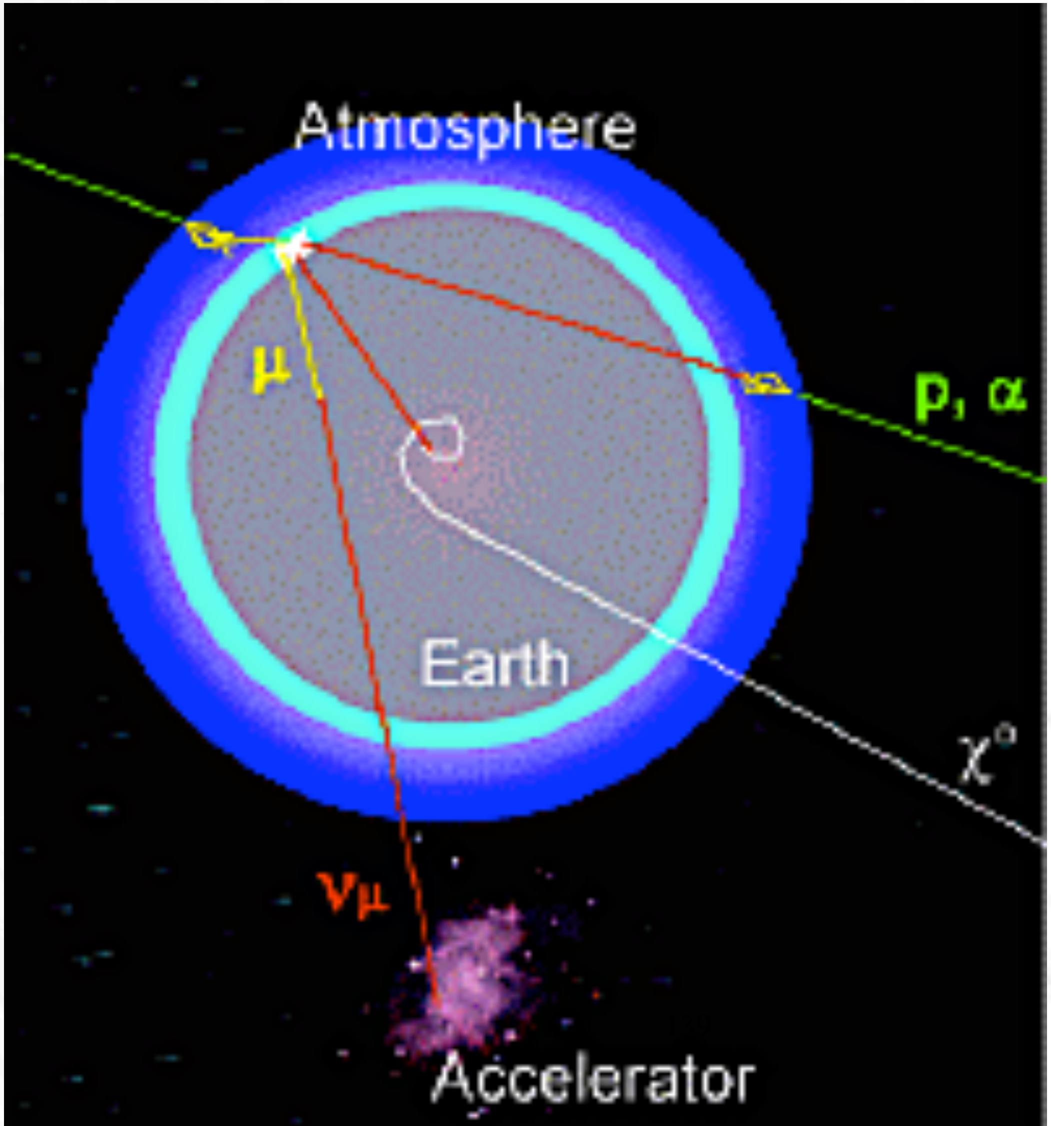

Experimental Detection of E<10^{17}eV Neutrinos

- Neutrinos coming from above are secondary from cosmic rays

- Neutrino coming from below are mixture of atmospheric neutrinos and HE neutrinos from space

- Earth is not transparent for neutrinos E>10^{15}eV

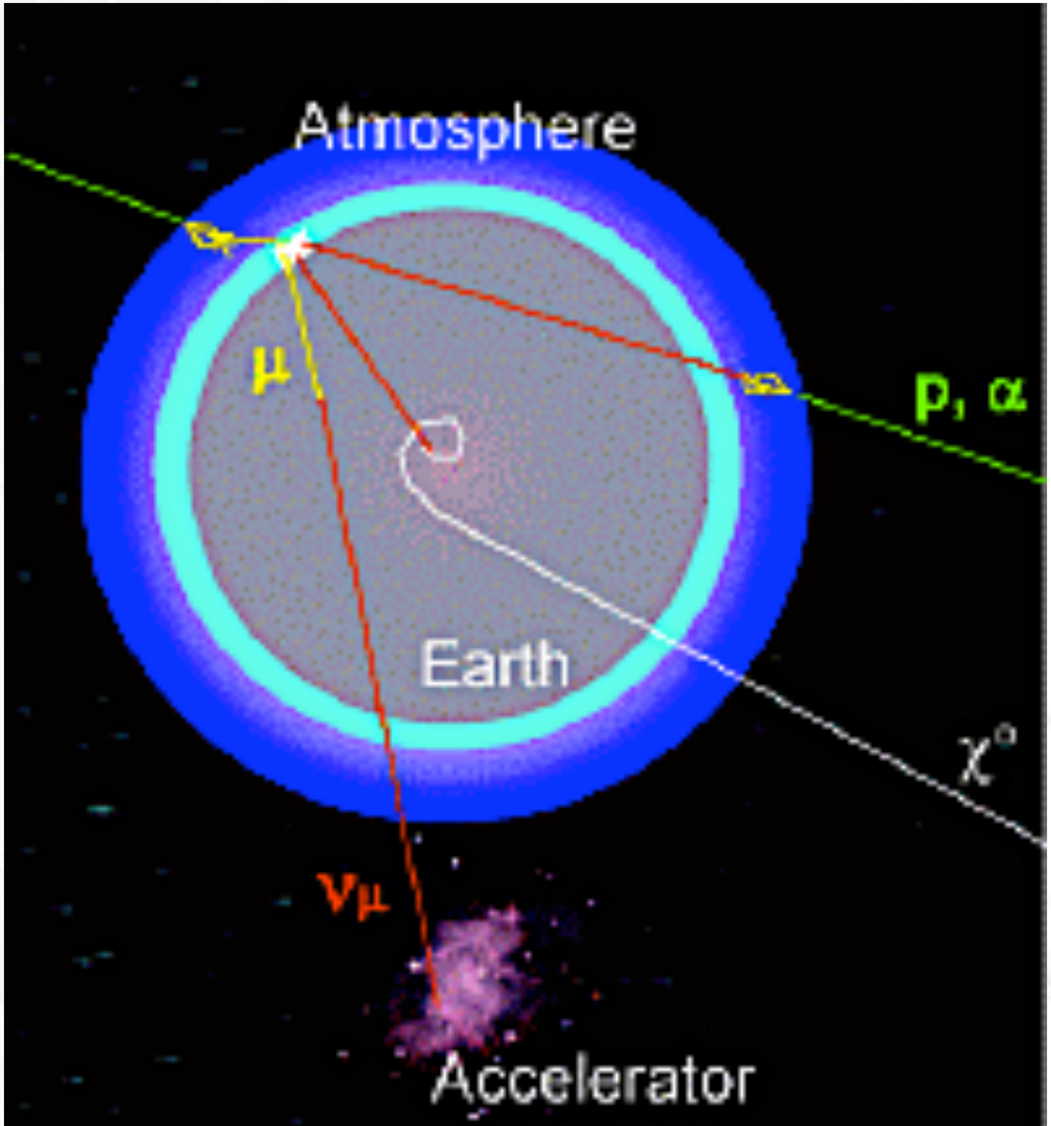

Experimental Detection of $E<10^{17}$eV Neutrinos

- Neutrinos coming from above are secondary from cosmic rays
- Neutrino coming from below are mixture of atmospheric neutrinos and HE neutrinos from space
- Earth is not transparent for neutrinos $E>10^{15}$eV
- Former experiments:

  MACRO, Baikal, AMANDA

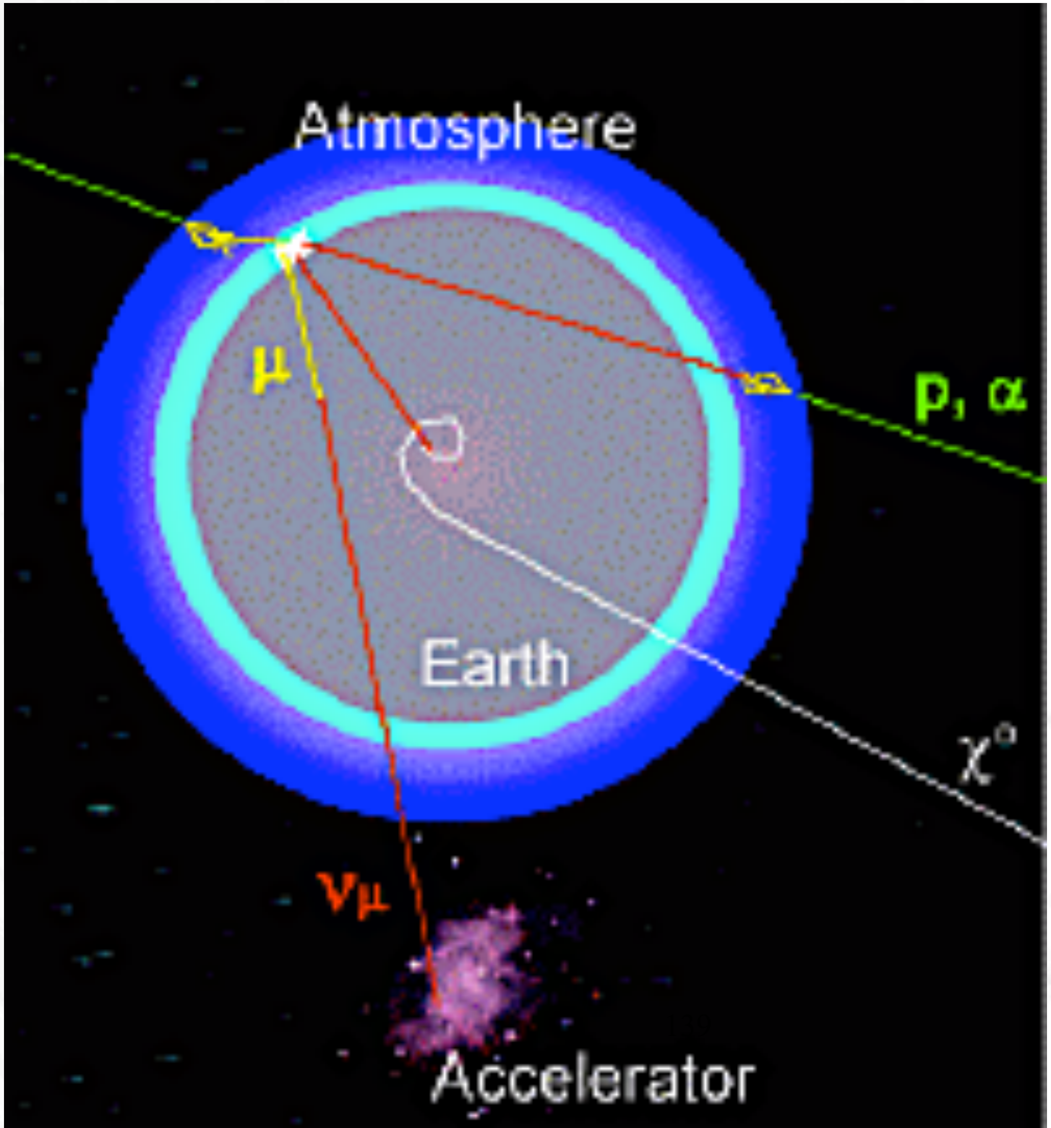

Experimental Detection of E<10^{17}eV Neutrinos

- Neutrinos coming from above are secondary from cosmic rays

- Neutrino coming from below are mixture of atmospheric neutrinos and HE neutrinos from space

- Earth is not transparent for neutrinos E>10^{15}eV

- Former experiments:
  MACRO, Baikal, AMANDA

- Present/future experiments:
  ANTARES, ICECUBE, KM3NeT

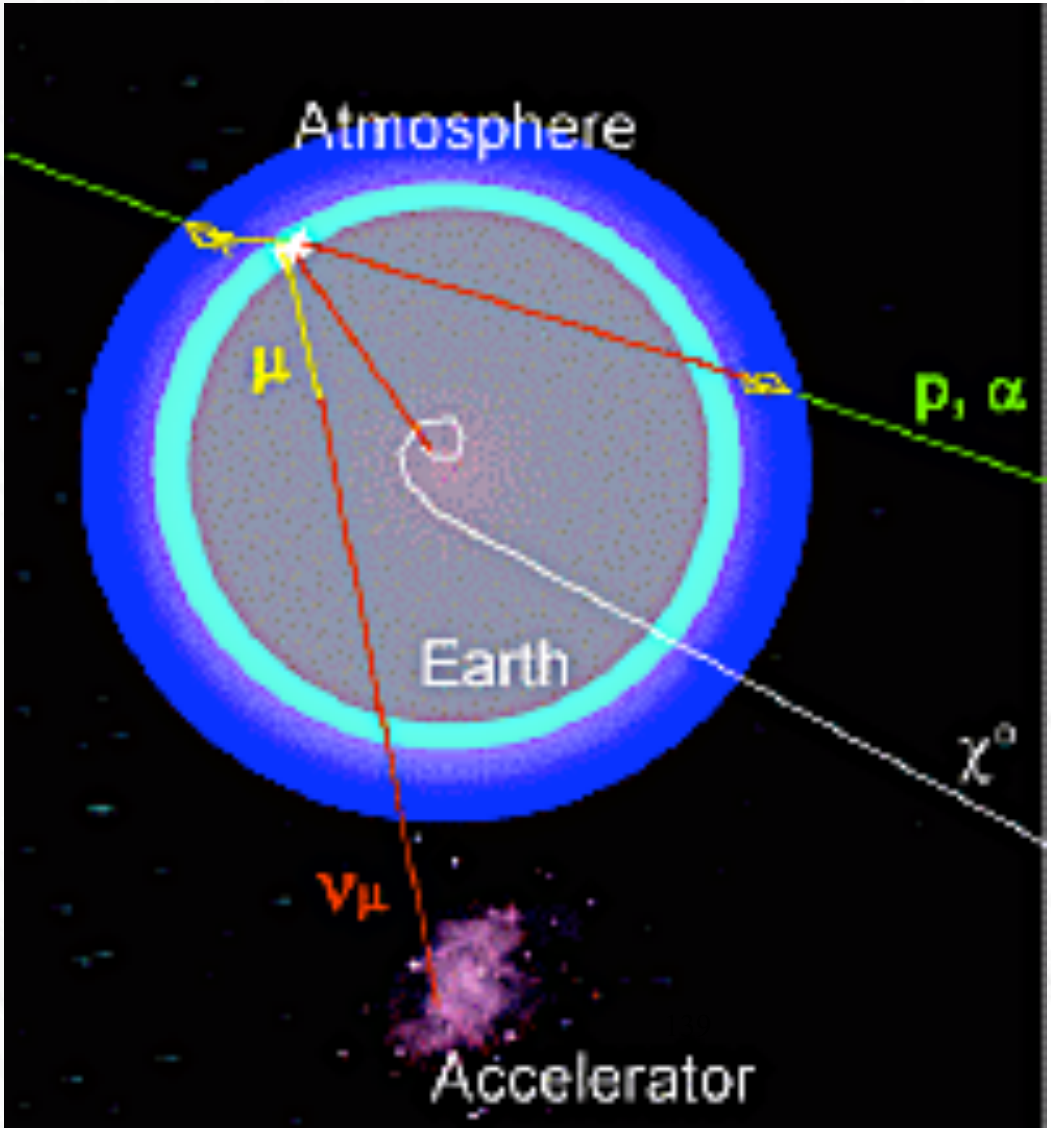

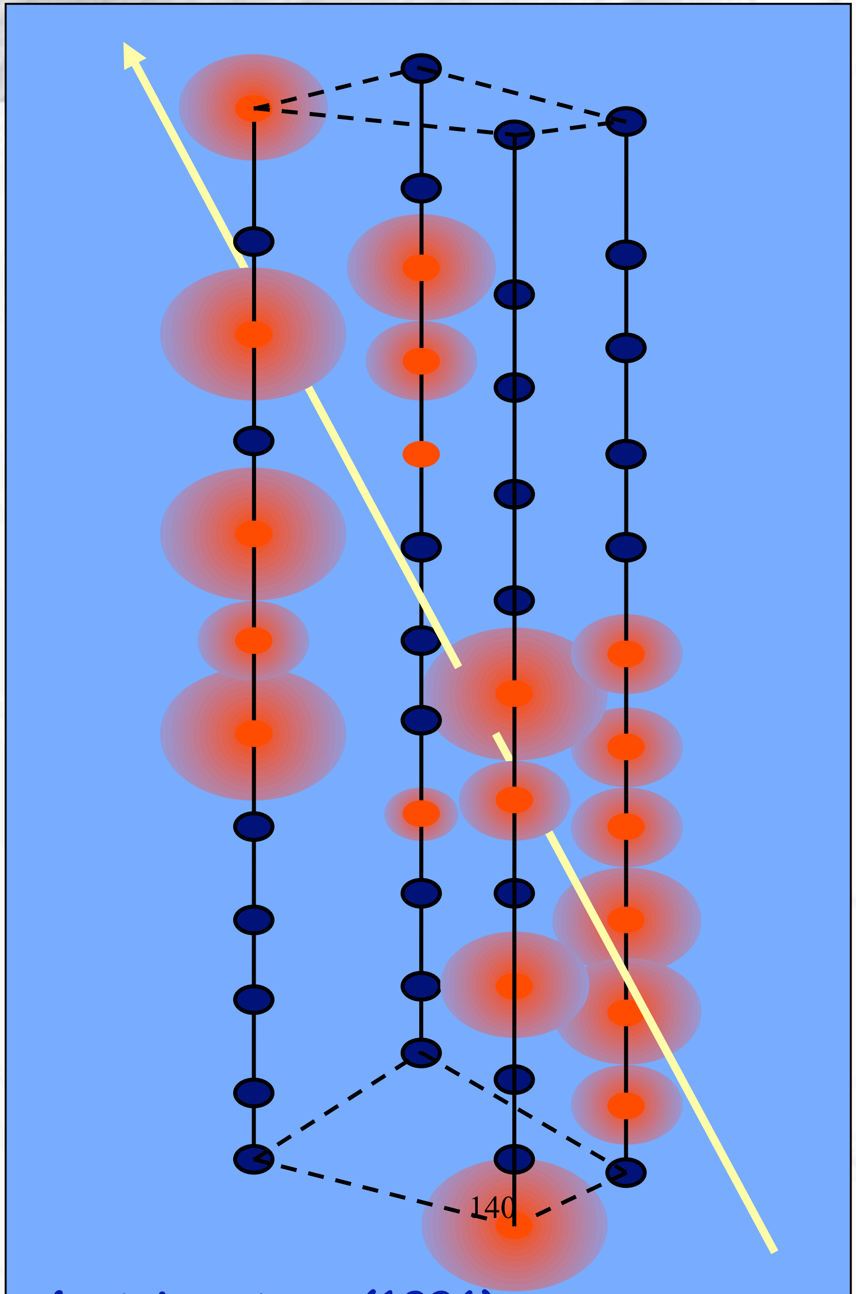

4-string stage (1996)

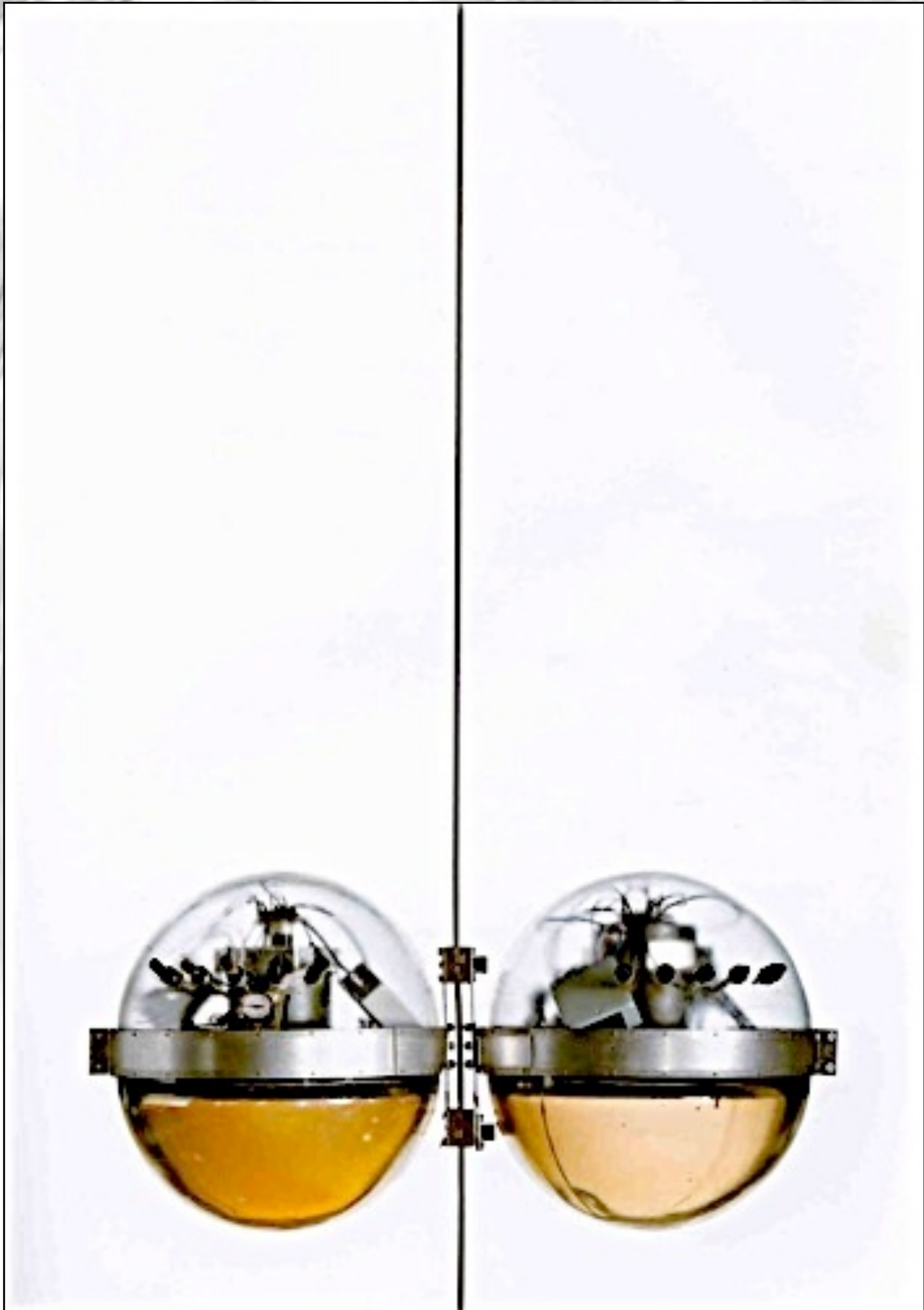

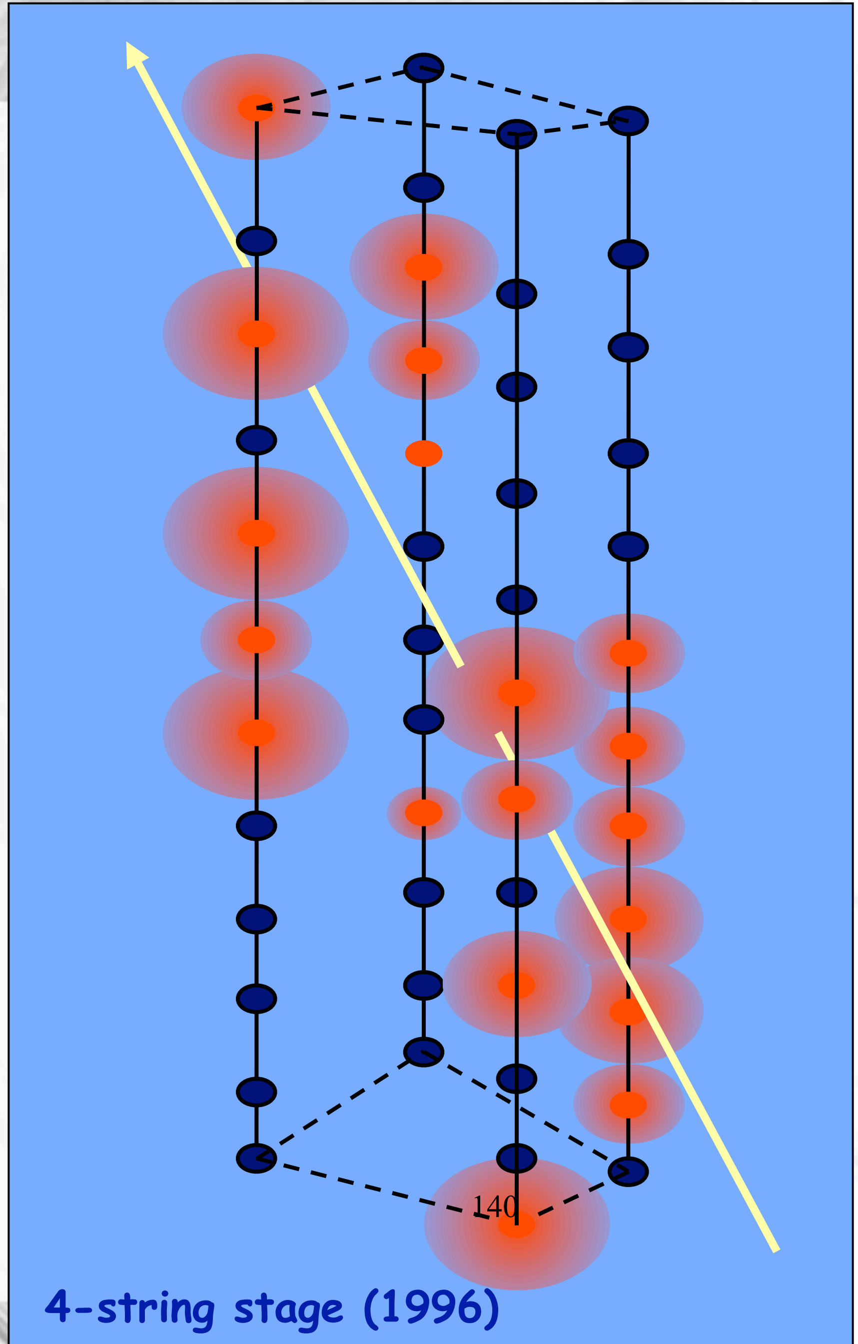
140
4-string stage (1996)

Lake Baikal

First underwater telescope
First neutrinos underwater

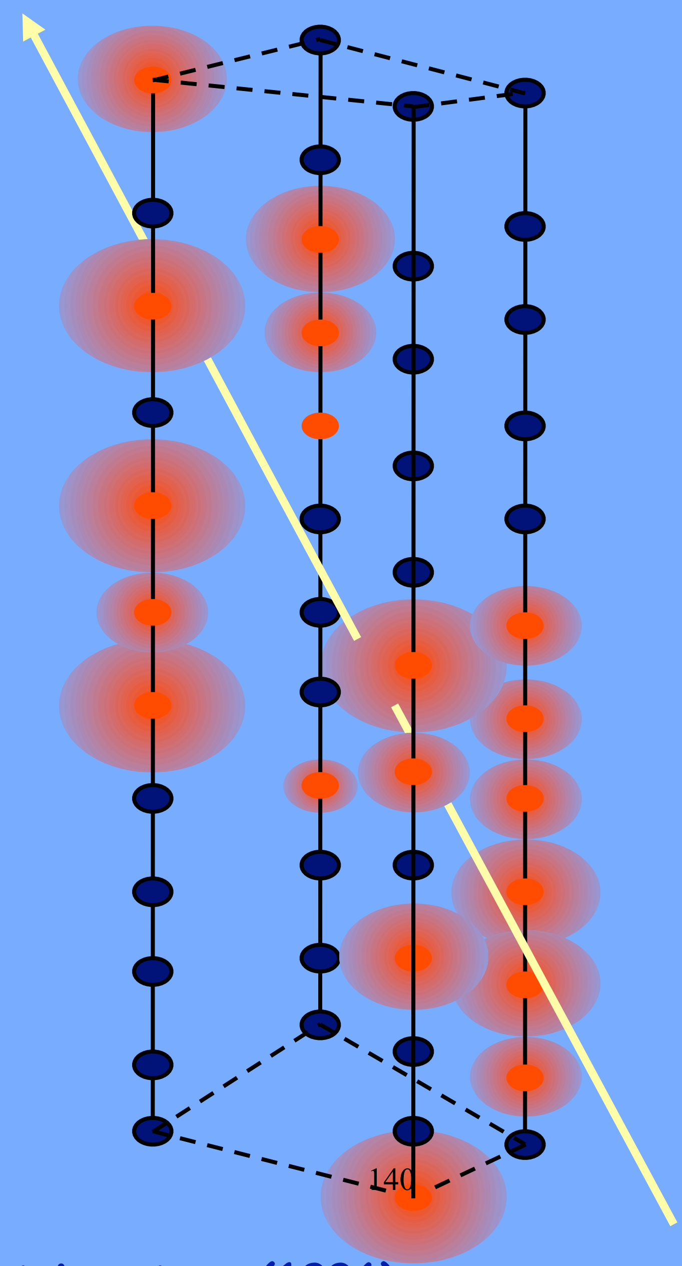

4-string stage (1996)

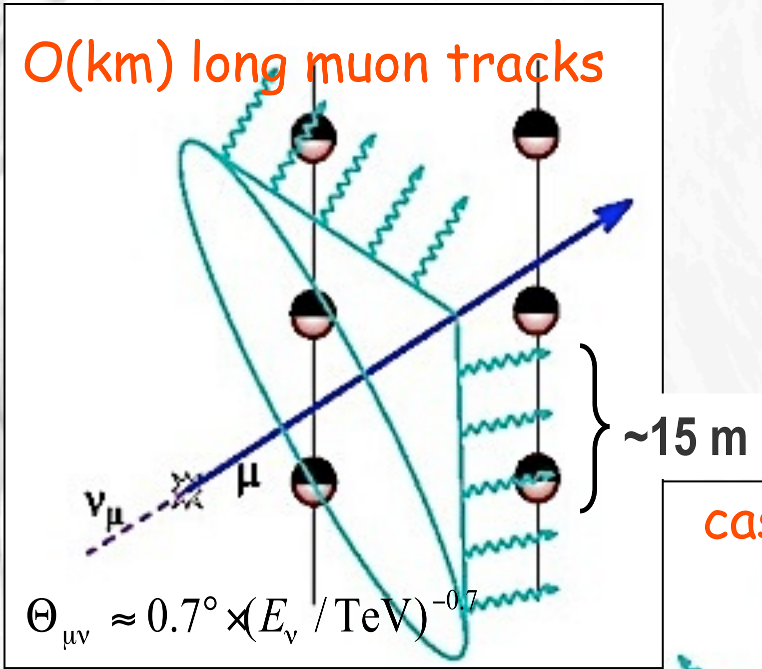

event reconstruction by Cherenkov light timing

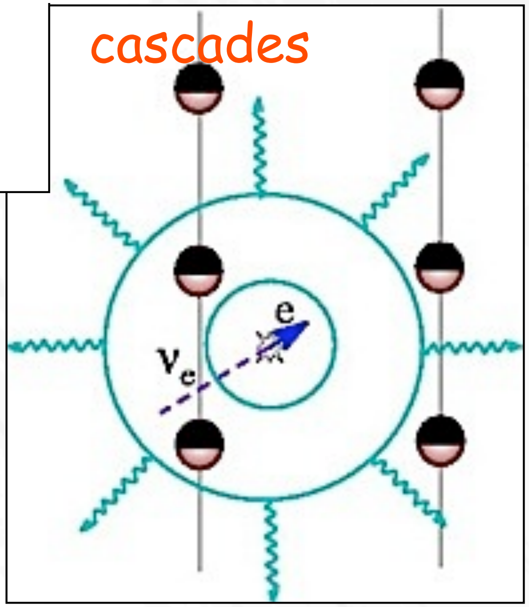

South Pole ice:
(most?) transparent
natural condensed material

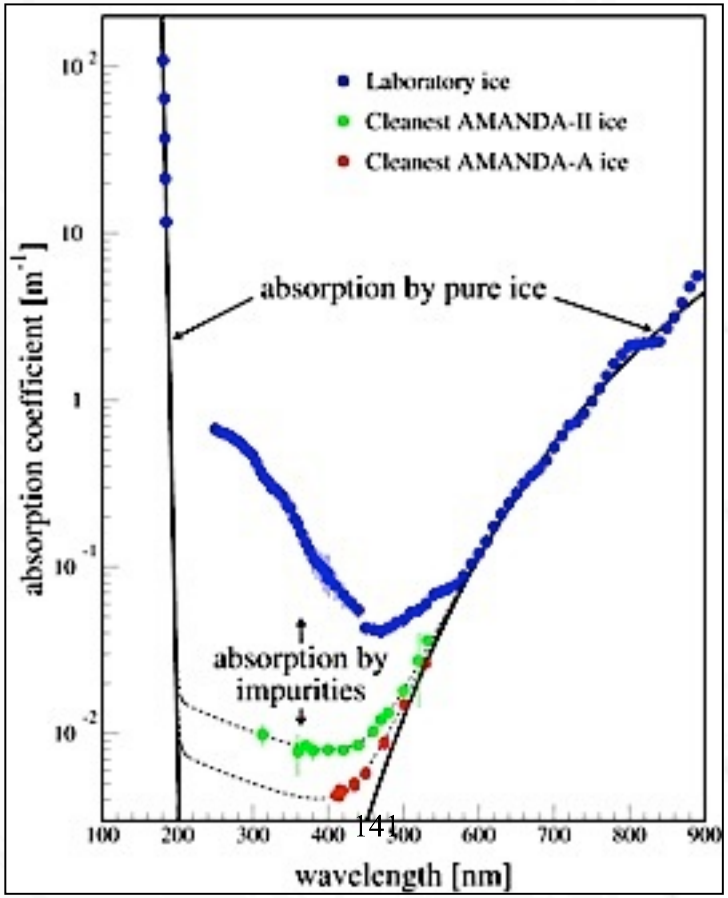

Longer absorption length → larger effective volume

Mediterranean Projects

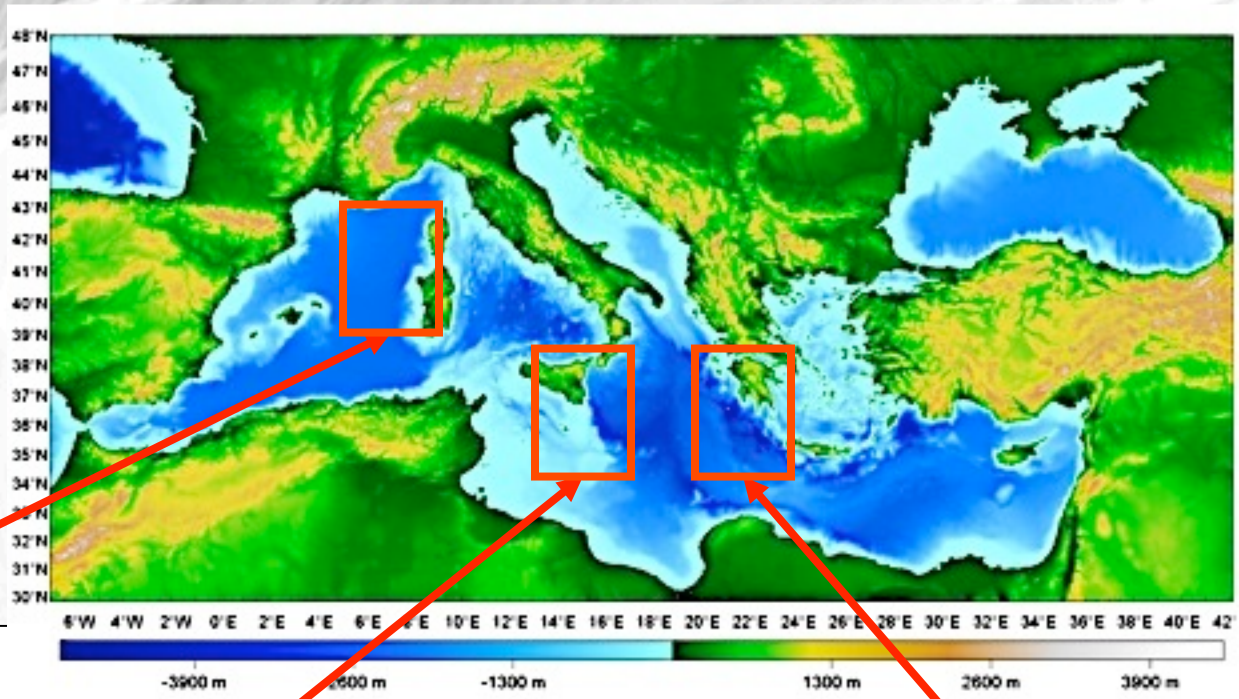

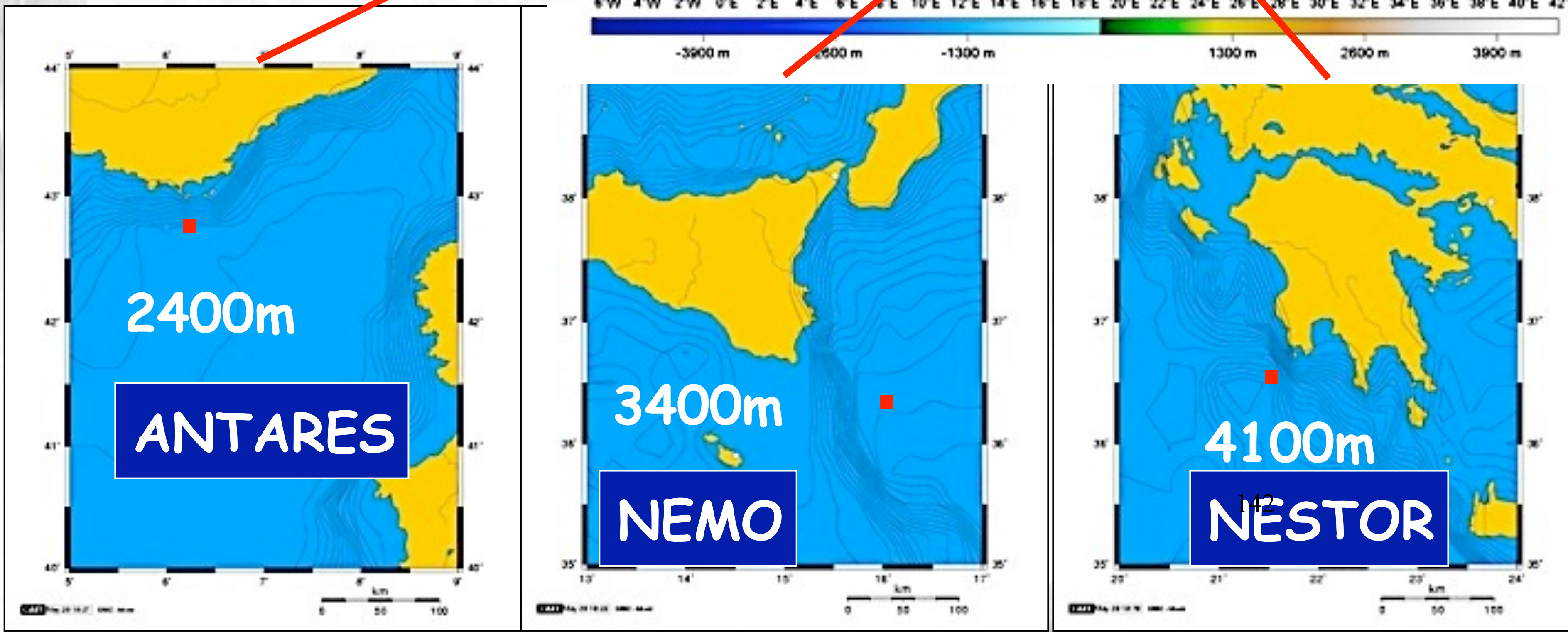

IceCube / Deep Core

- detects Cherenkov light from showers and muon tracks initiated by neutrinos
- detects ~220 neutrinos and 1.7×10^8 muons per day
- threshold 10 GeV
- angular resolution 0.4~1 degree

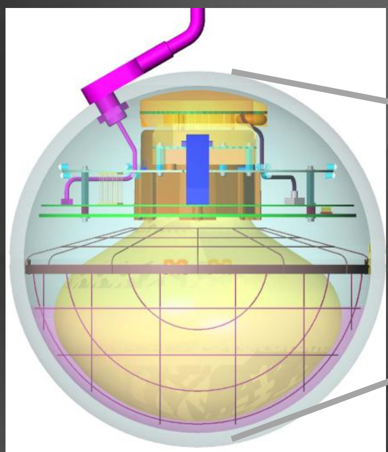

5320 Digital Optical Modules (DOM)

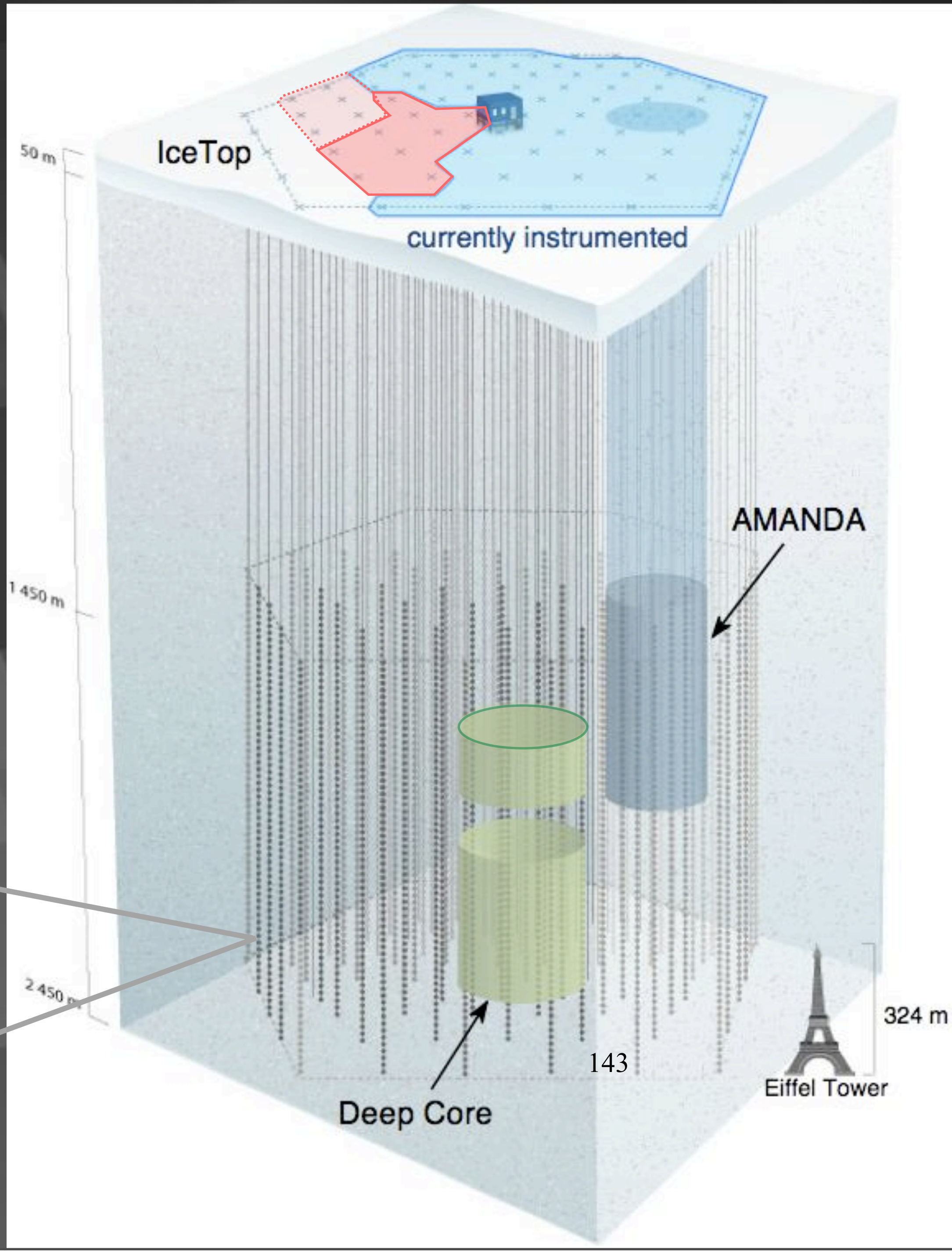

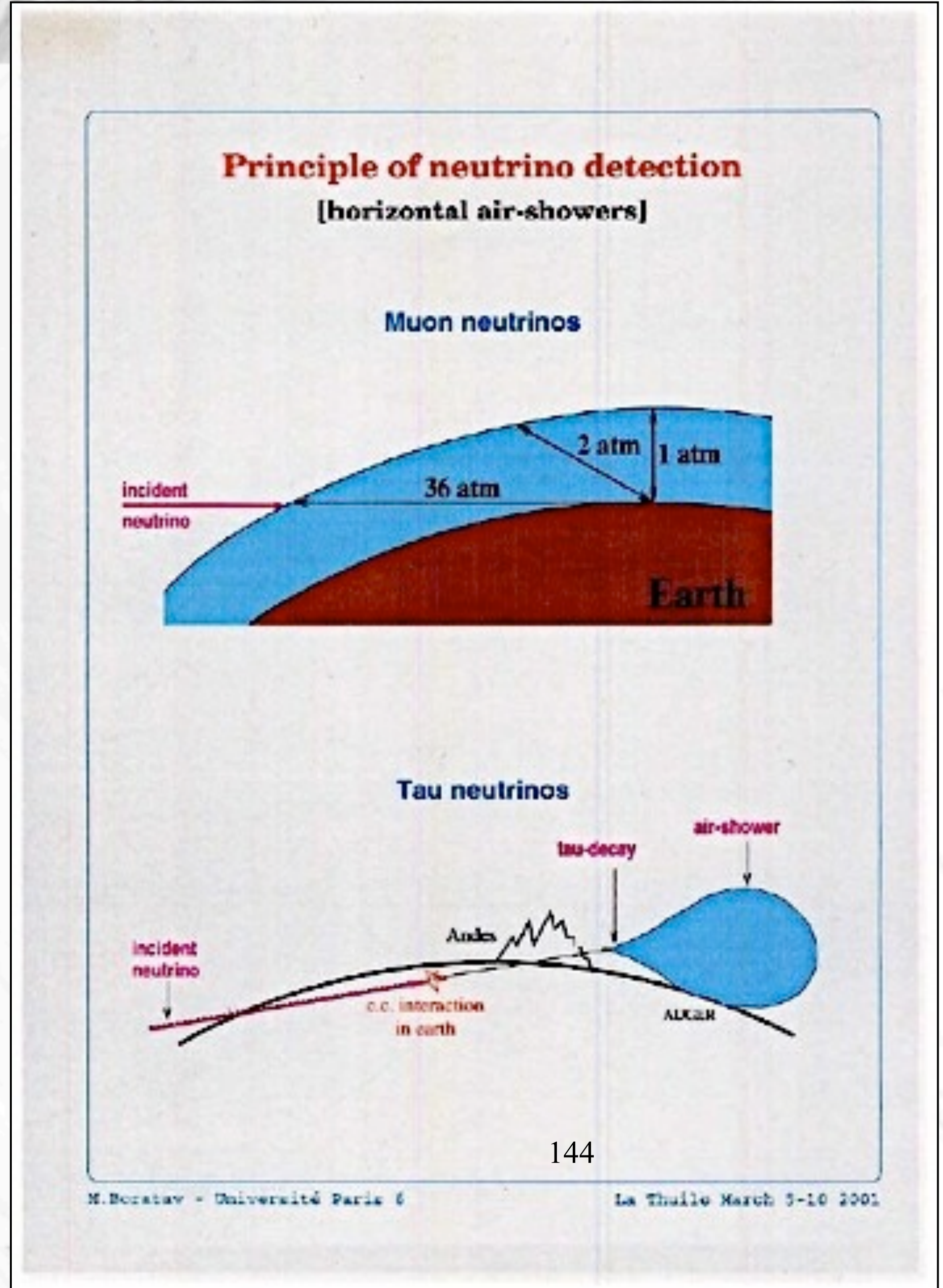
Principle of neutrino detection
[horizontal air-showers]
Muon neutrinos
2 atm
1 atm
36 atm
incident
neutrino
Earth
Tau neutrinos
air-shower
tau-decay
Andes
incident
neutrino
c.c. interaction
in earth
144
M.Boratav - Université Paris 6
La Thuile March 5-10 2001

- Neutrinos are not primary UHECR

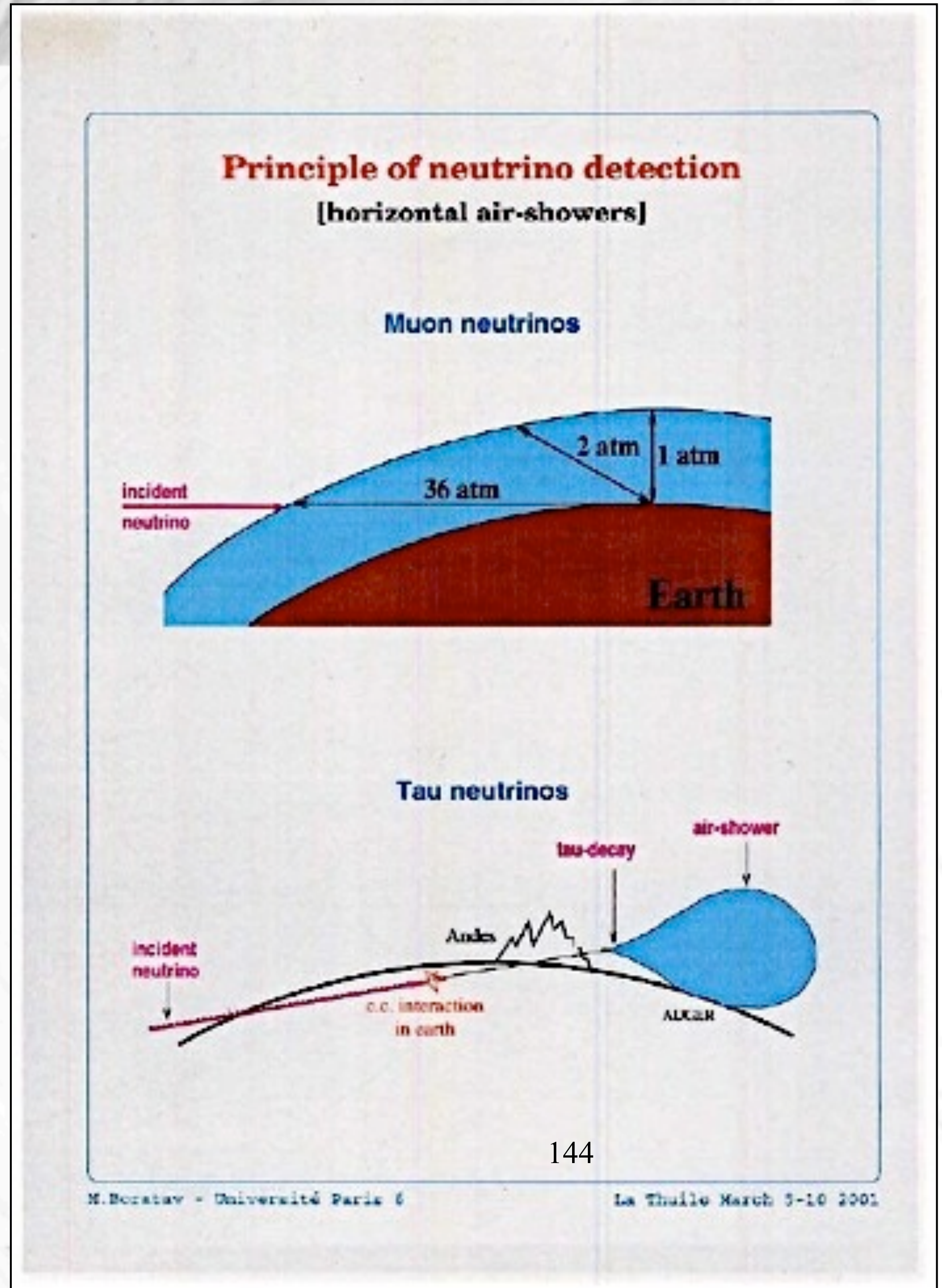

- Neutrinos are not primary UHECR
- Horizontal or Earth-skimming air showers – easy way to detect neutrinos

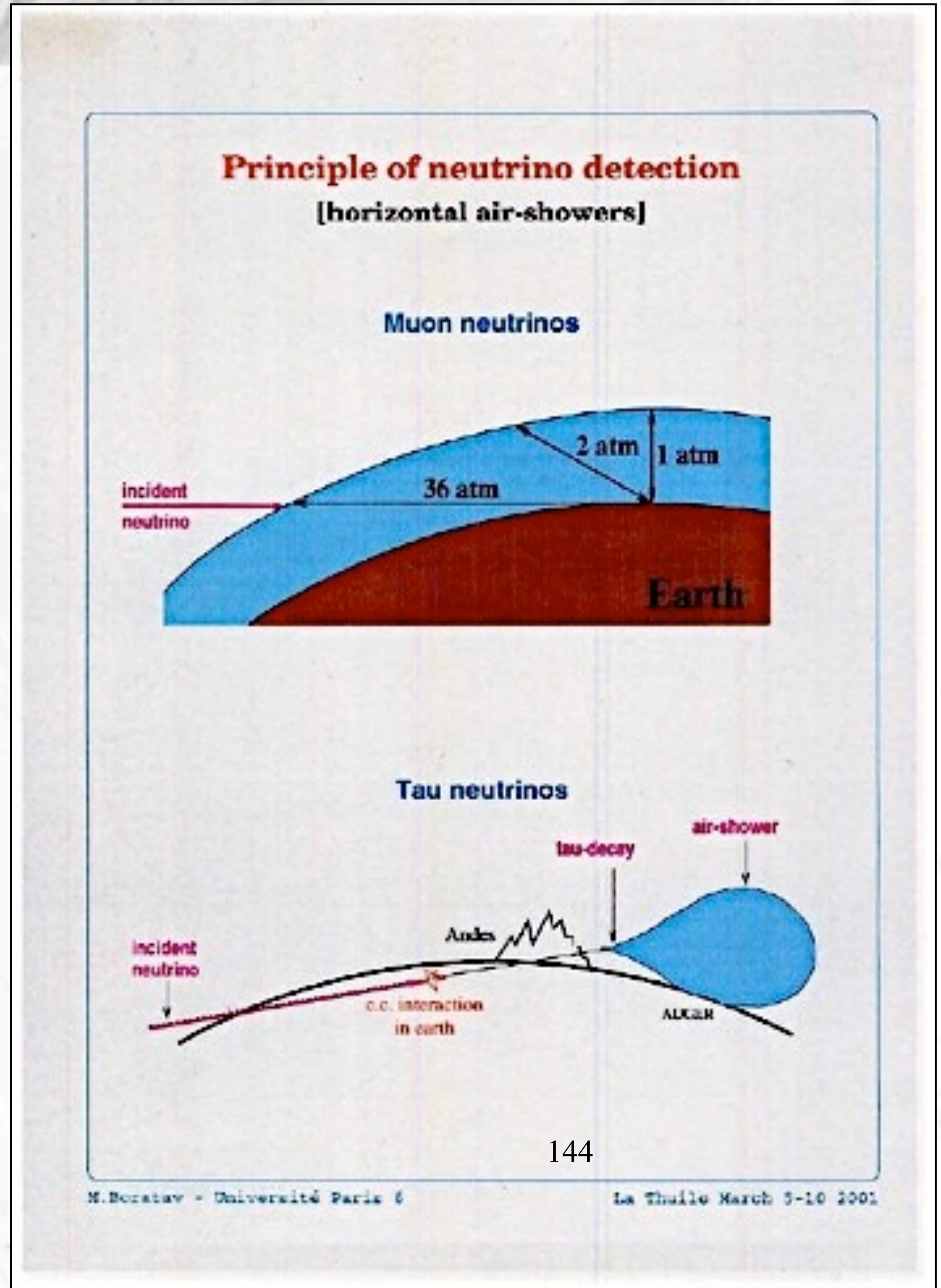

- Neutrinos are not primary UHECR
- Horizontal or Earth-skimming air showers – easy way to detect neutrinos
- Former experiments:

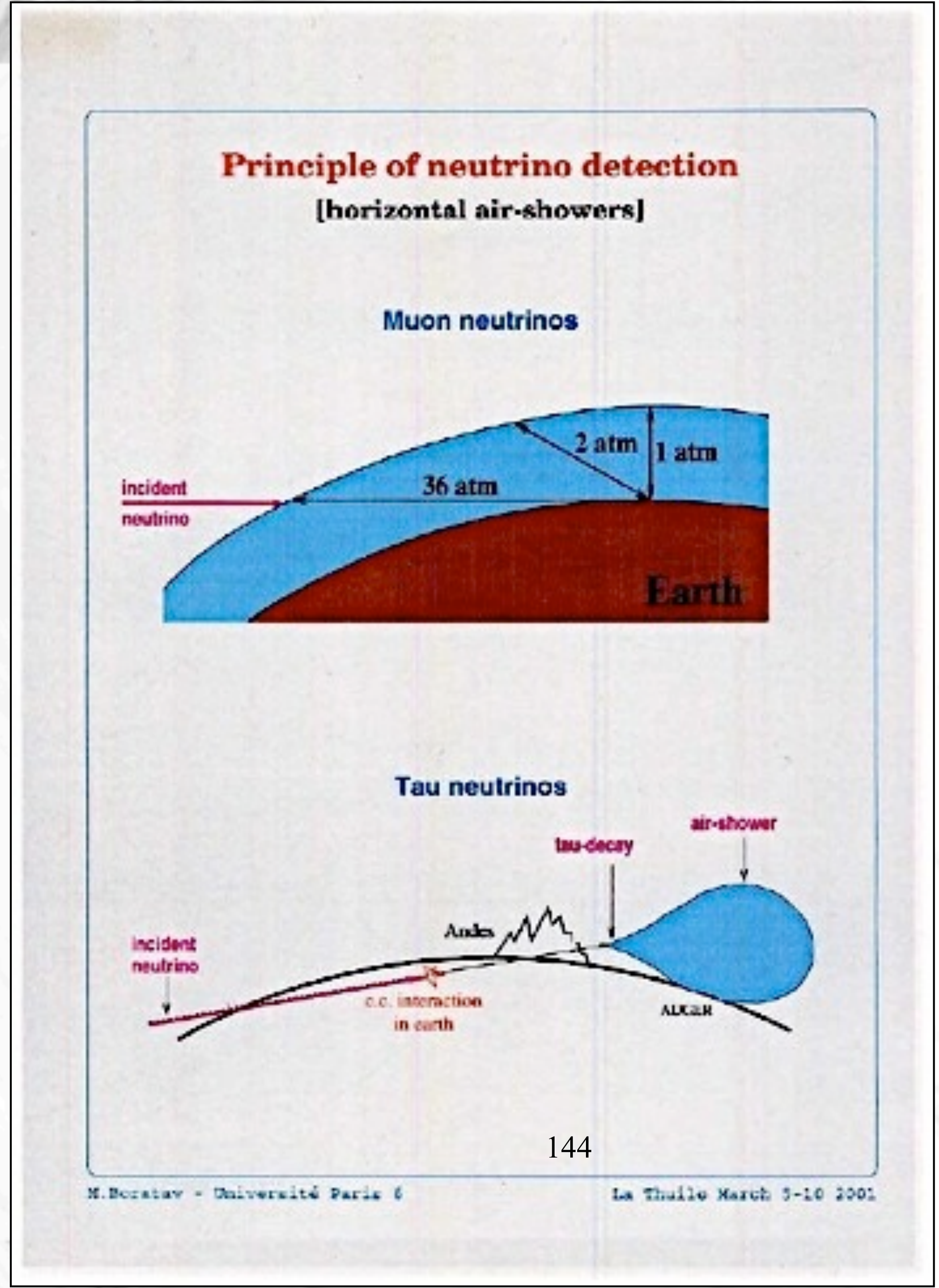

- Neutrinos are not primary UHECR

- Horizontal or Earth-skimming air showers – easy way to detect neutrinos

- Former experiments:

  Fly's Eye, AGASA

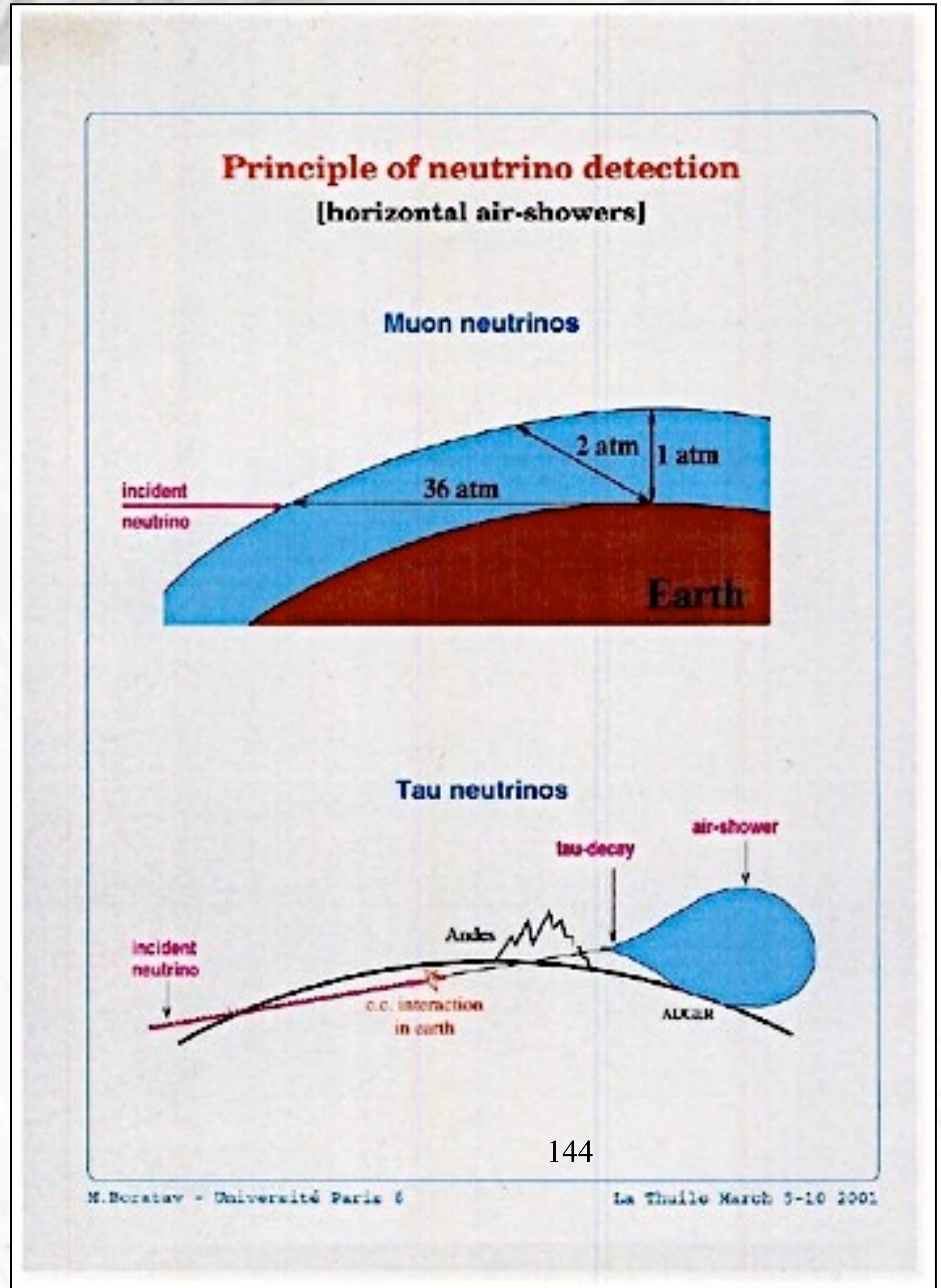

- Neutrinos are not primary UHECR

- Horizontal or Earth-skimming air showers – easy way to detect neutrinos

- Former experiments:

  Fly’s Eye, AGASA

- Present/future experiments:
  Pierre Auger, EUSO…

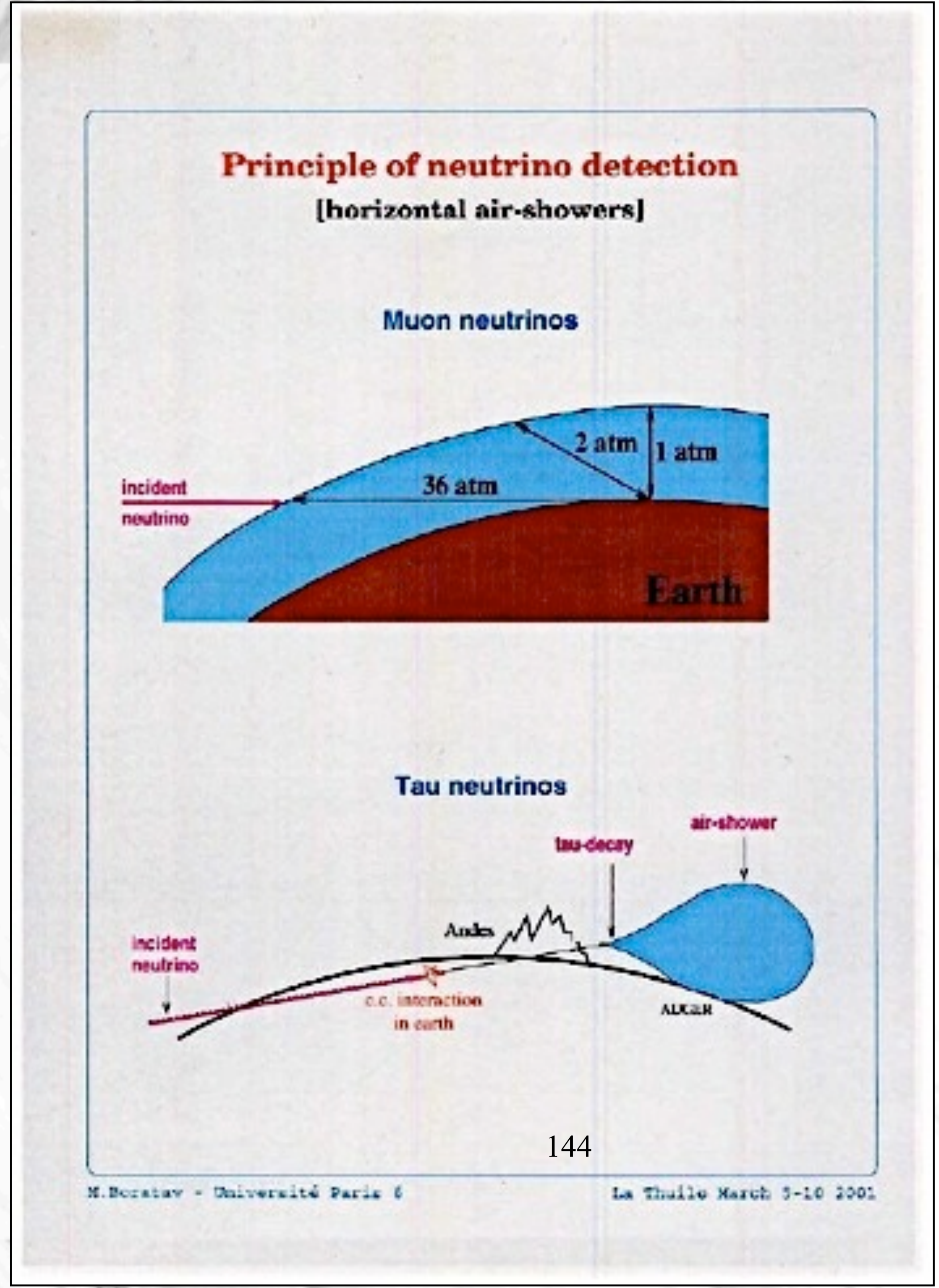

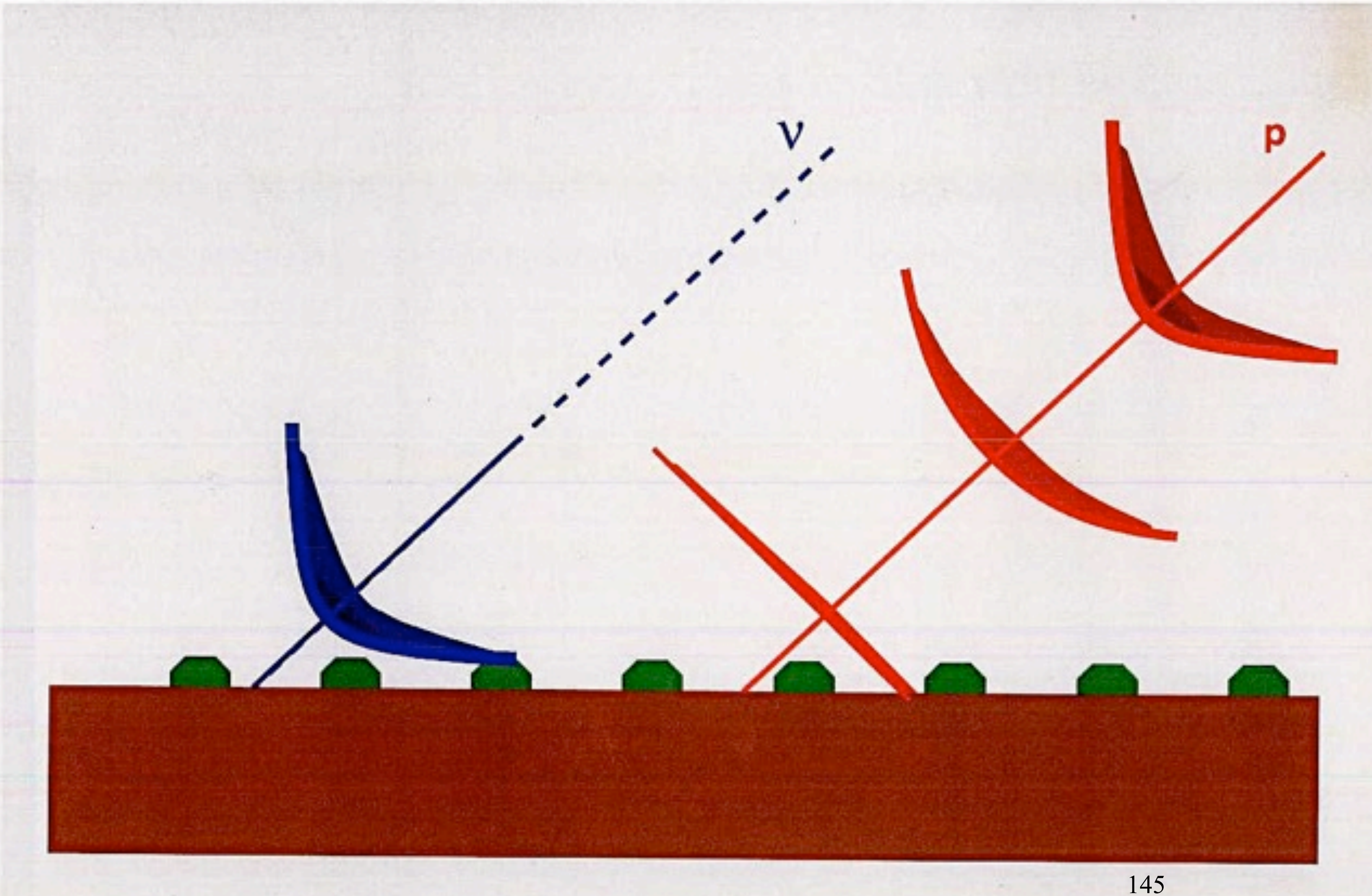

Curved “young” shower => neutrino
Flat “old” shower => hadron

Telescope Array Project

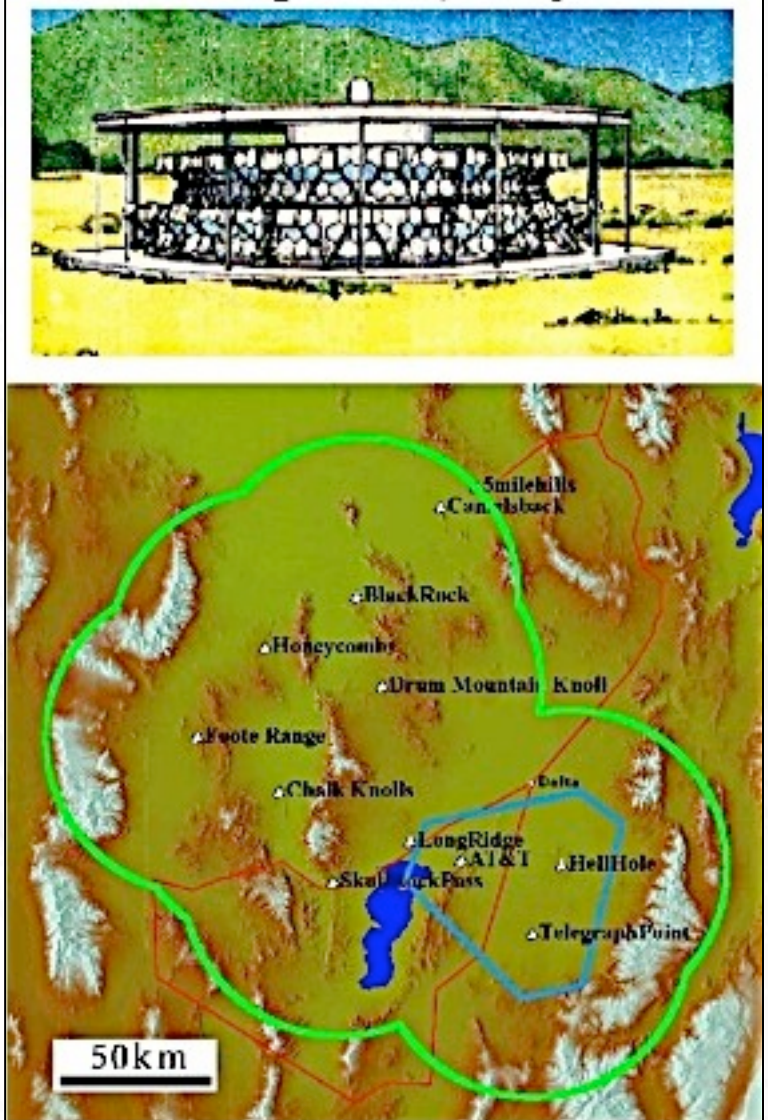

146

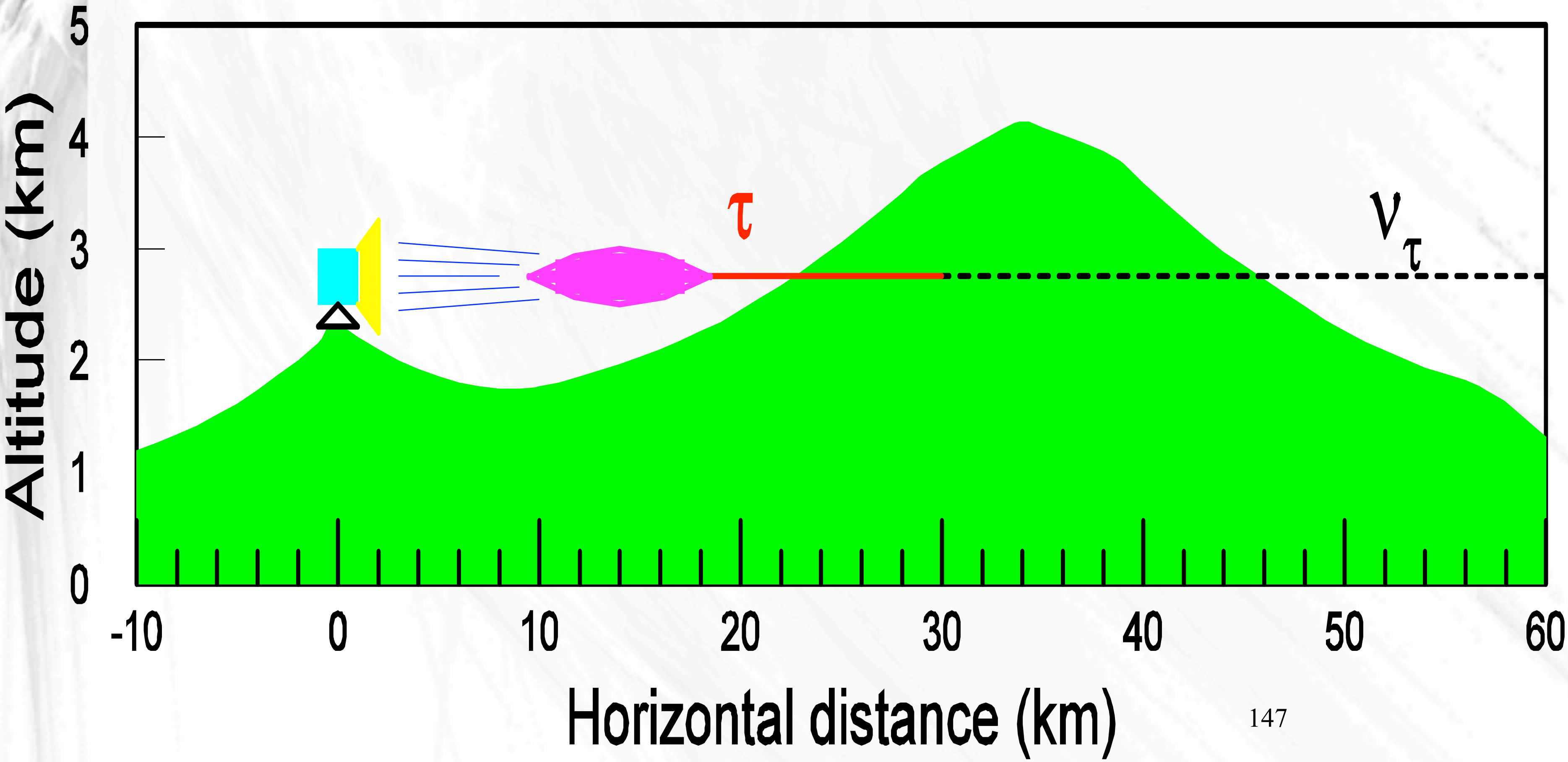
Altitude (km)
5
4
3
2
1
0
τ
ν τ
-10
0
10
20
30
40
50
60
Horizontal distance (km)

147

EUSO

ISS - The International Space Station

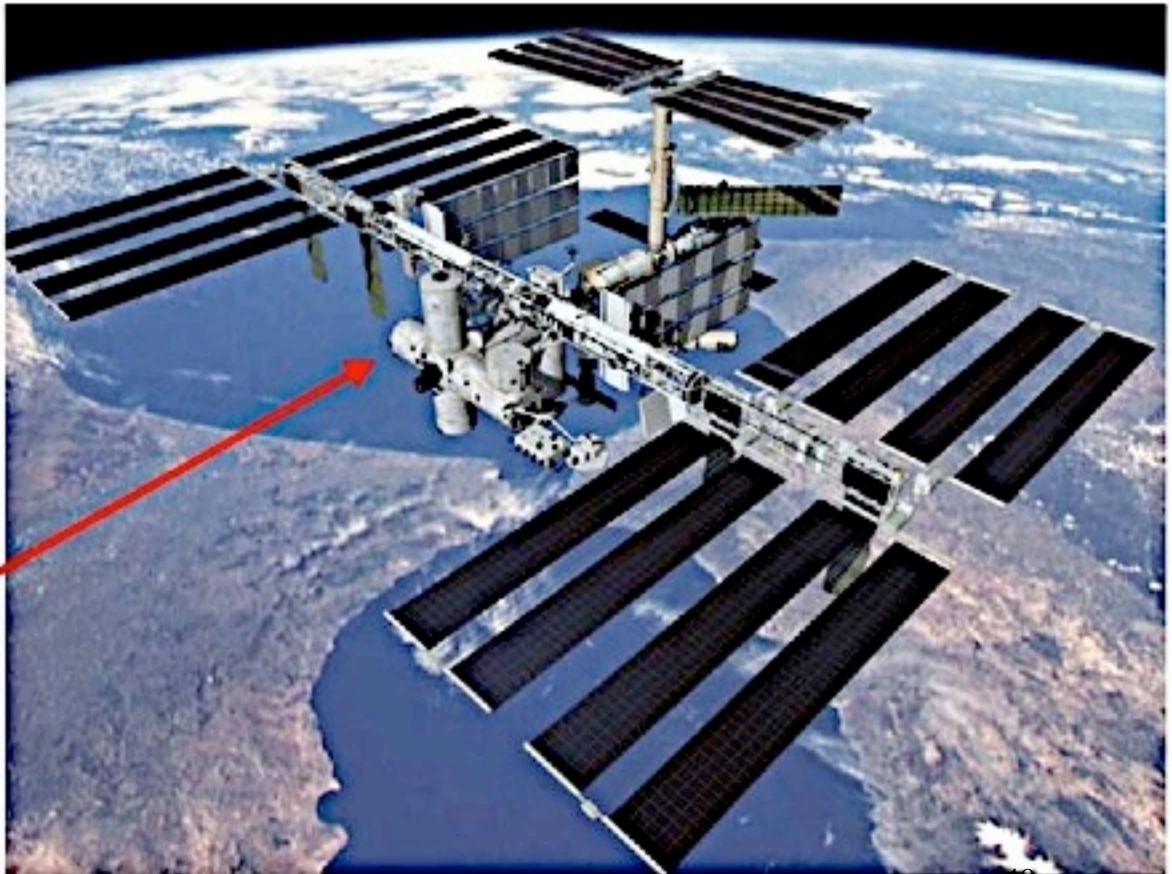

ESA Columbus Module

148

EUSO: Extreme Universe Space Observatory

Radio Detection of Neutrinos

$\nu_e + n \rightarrow p + e^-$

$e^- \rightarrow$ ... cascade

negative charge is sweeped into developing shower, which acquires a negative net cha
$Q_{net} \sim 0.25\ E_{cascade}$ (GeV).

$\Rightarrow$ relativist. pancake
~ 1cm thick, ∅ ~10cm

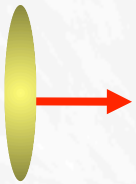

$\Rightarrow$ for λ >> 10 cm (radio)
coherence

$\Rightarrow$ each particle emits Cherenkov radiation

$\Rightarrow$ C-signal ~ E^2

$\Rightarrow$ C signal is resultant of overlapping Cherenkov cones

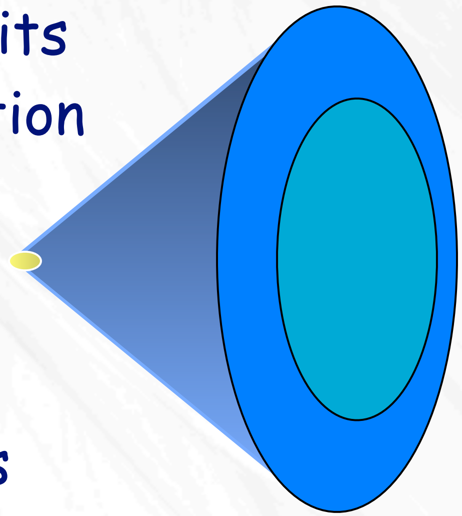

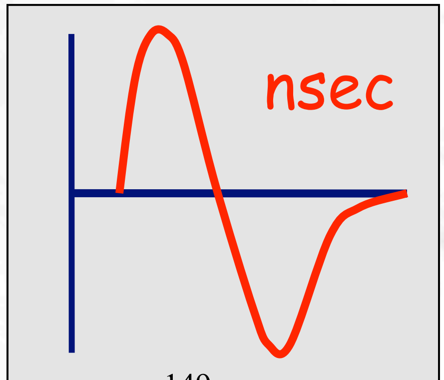

149

Threshold > 10^{16} eV

Lunar Regolith Interactions & RF Cherenkov radiation

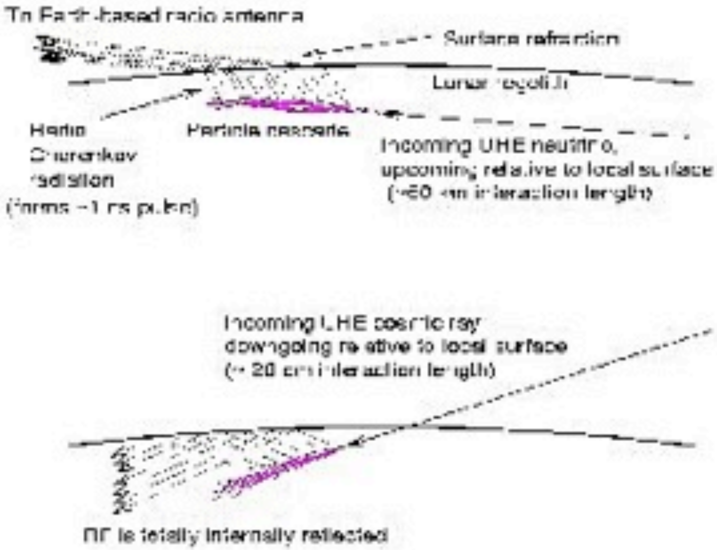

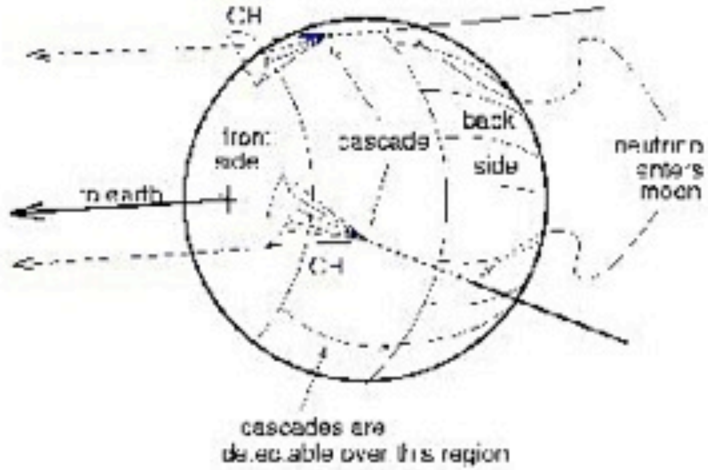

- At ~100 EeV energies, neutrino interaction length in lunar material is ~60km
- Rmoon ~ 1740 km, so most detectable interactions are grazing rays, but detection not limited to just limb
- Refraction of Cherenkov cone at regolith surface "fills in" the pattern, so acceptance solid angle is ~50 times larger than apparent solid angle of moon

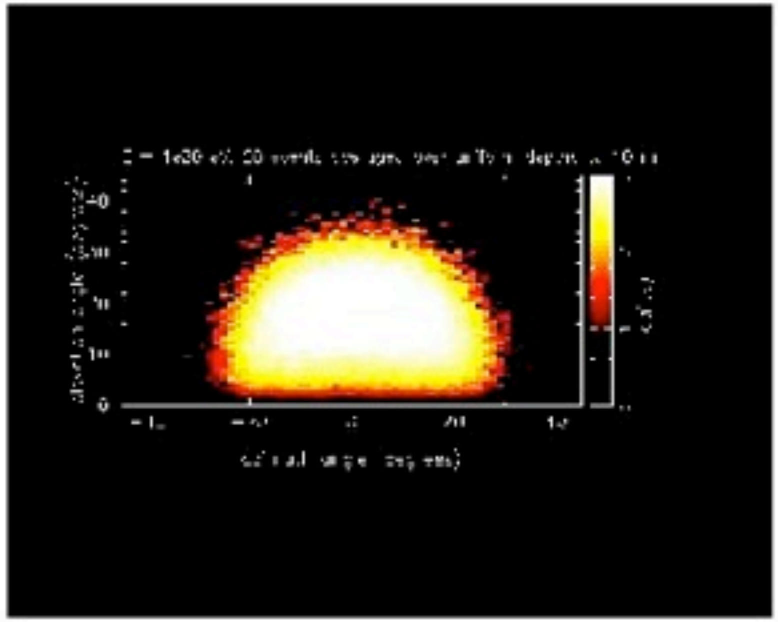

Lunar Radio Emissions from Interactions of ν and CR with > 10^{19} eV

Gorham et al. (1999), 30 hr NASA Goldstone 70 m antenna + DSS 34 m antenna

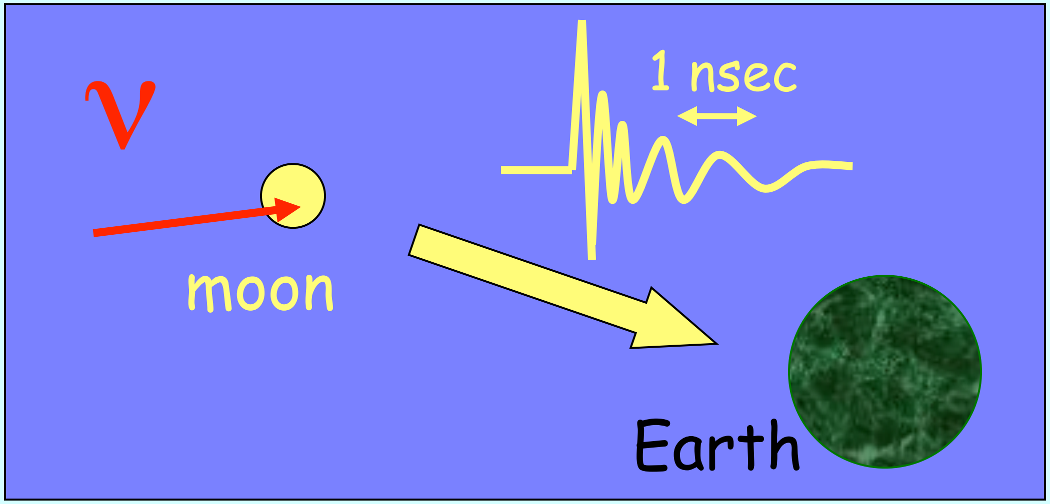

→ $E^2 \cdot dN/dE < 10^5\ eV \cdot cm^{-2} \cdot s^{-1} \cdot sr^{-1}$

at 10^{20} eV

Effective target volume
~ antenna beam (0.3°)
× 10 m layer

→ $10^5\ km^3$

South Pole

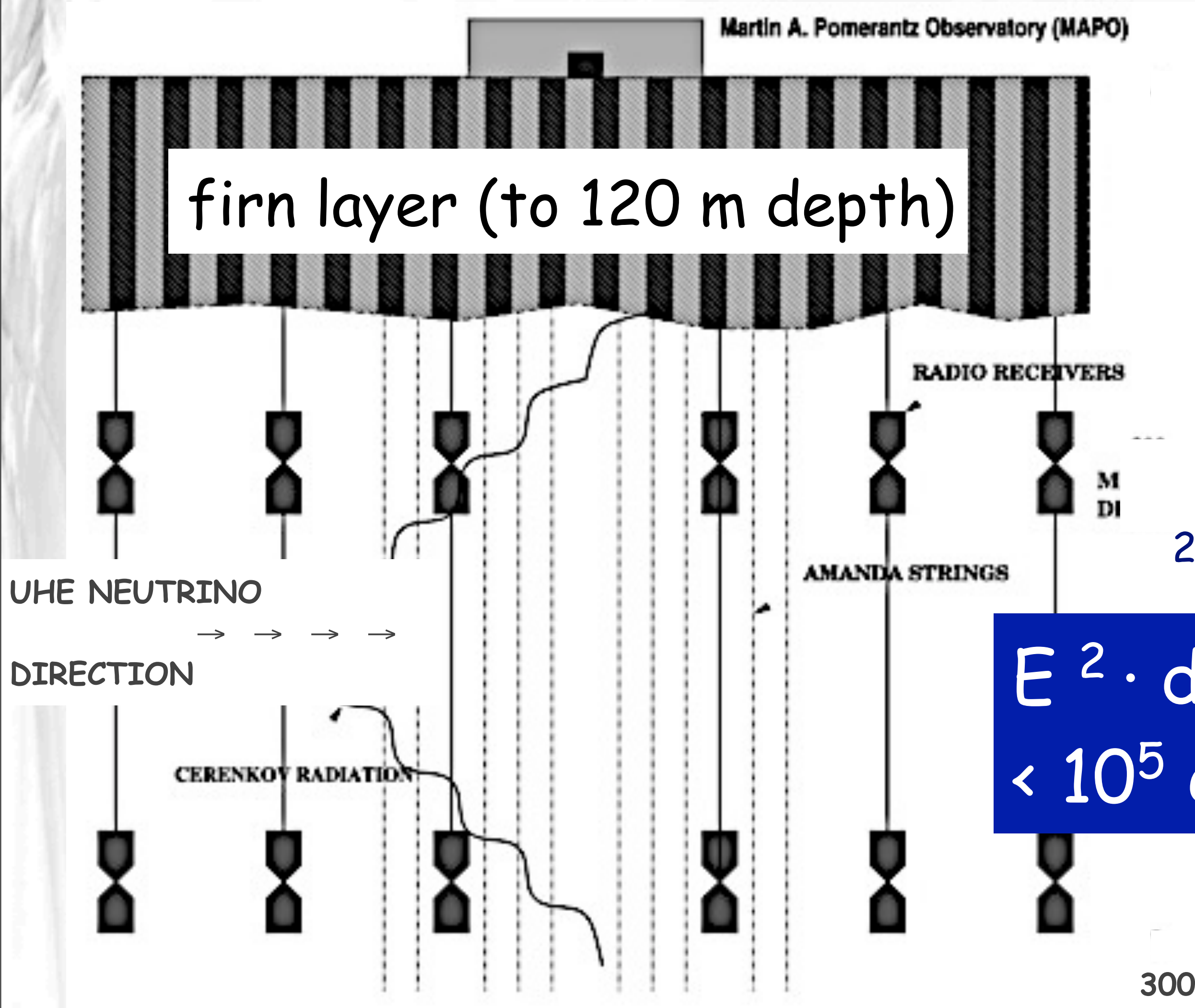

20 receivers +transmitters

$E^2 \cdot dN/dE$
$< 10^5\ eV \cdot cm^{-2} \cdot s^{-1} \cdot sr^{-1}$

at 10^{17} eV

Natural Salt Domes: Potential PeV-EeV Neutrino Detectors

- Natural salt can be extremely low RF loss: ~ as clear as very cold ice, 2.4 times as dense

- Typical salt dome halite is comparable to ice at -40C for RF clarity

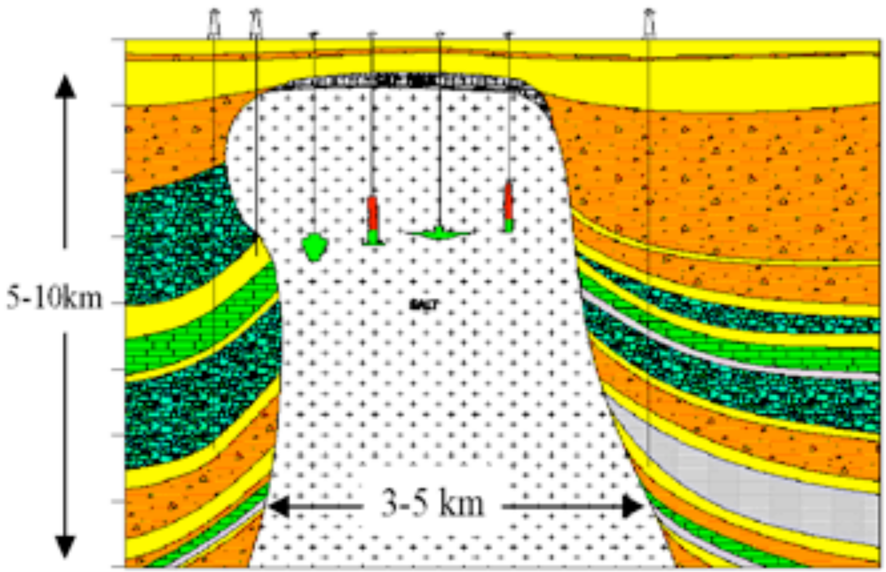

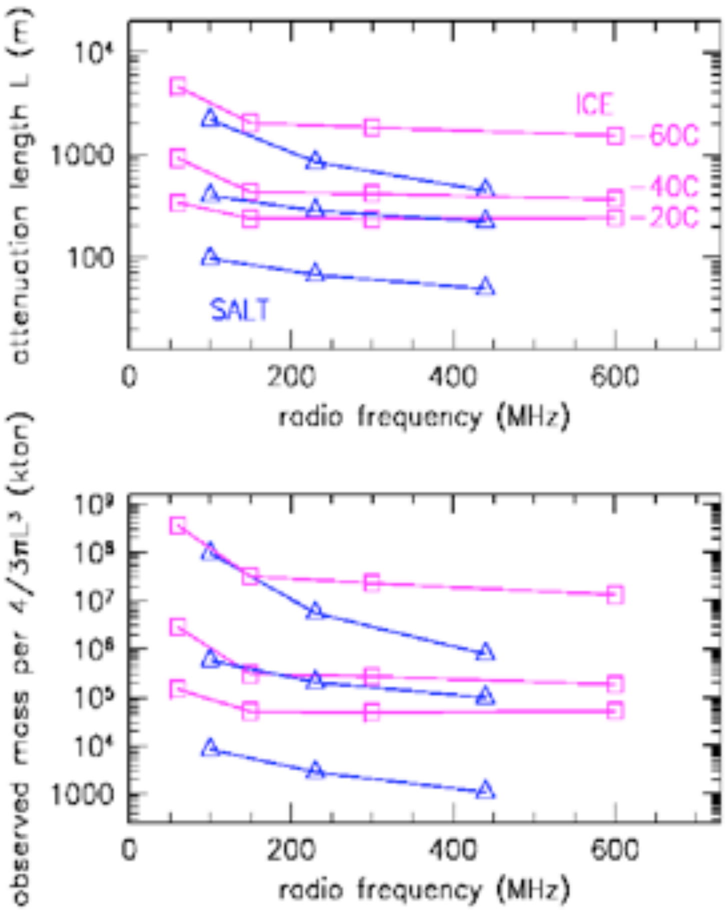

153

SALT curves are for (top): purest natural salt; (middle): typical good salt dome; (bottom) best salt bed halite.

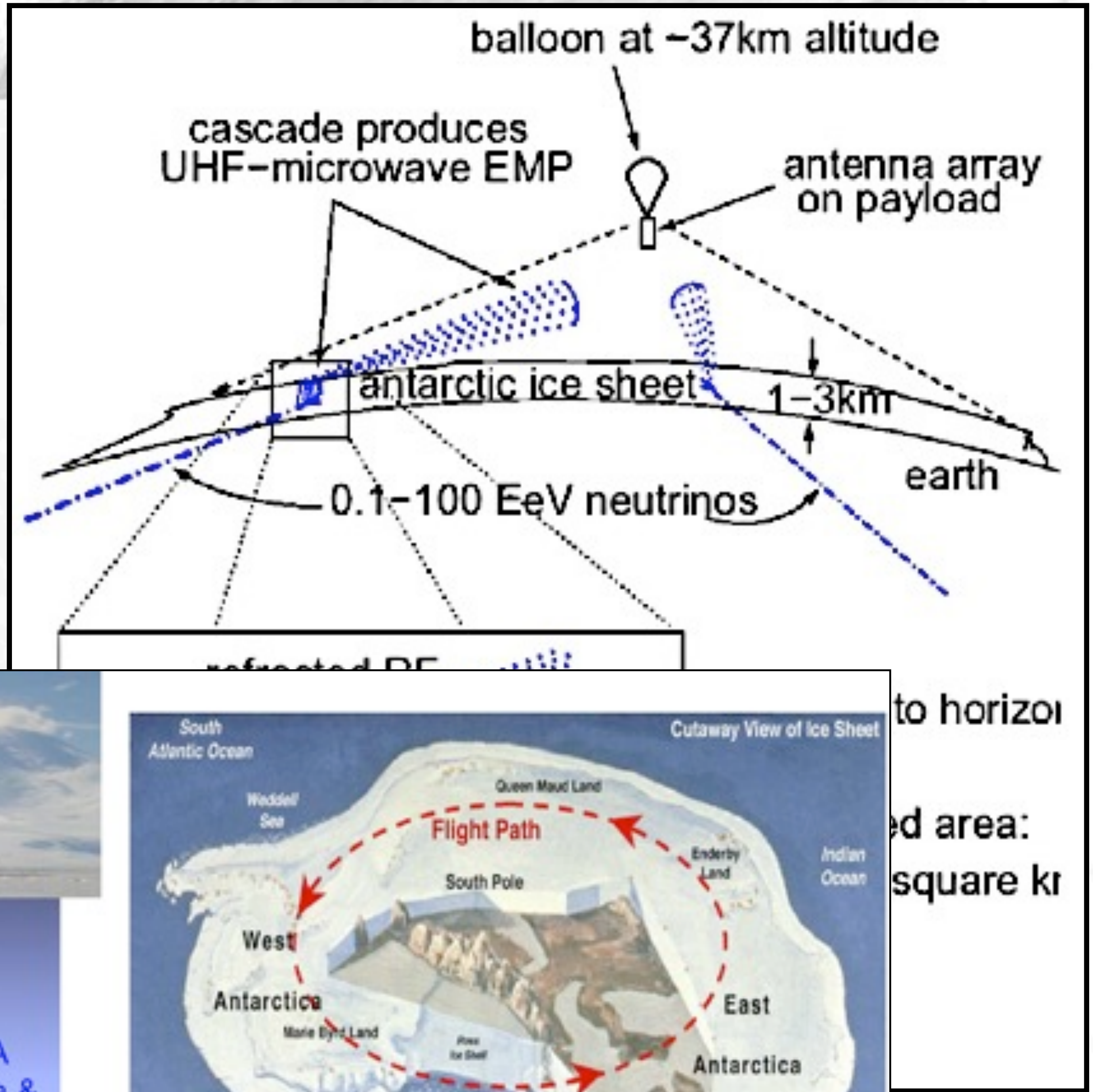
balloon at ~37km altitude
cascade produces
UHF–microwave EMP
antenna array
on payload
antarctic ice sheet
1–3km
earth
0.1–100 EeV neutrinos

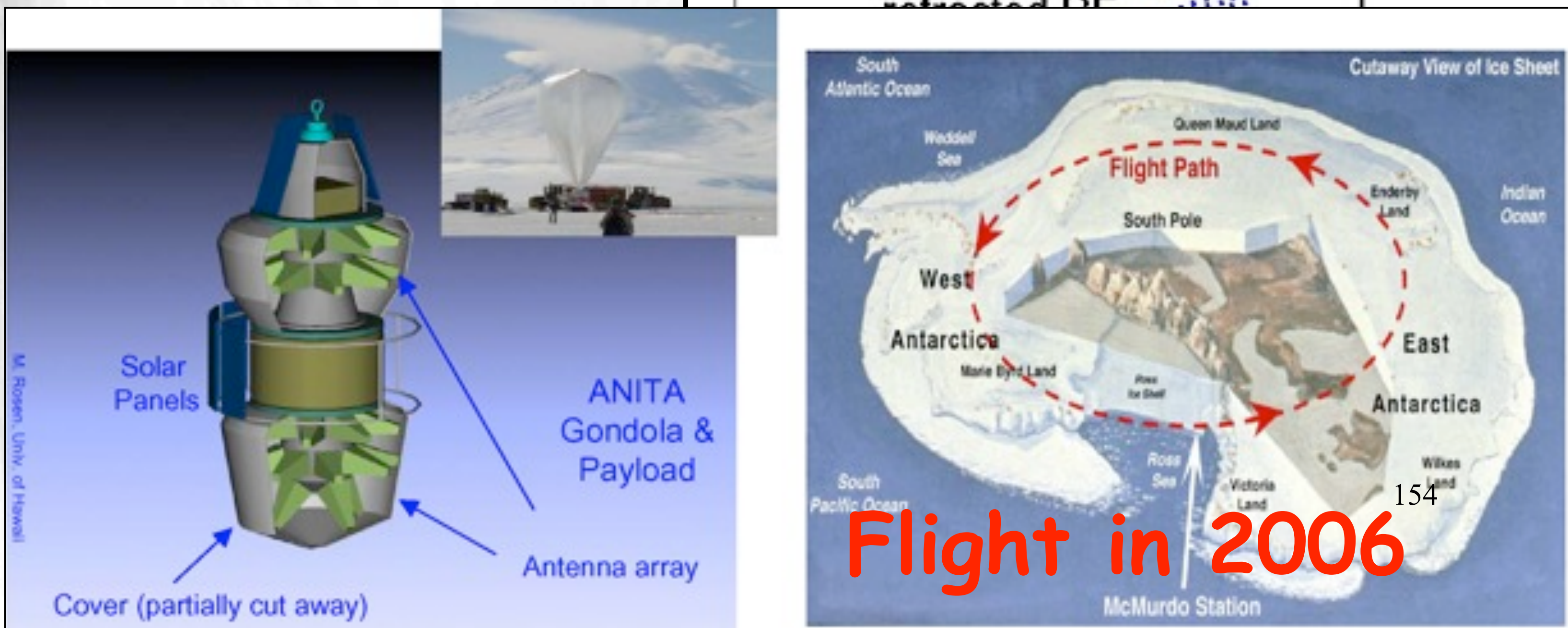
Solar
Panels
ANITA
Gondola &
Payload
Antenna array
Cover (partially cut away)
M. Rosen, Univ. of Hawaii
South
Atlantic Ocean
Cutaway View of Ice Sheet
Weddell
Sea
Queen Maud Land
Flight Path
Enderby
Land
Indian
Ocean
South Pole
West
Antarctica
East
Antarctica
Marie Byrd Land
Ross
Ice Shelf
Ross
Sea
Victoria
Land
Wilkes
Land
South
Pacific Ocean
154
Flight in 2006
McMurdo Station

Sensitivity of radio technique to UHE cosmic rays and neutrinos

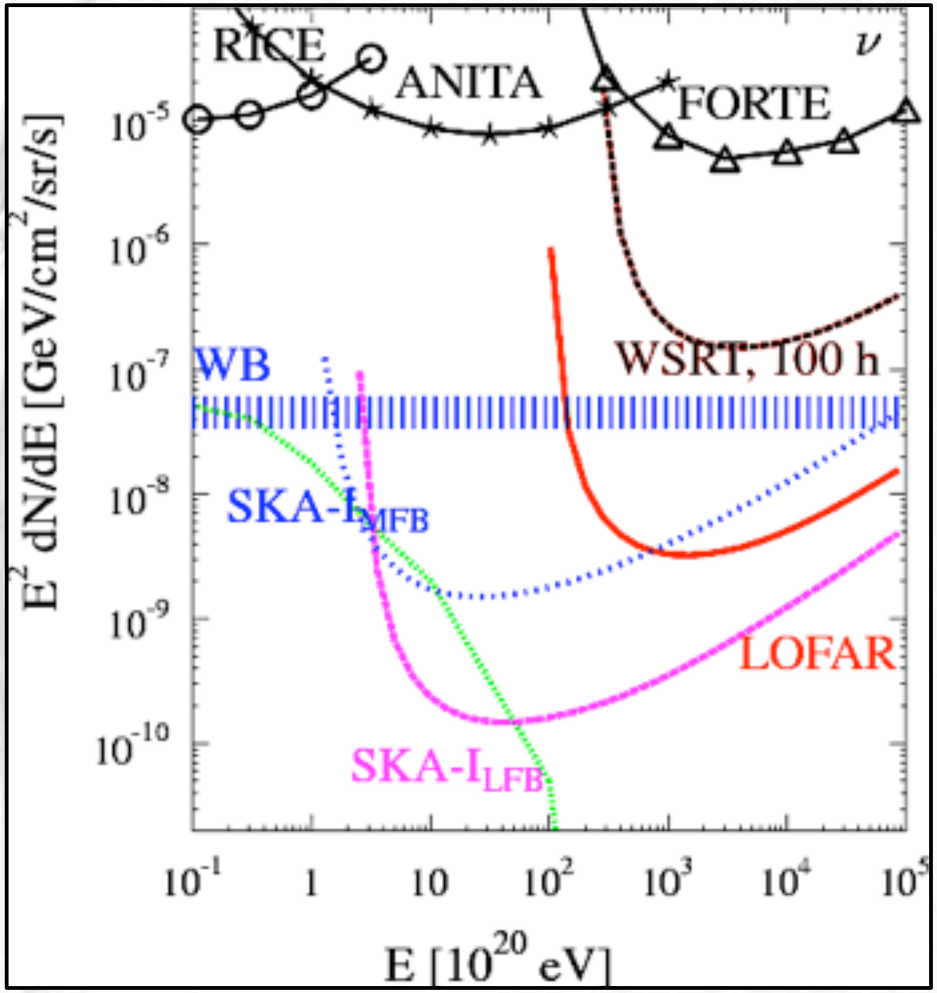

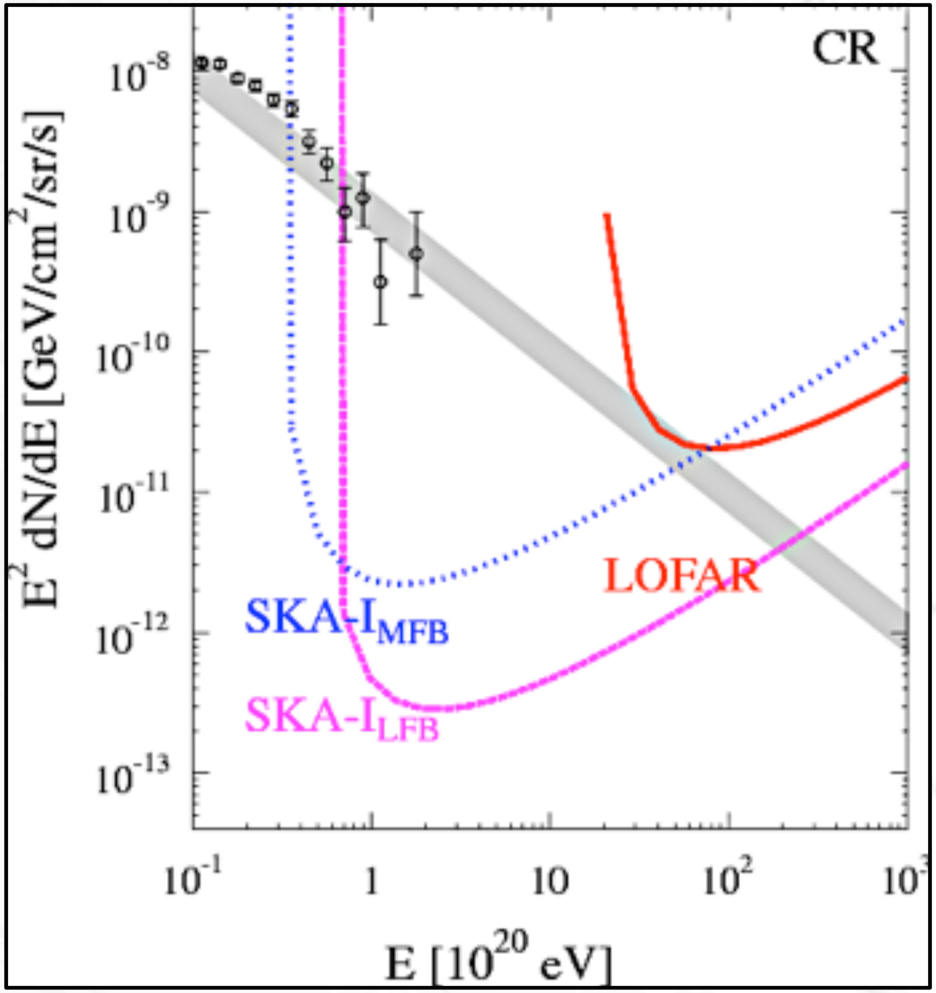

155

O. Scholten et al., arXiv:0810.3624

Acoustic detection of Neutrinos

Particle cascade → ionization

→ heat

→ pressure wave

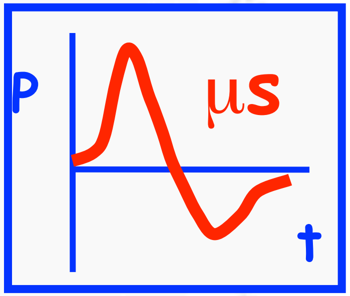

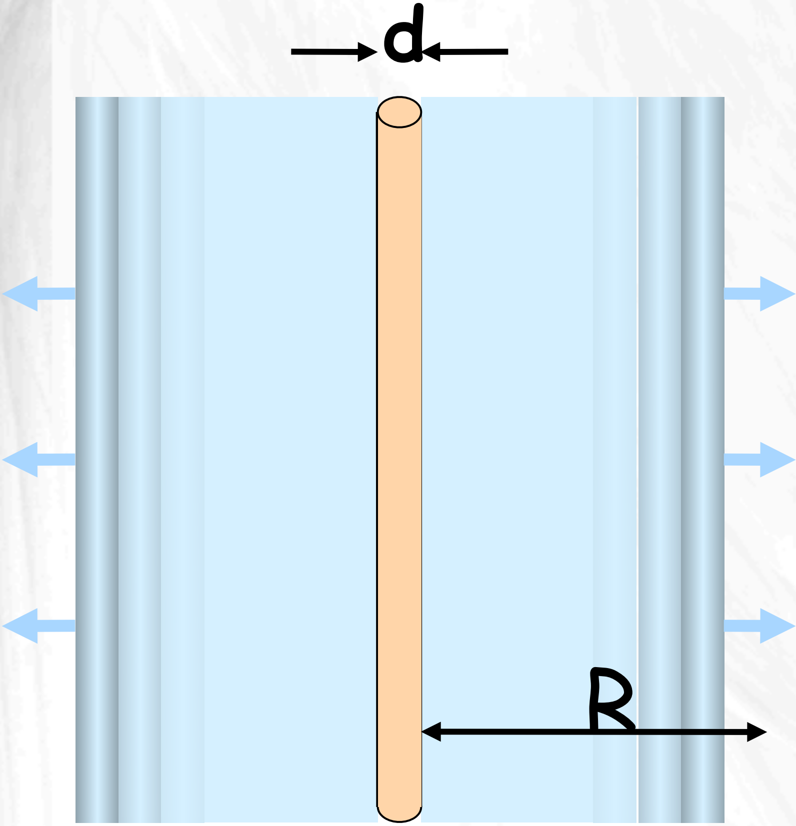

Maximum of emission at ~ 20 kHz

Attenuation length of sea water at 15-30 kHz: **a few km** (light: a few tens of meters)

→ given a large initial signal, huge detection volumes can be achieved.

Threshold > 10^{16} eV

Cosmic Rays, Gamma-Rays, Neutrinos, and Magnetized Sources

Various connections:
Magnetic fields influence propagation path lengths. This influences:

photo-spallation and thus observable composition, interpretation of ankle

production of secondary gamma-rays and neutrinos, thus detectability of their fluxes and identification of source mechanisms and locations.

Example:

Discrete Source in a magnetized galaxy cluster injecting protons up to 10^{21} eV

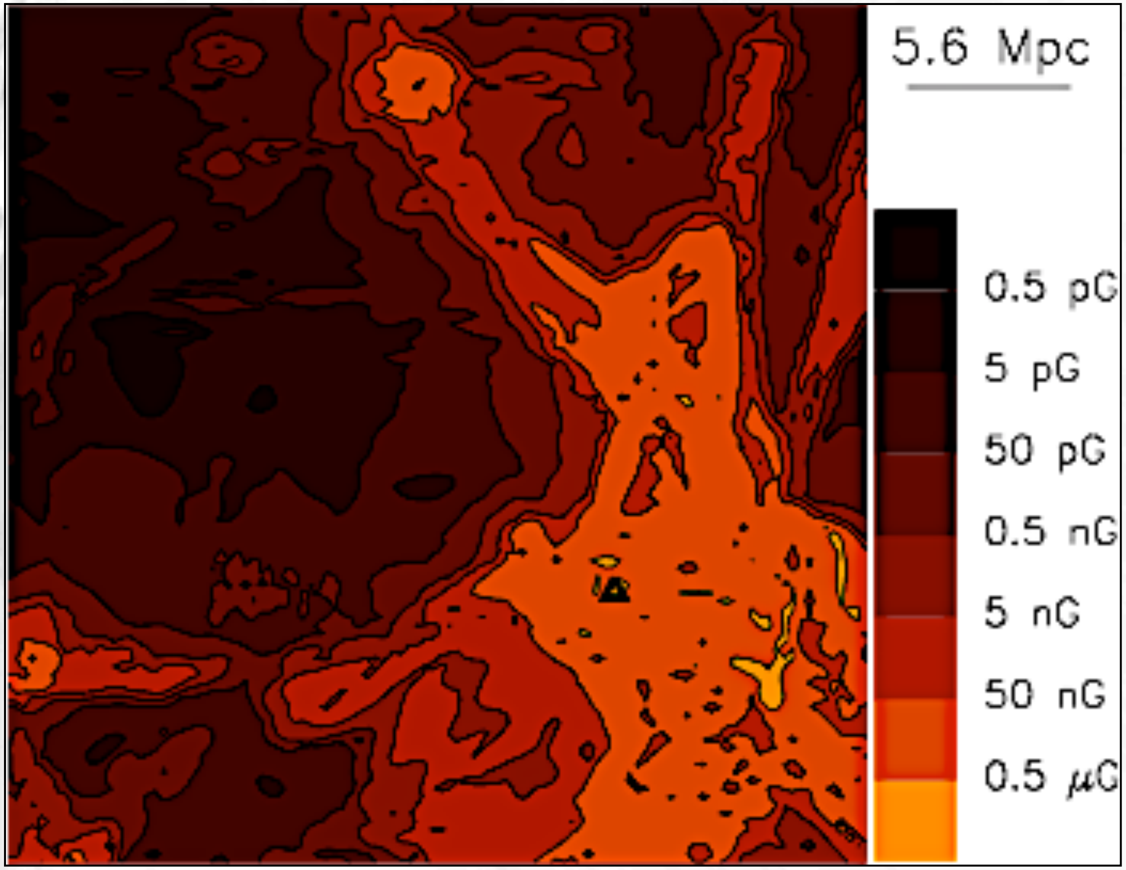

158

Armengaud, Sigl, Miniati, Phys.Rev.D73 (2006) 083008

Example:

Discrete Source in a magnetized galaxy cluster injecting protons up to 10^{21} eV

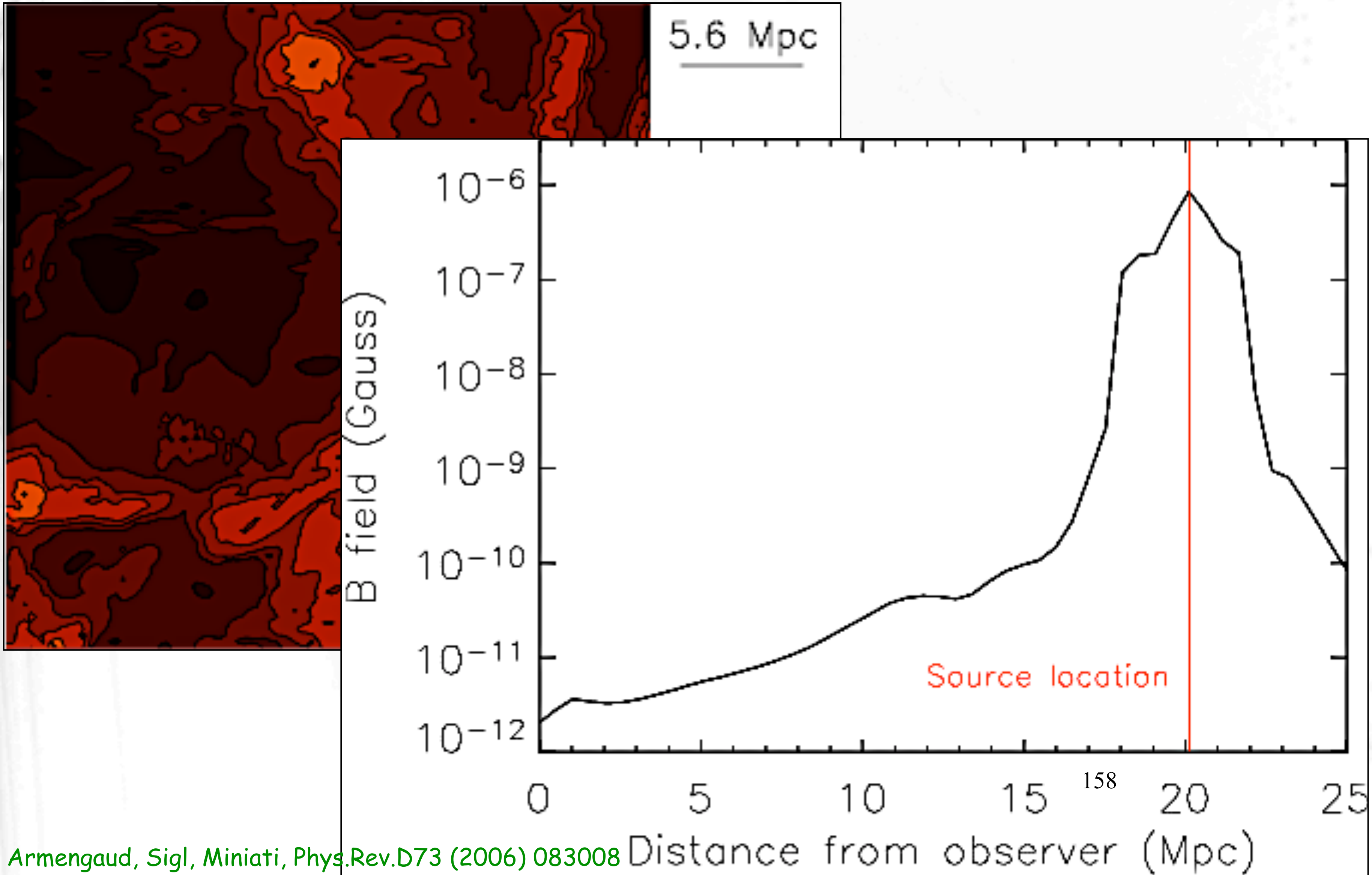

158

Armengaud, Sigl, Miniati, Phys.Rev.D73 (2006) 083008

Pair production by protons can dominate the GeV-TeV photon flux if injection spectrum is steep. Example for a cluster at 100 Mpc.

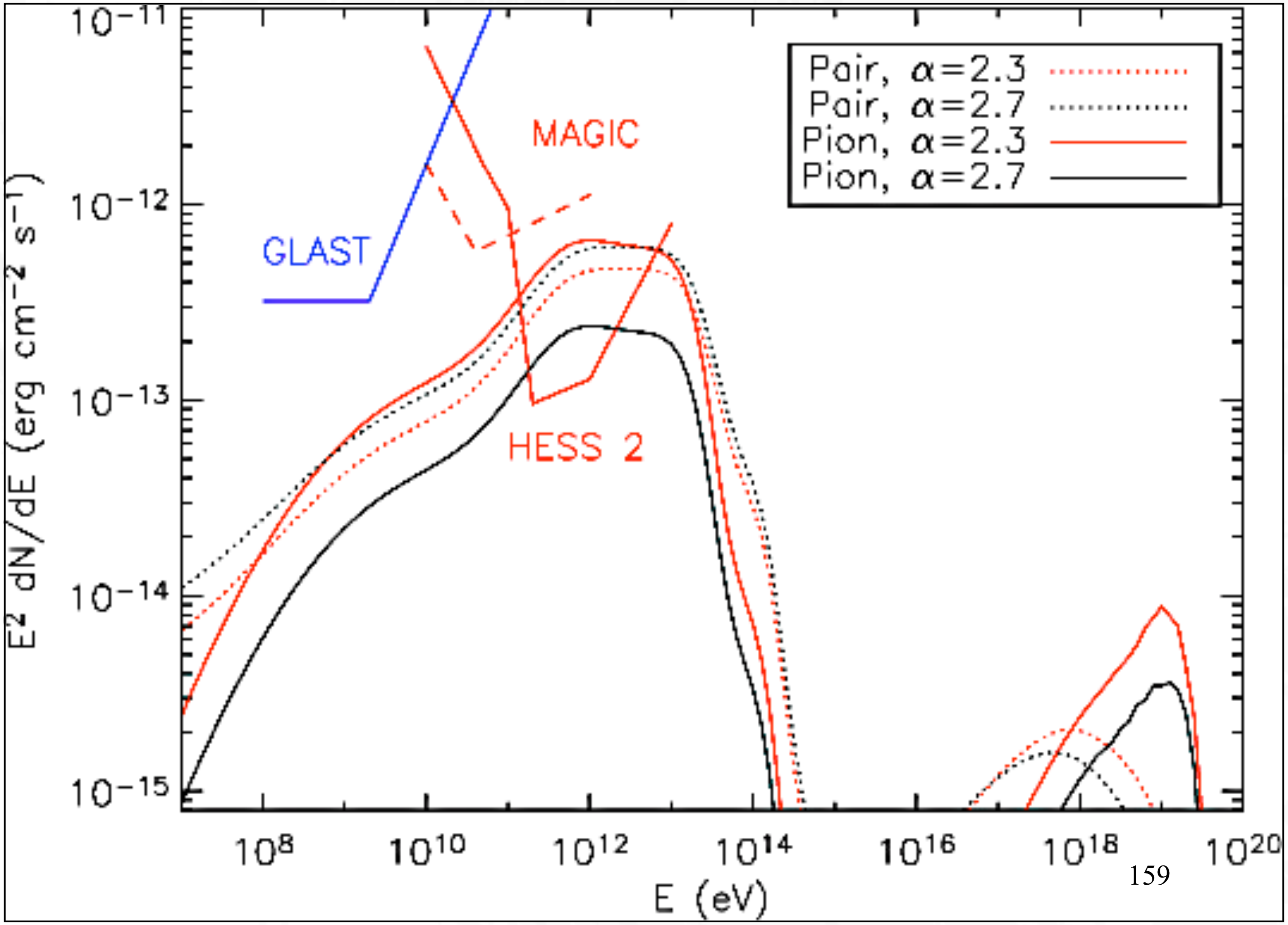

In a magnetic field B, pairs emit synchrotron photons of typical energy

$$E_{\rm syn} \simeq 6.8 \times 10^{11} \left(\frac{E_e}{10^{19}\,{\rm eV}} \right)^2 \left(\frac{B}{0.1\,\mu{\rm G}} \right) {\rm eV}$$

For pion production $E_e \sim 5 \times 10^{18}$ eV. Thus, in a 0.1 Gauss field, synchrotron radiation ends up below ~ 0.1TeV.

Pair production occurs for proton energies 10^{18} eV ≤ E ≤ 4×10^{19} eV which in ~ 0.1G fields thus ends up in synchrotron photons below ~ 1GeV. If the proton spectrum is steeper then ~ E^{-2}, the sub-GeV photon flux is dominated by synchrotron photons from pair production.

Source at 20 Mpc, $E^{-2.7}$ proton injection spectrum with 4×10^{42} erg/s above 10^{19} eV

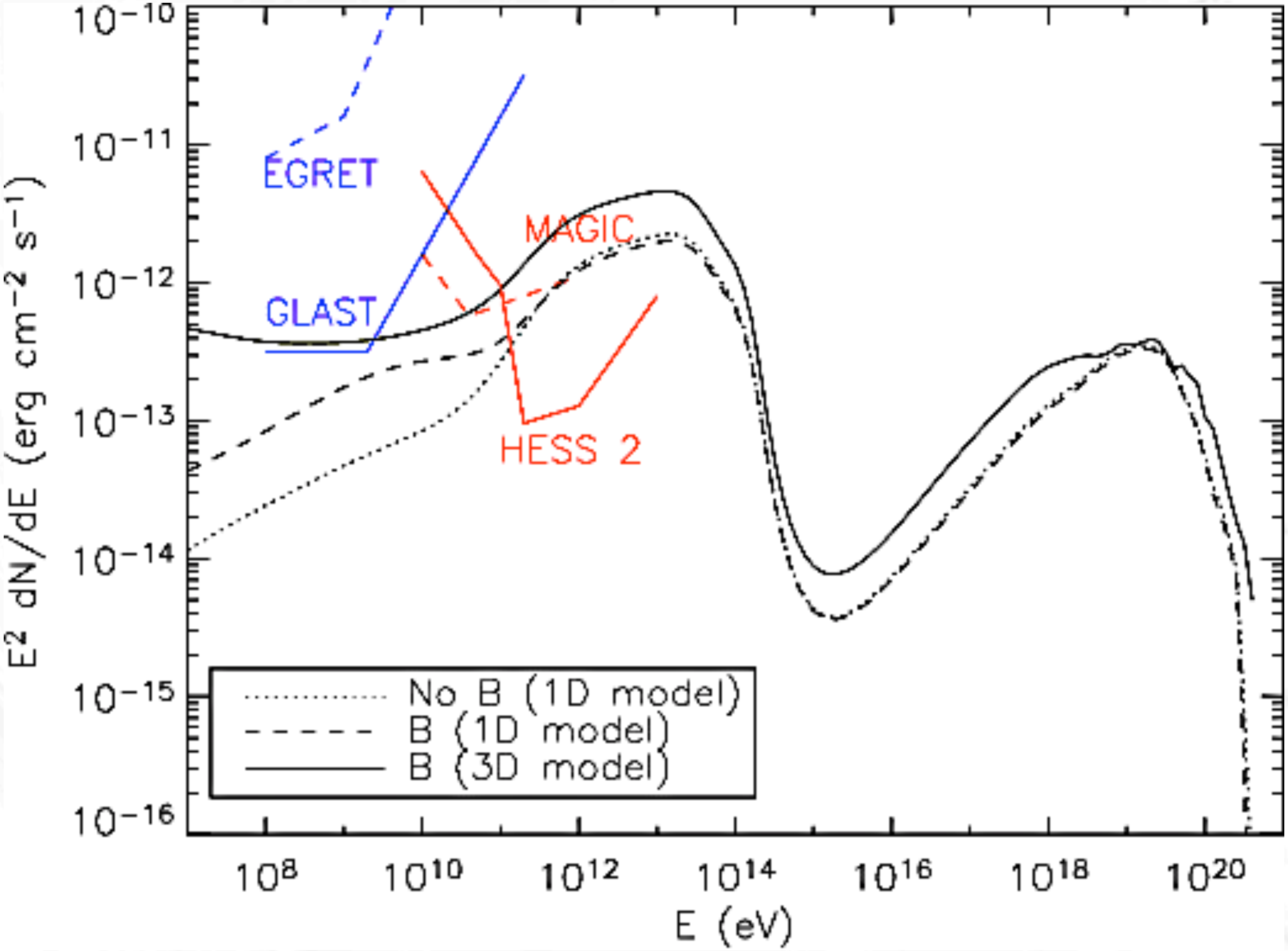

161

Source at 20 Mpc, $E^{-2.7}$ proton injection spectrum with 4×10^{42} erg/s above 10^{19} eV

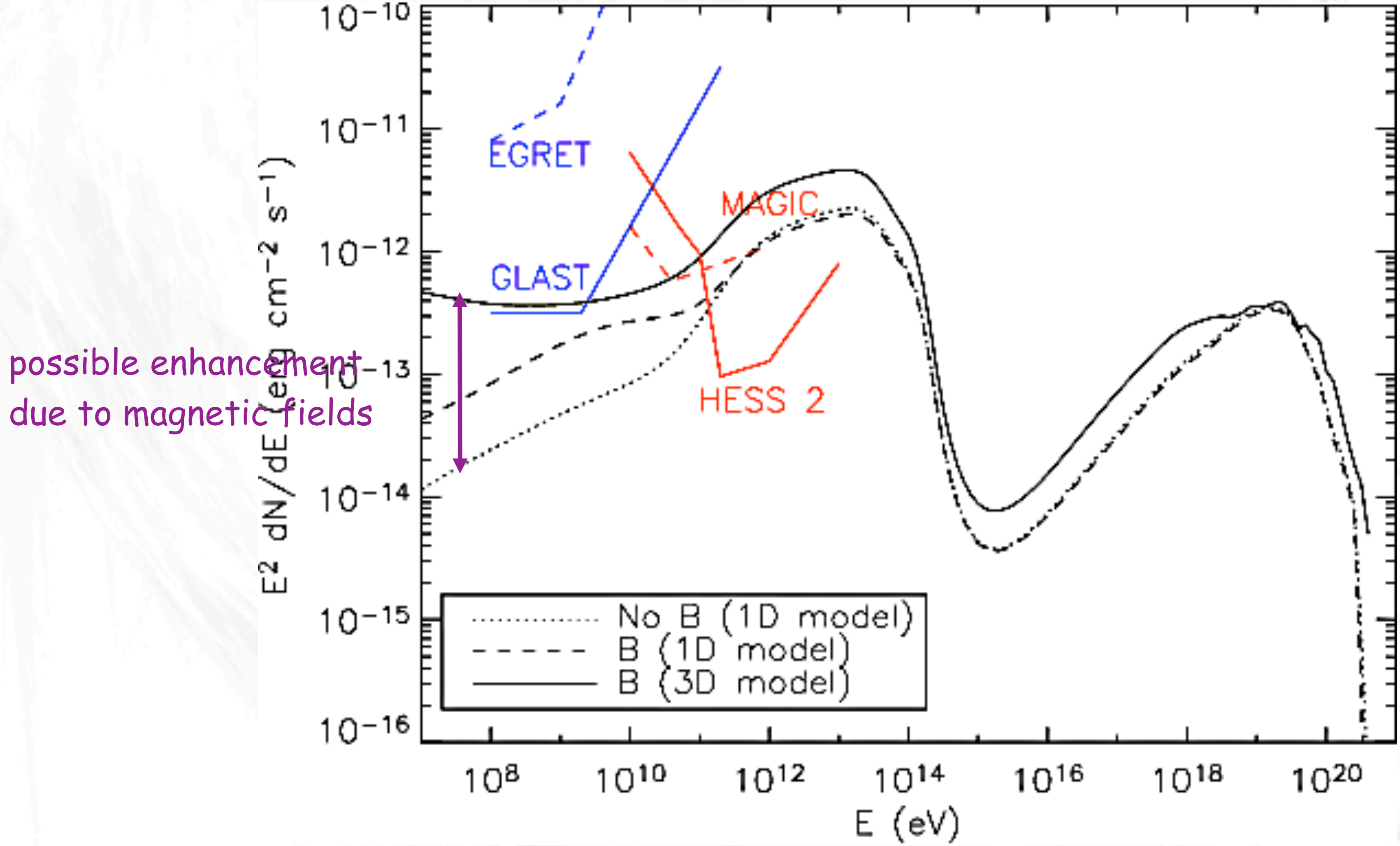

Note that the 3d structure of the field matters and leads to further enhancement of GeV γ-ray fluxes.

The source magnetic fields can give rise to a **GeV-TeV γ-ray halo** that would be easily resolvable by instruments such as HESS

In case of previous example, γ-rays above 1 TeV:

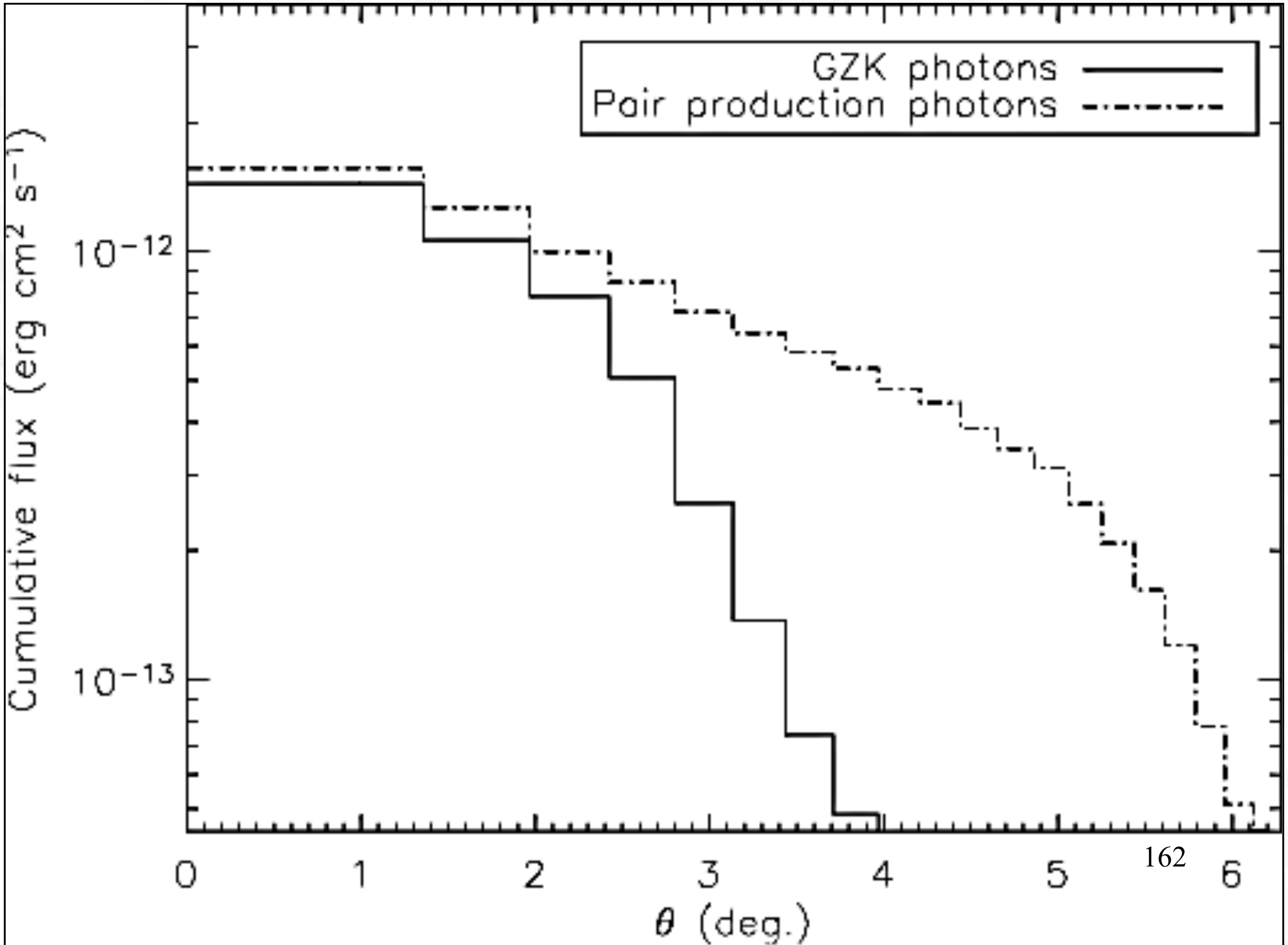

This is quite relevant for γ-ray astronomy in the GeV-TeV band

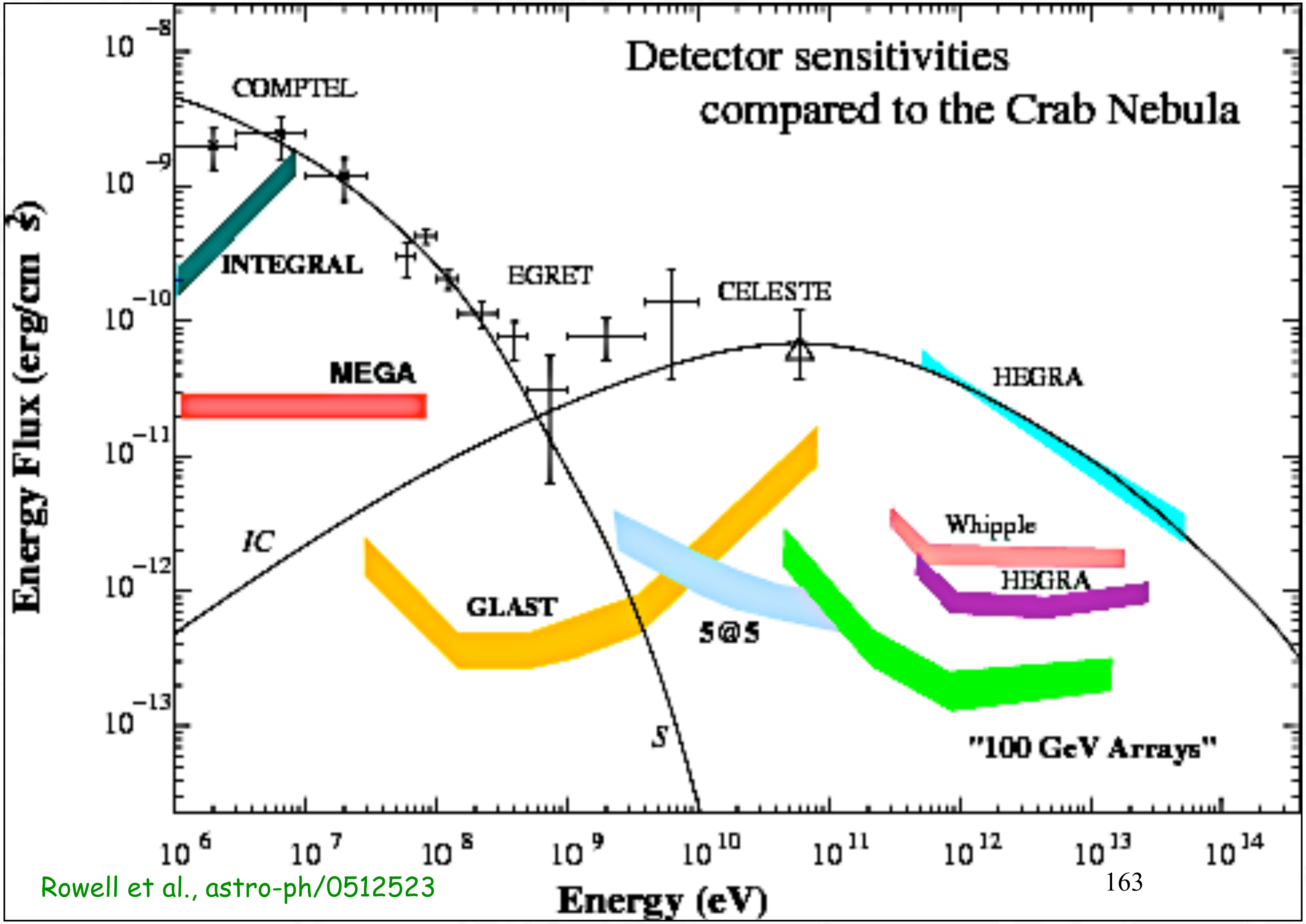

Rowell et al., astro-ph/0512523

The GZK neutrino flux can also be enhanced by magnetic fields

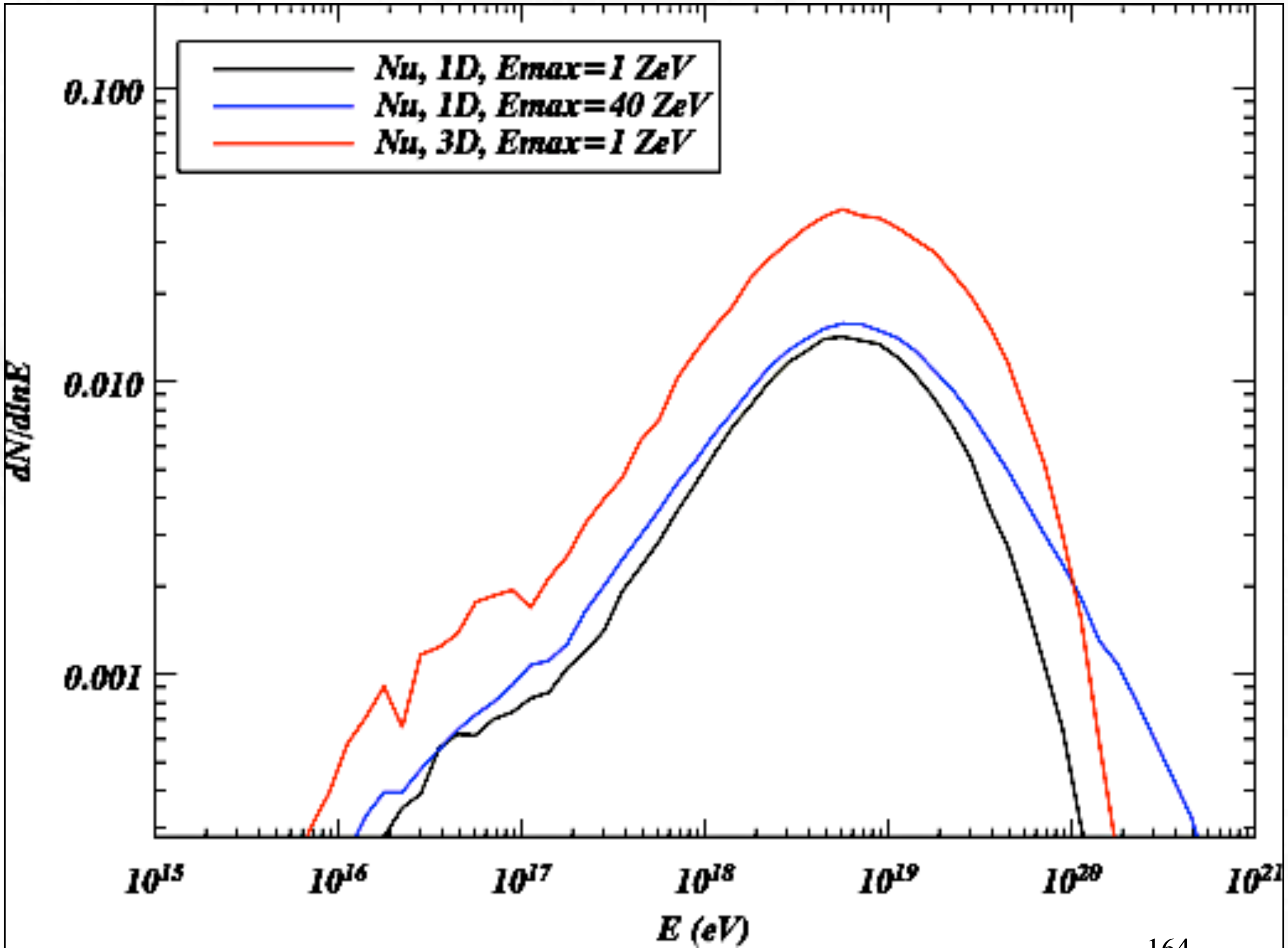

Maximal diffuse neutrino flux from magnetized galaxy clusters

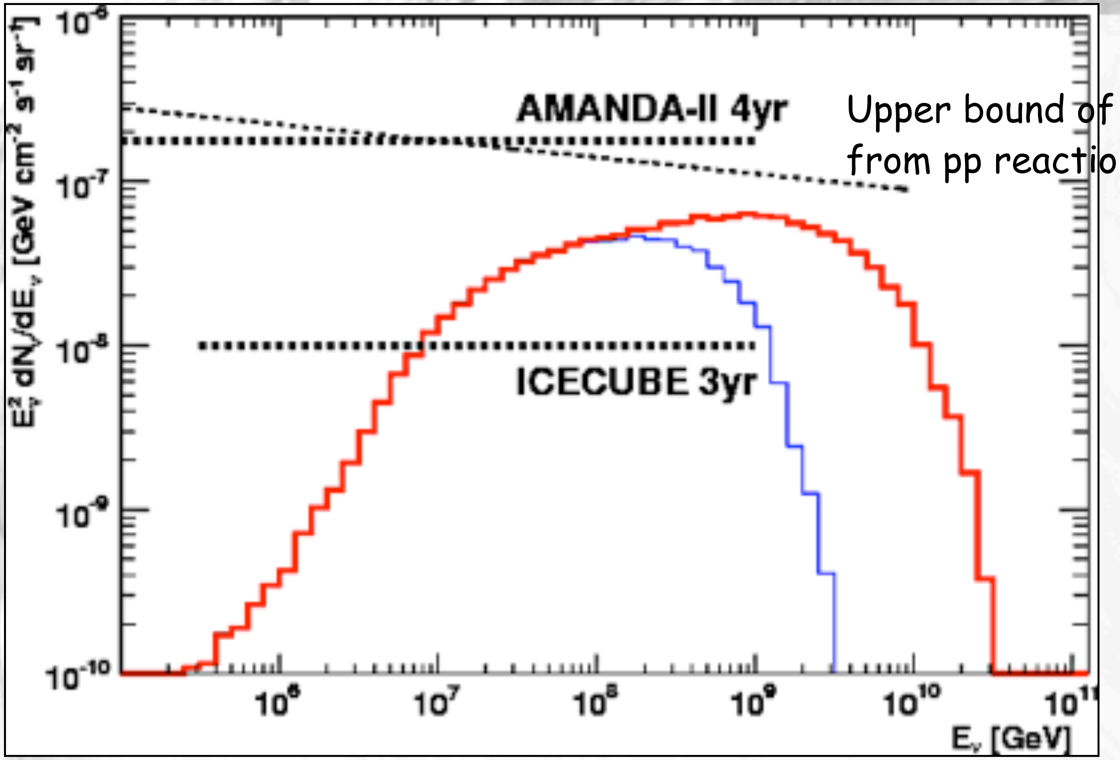

Upper bound of ν-flux from pp reactions

De Marco et al., Phys.Rev.D73 (2006) 043004

Shortcomings:

- overproduces UHECR flux by factors 10-40 if not blocked by magnetic horizon effects
- neglects neutrinos produced by photo-reactions outside the clusters

Maximal diffuse neutrino flux from magnetized galaxy clusters

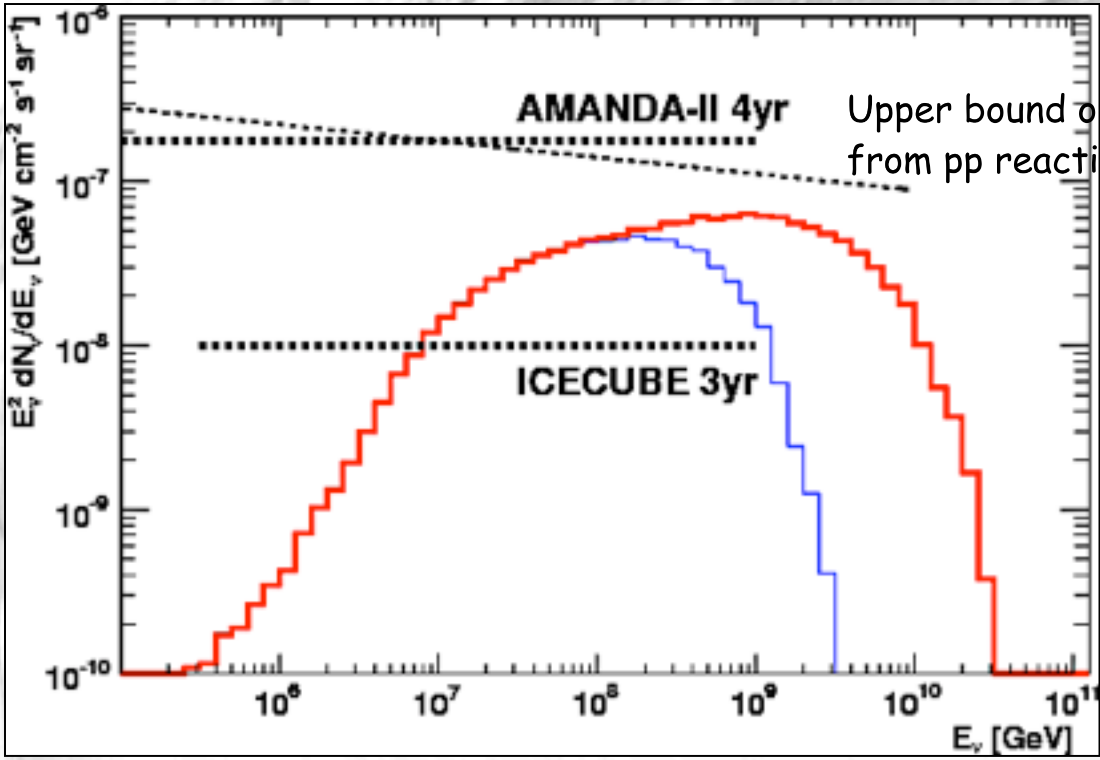

De Marco et al., Phys.Rev.D73 (2006) 043004

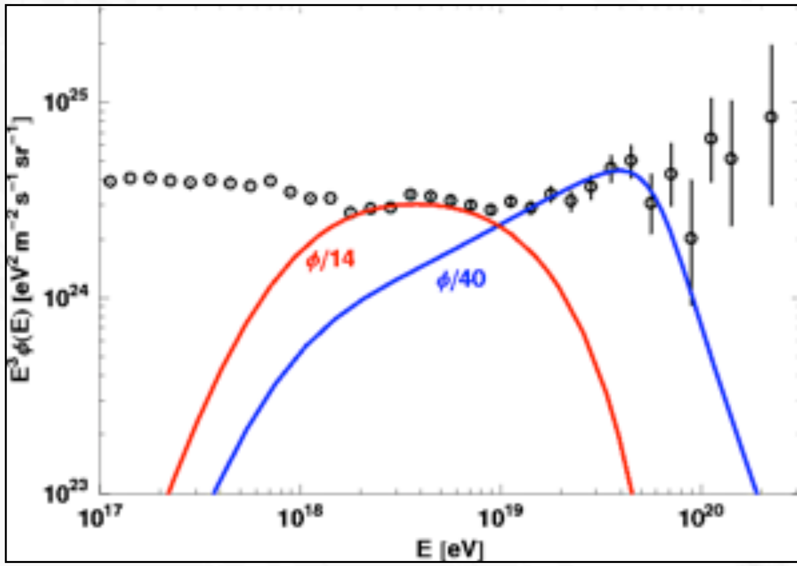

Shortcomings:

- overproduces UHECR flux by factors 10-40 if not blocked by magnetic horizon effects
- neglects neutrinos produced by photo-reactions outside the clusters

For example, γ-ray bursts, neutron stars.

In such sources, pions and/or muons could loose energy before decaying:

$$
\begin{aligned}
t_{\pi,\mu}(E) &= \tau_{\pi,\mu}\frac{E}{m_{\pi,\mu}} \propto E^1 \\
t_{\rm had}(E) &\simeq \frac{1}{n_p\sigma_h(E)} \propto E^0 \\
t_{\rm rad}(E) &\simeq \frac{1}{u_\gamma\sigma_{\rm rad}\eta(E)} \propto m^4_{\pi,\mu}E^{-1}
\end{aligned}
$$

where $\sigma_{rad} \propto E^{-1}$ and the inelasticity $\eta(E) \propto E^2$ in the non-relativistic regime. Then, for the loss rate $t_{loss}(E)^{-1} = t_{had}(E)^{-1} + t_{rad}(E)^{-1}$,
one has $j_\nu(E) \propto \min[1, t_{loss}(E)/t_{\pi,\mu}(E)] j_p(E)$ because $t_{loss}(E)/t_{\pi,\mu}(E)$ is the probability to decay within the energy loss time.
At low E hadronic losses dominate, whereas at high E radiative losses dominate.

Ando and Beacom, Phys.Rev.Lett. 95 (2005) 061103

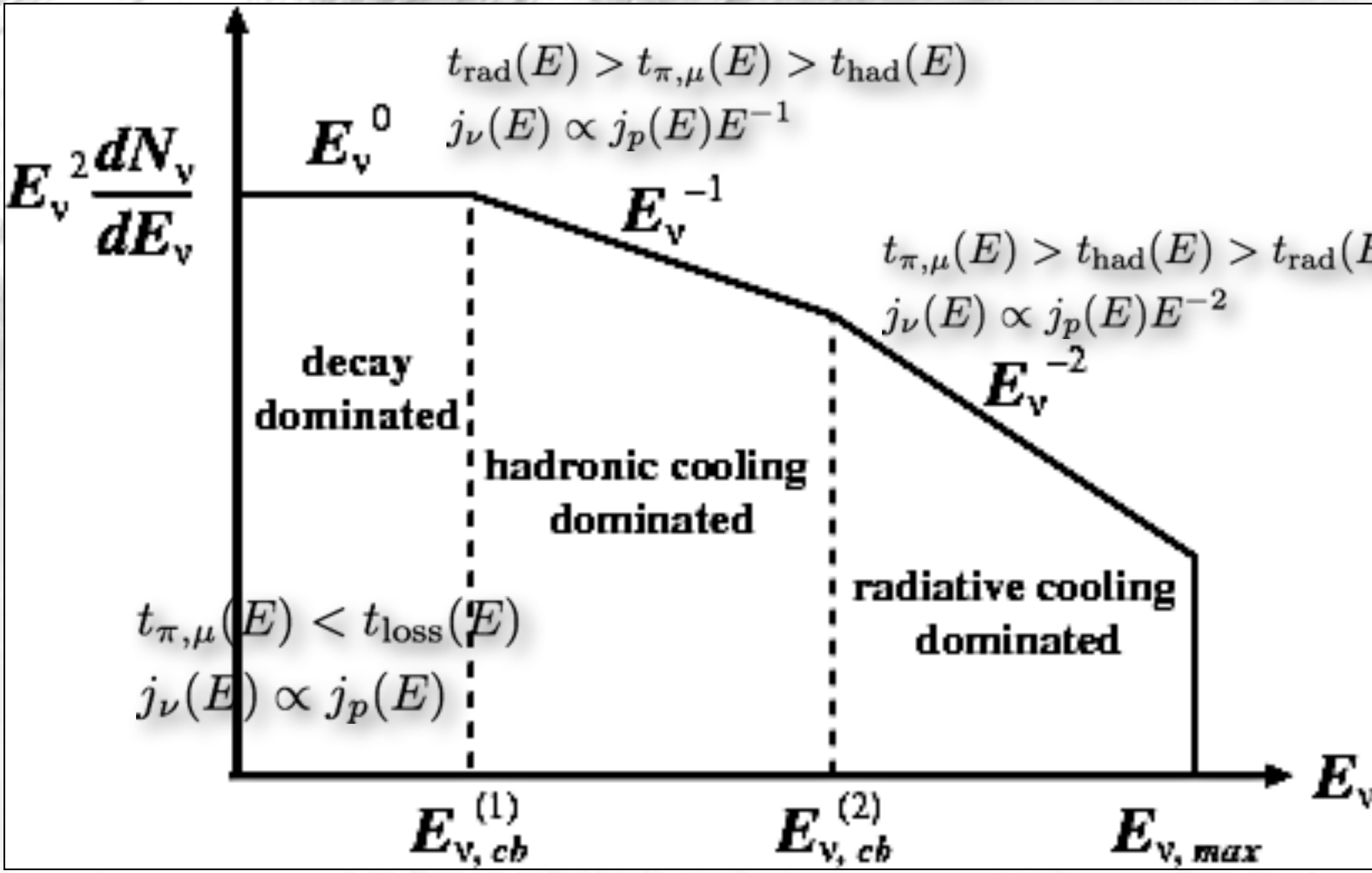

Note that $t_\mu \sim 100 t_\pi$ such that the critical energies are higher for pion decay. But pion decay into electrons is helicity suppressed, therefore, at high energies source fluxes should be muon neutrino dominated.

Testing Neutrino Properties with Astrophysical Neutrinos

- Oscillation parameters, source physics, neutrino decay and decoherence
- Neutrino-nucleon cross sections
- Quantum Gravity effects

For n neutrino flavors, eigenstates $|\nu_i\rangle$ of mass m_i, interaction eigenstates $|\nu_\alpha\rangle$ are related by a unitary $n \times n$ matrix U:

$$|\nu_\alpha\rangle = \sum_i U_{\alpha i} |\nu_i\rangle \,.$$

If at $t = 0$ a flavor eigenstate $|\nu_\alpha\rangle = \sum_i U_{\alpha i} |\nu_i\rangle$ is produced in an interaction, in vacuum the time development will thus be

$$|\nu(t)\rangle = \sum_i U_{\alpha i} e^{-iE_i t} |\nu_i\rangle = \sum_{i,\beta} U_{\alpha i} U^*_{\beta i} e^{-iE_i t} |\nu_\beta\rangle \,.$$

This implies the following transition probabilities

$$P(\nu_\alpha \to \nu_\beta) = \left| \sum_i U_{\alpha i} U^*_{\beta i} e^{-iE_i t} \right|^2 \,.$$

For flavors $|\nu_\alpha\rangle$ injected with relative weights w_α at the source, the flux of flavor $|\nu_\beta\rangle$ at the observer is then (averaged over the oscillations)

169

$$\phi_\beta(E) \propto \sum_\alpha w_\alpha P(\nu_\alpha \to \nu_\beta) \simeq \sum_{i,\alpha} w_\alpha \left|U_{\alpha i}\right|^2 \left|U_{\beta i}\right|^2 \,.$$

Examples for detectable flavor effects

Sensitivity to source physics: When both pions and muons decay before loosing energy, then $w_e : w_\mu : w_\tau \simeq \frac{1}{3} : \frac{2}{3} : 0$ and thus $\phi_e : \phi_\mu : \phi_\tau \simeq \frac{1}{3} : \frac{1}{3} : \frac{1}{3}$. If pions but not muons decay before loosing energy then $w_e : w_\mu : w_\tau \simeq 0 : 1 : 0$ and thus $\phi_e : \phi_\mu : \phi_\tau \simeq \frac{1}{5} : \frac{2}{5} : \frac{2}{5}$.

For unstable mass eigenstates introduce a factor $\exp\left[-(m_i/\tau_i)(t/E)\right]$.
In normal hierarchy if ν_2 and ν_3 decay completely, then $\phi_e : \phi_\mu : \phi_\tau \simeq \frac{3}{4} : \frac{1}{8} : \frac{1}{8}$.
In inverted hierarchy if ν_1 and ν_2 decay completely, then $\phi_e : \phi_\mu : \phi_\tau \simeq 0 : \frac{1}{2} : \frac{1}{2}$.

For quantum decoherence on scales smaller than t one always has $\phi_e : \phi_\mu : \phi_\tau \simeq \frac{1}{3} : \frac{1}{3} : \frac{1}{3}$.

Observed Flavor Ratios can be sensitive to source physics

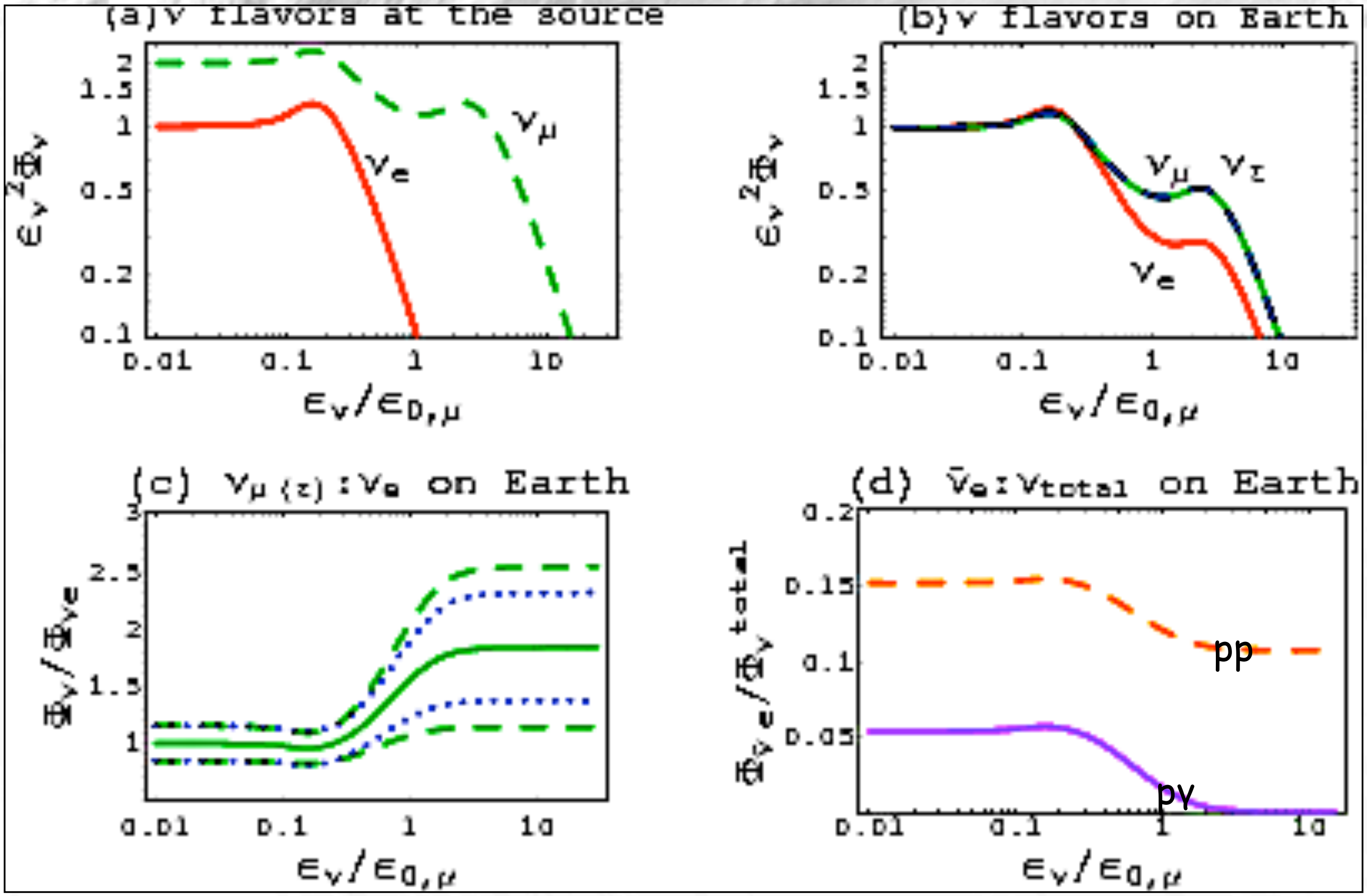

Kashti and Waxman, Phys.Rev.Lett. 95 (2005) 181101

Injection of pions of energy ϵ_π with spectrum $\propto \epsilon_\pi^{-2}$ with energy losses $\dot{\epsilon}_\pi \propto \epsilon_\pi^2$; $\epsilon_{0,\mu}$ is the energy at which decay equals synchrotron loss.

Observed Flavor Ratios can be sensitive to oscillation parameters

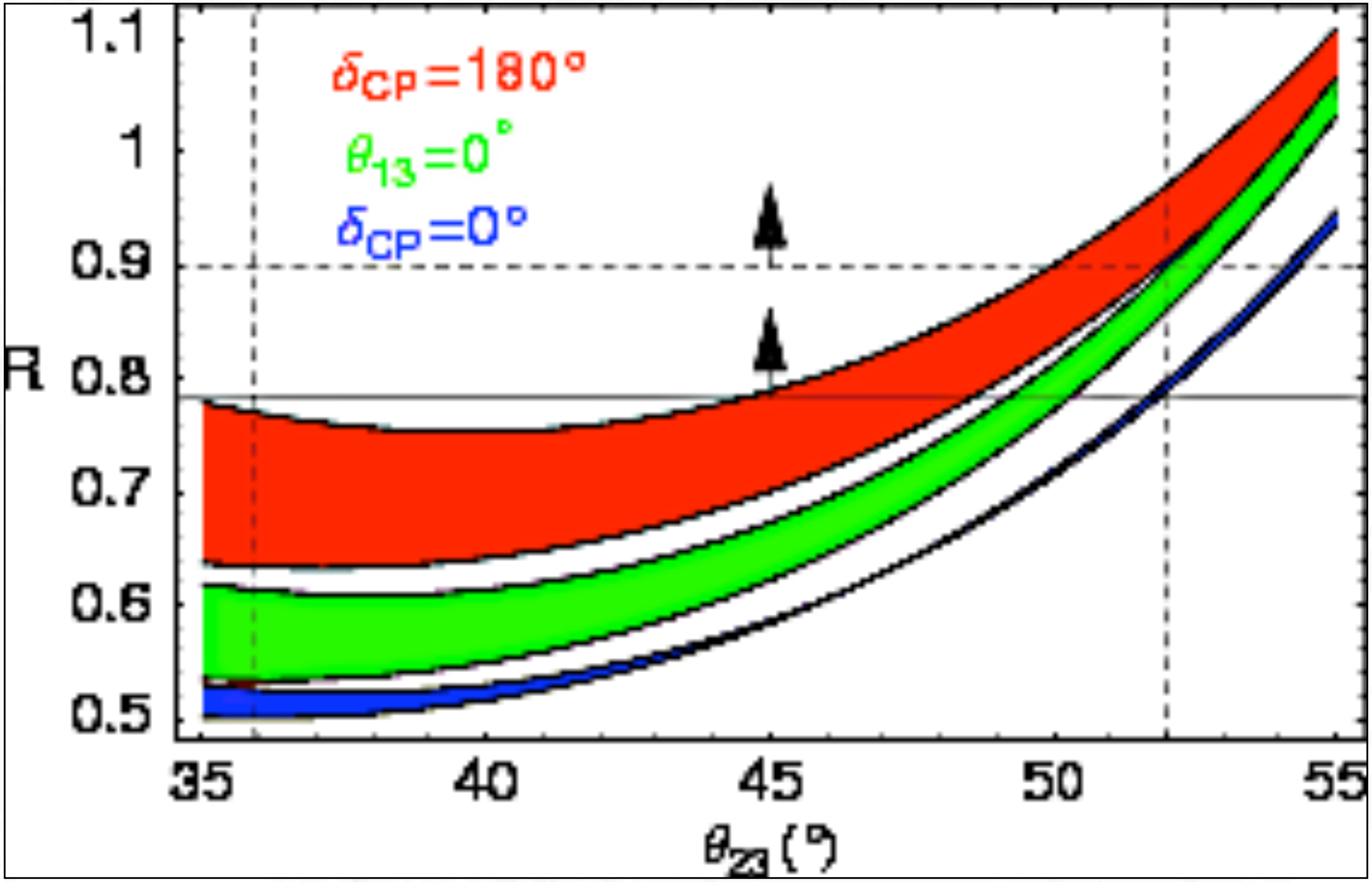

For a source optically thick to muons but not to pions: Pions decay right away, but muons loose energy by synchro before decaying

172

Serpico, Phys.Rev.D 73 (2006) 047301

Sensitivity of astrophysical neutrinos to oscillations: The Learned Plot

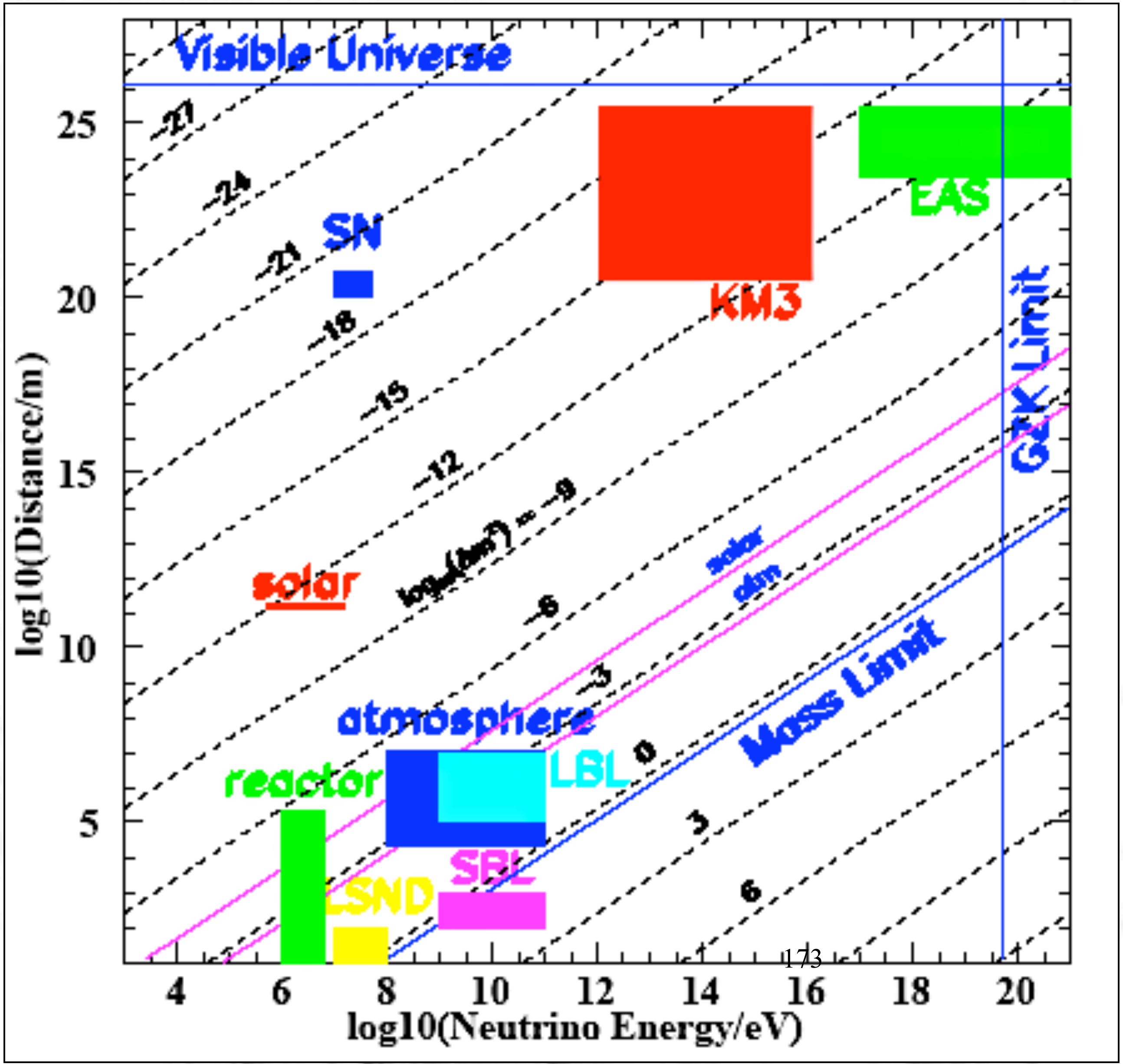

Oscillation phase is
$(L \, \Delta m^2 / 4 E_n)$
Numbers indicate
$\Delta m^2/eV^2$.

Probes of Neutrino Interactions beyond the Standard Model

Note: For primary energies around 10^{20} eV:

Probes of Neutrino Interactions beyond the Standard Model

Note: For primary energies around 10^{20} eV:

- Center of mass energies for collisions with relic backgrounds
  ~100 MeV – 100 GeV —> physics well understood

Probes of Neutrino Interactions beyond the Standard Model

Note: For primary energies around 10^{20} eV:

- Center of mass energies for collisions with relic backgrounds
  ~100 MeV – 100 GeV —> physics well understood
- Center of mass energies for collisions with nucleons in the atmosphere
  ~100 TeV – 1 PeV —> probes physics beyond reach of accelerators

174

Probes of Neutrino Interactions beyond the Standard Model

Note: For primary energies around 10^{20} eV:

- Center of mass energies for collisions with relic backgrounds
  ~100 MeV – 100 GeV —> physics well understood
- Center of mass energies for collisions with nucleons in the atmosphere
  ~100 TeV – 1 PeV —> probes physics beyond reach of accelerators

Example: microscopic black hole production in scenarios with a TeV string scale:

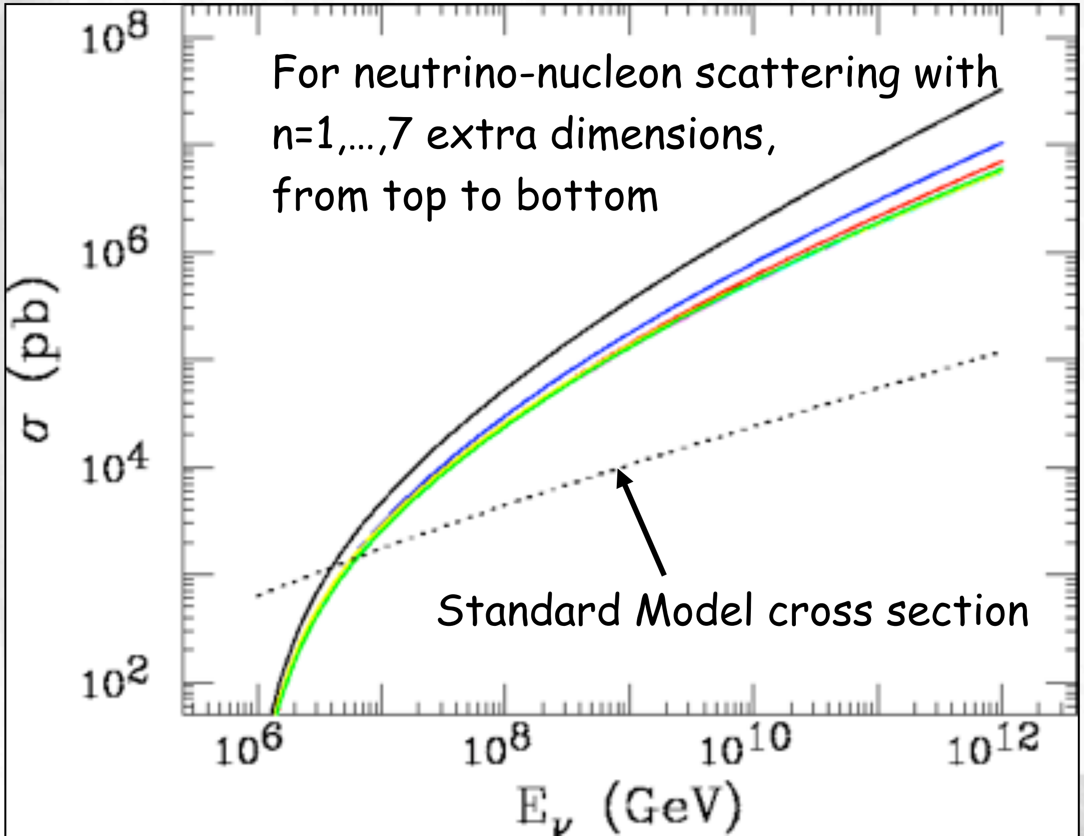

Feng, Shapere, PRL 88 (2002) 021303

174

Probes of Neutrino Interactions beyond the Standard Model

Note: For primary energies around 10^{20} eV:

- Center of mass energies for collisions with relic backgrounds
  ~100 MeV – 100 GeV —> physics well understood
- Center of mass energies for collisions with nucleons in the atmosphere
  ~100 TeV – 1 PeV —> probes physics beyond reach of accelerators

Example: microscopic black hole production in scenarios with a TeV string scale:

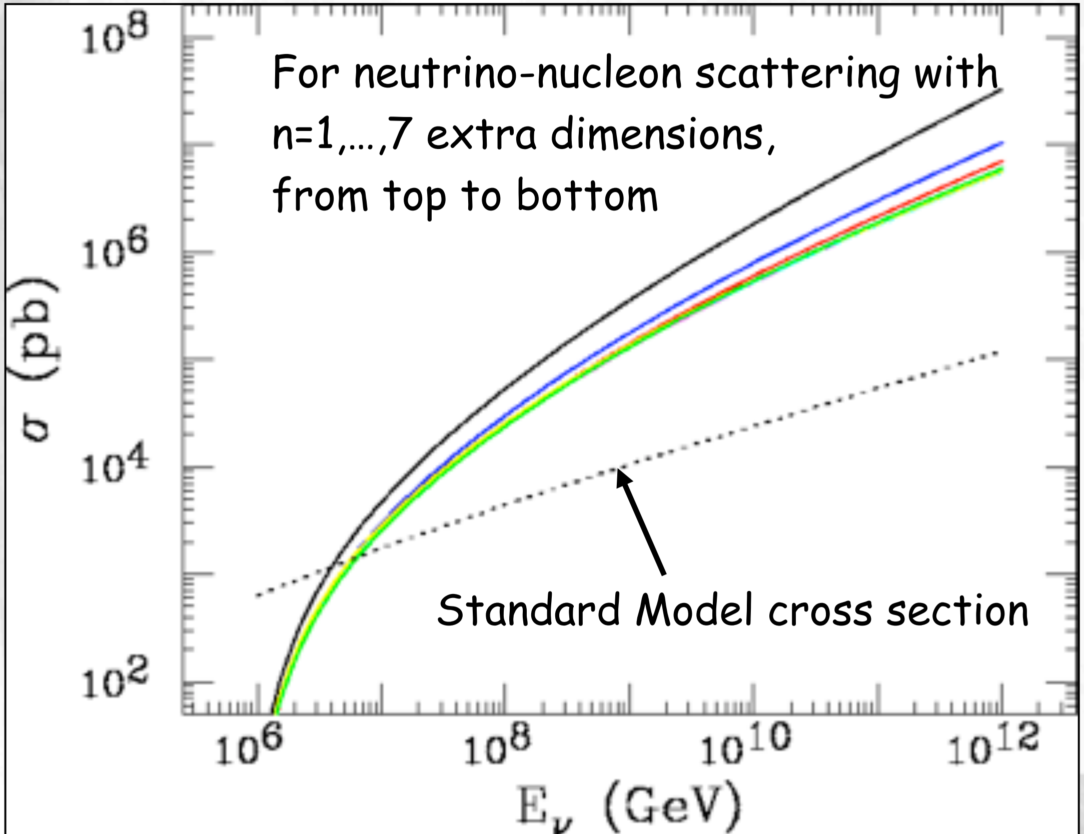

Feng, Shapere, PRL 88 (2002) 021303

This increase is not sufficient to explain the highest energy cosmic rays, but can be probed with deeply penetrating showers.

However, the neutrino flux from pion-production of extra-galactic trans-GZK cosmic rays allows to put limits on the neutrino-nucleon cross section:

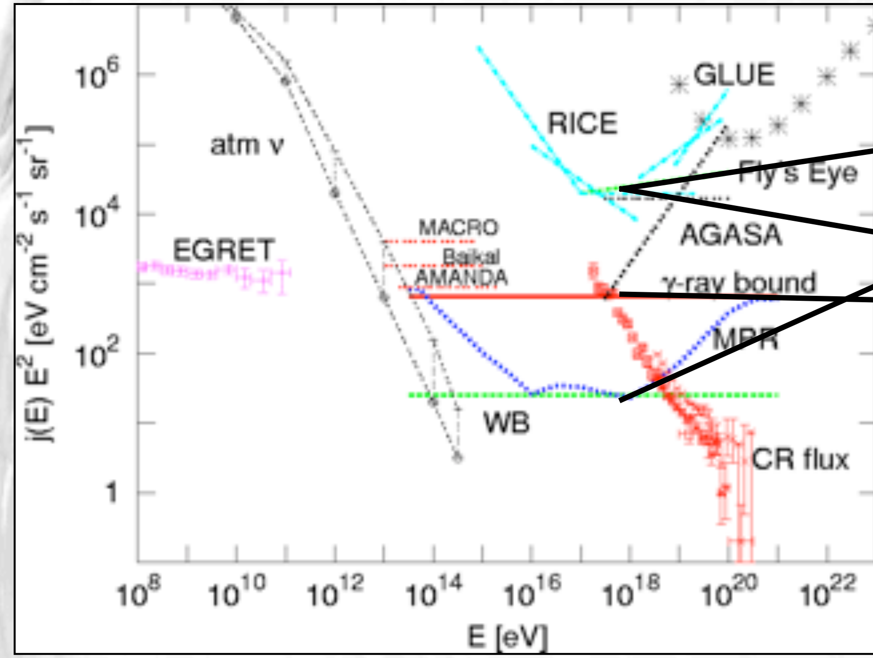

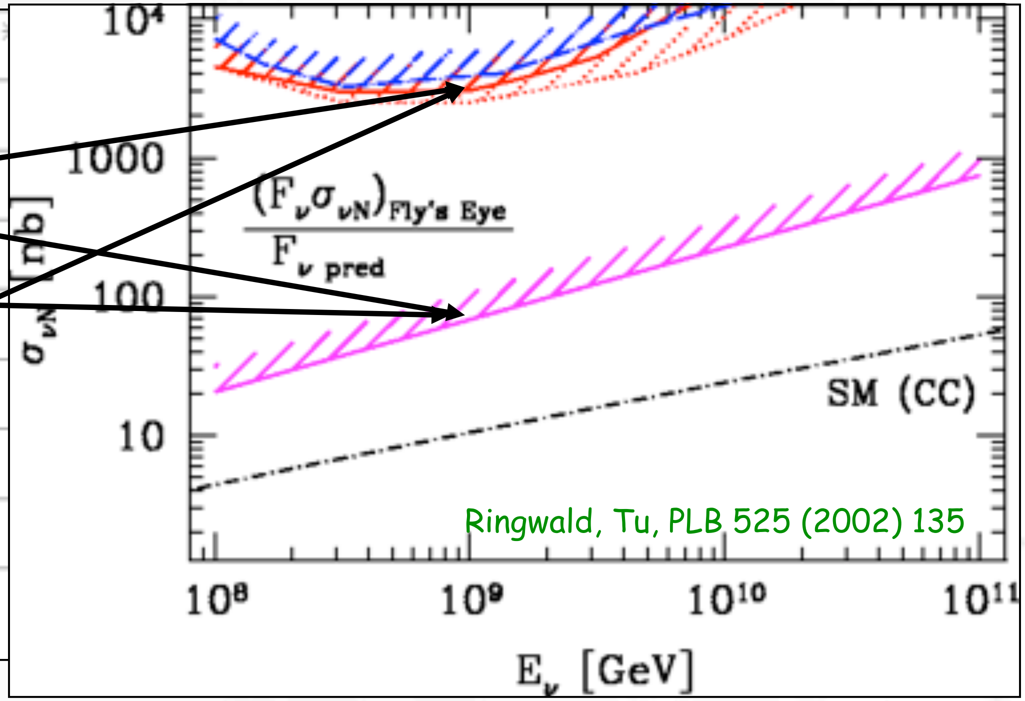

Comparison of this Nγ- ("cosmogenic") flux with the non-observation of horizontal air showers results in the present upper limit about 10^3 above the Standard Model cross section.

175

However, the neutrino flux from pion-production of extra-galactic trans-GZK cosmic rays allows to put limits on the neutrino-nucleon cross section:

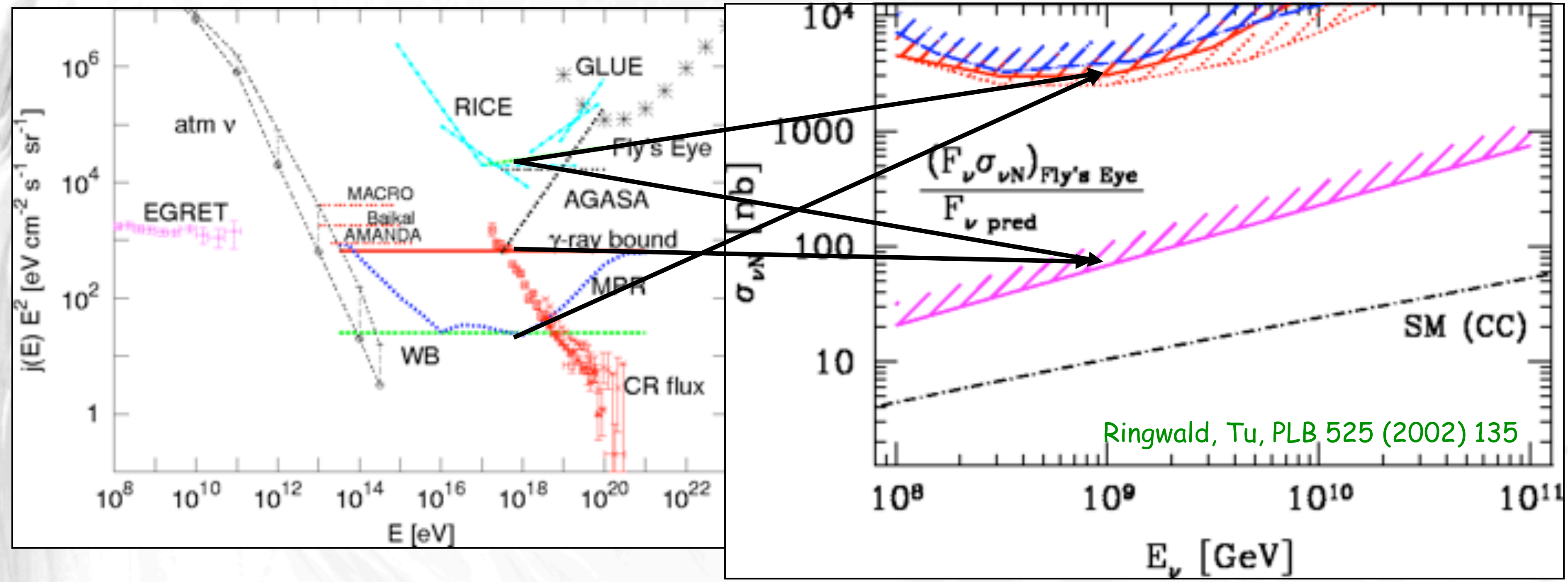

Comparison of this Nγ- ("cosmogenic") flux with the non-observation of horizontal air showers results in the present upper limit about 10^3 above the Standard Model cross section.

Future experiments will either close the window down to the Standard Model cross section, discover higher cross sections, or find sources beyond the cosmogenic flux. How to disentangle new sources and new cross sections?

Solution: Compare rates of different types of neutrino-induced showers

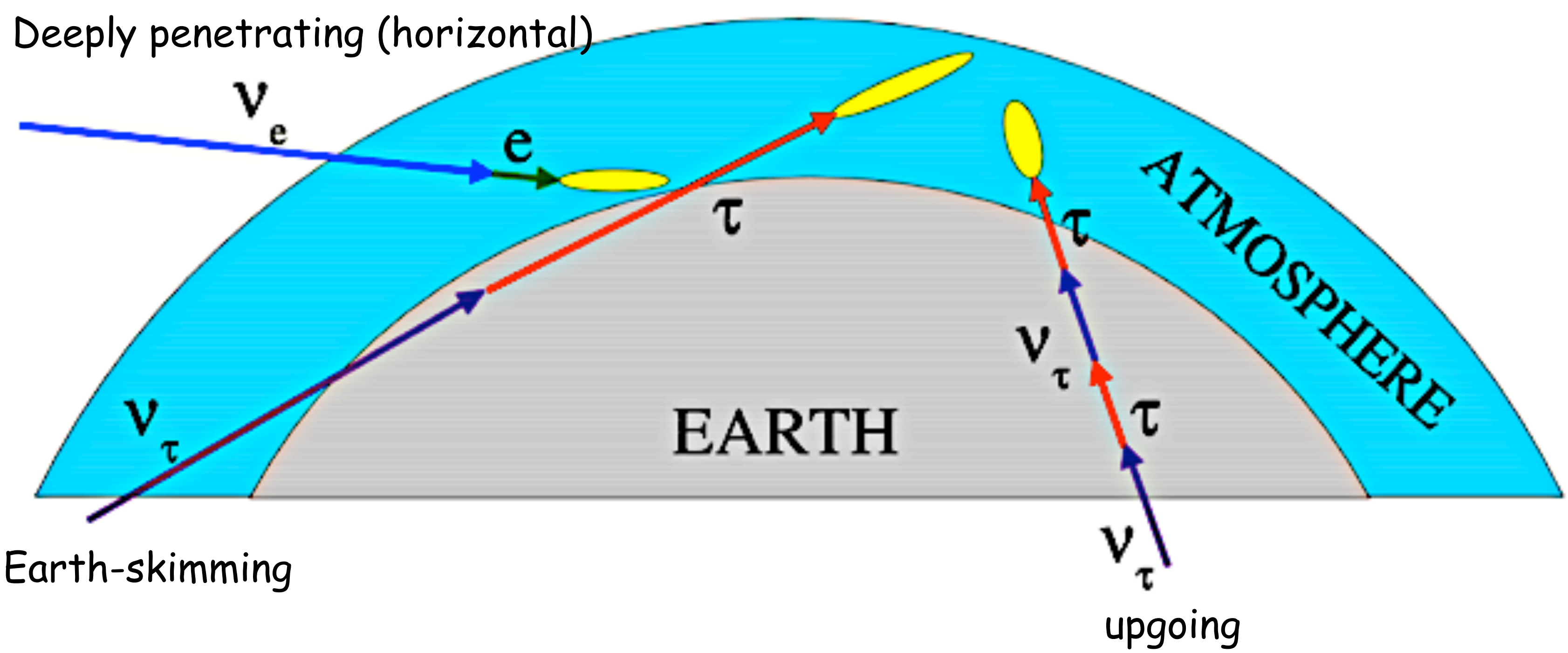

Figure from Cusumano

Earth-skimming τ-neutrinos

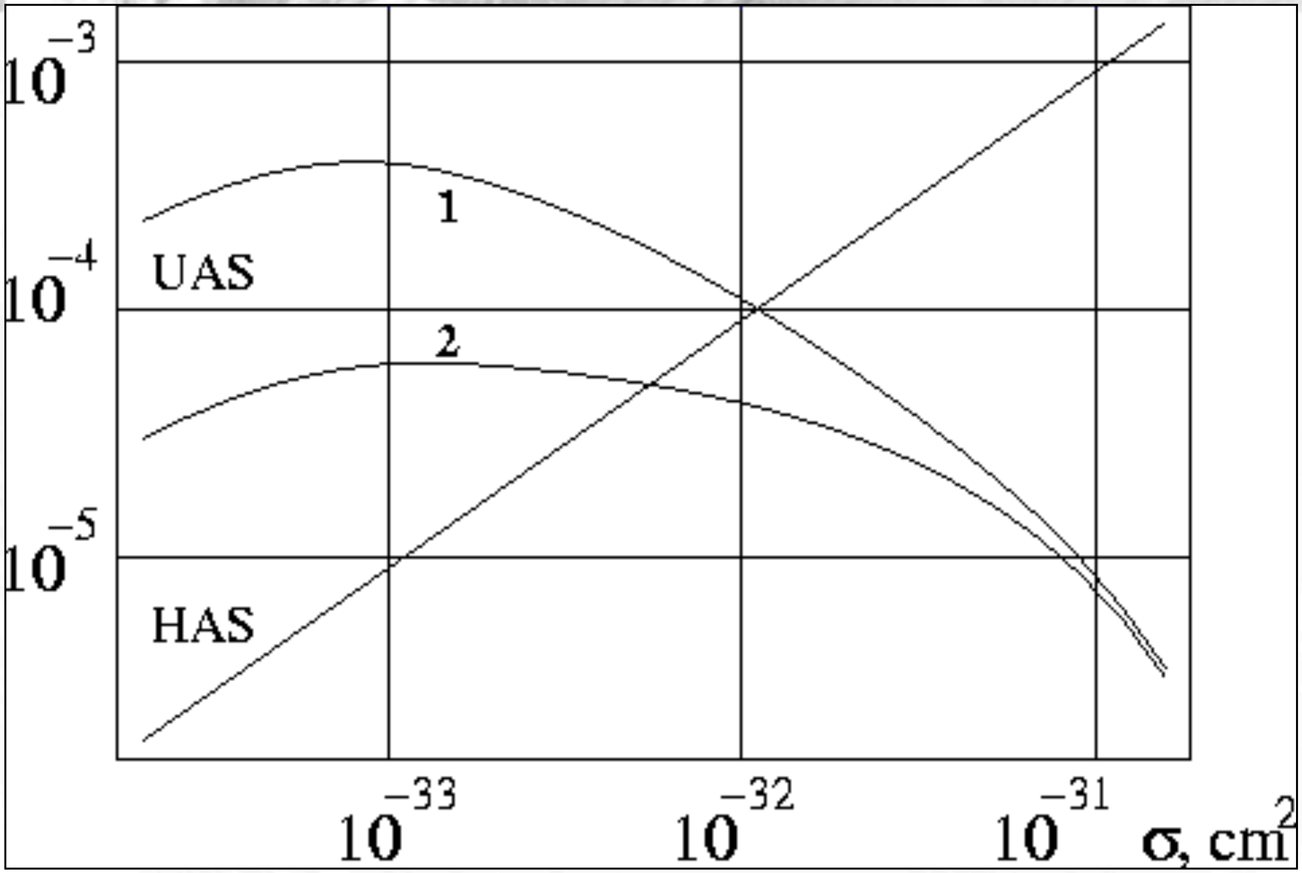

Air-shower probability per τ-neutrino at 10^{20} eV for 10^{18} eV (1) and 10^{19} eV (2) threshold energy for space-based detection.

Comparison of earth-skimming and horizontal shower rates allows to measure the neutrino-nucleon cross section in the 100 TeV range.

Kusenko, Weiler, PRL 88 (2002) 121104

Sensitivities of LHC and the Pierre Auger project to microscopic black hole production in neutrino-nucleon scattering

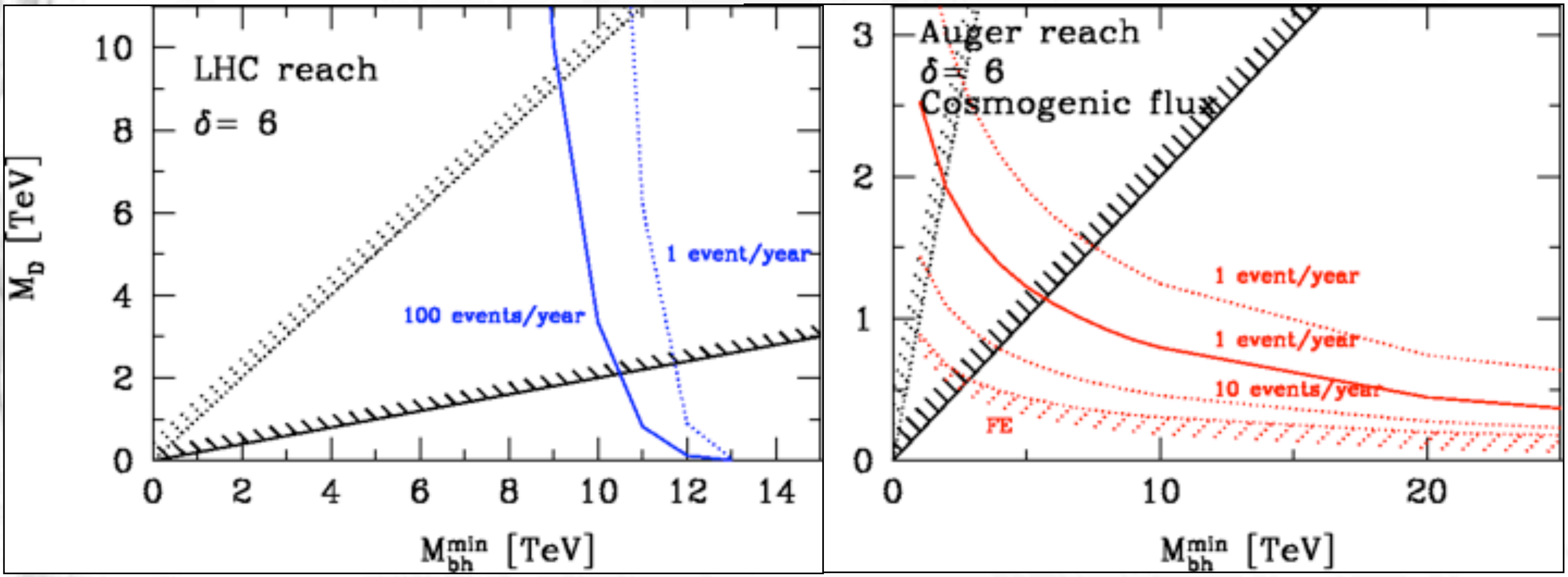

M_D = fundamental gravity scale; M_{bh}^{min} = minimal black hole mass

LHC much more sensitive than Auger, but Auger could "scoop" LHC

Ringwald, Tu, PLB 525 (2002) 135

Sensitivities of future neutrino telescopes to microscopic black hole production in neutrino-nucleon scattering

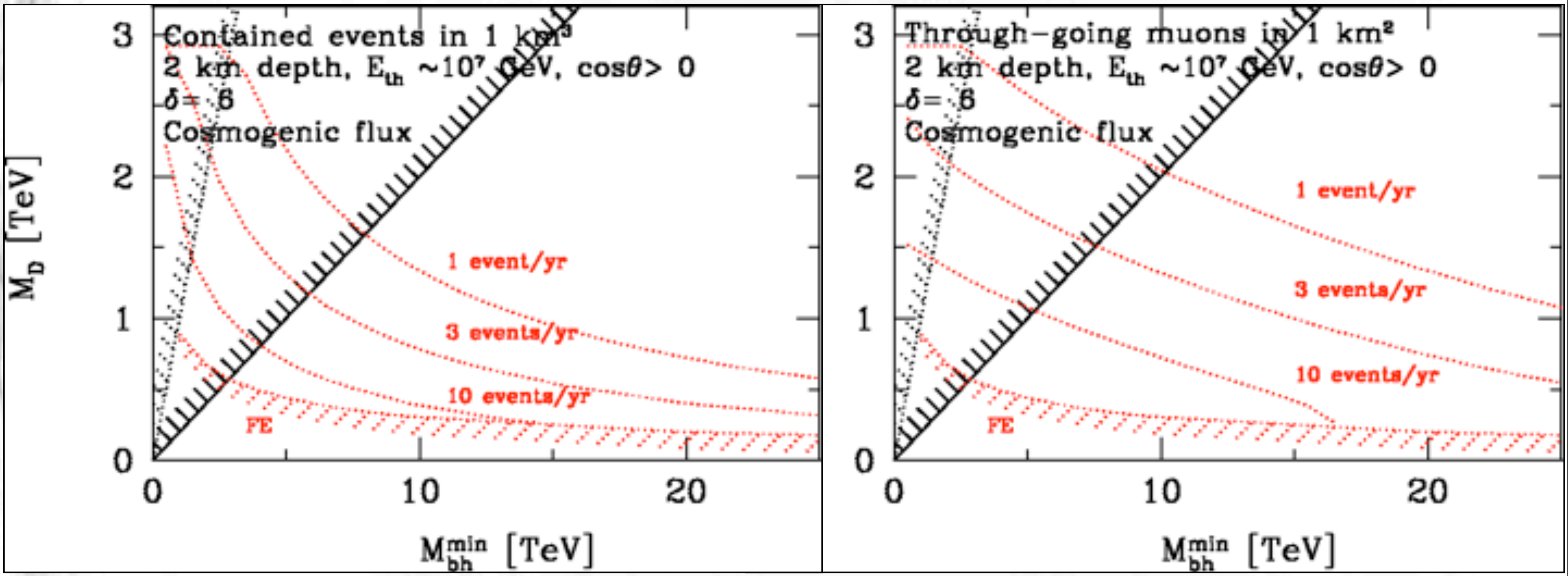

Contained events: Rate ~ Volume

Through-going events: Rate ~ Area

Ringwald, Kowalski, Tu, PLB 529 (2002) 1

Probes of Quantum Gravity Effects with Neutrinos

Dispersion relation between energy E, momentum p, and mass m may be modified by non-renormalizable effects at the Planck scale M_{Pl},

$$p^2 + m^2 = E^2 \left[1 - \sum_{n=1}^{\infty} \xi_n \left(\frac{E}{M_{\rm Pl}} \right)^n \right]$$

where most models, e.g. critical string theory, predict ξ=0 for lowest order.

For the i-th neutrino mass eigenstate this gives

$$p_i \simeq E + \frac{m_i^2}{2E} + \frac{1}{2} \sum_{n=1}^{\infty} \xi_n^{(i)} \frac{E^{n+1}}{M_{\rm Pl}}$$

The « standard » oscillation term becomes comparable to the new terms at energies

$$E \simeq M_{\rm Pl} \left(\frac{\Delta m^2}{M_{\rm Pl}^2 \xi_n} \right)^{\frac{1}{n+2}} \simeq 0.2\,, 2 \times 10^4\,, 1.8 \times 10^7\,, 1.7 \times 10^9\,\mathrm{GeV}$$

for n=1, 2, 3, 4, respectively, and $\Delta m^2 = 10^{-3}$ eV^2, for which ordinary Oscillation length is ~2.5(E/MeV) km. 180

See, e.g., Christian, Phys.Rev.D71 (2005) 024012

Other possible effects: Decoherence of oscillation amplitude with $\exp(-\alpha L)$:
Assume galactic neutron sources, L~10 kpc, giving exclusively electron-anti-neutrinos before oscillation. After oscillation the flavor ratio becomes 1:0:0 -> 0.56:0.24:0.20 without decoherence, but 0.33:0.33:0.33 with decoherence.

At E~1 TeV one has a sensitivity of $\alpha \sim 10^{-37}$ GeV (somewhat dependent on energy dependence of α)

Hooper, Morgan, Winstanley, Phys.Lett.B609 (2005): 206

Lorentz symmetry violations in the Nucleon Sector

Dispersion relation between energy E, momentum p, and mass m may be modified by non-renormalizable effects at the Planck scale M_{Pl},

$$E^2 - p^2 \simeq m^2 - \xi \frac{p^3}{M_{\rm Pl}} - \zeta \frac{p^4}{M_{\rm Pl}^2} + \cdots$$

where most models, e.g. critical string theory, predict $\xi=0$ for lowest order.

Introducing the standard threshold momentum for pion production, $N+\gamma \to N\pi$,

$$p_0 = \frac{2m_N m_\pi + m_\pi^2}{4\epsilon}$$

$$-\frac{p_0^3}{(m_\pi^2 + 2m_\pi m_N)M_{\rm Pl}} \frac{m_\pi m_N}{(m_\pi + m_N)^2} \left[2\xi \left(\frac{p_{\rm th}}{p_0}\right)^3 + 3\zeta \frac{p_0}{M_{\rm Pl}} \left(\frac{p_{\rm th}}{p_0}\right)^4 + \cdots \right] + \frac{p_{\rm th}}{p_0} = 1$$

Lorentz symmetry violations in the Nucleon Sector

Dispersion relation between energy E, momentum p, and mass m may be modified by non-renormalizable effects at the Planck scale M_{Pl},

$$E^2 - p^2 \simeq m^2 - \xi \frac{p^3}{M_{\rm Pl}} - \zeta \frac{p^4}{M_{\rm Pl}^2} + \cdots$$

where most models, e.g. critical string theory, predict ξ=0 for lowest order.

Introducing the standard threshold momentum for pion production, $N+\gamma \to N\pi$,

$$p_0 = \frac{2m_N m_\pi + m_\pi^2}{4\epsilon}$$

the threshold momentum p_{th} in the modified theory is given by

$$-\frac{p_0^3}{(m_\pi^2 + 2m_\pi m_N)M_{\rm Pl}} \frac{m_\pi m_N}{(m_\pi + m_N)^2} \left[2\xi \left(\frac{p_{\rm th}}{p_0}\right)^3 + 3\zeta \frac{p_0}{M_{\rm Pl}} \left(\frac{p_{\rm th}}{p_0}\right)^4 + \cdots \right] + \frac{p_{\rm th}}{p_0} = 1$$

Attention: this assumes standard energy-momentum conservation which is not necessarily the case.

Coleman, Glashow, PRD 59 (1999) 116008; Alosio et al., PRD 62 (2000) 053010

For $\xi \sim \zeta \sim 1$ this equation has no solution => No GZK threshold!

For $\zeta \sim 0$, $\xi \sim -1$ the threshold is at ~1 PeV!
For $\xi \sim 0$, $\zeta \sim -1$ the threshold is at ~1 EeV!

Confirmation of a normal GZK threshold would imply the following limits:

$|\xi| < 10^{-13}$ for the first-order effects.
$|\zeta| < 10^{-6}$ for the second-order effects.

Energy-independent (renormalizable) corrections to the maximal speed $V_{max} = \lim_{E\to\infty} \partial E/\partial p = 1-d$ can be constrained by substituting $d \to (\xi/2)(E/M_{Pl})+(\zeta/2)(E/M_{Pl})^2$.

$$\Delta t = -\xi\, d \frac{E}{M_{\rm Pl}} \simeq -\xi \left(\frac{d}{100\,{\rm Mpc}}\right)\left(\frac{E}{\rm TeV}\right) {\rm sec}$$

183

For $\xi \sim \zeta \sim 1$ this equation has no solution => No GZK threshold!

For $\zeta \sim 0$, $\xi \sim -1$ the threshold is at ~1 PeV!
For $\xi \sim 0$, $\zeta \sim -1$ the threshold is at ~1 EeV!

Confirmation of a normal GZK threshold would imply the following limits:

$|\xi| < 10^{-13}$ for the first-order effects.
$|\zeta| < 10^{-6}$ for the second-order effects.

Energy-independent (renormalizable) corrections to the maximal speed $V_{max} = \lim_{E \to \infty} \partial E/\partial p = 1 - d$ can be constrained by substituting $d \to (\xi/2)(E/M_{Pl}) + (\zeta/2)(E/M_{Pl})^2$.

The modified dispersion relation also leads to energy dependent group velocity $V = \partial E/\partial p$ and thus to an energy-dependent time delay over a distance d:

$$\Delta t = -\xi\, d \frac{E}{M_{\rm Pl}} \simeq -\xi \left(\frac{d}{100\,{\rm Mpc}}\right)\left(\frac{E}{\rm TeV}\right) {\rm sec}$$

183

for $\zeta = 0$. GRB observations in TeV γ-rays can therefore probe quantum gravity. The current limit is $M_{Pl}/\xi > 8\times10^{15}$ GeV (Ellis et al.).

Lorentz Symmetry Violation in the Photon Sector

For photons we assume the dispersion relation

$$\omega_\pm^2 = k^2 + \xi_n^\pm k^2 \left(\frac{k}{M_{\rm Pl}}\right)^n , n \geq 1 ,$$

and for electrons

$$E_{e,\pm}^2 = p_e^2 + m_e^2 + \eta_n^{e,\pm} p_e^2 \left(\frac{p_e}{M_{\rm Pl}}\right)^n , n \geq 1 ,$$

with only one term present. Polarizations denoted with ±. For positrons, effective field theory implies $\eta_n^{p,\pm} = (-1)^n \eta_n^{e,\mp}$. Furthermore, $\xi_n^+ = (-1)^n \xi_n^-$, so that the problem depends on three parameters which in the following we denote by

$$\xi_n , \eta_n^+ , \eta_n^-$$

for each n.

184

Consider pair production on a background photon of energy k_b and assume kinematics with ordinary energy-momentum conservation, with $p_e = (1-y)k$, $p_p = yk$. Using $x = 4y(1-y)k/k_{LI}$ with the threshold in absence of Lorentz invariance (LI) violation, $k_{LI}=m_e^2/\omega_b$, the condition for pair production is then

$$\alpha_n x^{n+2} + x - 1 \geq 0$$

where

$$\alpha_n = \frac{\xi_n - (-1)^n \eta_n^{\mp} y^{n+1} - \eta_n^{\pm}(1-y)^{n+1}}{2^{2(n+2)} y^{n+1}(1-y)^{n+1}} \frac{m_e^{2(n+1)}}{k_b^{n+2} M_{\rm Pl}^n} .$$

All combinations of $\xi_n, \eta_n^+, \eta_n^-$ can occur, depending on the partial wave of the pair, governed by total angular momentum conservation. All partial waves are allowed away from the thresholds.

The condition for photon decay is

185

$$\alpha_n x^{n+2} - 1 \geq 0$$

There are at most two real solutions $0 \leq x_n^l \leq x_n^r$ for pair production (lower and upper thresholds)

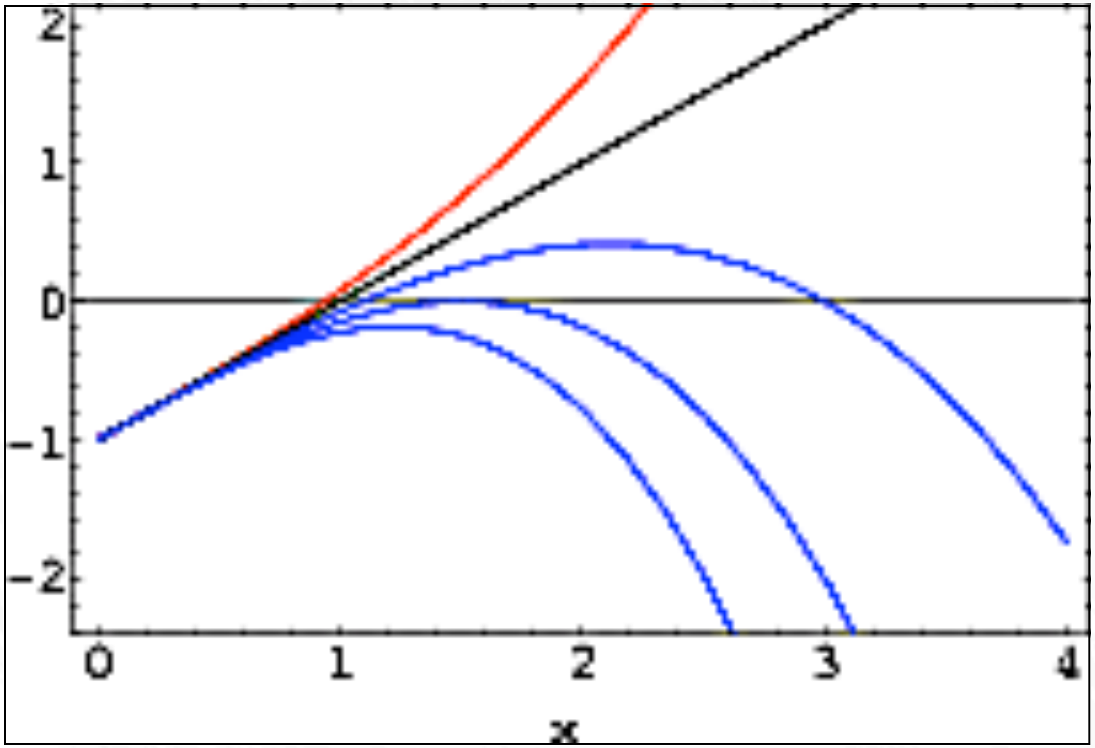

Galaverni, Sigl, Phys. Rev. Lett. 100 (2008) 021102.

For photon decay there is at most one positive real threshold.

186

Minimize/maximize these wrt. y

Current upper limits on the photon fraction are of order 2% above 10^{19} eV from latest results of the Pierre Auger experiments (ICRC) and order 30% above 10^{20} eV.

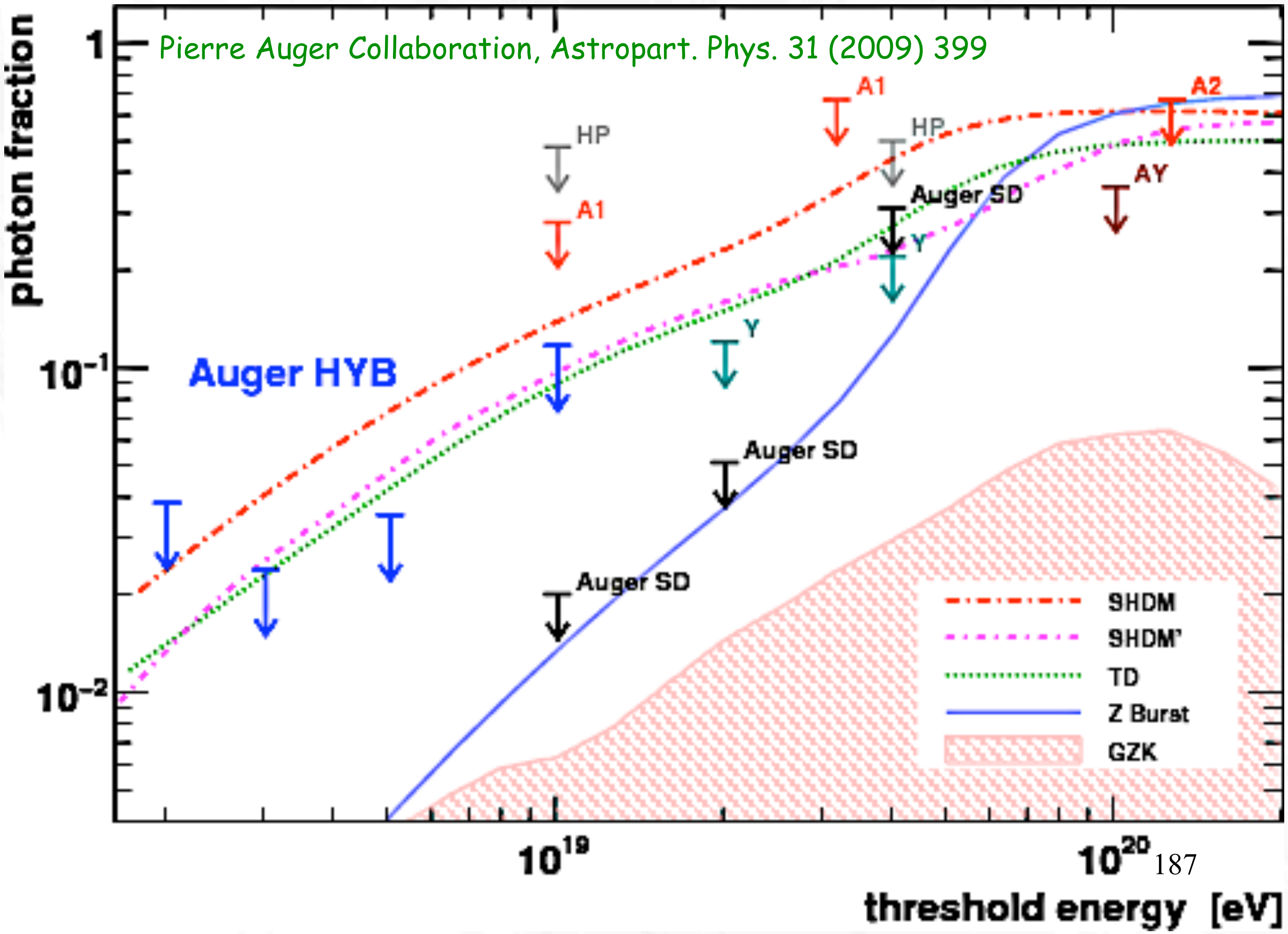

Future data will allow to probe smaller photon fractions and the GZK photons

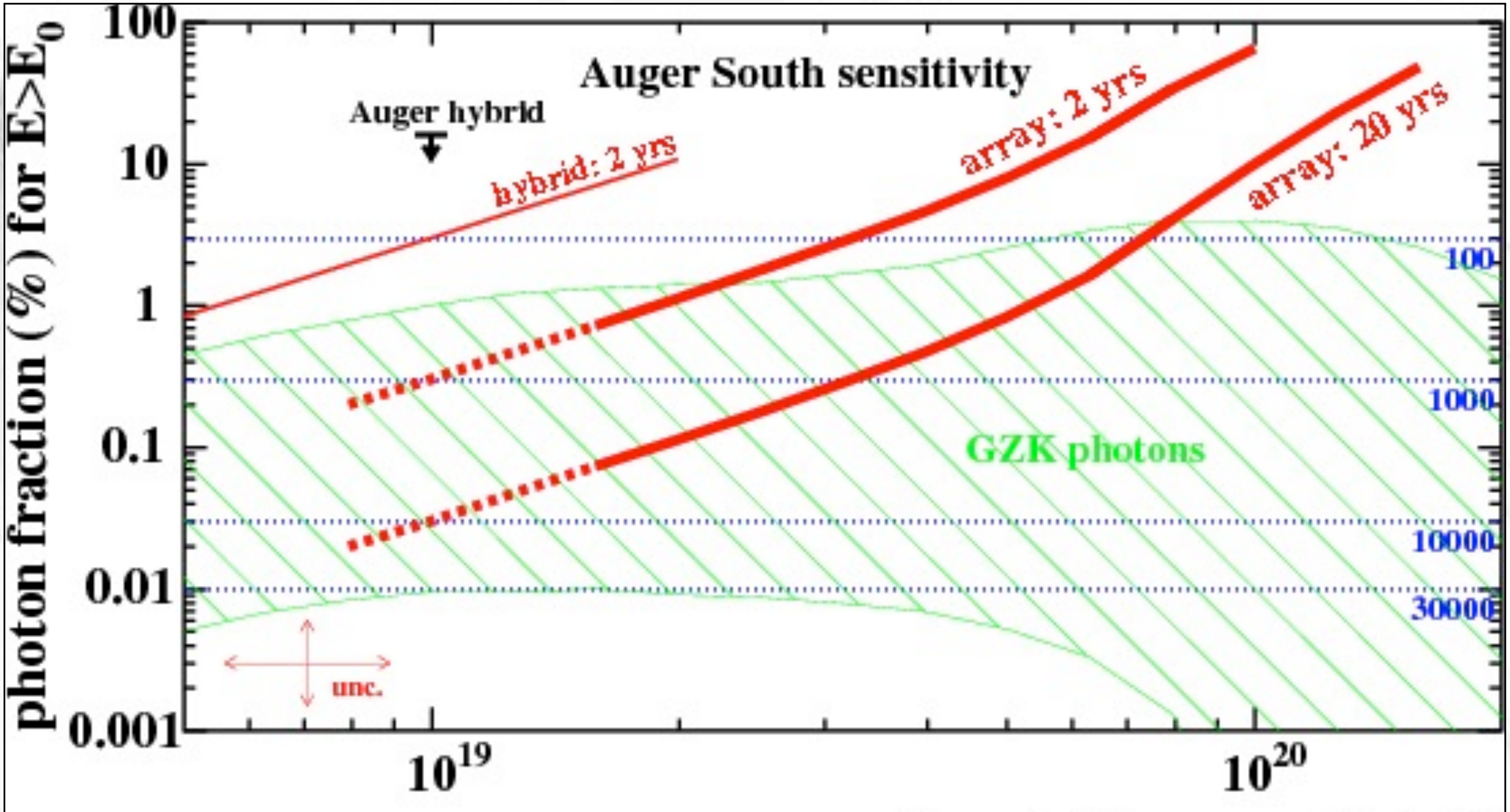

Risse, Homola, Mod.Phys.Lett. A22 (2007) 749.

In absence of pair production for 10^{19} eV < ω < 10^{20} eV the photon fraction would be ~20% and would thus violate experimental bounds:

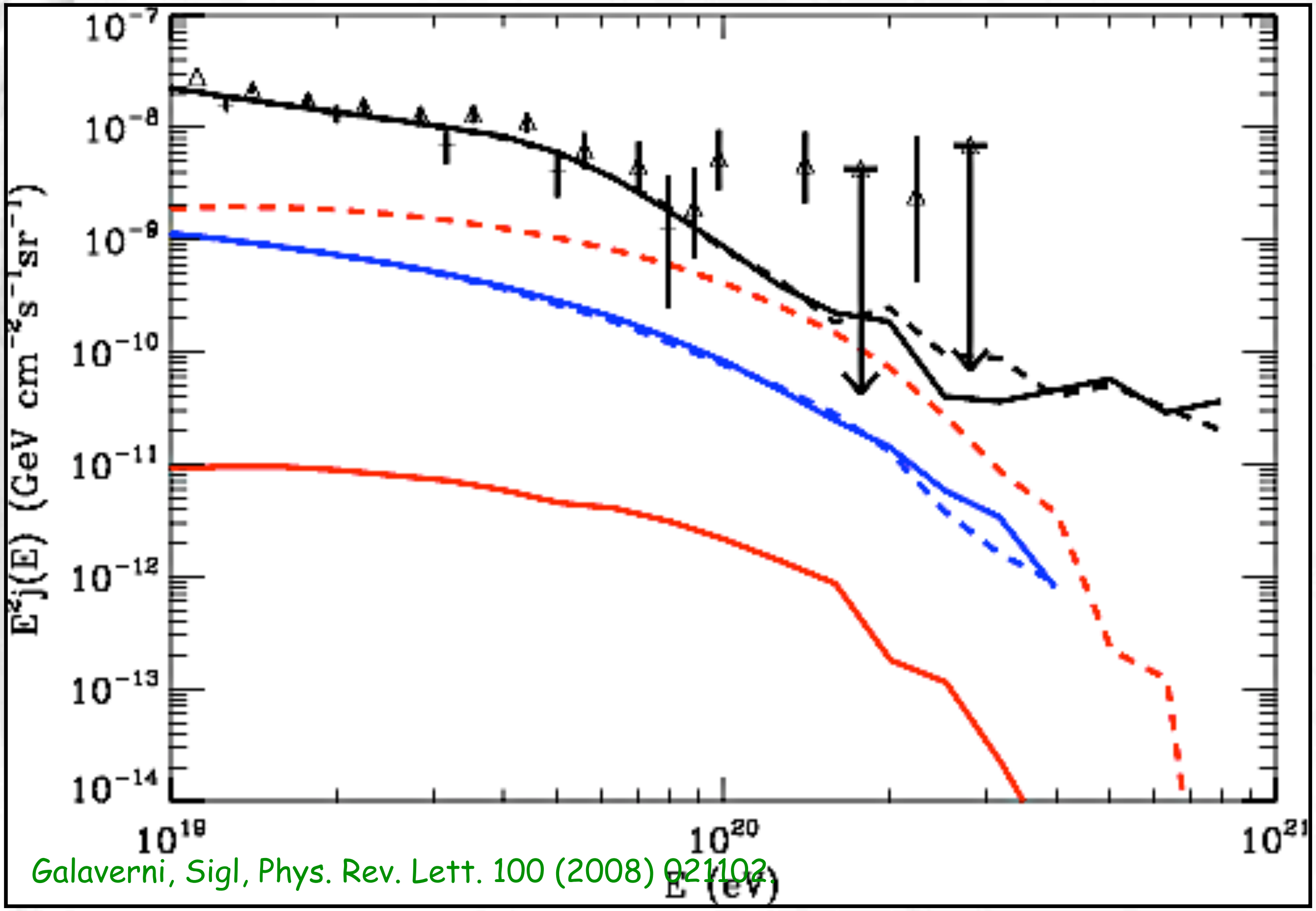

Galaverni, Sigl, Phys. Rev. Lett. 100 (2008) 021102.

189

In absence of pair production for 10^{19} eV < ω < 10^{20} eV the photon fraction would be ~20% and would thus violate experimental bounds:

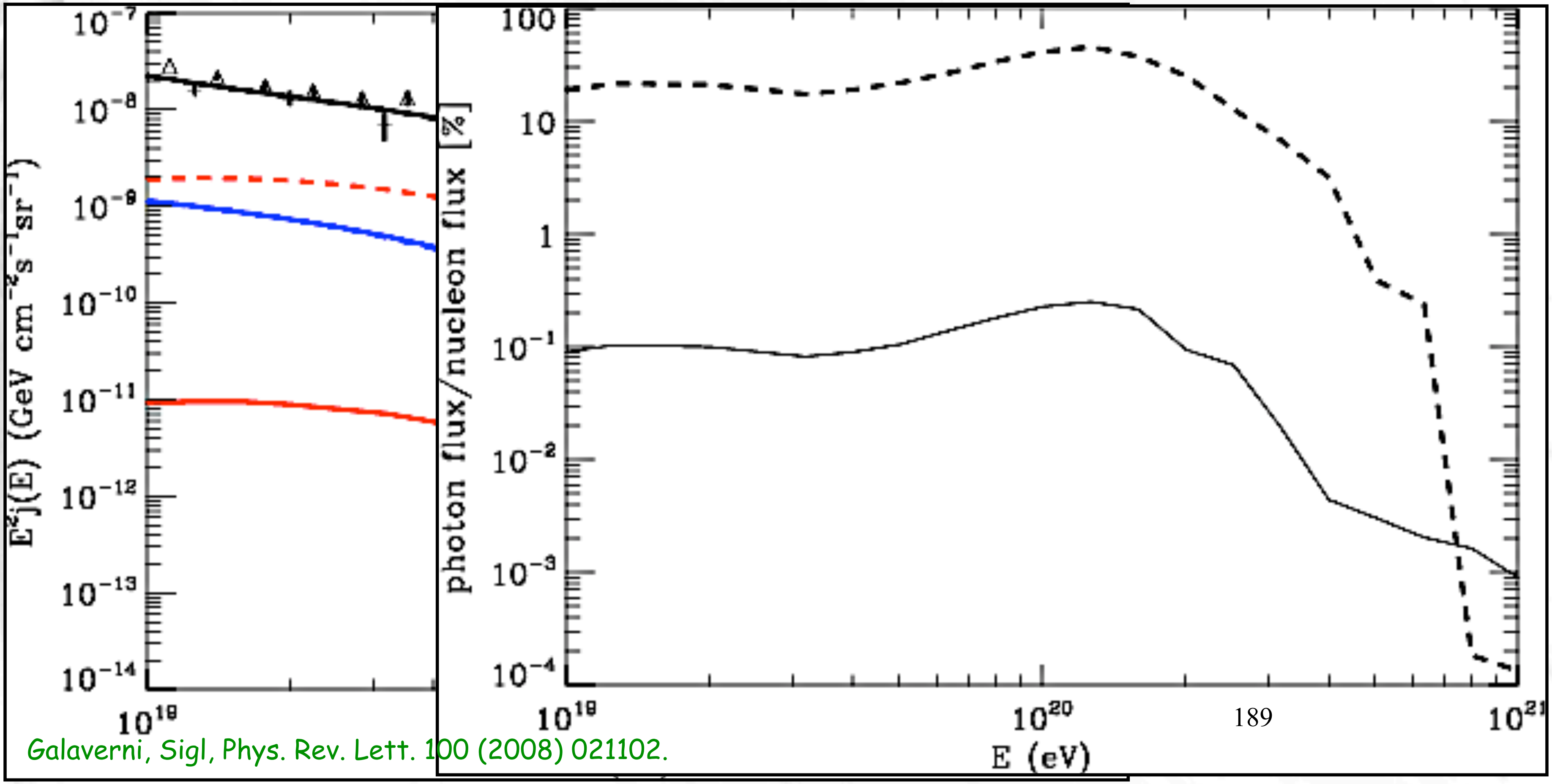

Galaverni, Sigl, Phys. Rev. Lett. 100 (2008) 021102.

A given combination $\xi_n, \eta_n^+, \eta_n^-$ is ruled out if, for 10^{19} eV < ω < 10^{20} eV, at least one photon polarization state is stable against decay and does not pair produce for any helicity configuration of the final pair.

In the absence of LIV in pairs for n=1, this yields:

$$|\xi_1| \leq 2.4 \times 10^{-15}$$

and for n=2:

$$\xi_2 \geq -2.4 \times 10^{-7}$$

If a UHE photon were detected, any LIV parameter combination for which photon decay is allowed for at least one helicity configuration of the final pair, for both photon polarizations, would be ruled out.

For n = 1, all parameters of absolute value < 10^{-14} ruled out

For n = 2, if absolute value of both the photon and one of the electron parameters is < 10^{-6}, the second electron parameter can be arbitrarily large even once a UHE photon is seen.

190

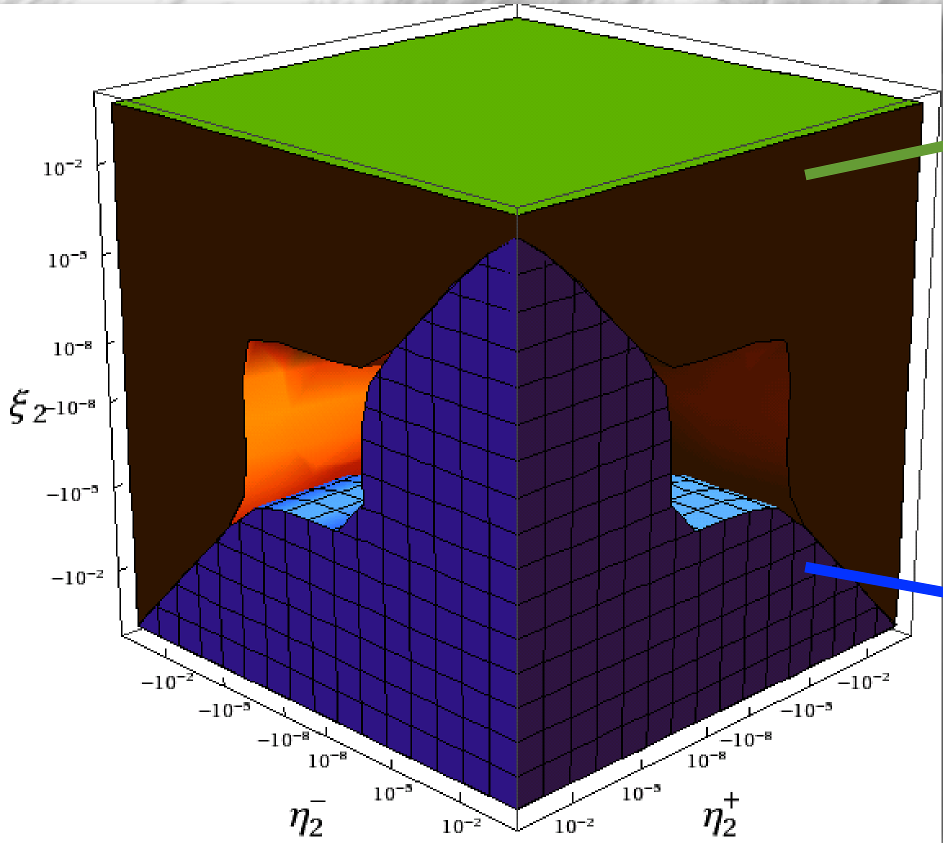

Such strong limits suggest that Lorentz invariance violations are completely absent !

Conclusions1

1.) The origin of very high energy cosmic rays is still one of the fundamental unsolved questions of astroparticle physics.
This is especially true at the highest energies, but even the origin of Galactic cosmic rays is not resolved beyond doubt.

2.) Above 60 EeV, arrival directions are anisotropic at 99% CL and seem to correlate with the local cosmic large scale structure.

3.) It is currently not clear what the sources are within these structures. Potential sources closest to the arrival directions require heavier nuclei to attain observed energies. Air shower characteristics also seem to imply a mixed composition.

4.) This is surprising because larger deflections would be expected for nuclei already in the Galactic magnetic field.

5.) A possible solution could be considerable deflection only within the large scale structure; but this would be a coincidence for galactic deflection

Conclusions2

8.) Both diffuse cosmogenic neutrino and photon fluxes depend on chemical composition (and maximal acceleration energy)

9.) Multi-messenger modeling sources including gamma-rays and neutrinos start to constrain the source and acceleration mechanisms

Conclusions2

6.) Pion-production establishes a very important link between the physics of high energy cosmic rays on the one hand, and γ-ray and neutrino astrophysics on the other hand. All three of these fields should be considered together.

8.) Both diffuse cosmogenic neutrino and photon fluxes depend on chemical composition (and maximal acceleration energy)

9.) Multi-messenger modeling sources including gamma-rays and neutrinos start to constrain the source and acceleration mechanisms

Conclusions2

6.) Pion-production establishes a very important link between the physics of high energy cosmic rays on the one hand, and γ-ray and neutrino astrophysics on the other hand. All three of these fields should be considered together.

7.) There are many potential high energy neutrino sources including speculative ones. But the only guaranteed ones are due to pion production of primary cosmic rays known to exist: Galactic neutrinos from hadronic interactions up to ~10^{16} eV and "cosmogenic" neutrinos around 10^{19} eV from photopion production. Flux uncertainties stem from uncertainties in cosmic ray source distribution and evolution.

8.) Both diffuse cosmogenic neutrino and photon fluxes depend on chemical composition (and maximal acceleration energy)

9.) Multi-messenger modeling sources including gamma-rays and neutrinos start to constrain the source and acceleration mechanisms

Conclusions3

11.) The large Lorentz factors involved in cosmic radiation at energies above ~ 10^{19} eV provides a magnifier into possible Lorentz invariance violations (LIV).

Conclusions3

10.) At energies above ~10^{18} eV, the center-of mass energies are above a TeV and thus beyond the reach of accelerator experiments. Especially in the neutrino sector, where Standard Model cross sections are small, this probes potentially new physics beyond the electroweak scale, including possible quantum gravity effects.

11.) The large Lorentz factors involved in cosmic radiation at energies above ~ 10^{19} eV provides a magnifier into possible Lorentz invariance violations (LIV).

Conclusions3

10.) At energies above ~10^{18} eV, the center-of mass energies are above a TeV and thus beyond the reach of accelerator experiments. Especially in the neutrino sector, where Standard Model cross sections are small, this probes potentially new physics beyond the electroweak scale, including possible quantum gravity effects.

11.) The large Lorentz factors involved in cosmic radiation at energies above ~ 10^{19} eV provides a magnifier into possible Lorentz invariance violations (LIV).

12.) Many new interesting ideas on a modest cost scale for low precision, high statistics ultra-high energy cosmic ray and neutrino detection (radio, acoustic, space based...) are currently under discussion.

194